The identification and quantification of surface change on limestone shore platforms of the Maltese Islands

Ritienne Gauci

Lead Supervisor: Dr Robert Inkpen

Second Supervisor: Dr Andy Gibson

Third Supervisor: Dr Malcolm Bray

A thesis submitted in partial fulfilment of the requirements for the award of the degree of Doctor of Philosophy in Geography at the University of Portsmouth

March 2018

Abstract

Despite the extensive international research on shore platforms over the past 190 years, very little is known about the platforms skirting the micro-tidal coasts of the Mediterranean region. This study investigates the surface change dynamics operating at supratidal levels on five shore platforms of the Maltese Islands, situated in central Mediterranean Sea. The lithology of the five selected shore platforms is Globigerina Limestone, with two platforms formed in the Upper Globigerina Limestone Member (UGLM) and another three having exposures in Lower Globigerina Limestone Member (LGLM) intermixed with conglomerate beds of variable thickness. The selected sites were considered as representative of the Maltese shore platforms in terms lithology and are situated in five different locations on mainland Malta.

The study was undertaken over a period of four years and used a multi-method approach aimed primarily to understand the behaviour of rock surface change on limestone supratidal surfaces. Morphological characteristics of each platform, in terms of weathering and erosion forms, were described from geomorphological field observations. The spatial and temporal variability of surface hardness was calculated with a N-type Schmidt Hammer. The mineralogical composition of the platforms was assessed with near-infrared spectroscopy (NIR) to determine whether the mineral component has a role in surface change dynamics. In addition, a rock exposure experiment with sixteen slabs was undertaken over a period of a year and a half in order to monitor the level of limestone susceptibility to inland subaerial weathering processes. *In situ* rates and modes of surface change were measured and quantified using the Traversing Micro-Erosion Meter (TMEM) on a spatio-temporal sampling network of 31 measurement stations.

Though the five selected platforms were generally known to be lithologically similar, differences in morphological forms were observed on each platform, with site-specific presence of weathering and erosion forms. Surface hardness results ftom the Schmidt Hammer indicated a lithological variability of the surface hardness, with the UGLM platforms (Blata l-Bajda and Ras il-Fenek) being the most heterogenous of the group and controlled by the presence of hardground beds within this member. The surface resistance of the LGLM platforms (Ponta tal-Qammieħ, Ponta tal-Munxar and

Ponta tal-Miġnuna) were less divergent than those in UGLM, but still exhibited variability in surface hardness at spatial scale on each platform.

The weathering rates recorded in the subaerial weathering experiment confirmed the overal surface hardness properties measured on the platforms. The main differences were observed on the UGLM slabs, with Blata l-Bajda slabs experiencing the highest rates of rock weathering, whilst those at Ras il-Fenek were the least responsive in their alterations. The weathering results of the LGLM slabs from Ponta tal-Qammieħ, Ponta tal-Munxar and Ponta tal-Miġnuna mirrored the same mix of results recorded for surface hardness for their respective exposures.

A good part of the surface morphologies observed on the platforms point to visible evidence of a salt-weathered environment in a supratidal conditions. Mineralogy results recorded a strong presence of calcite as the main mineral type but they also confirmed the evidence of variable levels of sodium chloride, which suggest that platforms are characterised by variable levels of salt dominance. The samples from the UGLM platform of Blata l-Bajda was found to be the most salt-dominated. The mineralogy results of the platform samples were further confirmed by those done on the sixteen weathered samples, which recorded loss of sodium chloride after a year and half of inland subaerial exposure.

The mean rate of surface change was measured to be -0.237 mma^{-1} and ranged from 0.097 mma^{-1} to -3.247 mma^{-1}. The rates were close to other results for limestone surfaces at supratidal levels in the Mediterranean, such as those published by Swantesson *et al.* (2004) and Mayaud *et al.* (2014). They were however found to be on the low side for rates published by Micallef and Williams (2009) for LGLM platforms. Analyses showed no spatial-temporal patterns in the rates of surface change across platforms or between platforms, although the behaviour of surface change of front and middle sections of the platforms were observed to be more comparable. The rates of surface change calcuated over a semi-annual and annual time-scale are more comparable than those calculated over a tri-monthly time-scale. The conclusions are that the rates of surface change on these platforms are largely lithologically controlled and that that lithological surface heterogeneity between and within platforms has influenced measured rates of surface change.

Keywords: shore platforms, micro-tidal, supratidal, limestone, Globigerina, Maltese Islands.

Table of Contents

List of Figures

List of Tables

List of Abbreviations

a.m.s.l	above mean sea level
ASTM	American Society for Testing and Materials
BC	Blue Clay
C_1	Lower Conglomerate Bed
C_2	Upper Conglomerate Bed
cm	centimetres
g	grams
GL	Globigerina Limestone
ISRM	International Society of Rock Mechanics
kg	kilograms
km	kilometres
LCL	Lower Coralline Limestone
LGLM	Lower Globigerina Limestone Member
m	metres
MEM	Micro-Erosion Meter
MEPA	Malta Environment Planning Authority
MGLM	Middle Globigerina Limestone Member
MIA	Malta International Airport
mm	millimetres
mma^{-1}	millimetres per annum
MRRA	Malta Resources and Rural Authority
NIR	Near-infrared spectroscopy
nm	nanometre
SAC	Special Area of Conservation
SH	Schmidt Hammer
TLGLHg	Terminal Lower Globigerina Limestone Hardground
TMEM	Traversing Micro-Erosion Meter
UCL	Upper Coralline Limestone
UCS	Unconfined Compression Strength
UGLM	Upper Globigerina Limestone Member

Glossary

Annual time period	A period of TMEM measurements taken over a time scale of one year.
Backshore	The supratidal area of the back of the platform, situated at extreme inland limit of the platform (close to the cliff-platform junction) and is only affected by waves during exceptional high tides or severe storms
Cliff-platform junction	The meeting point (or interface) between the vertical foot of the cliff and the platform surface
Cross-shore	The direction perpendicular to the shoreline
Foreshore	That part of a coast lying between the lowest low-water line and the average high-water line
Frontshore	The front part of the platform above the high water mark (at supratidal level)
Erosion rates	Rates of surface recession or surface lowering by erosion, usually represented in microns or mma^{-1}
Exposure periods	Periods of months in which an experimental exposure slab has been subjected to weathering processes in outdoor conditions
Platform gradient	The degree of inclination along a platform surface slope
Impact points	Single rebound measurements collected through a plunger impact by the Schmidt Hammer
Individual time period	A period of TMEM measurements of rates of surface change over a time scale of between three and four months

Intertidal	The area that is above water at low tide and under water at high tide (in other words, the area between tide marks)
Longshore	A direction parallel to the shoreline
Low tide cliff	A vertical seaward margin (or scarp) which terminates abruptly a subhorizontal shore platform
Measurement session	A single field trip session in which surface hardness and/or microtopography were measured on each platform.
Micro-tidal	Where mean spring tide range is less than 2m
Middleshore	A supratidal position in the middle section the platform width a cross-shore direction
Modes of surface change	The behaviour in surface change of a rock in relation to the pattern or sequence of surface lowering and/or surface rising through time
Platform width	Horizontal distance between seaward edge of the platform exposed at high ride and the landward cliff-platform junction
R value	A rebound value produced by the plunger of a Schmidt Hammer
Semi-annual time period	A period of TMEM measurements taken over a time scale of six months
Solution pits	A weathered surface micro-form with a diameter equal to or less 0.15 cm
Solution pools	A weatherd surface form with a diameter bigger than 0.15cm
Subtidal	The part of the coast below low tide that is always covered by water

Surf zone	The zone of wave action extending from the water (which varies with wave conditions, tide, surf, set-up etc.) out to the most seaward point of the breaker zone
Supratidal	The area above the spring high tide line, that is regularly splashed, but not submerged by seawater. Seawater penetrates these areas only during zone, spray zone or supralittoral zone
Surface change rate	A rate which denotes a positive and negative change in height of the rock surface and measured in mma^{-1}
Surface lowering (fall)	A negative change in height of the rock surface below an earlier level, calculated over a year scale and measured in mma^{-1} and denoted in negative values
Surface rise	A positive change in height of the rock surface above an earlier level, calculated over a year scale and measured in mma^{-1} and denoted in positive values
Test points	A rock surface area within which a number of impact points were measured with the Schmidt Hammer to calculate surface rebound and determine surface hardness

Declaration

I.D.: UP 640203

Name: Ritienne Gauci

Degree: Doctor in Philosophy in Geography

Title of Thesis: The identification and quantification of surface change on limestone shore platforms of the Maltese Islands

Total number of words: 91,148

Whilst registered as a candidate for the above degree, I have not been registered for any other research award. The results and conclusions embodied in this thesis are the work of the named candidate and have not been submitted for any other academic award.

This thesis has been subject to review by University of Portsmouth Faculty Ethics Committee. The letter from the Faculty Ethics Committee confirming the favourable opinion and the form UPR16 declaring the ethical conduct of the research are included in Appendix I.

_____

Signature of Candidate

21st March 2018

_____

Date

Acknowledgements

I would like to express my gratitude, in no order of merit, to the following contributors who have supported this research:

Heartfelt thanks go to my supervisory team at the Faculty of Science of the University of Portsmouth, led by first supervisor, Dr Robert Inkpen, Department of Geography, whose scholarly mentorship, acumen and unfailing support proved indispensable for the execution of this work. Sincere thanks are also due to second supervisor, Dr Andy Gibson, School of Earth and Environmental Sciences, for providing sound expertise and patient assistance with mineralogy tests. The helpful input from third supervisor, Dr Malcolm Bray, Department of Geography, was truly appreciated.

This project has been funded by the University of Malta Scholarship Grant and two University of Malta Research Grants (GEORP 001 & 002). I would like to thank both grant committees and the HR personnel for their generous assistance.

Sincere appreciation goes to Dr Stefano Furlani (University of Trieste) for accepting to construct the traversing micro-erosion meter for this research and for his on-going research interests on the Maltese Islands.

This research received insightful advice also from Dr Saviour Scerri (University of Malta), Dr Julian Evans (University of Malta), Dr Martyn Pedley (University of Hull), Arch. Adrian Mifsud (University of Malta), Dr Niccolo Baldassini (University of Catania), Dr Luca Foresi (University of Siena) and Dr Adnan Aydin (University of Mississippi).

Due gratitude goes to Mr Linley Hastewell (University of Portsmouth) for his honest friendship and discussions during our mutual PhD studies, Ms Emily Butcher (University of Portsmouth) for lab assistance, Ms Sandra Mather for last-minute rescue with mapping and Dr Antoine Vella for proof-reading assistance.

Invaluable defines the presence of two academic scholars for their generous mentorship: Professor John A. Schembri (University of Malta) for inspiring my career as a geographer to this very day and Professor Maria Attard (HOD Geography, University of Malta) for her precious trust in my work. Due recognition also goes to my other work colleagues at the University of Malta - Ms Candida Gerada, Ms Sephora Sammut, Ms Joanna Causon-Deguara - and my students for their patient understanding, especially in the final writing stages of this study. My deepest thanks also to Reverend Professor Dave Chester

(University of Liverpool Hope) for his encouragement and prayers for my personal well-being.

My friendship groups, both the real one (especially Ms Mireille Falzon and Ms Lucienne Calleja) whose intelligent adult conversations on literature, education, travel and children kept me sane, and the virtual ones on social media – the PhD and Early Career Researcher Parents, Full Draft Club and Virtual SUAW Parents Edition - without whom I would have felt more isolated in the challenging world of PhD parenting.

Finally, but perhaps most importantly, my academic career would never have commenced without the meaningful companionship of my husband Patrick, the love of our two young kids, Kate and André and the silent understanding of our families. They have all inspired me to give it my best shot, although I am sure they are all relieved that the writing is finally completed.

It takes a village to complete a thesis. I consider myself blessed to have had one.

Dedication

This work is dedicated to my family

Patrick, Kate, André

and my father, Joseph Abela.

Also dedicated to the loving memory of

my mother, Mary Abela

and

my brother-in-law, Silvio Gauci.

1 Introduction

1.1 Research Context

This thesis investigates the rates and modes of surface change on Globigerina shore platforms of the Maltese Islands (Central Mediterranean Sea) in order to contribute to knowledge on processes of change along the Maltese limestone micro-tidal coasts. Shore platforms have been attracting the research interests of coastal geomorphologists since the early nineteenth century when scholars such as Hawkins (1827), Ramsey (1846) and Dana (1849) introduced the earliest research works on such landforms. Fast forward 190 years, the shore platforms of the Maltese Islands, together with those along the Mediterranean coasts, remain scantily investigated and relatively unknown.

1.2 Shore platform research

The geomorphology of shore platforms is considered to be mainly a product of local geology, tidal regime, wave climate and weathering environment (Trenhaile, 2002a; Stephenson, Dickson and Trenhaile, 2013a). A large body of literature recognised the importance of wave erosion and weathering in the development of shore platforms and their surface morphology. However defining the relative contribution of each and their synergies in the control-process-form dynamics remain opens for debate (Viles, 2013). Trenhaile (2011) affirms that there is a wide acceptance for both wave and weathering processes to operate in tandem for shore platform development. The role of each of these processes varies spatially according to changes in geology and morphogenic drivers, and temporally with changes in climate, sea level, and intertidal and subtidal morphology.

To better address the wave-weathering debate, studies have investigated the forces resisting formation, the processes causing change and the balance between the two. The quantification and modelling of processes causing change on shore platforms became a standard objective of most platform studies, as well as

defining the lithological controls which determine the rate of morphological change. The development of the micro-erosion meter (MEM), the traversing micro-erosion meter (TMEM) and laser scanner since the late 1960's allowed for accurate quantification of the rates of surface change on shore platforms at sub-millimetre scale (Swantesson *et al.*, 2006; Stephenson and Finlayson, 2009; Stephenson, 2013). The *in situ* tests of surface hardness such as with Schmidt Hammer opened a new dimension in the investigation of rock resistance on shore platforms and revived the quantification of rock control in platform studies (Goudie, 2006, 2013, 2016; Viles *et al.*, 2011). Other aspects of geological contingency linked to structure, such as discontinuities and tectonics, are also paving the way for new insights on the role of meso-scale forms in platform evolution (Naylor and Stephenson, 2010; Goudie, 2016; Swirad *et al.*, 2016; Stephenson, Dickson and Denys, 2017).

Platform modelling has remained very central in linking the processes responsible for change to a specific platform typology (Dasgupta, 2010). The typology proposed by Sunamura (1992) – Type A for sloping platforms and Type B for sub-horizontal platforms - remains the one most widely used but also heavily debated. Other workers have tried to deviate from this typology (Section 1.3). Bird (2008), for example, included a third type of shore platform referred to as a structural platform and which coincides with a more resistant stratigraphic unit being subject to differential erosion by wave quarrying. Chelli *et al.* (2010) proposed alternative typologies for their studied platforms in Italy. Stephenson *et al.* (2013) also suggested that platforms should not be defined on the basis of a specific geomorphic element such as a seaward cliff.

The modelling of platform typology according to tidal range has a long pedigree and it is by now widely recognised that tidal range controls the elevation of the mean water surface and the extent to which wave erosional processes are concentrated within the vertical plane (Trenhaile, 2008). In micro-tidal settings the vertical extent of the intertidal zone is narrow and this is known to favour the formation of near-horizontal platforms due to wave erosion being

concentrated in a narrow zone (Trenhaile and Layzell, 1981). Some studies have increasingly defined sub-horizontal platforms as a weathering product, due to limited onshore extent of wave action. According to Stephenson and Kirk (2000) only 5 to 7 percent of the wave energy at the seaward edge reaches the cliff foot, causing limited wave erosion on the platform surface. Trenhaile and Kanyaya (2007) and Kennedy and Paulik (2007) also demonstrated the ineffectiveness of waves on sub-horizontal platforms in observing how waves break in front of, or directly over, the sharp low-tide cliff.

1.3 The need to study other boundary conditions in shore platform research

In the ever-growing wave-weathering debate, it is important to widen the geographic dimension of research in which shore platforms are studied (Stephenson and Naylor, 2010). To date most of the widely studied platforms are located along open-ocean coasts (mainly in North Atlantic and Pacific). The majority of the platforms studied were identified within two specific boundary conditions: high tide shore platforms assessed within intertidal levels (tide) and across different lithologies (geology). The traditional choice of such boundary conditions is based on the fact that many process-based studies deal with time-constraints. As a result, many platform studies focused their attention upon features which exhibited measurable change within a research project's lifespan of a few years related to a doctoral's research project or a grant (Trenhile and Porter, 2018). It is widely acknowledged that intertidal conditions produced larger magnitudes of rates of surface change compared to supratidal ones. Together with lithological differences from one geological unit to another in the same region, these conditions captured ample spatio-temporal data against which to investigate control-process-form dynamics. This skewed dimension of research further justifies the scope to extend platform research to other specific boundary conditions widen and strengthen comparative analyses in platform studies (Chelli *et al.*, 2010).

Within the micro-tidal setting, most works come from the southern hemisphere regions of New Zealand and southern Australia and within climate bands of tropical and subtropical world, as well as northern hemisphere regions of Japan and Korea (Gill, 1967; Trenhaile, 1987; Stephenson and Kirk, 1998; Trenhaile, 2008; Sunamura, Tsujimoto and Aoki, 2014; Kennedy *et al.*, 2017). These regions are considered different from the Mediterranean on a number of levels. Moses (2013) pointed out how tropical coasts, though micro-tidal and with low wave energy regimes (Davies, 1964), are also influenced by high exposures to wave energy from trade winds, monsoons and tropical cyclones (Trudgill, 1985, Davies, 1980). Semi-horizontal platforms in Southern Hemisphere regions have developed along oceanic coasts and have a sea level history of mid-Holocene high stands of +1 to +2 m and which subsequently fell to its present level after the middle Holocene (Pirazzoli, 1986). Recent models proposed that the sub-horizontal shore platforms over much of the Southern Hemisphere were in fact formed when the Holocene sea level was higher (Trenhaile, 2010).

In the Northern Hemisphere, the higher land-sea ratio and ice covered landmasses mark a more complex relation with post-Holocene deglaciation. Much less work on micro-tidal platforms comes from the Northern Hemisphere, in which areas formerly covered by ice sheets (such as parts of the British Isles) experienced relative sea level fall to its present level due to glacio-isostatic uplift. Much of the rest of the unglaciated Northern Hemisphere (such as in the Mediterranean region), saw its sea level rise to its present level, submerging former platforms (palaeoplatforms) and creating contemporary ones along shorelines over the last 3,000 to 4,000 years (Pirazzoli, 1993).

Comparability of platform development and typology between the Northern and Southern Hemisphere is problematic due to the complexity generated by local factors and their relative responses to past sea levels. Regionally dominant sub-horizontal platforms with low tide cliffs are documented to be found along the North Atlantic. Though the coasts of the Northern Hemisphere display a diverse range of tides and resultant platform typologies, only those in Canada and the

British Isles have been comprehensively studied. Sub-horizontal platforms with low tide cliffs are commonly associated with micro-tidal (but also meso-tidal) environments. They are recorded to have developed along western Newfoundland and Gaspé, Québec and their morphology is said to be comparable to those in similar tidal ranges in Australasia despite differences in climate (Trenhaile, 2008). In this case the platforms are still attributed to higher relative sea levels during the Holocene when formerly ice-covered landmasses around the North Atlantic were at relative lower elevations. The distribution of platforms around the British Isles is equally complex and determined not only by tidal ranges but also by glacio-isostatic adjustments, funnelling effects from embayed configurations and wave climate. Tidal range varies from a minimum of 1.75 m in SE Ireland up to 5 m in the south coast of England (Moses, 2014).

Within the micro-tidal regime, tidal range levels from 0-2 m and wave exposure may still produce different surface morphologies notwithstanding that they belong to the same lithology and tidal setting. Trenhaile (2015) pointed out how, within the same micro-tidal regime of limestone coasts in Bermuda, the profile morphology of the coast with a tidal range of 15 to 20 cm was substantially different from other more exposed coasts with a tidal range of 1 to 2 m. So it should not be discounted that same lithology and tidal range produces similar platform morphology.

With regard to the Mediterranean coasts, the first research gap identified is that only a handful of works have dealt with micro-tidal shore platforms in a semi-enclosed sea region which experienced a Holocene sea level trend inverse to that of the Southern Hemisphere (Robinson and Lageat, 2006; Swantesson *et al.*, 2006; Gómez-Pujol, Fornós and Swantesson, 2006; Andriani and Walsh, 2007; Furlani *et al.*, 2009, 2011, 2014; Chelli *et al.*, 2010; Chelli, Pappalardo and Pannacciulli, 2012; Causon Deguara and Gauci, 2017; Pomar *et al.*, 2017; Gauci, Schembri and Inkpen, 2017; Pappalardo, 2017). The European Shore Platform Dynamics (ESPED) project, funded by the European Union under MAST II programme (1998-2001) and the Italian platform project to characterise the platforms along the Ligurian

and Tyrrhenian Sea (Chelli, Pappalardo and Pannacciulli, 2012) were two steps in the right direction to address the lacuna of knowledge about Mediterranean shore platforms.

More research on sub-horizontal platforms in the Mediterranean is required as the current research based on higher Holocene sea levels does not fit well with the past sea level history of the Mediterranean. In fact the model of sub-horizontal platforms developed by higher Holocene sea levels, as proposed by Trenhaile (2010) does not explain the presence of sub-horizontal platforms in the Mediterranean, such on the Maltese Islands, when Holocene sea level rose to the present levels around the Maltese Islands (Furlani *et al.*, 2013; Micallef *et al.*, 2013). Additionally, it does not align with the theory that platforms are indicative of recent emergence such as by Kirk (1977) for the sub-horizontal shore platforms in southern New Zealand. The Maltese Islands are known to be tectonically stable and most shore platforms are found along coasts that have been studied for Holocene submergence rather than emergence (Furlani *et al.*, 2013).

Another research gap is that fewer works have studied the surface morphodynamics within a supratidal setting and across the same lithology. Within the context of the semi-enclosed Mediterranean Sea with limestones micro-tidal coasts, many sub-horizontal platform surfaces are exposed at supratidal levels. If weathering is such a dominant process on micro-tidal platforms, quantifying the *in situ* weathering rates on Mediterranean shore platforms across variable spatial and temporal scales is necessary in order to improve our understanding of the weathering mechanisms and be able to compare these results with other international studies with similar boundary conditions.

Studies of platforms in limestone lithology should be a priority given that one of the defining characteristics of the Mediterranean physical landscape is the prominent limestone rocky coast which accounts for 54 per cent of the total coastal length (Woodward, 2009). What percentage of this length represents shore platforms still remains unquantified, but the absence of such estimate is an

evident sign of the lack of attention given to this coastal landform. More studies on the limestone shore platforms along the low-tidal range coasts (a few decimetres) of the Mediterranean would provide a wider insights about weathering dominated platforms, already researched as primary role in the development of sub-horizontal shore platforms in Australasia and other warm environments (Bartrum, 1916; Wentworth, 1938; Bird and Dent, 1966; Healy, 1968; Robinson, 1977a, b; Mottershead, 1989; Stephenson and Kirk, 2000; Foote *et al.*, 2001).

Specifically, on the Maltese Islands, with a land surface of only 365 km ^{2} and a disproportionately long coastline of 272 km, 97 per cent of its coastline is a diverse assemblage of limestone landform systems and ranks as the highest in terms of the country's percentage composition of rocky coasts in the Mediterranean region (Woodward, 2009; Said and Schembri, 2010). Despite this, the number of studies on rocky coast processes is still small. Additonally, the few existing studies are mainly restricted to particular areas with a specific type of landform unit, such as sea cliffs by Farrugia (2008), bouldered beaches by Biolchi *et al.* (2015), Causon Deguara and Gauci (2017), landslides on the north-west of Malta by Devoto *et al.* (2012, 2013) and paleosinkholes in north-west Gozo by Soldati, Tonelli and Galve (2013) and Galve *et al.* (2015). Literature on local geology has to date only made subjective reference, based on visual observations, to rock erosion and weathering processes operating on shore platforms.

To date, Maltese shore platforms have not been scientifically researched as a geomorphological landform. Surface area calculations by Schembri (2003) estimated shore platforms to occupy 3.3 per cent of the total coastal area of the Maltese archipelago, whilst Biolchi *et al.* (2016) proposed a 15 per cent of the total coastal length of mainland Malta. To date, only one work i.e. by Micallef and Williams (2009) has attempted to quantify the processes of surface change on Maltese shore platforms. Beyond that, not much else has been produced in terms of research. As a result, the nature of the development of Maltese shore platforms within a micro-tidal regime is still not fully understood and many of their surface morphological features have yet to be scientifically described and measured.

1.4 Why study Maltese Globigerina shore platforms: the background narrative

In the previous sections, the choice of Maltese shore platforms was justified in terms of their representation as micro-tidal, sub-horizontal limestone platforms within a Mediterranean context, and for which previous researchers have identified a research gap and encouraged more work (Chelli *et al.*, 2010; Chelli, Pappalardo and Pannacciulli, 2012; Pappalardo, 2017). In addition to this, however, various important connections also exist between the maritime history of the Mediterranean Sea, the development of coastal land use on the Maltese Islands and the presence of shore platforms skirting along their shores. Whilst many just consider shore platforms as 'flat' rocky outcrops of no particular utility, their strategic presence at land-sea interface, especially in sheltered bays, provided efficiency of access for maritime and recreational purposes over the course of many centuries (Buttigieg, Vassallo and Schembri, 1997). Nevertheless, such a role has largely passed unnoticed due to the lack of research in connecting these landforms to such development. The following paragraphs aim to briefly contextualise the importance of shore platforms within the foreshore development of the Maltese coasts, as result of the geo-political events that unfolded over the centuries in the Mediterranean region. It is hoped that this short narrative will elucidate further what these landforms represented and further demonstrate the scope for more research.

Strategically located in the centre of the Mediterranean Sea, the Maltese Islands have long served as an important waterway outpost for various Mediterranean and European maritime powers. Table 1.1 illustrates how the use of shore platforms represents a long millennial history of human occupancy and colonisation dating back to Neolithic times (5000 BC). For early settlers, the coast served as the main survival link with nearby lands (such as with Sicily) for the supply and trading of goods. A few archaeological remains on shore platforms may indicate other uses of the platforms by early settlers, apart from that as access points to the sea. Archaeological examples include cisterns and historic cart ruts and these have served as an important indicator for sea level reconstruction carried out by Furlani *et al.* (2013) (Figure 1.1a, b). The maritime role of the

islands strengthened through the ages, culminating during the period of the Knights of St John and the British occupancy, who established the Grand Harbour area as the main seat of their maritime operations and optimised shore platforms for access to the fortified harbours and bays around the islands (Schembri, 2003) (Figure 1.1d).

Table 1.1: Growth of shore platform uses though the ages (Source: Compiled by Author)

Period	Date	Platform uses
Neolithic	no date	historic cart ruts
Bronze Age	1500-900 BC	cisterns, dye pits (?)
Roman	218-533	cisterns, small port operations
Norman	1194-1530	salinas
Knights of St John	1530-1798	military operations coastal defences salinas, fishing
British Empire	1800-1964	consolidation of maritime operations recreational uses ex. Victorian baths
Post-independence	1965-present	growth of mass tourism development of open public spaces intensification of retail facilities access services such as promenades, stairs, ramps other outdoor sports activities ex. fitness training, yoga use for filming industries salinas as ecotourism product

With more coastal protection in place, other industrial activities proliferated such as the salina industry, mostly (but not only) carried out on the sub-horizontal shore platforms in relatively softer Lower and Upper Globigerina Limestone (Gauci, Schembri and Inkpen, 2017) (Figure 1.1c, e). Today, with profound changes in the salt production by the world salt market over the last century, this extractive practice declined as an industry and currently holds more an artisanal status as a prime site for geo-tourism (Gauci, Schembri and Inkpen, 2017). Towards the end of the 19th century and the start of the 20th century, shore

platforms acquired such a popular recreational status by the middle and upper class that various swimming bath complexes were cut out from various shore platforms to accommodate safe and shallow waters for non-swimming bathers (Schembri, 2003) (Figure 1.1f).

During the 20th century and especially after independence from the British, the tourism sector and in particular mass tourism, was viewed as the alternative key to income, with annual tourist arrivals soaring from 28,000 (1960) to over 1.1 million in 2000 (Boissevain, 2004) and 2.3 million in 2017 (NSO, 2018). The rise of mass tourism had a profound effect on the coastal landscape, with the growth of many coastal localities and the absence of proper planning legislations. The foreshore was mostly seen as a way to maximise economic revenue from tourists, restricting most of Malta's accessible coast and maximizing capital to satisfy the demands of foreign consumers at the expense of local residents (Anderson and Schembri, 1991; Selwyn and Boissevain, 2004). Coastal stretches and embayments with shore platforms could not escape from a similar fate of frenzied development (Buttigieg, Vassallo and Schembri, 1997).

Today most of the shore platforms within recreational areas like Sliema, Buġibba, Qawra, St Paul's Bay, Baħar iċ-Ċagħaq, Marsaskala, Marsaxlokk and Birżebbugia are heavily encroached with retail facilities and services to accommodate the capitalistic demand of the tourism sector. A more encouraging note is the increase in public sensitivity to building development permits close to shore platforms, especially if these cut access to the sea or are in outside development zones (ODZ). The rapidly expanding network of several environmental NGOs (such as Nature Trust and Friends of the Earth) was crucial in monitoring development and sensitising civil society (Boissevain, 2004).

Figure 1.1: Historical land uses of Maltese shore platforms. a. Bronze Age pits at St George's Bay, Birżebbugia b. Cart-ruts at St George's Bay Birżebbugia c. Salini of the Darmanin family, Marsaskala d. Valletta fortifications at Fort St Elmo, with further contemporary land use encroachment in front of the bastion lines. e. Original salini (undated) hewn out of natural hollowed surfaces on Sliema shore platform. f. Victorian baths on Sliema shore platform (Source: Photos taken by Author)

1.5 Research Aims and Objectives

The impetus for this study is driven by the need to gain a more detailed understanding of the morphology at supra-tidal levels and surface change morphodynamics operating on micro-tidal shore platforms within the same limestone lithology. This will be achieved by choosing the relatively unknown shore platforms of the Maltese Islands as a study area and address the issues discussed above by adhering to the following three aims:

i. To provide a detailed morphological assessment (micro- and meso-scale) of five micro-tidal platforms of the Maltese Islands and critically review how the present morphological features relate to controls and processes operating on the platforms. This geomorphological information is key to understanding how the Maltese platforms place within the context of other published studies on limestone platforms in the Mediterranean - such as Andriani and Walsh (2007), Furlani *et al.* (2011), and Swantesson *et al.* (2006) - and elsewhere such as by Naylor and Stephenson (2010), Cruslock *et al.* (2010), Moura, Gabriel and Jacob (2011) and Marshall and Stephenson (2011);
ii. To extend the limited body of literature related to the identification and quantification of rates of surface change on supratidal platforms. This will allow data from shore platforms on the Maltese Islands to be compared with those from other studies and in so doing, address the problem of a lack of empirical comparison with Mediterranean platforms as recently reiterated by researchers such as Chelli *et al.* (2010) and Pappalardo *et al.* (2017); and
iii. To understand how specific *in situ* properties such as surface hardness and mineralogy determine platform spatial responses to processes of surface change or vice-versa.

The objectives set out to address the above mentioned aims are as follows and are also outlined in Table 3.3:

i. Create geomorphological maps for each of the five selected shore platforms by examining their surface morphology at micro- and meso-scale (Hypothesis no. 1, Table 3.3);
ii. Investigate the lithological control of the platforms by measuring in situ surface strength with the use of N Type Schmidt Hammer (Hypothesis no. 2 and 3, Table 3.3);
iii. Compare the lithological properties of each platform by examining the responses of each lithological sample to weathering with the set up of an outdoor experimental trial (Hypothesis no. 4, Table 3.3);
iv. Investigate the in situ mineralogical properties of each platform, through the use of the Near Infrared Spectroscopy (NIR) ((Hypothesis no. 5, Table 3.3); and
v. Measure and compare the rates and modes of surface change on each platform and experimental slab through the use of the Traversing Micro-erosion Meter (TMEM) (Hypothesis no. 6, 7 and 8, Table 3.3).

1.6 Thesis Outline

This chapter has introduced the research context by showing that the current state of research on Mediterranean shore platforms is currently unsatisfactory and requires further impetus. The present research paradigms on micro-tidal shore platforms do not provide sufficient data to allow comparisons of non-oceanic platforms, and especially for platforms in which the tidal range is only of few decimetres. There is the need to measure processes of surface change and how they operate at supratidal levels and identify how limestone surface properties respond to processes of change. Within this context, three main aims and five research objectives have been set out for the study.

Chapter Two provides the literature context for this study through a review of the body of research on shore platforms and with particular focus on works based on three boundary conditions: micro-tidal, limestone and supratidal environment.

The chapter provides a synthesis of the current state of knowledge of platform research and highlights in detail knowledge gaps about Maltese shore platforms. Literature on studies of Globigerina limestone surfaces and shore platform denudation on the Maltese Islands are also presented.

Chapter Three presents a detailed exposition of the methods and instrumentation used to collect field and laboratory data in this research. The study adopted a multi-method approach based on three strands of data collection: morphological investigation, geo-technical assessments (including lab mineralogy tests) and measured rates of surface change (Table 3,1). The morphological investigation was done through field geomorphological assessment of the platforms' surface. The geo-techncial assessments were based three test: 1. Surface hardness field tests (using the Schmidt Hammer); 2. Weathering exposure experiment; and 3. Mineralogy tests using the near infrared spectroscopy (NIR). The surface hardness test aims to gauge the surface resistance of the platform to erosion and weathering processes. Field analysis was supplemented by a series of exposure experiments. These were designed to gauge visually and quantitatively the relative susceptibility to weathering of each limestone exposure. Together with the mineralogy tests, the results will provide a better insight of the spatio-temporal parameters of the platforms' geo-mechanical properties and on the basis on these results infer the likely responses to processes to surface change. The measured rates of surface change were undertaken with the use of the Traversing Micro-Erosion Meter (TMEM) on a spatio-temporal scale.

Chapter Four presents the findings of the field investigations of the morphological features present on the platforms. The observations are presented in a series of detailed large–scale geomorphological maps in order to provide meso-scale evidence of how controls and processes have shaped the surface morphology of the platforms. The compilation of maps also helps to set the landscape context for a more informed visual comparison of these lithologically similar landforms and provide evidence of the extent of their morphological diversity.

Chapter Five presents the results of four other investigations related to both the weather conditions monitored during the study period and the surface resistance properties of the platform lithology. Included in this chapter is an analysis of climate data for the study period 2012-2016, an important factor in rock weathering.

Chapter Six presents results of the rates of surface change for platform and exposure blocks surfaces as measured by the TMEM. The rates were described and subsequently analysed through non-parametric tests on a spatial, temporal and spatio-temporal level in order to identify patterns of statistical similarities and differences at TMEM station level and platform level (spatial) and across annual, semi-annual and individual time periods (temporal).

Chapter Seven brings together the findings data presented in Chapters Five, Six and Seven to critically discuss the implication of the findings and the relative contribution of each to the study of processes of change on shore platform surfaces. A context of how these findings sit within the international research on platform studies is also highlighted.

The final chapter, Chapter Eight, presents a succinct summary the main outcomes of the research and reflects on the limitations of each instrument or technique used to examine shore platforms' surfaces and quantify their rates of surface change. The study's findings and their implications are evaluated within the context of environmental management of the Maltese coasts and avenues for further research and policy directions are recommended.

2 Literature Review

2.1 Research on rock coasts: introduction and context

Rock coasts occupy a very high proportion of the world's littoral and act as important sources of sediment for estuaries and beaches. The estimate of Emery and Kuhn (1982), i.e. 80% of the world's coastline, has often been quoted as the global figure representing rocky shores. Despite the wide geographical extent of rock coasts, their significance in coastal research is relatively recent when compared to soft sedimentary coasts. Until the mid-twentieth century, the focus of coastal research prevailed on beaches and other sedimentary coasts, since these landforms were perceived to have a greater human value. Rocky coasts scientists Trenhaile (2002) and Naylor, Stephenson and Trenhaile (2010) reiterate that modern research emphasis still continues to be on beaches, salt marshes, and other economically important coastal features and argue that this is due to global attention of the scientific community given to the phenomenon of global warming and related potential vulnerability of beaches to rising sea levels.

Although research on rock coasts is still relatively less well-examined, progress over the last four decades, has to be nevertheless acknowledged. Catalysts to such progress were the first two monographs entirely devoted to rock coast geomorphology published by Trenhaile (1987) and Sunamura (1992), who unveiled the vast research potential of rock coasts and the limited contribution to it by a fairly small number of geographically dispersed scientists.

Coastal research increasingly embraced the geomorphic system of rocky landforms in a diversity of settings and conditions (Naylor, Kennedy and Stephenson, 2014). Trenhaile (2012) defined such research growth not only in terms of increasing number of active rock coast researchers and of papers published, but also due to a wider recognition of the importance of rock coasts among a general coastal research population. The unprecedented increase of anthropogenic pressures and related hazards, impacts from climate change and

geo-heritage awareness have all been providing a practical need to understand rock coast dynamics and evolution at various sub-disciplines (Stephenson and Naylor, 2010; Kennedy, Stephenson and Naylor, 2014). Amongst the most notable developments, there were areas such as modelling the dynamics and behaviour of rock coast evolution, measuring of erosion at various spatial and temporal scales and applying a myriad of field and laboratory techniques in order to quantify the effects of multiple processes and rock controls. A unifying driver to all this, was the advent of new technologies which enabled the investigation of problems at scales and dimensions not previously explored (Kennedy, Stephenson and Naylor, 2014).

The challenge of how to relate the value of rock coast systems to wider geomorphological and earth science debates remains ever-present but thanks to a growing collaborative community of researchers from various parts of the world, rock coast research to date enjoys a stronger literature landscape. The recent work edited by Kennedy, Stephenson and Naylor (2014), *Rock Coast Geomorphology: A Global Synthesis,* provides evidence of this healthier state of works.

2.2 Shore platform: definition and research development

In attempting to understand the processes responsible for rock coast development, shore platforms were amongst the first landforms to be studied. Shore platforms are conspicuous landforms along much of the world's coastline and occurring in all but the very highest coastal latitudes, as well as lakes. The total percentage of coastline composed of shore platforms is unknown and thus they remain as an unquantified component of rocky shore environments (Stephenson and Kirk, 2006). In addition, these coastal landforms do not exist in isolation but are associated with a variety of morphological features such as cliffs, sea caves, ramps, notches, potholes, ramparts, solution pools, boulders and low-tide cliffs.

Although many workers agree that there is an inherent complexity in defining how shore platforms are formed (Trenhaile, 2006a), most workers define shore platforms as a resultant product of cliff recession. Trenhaile (2006a) defines them as "*rock surfaces created by the erosion and retreat of coastal cliffs*" (2006a: 956), whilst Stephenson and Kirk (2006) are more specific in terms of gradient and lithology and describe them as "*horizontal or gently sloping surfaces backed by a cliff, eroded in bedrock at the shore*" (2006: 873). However there is no overall consensus with regards to the definition parameters. In his IAG glossary for geological terms, Goudie (2014) defines it as "*a flat or gently sloping smooth or relatively smooth rock surface formed in the zone between high and low tide levels*" (2014:68). This latter definition does restrict the occurrence of shore platforms to those tidal ranges that can accommodate such landforms and disregards platforms formed along much narrower micro-tidal ranges and which occupy supratidal conditions.

Their genesis has been debated about for more than 150 years (De La Beche, 1839; Dana, 1849; Bartrum, 1916, 1924). Individual workers from a geographically diverse environment, started to investigate the origin and morphology of shore platforms and as a response to such diversity, a wide variety of terms were used to name this landform. Stephenson and Kirk (2006) listed at least twenty-five different terms synonymous with 'shore platform' used in the growing literature and each term had quite a different genetic and morphological meaning. The authors proposed that given "*the development of shore platforms and the processes involved are still not fully understood*" (2006: 873), the genetically neutral term 'shore platform' should considered more appropriate, as it has no genetic connotations. Much of the literature published over the last decade has in fact made use of this term.

As reviewed by many scholars, such as by Trenhaile (1980) and Stephenson (2000), much of the initial work and until the late 1960s was mostly characterized by qualitative and explanatory writing, with no attempt to quantify either the processes or the rates of erosion. Such work, which still exerts a strong influence

in modern texts, was descriptive and generally concerned with determining whether platforms are the product of wave erosion or weathering processes through morphological enquiry. However, the qualitative approach to the study of shore platforms hindered the possibility of comparative studies of local examples. In fact, Kirk (1977) stated that, as a result of such qualitative research, *"it is difficult to compare studies from one environment with another, and there are few hard data with which to rigorously test different hypotheses of shore platform development*"(1977: 573). Principally from the 1980s, there was a shift in the research paradigm from qualitative observations to quantitative analyses. Instruments such as the micro-erosion meters (MEMs) were developed to measure surface erosion. New field techniques such as photogrammetry were rapidly applied whilst supported by more sophisticated equipment and lab techniques to analyse rock properties (Dasgupta (2010).

Research on shore platforms proliferated inasmuch that periodical reviews were published to highlight such research growth, mainly by Trenhaile (1980), Stephenson (2000) and Dasgupta (2010). Trenhaile's (1980) paper is considered as the first scientific review on the topic, describing shore platforms as a neglected coastal feature given that the research "*reflects the activities of a rather small number of workers' and thus exhibits and only a minute sample of platforms that exist around the world*" (1980:1). In his work, the author reviewed how the research work was mainly carried out under the following main strands: 1. Processes of platform development; 2. Geological influence; 3. Genetic classification of platform evolutionary cycles; 4. Platform morphology and morphogenetic environment; 5. The role of tidal duration; and 6. Inheritance aspects and equilibrium.

Trenhaile's review work was followed up two decades later by Stephenson (2000), who re-confirmed Trenhaile's landmark description of shore platform as a neglected coastal feature and reiterated how "*20 years later this is still the case"* (2010: 312). Stephenson (2000) identified four major themes in shore platform research, namely: 1. the role of marine and subaerial processes on the

development of platforms; 2. morphology of platforms; 3. modelling the development of platforms; and 4. measurement of erosion rates on them. The last two themes were considered as the fastest-growing areas when compared to those carried out during Trenhaile's 1980 review. A decade later, Dasgupta (2010) highlighted "*the remarkable proliferation of research interests in shore platforms and much-improved data sets on the processes acting on them*" (2010: 183). He further built on the four themes proposed by Stephenson (2000) and identified newer themes of research that were enhancing the understanding of shore platform morphodynamics, such as the application of geo-informatics in understanding the dynamics of shore platforms and cliffs, focus on low wave energy environments, geological control on processes acting on platforms and their morphology, and inheritance.

At European levels, one of the most significant contributions to collaborative understanding of shore platforms was the European Shore Platform Erosion Dynamics (ESPED) project. This research project – the results of which were published in a special volume (Robinson and Lageat, 2006) - was primarily focused on examining current processes and recent landform evolution. Themes presented in the ESPED project ranged from micro-erosion meter and laser scanner studies of different lithologies and morphogenetic environments to chalk cliff recession and erosion studies and further discussions on inheritance. It is also worth noting that at the IAG Regional Conference in Malaysia (June, 2007), a few key messages emerged by members of the AIG/IAG rock coast working group about the definite growth in research on rock coasts, especially in the light of the ESPED project. Most notably, amongst these messages, was how shore platforms have become a much less neglected landform due to the remarkable proliferation of research interests in shore platforms over the last two decades (Naylor, Stephenson and Trenhaile, 2010; Kennedy, Stephenson and Naylor, 2014).

2.3 Platform typologies and related boundary conditions

Shore platforms have long been classified using a variety of environmental criteria. The latter would create specific conceptual boundaries within which one set of platforms would be distinguished from another, based on the environmental conditions in which they have developed, hence 'boundary conditions' (Kennedy, Stephenson and Naylor, 2014). The one most widely used is a tripartite classification based on elevation in relation to the tide: 1. High-tide platforms, would be platforms elevated at high tide and only submerged at this level; 2. Intertidal platforms are bound within the tidal range between the highest high-tide and the lowest low-tide and; 3. Low-tide platforms would correspond to platforms exposed only at low tide (Schwartz, 2006). Platforms in meso- and macro-tidal ranges regimes would be usually investigated at intertidal level, due to the multitude of morphodynamics triggered by the cyclical shifts of the tide. On the other hand, narrow tidal ranges make it difficult to examine platforms at intertidal levels and it is more likely that they would be examined in combination with supratidal levels as well.

Though relatively less in number, a few works have investigated platform surfaces at supratidal level i.e. that zone above the high tide where it is exposed to wave splash as seawater is thrown up onshore by breaking waves. Further landward sea spray may deposit dry salt deposits on land surfaces depending on suitably windy conditions. Mottershead (2013) argue that shore-normal zonation across this zone is defined by such highly variable conditions and by varying fluctuations of tides and weather conditions.

Another long-standing and widely-used traditional classification of rocky coast morphologies is that proposed by Sunamura (1983; 1992) in defining three major morphologies described hereunder and illustrated in Figure 2.1:

i. Shore platforms that slope gently (1-5^0) into the sea; they are sometimes called ramps and they usually extend from the cliff base to below the low tide level, without any major break of slope;
ii. Platforms that are nearly horizontal and terminate abruptly with a cliff or ramp at the seaward edge (also known as low tide cliff); they can occur above, within or below the intertidal zone; and
iii. Plunging cliffs in which shore platforms have not developed.

Sunamura (1983; 1992) distinguished between two platform morphologies by assigning the designations Type A to sloping platforms and Type B to sub-horizontal platforms (Figure 2.1). Platforms have been traditionally classified under such typology and within broader regions ever since. Much of the early literature placed the occurrence of sub-horizontal platforms in Australasia and Hawaii, and of sloping platforms around the storm waters of North Atlantic (North–east USA and Britain).

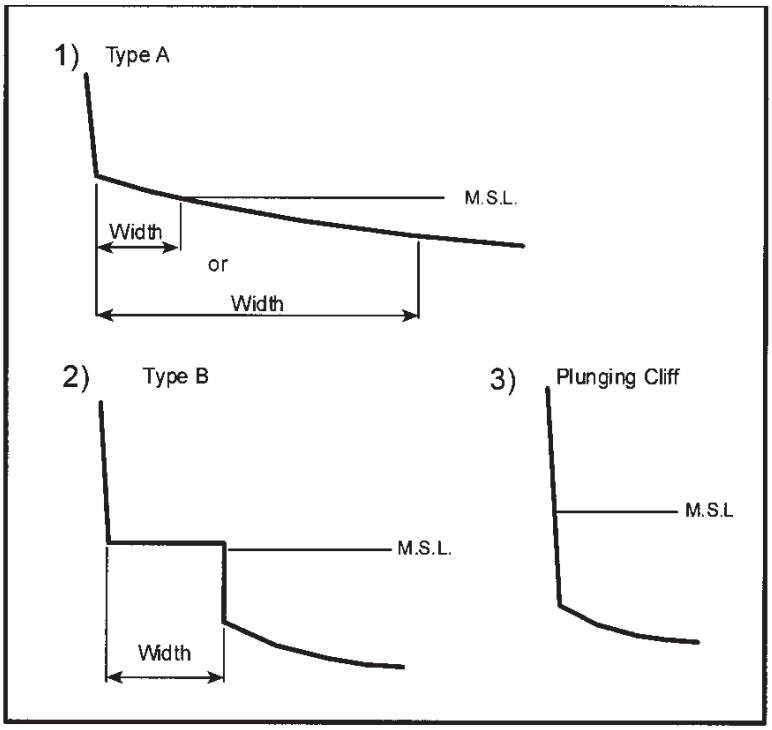

Figure 2.1: Three major morphologies of rocky coasts and two types of shore platform: 1) Type A; 2) Type B; and 3) plunging cliffs (Source: Sunamura, 1992).

Type B shore platforms are the focus of this present study. They are considered as typical of the micro-tidal regime of Australasia (Japan, Korea [East Coast] and New Zealand [Kaikoura Peninsula]) and in much of the tropical and subtropical world (Bartrum, 1924; Jutson, 1939; Edwards, 1941; Sherbon Hills, 1949; Cotton, 1963; Bird and Dent, 1966; Gill, 1967; Sunamura, 1992; Sunamura, Tsujimoto and Aoki, 2014; Choi and Seong, 2014; Dickson and Stephenson, 2014). Their width and elevation may vary considerably: from a few meters to hundreds of meters in width and formed at low-tide, inter-tidal elevations, and at a range of supratidal elevations up to several meters above high tide (Stephenson, Dickson and Trenhaile, 2013a).

On micro-tidal platforms, the vertical extent of the intertidal zone is narrow and this favours the development of near-horizontal shore platforms, with a seaward terminus present at the edge of the platform (Trenhaile and Layzell, 1981). Several workers also argue that sub-horizontal shore platforms were shaped by former sea-level high stands during the Holocene changes in sea level over much of the Southern Hemisphere (Trenhaile, 2010).

In line with the same argument about tidal range, it was assumed that sub-horizontal platforms were absent from the stormy North Atlantic due to inability of waves to cut horizontal surfaces, because of the wide range of elevations over which they operate (Sherbon Hills, 1972). However, it is now widely recognised that each type may be dominant in many other regions such as sloping platforms found in tropical and sub-tropical worlds (Trenhaile, 2006b). Regionally dominant sub-horizontal platforms in the North Atlantic were also found and investigated in micro- to mesotidal environments (Trenhaile, 1978; Trenhaile, 2008). They were described as morphologically similar to those in similar tidal environments in Australasia, notwithstanding the differences in climate (Porter *et al.*, 2010b).

Morphological differences between shore platforms in the southern and northern hemisphere, and more particularly in Australasia and Britain have been the subject of much debate. Trenhaile and Layzell (1981) suggested that

geological factors produce variations in platform geometry about morphological means which are determined by the morphogenic environments. Gill and Lang (1983) proposed that Type A and Type B profiles are different stages of development towards an ultimate profile of equilibrium and concluded that Type A and B platforms were not two distinct morphologies but rather two stages in one evolutionary process. However, Trenhaile (1987) argued that Type A and Type B terminology is not universal and only applies in micro- and mesotidal environments. Tsujimoto (1987) proposed a quantitative method to demarcate between Type A and Type B platforms and suggested that the distinction between Type A and Type B platforms is based on tidal range. Closer to more recent times, Stephenson (2000) reiterated how "*morphology is a notoriously ambiguous indicator of process and of process rates"* (2000: 312-3). In his review, the author stresses for the need to determine the universality of Sunamura's classification, given that clear relationships between platform morphology and the process environment have not been convincingly established; and this, notwithstanding and because of, the much-improved data sets of the processes acting on them from the previous decades.

Trenhaile (2012) also suggested that such a demarcation might not be possible given the considerable variations in the morphology of a shore platform within small areas, as a result of changes in rock structure, lithology and exposure to wave attack. In addition, the physical resistance of shore platforms depends upon their rock chemical composition, angle of dip, strike, bed thickness, joint pattern and density, degree of weathering and a myriad of other factors (Trenhaile, 2006b).

The presence or absence of the scarp is generally used in classifying the morphology as Type A or Type B. Confusion arises how to classify micro-tidal platforms that have no clear seaward scarp (such as Stephenson and Kirk, 2000a, 2000b; Kennedy and Dickson, 2006; Kennedy and Milkins, 2015). Classifying them as Type A may result ambivalent since Type A platforms have developed in different conditions in a macrotidal setting. Sites with mixed typologies have also

been observed in the Mediterranean such as by Chelli *et al.* (2010) and Chelli, Pappalardo and Pannacciulli (2012). The authors found it difficult to assign an A or B typology to the micro-tidal platforms in NW Italy and attributed this to the fact that the platform classification is based on oceanic shore platforms (coastlines of North Atlantic and Pacific Ocean), whereas the Mediterranean presents a different geo-dynamic setting. Stephenson, Dickson and Trenhaile (2013) prefer to use the terms 'near-horizontal' for platforms with gradients of less than about 1^0 in micro-tidal areas, and 'sloping platforms' which have gradients of greater than about 1^0 and generally found in mesotidal and macrotidal coasts.

The growth of platform studies over the past decades has helped to document how a wide variety of platforms that have formed in a large combination of environmental settings. With such growth further challenges are forthcoming, one of which is how researchers can contextualise their particular study within the proper boundary conditions of the system (Kennedy, Stephenson and Naylor, 2014). Though at regional level, tidal range and climate seem to have similar boundary conditions, this review section has shown that it is not always the case. In addition to that, geology and structure seem to play a major role in deviating from the obvious expected typologies and create their own boundary conditions. With specific reference to this research, the boundary conditions that were considered as the most appropriate in which to contextualise this research were three: 1. Lithology, by taking limestone as the rock unit component; 2. Tidal range, which is micro-tidal and hence automatically the choice falls also on sub-horizontal platforms; 3. Elevation of studies surfaces, which in this case is supratidal.

To better illustrate this theoretical context Table 2.1 shows the collation of studies for pertaining to each boundary condition (A-C), which studies have share two boundary conditions (1-3) and finally, which studies represent the combination of these three boundary conditions, similarly to this current research. What is immediately obvious is the amount of studies that have been devoted to

Studies of platforms with boundary conditions in either limestone lithology (A), with microtidal setting (B) or at supratidal levels (C). Works with a combination of these boundary conditions are listed in a tripartite classification based on lithology, tidal regime and elevation are illustrated in 1-4

Lithology Limestone A	Tidal Regime Microtidal B	Elevation Supratidal C
Hodgkin (1970)	Gill (1967)	Gill (1972)
Trenhaile (1972)	Gill (1972)	Mottershead (1982)
Trenhaile (1974a)	Takahashi (1974)	Mottershead (1989)
Trenhaile (1974b)	Sunamura (1978)	Trenhaile et al. (1999)
Torunski (1979)	Gill and Lang (1983)	Blancho-Chao et al. (2002)
Trenhaile and Layzell (1981)	Stephenson and Kirk (1998)	Cooper and Green (2015)
Schneider and Torunski (1983)	Thornton and Stephenson (2006)	
Spencer (1988)	Gomez-Pujol et al. (2007)	
Williams et al. (2000)	Hemmingsen et al. (2007)	
Naylor (2001)	Trenhaile (2008)	
Naylor and Stephenson (2010)	Porter et al. (2010a)	
Moura et al. (2011)	Porter et al. (2010b)	
Moura et al. (2012)	Naylor and Stephenson (2010)	
	Kennedy, Paulik and Dikson (2010)	
	Beetham and Kench (2011)	
	Ogawa, Kench and Dickson (2011)	
	Choi and Seong (2014)	
	Dickson and Stephenson (2014)	
	Kennedy (2016)	

Lithology and Tidal Regime Limestone and Microtidal 1	Tidal Regime and Elevation Microtidal and Supratidal 2	Lithology and Elevation Limestone and Supratidal 3
Kirk (1977)	Sunamura (1978)	Trudgill (1976a)
Robinson (1977a)	Gill and Lang (1983)	Trudgill (1976b)
Robinson (1977b)	Takahashi et al. (1994)	Trudgill (1979)
Stephenson (1997)	Dickson (2002)	Spencer (1981)
Torunski (1979)	Stephenson et al. (2004)	Spencer (1984)
Spencer (1985)	Davies et al. (2004)	Viles and Trudgill (1984)
Stephenson and Kirk (1998)	Kennedy and Dickson (2006)	Davies et al. (2004)
Stephenson and Kirk (2000a)	Furlani et al. (2007)	Moura et al. (2006)
Stephenson and Kirk (2000b)	Sunamura et al. (2014)	Moses et al.(2015)
Stephenson and Kirk (2001)	Kennedy and Milkins (2015)	
Taylor (2003)	Pappalardo et al. (2017)	
Stephenson et al. (2004)		
Cucchi et al. (2006)		
Furlani et al. (2008)		
Furlani et al.(2009)		
Stephenson et al. (2010)		
Inkpen et al. (2010)		
Marshall and Stephenson (2011)		
Kennedy et al.(2012)		

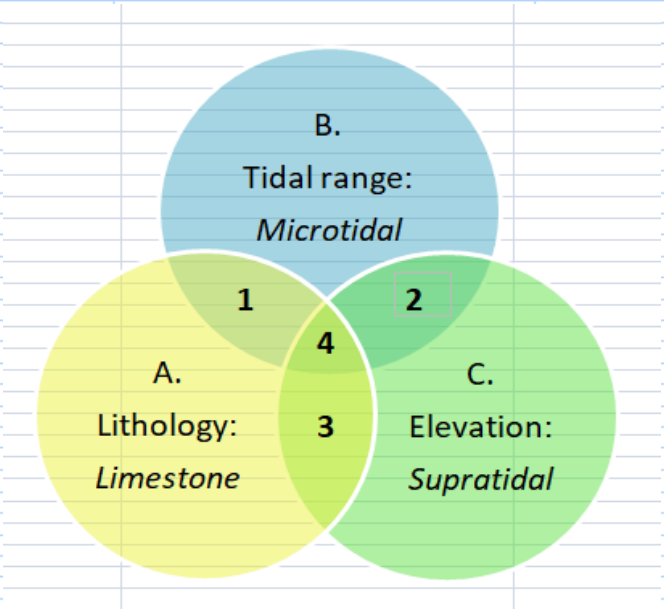

Lithology, Tidal Regime and Elevation Limestone, Microtidal and Supratidal 4
MacFayden (1930)
Torunski (1979)
Spencer (1981)
Moses and Smith (1994)
Stephenson (2001)
Gomez-Pujol et al. (2006)
Swantesson et al. (2006)
Furlani et al. (2011)
Chelli et al. (2012)
Cruslock et al.(2012)
Mayaud et al. (2014)
Pomar et al. (2017)

Table 2.1: Studies of platforms with boundary conditions in either limestone lithology (A), with micro-tidal setting (B) or at supratidal levels (C). Works with a combination of these boundary conditions are listed as a tripartite classification based on lithology, tidal regime and elevation, are illustrated in 1-4 (Source: Compiled by Author)

micro-tidal environments and for limestone lithology. More limited in number are the studies that investigated platform studies in a supratidal setting (Table 2.1). This latter boundary condition was considered a very important criterion for this research, as it provides a distinction between studies that have investigated limestone shore platforms in micro-tidal settings but under processes of surface change in intertidal conditions. The next section will examine better processes of change operating on shore platforms and elucidate how major differences in processes between the intertidal and supratidal zones create two distinct boundary conditions.

2.4 Processes of surface change on shore platforms

It is now widely acknowledged that a number of mechanisms operate on shore platforms, including waves, tides, frost, chemical and salt weathering, wetting and drying, bio-erosional or bio-protection, and mass movement (Stephenson, Dickson and Trenhaile, 2013a). The relative and absolute importance of these processes have varied through time, with changes in relative sea level and climate, and rock coasts often are relict features of environmental conditions that were quite different from today (Trenhaile, 2006a). Consequently, the precise role of each individual process in shore platform evolution remains elusive and complex to define (Naylor, Stephenson and Trenhaile, 2010).

2.4.1 Tidal processes

Tides – both in terms of range and duration - are responsible for important processes of change on shore platforms because they determine a number of dynamic factors such as the spatial and temporal extent of wave action across the platform surface, abrasion processes, the depths of water over which incoming onshore waves may break, wetting and drying processes, wave splashes and sea spray zone and related salt weathering and biological

zonation (Stephenson and Kirk, 2006). As tides control the elevation of the mean water surface and the degree to which wave erosional processes are concentrated within the vertical plane, they determine where, and to what degree, wave erosion takes place, not only within the tidal range but also at supratidal levels.

In the last few decades, several modelling attempts were made to correlate the spring tidal range to mean regional platform gradient (Trenhaile, 1987, 1997, 1999; Trenhaile *et al.*, 1999) (Figure 2.2). Although geological and other local factors may produce sloping and horizontal platforms along a coast, these studies demonstrated how the former are most common in areas with high tidal range and the latter in areas with low tidal range, as displayed in Figure 2.3. Trenhaile (1974a) found a correlation coefficient of 0.92 between platform gradient and tidal range in a macrotidal environment. The correlation coefficient decreased to 0.88 when data from eastern Québec were included for mesotidal tidal range. This suggests that, as tidal range becomes smaller, so does its influence on platform gradient.

Tidal processes translate into a strong and direct impact on intertidal platforms, depending on the seaward edge morphology of the platform, its gradient and elevation at sea level. Numerous studies have shown the efficacy of tides in contributing to mechanical processes such as abrasion, chemical processes such as water-layer weathering, salt weathering (Stephenson, 2000).

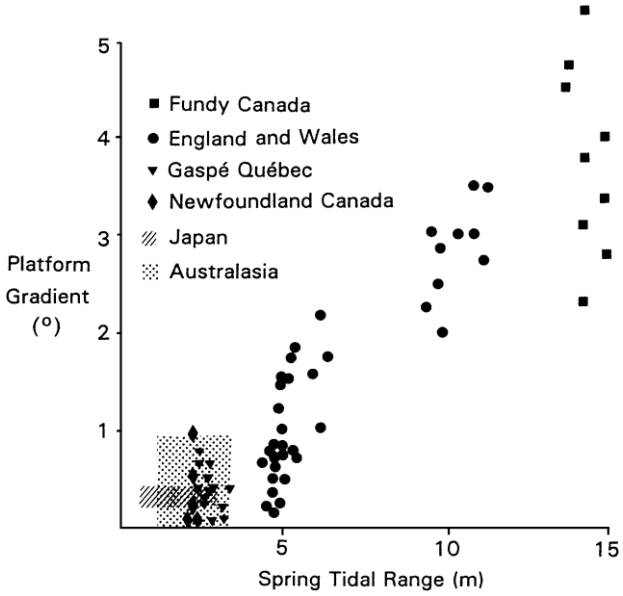

Figure 2.2: The relationship between shore platform gradient and tidal range. Each point represents the local mean of a large number of surveyed profiles (Source: Trenhaile, 2002)

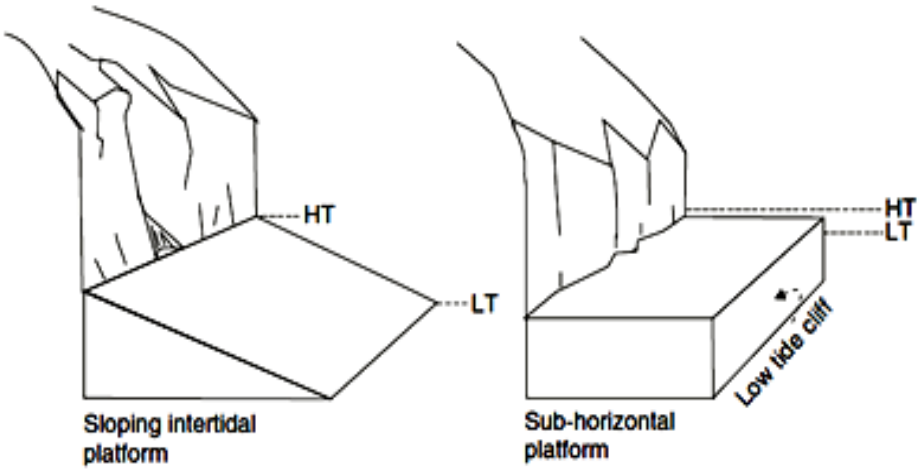

Figure 2.3: Diagrammatic sketch to demonstrate relationship between mean regional shore platform gradient and spring tidal range (Source: Trenhaile, 2004)

In controlling the immersion and exposure frequencies and durations, tides consequently control the intensity and spatial variability of weathering processes (Trenhaile, 2003, 2004). The strong correlation between wetting and drying frequency distributions and tidal range also provides a possible explanation for the gradient–tidal range relationship in areas where weathering rather than wave action is dominant. But even if weathering is to be accorded the primary role in platform formation, it must be explained how the responsible processes work in conjunction with tidal range to determine platform gradient (Trenhaile, 1987, 2004). Stephenson (2000) argued that there is no statistical basis to establish such a relationship, given that a few studies such as by Williams (1986) did not find a positive correlation.

Other coastal characteristics of platform morphology appear to be related to tidal factors. Cliff-platform junctions or notches are usually close to high tide level, although they are very sensitive to geological factors (Trenhaile, 1972). Tidal range may determine the elevation range of the ramp at the cliff base, and the low tide cliff, whereas the mean elevation of the platforms is associated with the tidally determined level of most frequent storm wave action (So, 1965; Trenhaile, 1972, 1978; Trenhaile and Layzell, 1981). These relationships suggest that despite differences in climate, tectonic history and wave regime, the morphology of shore platforms around the world varies in response to variations in tidal range.

2.4.2 Wave processes

The role of hydrodynamic processes on shore platforms is considered to be two-fold: firstly, to enable direct mechanical wear by the action of waves and secondly, to remove weathered and eroded sediment (generated by a range of processes) from the platform (Stephenson and Kirk, 2000).

The role of mechanical wave action and the studies investigating it have been amply reviewed by various rock scientists such as Trenhaile (2008, 2012)

and Stephenson, Dickson and Trenhaile (2013) and include breaking of wave shock, water hammer, air compression in joints, hydrostatic pressure, cavitation and abrasion as the main erosive processes. They are mostly effective when they are most restricted in extent and operate in a narrow zone where air and water alternate above and below the fluctuating waterline. Water shock, water hammer and air compression - which are probably the most significant erosional processes - only operate efficiently within the surf-breaker zone. Swell waves are considered to be more effective than shorter period wind waves in generating both shock pressures and sediment transportation on shore platforms (Noormets, Crook and Felton, 2004). On the other hand, quarrying of rock fragments by air compression and water hammer is considered the most effective process in the storm wave environment of the northern hemisphere (Trenhaile, 2012).

Until recently, the dominant view was that shore platforms are essentially wave-cut (Trenhaile, 1987, 1997, 1999; Tsujimoto, 1987; McKenna, Carter and Bartlett, 1992; Sunamura, 1992; Dickson and Woodroffe, 2005). Most of the examined platforms in the northern hemisphere were however oceanic and mostly associated with storm-wave environments. In Britain, they are also wide (100-250 m), gently sloping features (1-3^{o}), which rarely terminate abruptly at their seaward margins (So, 1965; Wright, 1967; Trenhaile, 1972). In Gaspe, Quebec, however, they are sub-horizontal and normally terminate abruptly in a low-tide cliff or ramp in similar storm-wave environment (Trenhaile, 1978).

In the Southern Hemisphere, the wave-cut platforms have also been reported from a swell-wave environment of Australasia and are oceanic in nature (Bartrum, 1924, 1926; Jutson, 1939; Edwards, 1941, 1951). Bartrum described these platforms which are found in exposed locations as being narrow and sub-horizontal, with abrupt seaward termini and with mean elevations 0.3 to 2.5 m above high tide level. Within a micro-tidal regime such elevations may mean that platforms are located at either intertidal, marginally at supratidal or a combination of both depending on the platform gradient.

Links between wave processes and platform gradient on shore platform remain uncertain and contradicting given the effect of variable lithology and structure along indented coastlines. So (1965) and (Sherbon Hills, 1972) suggested that steep gradients are linked with weak waves due to limited vertical erosion across the platform. Trenhaile (1974b) did find a relationship between platform gradient and fetch in southern Britain. However, other studies also recorded low platform gradient on the least exposed parts of Kaikoura peninsula in southern New Zealand (Kirk, 1977; Trenhaile and Layzell, 1980).

In the literature, much laboratory experiments and numerical modelling were taken to account for wave processes at the foot of cliffs and on platforms (such as by Sunamura, 1975, 1978a, 1978b; Tsujimoto, 1987; Sunamura, 1991). In addition to that, in the last 15 years wave characteristics have started to be directly quantified in the field and few of these are in micro-tidal settings. Stephenson (1997a) and Stephenson and Kirk (2000a) were the first to obtain deepwater wave parameters as well as those on the seaward edge and on the surface of platforms. They demonstrated how most of the energy possessed by the offshore waves is lost in reaching the platform edge due to shoaling and refraction and thus established that at micro-tidal Kaikoura, waves have no role in cliff retreat or shaping of the platforms (Stephenson and Kirk, 2000a). Stephenson and Thornton (2005) measured wave dissipation across a sub-horizontal platform in micro-tidal Marengo, Australia and recorded that energy across the platform was only 10–33% of that arriving at the seaward edge.

Beetham and Kench (2011) demonstrated that shore platforms are effective in reducing energy at gravity wave frequencies, as wave breaking is induced either at the platform edge, or across the outer platform surface. Marshall and Stephenson (2011) presented direct measurements of waves on four micro-tidal platforms and discovered that platform width did not control wave energy dissipation and that the latter was rather influenced by platform gradient and depth of water at the platform edge. Similarly, Trenhaile and

Kanyaya (2007) observed that waves generally break on the seaward edge of the platform in a meso and macro-tidal setting, but that during high spring tides, greater water depths allow fairly large waves to cross the platform. Kennedy, Paulik and Dickson (2011) observed that the elevations of sub-horizontal elevation tends to increase both with increase in wave action exposure and in water depth at the platform front. Most of these studies however, have investigated platforms mostly at intertidal levels, in a variety of tidal regimes and are exposed to open oceanic fetches. To date the mode and magnitude of wave dynamics on supratidal platforms on non-oceanic coasts remains not properly investigated.

The nature of the above-described processes would result in the following four key outcomes for horizontal platforms at supratidal levels and in sheltered seas and which were considered particularly relevant to this study:

i. Mechanical wave action would largely be concentrated along seaward scarp edge were plucking scars, surface pitting and notches tend to develop;
ii. At supratidal levels processes such as water shock, water hammer and air compression become more infrequent and storm episodic in a cross-shore direction;
iii. Platforms with large open fetches are bound to be relatively more exposed to the erosive power of swell waves rather than platforms in sheltered semi-enclosed seas; and
iv. The extent and magnitude of mechanical wave action on supratidal platforms would be determined by the force of the waves generated by storms, the depth water at which storm waves will break, the seaward morphology of the platform and its elevation beyond high tide.

Most of these early investigations of wave impacts at supratidal levels were based on morphological evidence or visual observations of waves reaching

rocky coasts. Wave quarrying on platform development has been examined in the field through the occurrence of fresh rock scars and coarse, angular debris consisting of joint blocks and other rock fragments. In a way, this trend has continued with recent literature such as by Swantesson *et al.* (2006) who investigated the impacts of wave quarrying through block and scar inventories and rock fragments calculations (process measurements). The effects of abrasion on rock coasts were also investigated by authors such as by Robinson (1977), Blanco-Chao *et al.* (2007) and Moses *et al.*, (2006) but such studies focus on processes primarily occurring in the intertidal zones.

2.4.3 Weathering processes

The role of weathering has often been accorded the primary role in the development of sub-horizontal shore platforms in Australasia and other temperate and tropical-swell wave environments around the Pacific fringe (Bartrum, 1916, 1926; Bird and Dent, 1966; Robinson, 1977a, 1977b; Mottershead, 1989; Stephenson and Kirk, 2000; Foote, Plessis and Robinson, 2001). However, there is no agreement on the precise mechanisms by which weathering may develop sub-horizontal platforms. Additionally, Viles (2013) remarked on the potential inter-connectivity between different mechanisms and stated that "*there is in reality a blurring of boundaries between processes whose names imply that they are distinctively different*" (2013:13).

Mottershead (2013) in his review on coastal weathering designed the process into a structured system in which materials and energy interact through a range of mechanical and chemical processes, leading the landscape to be modified by the alteration and movement of geomaterials (Figure 2.4). It is characterised as an open system in which material become available for other processes such as abrasion and mechanical wave action (as previously explained in Section 2.4.2). According to Trenhaile (2002), most weathering theories on shore platform now accept such type of system response and agree that shore platforms are created by the combined effect of wave and weathering

process and accord a major role to mechanical wave erosion in the removal of weathered rock. Much work about weathering has investigated the processes operating mostly on the intertidal shore platforms to determine the influence of water-layer weathering in platform surface lowering. Water-layer weathering refers to the accelerated geochemical weathering that occurs on shore platforms immediately above water level (Short, 2004).

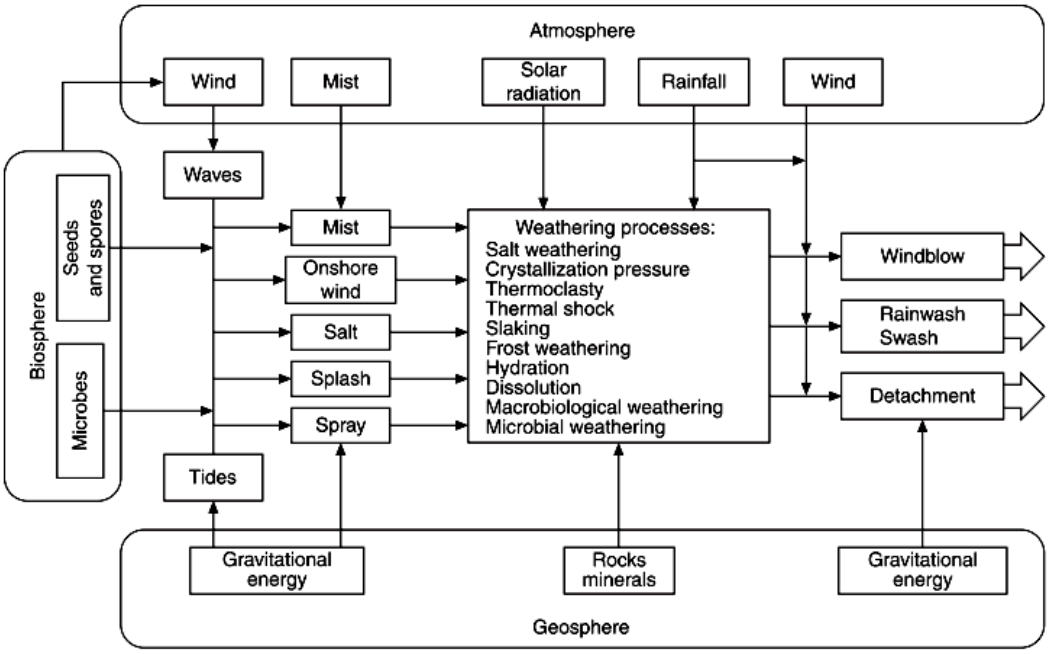

Figure 2.4: The coastal weathering system illustrating the relationships between energy and material flows and weathering processes (Source: Mottershead, 2013)

Shifting tides creates a zone within the mobile water level where such weathering occurs. Amongst the earliest works, Bartrum and Turner (1928) first suggested that all but seaward portions of platforms must be lowered by water layer levelling and leaving a residual ridge or rampart may be found at their seaward margin, where spray and splash may keep the rock moist, thereby preventing such process (Bartrum, 1935; Wentworth, 1938; Sherbon Hills, 1949). Some workers however considered that these horizontal platforms are the product of wave erosion and that any ramparts which exist are simply

associated with resistant rocks (Johnson, 1938; Edwards, 1941; 1951; Jutson, 1949; 1954; Gill, 1972).

Although, the exact mechanism of water-layer weathering is not very well understood (Trenhaile, 1987; Stephenson and Kirk, 2000b), most studies to date link this type of weathering processes specifically within the intertidal zone and is less effective in the supratidal zones. The combined actions of wetting and drying, thermal expansion in some rocks, the chemical action of salt spray, salt crystallization and the removal of solutions through rock capillaries require an alternately wet and dry environment in which to operate (Trenhaile, 1987) and several studies have shown how these operate at best in the intertidal zone (Stephenson and Kirk, 2000b; Kanyaya and Trenhaile, 2005; Porter *et al.*, 2010b) Quantification and understanding of individual processes were sought through field and laboratory experiments to examine the role of wetting and drying on the nature and variability of surface expansion and contraction on shore platforms (Stephenson and Kirk, 2001; Stephenson *et al.*, 2004; Trenhaile, 2006b; Hemmingsen, Eikaas and Hemmingsen, 2007; Porter and Trenhaile, 2007).

These findings clearly indicate that the role of wetting and drying is less regular and effective at supratidal conditions, especially if these supratidal zones on shore platforms are bounded from the intertidal zone by vertical seaward edge scarp, as in the case of sub-horizontal platforms and are situated above the limited extent of micro-tidal water level. However it does not mean that it is completely absent from supratidal zones. Stephenson and Kirk (2006) in fact report that it can occur up to 24 m above sea level where sea spray accumulates. Wetting and drying processes in these zones would be regulated episodic wetting by wave splash during heavy seas and by rainfall, which all lead to slacking form of rock breakdown (Kanyaya and Trenhaile, 2005; Mottershead, 2013).

Rock breakdown by salt weathering is very widespread and common on most shore platforms at high tide and supratidal levels. Cooke and Smalley (1968) identified three mechanisms for salt weathering: 1. Growth of salt crystals from solution; 2. Thermal expansion; and 3. Hydration pressure. The efficiency of salt weathering however depends on a number of factors such as degree of saturation and lithology (Cook, 1979). Mineralogy, texture, porosity, and strength may predispose particular rock types to the development of certain weathering forms (Mottershead, 2013). Cooke and Smalley (1968) explain how the degree of saturation of the solution is of great importance to salt weathering as higher saturation may accelerate internal rock breakdown through salt crystallisation. The authors remarked on how igneous rocks are less affected by salts, whilst chalk, limestone and sandstone are easily affected being more absorbing.

More specifically on supratidal platforms, Mottershead (1989) found that there is strong seasonality in the occurrence of these weathering mechanisms on shore platforms. Given the range of potential weathering mechanisms available in this context, it could be interpreted either that more frequent drying of the rock was causing more frequent crystallization or that more complete evaporation was exposing the rock to aggressive late-stage brine, or that the higher temperatures were directly creating greater thermal stress. Ambient atmospheric conditions and processes, with widely varying inputs of solar radiation and precipitation, can therefore condition the wetting and drying phases which in turn effect the short-term environmental events such as salt crystallization or temperature changes that are responsible for the detachment of weathered material (Mottershead, 1989; Takahashi *et al.*, 1994). These studies proved how much short-term climatic fluctuations can cause major micro-topographic variation of platform surfaces. Viles (2001) recognized that it is inherently difficult to quantify micro-climates, and how researchers are forced to rely on macro- climate data for surface change measurements.

The weathering of sedimentary rocks is recorded to produce a large variety of weathering forms at supratidal levels (Gill, 1972; Trudgill, 1976; Spencer, 1981, 1985, Mottershead, 1982, 1989; Viles and Trudgill, 1984; Moses and Smith, 1994; Cooper and Green, 2016). Polygonal pits and honeycombs have been described on weathered limestone surfaces (Bartrum 1936, Hills, 1949, Jutson, 1954; Cotton, 1963; Mottershead, 1982). Solution of carbonate rocks is held to be responsible for the formation of shallow basins with raised rims on sandstone platform (Emery, 1946). Wentworth (1939) linked the formation of limestone benches in Hawaii to solution by fresh ground or rain water, since warm water or sea water is normally saturated or supersaturated with bicarbonates.

Zonation of weathering forms has also been reported on supratidal platforms. In investigating limestone platforms in Mallorca, Moses and Smith (1994) reported how alveoli and fretted hollows mostly develop in the front part (spray zone) whist solution and pits are mostly located in the landward part of the platform. Such zonation indicated how susceptible is the weathering system to site-specific mechanisms and how the latter spatially operate in relation to the land-sea water interface.

2.4.4 Other Processes: Biological and Frost Weathering

Other processes such as biological and frost action are widely known to contribute to weathering of platforms surfaces. However, the review of scholarly work concerning these two processes will not be treated in much detail, as both processes have not been examined in this thesis.

A wide array of biogeomorphic processes operate in rock coasts and the role biological agency on rock coasts - especially for its efficacy on sedimentary surface such as in limestone and sandstone - is widely recognised (Moses and Smith, 1994; Spencer and Viles, 2002; Carter and Viles, 2005; Naylor, 2005; Gómez-Pujol, Fornós and Swantesson, 2006; Viles *et al.*, 2008; Naylor, Coombes

and Viles, 2012; Moses, 2013; Furlani *et al.*, 2014; Mayaud, Viles and Coombes, 2014). Biological weathering on platform surfaces is governed by factors including zonation of organisms, moisture availability, tidal characteristics, temperature, degree of exposure to sunlight and the salinity of water (Trenhaile, 1987). Stephenson (2000) sums up biological activity on shore platforms in two strands: 1. it causes erosion, which can be separated into bio-mechanical and biochemical components; and 2. it retards or prevents other erosional processes. Naylor, Viles and Carter (2002) have suggested that there is a third process - called bio-construction - that is carried out by the biota on platforms and is responsible for accumulation of sedimentary deposits. Bio-protection and bio-construction is increasingly being recognized in recent works that bio-protection was considered to be an important process on platforms (Carter and Viles, 2003, 2005; Naylor and Viles, 2002). Spencer and Viles (2002) also reviewed the long debate with regards to dissolution of rocky calcium carbonate coasts by sea water, and signalled a general consensus that this is a relatively unimportant process in tropical waters.

At supratidal levels, recent studies have elucidated how biological activity contributed to short-term surface change. Gomez-Pujol, Stephenson and Fornos (2007) published two-hourly surface changes on a supratidal cliff face and explained how surface change is caused by the expansion and contraction of lichen thalli following absorption of moisture and drying out of the cliff surface. How such process may lead to weathering needs to be further examined. A similar investigation by Mayaud, Viles and Coombes (2014) on a coastal supratidal limestone in France revealed surface change related largely to insolation in the morning and evening when thermal gradients were steepest and how the presence of a biofilm intensified rock expansion, but delayed surface response to microclimatic variability. Preferential responses to specific ambient conditions may also determine spatial presence of biological agency on platform surfaces. The recent work by Pomar *et al.* (2017) showed how limestone biopits on supratidal platforms were mostly distributed in shaded exposures and sheltered areas, away from prevailing winds and waves, direct

insolation and desiccation. These studies continue to confirm the extent to which processes on supratidal limestone platforms can be site-specific.

Several studies over the last seven decades have also demonstrated the effects of frost-weathering (freeze-thaw cycles, ice action) in the development of platform in high latitudes and related storm wave environments, whereby rapid cliff recession and the formation of coastal benches in these regions has been attributed to frost-shattering and the removal of weathered debris and ice action (as reviewed by Stephenson, 2000 and Dagsupta, 2010).

2.5 Controls on surface change on shore platforms

2.5.1 Lithology

Rock coast geomorphologists have long investigated the dynamic interactions between the forces that cause erosion of rock coasts and the forces that resist it. As stated by Naylor and Stephenson (2010) the role of geology in coastal geomorphology continues to be an area requiring further work. Certain aspects such as lithological control on processes acting on platforms and their morphology, and inheritance, were recognized quite early (such as by Johnson, 1919; Edwards, 1941; Trenhaile, 1971, 1974). The mean elevation of platform was observed to increase with rock hardness (Gill, 1967, 1972) as does the height of the cliff-platform junction (Wright, 1970; Trenhaile, 1971, 1972). Theory suggests that platforms become steeper and narrower as rock hardness increases (Trenhaile and Layzell, 1979). Gradients are generally steep on resistant rocks, but the relationship between width and rock hardness remains ambivalent (Trenhaile, 1972, 1978, 2000; Davies *et al.*, 2006).

In recent years lithological controls on platforms have been studied in greater detail (such as by Woodroffe *et al.*, 1992; Brooke *et al.*, 1994; Trenhaile, 2002; Dickson, Kennedy and Woodroffe, 2004; Kennedy and Dickson, 2006; Thornton and Stephenson, 2006; Blanco-Chao *et al.*, 2007; Cruslock *et al.*, 2010; Kennedy, 2010; Naylor and Stephenson, 2010). Many field observations of sub-

horizontal platforms have proposed that lithological resistance may determine shore platform elevation, with shore platform elevation increasing with increase in rock resistance (such as by Gill, 1967; Kirk, 1977; Gill and Lang, 1983; Kennedy and Dickson, 2006; Thornton and Stephenson, 2006). These observation were supported by previous results from Sunamura (1991) who examined the relationship between the assailing force of waves (Fw) and the resisting force of the platform rock (Fr) and also proposed that deeper waters at the shoreline favour such high elevations. This latter conjecture was confirmed in a recent study by (Dickson, 2006). Less scholarly agreement seems to be reached with respect to lithological controls on platform width. A few studies such as by Agar (1960), Everard *et al.* (1964) and Takahashi (1977) noted that wider platforms form where lithological resistance is weakest and that more resistant rocks limit the widening extent of the platform. However, in some areas, resistant rocks are associated with wider platforms, whereas less resistant rocks have narrower platforms (such as by Edwards, 1941 and So, 1965).

Trenhaile (1980, 2001) argued that lithology may influence platform development and related morphology as follows:

i. Lithology and mineralogy control the efficiency of the processes operating on shore platforms. Chemical processes might be more dominant on rocks that are capable of absorbing large quantities of water. Platform profiles might be indicative of how many geological factors might control erosional processes. For example, Gill (1972) has noted gentle sloping platforms are associated with soft non-soluble rocks in SE Australia, whereas highly soluble rocks surfaces are horizontal;
ii. Structure and lithology of the cliff and platform determine the type of accumulating deposit present at the cliff foot and which in turn influence processes (such as abrasion) operating at the cliff foot and rate of recession; and

iii. The resistance of the rocks to the processes operating on them determines the degree to which platforms are inherited features. Trenhaile (1980) opined that "*shore platforms, in all but resistant rock areas, are contemporary features on or close to a state of dynamic equilibrium*" (1980: 16).

This study will attempt to investigate more in detail some of the aspects mentioned in point (i) as described above, primarily mineralogy and surface hardness. Though point {ii) and (iii) will not be investigated in this study, they do highlight the extent to which lithology may influence processes of development and surface change on shore platforms.

The efficiency of wave abrasion and quarrying is not solely dependent on tidal range; rock properties also play an important role. A recent study by Moses *et al.* (2006) indicated that softer rocks are abraded more easily than harder rocks. Kennedy and Beban (2005) have asserted the fact that in highly jointed rocks, such as the greywackes of Wellington, New Zealand, waves have great potential to pluck hand-size clasts.

In recent platform studies, rock resistance is often researched on the basis of rebound value, obtained through the use of instruments such as a Schmidt Hammer (Dickson *et al.,* 2004; Kennedy, 2010; Kennedy and Beban, 2005; Kennedy and Dickson, 2006; Kennedy and Paulik, 2007; Stephenson and Kirk, 2000b; Taylor, 2003; Thornton and Stephenson, 2006). Other factors such as structural properties, mineralogy and moisture content also need to be considered (Augustinus, 1991). The Schmidt Hammer has become a routine field instrument to provide (but not only) a measure of rock surface strength or durability. Its use has grown to assess a variety of field characteristics: relative compressive strength for comparative purposes between sites, to measure changes in mechanical strength as a result of weathering or abrasion (Goudie, 2006). For example, Trenhaile *et al.* (1999) and Stephenson and Kirk (2000) used the instrument to infer differences in the degree of weathering between

the upper and lower portions of shore platforms. Dickson, Kennedy and Woodroffe (2004) used it to assess how discontinuities impact the relative resistance of the rocks around the coast of Lord Howe Island (Southwest Pacific). Blanco-Chao *et al.* (2007) identified abrasion strips on rock platforms in western Galicia, which recorded higher R values.

2.5.2 Structure

Platform profiles may be strongly influenced not only by lithological factors but also by structure. Rock dip and strike, bed thickness, joint density and variations in the strength of the beds usually determine the susceptibility to erode the platform at meso-scale levels and influence also surface roughness. Everard *et al.* (1964) suggested that, in steeply dipping rocks, platforms are widest when the strike is perpendicular to the cliff, whereas in gently dipping strata they are widest when the strike is parallel to the cliff face. Storm waves, splash and spray produced supratidal ledges in gently dipping rocks (Jutson, 1939).

The effects of rock structure can vary significantly across shore platforms and can add other complexities in the assessment of rock hardness as a lithological control. As Trenhaile (2012) pointed out *"the resistance of a rock to wave erosion often reflects the exploitation of joints, bedding planes and other structural weaknesses, and it may have little relationship to the strength of the rock itself"* (2012: 181).

There has been a recent emergence of a good number of studies which emphasized the role of structure as a primary control parameter for shore platform erosion as a meso-scale level. Kennedy and Dickson (2006) observed how the lower platforms corresponded to a jointed morphology whereas higher platforms lacked such structure. Where joint surfaces are open waves can be very efficient in removing blocks (Kanyaya and Trenhaile, 2005), with wave

quarrying occurring along these planes (Bird and Dent, 1966) and on highly jointed platforms (Kennedy and Beban, 2005a).

Meso-scale controls, such as rock mass properties of bed thickness and density of discontinuities, have been found to be important determinants of platform surface morphology across a range of rock types, including Blue Lias limestone (Cruslock *et al.*, 2010) and chalk (Hénaff *et al.*, 2006; Dornbusch & Robinson 2011). Platforms in these two rock types are considered to be the most intensively studied over the longest time period for the British Isles (Moses, 2014). Dornbusch and Robinson (2011) had observed that step retreat on chalk platforms in the SE England were highly variable in space and time (0.6–5.0 mma^{-1}). but were of similar magnitude to surface downwearing. This result differs from that previously published by Trenhaile (2008), who from field observations on the Blue Lias limestones of south Wales, concluded that step erosion is more rapid than vertical downwearing of the platform.

Geological structure appears to also play an important role (more than composition) in controlling the nature and scales of erosion of shore platforms in Sweden and Wales, especially quarrying and block removal of near-horizontally bedded limestones. Wave quarrying was found to be most effective where waves, surf and swash can impact upstanding irregularities, as in horizontally thinly bedded rocks with seaward-facing scarps, and in steeply dipping strata where differences in rock resistance produce uneven platform surfaces with upstanding beds of resistant strata (Trenhaile, 1972; Cruslock *et al.*, 2010; Naylor and Stephenson, 2010).

Kennedy (2010) also concluded that rock structure plays a significant role in the morphology and spatial extent of shore platforms in Sydney Harbour. He demonstrated that platform width is often governed by geological controls as well as waves. Trenhaile and Kanyaya (2007) concluded that waves are able to quarry large joint blocks and other rock fragments from sloping platforms;

however they less effective on sub-horizontal surfaces, where the waves break at the seaward edge.

2.6 Quantified measurement of surface change on shore platforms

Early inferences of erosion rates were constructed in a descriptive manner through morphological and sedimentary evidence (Trenhaile, 1980). Prior to 1970s, attempts to calculate rates of surface lowering on platforms relied on techniques such as weathering of dated inscriptions (Emery, 1941), chemical analysis of pool water (Revelle and Emery, 1957) and the use of scour pins (Hodgkin, 1964). Instruments and techniques to measure annual millimetric scale of surface change were hard to come by before the 1970s. This lack of information held back the growth of the theories of landform evolution, which ultimately could only be tested through knowledge of erosion rates. Two important rates were needed for such theories: vertical erosion (which the vertical lowering of its surface) and horizontal erosion (which is the increase in the distance between the platform edge and the cliff line caused by cliff retreat).

In 1970, however, a new technique was introduced that enabled very accurate measurements. The micro-erosion meter (MEM) was introduced by High and Hanna (1970) as a technique for measuring small rates of erosion on bedrock. A measurement is made of the height of a rock surface relative to some fixed datum. The instrument consists of a micrometer dial gauge and attached micrometer probe which is mounted onto a tripod framework. The tripod gives the instrument stability and it rests on three reference studs drilled securely into the rock. The measurement of the surface height of the rock relative to the studs can be made at repeated intervals, yielding results of surface lowering in mm/yr. Initial meters had probes which were fixed and the tripod could be rotated to three positions, yielding three measurement points (Trudgill, 2004).

The MEM was subsequently modified by Trudgill, High and Hanna (1981) and Trudgill (1983) to allow a greater number of measurements to be made.

The modified meter, known as the traversing micro-erosion meter (TMEM), uses a traversing mechanism with a tripod base plate which could be rotated and additionally the dial gauge could itself be placed in several reference positions, thus enabling a much larger number of points to be measured. The TMEM was further modified by Stephenson (1997) to allow digital recording and direct transfer of data to a PC. As far as downwearing is concerned, the introduction of the Micro-Erosion Meter (MEM), and its variant the Traversing MEM (TMEM), has enabled far more accurate measurement of erosion rates on platforms in various studies (Table 2.2). In his review, Trenhaile (1980) reported an initial global rate of platform downwearing ranging between 0.0001 mma^{-1} and 0.035 mma^{-1}, being the greatest in exposed wave-dominated environments. Backwearing erosion rates (across the platform's horizontal plane) have generally been found to be of higher magnitudes and ranged from the negligible to as much as 50-75 mma^{-1} (Sunamura, 1973; Kirk, 1977). Globally, Stephenson and Kirk (2006) reported erosion rates in the range of between 0.5-1.5 mma^{-1} with a mean of 0.95 mma^{-1}. Slightly higher is the mean figure measured only by MEM/TMEM as reported by Stephenson and Finlayson (2009) i.e. of 1.486 mma^{-1}.

Today most workers agree that a global mean erosion rate is not truly indicative given that erosion rates at different locations will vary considerably from this mean rate (Stephenson and Finlayson, 2009). It is widely acknowledged how much MEM and TMEM rates widely range even for the same lithology and vary from site to site due to the local wave and tide dynamics, ambient conditions, as well as structural properties of the rock. For example, for tropical limestones, Stephenson and Kirk (2006) quoted an overall figure of 1.97 mma^{-1} and 1.25 mma^{-1}, whereas for temperate limestones and mudstones the figures are 1.13 mma^{-1}, 1.48 mma^{-1} and 1.53 mma^{-1}. In his review, Dagsupta (2010) presents a summary of published erosion rates and shows the mean erosion rates on shore platforms cut in different lithologies, excluding those developed in unconsolidated till and reef limestone (Table 2.2).

Table 2.2: Measured rates of erosion on shore platforms, as listed by Dagsupta (2010)

Location	Instrument	Duration (yrs)	Rate or range of erosion (mm/yr)	Lithology	Source
Kaikoura Peninsula, New Zealand	MEM	30	1.090	Mudstone and limestone	Stephenson et al. (2010)
Kaikoura Peninsula, New Zealand	TMEM	10	0.901	Mudstone and limestone	Stephenson et al. (2010)
Quebec and Nova Scotia, eastern Canada	TMEM	3–6	0.242 1.254 0.722	Argillite Sandstone Basalt	Porter et al. (2010a) Porter et al. (2010b)
Galicia, Spain	TMEM	1	0.130–1.800	Granite	Blanco-Chao et al. (2007)
Kent, UK	TEB	1	1.750	London clay	Charman et al. (2007)
The English Channel coast, UK and France	MEM	3	3.650	Chalk	Foote et al. (2006)
Sweden Mallorca, Spain	MEM	3	0.004 0.090	Igneous (granite, ortho-gneiss and dolerite) Carbonate (limestone and dolomite)	Swantesson et al. (2006)
Sweden Mallorca, Spain	TLS	3	0.005 0.130	Igneous (granite, ortho-gneiss and dolerite) Carbonate (limestone and dolomite)	Swantesson et al. (2006)
Victoria, Australia	TMEM	3.4	0.302	Greywacke and siltstone	Stephenson and Thornton (2005)
Kaikoura Peninsula Raramai Arch, Kaikoura Akaroa Harbour, Banks Peninsula Lake Waikaremoana	MEM and TMEM Bedstead Frame	2.50 2.50 2.36 2.63 3.20	1.410 1.190 0.780 0.290 9.130 2.560	Mudstone Limestone Greywacke Basalt Mudstone All lithologies	Taylor (2003)
West coast, Portugal	MEM	2	0.200–3.400 2.000–4.000 0.400–1.000 0.200–2.800 1.750	Greywacke Marl Limestone Shale All lithologies	Andrade et al. (2002)
Tombadoiros, Portugal	TMEM	0.26	0.153	Limestone	Neves et al. (2001)
Kaikoura Peninsula, New Zealand	TMEM	2.19	1.233 0.875 1.983 0.733 1.130	Mudstone Limestone Mudstone (type-A) Mudstone (type-B) Mudstone and limestone	Stephenson and Kirk (1998)
Kaikoura Peninsula, New Zealand	MEM	20	1.430	Mudstone and limestone	Stephenson and Kirk (1996)
Devon, UK	MEM	7	0.625	Supra-tidal green schist	Mottershead (1989)
Gower, south Wales	MEM	1	0.033 (intertidal) 0.135 (spray zone) 0.020 (ledge)	Limestone	Shakesby and Walsh (1986)
Victoria, Australia	MEM	2	0.370	Greywacke	Gill and Lang (1983)
Northern Adriatic	MEM	1	0.571	Limestone	Torunski (1979)
Kaikoura Peninsula, NZ	MEM	2	1.530	Mudstone and limestone	Kirk (1977)

From these works, Dagsupta (2010) calculated a global mean erosion rate of 0.397mma^{-1}, 1.282 mma^{-1} and 0.625 mma^{-1} for igneous, sedimentary and metamorphic rocks respectively. These figures show that there is a large variation in erosion rates due to change in rock characteristics, with chalk having a considerably higher erosion rate than all other rocks considered in the work (Dagsupta, 2010). The rates published in Table 2.2, are also mostly related to measurements for intertidal zones and relatively fewer works have been specified as being supratidal. Given the difference in morphodynamics present at these two tidal zones, rates between these two zones may also not be comparable. Table 2.3 presents the findings for erosion rates at supratidal levels calculated on short-term (diurnal) and long-term scales (seasonal annual and decadal) scales. These works provide important insights with regards to surface change measurements with MEM and TMEM. Erosion rates are also widely variable within the supratidal zone, even when considering the lithologically similar rocks such as limestone (Torunski, 1979; Shakesby and Walsh, 1986; Moses *et al.*, 2015).

Limestone shore platforms are not only characterized by a large variety in morphology. Many workers seemed to also agree that limestone surfaces are highly heterogeneous in their surface change dynamics at micro-scale. In their study, Inkpen *et al.* (2010) concluded that limestone coasts do not display a consistent mode of surface change, both over the short- and long-term scales. Mayaud, Viles and Coombes (2014) claimed that petrographic variations within the limestone could lead to differential responses to insolation, both at the surface and inside the rock mass. The heterogeneity of limestone also directly translates into a large variation of surface hardness. In his review, Goudie (2006) listed how numerous studied types of limestone had an R value ranging from 9.0 to 61.9. Given such a large range in surface hardness, it

Table 2.3: Rates of surface change measured at supratidal levels (Source: Compiled by Author)

Rates of surface change measured at supratidal levels				
Rates of change (mm/yr)*	**Lithology**	**Location**	**Method**	**Reference**
0.26	Calcarenites	Aldabra Atoll, Indian Ocean	MEM	Trudgill (1976)
0.6	Greenschist (platform)	SW England	MEM	Mottershead (1977)
0.09-0.62	Aldabra Limestone	Aldabra Atoll, Indian Ocean	MEM	Trudgill (1979)
0.09-0.11	Takamaka Limestone	Aldabra Atoll, Indian Ocean	MEM	Trudgill (1979)
0.07-0.155	Turonian Limestone (Upper Cretaceous)	Gulf of Trieste, Adriatic Sea	MEM	Torunski (1979)
0.2653-0.7882	Calcarenites	Cayman Island, Caribbean Sea	MEM	Spencer (1981)
0.04-1.3	Horizontal greywacke	Victoria, Australia	MEM	Gill and Lang (1983)
0.55-0.64	Greenschist platform	SW England	MEM	Mottershead (1982)
0.35	Calcarenites	Aldabra Atoll, Indian Ocean	MEM	Viles and Trudgill (1984)
0.020-0.297	Limestone	Gower, South Wales	MEM	Shakesby and Walsh (1986)
0.09-1.77	Reef limestone (Pleistocene)	Grand Cayman,Caribbean Sea	MEM	Spencer (1985)
0.625	Greenschist platform	SW England	MEM	Mottershead (1989)
0.92-2.90	Sandstone blocks	Japan	MEM	Takahashi et al. (1994)
0.007-0.482	Cretaceous Limestone	Mallorca (Balearic Islands)	MEM, Laser Scanner, biological survey	Swantesson et al. (2006)
0.003-0.814	Upper Miocene Reef Limestone	Mallorca (Balearic Islands)	MEM, Laser Scanner, biological survey	Swantesson et al. (2006)
0.004-0.369	Upper Miocene Calcerenite	Mallorca (Balearic Islands)	MEM, Laser Scanner, biological survey	Swantesson et al. (2006)
0.011-0.997	Jurassic Dolomite Breccias	Mallorca (Balearic Islands)	MEM, Laser Scanner, biological survey	Swantesson et al. (2006)
0.001-0.003	Granites	Costa Brava (Catalonia)	MEM, Laser Scanner, biological survey	Swantesson et al. (2006)
0.193 to -2.086**	Greywacke	Apollo Bay, Australia***	TMEM	Stephenson et al. (2004)
0.126 to -0.261**	Sandstone (cliff face)	Marengo Bay, Australia	TMEM	Gomez Pujol et al. (2006)
9.16	Middle Globigerina Limestone	Malta	Rock profiler	Micallef and Williams (2009)
0.49-1.09	Lower Globigerina Limestone	Malta	Rock profiler	Micallef and Williams (2009)
1.38	Upper Coralline Limestone	Malta	Rock profiler	Micallef and Williams (2009)
0.77	Lower Coralline Limestone	Malta	Rock profiler	Micallef and Williams (2009)
9.0-14.0	Middle Globigerina Limestone	Malta	TMEM	Furlani et al. (2014)
0.31 to -0.26	Tertiary Limestone (bare rock)	Massif des Calanques, France	TMEM	Mayaud, Viles and Coombes (2014)
0.50 to -0.17	Tertiary Limestone (bio-film colonised rock)			
0.095	Holocene and Quaternary reef limestones and aeolianites (boulder)	Thailand	MEM	Moses et al. (2015)
** Positive rates denote surface lowering; negative rates denote surface rises*				
***mm*				
**** only supra-tidal around new and full moons*				

would be incorrect to expect all limestone surfaces to weather and erode at the same magnitude and in the same mode, even in circumstances in which the external environmental parameters had to be constant.

Short-term surface changes at supratidal levels, with surface rises and falls have also been reported in various studies such as Mottershead (1989), Stephenson *et al.* (2004) Gómez-Pujol, Stephenson and Fornós (2007) and Mayaud, Viles and Coombes (2014). They recorded fluctuations in surface rises and lowering corresponding to lithological and biological responses to micro-ambient diurnal conditions. Mayaud, Viles and Coombes (2014) suggested that such short-term behaviour may be the result of rock 'memory' which is sensitive to microclimatic fluctuations and created hotspots of expansion and contraction at the centimetre scale. Their conclusion is that surface change on supratidal limestone is highly heterogeneous in space and time.

Apart from the varied magnitude of changes, the causes behind short-term surface changes also varied between studies. Mayaud, Viles and Coombes (2014) reported that, despite surface colonization, rock surfaces behaved with maximum contraction or expansion at the start of the day and then displayed maximum examples of the opposite behaviour later in the day. Gómez-Pujol, Stephenson and Fornós (2007) on the other hand, claimed an opposite trend: a much higher proportion of falling points in the morning and rising points in the afternoon on their colonized sandstone surfaces at Marengo Bay. Stephenson *et al.* (2004) speculated that the surface rise at supratidal greywacke at Apollo Bay are a temporary or delayed response to drying in view of the fact that Apollo Bay is only supratidal around new and full moon and consequently it is exposed to wetting and drying conditions. The implication behind these recorded diurnal surface changes on supratidal surfaces is also that TMEM measurements – especially if done on longer time-scales – need to be scheduled at the same hour during the day in order to capture as much as possible a comparable present state of surface response from one measurement period to another. Given the supratidal position of these surfaces, the role of tidal

variations has relatively a less direct impact on processes of surface change. This also applies in the context of the Maltese Islands, which has a very small tidal range (0.206 m during spring tide and 0.046 m during neap tides, as per Drago, 2009) and with most platform supratidal surfaces terminating in a low steep scarp.

A few studies did measure rates over longer timescales. The Mottershead (1989) study used the MEM over a period of seven years to calculate a mean lowering rate on supratidal greenschist on the Start-Prawle Peninsula in UK and identified salt spray weathering as the principal agent of erosion. Field observations revealed a consistent seasonal variation with a clear summer maximum, clearly indicating a climatic control. The author attributed such seasonal patterns of surface change – which include surface rises and falls – to a variety of weathering mechanisms such as frequent drying of the rock (causing more frequent crystallization), evaporation which exposes rock surfaces to aggressive brine or higher temperatures which were directly creating greater thermal stress or differential expansion of halite in the rock pores. Surface rises are therefore not a temporary or occasionally phenomenon but may be a more a regular process that extends to longer term scales.

The heterogeneous behaviour of short-term surface change on supratidal surfaces may imply that in order to get a better representation of surface change for longer time-scales, a better coverage with a larger number of bolt sites is required. In relation to this, Viles and Trudgill (1984) presented erosion rates from Aldabra Atoll, based on an 11-year period, and attempted to test the validity of extrapolating shorter-term data to longer periods. To do this, they predicted the total erosion that would occur in 11 years by extrapolating from a two-year dataset and compared this result with erosion measured over the 11-year period. The shorter-term measurements were within an order of magnitude of the long-term rates, with a 10% difference in mean rates. Viles and Trudgill (1984) concluded that the use of a 'small' number of sites was suspect and that a 'larger' number of MEM sites were needed to gain acceptable

data. They did not suggest the number required. Attempts to extrapolate shorter-term data were thought to be invalid, except to establish an order of magnitude, and extrapolation should be done with a degree of caution. Mottershead's (1989) proposed that 30 individual measurements provided a valid erosion rate and this was confirmed be statistically valid by Stephenson and Kirk (1996).

2.7 Current state of research on Maltese shore platforms and justification for study

Though shore platforms on the Maltese Islands cannot be considered as spectacular or monumental geomorphological landforms in any way, the information presented in the Introduction (Chapter 1) bears testament to the following important considerations about Maltese shore platforms:

i. The examples of prehistoric and historic features, provided in Chapter 1, are a reminder about how much shore platforms not only hold important heritage elements that connect us with past civilisations and traditional practices but also hold links to the understanding of how these civilisations related to the coast and its past environmental conditions;
ii. The high level of land use development experienced on the foreshore has obliterated a large number of shore platforms from their natural state and the remaining ones exist in an endangered status due to the constant pressure from further building encroachment and land reclamation projects;
iii. In being located at the foreshore, shore platforms remain highly exposed to major risks of environmental change, such as climate change-driven effects of storm surges and sea level rise; to date, we have yet no data on how these platforms may respond to these changes; and
iv. The intensive use of these platforms has increased their level of vulnerability to the effects of environmental changes listed in [iii]

and with knock-on effect on related coastal activities (such as recreation, tourism, maritime operations and salt making practices) which to date remains largely under assessed.

An important conclusion highlighted by Buttigieg, Vassallo and Schembri (1997) dealt with the importance of collecting more scientific data on the physical properties of shore platforms in the hope to facilitate better both the management of these platforms at policy level and for more public awareness on their proper use and geo-heritage value:

> *"The way forward for more public awareness on shore platforms is to highlight their importance primarily through further studies on their physical properties…Basic information needs to be gathered by means of an overall study followed by constant monitoring of the physical conditions that affect shore platforms in the Maltese Islands"* (1997: 87).

Not enough is known about the lithological properties of Maltese shore platforms, other than that they are formed in Globigerina Limestone. A number of studies exist on the Lower Globigerina Limestone Member but they are mostly treated from an engineering perspective as a building stone. As shown in Table 2.4, studies about the deterioration of LGLM are mainly focused lab tests to assess the geo-mechanical and geo-chemical properties of the member as a building stone, primarily for the Franka and Sol variant. There is still lack of scientific research about *in situ* surface deterioration processes and especially on how such processes operate on natural limestone landforms.

To date, surface erosion rates for Maltese shore platforms are limited to two studies. In the first one, Micallef and Williams (2009) used a rock profiler (constructed specifically for this study) in order to investigate micro-profile changes of the limestone surface on nineteen shore platforms sites with four different lithologies over a study period of between three to five years. The chosen lithologies were Lower Coralline Limestone (LCL, Mtarfa and Tal-Pitkal Member), Globigerina Limestone (GL, Lower and Middle Member, LGLM.

MGLM) and Upper Coralline Limestone (UCL, Xlendi Member) (See Section 4.2 for a brief description of Maltese limestone stratigraphy).

Table 2.4: Summary of published studies on Lower Globigerina Limestone Member as a building stone (Source: Compiled by Author).

Summary of published studies on Lower Globigerina Limestone Member as a building stone	
Name of studies published	Vannucci *et al.* , 1994; Torfs and Van Grieken, 1997; Vella, Testa and Zammit, 1997; Fassina, Cassar and Torpiano, 1997; Fitzner, Heinrichs and Volker, 1997; Cassar, 1999; Cassar and Vannucci, 2001; Cassar and Vella, 2003; Cassar, 2004a,b ; Gatt, 2006; Rothert *et al.* , 2007; Sammut *et al.* , 2014; Diana, Cassar and Zammit, 2014; Baratin and Acierno, 2016; Cabello-Briones and Viles, 2017.
Aims of studies	To identify causes of Globigerina Limestone detoriation as a building stone
	To formulate non-invasive restoration techniques to conserve the limestone heritage of the Maltese Islands
Physical properties examined	The mechanisms of capillary rises of salt-laden moisture and their resultant accumulation
	The thermodynamic changes in soluble salts driven by crystallisation and dissolution cycles.
Main outcomes of these studies	A great variability exists in the weathering patterns of LGLM
	The mineralogical and/or geochemical composition drive the weathering behaviour of the LGLM
	The textural features affect compressive strength and its porosity, which permits rising dampness (responsible for that salt crystallisation process that defaces masonry stone)
	LGLM (Franka variant) reveal a high total porosity, reaching values of up to 40% and with variations between 24 and 37% depending on location and depth
	Characteristics of pore sizes and distribution are considered to be an important control on the internal capillary movement of soluble salts and its resultant weathering processes
	Subefflorescence of soluble salts, in particular chlorides but also sulphates and nitrates, is considered to be the primary cause of deterioration salt crystallisation is considered more damaging than efflorescece due to associated expansion which disrupts the internal structure and cause loss of surface
	The formation of a compact superficial calcite crust (1-2cm) increases salt accumulation leading to material detachment by granular disintegration and flaking within the cavities
	Alveolar weathering i.e. a form of back-weathering driven by a honeycomb structure, and together with scaling and flaking, is considered to be the principal processes of deterioration, followed by powdering and deep weathering.

This cited study provided for the first time annual mean surface lowering rates for the Maltese coasts according to the following lithologies: 0.77 mma^{-1} for LCL, 0.74 mma^{-1} for LGLM, 9.16 mma^{-1} for MGLM and 1.38 mma^{-1} for UCL.

The authors attribute the variations in rates to site-specific degree of exposure (mostly in relation to storm wave incidents), mechanical wave erosion, solution and salt-crystallization processes active at each site. The key findings of the study were the following:

i. A considerable range of mean surface lowering values at micro-scale were recorded and they were observed both spatially (at each site, on the same bedrock and at the same profiling site) and temporally (at inter-annual level);
ii. The annual mean surface lowering rates for Globigerina Limestone shore platforms had the highest variability i.e. ranging from 0.74 mma^{-1} (LGLM) to 9.16 mma^{-1} (MGLM) and these data were partially related to how different geological sub-divisions within the Globigerina Limestone may vary in their resistance to erosion;
iii. No correlation was recorded between the direction of exposure and mean surface lowering rates;
iv. On a temporal scale, mean rates have been influenced by difference in episodic storm conditions between the two study periods (1992-1995 and 1995-1997), with a storm event ratio of 1:4 between the two periods;
v. LCL recorded lowering rates similar to the Globigerina Limestone due to presence of weak-beds and carbonate composition in the former, which make it susceptible to a degree of erosion and weathering higher than originally expected;
vi. The higher mean rates in UCL were attributed to its pitted karst surface which retains sea water and thus enhances weathering; and
vii. Some of high mean rates measured in salini pans (Qawra, Malta) were linked to salt crystallisation within surface rock pores due to high summer temperatures, high seawater salinity in the Mediterranean (about 36ppm) and increased permeability of local limestones.

As a first study for Malta, with findings discussed as a comparable work with other international research on shore platforms, the paper by Micallef and Williams (2009) presents a number of shortcomings. The authors conclude by stating that the recorded mean surface lowering rates seem to be within the range outlined in other studies and cite the work of Trudgill (1976), Robinson (1977), Spencer (1981) and Mottershead (1982). The four cited works have used the micro-erosion metre and, in citing them, Micallef and Williams (2009) wished to demonstrate that the data obtained with the profiler is comparable with that of the micro-erosion metre. In view of the inherent complexity of shore platforms - so well-acknowledged in the literature - direct comparisons of these cited studies with the micro-tidal limestone coasts of the Mediterranean need to be treated with caution. Trudgill (1976) and Spencer (1981) studied young reef limestone on elevated platforms in Aldabra Atolls and Cayman Islands respectively. Though these sub-aerial limestone platforms were both located in sheltered micro-tidal conditions, they are also set in a sub-tropical climate with annual rainfall means of 1142 mma^{-1} (Trudgill, 1976) and 1495 mma^{-1} (Spencer, 1981). Robinson's shore platforms were studied in the temperate climate of north-east Yorkshire and geologically set in Lower Jurassic shales with tidal conditions between 2 mm to 4.6 mm. Mottershead's study, also set in a British temperate climate, observed the metamorphic green schist with macro-tidal conditions of East Prawle (South Devon).

The four cited works have observed platforms in physical settings quite different from those of the Maltese platforms. A more fitting comparison would have been with the Upper Miocene reef limestones (0.003–0.814 mma^{-1}) and Upper Miocene calcarenites (0.003-2.095 mma^{-1}) of the Balearic Islands, studied by Swantesson *et al.* (2006) and the Upper Miocene calcarenites (0.80–1.18 mma^{-1}) by Gómez-Pujol, Fornós and Swantesson (2006). These studies - apart from being relatively more recent - studied limestone platforms in a similar Mediterranean climate, within an island setting of a semi-enclosed sea (and not oceanic), and having limestone coasts of a depositional age close to that of the Maltese limestone.

The authors also acknowledged that a high variability in rates at different spatial and temporal scales was recorded. Yet, they limit to present their calculations as mean erosion rates for each site over the whole study period, which tends to obscure the variability of erosion and the possible mechanisms driving it. The mean rates displayed in their Table 1 (2009: 740) show that the use of averages can be misleading and does not give a detailed narrative about the measured levels of variability during the study period. No parametric tests of difference were carried out to test whether the differences between the nineteen sites were statistically significant.

The study also lacks essentially a morphological description of the selected platforms. It provides neither detailed data about their physical properties (other than that lithological and locational) nor pertinent justifications for the scientific qualification of these sites as shore platforms based on international literature. This information would have been essential given the absence of literature on Maltese shore platforms and their physical characterisation as a geomorphological landform. In fact, though it is generally assumed that variance in lithological resistance at sea level produces shore platforms on the Maltese coasts and that most platforms are in fact in GL, there is yet no defined information on how other lithologies of alternating resistance at sea level may be producing shore platforms. It is not altogether clear if the sites of Micallef and Williams (2009) in MGLM, LCL and UCL are actually 'shore platforms' *in sensu stricto*, given that the term 'sloping rocky shores' was also used in the text (2009: 741)[1]. No other studies were ever published again with the use of the rock profiler on Maltese shore platforms.

The second work was a review paper by Furlani *et al.* (2014) on Mediterranean rocky coasts, in which surface erosion rate of between 9-14 mma^{-1} for an unspecified shore platform in MGLM was recorded over a study period of one year. The rate, obtained with a TMEM, was listed down as part of compilation list of erosion rates for shore platforms and coastal bedrock on the

[1] Professor Anton Micallef was contacted for further enquiry about his paper. No reply was forthcoming.

Mediterranean rocky coasts. No discussion about the source of this measured rate was presented in this review paper.

Given the lack of scientific studies on Maltese shore platforms, inaccuracies in their geological mapping have been encountered during this current research. These will be further elaborated and presented in a corrected format in one of the findings chapter (Chapter 4). Such findings continue to confirm the need to collect more scientific data to correctly characterise the physical properties of Maltese shore platforms and thus build a research landscape with more specific and accurate data. Twenty years down the line from the recommendation put forward by Buttigieg, Vassallo and Schembri (1997), it is hoped that the study presented here will partially address their call about the need for more scientific research on Maltese shore platforms.

3 Methodology

3.1 Introduction

The general outline of the research framework adopted for this study is illustrated in Figure 3.1. As explained in the Introduction (Chapter 1), the first phase of the research consisted in formulating the aims and objectives of the research and to target a specific number of research questions as the main hypothesis framework. In view that research on Maltese shore platforms was limited (Chapter 2, Section 2.7), curtailing the number of research questions was challenging, given the potential in addressing the various neglected research areas. Additionally, the extensive foreign literature available on shore platforms was in a way counterproductive to the streamlining process of the research questions. Establishing the relevant boundary conditions of this study has helped to prioritise the review process and select which papers were core and peripheral to such boundary conditions. The review work and delineation of boundary conditions subsequently helped to define better the aims and objectives (outlined in Chapter 1) and design the methods accordingly.

3.2 Methodology Design

Careful definition of the research questions at the start pinpoints where to look for evidence and helps determine the methods of analysis to be used further on in the study. In the planning stage of this research, numerous fieldtrips were undertaken to determine what type of approach to use in selecting case-studies to examine in depth, which instruments will be employed, and finally, which data gathering and analysis approaches to adopt. These will be discussed further in Section 3.2.1 and 3.2.2.

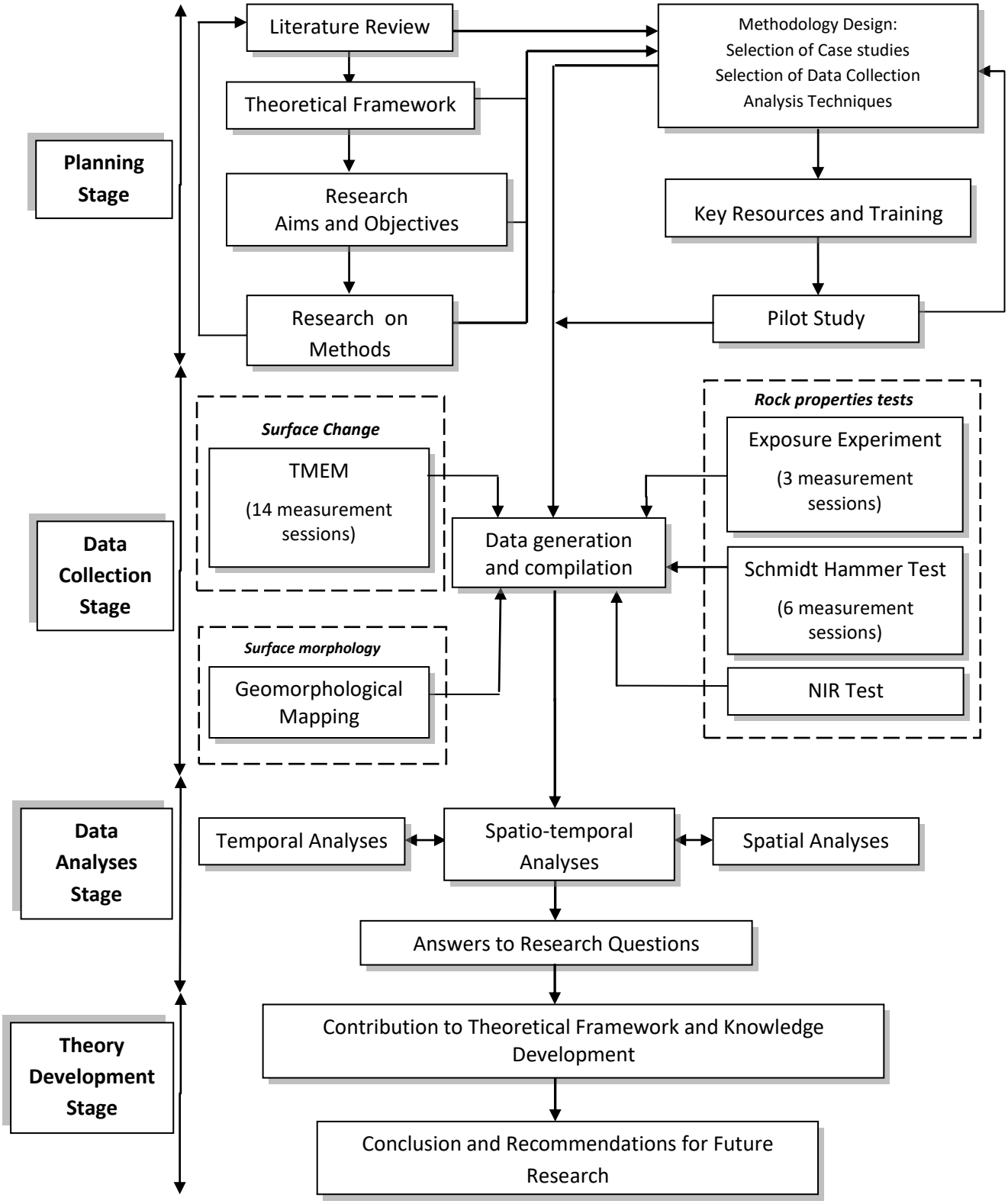

Figure 3.1: Systems diagram illustrating the research framework (Source: Developed by Author)

3.2.1 Site selection

In this research, the empirical inquiry was based on a selection process of shore platform sites on the Maltese Islands in order to investigate the phenomenon of shore platform erosion. The choice of sites was considered indispensable in order to remain pertinent within the aim and objectives of the research and to manage at best the data collection process and analyses within the stipulated time-frames. The selection criteria underpinning the choice of shore platform sites consisted of a set of essential criteria and another set of preferred criteria, listed as follows:

i. Essential criteria:
    a. Lithology – the lithology had to be Globigerina Limestone, given that most platforms on the Islands develop from this lithology when located close to sea level;
    b. Backed by cliffs – in view of the fact that most literature on shore platforms focuses on shore platforms backed by cliffs, this type of environment was chosen for this research. This may allow the research to eventually pave the way for other projects which might investigate the dynamics of the two systems as a cliff-platform system and its response to coastal erosion processes;
    c. Exposure to winds and waves – a fourteen-year study conducted by MMA (2003) showed that the wave climate of the Maltese Islands is dominated by incident offshore wave roses and offshore winds from the northwest. The offshore wave rose and local wind rose are directionally similar. Thus, the wave climate is controlled by steep sea waves generated by local winds rather than swell waves. In view of this, wave exposure – as a criteria – has been inferred in relation to exposure to local wind direction, 20.7% of the days dominated by the prevailing northwesterly winds (Galdies, 2011).

d. Size: the platform needed to be sufficiently large in order to be able to set up at least two transects perpendicular to the shoreline, in which three TMEM stations (front shore, middle shore and backshore) could be set up at sufficient distance from each other; and
e. Supratidal elevations: measurement stations needed to be set up close to sea level in as much as further inland from sea level. Thus stations located in the front sections can then be compared to the middle sections and backshore areas.

ii. Preferred criteria:
    a. Accessibility – the level of accessibility to these sites had to be reasonable in order to be able to reach the platform with all the necessary equipment. High and safe accessibility was preferred in this case;
    b. Level of use – shore platforms are highly used for bathing and other recreational summer activities. Thus it is not advisable to choose shore platforms that have such a high anthropogenic use which might compromise data collection procedures. Low level of use was preferred in this case;
    c. Travel distance: this relates to the time and mode required to reach the sites. Low distances and one use of transport mode were preferred; and
    d. Travel mode: this refers to the type of transport required to reach the site; one mode of transport was preferred.

These criteria were formulated after a careful examination of the platform studies available in the literature and how a study with such criteria could potentially fill the gaps in knowledge which were identified and discussed earlier (Section 1.3 and Section 2.3).

In Biolchi *et al.* (2016) it was calculated that 15% of the Maltese coastline consists of shore platforms, generally described as Type B platforms.

It was reported by the authors that these platforms develop along bedding planes following their slope, are never submerged and that usually a deeply carved abrasion notch occurs at mean sea level. For this study, fourteen sites were identified as fitting to the above-mentioned criteria and having the potential to provide sufficient comfort in addressing the specific targets of this research.

As displayed in Figure 3.2 and Table 3.1, these selected case studies possess different essential criteria in terms of geographical location, exposure to wave action and lithology. However, overall they also share a number of essential criteria as illustrated in Table 3.1.

Conversely, a wider range of results was obtained for the preferred criteria and these ended up becoming a weighing factor in the selection process. Transport logistics, accessibility and feasibility of travel mode were the main secondary criteria that were retained to helped in maximising field trip times. For this reason, the shore platforms in Gozo were not included. Given that most platforms on the Maltese Islands are in LGLM and UGLM and one of the main scopes of this research was to garner a proper representation of Globigerina shore platforms, the Gnejna Bay platform in MGLM was not considered. The latter platform was also not sufficiently large for the intended transect sampling method. Accessibility and low level of use were two criteria that counterweighed each other. High level of use, such as Sliema Bay platform was not considered ideal given the need to set up permanent TMEM stations. Low accessibility, although a positive factor in terms of minimising anthropogenic disturbances, would translate in logistic issues in reaching the site with the equipment such as St Lucian Headland. In view of the fact that very limited research has been undertaken on the surface rock erosion of Maltese shore platforms, this study is being considered amongst the first to offer a representative samples for shore platforms on the Maltese Islands.

Figure 3.2: Aerial image of the Maltese Islands with numbered locations 1-14 identified as possible case studies for the purpose of this study (Source: Base Image from MEPA, 2013; Modified by Author)

Table 3.1: Assessment matrix of the selection criteria applied to the fourteen shore platform sites considered for this study. Green shading indicates the five platform sites chosen for this study (Source: Developed by Author)

Name of Sites			Essential Choice Criteria					Preferred Choice Criteria			
		Location	Lithology	Cliffs	Exposure	Supratidal Elevations	Good Sampling Size	Good Accessibility	Low Level of use	Short Travel Distance	One Transport Mode
1	Għar Qawqla, Marsalforn	Gozo	LGL	✓	N	✓	✓	✓	✓	×	×
2	Qbajjar Bay, Marsalforn	Gozo	LGL	✓	N	✓	✓	✓	✓	×	×
3	Xwejni Bay, Marsalforn	Gozo	LGL	✓	N	✓	✓	✓	✓	×	×
4	Xatt l-Aħmar, Mġarr	Gozo	LGL	✓	SE	✓	✓	×	✓	×	×
5	Ponta tal-Qammieħ, Marfa Ridge	Malta	LGL	✓	NW	✓	✓	×	✓	✓	✓
6	Blata l-Bajda, Selmun	Malta	UGL	✓	NE	✓	✓	✓	✓	✓	✓
7	Ponta tal-Miġnuna, St Thomas Bay	Malta	LGL	✓	NE	✓	✓	✓	✓	✓	✓
8	Ponta tal-Munxar, St Thomas Bay	Malta	LGL	✓	NE	✓	✓	✓	✓	✓	✓
9	Ras il-Fenek, Delimara	Malta	UGL	✓	SE	✓	✓	✓	✓	✓	✓
10	St Peter's Pool, Delimara	Malta	UGL	✓	SE	✓	✓	✓	✓	✓	✓
11	Delimara Bay, Delimara	Malta	UGL	✓	SE	✓	✓	✓	✓	✓	✓
12	St Lucian Headland, Birzebbuġa	Malta	LGL	✓	SE	✓	✓	×	✓	✓	✓
13	Ġnejna Bay, Mgarr	Malta	MGL	✓	NW	✓	×	✓	×	✓	✓
14	Sliema Bay (aka Exiles), Sliema	Malta	LGL	✓	NE	✓	✓	✓	×	✓	✓

To satisfy this outcome, the choice of shore platforms was restricted to the following five shore platform sites:

i. Ponta tal-Qammieħ, Marfa Ridge, Malta
ii. Blata l-Bajda, Selmun, Malta
iii. Ponta tal-Miġnuna, St Thomas Bay, Malta
iv. Ponta tal-Munxar, St Thomas Bay, Malta
v. Ras il-Fenek, Delimara, Malta (Figure 3.3).

The choice of these above-listed five sites incorporated a set of criteria reflecting the following physical properties of the platforms (Table 3.2):

i. Geology: the majority of Maltese shore platforms develop from the differential erosion created by the stratigraphy characteristics of either [a] relatively more resistant Lower Globigerina Limestone (and related presence of conglomerate beds) with the overlying marly MGLM or [b] with the relatively more resistant lower yellow marl bed of the UGLM with the overlying middle grey marl bed of the UGLM;
ii. The sites of Ponta tal-Qammieħ, Ponta tal-Miġnuna and Ponta tal-Munxar satisfy criteria [a] whilst Blata l-Bajda and Ras il-Fenek satisfy criteria [b] (Table 3.2);
iii. Orientation to wind/wave direction: the five sites chosen have different orientations in relation to local incoming wave/wind direction. The platforms oriented North-west and North-east are more exposed (in that order) to incoming wind/wave action due to the wind/waves coming from those two prevailing directions:
    a. Ponta tal-Qammieħ: North-west
    b. Blata l-Bajda: North-east
    c. Ponta tal-Miġnuna: North-east
    d. Ras il-Fenek: South-east
    e. Ponta tal-Munxar: North-east.
iv. Elevation: the chosen shore platforms ranged in mean elevation from as close to 1m a.m.s.l to elevations at 11m a.m.s.l. (Table 3.2). The height above sea level were taken using GPS Status® application;

Table 3.2: Main physical characteristics of selected shore platforms (Source: Developed by Author)

Name	Location	Orientation (mag)	Mean Elevation (m) a.m.s.l	Total Platform Area (m^2)	Max. Length (m)	Max. Width (m)	Main Lithology	Morphology	Platform Type	Backshore properties
Ponta tal-Miġnuna	St Thomas Bay, Malta	148.65 SE	≤ 6	3589	31	113	Lower Globigerina; Hardground conglomerate outcrops	Gentle sloping to east; sub-horizontal into low cliff edge to the west	Type B	Middle Globigerina Cliffs
Ponta tal-Munxar	St Thomas Bay, Malta	75.16 W	≤ 6	592	65	22	Lower Globigerina Limestone	Dipped to the south; low cliffs to the north and gentle sloping to the south	N/A	Middle Globigerina Cliffs
Ras il-Fenek	Delimara, Malta	145.36 SE	≤ 11	584	74	64	Upper Globigerina Limestone with interbedded phosphatic beds	Sub-Horizontal and stepped; bordered by low cliffs	Type B	Upper Globigerina grey marl beds and upper yellow marl beds
Blata l-Bajda	Selmun, Malta	60.97 NE	≤ 2	5427	120	30	Upper Globigerina with yellow beds at sea level	Sub-horizontal	Type B	Upper Globigerina with grey marl and yellow beds.
Ponta tal-Qammieħ	Marfa Ridge, Malta	262.53 NW	≤ 9	3435	109	177	Lower Globigerina; Hardground conglomerate outcrops	Sub-horizontal Gentle sloping northwest; low-cliffs to south-east	Type B	Middle Globigerina Cliffs

Figure 3.3: The selected five shore platforms: a. Ponta tal-Miġnuna (St Thomas Bay) b. Ponta tal-Munxar (St Thomas Bay); c. Ras il-Fenek (Marsaxlokk); d. Blata l-Bajda (Selmun); e. Ponta tal-Qammieħ (Mellieħa)(Source: Photos taken by Author).

v. Shape: they differ in shape in being either semi-circular (Ras il-Fenek, Ponta tal-Miġnuna) or more elongated (Ponta tal-Qammieħ; Blata l-Bajda and Ponta tal-Munxar);
vi. Size: size was measured as the whole platform surface area bounded between the shoreline and the cliff-platform junction. Their total surface areas ranged from 584 m^2 for Ras il-Fenek to Blata l-Bajda being the largest with 5,427m^2 (Table 3.2);
vii. Platform width (max): this was measured as the maximum length in metres from the cliff –platform junction to shoreline in a cross-shore direction. The width dimensions varied from 22 m to 177 m;
viii. Platform Length (max): this was measured as the maximum length of the platform in an alongshore direction (as a straight line distance). The width dimension varied from 30 m to 109 m; and
ix. Accessibility: in terms of accessibility, they all presented a varying degree of reasonable walking access such as those at St Thomas Bay (Ponta tal-Miġnuna and Ponta tal-Munxar) which were easily reached from the main road within five minutes. The other three sites required a longer walking fieldtrip: Ras il-Fenek (20 minutes) Blata l-Bajda (30 minutes) and Ponta tal-Qammieħ (40 minutes).

3.3 Data collection and methods parameters

A framework of data gathering must ensure that the designated data gathering tools are chosen and exercised systematically and appropriately in collecting the evidence from the field. Within this context, a series of decisions were taken in relation to selection of the following aspects of research:

i. The number of sites to be selected;
ii. The equipment to be used in field;
iii. The temporal frequency of data collection; and
iv. The data analyses to be performed once the data was collected.

Table 3.3 outlines the investigated parameters and the techniques or instruments used to test the relevant hypotheses which frame the research

Table 3.3: Main themes and hypotheses, according to their respective investigated parameters and instrument/technique used (Source: Developed by Author)

Research Theme	Hypotheses		Investigated parameters	Instrument/Technique Used
Geomorphological features	1	Globigerina shore platforms share common geomorphological features, primarily inherent of their geological characteristics.	Surface morphology at micro- and meso-scale	Geomorphological mapping
Mineralogical and geo-mechanical properties	2	Globigerina shore platforms share similar properties of surface hardness	Surface rebound values in cross-shore direction and in different seasons	N-type Schmidt Hammer
	3	Surface hardness on Globigerina shore platforms is subject to spatio-temporal variability	Surface rebound values in cross-shore direction and in different seasons	N-type Schmidt Hammer
	4	Globigerina shore platforms consist of a limestone lithology susceptible to similar rates of weathering	Rock sample surface change, percentage weight change and debris loss	Exposure trials with micro-catchment basins and TMEM
	5	The mineralogical properties of the Globigerina shore platforms influence lithological control and rates of surface change	Rock mineralogy: identification of mineral type and mineral group	Near Infrared Spectroscopy
Rates of surface change	6	Rates of surface change are directly related to cross-shore spatial dynamics across each platform	Rock surface change within each TMEM station	TMEM
	7	Rates of surface change on each platform are influenced by temporal and seasonal parameters	Rock surface change within each TMEM station	TMEM
	8	Platforms share common spatio-temporal patterns of surface change	Rock surface change within each TMEM station	TMEM

themes of this study. The TMEM was considered as the core method in this study to be employed in order to identify and quantify rock surface change on spatial and temporal scales. The geomorphological mapping, the geological tests (NIR, Schmidt Hammer, rock exposure trials) provided supporting data which may help to identify the control parameters that may be influencing the rates and modes of surface change captured by the TMEM.

The acquisition of the some of the above-mentioned equipment involved a lengthy preparatory phase, with the former starting quite in advance, given that some of the needed tools chosen for this research (such as the TMEM) are expensive acquisitions and needed to be obtained through a lengthy funding application process with the University of Malta Research Grants Schemes. Additionally training was required to cover the basic concepts of the equipment, hardware and software management and proper applications of the tool in the field (Figure 3.1).

3.4 Data Collection Process

3.4.1 Geomorphological assessment and mapping

Dramis, Guida and Cestari (2011) described geomorphological maps as providing a "*full objective description of landforms (morphography) identified with specific names and depicted with their correct shape or, where not allowed by the map scale, by appropriate symbols"* (2011:39). Geomorphological maps would include information on spatial properties, origin, evolution and relative age of landforms, their present activity and effective processes, as well as the type of bedrock and near surface deposits.

Knowledge of all the conditions that frame the morphological make-up of the platform (such as geometric properties, lithology and structure) is essential to understand the extent and mode of erosional or sub-aerial operations, and how site-specific lithology and structural controls are responding to these forces. As previously explained in Section 3.2, an intensive type of case-study approach was required in order to identify and quantify rates of surface change through

the installation of TMEM stations. However, producing a geomorphological map of the whole platform was considered an important requirement for the following reasons:

i. It provides a better physical context in which to compare morphological similarities and differences between the selected Globigerina platforms. This addresses the first research questions about whether Globigerina shore platforms are morphologically similar platforms and if not, to what extent are they different;
ii. It helped to present a better idea of the platform environment where the TMEM stations have been placed and to contextualise better the site-specific conditions of each station; and
iii. The mapped morphological products may help to infer erosional and/or weathering forces present across the platform and potentially linked to the rates and modes of surface change across the different TMEM stations. This was observed to be a missing element in many TMEM studies.

To date, very few works have published geomorphological maps at a sufficient small scale to incorporate mapping of platforms, such as by Hénaff, Lageat and Costa (2006) and Cruslock *et al.* (2010). Geomorphological maps of Maltese shore platforms have never been published to date. A morphodynamic perspective was adopted for the creation of a five geomorphological maps for the selected platforms. Geology, structure, weathering and erosion forms were all sketched over a number of field visits between 2012 and 2013. Field observations led to the discovery of a number of lithological misinterpretations present on the national geological map produced by Pedley (1993) and which will be presented in Chapter 4. These observations were later confirmed with additional site visits with local geologist Dr Saviour Scerri and consultations with other scholars who previously investigated Maltese stratigraphy such as Dr Martyn Pedley (University of Hull), Arch. Adrian Mifsud (University of Malta), Dr Niccolo Baldassini (University of Catania) and Dr Luca Foresi (University of Siena). The smallest scale available for base maps from local ERA mapping agency was in the form of 1:2,500 survey sheets. Such a scale does not provide sufficient detail of each platform. Base maps were reconstructed by producing outline maps using Google Earth satellite images and adding geological and

geomorphological information (including symbology) from the small number of maps available such as Pedley (1993) and Biolchi *et al.* (2016). However both these works were not at a sufficient small scale (1:25,000) and thus more detailed information was added to the maps through site visits. All the information was collated together using Adobe Illustrator software.

3.4.2 Traversing Micro-Erosion Meter (TMEM)

3.4.2.1 Scope of the investigation

This study is a first in investigating rock surface change on a number of Maltese shore platforms with the use of a traversing micro-erosion meter (TMEM). The aim was to measure rates and modes of surface change on Globigerina shore platforms and provide spatio-temporal statistical comparisons. The choice of instrument was based on the fact that most recent literature about micro-erosion studies on shore platforms used the TMEM (Stephenson, 2013).

3.4.2.2 The instrument model: a brief description

Dr Stefano Furlani – a micro-erosion researcher and key user of the TMEM from the University of Trieste – offered to construct and make available the instrument within a few months of production[2]. Supporting equipment included a calibration plate, digital lead, positioning plate and 48 titanium studs. The 48 titanium studs provided 16 triangular TMEM stations, each made up of two round-headed studs (Model L26 no. 50) and one flat-headed stud (Model L24 no. 25). In April 2012, Dr Stefano Furlani provided the TMEM instrument and a five-day training session was organised, in order get technical and field-based training related to the following:

i. The *in situ* installation of TMEM stations;
ii. Field-based training related to the measurement to rock surface heights using the TMEM;
iii. Maintenance and calibration of the TMEM instrument; and
iv. Data transfer into spreadsheets using Excel.

[2] Funding from the University of Malta Research Grant Schemes was allocated as follows: €3000 for the UoM GEORP 01-02 project and €4200 were allocated by the UoM GEORP 01-03 project.

The TMEM manufactured for this research has a digimatic indicator Mitutoyo Corp® Model IS-S112B (Code No. 543-690B). The instrument is equipped with a millimetre-resolution electronic dial gauge and the readings can be directly downloaded on a laptop computer. The electronic dial gauge Mitutoyo Corp® Model IS-S112B (Code No. 543-690B) has a resolution of 0.001 mm, a manufacturing accuracy of $\pm$0.003 mm and a range of 12.7 mm. The bottom part of this digital gauge was equipped with a three legged support that rests on tripod position plate with six position spheres (0.6 mm in diameter) located on each of its three sides. Each position along the three sides is identified with the use of a letter or number character: A, B, C, D and E for one side; a, b, c, d and e for the second side; 1, 2, 3, 4 and 5 for the last third side. Each specific position of the TMEM is then identified with a specific unique code consisting of one letter/number character for each side such as Aa1, Aa2, Ab4 and so forth. A total of 22 equidistant points were selected for this study (Figure 3.4) to measure rock surface change as part of the hypotheses statements (No. 6-8) listed in Table 3.3.

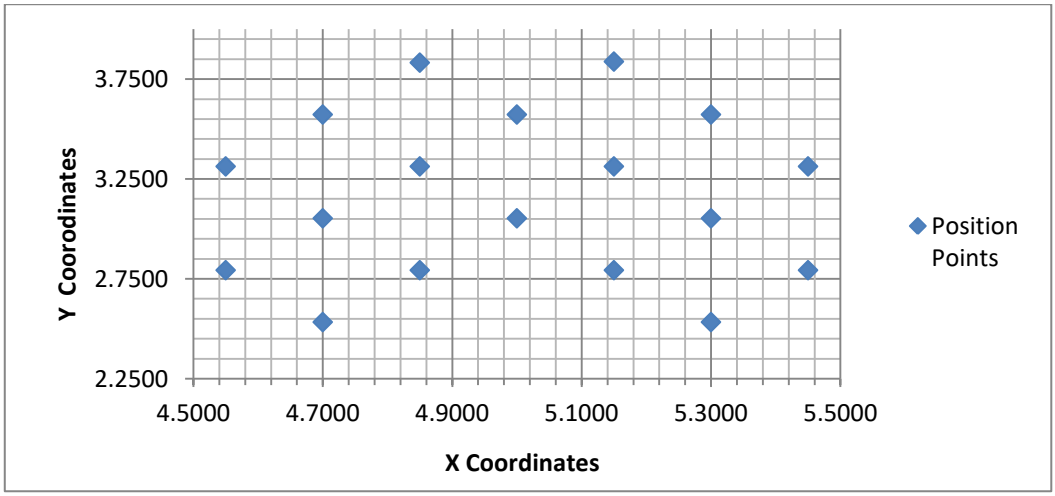

Figure 3.4: Position points of readings within the TMEM station according to their X and Y co-ordinates (Source: Developed by Author)

The base of the tripod plate has three titanium pins that lock into the three titanium bolts installed on site: two with semi-spherical heads and one with flat heads (Figure 3.5). Bolt holes were drilled in the rock with a cordless driller to a depth of 5 cm. Bolts were cemented inside the holes with a rapid-

drying cementing powder (Figure 3.6). Once locked in position over the bolts, the TMEM is moved over the triangular tripod along the 18 position spheres. The exact relocation of the tripod plate on the fixed studs follows what is known as the 'Kelvin Clamp Principle': a principle in which the spheres in the tripod plate lock in the bottom fixed studs and thus an actual re-positioning of the instrument over a period of the time is possible and reliable (Forti *et al.*, 2006; Furlani and Cucchi, 2008).

A calibration steel base was constructed and used regularly to check calibration error/changes of the instrument during the study period (Figure 3.5). The best method was considered to be the calibration of the instrument twice prior to reaching the site, then re-checking (twice) *in situ* prior to measuring the TMEM stations and a final re-checking (twice again) post-situ after the data collection. The average of the two in situ calibrations was used as reference position when processing the *in situ* rock surface height data. More detail of the related procedures is given further on in Section 3.4.2.6.

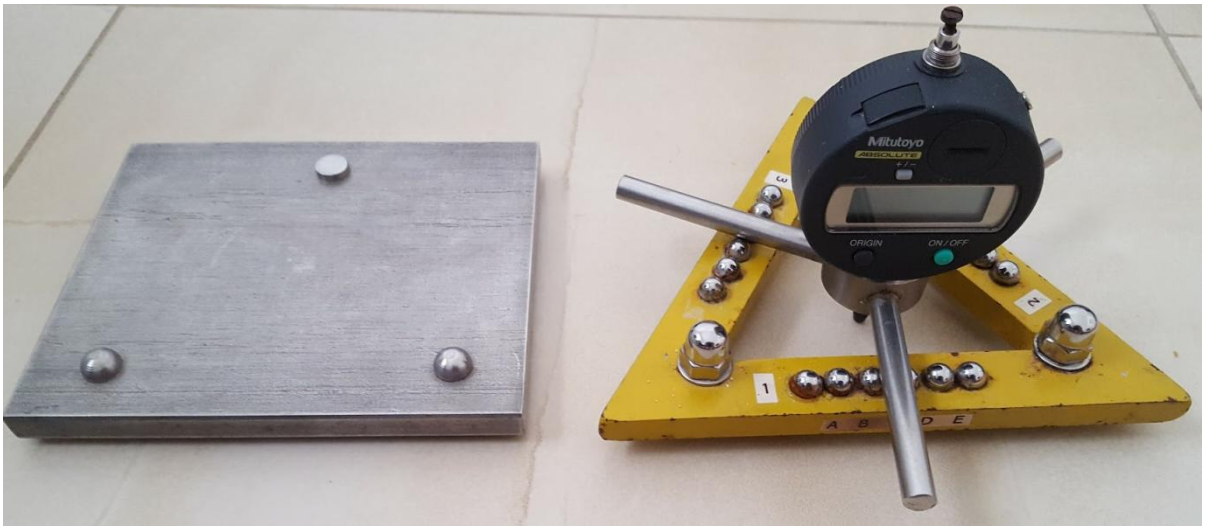

Figure 3.5: The TMEM with digimatic indicator Mitutoyo Corp® Model IS-S112B (Code No. 543-690B) mounted on three-legged support, resting on the tripod position plate and the calibration plate next to it (Source: Photo taken by Author)

3.4.2.3 Installation of TMEM stations for pilot study

In April 2012, sixteen TMEM stations were set up in five coastal sites on mainland Malta, with each site having three TMEM stations placed along a

transect in a cross-shore direction with as a set of three TMEM stations positioned in the front, middle and back sections of the platform. The aim of this transect sampling was to obtain a comparative analysis of rock surface erosion in relation to distance from the shoreline. This cross-shore sampling method has been previously in other studies, such as by Porter *et al.* (2010a), to identify any spatial variation in surface erosion rates with increasing distance from shoreline. In the case of Ponta tal-Munxar, given that the platform is comparatively narrower, there was no sufficient space to place TMEM stations in the middle section. Therefore two transects were set up, each with a TMEM station in the front and back sections of the platform (Table 3.4).

Table 3.4: Number of stations per shore platform site for pilot study

Research Status	Case-study location	No. of TMEM Stations
Pilot Study Sites	Ponta tal-Qammieħ (Marfa Ridge)	3
	Blata l-Bajda (Selmun)	3
	Ponta tal-Miġnuna (St Thomas Bay)	3
	Ponta tal-Munxar (St Thomas Bay)	4
	Ras il-Fenek (Delimara)	3

The following equipment was used for the installation of the TMEM stations as follows:

i. 48 titanium studs: 32 round-headed studs (Model L26 no 50) and 16 flat-headed stud (Model L24 no 25) with a depth of 2.5 cm. These dimensions were the standard dimensions produced (Figure 3.6a);
ii. 18V Cordless driller Economy by Ferm® and EBFL-18 Economy by Ferm® charger (Figure 3.6b);
iii. 3 Twist drill bits: 1/16 (0.406 mm), 1/32 (0.812 mm) and 1/64 (1.63 mm) (Figure 3.6c);
iv. TMEM Triangular stud position plate (Figure 3.6d); and
v. Rapid drying cement powder (Figure 3.6e).

Each station consisted of three titanium studs (two semi-spherical and one flat shaped) which support the triangular base on which the digital TMEM is placed to take trasversing readings of relative rock surface heights. The TMEM is equipped with an electronic dial gauge and has a resolution of 0.001 mm.

Twenty-two digital readings were periodically measured at each station every three months and the study covered a period from April 2012 to August 2013. A total of four cycles of TMEM readings were measured at each site during this period of one year and three months as part of the pilot study.

Figure 3.6: Tools for the installation of TMEM stations: a. Titanium studs; b. Cordless driller; c. Twist drill bits; d. TMEM position plate; e. cement powder (Source: Photo taken by Author)

3.4.2.4 Outcome of pilot study: procedures for further set-ups

After four field sessions, more confidence in the data gathering was established. A few research barriers were also encountered which needed to be managed to ensure future undisturbed continuation of data collection. The identified barriers and solutions addressed were the following:

i. Two TMEM frontshore stations were lost due to studs' removal by human tampering. It was decided that future frontshore studs will not be placed close to accessibility points, favourite fishing or bathing spots close to shore ladder locations;
ii. All bolts need to be covered with a special paste made up of natural globigerina debris and cement powder to camouflage better the presence of

the studs from any acts of vandalism by platform users. It was found that this paste had the right consistency and colour to cover surficially the studs, without attaching too strongly to them and thus be able to dust them off easily in subsequent measurement sessions;

iii. Backshore stations cannot be placed too close to the cliff line because they might end up being covered by falling cliff debris. A threshold distance of at least one metre was established from the cliff-platform junction;

iv. Frontshore stations situated in highly exposed parts of the platform might need to be relocated one or two metres from the shoreline given that they cannot withstand continuous wave pounding after a few cycles. The other option would be to design new studs with a longer leg frame in order to secure a better installation of these studs against the pounding action of the waves;

v. Most fieldwork was better done in early mornings to avoid curious on-lookers and thus minimise the risk of human tampering of the stations and as much as possible outside the hunting season;

vi. Before the third measurement session, the measuring probe of the TMEM was temporarily blocked, probably due to sea spray contamination. After routine checks and maintenance with a valve oil the probe became functional again. However, to make sure that that the future data collection remains viable, the origin point of the instrument was reset and the third cycle readings were not retained to maintain confidence in the dataset; and

vii. More regular cleaning and maintenance of the instrument were undertaken in order to avoid a similar malfunction, explained in [vi].

3.4.2.5 Development of TMEM network with a second transect

Over the study period (April-May 2012 to August 2016), a total of 42 TMEM stations were installed and monitored. The study period comprised a total of 14 measurement sessions (Table 3.5 and Appendix II). The TMEM stations were laid out in a cross-shore direction along two transects, with three TMEM stations along each transect on each platform (Appendix III). A total of 11 TMEM stations were replaced due to damage or loss over the course of the study. To keep track of these replacements, a matrix was created to keep tab of each

Shore Platform Site	TMEM Stations	Measurement sessions of surface change													No. of Sessions
		1	2	4	5	6	7	8	9	10	11	12	13	14	
Ponta tal-Mignuna	MPM 1a														1
	MPM 1b														12
	MPM 2a														6
	MPM 2b														7
	MPM 3a														1
	MPM 3b														5
	MPM 3c														6
	MPM 4a														1
	MPM 4b														12
	MPM 5														13
	MPM 6a														3
	MPM 6b														9
Ras il-Fenek	MRF 1a														2
	MRF 1b														9
	MRF 2a														2
	MRF 2b														9
	MRF 3														9
	MRF 4														9
	MRF 5														9
	MRF 6														13
	MRF 7														9
Blata l-Bajda	MBB 1a														2
	MBB 1b														9
	MBB 2														13
	MBB 3														13
	MBB 4														9
	MBB 5														9
	MBB 6a														4
	MBB 6b														4
Ponta tal-Qammieh	MPQ 1														13
	MPQ 2														13
	MPQ 3														13
	MPQ 4														9
	MPQ 5														9
	MPQ 6														9
Ponta tal-Munxar	MMX 1a														4
	MMX 1b														8
	MMX 2														13
	MMX 3a														4
	MMX 3b														3
	MMX 3c														3
	MMX 4														13
	MMX 5a														1
	MMX 5b														8
	MMX 6														9
Total No. of Sessions															**342**

Figure 3.7: List of TMEM stations used per platform (with replaced ones indicated by a, b and c letter) and measurement sessions (Source: Developed by Author)

replacement (Figure 3.7). The replaced TMEM stations retained the original name but with 'a', 'b' or 'c' label added to denote successive replacement where appicable. This matrix helped to eventually visualise better the length of monitoring done for each station over the course of fourteen measurement sessions. The positions of these stations are illustrated in the geomorphology maps presented in Chapter 4.

Table 3.5: Number of stations per shore platform (Source: Developed by Author)

Research Status	Platform site	No. of TMEM Stations set up	No. of TMEM stations replaced	Total no. of TMEM stations installed	Percentage of TMEM replaced
Definite Project	Ponta tal-Qammieħ	6	0	6	0
	Blata l-Bajda	6	2	8	33
	Ponta tal-Miġnuna	6	3	9	50
	Ponta tal-Munxar	6	4	10	66
	Ras il-Fenek	7	2	9	28

3.4.2.6 Instrument calibration, error checks and corrections

The basis for accurate three-dimensional measurements with the TMEM lies in monitoring and recording the precision of the instrument in measuring vertical heights (distances) between the TMEM instrument probe and a flat plane. This flat plane, represented by the calibration plate, is used as a 'reference plane' on two accounts:

i. It becomes a measured surface along which deviations from the three control points and their zone parameters are referred; and
ii. It provides a set of control points reference values, along which to benchmark the actual *in situ* rock surface height measurements.

Any slight variations in calibration constants for any specific point (across a period of time) may have a subtle but important effect on *in situ* measurements and their relative change calculations. It is important to log such

variations and ensure that the calibration plate is smooth, free from any contaminants or loose dust. Should variations in the calibration values be observed, *in situ* measured changes may require to be corrected from such calibration variations in order obtain comparable *in situ* measurements from one period to the next (S. Furlani, Pers. Comm., 12/4/12).

In this research, the reference plane measurements were obtained from the calibration method, by locking the TMEM tripod on top of the calibration plate, position the TMEM instrument on top of the tripod and then pass the instrument on the chosen twenty-two position points along the tripod to obtain relative control points measurements (Figure 3.5). This should be done prior to taking *in situ* measurements. Initially, this method was undertaken once in an indoor ambience - prior to going in the field – in order to have a stable desk and minimise any physical instability in the recording of these control-points measurements. With successive uses of the instrument over a longer period of time and further transportation and exposures to outdoor coastal environments, additional checks and balances in the use of the instrument were undertaken *in situ* and *post situ*. These were primarily two:

i. Conducting a double calibration in order to ensure that the Mitutoyo Corp® dial indicator was still operating within the of +/- manufacturing accuracy of ±0.003 mm. This double calibration was carried out throughout the last eight cycles; and
ii. Calibrating in a tripartite pattern of *pre situ* (indoor), *in situ* (on the field) and *post situ* (indoor) during the last six cycles in order to keep a check on the magnitude of the calibration variations during the data collection period.

Two mathematical corrections were undertaken to the field measurements:

i. Position point correction: The Mitutoyo Corp® dial indicator of the TMEM has a position point which initially always started from a zero position point. The continuous and intensive use of the

instrument had a 'loosening' effect on the zero position of the probe; by the 6th measurement period, it was observed that it had started to position a few microns below the zero reading. Thus, the position point of the dial indicator was recorded prior to taking measurements and then corrected from the field measurements.

ii. Calibration correction: Calibration variations were corrected from *in situ* measurements when calculating the actual change in rock surface heights from one period to the next. Once the TMEM field data was collected and inputted in Excel spreadsheets, actual changes in rock surface heights between two time periods were calculated with a three-step calculation as follows:
    a. a subtraction of *in situ* readings of the current time period from the in situ readings of the previous time period;
    b. a second subtraction of the average calibration of the current time period from that of the previous time period; and
    c. a final subtraction in which the magnitude of average calibration variation between the two periods obtained in step [b] is subtracted from the *in situ* surface height change, previously obtained in step [a].

The above-described mathematical procedure is represented in the following equation:

$$\text{Corrected surface change between two time periods} = (R_2\text{-}R_1) - (Av.Cal_2\text{-}\ Av.Cal_1)$$

Equation 1

Where

R_2 In situ reading taken in the current time period

R_1 In situ reading taken in the time period previous to R_2

$Av.Cal_2$ Average calibration reading of R_2

$Av.\ Cal_1$ Average calibration reading of R_1

One worked example of Equation 1 is provided in the following box:

Corrected surface change of Aa1 Station MPB 1b (Selmun) between 14th time period and 13th time period:

R_{14} 4.704

R_{13} 4.714

$Av.Cal_{14}$ 1.328

$Av.\ Cal_{13}$ 1.331

Corrected surface change = $(R_{14}\text{-}R_{13}) - (Av.Cal_{14}\text{-}\ Av.Cal_{13})$

= (4.704 – 4.714) – (1.328-1.331)

= (-0.010) – (-0.003)

= -0.007

With regard to the subtraction method used to correct the calibration variations between two time periods, two methods were considered:

i. Subtracting the calibration variation according to individual variation values present at every single point - which we refer to as an 'individual point correction method'; or
ii. Use a representative average calibration value for that time period to correct the surface change of all the twenty-two points, which we refer to as the 'averaging correction method'.

The second method i.e. the 'average correction method' was chosen, given that the pattern of calibration variation between two time periods was consistent and uniform across the twenty-two points. Thus the averaging method was not going to misrepresent any points having relatively larger or smaller deviations from the representative average. For those time periods where a double calibration was performed, the average calibration between the two data sets was calculated and then the total average was calculated for all the twenty points. For those time periods, where the *in situ* calibrations were performed, those were preferred over the indoor ones; in the absence of *in situ* calibrations such as in the first eighth cycles, the average calibration of the indoor values was used.

The double calibration procedure ensured no instrument error in the Mitutoyo Corp® dial indicator, since it was always operating within the +/- manufacturing accuracy of ±0.003 mm. With the tripod and the calibration plate remaining physically in unchanged states, the only reason for such intermittent shifts in calibration was attributed to be the central connection between the dial gauge and the three-legged base. It was observed that the magnitude of calibration variations was mostly higher, after a period of instrument inactivity, from one time-period to the next. It never varied during the same measurement session of a particular site. A potential mechanical shift in the central connection between the dial gauge and the three-legged base would explain why the degree of calibration variation occurred uniformly across all the 22 measuring points. Given that any physical examination of the instrument may have compromised the continuation of the measurement periods, it was decided to continue the data collection, whilst keeping all necessary checks and balances on the calibration values for accurate post-calculation corrections. Once the corrections for position point and calibration were done, the final rates of surface change (in mma^{-1}) between time periods were further calculated using the following formula:

$$\text{Rates of Surface Change } (mma^{-1}) = \left(\frac{\text{Surface Change between Two Time Periods (mm)}}{\text{Total Number of Days between Two Time Periods}}\right) \text{ x } 365$$

Equation 2

The rates were then used for statistical comparisons and calculations between time periods and sites. In this thesis, negative values represent lowering of the rock surface heights (indicating erosion) whilst positive ones represent rising of the rock surface heights (indicating accretion). This method is different from the one employed in most TMEM studies, in which erosion was represented by positive values and accretion by negative values (Table 2.2, Chapter 2). The reason behind the current choice of method was that during the data collection process, comparison of readings was being carried out between a current time-period and the previous one. Thus, losses and gains of the surface change between the two time periods were easier to comprehend with

backward subtractions, in which the surface loss was represented by negative values and surface gains were represented by positive values.

3.5 Rock properties assessment

3.5.1 Measurement of rock surface hardness with N Type Schmidt Hammer

3.5.1.1 Scope of the investigation

The role of lithological control in influencing rock resistance to erosion and weathering processes has increasingly become a key discussion in many platform studies in the last few decades (See Chapter 2, Section 2.5.1) (Robinson and Moses, 2011; Goudie, 2016). This investigation builds on these established works in trying to characterize the surface hardness properties of some of the Maltese shore platforms. Determining the spatial extent of surface hardness properties across the platform can elicit a better understanding of the control-process dynamics that may influence the rates of surface change measured in this study. This investigation tested hypothesis no. 2 (outlined in Table 3.3), in determining the extent of rock surface hardness across each platform and whether there is spatio-temporal variability within each platform and between platforms.

Surface rock hardness was also measured as rebound values (R values) obtained from an N type Schmidt Hammer along the two transects laid out to install the six TMEM stations (Figure 3.8). The Schmidt Hammer, devised in 1948 by E. Schmidt, was originally intended for *in situ*, non-destructive tests on concrete hardness (Day, 1980; Viles *et al.,* 2011). It measures the distance of rebound, or rebound value, of a controlled impact on a rock surface (Goudie, 2013). Over the last sixty years, the application of the instrument grew and diversified in a wider research context and has evolved into different models with different functions (Viles *et al.,* 2011). In recent years, it has become a routine standard tool to assess lithological control and rock weathering on various shore platforms (Goudie, 2006).

The two mostly used hammers by geomorphologists are the N type and L type (Selçuk and Nar, 2016). The N type provides impact measurements for rock types ranging from weak to very strong with compressive strengths (*c.* 20–250 MPa). The L type hammer has an impact three times lower than the N type (0·735 compared to 2·207 Nm) and is mostly for weak rocks and those having thin crusts (Viles *et al.*, 2011). ASTM (2005) standards for testing of rock hardness, D5873-14, do not specify a hammer type, but suggest that the use of this instrument is best suited for rocks which have UCS in the range of 1–100 MPa. Aydin and Basu (2005) describe how both types of hammers have been used in rock engineering for strength estimation of various rocks having UCS up to approximately 350 MPa. For the current study, the N-type hammer was used. Comparative studies between the two hammers, such as by Aydin and Basu (2005), confirm that the N type hammer performs better as the higher impact energy (2.207 Nm) represents the intact rock strength more reliably. They also reported that it produces a lesser scatter in the data, and is more efficient than the L type hammer in predicting uniaxial compressive strength.

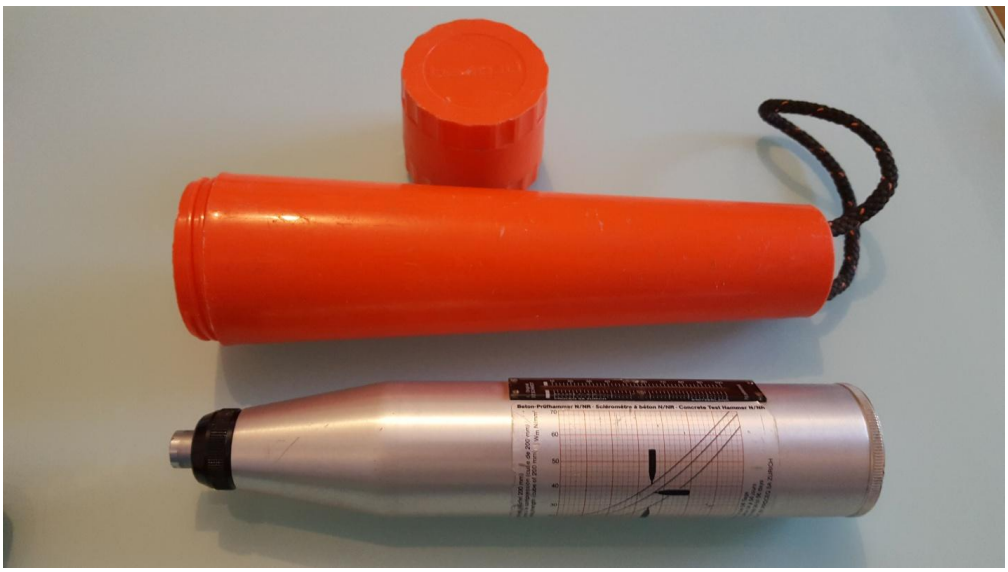

Figure 3.8: The N Type Schmidt Hammer used in this current research (Source: Photo taken by Author)

3.5.1.2 Method to obtain a representative R value: choice and justification

As seen in Appendix IV, the literature abounds with numerous studies about selective methods that can be used to obtain a representative R value for various lithologies. Amongst the most well-known and highly-used methods are those of the International Society for Rock Mechanics (ISRM) (2007) and the ASTM (2005) (Selçuk and Nar, 2016). Without disregarding the science behind these, this current study has opted not to use one particular selective method but rather implement a criteria-based procedure based on the following set of arguments already published in the literature:

i. Mean R value representation: Two studies have so far used N-type Schmidt Hammer on Maltese limestone boulders: Biolchi *et al.* (2015) and Causon Deguara and Gauci (2017). Both studies have used the ISRM (2007) method to calculate the density of Maltese limestone boulders. However, some authors, like Torabi, Ataei and Javanshir (2011), discourage the use of selective methods such as ISRM (2007), given that it skews the mean R values towards the upper 50% of the data structure and discards the lower half. The authors reiterate that lower R values may not necessarily be the result of test deficiencies but rather the reaction from inherently heterogeneous and/or weaker structures present in certain lithologies. In a recent study by Karaman and Kesimal (2015), the authors demonstrated how the averaging method was slightly more reliable when compared with two selective methods. They conclude that a mean R value provides a better representation of the overall rock hardness and acts as a more robust indirect indicator of properties such as unconfined compressive strength. Niedzielski, Migoń and Placek (2009) investigated the minimum sample requirements for Schmidt Hammer tests and concluded that the elimination of low values may have variable effect from negligible to significant, depending on rock type and significance level. Their recommendation was for researchers to choose a method that is primarily guided by the purpose of study;

ii. Rock surface response to hammer impact: Other selective methods can produce more skewed results than ISRM (2007), especially in terms of rock surface behaviour to hammer impacts. Guney *et al.* (2005) tested limestone surface hardness by comparing the readings of N-type and L-type hammers against three selective procedures: 1. Poole and Farmer (1980); 2. Hucka (1965); and 3. ISRM (2007). Refer to Appendix IV for an outline of these methods. ISRM (2007) yielded lower R values than the other two tests. The authors attribute primarily this result to two main reasons: 1. ISRM is based on the mean value of ten separate points, whereas the other two procedures take the peak value out of five or ten impacts on the same point; 2. repeated impacts on the same point, as performed by Poole and Farmer (1980) and Hucka (1965), may lead to an increase in the rock elasticity on the impact point and consequently induce a surface behaviour misrepresentation of the entire rock sample; and

iii. Lithological heterogeneity: Several other authors, such as Amaral, Rosa and Fernandes (1999), Aydin (2009) and Liang *et al.* (2015) have acknowledged the large variability of rock hardness present in certain lithologies and most significantly in limestone by Goudie (2006). Amaral, Rosa and Fernandes (1999) highlight the need to understand the variations in the hardness because they are precisely related to the material heterogeneity. They propose for all R values to be taken into account. Likewise, Aydin (2009), in his review work of the ISRM (2007) method, also suggested that all values should be used to calculate summary statistics and no values (high or low) should be discarded.

Given that the present study is a first in presenting findings related to surface hardness properties for Maltese shore platforms and that such information is still largely unknown and unquantified, it was considered important to provide a meaningful representation of their surface rock hardness based on the whole spectrum of single impact points. Thus for the purpose of this study, it was decided to collect individual readings as separate

impact points and to consider the mean R value of all individual readings as a representative value.

3.5.1.3 Number of impact points: choice and justification

The number of impact points per 'test point' and the number of measurement periods were two important considerations when determining the number of single impact points in this test. In this study, 'test point' refers to a specific point on the shore platform where a set of single impacts were taken in a downward-facing non-horizontal position and within at least one plunger distance apart.

At each test point, impact points were recorded in an area of 20 cm by 20 cm according to ASTM (2005) specified procedure. Similarly to Williams and Robinson (1983) the rock surface was not prepared with the carborundum stone since it was the intention of this study to capture the hardness properties of the rock surface in their natural state and in line with the same surface conditions in which the TMEM stations have been set up. In the terms of hammer operation procedures *in situ*, all the readings were taken according to the guidelines set by ASTM (2005) (excluding the sampling requirements) and the recommendations listed in Goudie (2013).

Within the selective methods listed in Appendix IV, one can notice the extremely wide range of procedures applied to Schmidt Hammer test. In this regard, Niedzielski, Migoń and Placek (2009) explained how the minimum number of test points was never consistently and rigorously considered in geomorphological studies. Such decision was always based on intuition rather than statistical criteria and this led to the number of impacts at any one site ranging from 5 to 50 impact points. From the statistical tests run by Niedzielski, Migoń and Placek (2009), it was concluded that fine-grained sedimentary rocks require lower values of minimum sample size: not more than 15 impact points. Applying this result *in situ* for this current study however required the additional consideration of other *in situ* conditions such as discontinuities,

Table 3.6: Length of transect, number of test points and number of impact points per platform site (Source: Developed by Author

Name of platform site and locality	Length of Transect (m)		No. of test points per transect*		No. of impact points**		No. of impact points***		Total no. of impact points per transect		Total no. of impact points per platform
					6th-7th measurement session		8th-11th measurement session		All sessions		
	Transect 1	Transect 2	Transect 1	Transect 2	Transect 1	Transect 2	Transect 1	Transect 2	Transect 1	Transect 2	
Ras il-Fenek (Marsaxlokk)	54.5	56.4	11	11	110	110	440	440	550	550	1100
Ponta tal-Miġnuna (St Thomas Bay)	20.4	23.8	10	10	100	100	400	400	500	500	1000
Ponta tal-Munxar (St Thomas Bay)	44.2	53.9	12	12	120	120	480	480	600	600	1200
Ponta tal-Qammieħ (Mellieħa)	99.1	95.1	15	15	150	150	600	600	750	750	1500
Blata l-Bajda (Selmun)	89.9	73.9	14	12	140	120	560	480	700	600	1300
Total no. of impact points per transect					620	600	2480	2400	3100	3000	6100

** 'Test point' refers to a specific point on the shore platform where a set of single impacts R readings were taken within at least one plunger distance apart*

***Five impact points per test point*

****Ten impact points per test point*

weakness planes and surface irregularities (Sheorey *et al.*, 1984). The repetition of the test over a set of measurement sessions also needed to be factored in the decision about the number of impact points, as the former would determine the amount of R values to be generated and which subsequently needed to be analyzed within a reasonable time-frame.

Given the surface variability present at each platform, it was preferred to have a higher number of test points along each transect and consequently a relatively lower number of individual impact readings per test point. This method was considered better in terms of achieving a uniform spatial distribution of readings along each transect. In view of the high volume of test points chosen along each transect and the planned measurement periods, the minimum number of impact points established in the literature, i.e. 5 impact points, were initially implemented in the first two measurement sessions (Table 3.6). Initially it was planned to collect only four measurement sessions based on five separate impact points to cover an annual time frame. In the light the ease and rapidity at which the R values were collected and the recommendations found in the literature to increase sample size for highly variable lithologies in order to minimize the margin of error (Day 1980), the impact points were scaled up to ten and four other measurement sessions, 8^{th}-11^{th}, were collected with ten impact points per test point (Table 3.6).

A total of six measurement sessions (from February 2014 to August 2015) were undertaken and these align with the 6^{th} to 11^{th} measurement sessions of the TMEM data collection (Appendix II). For this reason, reference to the measurement sessions of the Schmidt Hammer data will bear the same name used for the TMEM measurement sessions i.e. 6^{th}, 7^{th} measurement session and so forth.

3.5.1.4 Normalisation method for the non-horizontal R values: choice and justification

The testing procedure involved taking a number of readings along the two transects on each shore platform with the instrument in a vertical position

and in a perpendicular direction to the platform horizontal surface. To remove the effect of gravity, rebound values were normalized with reference to the horizontal direction according to a formula method proposed by Basu and Aydin (2004). This latter method proved more accurate than the conventional on two accounts:

i. The conventional method – as stipulated by ISRM (2007) and ASTM (2014) – normalizes rebound values by using the correction curves provided by the manufacturer. However, such correction curves are not always accurate in normalizing rebound values from different rock surfaces given that the instrument is designed for concrete surface testing; and
ii. The manufacturer correction curves are often limited to two or four impact directions.

The normalization method by Basu and Aydin (2004) can be used for any type of Schmidt Hammer fired in any direction. Through experimental studies, Basu and Aydin (2004) demonstrated the validity of their normalization formula when applied to a wide range of rock materials. In this study, in order to achieve maximum accuracy, the normalisation was done to each individual non-horizontal reading before mean R values were processed in Microsoft Excel® spreadsheets (See Appendix VI). The normalised values were recorded and displayed up to one decimal point and summarised in Table 5.5.

3.5.1.5 Statistical treatment of the two types of impact point datasets for variance

Given that the two initial measurement sessions were based on five impact points rather than ten, statistical comparisons were undertaken to check whether the five-impact point method was statistically similar to the ten impact point method. The reason for this checking exercise was to understand whether the datasets taken on the 6th and 7th measurement sessions could be included with the successive four measurements sessions for analyses.

For this checking exercise, the datasets of Transect 1 from the 8th to 11th measurement sessions were split up further into three datasets: 1. Mean R values of the first five impact points; 2. Mean R value of the second five impact points; 3. Mean R value of the whole dataset based on ten impacts points. Mean R values were normally distributed, as assessed by Kolmogorov Smirnoff (KS) test ($p > .05$). On the basis of the KS Test, it was decided to conduct Independent Sample T-Tests using the mean R values of Transect 1 for the five studied platforms. A total of 40 T-tests were carried, which was considered adequate as a checking exercise to compare the R value variability between the two datasets.

Table 3.7 displays the *p* values confirm that there is a high degree of similarity between the two tested datasets, with *p* values ranging from 0.503, $t(26)=0.680$ to 1.00, $t(18)=0.000$. This confirms that the mean R values of the datasets with five impacts points are equally representative as those based on the ten impact points. This result confirms the observations of Poole and Farmer (1980) and Sheorey *et al.* (1984) which show how the variability of individual readings levels off within the first five impacts. On the basis of this result, it was decided to retain the mean R values of the 6th and 7th measurement sessions.

Table 3.7: Independent Sample T-test to rest variability of means based on 5 impact points when compared with that based on 10 impact points (Source: Developed by Author)

Session No.	Test No.	Ras il-Fenek	Ponta tal-Miġnuna	Ponta tal-Munxar	Ponta tal-Qammieħ	Blata l-Bajda
8th measurement session	Test 1	0.743	0.957	0.709	0.918	0.851
	Test 2	0.696	0.959	0.665	0.930	0.889
9th measurement session	Test 1	1.000	0.817	0.794	0.768	0.883
	Test 2	0.984	0.834	0.813	0.793	0.871
10th measurement session	Test 1	0.962	1.000	0.697	0.967	0.519
	Test 2	0.960	0.991	0.706	0.953	0.503
11th measurement session	Test 1	0.933	0.875	0.560	0.863	0.937
	Test 2	0.924	0.858	0.555	0.882	0.969

3.5.1.6 Estimation of Unconfined Compression Strength (UCS) and Rock Density.

In the study of rock mechanics, rock hardness is perhaps the most frequently used index for indirect determination of unconfined compression strength (UCS). Over the past five decades, a number of empirical correlation coefficients (linear or curvilinear) have been proposed for various lithologies to establish rock hardness as a predictor of UCS. These coefficients have been reviewed and summarized by various authors (Goudie, 2006, 2013; Yagiz, 2009; Karaman and Kesimal, 2015; Yilmaz *et al.*, 2016). Correlation coefficients between R values and UCS for sedimentary rocks have been found to be wide ranging: from 0.77 by O'Rourke (1989) to 0.98 by Yilmaz and Sendir (2002). Such a variability is highly dependent on a number of factors such as the geological properties of the tested sedimentary samples, instrument's use (N type or L type) and its position (vertical or horizontal) and equations method (ex. adding other properties such as porosity and rock dry density) (Hebib, Belhai and Alloul, 2017).

Many of these hardness tests were tested on laboratory samples and, thus, various proponents still advice for caution on the use of these coefficients with *in situ* R values and to apply equation models which are rock specific (Yılmaz and Sendır, 2002; Fener *et al.*, 2005; Odediran and Mopa, 2014). In line with these recommendations, the UCS values presented here will be used as an approximate measure for the general descriptive statistics and the coefficient of Katz, Reches and Roegiers (2000) was chosen given that it was derived from testing on limestone lithology and based on N-type hammer. Apart from being considered a reasonable measure by various authors (such as by Odediran and Mopa, 2014), this equation model has also one of the highest correlation coefficients with UCS i.e. 0.96.

Katz, Reches and Roegiers (2000) also correlated R values to the density of the rocks. This formula was also chosen in the study of Maltese limestone boulders (Biolchi *et al.*, 2015; Causon Deguara and Gauci, 2017). In these

studies, the boulder density was associated to averaged HR value assigned to each block by means of Equation (3):

$$\rho = 1308.2\ln(HR)/2873.9$$

Equation 3

where ρ is the density unit expressed in kg m $^{-3}$ and HR stands for Hammer Rebound value.

The UCS and dry density values were included in the overall descriptive statistics of each transect (Table 5.5) and were calculated on the mean R value of each transect. Notwithstanding the existence of good to strong empirical relationships between R values and UCS, the notion explained by Day (1980) still holds a lot of relevance to this present study; in that, surface hardness, as measured by the hammer, may be a better measure of resistance to erosion rather than of bulk compressive strength. The statistical treatment of these two measures is only meant to provide some indicative measures of the Maltese limestone. These measures will be placed and discussed both within the local context of other tests done on Globigerina limestone and also in an international context where similar data were published for other limestone lithologies such as by Yagiz (2009), Karaman and Kesimal (2015) and Hebib, Belhai and Alloul (2017).

.

3.5.1.7 Statistical treatment: software used

All R values were inputted and normalised using Microsoft Excel® 2010. The descriptive statistics (mean, median, mode, range, minimum and maximum values, sample variance, standard deviation, sample variance, co-efficient of the variance, UCS, kurtosis and skewness) and graphs (frequency graphs, bar graphs and box plots) were produced with Excel Data Analysis add-on tool. Bulmer's skewness classification (Bulmer, 1979) was used to interpret the skewness level of the R value datasets (Section 5.4.3). The K-means clustering

and independent sample t-tests were performed with IBM SPSS Statistics 24® (Section 3.6).

3.5.2 Weathering Exposure Experiment with micro-catchment basins

3.5.2.1 Scope of the investigation

The aim of this exposure experiment was to monitor more closely the responses of limestone samples (extracted from each platform) to weathering, in order to both understand whether (and to what extent) their rates and modes of surface change may be influenced by weathering processes and record changes in quantified outcomes (See Table 3.3). Exposure trials have been successfully used in geomorphology to monitor rock surface change responses to micro-ambient conditions (Moses, 2000; Viles, 2005; Furlani and Cucchi, 2008) and recently even in heritage science such as the effect of the temple open shelters on Globigerina Limestone deterioration rates (Briones, 2015; Cabello-Briones and Viles, 2017). They aimed to monitor the response of stone samples to specific ambient conditions. The variability of the lithological responses to sub-aerial weathering may shed important indications about the geotechnical properties of rocks (Pinho *et al.*, 2006). There is as yet no standard protocol for such experiments and their design is mostly guided by the intended scope of the study.

In the light of numerous studies undertaken about the deterioration of LGL building block (Section 2.7), a freshly cut LGL block (sample no. 5), was included in the experiment for a comparison with the platforms rocks. This is the first time that such a comparative work was actually undertaken in comparing rates of deterioration between a cut slab and natural rock and also in using TMEM as a tool to measure rock surface change on such samples.

3.5.2.2 Experimental design and sampling strategy

The experimental design was made up of three parts:

i. Experiment A: qualitative assessment, based on ISRM (1981) classification of rock mass weathering, aimed to provide an additional evaluation of the geo-technical behaviour of the extracted samples (in LGLM and UGLM) in response to sub-aerial weathering and to classify the resultant effects;
ii. Experiment B: measurement of weight loss and debris loss in the micro-catchment in order to obtain a quantified measure of the altered weathered state of each slab as a mass; and
iii. Experiment C: measurement of the rates of surface change on the TMEM station on each slab, in order to obtain a comparative analysis with the rates measured *in situ.*

For Experiment A, in order to minimise the subjectivity in describing the state of weathering of rock materials as per (a), this study made use of the recommendations of Pinho *et al.* (2006) in using the ISRM (1981) classification system, known as Basic Geotechnical Description of Rock Masses (BGD) (Table 3.8). The authors considered this system, used worldwide, as an appropriate system offering a good standardized basis to characterise the effects of weathering and classify the degree of weathering according to a graded scale. This method is normally applied for assessment of rock mass weathering at field size scale. However, this method was considered appropriate enough to apply at smaller scales for the experimental slabs in order to ensure minimal bias in the assessment of weathering criteria. Sample discoloration and texture changes were assessed visually and the findings were presented in a descriptive, qualitative format (Section 5.5.1).

With reference to Experiment B, this study used a similar simple methodology based on exposure trials, micro-catchment and non-destructive analyses. Fifteen blocks were extracted from the surface of the platform sits (Table 3,9). The block dimensions ranged in thickness between 15-22 cm and had a surface area which ranged between 50 – 150 cm^2 (Figure 3.9). Their surface finish was natural weathered surface. They were exposed to inland sub-aerial conditions in order to monitor rock surface change away from the coastal

in situ conditions from where they were originally found. A sample was extracted from the front part and back part of each shore platform surface, close to the transects that were laid out for the TMEM site monitoring.

Table 3.8: Scale of rock mass weathering according to ISRM (1981)

Term	Grade	Description
Unweathered (fresh)	W1	Rock mass shows no loss of strength, discoloration or other effects due to weathering. There may be slight discoloration on major rock mass defect surfaces or on clasts.
Slightly Weathered	W2	The rock mass is not significantly weaker than when unweathered. Rock may be discoloured along defects, some of which may have been opened slightly.
Moderately Weathered	W3	The rock mass is significantly weaker than the fresh rock and part of the rock mass may have been changed to a soil. Rock material may be discoloured, and defect and clast surfaces will have a greater discolouration, which also penetrates slightly into the rock material. Increase in density of defects due to physical disintegration process such as slaking, stress relief, thermal expansion/ contraction and freeze/thaw.
Highly Weathered	W4	Most of the original rock mass strength is lost. Material is discoloured and more than half the mass is changed to a soil by chemical decomposition or disintegration (increase in density of defects/fractures). Decomposition adjacent to defects and at the surface of clasts penetrates deeply into the rock material. Lithorelicts or corestones of unweathered or slightly weathered rock may be present.
Completely Weathered	W5	Original rock strength is lost and the rock mass changed to a soil either by chemical decomposition (with some rock fabric preserved) or by physical disintegration.

The following experimental procedures were undertaken:

i. Measurement of samples' dry weight in January 2015 (pre-exposure), July 2015 and July 2016;
ii. Measurement of dry weight of sediment loss from these samples in July 2015 and July 2016;
iii. TMEM monitoring over a period of four measurement sessions, starting from January 2015 to July 2016. A total of 27 TMEM stations were installed on these samples (Table 3.10); and
iv. Mineralogy tests of samples after exposure with NIR (See Section 3.5.3).

For procedures [i] and [ii], each sample was left to dry at room temperature for 48 hours before exposure to sub-aerial inland conditions. This method was preferred than oven drying at higher temperatures in order not to alter the mineral composition of the samples, as inherited from the platform coastal environment, The dry weight and its resultant debris losses were subsequently measured on a Silvercrest® digital scales (Figure 3.10a). In order to collect the sub-aerial debris loss each sample was placed on a stainless steel grid and the grid was then placed on top of a deep plastic container basin, which acted as a catchment basin for the sediment (Figure 3.10b and c).

With regard to experiment C, as shown in Table 3.10, 27 TMEM stations were installed on the 16 rock samples (Figure 3.10d). The freshly-cut block in Lower Globigerina Limestone was also added to the group of tests in order to facilitate comparison of erosion behaviour between natural rock surfaces and a freshly cut one. Nine rock samples had more than one TMEM station installed. Rocks with two TMEM stations had the rock surface area sub-divided into a Left and a Right (Figure 3.a) area whilst measurements on rocks with three stations were subdivided into a 'Left', 'Centre' and 'Right' areas (Figure 3b). Data collection procedures for TMEM measurements of rock surface heights were the same as the ones adopted for shore platform TMEM stations (See Section 3.4.2).

Table 3.9: Details of experimental slabs extracted from each shore platform site according to platform position and transect (Source: Developed by Author)

Sample No.	Shore platform site	Platform Position	Transect No.	No. of TMEM stations
1	Blata l-Bajda	Front	1	2
2	Ponta tal-Qammieħ	Front	1	3
3	Ponta tal-Miġnuna	Back	2	1
4	Ponta tal-Munxar	Back	2	1
5	Globigerina Block Sample	N/A	n/a	2
6	Ras il-Fenek	Front	1	1
7	Ponta tal-Munxar	Back	1	2
8	Ponta tal-Munxar	Front	2	2
9	Blata l-Bajda	Front	1	2
10	Ras il-Fenek	Back	2	2
11	Ponta tal-Miġnuna	Back	2	1
12	Blata l-Bajda	Back	1	3
13	Ponta tal-Miġnuna	Front	1	2
14	Ras il-Fenek	Front	1	1
15	Ponta tal-Qammieħ	Back	1	1
16	Ponta tal-Qammieħ	Front	1	1

Table 3.10: Details of total number of rock samples extracted from each shore platform site and total number of TMEM stations per platform site (Source: Developed by Author)

Name of shore platform site	Localion	No. of samples	No. of TMEM stations
Blata l-Bajda	Selmun	3	7
Ponta tal-Miġnuna	St Thomas Bay	3	4
Ponta tal-Munxar	St Thomas Bay	3	5
Ponta tal-Qammieħ	Marfa Ridge	3	5
Ras il-Fenek	Marsaxlokk	3	4
Globigerina Block Sample	N/A	1	2
Total no. of samples		16	27

Figure 3.9: Sixteen experimental slabs prepared with TMEM stations to measure surface rock erosion by sub-aerial weathering (Source: Photos taken by Author)

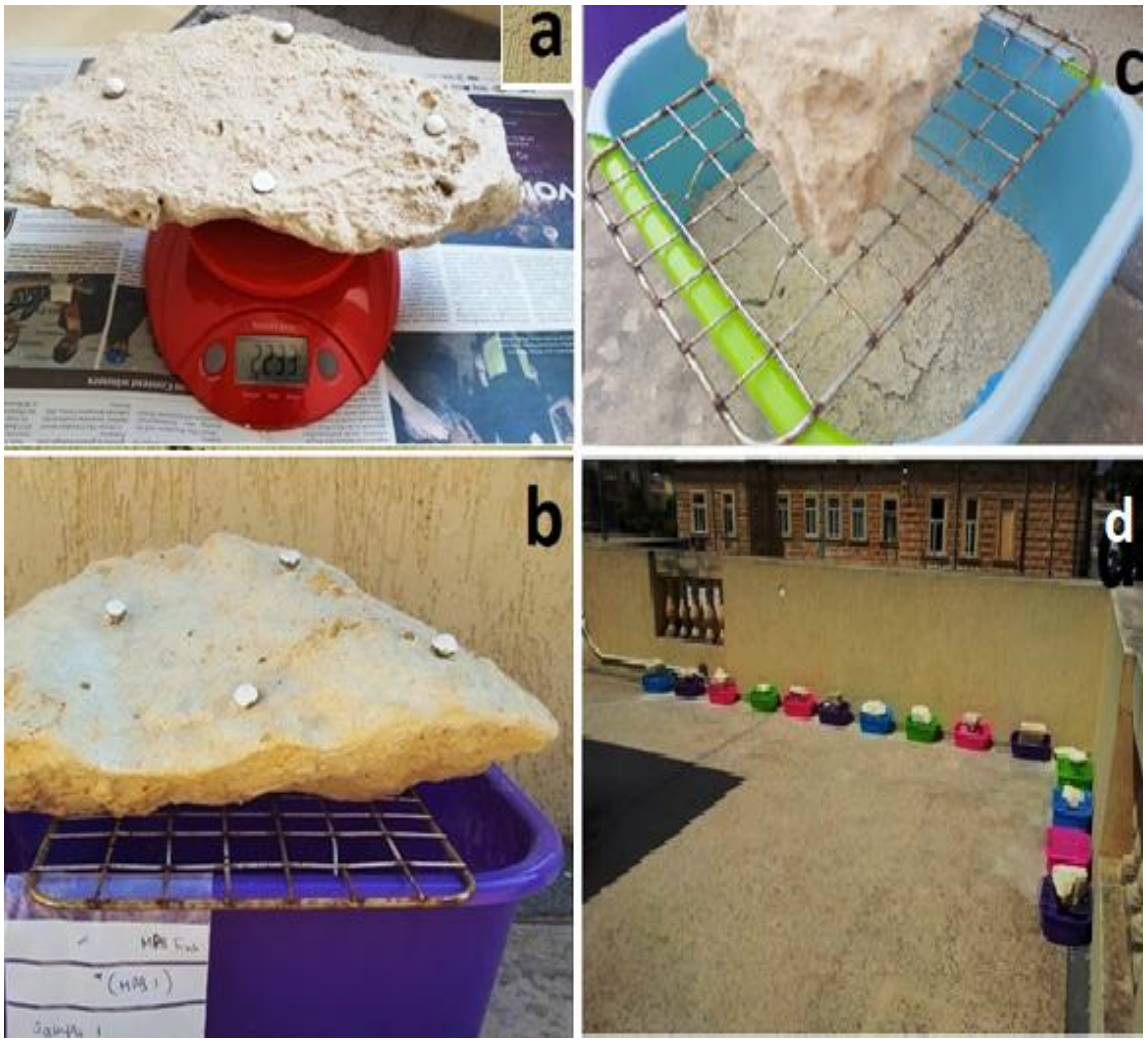

Figure 3.10: a. Dry measurement of experimental slab b. Close up of entrapment basin with steel wire mesh underneath experimental slab and sample collected for NIR tests; c. Debris fall out inside one of the microcathment basin; d. Layout of experimental slabs outdoors (Source: Photos taken by Author).

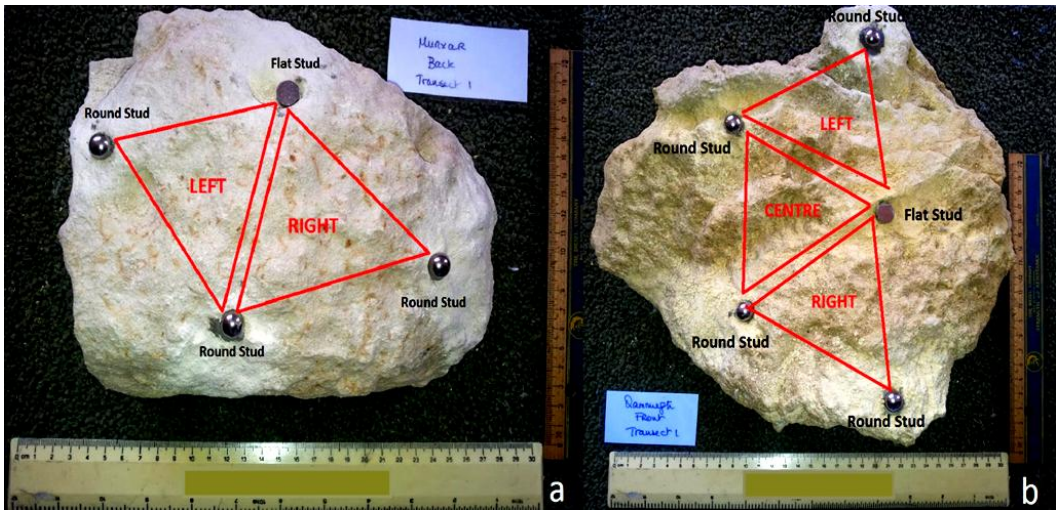

Figure 3.11: a Left and Right measurement areas on Ponta tal-Munxar experimental slab (Back position, Transect 1, Sample No. 7); b. Left, Centre and Right measurement areas for Ponta tal-Qammieħ (Front position, Transect 1, Sample No. 2) (Source: Photos taken and modified by Author)

3.5.3 Mineralogy test: Near Infrared spectroscopy (NIR)

3.5.3.1 Scope of investigation

It is well known that, although limestone is composed mainly of calcite, it may show significant variations in minor mineral composition and texture, resulting in a complex and contrasting weathering behaviour (Kramar *et al.*, 2010). The aim of this investigation was to identify the mineralogical properties of the platform surface in order to determine to what extent they may influence rates and modes of rock surface change. This investigation aimed to address hypothesis no. 4 in determining whether mineralogical composition may affect patterns of surface change (Table 3.3).

3.5.3.2 Theoretical Background

Spectroscopy is described as the study of light as a function of wavelength that has been emitted, reflected or scattered from a solid, liquid, or gas (Reich, 2005). As photons enter a mineral, some are reflected from grain

surfaces, some pass through the grain, and some are absorbed. Those photons that are reflected from grain surfaces or refracted through a particle are said to be scattered. Scattered photons may encounter another grain or be scattered away from the surface so they may be detected and measured. Photons may also originate from a surface, a process called emission. All natural surfaces emit photons when they are above absolute zero. Emitted photons are subject to the same physical laws of reflection, refraction, and absorption to which incident photons are bound.

There are four general parameters that describe the capability of a spectrometer: 1. spectral range, 2. spectral bandwidth, 3. spectral sampling and 4. signal-to-noise ratio (S/N). Spectral range is important to cover enough diagnostic spectral absorption to solve a desired problem. There are general spectral ranges that are in common use, each to first order controlled by detector technology: a) ultraviolet (UV): 0.001 to 0.4microns, b) visible: 0.4 to 0.7microns, c) near-infrared (NIR): 0.7 to 3.0microns, d) the mid-infrared (MIR): 3.0 to 30 microns, and d) the far infrared (FIR): 30microns to 1 mm.

NIR spectroscopy, predicts different minerals present in the sample as a function of their near infrared (NIR) diffuse reflectance spectra. The variety of absorption processes and their wavelength dependence allows deriving information about the chemistry of a mineral from its reflected or emitted light. In the field of rock mechanics, its overall objective is to probe a rock sample in order to acquire qualitative information coming from the interaction of near-infrared electromagnetic waves with its constituents. Accordingly, the energy of the spectrum is reduced thereby generating an absorption spectrum whose position in the spectra region indicates the type of bonds and in many cases the minerals associated with them. The non-destructive reflection spectroscopy has been utilized to identify all common clay minerals as well as sulfates, hydroxides and carbonates (Viscarra Rossel *et al.*, 2009) .

Clark (1999) outline various advantages in the use of NIR spectroscopic analyses for mineralogy tests: it is sensitive to specific chemical bonds in materials and unlike some diagnostic methods, like X-ray diffraction it is

sensitive to both crystalline and amorphous materials. In terms of laboratory procedures, it is fast (one minute or less per sample), non-destructive, non-invasive, suitable for in-line use, nearly universal application and requires minimum sample preparation demands. He also mentions some of its well-known disadvantages. It is considered too sensitive to small changes in the chemistry and/or structure of a material and thus, variations in material composition may often causes shifts in the position and shape of absorption bands in the spectrum. Thus, with the vast variety of chemistry typically encountered in the real world, spectral signatures can be quite complex and sometimes unintelligible or misinterpret. The latter problem, however, is slowly being resolved with increased knowledge of the natural variation in spectral features.

By comparison to other rock types, limestones have received little attention by researchers in spectral techniques. As with other carbonate rocks, limestones tend to be composites of grains (typically sand, silt, calcite or shell fragments), within a carbonate cement. The presence of even a small amount of clay or iron in the cement can mask the spectral signature of other minerals. This makes the isolation of prominent or specific features difficult, especially if the tested rock type is homogeneous in colour (Stoner and Baumgardner 1981).

The primary spectral features of carbonate rocks, including limestones are thought to be the result of clay minerals held within the sedimentary matrix (Hunt and Salisbury, 1976). They attributed absorption features at 400, 430, 450, 510, 550, 700, 870, and 1000 nm to these clays within carbonates. Hunt and Salisbury (1971) also identified 7 sharp asymmetrical absorption features between 1735 and 2600 nm which they attributed to the presence of carbonate minerals, though none are diagnostic. It has been suggested that the amount of carbonate or calcite can be related to bands around 1800, 2330, 2350 and 2360 nm (Ben-Dor and Banin 1990, Hunt and Salisbury, 1971), although these wavelengths also coincide with other minerals and hence are not diagnostic.

3.5.3.3 Description of the field investigation

The mineral composition of both the platform surfaces and the weathered blocks from the exposure experiment were investigated. A total of 47 samples – corresponding to 31 intact (non-powdered) samples from *in situ* (in the vicinity of the TMEM stations) and another 16 intact samples from the outdoor experimental slabs – were extracted in July 2016 for NIR tests (Figure 3.12). The samples were scraped platform surface and ranged in size between 50-100g. Spectrum plots for individual sample were generated to facilitate quantitative analysis of the rock mineralogy properties and provide stronger discussion in relation to the rock surface change data generated by the TMEM.

3.5.3.4 Lab procedures (NIR)

All samples were dried at 40^0 C for 48 hours before testing using the ASD Labspec5000 with a 5 mm fore-optic. For the spectral tests, 40^0 C is used as primary drying temperature so as to drive off water, without damaging any clay or salt crystals that might be present (Pers. Comm. A. Gibson, 18/06/2018). Analyses have been carried out using The Spectral Geologist Core® (TSG) v. 7.0. As displayed in Table 3.13, rock sample data were labelled according to 'scalars' – columns against which measurements can be attributed. This allows data to be sorted according to attributes in each scalar. These scalar data are presented as part of the findings in Chapter 5 (Section 5.3).

Figure 3.12: a. Extraction of sample from the platform surfaces ; b. Field tools used for the extraction: GPS, two geological chisels, and sample plastic bags; c. An example of a packed sample extracted from *in situ* close to MRF Station 1b, Ras il-Fenek (Source: Photos by Author)

Table 3.11: Labelling procedure for samples (Source: Labelling by A. Gibson; Compiled by Author)

Scalar	Classes Used
Site	MPQ = Malta Ponta tal-Qammieħ MPB = Malta Blata l-Bajda MPM = Malta Ponta tal-Miġnuna MMX = Malta Ponta tal-Munxar MRF = Malta Ras il-Fenek
Location	1 – Frontshore, Transect 1 2= Middleshore, Transect 1 3= Backshore, Transect 1 4= Frontshore, Transect 2 5= Middleshore, Transect 2 6= Backshore, Transect
Material	Limestone, conglomerate, fired sample
Surface	Fresh
Colour	Light, darker, phosphatic grey, algal

The mineralogical dataset at this stage used pre-defined standard attribution tables, which are in-built in the TSG software to provide information about the spectral signatures of each mineral type and mineral group. Though these standard mineralogy signatures are not calibrated to the Malta samples, they still offer a good indication of the minerals present in the samples. The initial output from the software would be spectral curve graph lines, each with their corresponding wavelengths, shapes, and strengths and which are the keys to understand the mineralogical properties of the tested samples. As seen in Figure 3.13, spectral lines are well-defined (in wavelength) wavelength/frequency regions in the spectrum in which excess photon energy appears as emission lines and missing where photon as absorption lines. Each spectral curve is analysed using a range of curve-fitting algorithms stored in the TSG software, in order to match each sample to a pre-defined library spectra of mineralogical properties. Rather than provide a quantitative assessment, the TSG software provided an index which indicates what proportion of the target

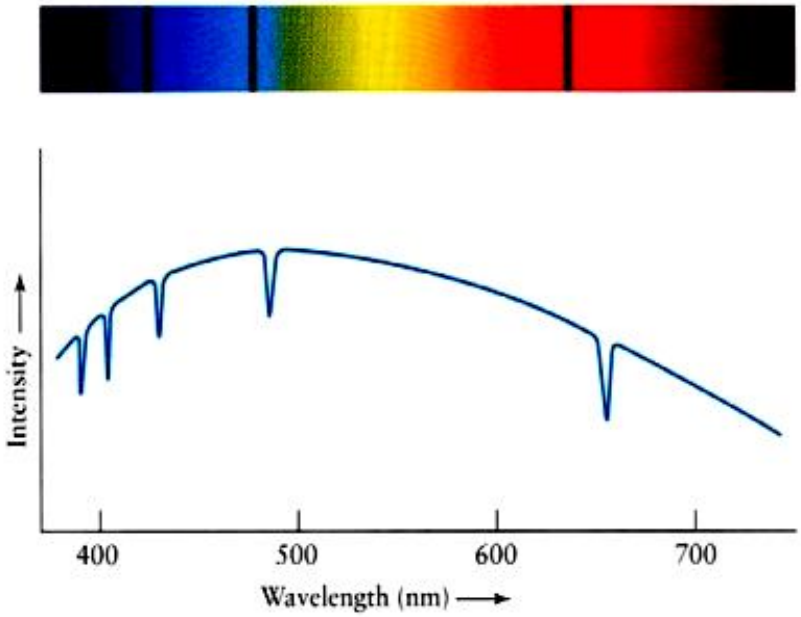

Figure 3.13: A simplified example of a typical spectral signature as a graph (below) and as a recorded spectrum (top) (Source: Screenshot by Author, 2017).

signature is likely to be composed of, after matching it with the closest available library spectra signature.

The digital spectra of seven samples were then re-checked using XRD technique. The samples were oven dried at 50^0 C for 24 hours before being ground using a planetary grinding mill with an agate container. The temperature requirement for XRD test is slightly higher than that for NIR tests. XRD preparation follows a different protocol as it is a destructive test and samples are not retained or re-used (Pers. Comm. A. Gibson, 19/6/2018). Samples were ground to less than 5□m. Samples were subsequently pressed into circular sample holders and tested using a PANalytical XPert3 Powder XRD fitted with a copper tube. Samples were tested on 6th June 2017 at a high resolution with each scan lasting around 45 minutes. Data was collected using PANalytical DataCollector software and exported as .csv files. Analyses of results were carried out using PANalytical Highscore Plus (V4). The software was used to automatically compare sample results to an extensive mineralogical

database that identifies similarities between peaks in the measured trace and those of known samples. Results were then interpreted manually by operator selection of matches - a decision based upon an index score for similarity, visual interpretation of peak matches and knowledge of the mineralogical context of samples.

Ambiguous spectral signatures were then further corroborated with X-ray powder diffraction (XRD). As a technique, XRD is widely used in the study of crystalline structures and to identify unknown crystalline materials such as minerals, which is a critical component to studies in geology (Bunaciu, Udriştioiu and Aboul-Enein, 2015). As a technique, it is known to provide less unambiguous mineral determination and the results produced are relatively straightforward to interpret. Samples close to MPQ5, MPM3, MPB1, MMX3, MMX2 and MPB4 were selected for XRD Tests. An additional sample with black crust coating was extracted from a limestone building facade from Pembroke (Malta), and used as a comparative sample in view of the various literature about the formation of gypsum crust on Mediterranean limestone (Gomez-Heras *et al.*, 2008; Fronteau *et al.*, 2010; Smith *et al.*, 2010).

3.5.4 Weather data collection

The description of the general climate conditions is presented in this section and based on the official weather data source provided by the National Meteorological Office in Malta International Airport plc in Luqa. Apart from giving a background context of the climate conditions experienced during the study period, these data highlight whether these conditions experienced during the study period followed the typical trends of a Mediterranean climate and, if not, what sort of climate anomalies were recorded by the national authority. Monthly weather data was collected for the year 2012-2016 to provide the background to climate trends present on the Maltese Islands during the study period. The weather trends collected were as follows:

i. Mean Maximum and Minimum Temperature
ii. Lowest and Highest Maximum Temperature
iii. Lowest and Highest Minimum Temperature

iv. Atmospheric pressure
v. Humidity
vi. Total rainfall
vii. No of rainy days
viii. Mean wind force.

3.6 Data Compilation and Presentation

This part of the research involved the presentation and analyses - in descriptive and inferential format - of the field and laboratory results as follows:

i. geomorphological mapping of the platforms;
ii. the micro-topographic height data from the TMEM;
iii. weathering data from exposure experiments;
iv. Schmidt Hammer rebound (R) values; and
v. Near-infrared spectroscopy (NIR) laboratory tests.

Field data results were compiled as follows:

i. Maps: Field data for geomorphological mapping was compiled using Adobe Illustrator; and
ii. Table formats, line graphs, bar graphs, box plots and frequency graphs: Microsoft Excel was used to compile and present data related to micro-topographic height data measured with TMEM, Schmidt Hammer R values, exposure experiment, erosion and weathering forms, weather information and all inferential results.

All the data was presented and discussed from Chapter 4 to 7 as part of the study findings.

3.6.1.1 Descriptive and Inferential Analyses

The results were subsequently analysed with statistical inferences using SPSS Version 23 and presented in table formats. The core of the analyses was rock surface change – as measured by the TMEM – in order to quantify rates of

rock surface change and determine to what extent these rates vary spatially and temporally Table 3.3. The analyses of the remaining investigated themes served to inject further information about how the observed rock surface change may be influenced by lithological properties and morphology.

Three spatial dimensions were explored in these analyses of the TMEM data as follows:

i. Differences between the twenty-two measuring points within one TMEM station;
ii. Differences between the TMEM stations within the same shore platform in a cross-shore direction (front, middle and back stations); and
iii. Differences between one platform and another (Table 3.12).

Several temporal periods were also investigated on site and in the exposure experiment. These are described as follows:

i. TMEM:
    a. The study period comprised 14 measurement sessions from which a 12 individual time periods (3-4 months) were analysed (Table 3.13);
    b. Annual time periods: in total, 182 annual periods were examined i.e. 34 for Blata il-Bajda, 35 for Ponta tal-Miġnuna, 42 for Ponta tal-Qammieħ, 33 for Ponta tal-Munxar and 38 for Ras il-Fenek. The results are presented in Chapter 6, Table 6.14;
    c. Semi-annual time periods: in total, 241 time periods were examined i.e. 43 for Blata il-Bajda, 51 for Ponta tal-Miġnuna, 51 for Ponta tal-Qammieħ, 45 for Ponta tal-Munxar and 51 for Ras il-Fenek. They were labelled as A2 to I2. The results are presented in Chapter 6, Table 6.15;
    d. Individual time periods (3-4 months): a total of 292 periods were examined across the five stations as follows: 55 at Blata l-Bajda, 59 at Ponta tal-Miġnuna, 60 at Ponta tal-Qammieħ, 56 at Ponta tal-Munxar and 61 at Ras il-Fenek; the range of three to four months was due to bad weather and/or inability to access sites in

the right weather conditions). The results are presented in Chapter 6, Table 6.16.

Table 3.12: Description of the spatial framework used for the statistical analyses of the TMEM stations

Platform Site	TMEM Station Code	Transect Position	Front	Middle	Back
Ponta tal-Qammieh	MPQ	Transect 1	MPQ1	MPQ2	MPQ3
		Transect 2	MPQ4	MPQ5	MPQ6
Ponta tal-Munxar	MMX	Transect 1	MMX1a		MMX2
			MMX1b		
		Transect 2	MMX3a		MMX4
			MMX3a		
			MMX3c		
		Transect 3	MMX5a		MMX6
			MMX5b		
Blata il-Bajda	MBB	Transect 1	MBB1a	MBB2	MBB3
			MBB1b		
		Transect 2	MBB 4	MBB 5	MBB6a
					MBB6b
Ponta tal-Mignuna	MPM	Transect 1	MPM1	MPM2a	MPM3a
				MPM2b	MPM3b
		Transect 2	MPM4	MPM5	MPM6a
					MPM6b
Ras il-Fenek	MRF	Transect 1	MRF1a	MRF2a	MRF3
			MRF1b	MRF2b	
		Transect 2	MRF4	MRF5	MRF6

ii. Exposure Experiment:
   a. Total exposure period of the exposure experiment, which was calculated from pre-exposure period (February 2015) to 3rd exposure period (August 2016); and
   b. Individual exposure period: two exposure periods were measured: a first one of six months (Feb-Aug 2015) and a second one of one year (Aug 2015-Aug 2016).

Table 3.14 illustrates the analyses framework of this study according the each investigated theme and its relevant hypothesis testing. Kolmogorov-Smirnoff (KS) tests were undertaken in order to check normality of data distribution before conducting the correlation and analyses of variance tests. Most of the TMEM data resulted having a non-normal distribution and this was to be expected. As well-argued by Robinson (1976) in his review about statistical analysis of TMEM data, coastal erosion rates are high variable in magnitude and susceptible to sporadic events. As a result, he argues that rates will have a markedly skewed distribution and thus normal distribution is rarely achieved. Robinson (1976), in fact, recommended non-parametric tests for TMEM data analyses, such as Mann Whitney-U tests and Kruskall-Wallis H tests for the analyses of variance between two or more independent samples. KS tests were performed for the rest of the investigated themes as well and parametric methods, as indicated in Table 3.14 were only used when KS Test confirmed normal distribution.

Table 3.13: Description of single measurement sessions paired into time periods to represent individual, semi-annual and annual time periods. Period labels were given to semi-annual and annual time periods to simplify reference to them in the inferential tests. Cells in grey shading indicate annual time frames according to the start of study period i.e. from April-May 2012.

Individual Time periods	Semi-annual time periods		Annual time periods	
(3-4 months)	(6 months)	Period Label	(12 months)	Period Label
2_1	4_2	A2	5_1	A
5_4	6_4	B2	6_2	B
6_5	7_5	C1	8_4	C
7_6	8_6	C2	9_5	D
8_7	9_7	D2	10_6	E
9_8	10_8	E2	11_7	F
10_9	11_9	F2	12_8	G
11_10	12_10	G2	13_9	H
12_11	13_11	H2	14_10	I
13_12	14_12	I2		
14_13				

Table 3.14: Choice of inferential tests according to the investigated theme and tested null hypotheses (Source: Developed by Author)

Theme of Investigation	Null Hypotheses Tested	Inferential Test	No of Tests done
Rock hardness of platform surface	There are no differences in the statistical properties of surface hardness between platforms	K-means clustering method	3
	There are no differences in the percentage distribution of R values classes between platforms		3
	There are no differences in the percentage distribution of R values classes between TMEM stations		3
	There are no differences in rock surface hardness on platforms between summer and winter	Independent Sample T-test*	20
	There are no differences in rock surface hardness on platforms differs between the front and back sections		1
Exposure experiment	Percentage loss of weight does not correspond with amount of debris loss	Spearman Rank**	1
	There are no differences in the percentage loss of weight between the frontshore and the backshore samples	Independent Sample T-test*	1
	There are no differences in rates of surface change between individual exposure periods	Mann Whitney U-Test	46
	There are no differences in the rates of surface change across all stations for each exposure period	Kruskal Wallis H Test	4
	There are no differences in rate of surface change across annual exposure periods between front and back samples		2
	There are no differences in mean rates of surface change across individual exposure periods between front and back of platform samples		4
	There are no differences in the rates of surface change on each station between each individual exposure period		17
Spatial patterns of surface change	There are no differences in annual rates between the front, middle and back of each platform	Kruskal Wallis H Test	40
	There are no differences in individual period rates between front, middle and back sections of each platform		55
	There are no differences in the individual period rates between front and middle sections of each platform	Mann Whitney U-Test	72
	There are no differences in the individual period rates between front and back sections of each platform		98
	There are no differences in the individual period rates between middle and back sections of each platform		77

Theme of Investigation	Null Hypotheses Tested	Inferential Test	No of Tests done
Temporal patterns of surface change	There are no differences in paired comparisons of annual rates on each platform	Mann Whitney U-Test	504
	There are no differences in paired comparisons of semi-annual rates on each platform		824
	There are no differences in paired comparisons between annual and semi-annual rates on each platform		1464
	There are no differences in paired comparisons between individual measurement periods on each platform		1151
	There are no differences between all individual time periods for each station		36
	There is no correlation between seasonal change and rates of surface change	Spearman Rank**	58
Spatio-temporal patterns of surface change	There are no differences in individual time period rates between front, middle and back stations across all platforms	Kruskal Wallis H Test	12
	There are no differences in individual time period rates between all front stations across all platforms		12
	There are no differences in individual time period rates between all middle stations across all platforms		12
	There are no differences in individual time period rates between all back stations across all platforms		12
TOTAL			**4532**

** KS test showed normal distribution of data*

*** KS Test showed non-normal distribution of data*

Figure 3.14 illustrates the statistical framework used to analyse the datasets and produce a clear data narrative about the rates of surface change at each site within the context of different temporal and spatial contexts. Every single dataset with *p* value results were categorised into percentage distributions of *p* values having H_0 acceptance, H_1 acceptance and no pattern. If the tested data set results with 50% of *p* values that accept H_0 and 50% that reject H_0, then it is no certain that there is any pattern in the analyses can be inferred.

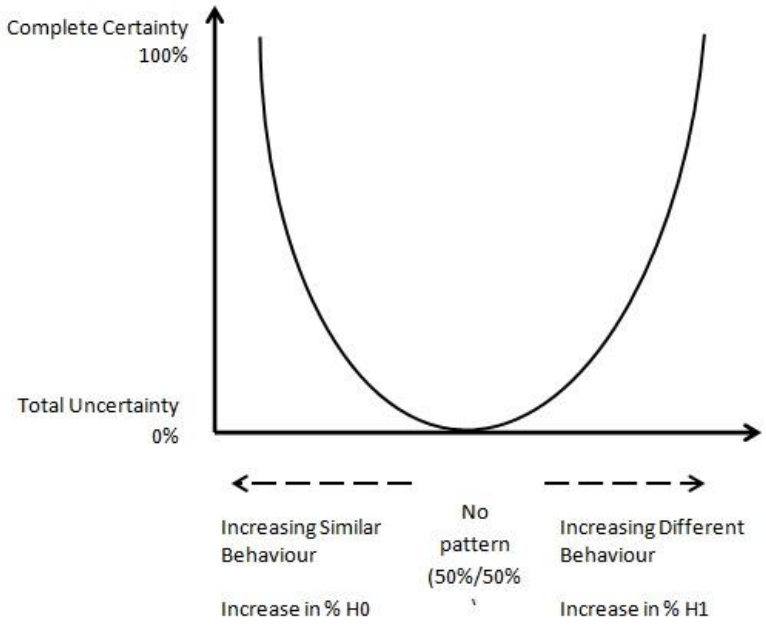

Figure 3.14: Illustration of relationship between degree of certainty or belief in a general pattern and the percentage of statistical tests that accept null hypothesis (Source: Developed for this study by R. Inkpen)

If the statistical comparisons produce 60% accept H_0 and 40% reject H_0, there is an increasing certainty that there is a pattern in the surface-change behaviour of the sites and that is one of increasingly similar or the same behaviour. As the % acceptance of H_0 increases, so does the certainty or belief, heading towards complete certainty, that sites are showing similar or the same behaviour in terms of their surface change. Likewise, as the % of rejections of H_0 increases beyond 50% toward more H_1 acceptance, then there is increasing certainty that the sites are showing increasing different behaviour in their erosion rates.

This idea is further illustrated in Table 3.15 as a hypothetical example. Multiple tests between individual time periods are being compared between the front and middle stations on four platforms. The 50% threshold was used in order to quantify any deviation from that threshold in terms of H_0 rejection and thus imply a consistent presence or absence of a pattern. For platform A, only a

maximum of 25% of the statistical tests have outcomes that accept the null hypothesis, suggesting that there is likely to be statistically significant differences in rates of surface change in most time periods between the front and middle stations of the platform. For platform D, over 76% of the statistical tests have outcomes where the null hypothesis is accepted implying that it is likely that there are few, if any, time periods for which the rates of surface change are statistically significant different between the front and middle stations on this platform. For both platforms A and D, a general pattern of behaviour for rates of surface change can be inferred from summarizing the statistical test outcomes. For platform B the outcomes of the statistical tests suggest that there may be a tendency for rates of surface change to be statistically different between time periods but that this pattern is not as strong as for platform A. For platform C there is no certainty that any general pattern can be discerned from the statistically tests as the outcomes are as likely to accept as to reject the null hypothesis.

Table 3.15: An example of visualization of multiple comparative statistical tests between time periods of rates of surface change

Name of Platform	TMEM Stations	Percentage of *p* values accepting H_0				
	Front vs Middle	0-25%	26-49%	50%	51-75%	76-100%
A	A1 vs A2					
	A4 vs A5					
B	B1 vs B2					
	B4 vs B5					
C	C1 vs C2					
	C4 vs C5					
D	D1 vs D2					
	D4 vs D5					

When interpreting these figures the arbitrary nature of the divisions need to be borne in mind. It was felt, however, that given the number of statistical tests run and the need to initially discern general patterns the choice of the 25% boundaries was felt to provide divisions magnitude useful in distinguishing

general patterns of behaviour in relation to the acceptance of the null hypothesis. The initial impressions were always supplemented by a more detailed and nuance analysis of the nature of these general trends.

3.6.1.2 NIR data analyses

Samples were sorted according to site and the combined spectral signatures were considered to determine the 'bulk' mineral components at each site using the 'Overview Assemblage Histogram' tool. This can be observed at two levels: group level or mineral level (Figure 3.15). Without calibration it is appropriate to consider the group level graph, which is presented as Figure 5.8 in Chapter 5. The software does provide percentage figures which indicate which mineral groups make up the spectral signature of that site. This is a useful measure which indicates which minerals and mineral groups are present at each site.

The results of these percentage groups are presented as Table 5.1 in Chapter 5. On the other hand, the mineral groups do have to be considered with some manual intervention, with specific mineral names indicated by pre-defined library spectra and which thus would require some interpretation within the context of which minerals are likely to be present at site. The percentages of the mineral group are presented in Chapter 5 as Table 5.2. Two spectra images – one for the platforms sites and one for the roof samples, are presented in findings of Chapter 5. These spectra images, displayed as long strips with varying colour and dark or light vertical "lines" represent the spectrometer output in terms of spread the light into its component wavelengths.

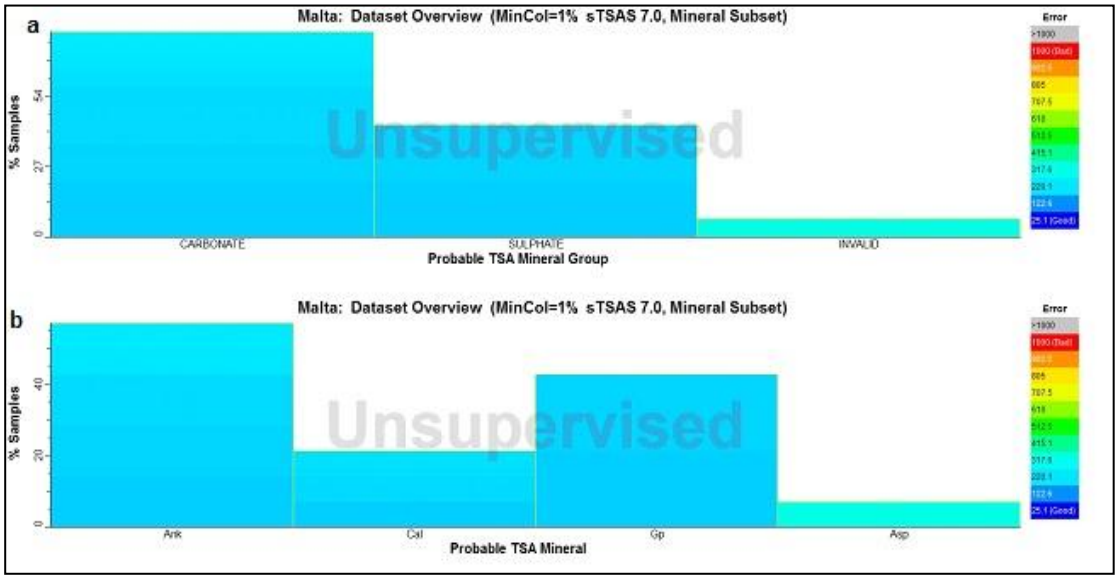

Figure 3.15: a. Overview assemblage histogram of a MRF platform sample – Group Level; b. Overview assemblage histogram – Mineral Level of an MRF platform sample

4 Field investigation of surface morphology

4.1 Introduction

This chapter aims to provide a more detailed geomorphological assessment of the physical setting of the studied platforms in terms of site and situation, their litho-stratigraphy and structure, presence of weathering and erosion forms. It aims to demonstrate how the five studied platforms exhibit a wide range of geomorphological characteristics, despite being broadly classified within the same lithostratigraphy i.e. Globigerina Limestone. The results of the detailed field assessment indicate that rock structure and resistance are both important site-specific determinants of platform morphology at a variety of scales and provided a better landform context against which the quantified rates surface change across each platform may eventually be related to. It has helped to elicit stronger comparisons and assimilations about the physical mechanisms of surface change operating on the five studied platforms.

The following sections give an overview of the Maltese limestone stratigraphy (Section 4.3) and describe the results of the field investigations described above (Section 4.4-4.6). Details of site, situation and access to each platform are also presented beforehand in order to convey the locational characteristics of each site, especially in relation to the islands' structural setting. As previously explained in Chapter 3 (Section 3.2.1), access to site was an important choice criterion in terms of site selection process and fieldwork logistics. Hence, details related to type and levels of access to each platform are also provided.

4.2 Maltese limestone stratigraphy: a brief overview

The Maltese Islands are an archipelago of three main islands (Malta, Gozo and Comino) and are located in Central Mediterranean (Figure 4.1). The exposed lithostratigraphy of the Maltese Islands is almost entirely built from late Oligocene to late Miocene marine sedimentary rock which formed in shallow seawaters (0–150 m) on a stable near-horizontal platform. Most of the widespread outcrops belong to the Miocene age (Carbone *et al.*, 1987) (Table 4.1).

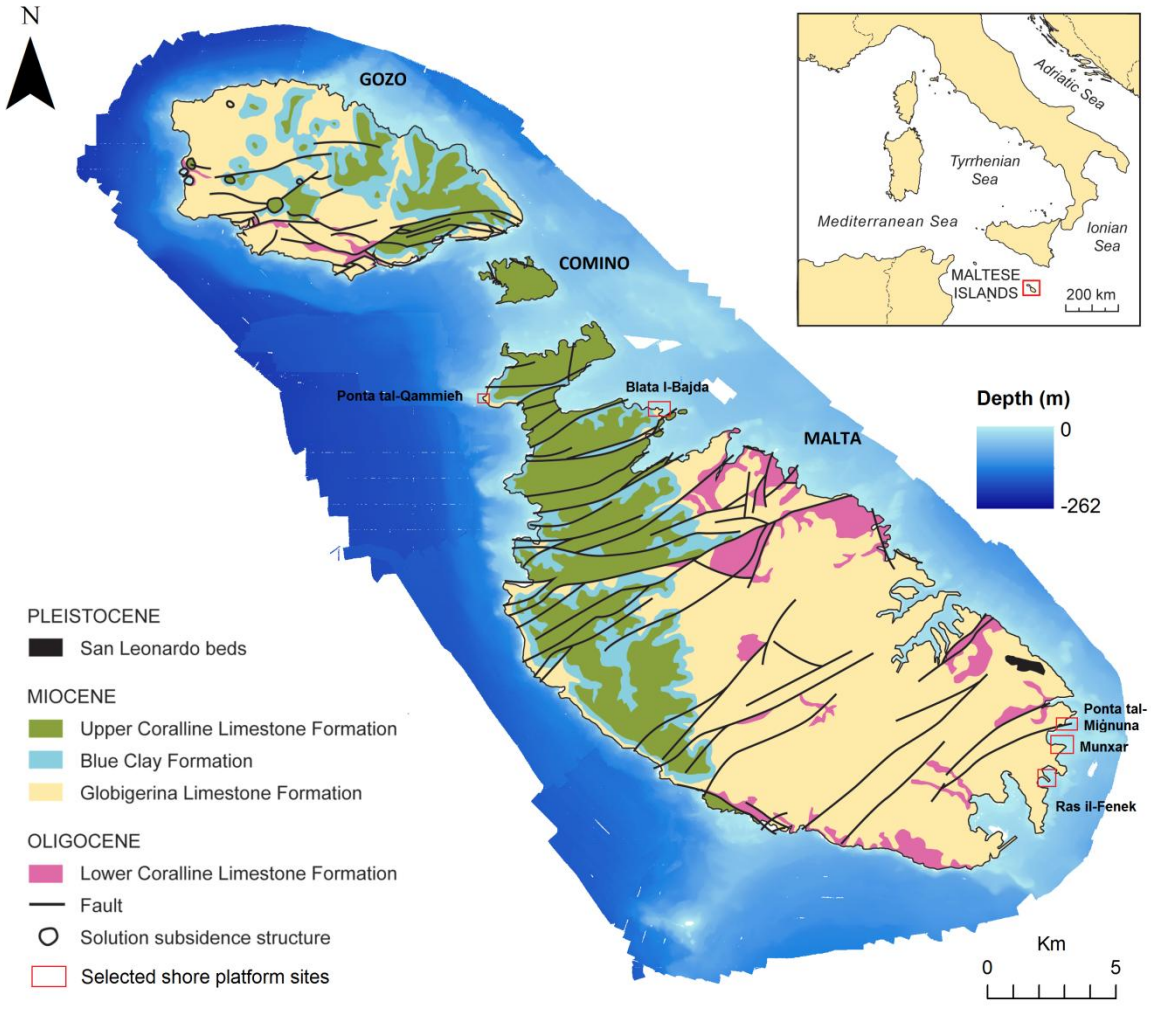

Figure 4.1: The Maltese Islands' geology and bathymetry, with labelled inserts indicating location of selected shore platform sites. (Source: Geological map redrawn from Pedley, 1993; Bathymetric map from ERDF LIDAR data, 2012)

Table 4.1: Description of exposed limestone stratigraphy of the Maltese Islands and main sub-divisions of the Globigerina Liméstone

(Source: Compiled by Author from Pedley *et al.,* 1978, 1992; Alexander, 1988; Cassar 2002).

Epoch	Stage	Years	Formation	Member	Member Thickness	Main sub-divisions of the Globigerina Limestone
		BP Mya			(m)	(Rehfeld and Jansseen, 1995)
Late Oligocene	Chattian	>23	Lower Coralline Limestone	Maghlaq	>38	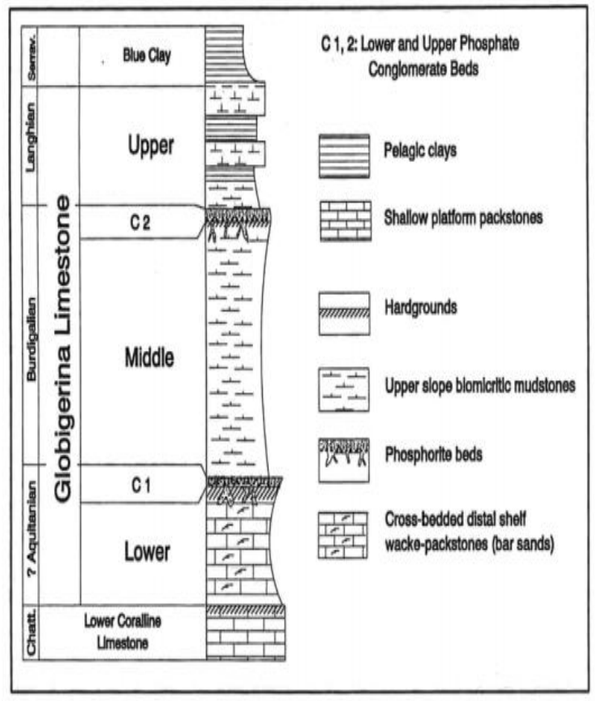
	Chattian			Attard	10-15	
	Chattian			Xlendi	0-22	
	Chattian			Il-Mara	0-20	
Late Oligocene	Chattian	23-20	Globigerina Limestone	Lower Globigerina Limestone	0-80	
				Lower Main Conglomerate (C_1)	0.1-0.4	
Late Oligocene-Early Miocene	Late Chattian-Late Burdgalian	20-15		Middle Globigerina Limestone	15-38	
				Upper Main Conglomerate (C_2)	0.1-0.3	
Middle-Late Miocene	Late Burdigalian-Langhian	15-13		Upper Globigerina Limestone	8-26	
Late Miocene	Serravallian-Early Tortonian	13-12.1	Blue Clay		15-75	
	Middle-Late Tortonian	13-11.5	Greensand	Gelmus	0-11	
Late Miocene	Late Tortonian	12-7.5	Upper Coralline Limestone	Ghajn Melel	0-13	
	Late Tortonian			Mtarfa	12-16	
	Late Tortonian			Tal-Pitkal	30-50	
	Early Messinian			Gebel Imbark	4-25	
Pleistocene	Calabrian	>2.5	Quaternary deposits	San Leonardo Beds.	0-10	
				Valley fills	0-7	
				Raised Beach deposits	0-3	
				Tufa and Travertine Deposits	0-16	

Lithostratigraphy mainly after Murray (1890); chronostratigraphy after Felix (1973); biostratigraphy after Baldassini and Di Stefano (2016)
Sources: Pedley et al., 1978, 1992; Alexander, 1988, Cassar 2002)

The stratigraphy succession consists of five main formations of about 250 m in thickness, with horizontally stratified limestones, subsidiary marls and clays which are distinct from each other in terms of sediment grain size and relative depth of deposition (Pedley, 1975, 2011; Pedley, House and Waugh, 1976) (Table 4.1). From these five sedimentary formations, this study mostly concerns the Globigerina Limestone (GL). The lithostratigraphy of the GL has been amply described in various studies (Pedley, 1975; Pedley, House and Waugh, 1976; Bennett, 1979; Pedley and Bennett, 1985; Pratt, 1990; Rose, Pratt and Bennett, 1992; Gatt, 2006; Baldassini and Di Stefano, 2015, 2017). It owes its name due its abundance in planktonic foraminifera of Globigerina and consists of a yellow to pale grey, biocrimitic limestone with locally abundant macrofossils.

In response to a combination of tectonic controls, eustatic fluctuations, storm activities and related erosional episodes in Central Mediterranean region during the late Oligocene-late Miocene period, the depositional setting of the GL was influenced by a series of sedimentary intervals and associated hiatuses, leading to the subdivisions of the GL into three different members - Lower, Middle and Upper Globigerina Limestone Members (LGLM, MGLM and UGLM). As seen in Table 4.1, these members are bounded by phosphorite conglomerates, hardgrounds and omissionground (Rizzo, 1932; Pedley, House and Waugh, 1976, 1978; Rose, Pratt and Bennett, 1992; Rehfeld and Janssen, 1995; Baldassini and Di Stefano, 2017).

Shore platforms have mostly formed in the LGLM and UGLM surfaces. The LGLM is considered to be a series of massive-bedded biomicrites and biomicrosparites, wackestones and packstones, associated with the warm climatic phase of late Chattanian (Baldassini, Mazzei and Foresi, 2013; Baldassini and Di Stefano, 2015, 2017). It is subdivided into two principal beds, known as sub-facies, from the base to the top as follows:

i. Sub-facies A: Colloquially termed as 'Soll' (Aquilina, 1987a), this base of the LGLM is characterised by a typically grey or yellow globigerinid clayey carbonate, with well-preserved bedding planes

and occasionally interspersed with beds of bluish-grey clayey or marly limestone. It is considered to have a higher non-carbonate fraction and an overall lower porosity; and

ii. Sub-facies B: Colloquially termed as 'Franka', or freestone (Aquilina, 1987b), this bed is composed of soft white to yellow medium to fine-grained calcarenite. It is considered a well-bedded limestone with parallel bedding or cross-laminations.

The UGLM consists of alternate facies of hard limestones, wackestones and calcareous marls and mudstones (Baldassini and Di Stefano, 2017). Felix (1973) subdivides (from bottom to top) this uppermost member of the GL in the following four beds:

i. Phosphorite pebble bed at the base, known as Upper Main Phosphate Conglomerate bed (or C_2);
ii. Yellow to orange hard and compact limestone, which is considered as a foraminiferal wackestone facies;
iii. Grey marly middle bed, which is a calcareous grey marly facies (mudstones) and described by John, Mutti and Adatte (2003) as 'Clay Rich Interval', due to an increase of clay content; and
iv. Yellow to orange hard and compact limestone, with foraminiferal wackestone facies and bioturbated limestones.

The two main phosphorite beds are C_1 and C_2 Conglomerates. The C_1 varies in thickness between 10-40 cm and contains sub-angular dark brown phosphatic pebbles and sub-rounded light brown phosphatised cobbles, mixed with whitish marl limestone deposits and fossils (Baldassini and Di Stefano, 2015). The C_2 Conglomerate is 10–30 cm thick and is formed by very small phosphatic deposits (about 1 mm in diameter) and sub-angular pebbles (which never exceed 5 cm in diameter) mixed with yellowish carbonates and fossils (Baldassini and Di Stefano, 2015). A third phosphorite bed was identified by Carbone *et al.* (1987) at the boundary between the LGL and LCL.

4.3 Delimara Peninsula: shore platform of Ras il-Fenek

4.3.1 Access to the shore platform of Ras il-Fenek

The shore platform of Ras il-Fenek (35°50'14.67"N, 14°33'52.05"E) is situated at the tip of a narrow rural promontory, which is not accessible to vehicle traffic. The shore platform can only be reached via a footpath situated en route of Delimara Road, a local access road that crosses the Delimara peninsula and links the peninsula with the main traffic network from Marsaxlokk. The area of Xrobb l-Għaġin is not serviced by public transport and the promontory can only be accessed via a footpath (0.7 km) from Delimara Road and it takes approximately 20 minutes to reach the platform.

4.3.2 Background: Site and Situation

The promontory of Ras il-Fenek and its shore platform are located in a coastal area known as Xrobb l- Għaġin situated between the town of Marsascala and Marsaxlokk in the south eastern part of Malta (Figure 4.2). Ras il-Fenek forms part of a sequence of promontories skirting the coast of Delimara peninsula. The litho-stratigraphy of these promontories is composed of UGLM and MGLM and the landforms are flanked by a series of either narrow inlets (Peter's Pool, Qala t-Tawwalija, Il-Kalanka tal-Gidien) or circular embayments (Ħofra l-Kbira and Ħofra ż-Żgħira).

As seen Figure 4.2b, the litho-stratigraphy of the peninsula's hinterland mostly consists of UGLM whilst the coastal promontories are characterised by a series of cliff outcrops in MGLM and/or UGLM and shore platforms in UGLM (Pedley, 1993). Two inferred faults - one in a NNE-SSW direction and another in a NE-SW direction – intersect at the upper and lower part of the peninsula respectively. As illustrated in Figure 4.2b the NNE-SSW fault contributed to a dip of the eastern coastline in easterly and south-easterly direction with an inclination varying between $2\text{-}6^0$, with the result that only UGL member is exposed above sea level.

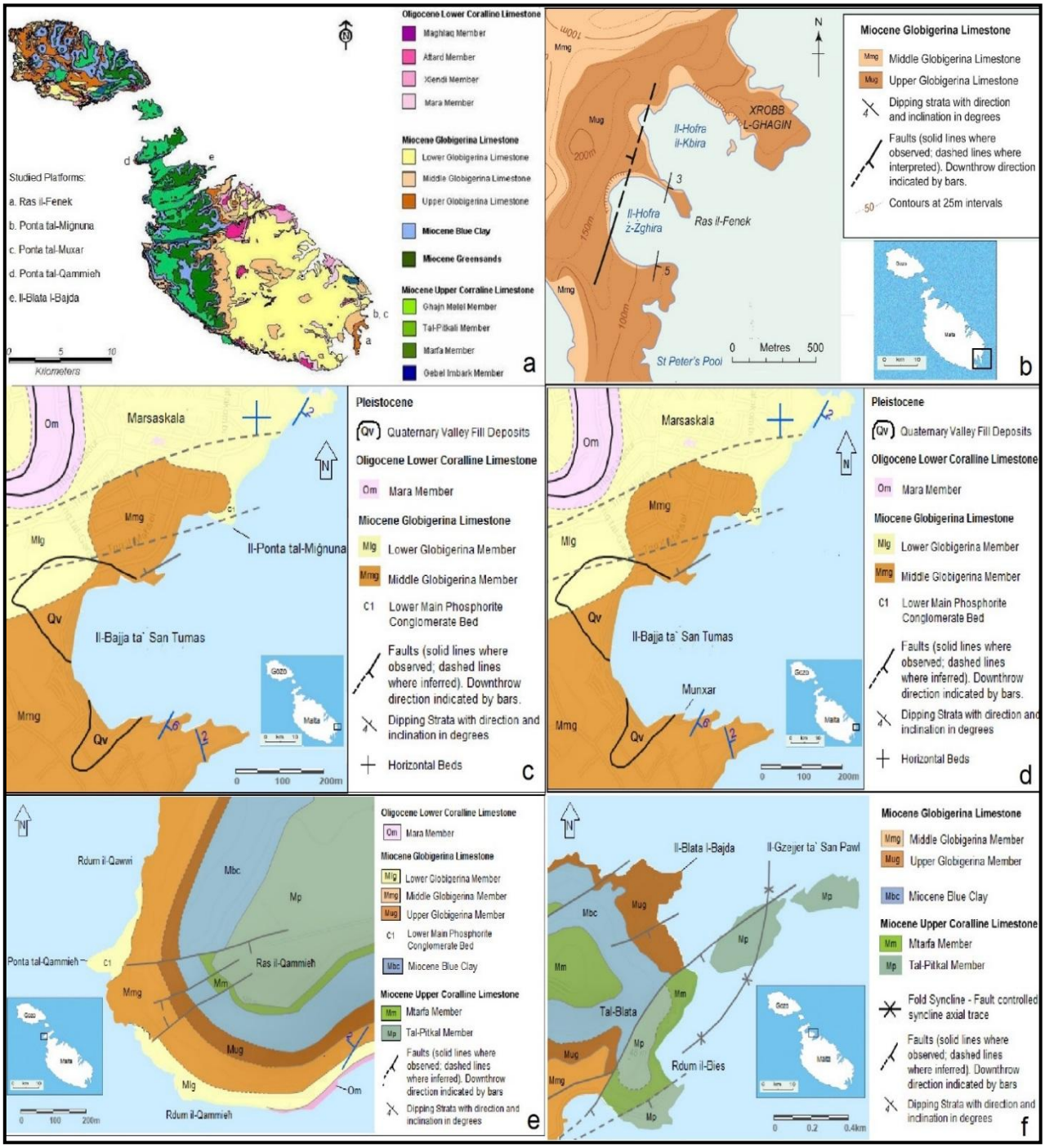

Figure 4.2: a Geological representation of the Maltese Islands and the five studied platforms; b. Ras il-Fenek; c. Ponta tal-Miġnuna; d. Ponta tal-Munxar; e. Ponta tal-Qammieħ; f. Blata l-Bajda (Source: Redrawn and modified from Pedley, 1993)

The promontory of Ras il-Fenek separates the two sub-circular embayed areas in MGLM, known as Ħofra ż-Żgħira (in Maltese, Ħofra means hole, ż-Żgħira means small) and Ħofra l-Kbira (in Maltese, Ħofra means hole, l-Kbira means large) (Figure 4.2b). The inner cliff recess of Ħofra ż-Żgħira is fringed by a narrow beach with coarse-grained UGLM deposits. Ras il-Fenek is dipped at 3^0 in a south-easterly direction whereas, further south, il-Ħofra ż-Żgħira is dipped in a similar direction at 5^0. The morpho-genesis of these two sub-circular bays is attributed to the presence to two ancient drainage lines that converged into the area (Soldati, Tonelli and Galve, 2013). The 3-5^0 dip, with a NNE strike present in the seaward exposed sections, are landward bounded by the relatively softer MGLM (Soldati, Tonelli and Galve, 2013). The combination of fluvial erosion at the exposed unit of UGLM and preferential marine erosion along where stream valleys reached the sea, created a retrogressive erosion of the dipped UGLM and subsequently lead to the inland removal of the MGLM beds. Wave refraction processes along the softer MGLM outcrops, flanked by more resistant UGLM outcrops, receded the shoreline into a semi-circular embayment. Two truncated valleys can still be observed at the top of the MGLM cliffs (at c. 125 m a.m.s.l) in the inner recess of il-Ħofra ż-Żgħira.

The sub-circular coasts of Xrobb l-Għaġin are scheduled as Areas of Ecological Importance (AEI) Level 2 and Sites of Scientific Importance as defined by Structure Plan Policy ME01, as UGLM allows specific coastal vegetation communities to colonise. Generally, the most dominant habitats are the steppe and garigue. The cliffs are also classified as Area of High Landscape Value (AHLV) Level 2 (i.e. protected or identified for protection in accordance with Policy RCO 1 of the Structure Plan) in accordance with Government Legal Notice 400 of 1996 (MEPA, 1995). In accordance with Structure Plan Policy RCO14, the greater part of the Delimara Peninsula is designated as a National park, as outline in policy MD01 of the Marsaxlokk Local Plan (1995). Futher land-use information is provided in Appendix V.

4.3.3 Morphological field assessment and mapping

A multi-levelled, elevated shore platform dominates the tip of Ras il-Fenek in a south eastern direction (Figure 4.3). It can be considered a Type B shore platform i.e. a nearly horizontal platform, which extends from the base of a cliff and ends in a low-tide cliff above sea level. With an area of 3,794.5 m^2, the platform is situated at elevation heights between 6 and 11 m a.m.s.l. The gradient of the platform is not more than 2^0 (Figure 4.4).

As explained in Section 4.2, UGLM generally consists of a sequence of three alternating horizontal beds of lower yellow limestone, middle grey marls and upper yellow limestone. However, as confirmed also by authors such as by Foresi *et al.* (2011) and Bianucci *et al.* (2011), the UGLM along the Delimara peninsula is markedly different from the rest of the island due to the presence of a number of hardgrounds with bioturbation characteristics within it. Bianucci *et al.* (2011) described three well-developed hardgrounds present in the lower yellow limestone bed, while several less well-developed ones are said to be observed in the upper yellow limestone bed. The phosphatised sediments in these hardgrounds give indurate characteristics to the UGLM surface, unlike other soft and flaky UGLM exposures such as at Blata l-Bajda Selmun (See Section 4.6).

Rehfeld and Janssen (1995) interpreted the development of these hardgrounds (above the C_2 bed in the UGLM) as a condensed sedimentary unit which developed in the course of a renewed cyclical transgression (transgressive surge) i.e. small scale oscillations during sea level lowstand, during which sedimentation rates were low due to increased bottom currents. Conditions of deposition were still evidently more sheltered and bottom conditions more stable, enough for the preserved fauna to be similar to that found in other parts of UGLM (Bianucci *et al.*, 2011).

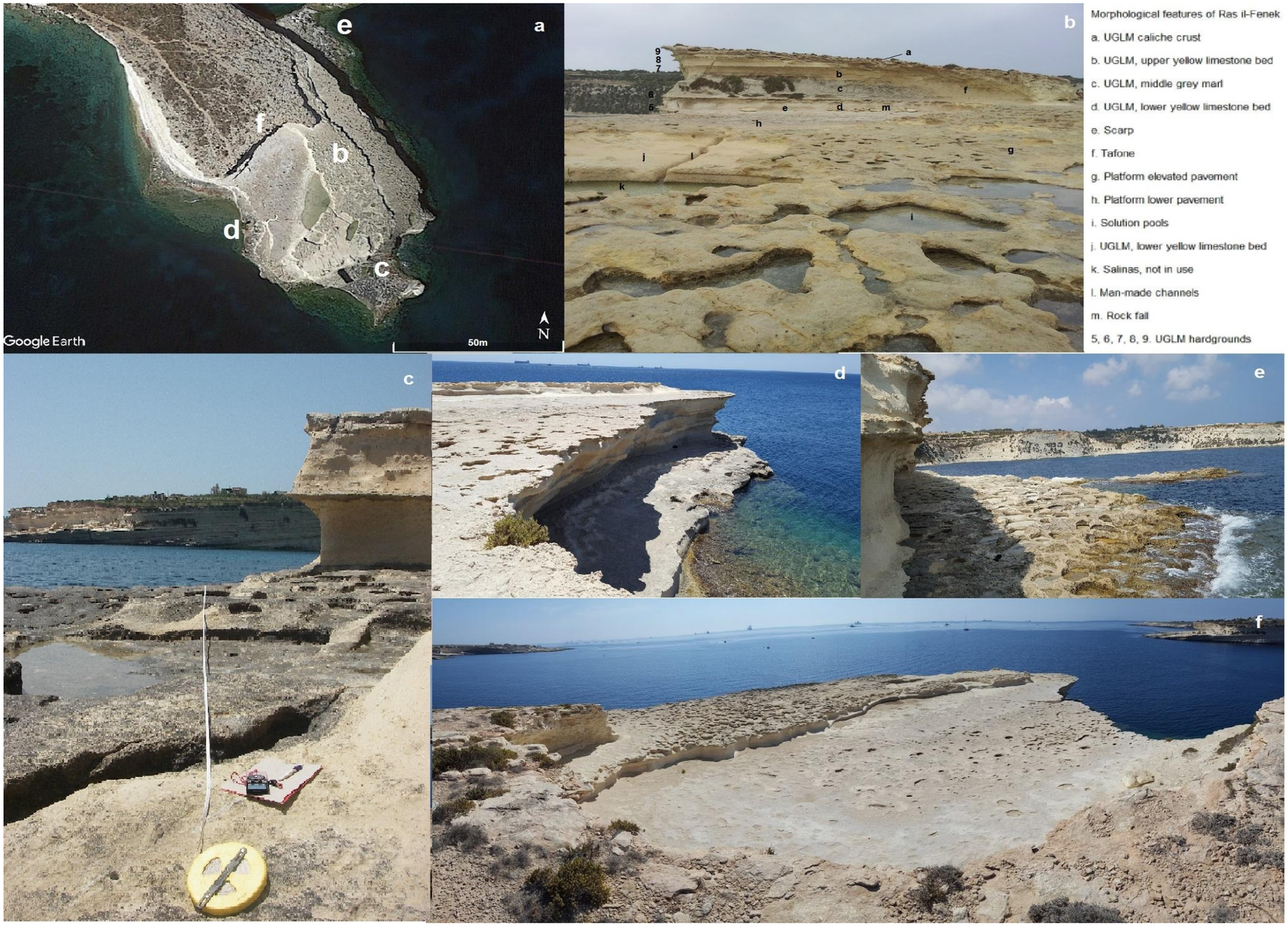

Figure 4.3: Main morphological characteristics of Ras il-Fenek: a. Google Earth image of Ras il-Fenek; b. Main morphological features of the platform pavement features and the cliff section; c. Lower pavement, with solution pools and low tide cliff in UGLM lower yellow limestone bed in the background and a man made channel in the foreground; d. Lower hardground pavement as a bench; e. Karstified limestone outcrops at sea level on the NE side of the platform; f. Panoramic view from UGL cliffs of the upper and middle pavement of the platform (Source: Photos taken by Author)

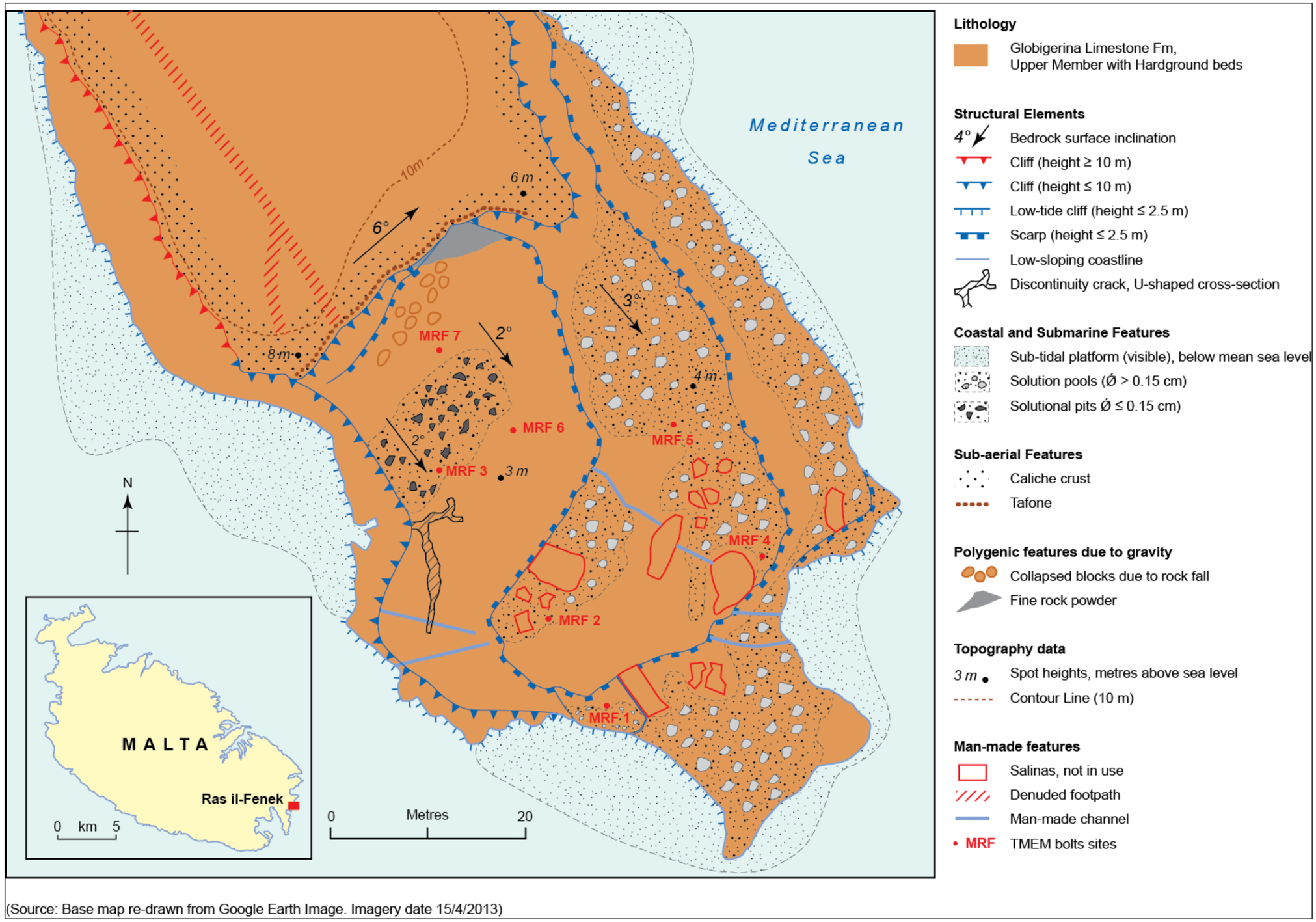

(Source: Base map re-drawn from Google Earth Image. Imagery date 15/4/2013)

Figure 4.4: Geomorphological map of Ras il-Fenek (Source: Base map from Google Earth, Compiled by Author)

The platform of Ras il-Fenek has developed within the lower yellow limestone bed, which is positioned in contact with mean sea level and receives direct wave action (Figure 4.2b and Figure 4.4). The platform is backed by UGLM cliffs in middle grey marl beds and capped by the upper yellow limestone bed. These two beds would have retreated to the present position due to the differential response behaviour to marine erosion at sea level. The middle grey marls, in being less resistant than the lower and upper yellow limestone, would have retreated faster. Such a recession would produce two results: 1. the undercutting and eventual collapse of the upper yellow limestone; and 2. the exposure of sub-horizontal platform by the resistant lower yellow bed.

In total, nine beds of thin phosphatised hardgrounds were identified in this study, along the vertical cross-section of the UGLM (Figure 4.3b). Three of these hardgrounds constitute the platform surface. The lower yellow limestone bed, which starts at mean sea level, has a total of six hardgrounds, with the fifth and sixth hardground corresponding the lower and upper levels of the platform surface respectively. The base of middle grey marl layer is bounded by the sixth hardground bed and does not exhibit any hardground bed within its section. The top 0.5 m of the middle grey layer gradually transit into yellow marly limestone bed, before another three hardgrounds subsequently develop in the upper yellow limestone bed. The upper bed ends with a distinct colour darkening from light to dark beige. This colour change corresponds both to a progressive decrease of the calcareous marl thickness and an equivalent increase in indurate limestone. This upper yellow bed terminates at the surface with a hardened pseudo-bedded layer of caliche crust. These type of calcareous crust laminae, with irregular and crumbly carbonates in-fills, are very common sub-aerial structures on many limestone surfaces in semi-arid areas (James, 1972). They form through the semi-arid combination of alternating short periods of rainfall (which lead to initial dissolution of carbonates) and intense evaporation (leading to capillary rise of soluble carbonates). Carbonates reprecipitate as calcite crystals and act a void-filling cement to form laminar crusts. James (1972) report that limestone coasts favour this crust formation

due to the additional input of calcium carbonate ($CaCO_3$) from salt spray on the near surface waters.

The exposed hardground surfaces provided additional rock resistance to coastal weathering and erosion processes and created a stepped platform surface in three pavement levels. The sixth hardground bed corresponds to the upper platform pavement; it extends from the base of the western end of the cliffs and covers the eastern and front side of the platform in a semi-circular direction (Figure 4.3b). It ends landward with a semi-circular scarp of 108m long and 1.5 m high. The total area of this elevated pavement is 1,293 m^2. The fifth hardground bed, situated at c.1.5 m below the sixth one, corresponds to the sub-horizontal middle pavement of the platform and outcrops in three separate sections of the platform: western side, eastern edge and front section. In total they have an area of 1994 m^2. The lowest pavement level is formed by the first hardground bed of the sequence and is situated at the tip of the peninsula close to mean sea level (Figure 4.3c). It has also developed a small inaccessible bench on the western side of the platform (Figure 4.3d) and a loop shaped rock exposure section on the eastern side of the platform (Figure 4.3e). Together, these three hardground exposures cover a total surface area of 1494 m^2.

The elevated pavement formed by the sixth hardground bed has a rugged surface morphology. Due to its highly bioturbated characteristics, the elevated pavement is densely hummocky with numerous flat-floored pools (Figure 4.3b). In the seaward section of this pavement, sea water, sea spray and rainwater collect in the pools forming transient but irregularly shaped solution pools. The physical effects of wetting and drying and physicochemical effects of salt crystallisation from drying spray in supratidal conditions have not yet been studied on the Maltese coasts. Bird (2011) affirms that in many cases it is difficult to separate the two processes.

Parts of the seaward section of this elevated pavement also exhibit removal of hardground surface and exposure of outcrops of the lower yellow limestone layer. The less resistant outcrops were modified with rectangular deep salinas, ranging in between 1.5 m^2 to 21 m^2 in size, hewn out of the UGLM

(the date of their construction is unknown and they are no longer in use). This stripping of the hardground beds would point to the possibility that, though this platform pavement is relatively well elevated above sea level, its seaward parts may still receive enough wave quarrying from high energy storm waves and, as a result, erode the surface front parts of the pavement. During the winter field visits, it was noticed that wave splashes reached the central part of the middle pavement. Sea water fills the salinas and accumulates in the seaward parts of the middle pavement, behind the escarpment line formed by the overlying hardground bed. The middle pavement is relatively more planar and is characterised by less bioturbated characteristics than the elevated bed (Figure 4.3f). Thus, it has a less karstified morphology that can trap and generate solution pools. It has mostly small solution pits ($\emptyset \leq 0.15$ cm) distributed on the platform pavement in an NNE-SSW direction.

The third exposed hardground pavement is found at the base of the platform and has a more pitted karst surface, heavily covered with numerous circular pools which are not larger than 1 m in diameter (Figure 4.3c). A micro-pitted surface has also developed at this level, whereas not so well developed on the upper levels of the platform surface. Given the low-tidal regime and the elevated position of the platform, the intertidal zone is very restricted. Only one or two metres along the edges of the platform show a micro-pitted morphology. The platform is also surrounded by a sub-tidal platform, also in UGLM, at sea depths between 1-5 m below mean sea level (Figure 4.4). The visible part was measured to have an area of c. 1,638 m^2 and it extends to parts where it emerges above sea level on the eastern side of the platform. The bathymetry beyond the sub-tidal platform rapidly drops to deeper waters ranging from -5 to -10 m.

The platform is backed by UGLM cliffs in middle grey marls and capped by the overlying upper yellow limestone bed (Figure 4.3b and Figure 4.4). They range in height between 8 and 6m a.m.s.l and change from a horizontal strata bedding on the western side, to a more cross-bedded strata on the eastern side, with the surface dip on 6^0 in a NNE direction. They close off the back of the

platform with a cliff line which is c. 80 m long and trends in a SW-NE direction (Figure 4.4). The cliff-platform junction has a stepped morphology due to the exposed presence of the sixth hardground, which forms a scarped base and from where the UGLM middle grey marl bed outcrops with irregular sloping profiles. This middle bed seems to weather out substantially into crumbly and recessed forms in an easterly direction. The combination of this highly weathered bed with the overlying calcrete crust in the overlying yellow limestone bed, created a tafone shaped cliff, having a cavernous inner wall made up of a weathered interior and an overlying overhang (Figure 4.3b). The recession of the grey marl undercuts and destabilises the overlying yellow limestone bed. It produces fractures and cliff crumbling (i.e. the detachment of large stone compact stone pieces into crumb-like shape) and eventual rock fall collapse at the cliff-platform junction.

Apart from cobbles and boulder sized deposits in UGLM, the base of the cliff is also covered with fine stone powder sediment (rock meal) due to the highly weathered properties of the UGLM (Figure 4.4). Prevailing north-westerly winds borne from the back of the promontory would be responsible for the sub-aerial shedding of this fine sediment from the overlying cliffs, whilst north-eastern and southern-borne winds would facilitate its transportation and accumulation on the eastern section of the platform near the cliff-platform junction. It also becomes in-fill sediment for the numerous flat-floored pools present in the backshore.

4.4 St Thomas Bay: shore platforms of Ponta tal-Miġnuna and Ponta tal-Munxar

4.4.1 Access to the shore platforms of Ponta tal- Miġnuna and Ponta tal-Munxar

Compared to the other shore platforms situated just below the coastal promenade of St Thomas Bay, the ones at Ponta tal-Miġnuna and Ponta tal-Munxar are the least accessible of the lot. This lower grade of accessibility has left both platforms as more quiet bathing areas, sought after only by well-informed bathers residing in the vicinity. This semi-secluded aspect drove in

part the choice of the platforms for this study in order to ensure the least possible disturbance to the TMEM stations.

The Ponta tal-Miġnuna shore platform (35^0 51'24.20"N, 14^0 34'19.99"E) is the first of a sequence of shore platforms skirting along the 2.9 km coastal stretch of St Thomas Bay (from Ponta tal-Miġnuna to Ponta tal-Munxar) whilst the shore platform at the Munxar promontory (35^0 51'16.08"N, 14^0 33' 50.02"E) is the last one on the other side of the bay (Figure 4.2c). Access to Ponta tal-Miġnuna would require more familiarity with the local secondary road network radiating out from the main road of Triq il-Qaliet. This network would lead you to an undeveloped cul-de-sac overlooking the cliffs of St Thomas Bay. The platform would then need to be reached via a footpath from the top of the cliff escarpment through a narrow winding path meandering down along its cliff facade. A metal railing has recently been installed along this path to ensure a higher level of safety and facilitate better its access.

The shore platform at the Munxar promontory is also only accessible via a footpath. An elevated metal rod acts as road barrier at the beginning of the Munxar promontory to stop vehicle traffic and allow only access on foot via a wide pathway skirting along the top of the promontory vertical cliffs. The shore platform is the only accessible platform along this promontory.

4.4.2 Background: Site and Situation

The shore platforms at Ponta tal-Miġnuna and Ponta tal-Munxar are situated opposite each other across St Thomas Bay on its northern and southern littoral side respectively. The bay is a secluded shallow bay (≦ 10 m in depth) in the south-east part of Malta and can be reached via the nearby seaside town of Marsaskala or from the inland village of Żejtun (Figure 4.2 c, d). The bay is semi-enclosed in a north-easterly direction between two headlands i.e. Ponta tal-Miġnuna and Ponta tal-Munxar. The two promontories are situated at a distance of 800 m from each other and the inner recess of the bay has a central axis of 780 m long. Most of the bay's bathymetry between the two headlands does not exceed depth of -10 m.

A combination of a fault and two inferred faults trend WSW-ENE across the northern side of St Thomas Bay, with one of the inferred faults cutting in a northern downthrow through the shore platform at Ponta tal-Miġnuna (Pedley, 1993). Dipping strata of 6^0 in a SE direction and of 2^0 in an ENE direction are observed at the Munxar peninsula, whilst the northern side has retained uniform horizontal bedding (Figure 4.2c and d). MGLM dominates the area, with an outcrop of LGLM starting off from Ponta tal-Miġnuna in a northerly direction and with Pleistocene valley fill deposits flanking the corners of the bay's inner recess. The site-specific combination of lithology-structure has created a contrast in the physical setting of the bay, with LGLM shore platforms skirting just above mean sea level at the base of MGLM cliffs on the northern side of the bay, whilst a thicker strata of MGLM produced higher cliffs with very few shore platform along the shores of the Munxar promontory at elevations ranging from 6 m to 20 m a.m.s.l. Baldassini (2012) explained how the MGLM consists of three depositional units, with the top depositional unit outcropping at St Thomas Bay and the lower two units exposed only along the north-western coast of mainland Malta. The presence of Pleistocene valley deposits correspond with the mouth of two shallow valleys situated on each side of the bay's inner recess (Figure 4.2c, d). A study conducted by Dr Paul Farres (Pers. Comm., 12/11/2012) identified valley sediments from Globigerina Limestone landscapes, which have different properties from those formed over Upper Coralline Limestone, in terms of their responses to weathering and potential regolith formation. The weathering process produced a calcareous mud containing small rock granules and an inverted soil profile characteristics.

4.4.3 Morphological field assessment and mapping

4.4.3.1 Ponta tal-Miġnuna

This shore platform is considered to be the largest one at St Thomas Bay with a surface area of 3589 m^2 (Figure 4.5 and Figure 4.6). Its central axis is

Figure 4.5: Main morphological characteristics of Ponta tal-Miġnuna a. View of the western section of the platform; b. C_1 bed at the seaward section; c. Detachment scarp of the SW-NE fault and contact point between C_1 bed and MGLM at the cliff-platform junction; d. Orthogonal joints; e. Joint-bounded bouldered perimeter; f. Solution pools on the C_1 bed g. Composite MGLM cliffs (Source: Photos taken by Author).

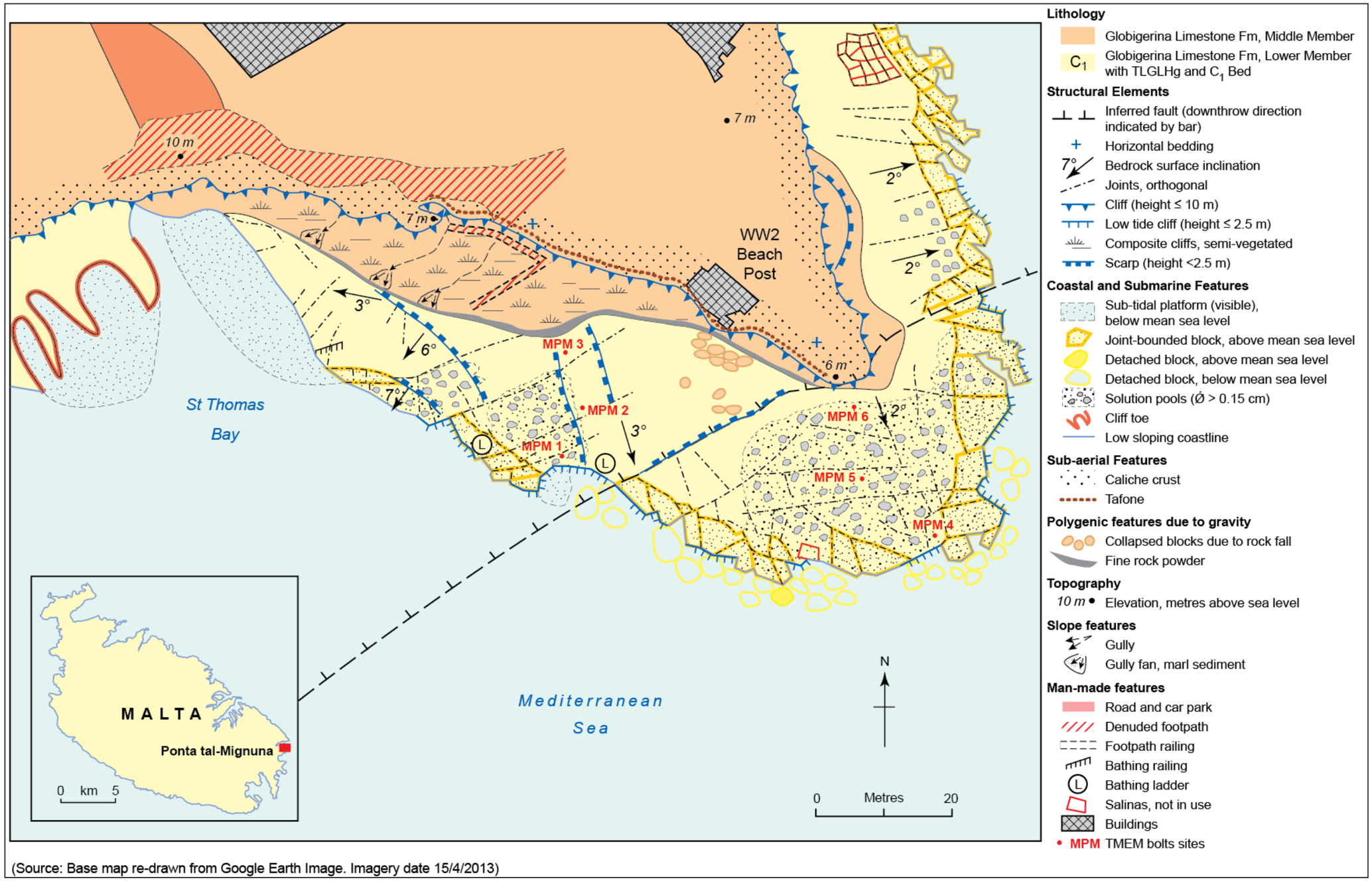

(Source: Base map re-drawn from Google Earth Image. Imagery date 15/4/2013)

Figure 4.6: Geomorphological map of Ponta tal-Miġnuna (Source: Base map from Google Earth and compiled by Author, 2016)

oriented south-east (148^0) and its elevation ranges from 0 to 5 m a.m.s.l. On the western side, the platform ends with a low tide cliff and plunges to depths between 1.5 to 7 m. The eastern side slopes gently below sea level to depth of 1.5 m at 10 m away from the shoreline (Figure 4.5 and Figure 4.6). Its maximum width i.e. from the edge to the platform-cliff junction is of 31 m and its maximum length i.e. from the western edge to the eastern edge is of 113 m. Given the platform elevation and the low tidal range on the Maltese Islands, most of the surface features on this platform exist in a state of supratidal conditions. The platform exhibits variations in surface morphology due to changes in rock litho-stratigraphy, structure and exposure to wave attack.

From a lithology point of view, its morphology corresponds to a distinct discontinuity surface that acts as a stratigraphic break between the MGLM and the LGLM members and it is mainly characterised by a phosphatized hardground, known as the Terminal Lower Globigerina Limestone Hardground (Rose, Pratt and Bennett, 1992) and the overlying ubiquitous C_1 bed rich in phosphatic nodules (or pebbles)(Section 4.2). The phosphate bed between the two is only about 2 cm thick and not as well-developed as in other places like Qammieħ (See Section 4.4). In fact it is hardly developed but phosphate pebbles and granules can be seen in the hummocky surface of the platform. The hummocky surface is actually the scour surface at the base of the phosphate conglomerate bed, such as the one situated at Qammieħ (S. Scerri, Pers. Comm., 4/08/2017). The platform-cliff landform system at Ponta tal-Miġnuna is therefore the combined result of a resistant outcrop of LGLM capped by TLGLHg, a thinly bedded C_1 bed and overlying retreating soft marl cliffs in MGLM (Figure 4.5b).

Holocene rise in sea level and resultant wave-pounding action caused the retreat of MGLM marls at a relatively faster rate, exposing a shore platform corresponding to the stratigraphy contact between the two lithological units and revealing a surface morphology rich in bow-form burrow with *Glyphichnus*-mode of preservation at top of LGLM (Gruszczyński *et al.*, 2008). The upper surface of the C_1 bed is mainly planar and characterized by a

phosphatic polycyclic layer which covers the clasts (Pedley and Bennett, 1985). The overall elevation of the platform was determined by the position and thickness of the bedding planes within resistant strata of C_1 bed, TLGLHg and LGLM in the relation to both the overlying less resistant strata of the MGLM marls and the point of contact of contemporary mean sea level.

The C_1 bed was observed to be thicker in the outer exposed parts of the platform and then becomes gradually thinner in a westerly direction (Figure 4.5a). The resistant outcrops in LGLM have been observed in various parts of the platform even at sub-littoral level. In fact, on the western side, the platform continues to slope gradually below mean sea level at a distance of 10 m from the shoreline, revealing a submerged platform of 333 m^2 in shallow sea waters of not more than 1.5 m in depth. Other shallowly submerged platforms in LGLM skirting the MGLM cliff toes were observed in a westerly direction along the bay.

The structure of the platform has been shaped not only by lithological difference in resistance to wave processes but also by tectonic controls. As explained in Section 4.4.2, a WSW-ENE inferred fault in a northern downthrow direction runs across the northern side of St Thomas Bay, cutting through the shore platform and the edge of the MGLM cliff escarpment at Ponta tal-Miġnuna (Figure 4.6). A series of four scarps of not more than 1.25 m in height have developed in different directions through the platforms and created sections of multi-levelled surfaces with different gradients (Figure 4.5c). Gentle sloping gradients ($\leq 5^0$) were recorded towards the western side of the platform (where a railing was set up to facilitate walking access to sea); sub-horizontal gradients were recorded on the more elevated and exposed part of the platform on the eastern side (where two ten-rung ladders have been installed).

Geological structure plays an important role in terms of the joints present on the platform because the spacing and number of joints has determined the size and scale at which erosion occurred across the platform, especially at the seaward perimeter (Figure 4.5d). A number of orthogonal pressure release joints dissect deeply in the surface of the platform and are

particularly located around the WSW-ENE inferred fault and across the exposed part of the platform (Figure 4.6). They do not vary greatly in appearance and arrangements, although their dimensions visibly ranged from 0.25 m to 0.75 m in width and their depths ranged from 0.15 m to 0.95 m depth. Given their close location to the inferred fault, one can assume that their genesis may be attributed to the brittle deformation of the bedrock due to the stresses driven by the fault displacement. Microfissures ranging from 2-10 cm and up to 1 cm deep were also observed to follow along these orthogonal joints.

The development of these joints has not only determined the surface morphology of the platform but also influenced the response of the platform to mechanical wave erosion. Wave quarrying is in fact important on horizontally-bedded rocks with seaward-facing scarps because they provide steep surfaces that can be impacted by waves, surf, and swash (Trenhaile, 2011a). Additionally, the micro-tidal regime concentrates wave quarrying by water hammer, shock pressures, and air compression in the narrow zone between the wave crest and just below the mean sea level, generating a high wave pressure on the rock discontinuities along the edge (Trenhaile, 1987; Porter *et al.*, 2010a). Wave quarrying hence widened and weakened the joints at the seaward edge, and dislodged substantially large blocks to the extent of creating a boulder-strewn perimeter with c. 90 joint-bounded blocks at supratidal level (Figure 4.5e). The blocks vary widely in size between 12 m^3 to 350 m^3, with some of the smaller clasts imbricated amongst larger boulders (Figure 4.6).

A field inspection of the sub-tidal morphology around the platform also revealed a number of disconnected boulders that have collapsed into the sea (Figure 4.6).The compression of air in joints by large storm waves may provide enough hydraulic lift to dislodge large blocks and transport them in the sea (Biolchi *et al.*, 2015). These blocks were mostly observed to be found around the south-east tip of the platform at depths ranging between 1.5 to 10 m below mean sea level. Most of them were observed to be covered with seaweed growth indicating a not-so-recent collapse.

Though the platform surface is not characterised by abrasive potholes, a number of such potholes, with rounded smooth boulders trapped inside them, were also observed on the shallow parts of the seabed at circa 7 m deep. It is well documented that abrasion can take place at any depth at which the material can be agitated by wave-generated shear stresses, and that it is generally most effective at, or close to, the water surface (Robinson, 1977a; Trenhaile, 1987). Their presence would suggest high-energy agitated waters on this exposed part of the sea bed and in turn, indicate that the outer part of the platform may also be impacted by such high-energy waves. The extent of such impact however is not altogether clear, given that the outer part of the platform is also bordered by a low-tide cliff of 2-3 m above sea level. The seabed morphology changes in a westerly direction: from deep waters with abrasion pools and large clasts or boulders in LGLM to shallow waters with a mix of numerous smaller MGLM cliff boulders and cobbles, interspersed in thick beds of *Posidonia oceanica* meadows. The presence of large MGLM members decreases rapidly in number and size in an easterly direction, implying either a more sheltered part of the platform that generates less disjointed boulders or else active re-working of the large boulders into smaller clasts further inside the bay.

Pitting surfaces i.e. small corrosion hollows of a few millimetres in depth, were also observed in the first 5m from the edge of the platform and also within the flat bottom of the solution pools. The pits are usually small in diameter (ranging between 2 and 5 mm) and observed to occur mostly within the seaward zone of the platform, at a few metres above the normal wave action. This zone is still periodically exposed to heavy sea spray and wave over washes during stormy weather. The wetting and drying process is more effective in semi-arid arid climates like that of the Mediterranean because the frequent desiccation in dry weather alternates with wetting by occasional erratic rain as well as swash and sea spray. In the supratidal conditions of the Maltese platforms, the mechanical effect of alternate wetting and drying is considered to be also accompanied by the physiochemical effect of salt crystallization from drying spray which leads to the decrepitation of the rock surface and resultant

production of rock fragments which are then removed by wave sluicing. As previously mentioned, the eastern exposed-side platform surface is characterized by a thicker conglomerate bed with ridges of more resistant rugged nodules interweaving between planar outcrops of non-nodular bed formation and terminal hardground. These planar surfaces within the rugged outcrops act as catchment areas where sea spray, salt water, and rainwater get deposited and turn into salt evaporate pools upon drying, creating a network of flat-floored pools known as solution pools (Figure 4.5f and Figure 4.6).

Salt crystallization is also an underlying process manipulated for the production salt on Maltese shore platforms (Gauci, Schembri and Inkpen, 2017). Ponta tal-Miġnuna has c. 25 salini (average area of 3 m^2 each) etched out from these solution pools in order to facilitate salt production by insolation. These are currently not in use. Their presence is however not uncommon in the vicinity of the Marsaskala coast, where numerous salini patch its coastal zone and some of them are still in active production to date. Nonetheless, their presence is an evident sign of effectiveness of Globigerina lithology, evaporation and sea water in creating salt crystallization processes in these rocky areas and thus salt weathering on these platforms may also be an important agent of surface change.

An examination of the MGLM cliffs backing the platform provides further insights into the responses of the cliff-platform system to contemporary forces of surface change. The cliff has a minimum thickness of 2 m on the eastern side of the platform, increasing to 10 m in a westerly direction (Figure 4.6g). The thickness of the MGLM is not the only property that changes in an easterly direction. Compared to the relatively more vertical MGLM cliffs around St Thomas Bay, the cliff line above the shore platform at Ponta tal-Miġnuna has a more composite profile, consisting of two or more major steep faces in the lower section of the profile and overlain non-homogenously by more gentle slopes and concave overhangs along the upper mid-section (Figure 4.5g).

At the top, the cliff starts with a pseudo-bedding and pseudo-cross bedding crust that has developed due to the formation of shrinkage cracks

(developed by shrinkage of the clay content) which later get filled with caliche crusts and saline solutions through evaporation-induced capillary rise. Deposition of cementing minerals like calcium carbonate, silica and iron produce a crust resistant to physical and chemical weathering (James, 1972). Halophytes such as Golden Samphire (*Inula chritmoides)* were also observed above the caliche crust layer; plants are also known to contribute to the formation of caliche crusts since they take up water through transpiration and leave behind the dissolved calcium carbonate, which precipitates to form caliche. This is a common feature of MGLM exposures especially close to sea level where water for capillary rise is available (S. Scerri, Pers. Comm, 4/08/2017). The presence of this indurate crust above the relatively MGLM softer marls also developed a tafone morphology along the cliff upper line (Figure 4.6). It is a long cavernous feature – 10 m long, 2 m high and 1.5 m deep - and is characterised by weathered concave inner wall beneath a large continuous overhang of calcrete crust (Figure 4.6). The marly interior faces of the tafone are highly flaky and powdery, and their weathered properties have generated fine powdery sediment (rock meal) deposited on the tafone floor.

The MGLM cliffs present various composite profiles, with cliff crumbling as a very common weathering form along the exposed cliff faces of the MGLM. Composite cliffs are fairly complex systems and no single explanation can take into account different lithologies and locations (Trenhaile, 1987). A possible reason for the difference in cliff profiles around St Thomas Bay may be attributed to the presence or otherwise of underlying shore platforms. Part of the cliffs no platform has developed a steeper morphology, indicating that they are more directly exposed to direct wave impact and related steepening processes. Those armoured with a shore platform acquire a protective buffer against mechanical wave erosion. With the stabilisation of the Holocene sea level rise, the cliff line above the platform bedding plane may have retreated from a higher energy sector of the coast into a more sheltering position beyond wave reach. With the slowing down of wave erosion, sub-aerial denudation processes would have taken over (especially in the upper section of the cliffs)

transforming vertical cliffs into composite cliffs and even into degraded bluffs (Bird, 2011).

In sections with less consolidated material or capillary rise, the lithology of the MGLM is mostly sensitive to sub-aerial processes of wetting and drying which cause alternate swelling and contraction and the eventual development of cracks, angular fractures and disjointed blocks along the cliff facade. Disjointed blocks on steeper cliff profiles are more sensitive to gravity-induced falls and eventually collapse at the toe of the cliff. A few of these collapsed blocks were observed on site, close to the section of the cliff that had the largest and deepest overhangs. The western end of the cliff section is sliced though by the inferred fault, causing a displacement of the MGLM base by approximately one metre.

Three gulley slopes, ranging in width between 0.5 to 1.5 m, dissect the top of the cliff on the western side of the platform (Figure 4.6). The gullies extend headward from the steeper slopes into the lower sections of the cliff and deposit limestone marl sediment in fan formation at the base of the cliffs. The headcut of these gullies feeds from a drainage line situated at the top of the cliff which washes surface rainwater run-off from the inclined footpath. Both the headcut and the mid-slope were measured and found to be 0.7 to 1.0 m deep, and mostly have U-shaped cross-sections. The intense erratic rainfall, so typical of the Maltese Islands, mobilises marl sediment into debris flow along the gully slope channels. The flatter profiles and slower seepage of rainwater produced by the exposed harder pseudo-crust (which also traps more water in its rugged micro-topography) or by coastal slumping have allowed the growth of several halophytic succulents, such as the Golden Samphire (*Inula chritmoides).*

Though the morphology and rates of surface change for cliffs are not examined in this thesis, the various erosion and weathering forms present along these cliffs provide a number of important indications that feed into the purpose of this study on platforms. Firstly, the examination of the lithological responses of the MGLM to atmospheric processes and biological agents are quite distinct from those for Upper and Lower Globigerina limestone. All the

above morphological evidence reaffirms once again the notion of how much the Globigerina Limestone exhibits a wide range of surface morphologies in response to forces of surface change. Secondly, it shows how much the platform as a landform also operates in tandem with the cliff as a coupled system and is largely influenced by difference in lithological responses between the relatively more resistant LGLM (and its conglomerate outcrops) and the softer MGML. Last, the presence of more weathering forms on the cliffs overlooking western side of the platform (such as composite profiles, meandering gullies, debris of the end of the gullies, vegetation outcrops) are indicative of a relatively more sheltered aspect away from any direct impact of the waves. On the other hand, the steeper cliff faces on the eastern side may indicate more exposure to wave action during storm events.

4.4.3.2 Ponta tal-Munxar

With a shoreline perimeter of 219.8 m and a surface area of 919.2 m^2, the platform has a central axis orientation towards 84^0 ENE and has a strong back tilt of 6^0 towards south-east (125^0) (Figure 4.7d). The adjacent headland of L-Ghassa tal-Munxar also has a strong back tilt of 6^0 towards south-east. It extends into the sea in a tongue-like shape with the longest axis of 93.4 m in parallel with both to the shoreline and the vertical cliffs across the inlet. Its elevations range from mean sea level at its extreme tip and along its southern shoreline to 5 m a.m.s.l along its northern side in a landward direction (Figure 4.7d).

The atypical dipped position of the platform in relation to the cliff line morphology (Figure 4.7 a, b) and the overall topography and bathymetry of the area indicate the possibility of a small fault with downthrow towards the north-west. Such small normal faults often have a displacement of less than one metre and are not uncommon within the GL elsewhere (M. Pedley, Pers. Comm., 31/07/2017). Some support for the existence of a normal fault comes from the Pedley's geological map (1993). Although it does not show any inferred fault line in the area, it indicates unusually steeper dips in this area of around 6^0 and which are higher than the gentler regional dip of 2^0 or 3^0. Hence, it is quite

Figure 4.7: Main morphological characteristics of Ponta tal-Munxar: Back to front (W-E) view of the platform; b. Dipped platform to SE, with backing cliffs in MGLM and Quaternary valley-fill in the background; c. Erosional scarp along low-tide cliff; d. Inlet waters with visible sub-littoral platform and broken clasts below sea level; e. Cliff-platform junction covered in rock collapse material, and with coarse-grained beach in the foreground; f. Close up of rugged platform surface in GL (Source: Photos taken by Author)

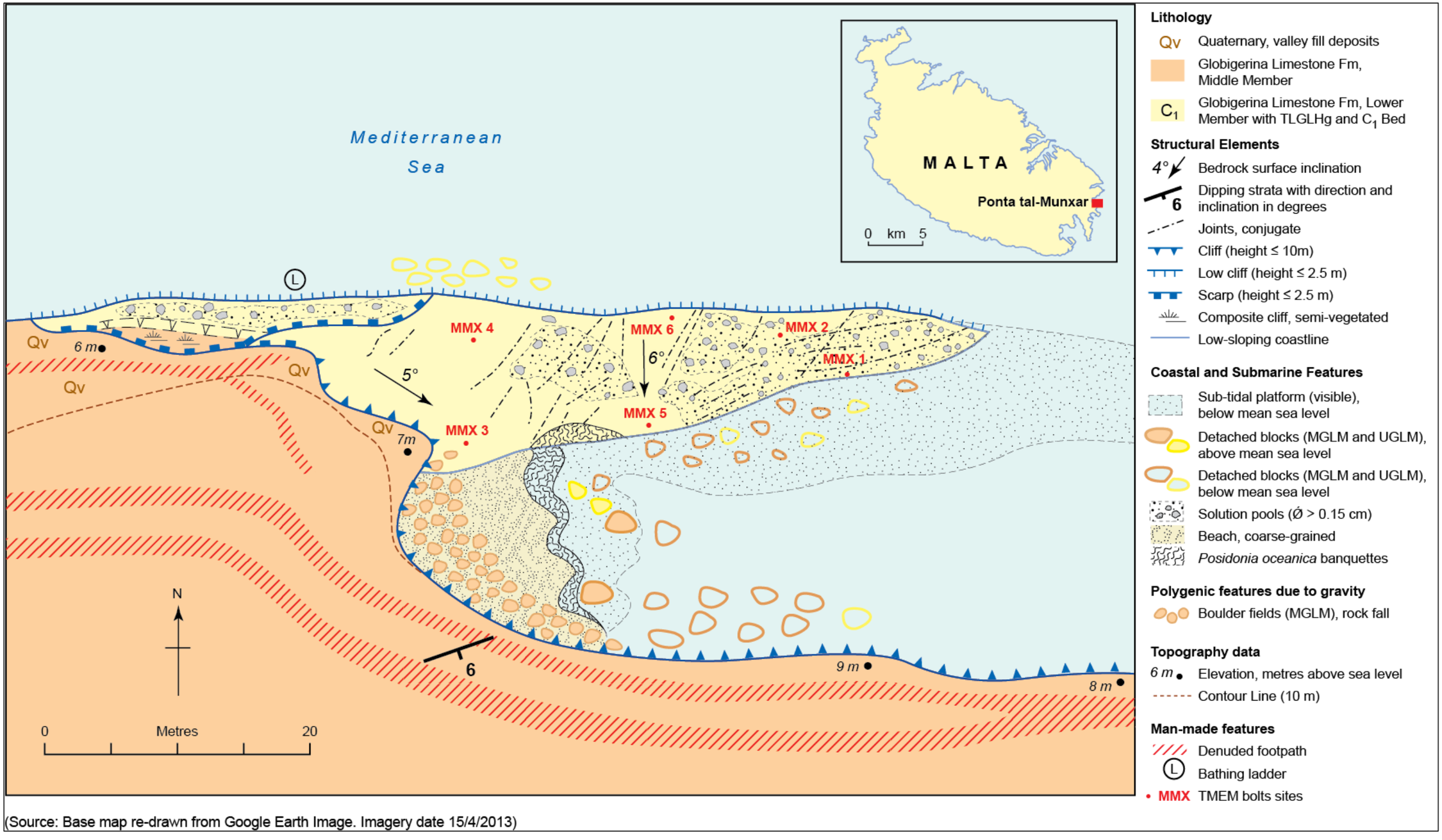

(Source: Base map re-drawn from Google Earth Image. Imagery date 15/4/2013)

Figure 4.8: Geomorphological map of Ponta tal-Munxar (Source: Base map from Google Earth and compiled by Author)

possible that there are small displacements in the immediate vicinity of the platform in question. The platform continues to slope gently below sea level to shallow submerged depths of not more than 1.5 m and reaches a length of 33 m from the shoreline. The submerged part has an area of c. 150 m^2 and given the low-tidal range present on the Maltese Islands, this submerged part is never exposed. It is also asymmetric in shape and slopes gently towards the inlet on the southern side in line with the rest of the exposed platform (Figure 4.8).

This shore platform is the one of the very few existing outcrops from a longer sequence of submerged platforms at the base of Munxar's vertical cliff coast. The latter is mostly characterised by low rectilinear cliffs in Quaternary valley-fill deposits and relatively higher and densely fractured MGLM cliffs (Figure 4.7b and Figure 4.8). The identification of the platform lithology was not as straightforward as originally thought. The lithology is marked as MGLM in Pedley (1993) and later reconfirmed by M. Pedley (Pers. Comm., 31/07/2017) as corresponding to one of the relatively well lithified beds within the lower part of the MGLM. However, a marine paleontological work by Foresi *et al.* (2014) on St Thomas Bay points towards the presence of a thin conglomerate bed C_1 at the base of the cliff and thus suggesting that the platform outcrops in TLGHg and overlies LGLM which is found closer to sea level (Figure 4.7c). This relative position plus the presence of an intensely bioturbated surface of the platform seemed to point towards being a TLGHg surface in pelagic carbonates rather than a lithified bed in MGLM. This was confirmed by Foresi in a further communication with the author (Pers. Comm., 22/08/2017). Subsequent on-site visits and discussion with Dr Saviour Scerri confirmed Foresi's observation, with the identification of the C_1 bed at the base of the cliff and the well-visible LGL outcrop below the hardground escarpment (Figure 4.7b).

The presence of other sub-tidal platforms was also observed along the base of Munxar cliffs, particularly at Munxar Point, which is mostly known for the presence of shallow reef conditions created by the presence of this lithified bed at submerged conditions. Interestingly, the reef conditions present along this bay, the physical configuration of St Thomas Bay, its exposure to strong

Gregale winds and the findings of four small antique anchors continue to date to fuel a hypothesis that Munxar may actually be the shores where apostle St Paul (patron saint of Malta) was shipwrecked on his way to Rome (60 A.D.), the events of which are described in Acts 27:14 (Gerada Gatt, 2014).

The shallow semi-enclosed inlet created by the platform in parallel position with Munxar cliffs is c. 31.8 m wide and 44.3 m long (Figure 4.8). It has trapped enough incoming longshore sediment to build a small coarse-grained beach above the submerged beds found in the inner recess zone between the platform and the cliffs (Figure 4.8). The beach sediment is a mix of pebble (Ø 4-64 mm), gravel deposits(Ø 2-4 mm) and a large abundance of empty shells of the marine snail *Tricola pullus* (identified by Evans J., Pers. Comm. 19/08/2017) The beach is c. 15 m long and 7m wide. Given the exposed coastal configuration along which Maltese shore platforms have formed, it is quite uncommon to find similar beach deposits accruing so closely to shore platforms and at relatively such low elevations. Banquettes of *Posidonia oceanica* are frequently deposited on this beach after stormy conditions (Figure 4.8).

The backshore of the beach is backed by heavily-jointed MGLM cliffs ranging in elevation between 4 to 7 m above sea level (Figure 4.7b). Foresi *et al.* (2014) constructed a bio-stratigraphy of the cliffs at Munxar and characterised the cliffs as an alternating sequence of three layers of light beige to greyish calcareous marls and light beige to greyish limestone and marly limestone. The bedding planes of the cliffs are dipped at 6^0, with distinct bands of several beds across the cliff profile. The bottom bed has a relatively softer marl texture giving a gentle concave profile to the base of the cliff. The top part is characterised by more angular joints, which have developed as a result of repeated swelling and contraction within the member. The western end of the MGLM cliffs, which overlooks the shore platform, is capped by terra rossa Quaternary valley-fill deposits. Their thickness increases landward into low cliffs in the inner recess of the bay.

The cliff is the backshore limit for both the beach and the platform and is covered by clasts and boulders of varying sizes as a result of frequent cliff

collapse (Figure 4.7e). This cliff toe debris provides input material to sustain the sediment supply of the beach. On the other hand, the presence of the beach in front of the cliff provides abrasive material for more intense mechanical wave erosion. On various fieldtrip visits, it was observed that the backshore sediment is extremely dynamic and changeable to the direction of incoming waves. The position of rock fall accumulations was noticed to shift along the cliff-beach junction, indicating a dynamic wave environment (Figure 4.7d). The presence of other clasts and boulders in the shallow inlet waters may indicate that some of the cliff material is eventually transported by wave action towards the sea or else transported inshore due to breakage from the submerged parts of the platform (Figure 4.8). The presence of this material may represent a stronger abrasive component in the waver erosion dynamics of the bay.

In relation to its overall site setting, the platform is exposed to an open fetch from a north-easterly direction. It is from this direction that the Gregale wind, i.e. a strong, cool, north-easterly wind, is generated when low-pressure systems move southwards and produce an impactful wave climate. The elevated side of the platform is in fact more exposed to such breaking waves from north-east, particularly during Mediterranean cyclonic storms or when strong winds blow onshore. The platform's elevated side, which is exposed to such north-easterly conditions, rises from sea-level in a series of low-stepped scarps, which then decrease in number and elevation as the platform slopes southwards to sea level at a gradient of 6^0 (Figure 4.7c). The receding stepped scarps may be an indication of step backwearing due to the wave quarrying and variation in lithological resistance to wave impacts. There is a distinct contact point between the top bioturbated bed of the platform and the exposed underlying bed with a smoother surface. This contact point may act as a line of weakness along which breakages occurring along the numerous fractures found along the top bed of the platform. With the recession of this top bed the underlying smoother beds are exposed. Numerous clasts were observed in the sub-tidal zones of the platform (Figure 4.7d). The clasts on the southern side originate from the submerged parts of the lithified bed, whilst the clasts on the

northern side consist of broken deposits from the scarp and the lithified bed located on the exposed northern side of the platform.

The underlying uniform LGLM bed drops into the sea as a steep low scarp to depths of between 2 to 4 m below sea level along the northern side (Figure 4.8). A ten-rung ladder has also been installed to ease bathing access. In view of the fact that this elevated scarp is subject to frequent impact of waves and sea spray, its limestone surface is heavily pitted with a dark intricately weathered morphology from sea level to 1.5 m a.m.s.l. On a number of field visits, erosion scars from mechanical wave erosion were observed along the scarp directly above sea level. These erosion scars initially exposed a pale smooth surface which contrasted with the surrounding dark solution-pitted surfaces. Such scars do not however take more than a year to re-establish as dark surfaces. Pitted dark surfaces were less observed in the southern sloping side of the platform and extend only to distance of between 0.5-1.5 m from the shoreline. Given that the prevailing winds are from the north-east, this southern side of the platform is more sheltered from wave action and sea spray and hence the extent of pitted surface morphology is limited landward.

A dense network of conjugate joints intersects obliquely across the platform (Figure 4.8). They are quite irregular in form, spacing, and orientation and so cannot be readily grouped into distinctive joint sets such as the orthogonal types. With dihedral angles measured between 35° to 45° within a joint system, these conjugate joint sets are spread out across whole platform in different directions. Their length ranges from 1 to 8 m. Some (but not all) of the deepest discontinuities (≤0.9 m in depth) are found to be oriented north-east and cut transversally across the platform at c. 75^0 to 90^0 with the northern edge. Their enlargement may be attributed to a higher level of exposure to wave quarrying and solution processes produced by wave impact and sea spray deposit respectively from the north-east. An additional process of enlargement would occur by sea water flowage from on-shore waves which would channel sea water downwards through these joints along the 6^0 gradient in a south-

westerly direction. The base of these discontinuities is in fact filled with salt evaporates and fine sediment thinning out in a southward direction.

There is not enough information on the origin of these joints at Munxar. Actually not much information exists on any joints found on the Maltese Islands. Given their characteristics and presence on a heavily-bedded sedimentary lithology, the most plausible reason inferred would be that they are tectonically-driven release joints formed near the surface during uplift and erosion. As bedded sedimentary rocks are brought closer to the surface during uplift and erosion, they cool, contract and become relaxed elastically. This causes stress build-up that eventually exceeds the tensile strength of the bedrock and results in the formation of jointing (S. Scerri, Pers. Comm., 12/08/2017).

Some flat-floored solutions pools (mostly of a diameter of $\leq$0.5m) have formed in the most exposed parts on the platform i.e. on the smooth LGLM outcrops and on the edges of the hummocky TLGHg surface on the northern side and along the seaward end of the platform (Figure 4.7f). The morphology of these pools is very typical of other pools found on Globigerina shore platforms, although those found on the hummocky bed do not have outer rims of uniform height due to the uneven topography of the platform's surface.

In nutshell, this platform is characterised by the following atypical characteristics:

i. The platform is aligned parallel to the coastline, rather than perpendicular as most platforms;
ii. It is not the typical sub-horizontal structure; innhstead, it is backward dipped away from the sea (to the south) with a 6^0 gradient; and
iii. A coarse-grained beach is located on its southern side; whereas most shore platforms in Malta are not flanked by beach deposits.

4.5 Marfa Ridge: shore platform of Ponta tal-Qammieħ

4.5.1 Access to shore platform of Ponta tal-Qammieħ

There is very little disturbance at Ponta tal-Qammieħ (35°58'16.70"N, 14°19'23.56"E) since the site is relatively inaccessible from the promontory of Ras il-Qammieħ and the underlying *rdum* landforms. The platform needs to be reached on foot from Ras il-Qammieħ, via the elevated LGLM platforms and then cross over the *rdum* faulted sections in BC and MGLM in order to reach the other side of Ras il-Qammieħ where the platform is situated at Ponta tal-Qammieħ. The whole journey of c.1.8 km takes approximately one hour to complete one-way.

The level of access difficulty to this platform (Section 3.2.1, Table 3.1) was counterbalanced by a number of site-specific factors that make this platform different from the other chosen ones and thus conditioned its choice. First, the platform is relatively undisturbed and the risk of losing the TMEM stations was relatively low. In fact none of the stations needed to be replaced during the study period (Table 3.7). It was also the only platform directly exposed to the NW direction and, lastly, it is positioned along the exposed site of a promontory rather than enclosed within a recessed bay.

4.5.2 Background: Site and Situation

The shore platform of Ponta tal-Qammieħ extends from the headland area of Qammieħ situated on the western edge of Marfa ridge (Malta) and is located within the limits of the town of Mellieħa (Figure 4.2e). The Qammieħ area is located north of the Great Fault and coincides with its ridges and trough systems which position Marfa ridge as the last ridge on the island of Malta. The litho-stratigraphy of the area has been researched quite extensively as Marfa Ridge is the result of tectonic uplift by the Pantelleria Rift system and as a result has exposed the whole stratigraphic sequence of the Maltese lithology (Gianelli *et al.*, 1972; Pedley and Bennett, 1985; Carbone *et al.*, 1987; Rose, Pratt and Bennett, 1992; Baldassini, Mazzei and Foresi, 2013).

With its highest elevation reaching 129 m a.m.s.l at Ras il-Qammieħ, the landscape is typified from top to bottom by heavily fractured UCL plateaus (in Mtarfa Member and Tal-Pitkal Member) which cap the underlying sloping taluses of Blue Clay and the resultant boulder scree that collapsed from the unsupported UCL plateaus. The scree may extend from the UCL-BC junction all the way down to sea level and beyond and creating boulder-strewn coasts known locally as 'rdum'. Some parts of the more elevated Qammieħ parts include a full stratigraphic sequence which ends with the exposures of GL as elevated platforms and underlying vertical LCL cliffs (Figure 4.2e). A main W-E fault slices through Marfa Ridge from Rdum il-Qawwi with a northern downthrow and as a result, it has lifted Qammieħ area as the highest part of the Marfa Ridge and exposed a more complete stratigraphic sequence (Figure 4.2e).

Three small parallel faults also trend in an ENE-WSW direction from Ras il-Qammieħ in a seaward direction at a distance of between 50-70 m away from each other. Two of these faults have a SSW downthrow, whilst the third fault has a downthrow in a NW direction. The downthrow orientation of these three faults conditioned the contact point between sea level and the litho-stratigraphy at Ponta tal-Qammieħ, by bringing the MGLM close to sea level and submerging the underlying LGLM. This interrupted the LGLM exposure along Rdum il-Qammieħ coast and transformed this section of the coast into an rdum landscape for which the area aptly was named after. A third fault (with a NW downthrow) positions LMGL as an elevated platform along the south-east side of Rdum il-Qammieħ, whilst the upper fault with a SSW downthrow direction places LMGL as shore-level as a shore platform known as Ponta tal-Qammieħ and is backed by MGLM cliffs. Thus, tectonic structure has helped to create one of the very few shore platforms along the NW side of Malta. This region is mostly well-known for its rdum coastlines, rectilinear cliffs such as Ras il-Pellegrin and sporadic embayed beaches of sandy or mixed coarse-clastic sediment such as Fomm ir-Riħ, Ramla tal-Mixquqa or Ġnejna. Very little mention is however ever made about the geomorphological significance behind such a unique platform development in the area.

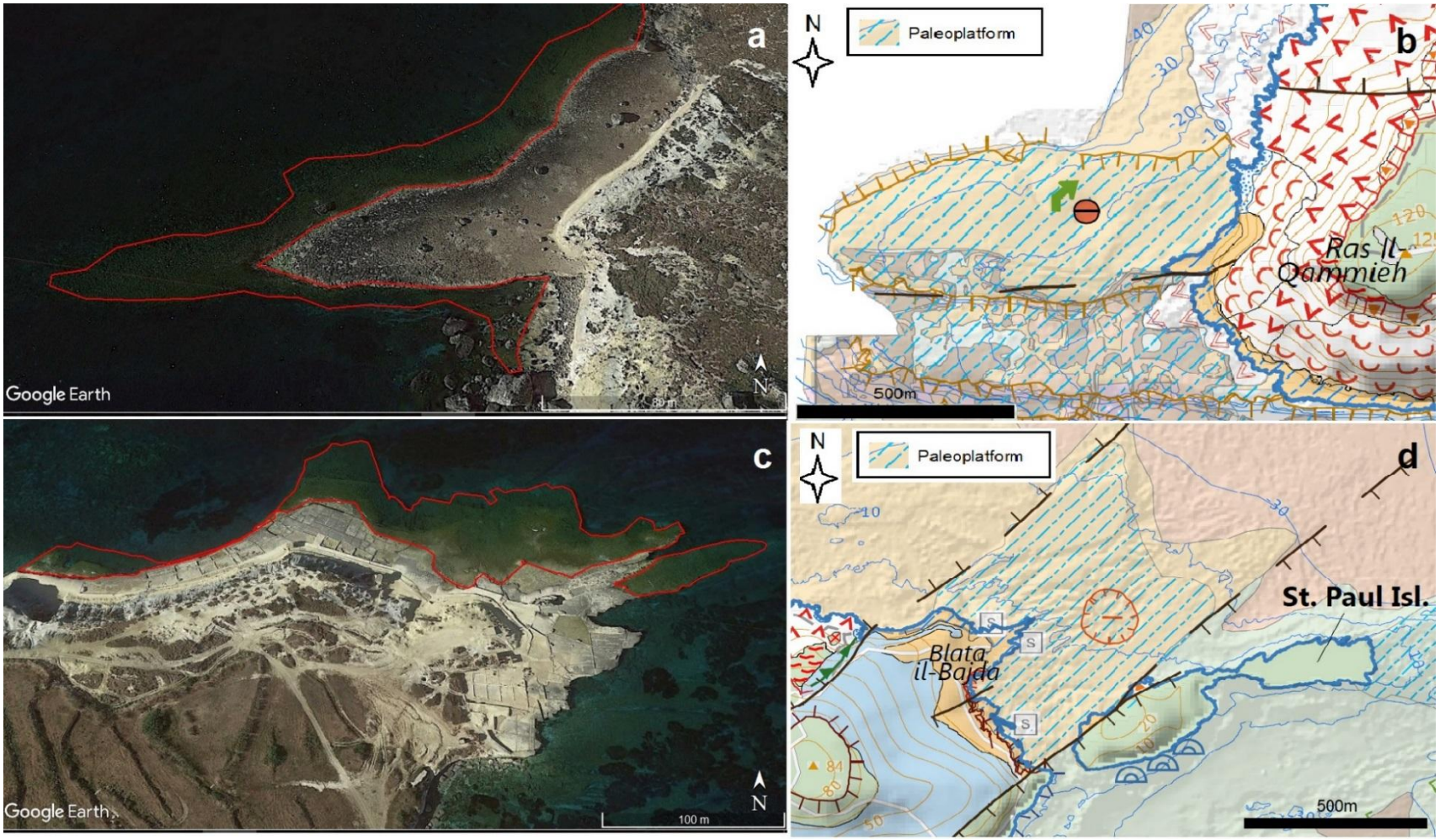

Figure 4.9: a. Subtidal platforms as visible from Google Earth for Qammieħ and c. Blata l-Bajda with perimeter outlined; mapping of the paleoshorelines for Qammieħ (b) and Blata l-Bajda (d) according to Prampolini *et al.*, (2017)

Snorkelling surveying and Google Earth image analyses, conducted by the author, showed how the entire platform is within a relatively shallow bathymetric zone of not more than 10 m in depth and the highest elevation was recorded to be of c. 4 m above sea level. From the tip of the platform till its north-east end, the platform visibly slopes gently below sea level at a distance of c. 27 m from the shoreline and reaches depths of c. 1.5 m below sea level. The submerged visible part at the tip of the peninsula is more extensive and measured a distance of c. 139 m from the tip. This total visible submerged part of the platform was recorded to have a seaward perimeter of 520.6 m and a total surface area of 7,486 m^2 (Figure 4.9a).

Yet, a recent palaeo-geographic reconstruction by Prampolini *et al.* (2017) of the bathymetry and sea floor morphology of the north-west of Malta, reveals two interesting facts about the paleo-landscape of Ponta tal-Qammieħ (Figure 4.9c). First, the study suggests the possibility of a seafloor fault displacement trending in a westerly direction along the southern edge of the platform. The inferred fault was mapped as extending offshore over a distance of c. 640 m and reaching depths of -40 m. This fault line was inferred from acoustic back-scatter evidence which traced how bathymetric depth contours deviate in a typical fault-displacement manner.

A second finding was the presence of a much more extensive submerged palaeo-platform belonging to a paleolandscape during the last glacial maximum when sea level lowstands were c. -130 m. According to Micallef *et al.* (2013) paleoshore terraces on the Maltese Islands were shaped between 60 kyr and 20 kyr (Figure 4.9c). These terraces were interpreted as shore platforms formed by subaerial weathering during maximum lowstand exposure at 20kyr and subsequent wave erosion during post-glacial sea level rise which retreated landward the coastline. Prampolini *et al.* (2017) map the Qammieħ paleoplatform as extending offshore in a westerly direction over a distance of c. 0.9 km from the present shoreline and reaching bathymetric depths of -40m. It terminates with a structural scarp edge which encircled the entire palaeoplatform and ended landward along the exposed scarp edge of the

present shore platform on the southern side (Figure 4.9c). Based on the dimensions mapped by Prampolini, it was estimated to have a surface area of 568,000 km^2. This study confirms therefore that the shore platform at Ponta tal-Qammieħ is the only remaining exposed part of this paleoplatform, following post-glacial sea level rise in the Holocene which drowned 450 km^2 of former terrestrial and coastal landscape of the Maltese Islands (Micallef *et al.*, 2013).

4.5.3 Morphological field assessment and mapping

The shore platform at Ponta tal-Qammieħ is the largest platform in this study with a perimeter of 496.7 m and a total surface area of 7327.9 m^2 (Figure 4.10) Its longest cross-shore axis - from the cliff-platform junction to the tip - is 215.2 m and is oriented at 260^0 (WSW). Its longest parallel axis is 326.5 m in width. The cliff-platform junction is 131.8 m long. The elevation of the MGLM cliffs increases from 9 to 15 m in a north-easterly direction in line with the closest fault in the area trending ENE-WSW with a SSE downthrow (Figure 4.2e). This fault has brought the MGLM in juxtaposition with the LGLM at mean sea level. The platform gently dips in a north-easterly direction with a parallel gradient of 5^0 from the low cliff edge which then gradually decreases to 3^0 in the northern end, where the platform terminates at mean sea level and the MGLM comes once again in contact at mean sea level.

The platform edge slopes from the backshore to the foreshore at a 6^0 gradient but the northern sections have a gentler cross-shore gradient of 4^0. As seen in Figure 4.2e, within this structural setting, the platform is flanked on both sides by *rdum* landforms in MGML. Their presence has limited substantially the accessibility of the platform from land. A number of large boulders in UCL have also been transported from the upper *rdum* areas and deposited on the platform. This may indicate that the earthflow and landslide dynamics in the area are quite active. Substantial quantities of boulders have also fallen in the nearshore waters on the southern side of the platform. This adds a dynamic input to the platform system, not encountered on the other platforms. It confirms the importance of investigating the cliff-platform coupled

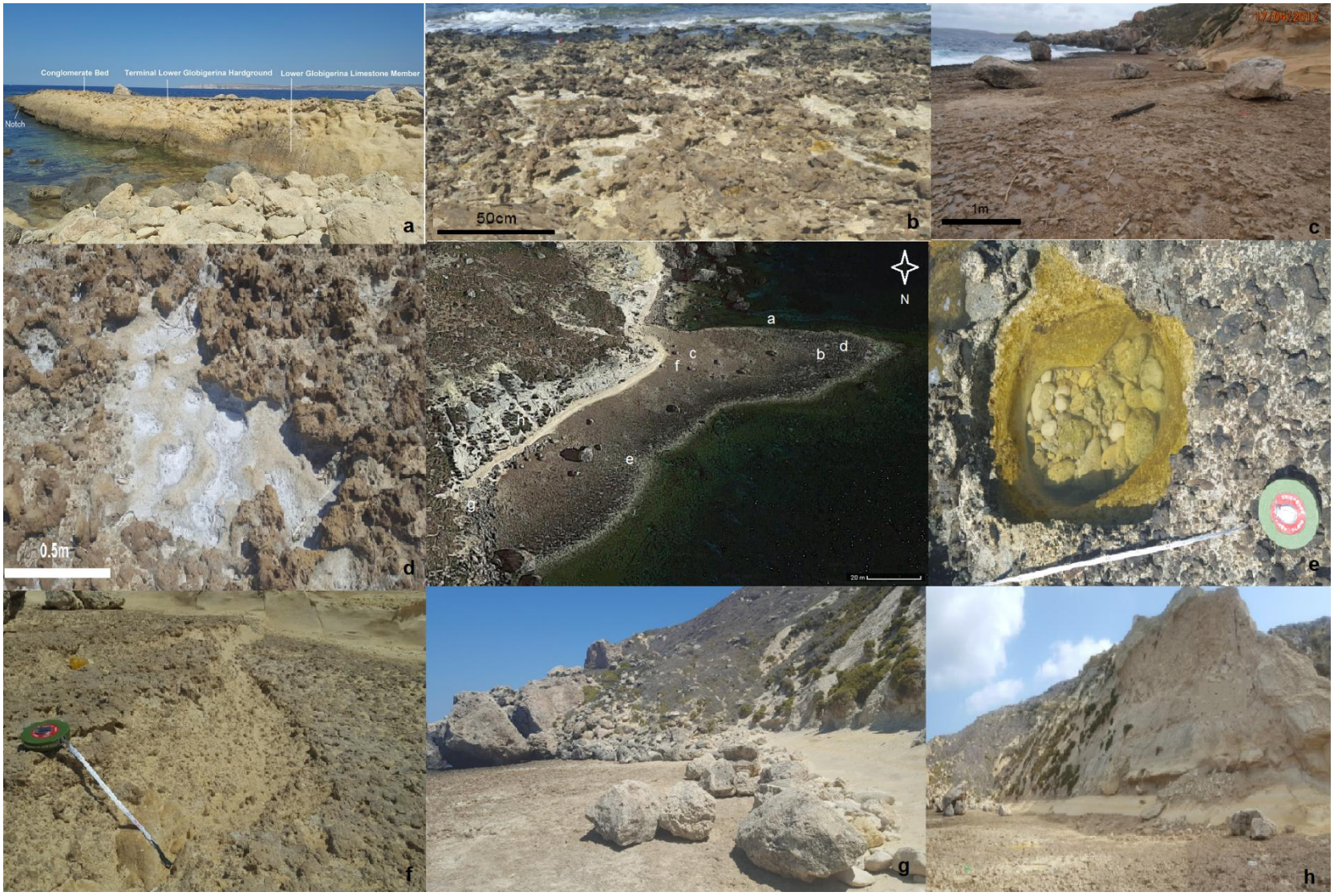

Figure 4.10: Main morphological characteristics of Pont tal-Qammieħ a. South low-tide cliff with stratigraphy of C_1 bed, TLGHg and LGLM; b. Foreshore in thick C_1 bed; c. Backshore in thin C_1 bed; d. Dry solution pools in C_1 bed; e. Abrasion pools in foreshore zone; f. Detachment scarp along W-NNE fault; g. Mixed boulder fields from rock falls and landslide; h. MGLM cliffs close to W-NNE fault (Source: Photos taken by Author)

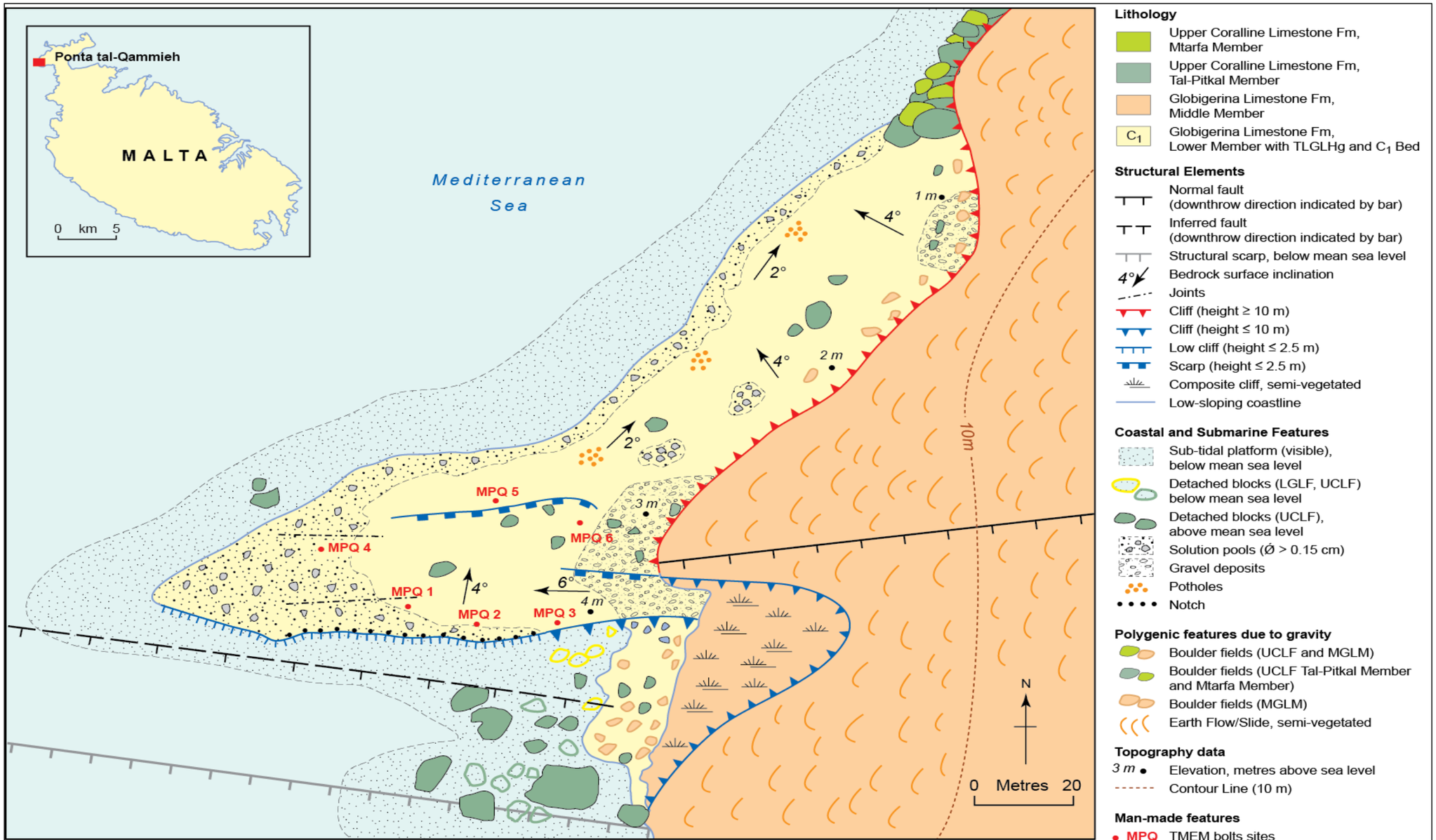

(Source: Base map re-drawn from Google Earth Image. Imagery date 15/4/2013)

Figure 4.11: Geomorphological map of Ponta tal-Qammieħ (Source: Base map from Google Earth and compiled by Author).

system in order to fully assess the morphodynamics systems that contribute to processes of change on the platform surface.

The lithology of the platform corresponds to a well-developed C_1 conglomerate bed, overlying TLGLHg and LGLM and backed by steep sloping MGLM cliffs (Figure 4.10a). In this region, the bed provides an effective lithostratigraphic marker to separate the LGLM from the MGLM. In fact, the C_1 bed at Qammieħ is such a good representative example that its genus term was renamed as 'Qammieħ bed' by Bennett (1979) and subsequently as 'Qammieħ Conglomerate Bed' by Rose, Pratt and Bennett (1992). The C_1 bed at Ponta tal-Qammieħ is quite a prominent hard bed, one metre in thickness and composed of brown phosphatic nodules, glauconite granules and a diverse array of allochthonous fauna in a phosphotized state such as molluscs, echinoids, pteropods and solitary corals (Figure 4.10b). These occur in the form of moulds and casts within the conglomerate level and are intermixed with unphosphatized fauna assemblages such as ostreids, pectinids and bryozoans (Baldassini, Mazzei and Foresi, 2013). Carbone *et al.* (1987) also observed extensive filling of the burrowed systems with phosphorite intraclasts and cream, planktonic foraminiferal wackestones and packstones. The surface lithology of this platform is therefore made extremely complex and varied not only by the presence of thick conglomerate clasts but also compounded by the rich presence of fossils within its grain structure.

The planar development of the C_1 bed on the platform is not uniform in thickness. It is more developed in a homogenous bioturbated surface in a seaward direction, and decreases in thickness towards the backshore area, where more TLGLHg outcrops are exposed in the upper central parts of the platform (Figure 4.10c). This has conditioned the surface roughness of the platform, with more rugged sharp mounds and flat-depressions in the front (Figure 4.10b) and mid-sections of the platform and relatively smoother surfaces at the backshore (Figure 4.10c), where the bed thins out and exposes either hardground and extends into MGLM (in closer proximity to the cliff platform junction). The combination of this lithological characteristic, together

with the fact that the front and mid sections of the platform are subject to more wave action from the north-west and north-east, have resulted in the development of a dark, heavily karstified foreshore with numerous flat-floored solution pools and solution-pitted surfaces (Figure 4.10d). The increase in conglomerate thickness in a seaward direction and the proximity to wave action may therefore produce different responses to weathering and erosion processes when compared to the thinner sections but less exposed sections at the back of the platform.

A notch was also identified at the base of the low-cliff side extending from the cross-shore mid-section of the platform base to about 39.4 m in a westerly direction. From mean sea level it extends to a maximum height of 1.5 m and a maximum depth of 1 m. Rocky substrate limpets were observed in the inner recess of the notch, The organisms are typical of the mediolittoral zone and tolerate more or less regular immersion in seawater but not continuous submersion (Schembri *et al.*, 2005). The notch is present only in the middle section of the platform cliff. It thins out in landward direction, whereas in a seaward direction, the scarp line is interrupted by the sloping gradient and the presence of irregular karst topography at the exposed seaward edge of the platform (Figure 4.11). The development of the notch along the low-cliff side indicates mechanical wave action coming from a prevailing west-north-westerly direction. To what extent such mechanical wave action is influencing rates of change on the platform surface in the immediate supratidal vicinity can only be inferred by the presence of another two morphological features located above the notch: the solution pools on exposed LGLM surface and the backwearing scarp above the low-tide cliff.

The first type of pools is mostly formed on relatively smoother LGLM exposures found the middle section of the platform (along the low cliff side) (Figure 4.10). The pools in the exposed sections are shallow with a diameter of between 0.4 m to 1 m wide and a rim height of between 0.1m to 0.2m high. They do not vary so much in dimension and shape: they are mostly spherical and regular in shape. Their development has occurred on LGLM surfaces that have

been stripped off from the overlying C_1 bed, the limit of the erosional stripping is marked by a backwearing scarpline, 0.5 m in height, above which the platform reaches its present elevations with the hardground and overlying C_1 bed.

A second type of solution pools are localised mostly along the foreshore part of the platform at cross-shore distances between 4 to 12 m away from the shoreline. They are morphologically different from the ones on the LGLM exposures, since they have formed in the thicker and rugged C_1 bed (Figure 4.10d). Although they generally have a flat basin, (some with smaller circular sub-depressions in them), the rugged morphology of the surrounding C_1 bed has shaped these pools into irregular, roughly-edged forms having steep sides and overhanging lips. Their depth is generally within the range of 0.3 m to 0.6 m, their width was measured to vary from 0.2 m to 6.5 m in diameter. Some of these irregular forms are the result of coalescence of several smaller pools into singular larger units. Some of the largest pools were measured in the platform area close to the faulted section and at the tip of the platform. Most of the pools located within three metres from the shore remain perennially wet with sea water all year round. Landward, these pools become pronouncedly drier especially in summer and consequently sea water evaporation develops white salt evaporates which cover uniformly the flat bottom of these pools (Figure 4.10d). The combined mechanisms of lithological-controlled roughness, wave action and evaporation seem to be work synergistically in the development of these solution pools which form from the entrapment of onshore sea water in surface depressions, which then evaporates to create salt weathering.

Mechanical wave action in the foreshore areas, specifically in the three areas along the breaker zone, is evidenced by a network of marine potholes (Figure 4.10e). A total of 17 potholes (some inter-connected) were observed to be deep-sided, conical in shape and some (though not all) had trapped abrasive material at the bottom (Figure 4.10e). The abrasives were found to be coarse and rounded material ranging from cobbles to gravel deposits. The lower section of the potholes were smoother and polished whilst the upper sides were

rougher and pitted. Such vertical zonation of surface roughness within the potholes would suggest more active abrasive processes by the gyratory flow of the abrasives in the lower sections of these potholes. The presence of these potholes would therefore indicate a wave dominant zone, with mechanical erosion facilitated by the supply of clasts which get plucked off from C_1 bed surface and act as abrasives in the area. Measured rates of surface change may therefore be varied depending on such type of site-specific mechanisms and controls.

When considering the relative vicinity of this platform to a normal fault, there is relatively minimal discontinuous structure within this unit and very few joints and fractures (Figure 11). Two low detachment scarps trends across the platform from the cliff-platform junction to the shoreline in a westerly direction. Both scarps mark the continuation of the ENE-WSW fault dissecting through the overlying MGLM cliffs from the overlying UCL plateau at Ras il-Qammieħ. Both scarps reach a displacement vertical level of not more than 0.4 m (Figure 4.10f). They were both measured to have lengths of 18.3 m (upper part of platform) and 37.6 m (mid and lower part of platform). The central part of the scarp exposes well the planar and underlying convoluted characteristics of the conglomerate bed above the LGLM.

Two cross-shore joints also intersect in a similar ENE-SWS direction the front section of the platform. They are 18 m and 25 m long and not more than 0.2 m wide and 0.4 m in height. They have a relatively smooth U-shaped cross-section with flat and pitted floor characteristics, which would suggest widening from salt spray solution. The presence of these joints was not deep enough to develop a joint-bounded bouldered perimeter as observed at Ponta tal-Miġnuna. Continuous wave quarrying and solution weathering by sea spray have however developed a series of vertical joints which dissect the low-cliff convex shaped edge of the platform.

The platform surface is also characterised by a series of boulder fields and finer sediment accumulations. The two main boulder clusters, made up of both UCL and MGLM deposits, flank the outer extreme ends of the platform and

are situated at the foot of the MGLM earthflows coming in direct contact with mean sea level (Figure 4.11). The dimension and distribution of these deposits is quite varied and intermixed; their dimensions range from cobble sized (Ø 64-256 mm) to boulder megaclasts (Ø over 256 mm). They are additionally surrounded by smaller deposits in pebble (Ø 4-64 mm) and gravel (Ø 2-4 mm) size. The reason for such variable dimensions is that these boulders fields have accrued from a mix of sediment sources. The larger deposits were sub-aerially transported downwards by rock falls, rock topple and rock sliding from the overlying *rdum* systems (Figure 4.10g). The smaller deposits were transferred downwards by the MGLM earthflow systems, whereas the relatively more rounded gravel and pebble sediment would have been transported onshore by wave action and trapped onshore between the larger sediment.

Apart from these boulder fields, another two distinct sets of finer sediment accumulations were identified at the backshore (Figure 4.11). The first one is generated by the loose consolidated nature and densely jointed structure of the exposed MGML grey marls, where slumping occasionally occurs along these beds. Mass wasting material gets washed downslope and accrues along the concave-upward base of these marls. This process is mostly driven by sub-aerial processes with wetting and heavy rainfall considered as principal triggers for slide lubrication and loading of the material mass (Stephenson, Dickson and Trenhaile, 2013a).

The second type of sediment deposits are pockets of well-sorted gravel sediment that were identified at the backshore of the platform. This sediment was mostly found to accrue either in hollows and depressions formed by the rugged surface of the C_1 bed and underlying TLGLHg or close to the boulder field present on the northern section of the platform. The possible source of this gravel may be marine, from where initially it is washed ashore and then transported by aeolian processes at the back of the platform and is deposited as well-sorted sediment with a low variance in size. The presence of such sediment at the landward margin of a platform is generally considered quite

typical on many platforms and its abrasive role is mostly significant along the cliff-platform junction (Stephenson, Dickson and Trenhaile, 2013a).

The MGLM cliffs skirting along this platform are steep sloping and mostly densely vegetated in the upper sections (Figure 4.10h). Stratigraphically, they generally consist of an uneven horizontal sequence of yellow calcareous limestone at the base, thick sections of grey limestone and marly limestone in the mid-section of the cliffs, and thinner inter-bedded strata of yellow calcareous limestones and greyish limestone marls at the top sections. Some of the more resistant marls produce overhangs overlying relatively weaker ones, which break and collapse when over-steepened by the underlying weaker marl. The more elevated northern sides of the cliff have a more uniform steep sloping profile and are thickly covered with a dense matt of Mediterranean salt steppe. The southern side of the platform, close to the low-cliff edge, is backed by a faulted and composite-type of cliff morphology. Cliff crumbling is also present along the various exposed faces of these cliffs. The composite profile of this cliff section is attributed to the combined result of fault displacement and its relative position in the sheltered side of the platform, where it is better buffered by the wide frontal expanse of the platform and less exposed to onshore high impact waves generated by the north-westerlies and the north-easterlies. Sub-aerial processes are therefore more effective in the overall contemporary profile evolution of this part of the cliffs.

4.6 Selmun: shore platform of Blata l-Bajda

4.6.1 Access to shore platform of Blata l-Bajda

The shore platform of Blata l-Bajda (35°58'02.82"N, 14°23'45.43"E) can be accessed from two main departure points: either from Fort Campbell hill (84m a.m.s.l) or from Mistra Battery (en route from Mistra Bay). Two off-road pathways connect Fort Campbell to Blata l-Bajda: a 1.3 km front route or a 1 km back route, both leading steeply down from the hill. Both these routes are not accessible for vehicle traffic and can only be reached on foot in 30 minutes. The Mistra Battery route is also an off the beaten coastal track from Mistra Battery

and also not accessible by vehicle. The route is 1.3 km long and Blata l-Bajda can be reached in a 25 minute journey on foot.

4.6.2 Background: Site and Situation

The shore platform of Blata l-Bajda is situated within the coastal area of Selmun in the north-east part of Malta, in the vicinity of the localities between Mellieħa and Xemxija. Selmun form part of the Mellieħa locality boundary and covers a total land area of 3.21 km^2. The north, east and the south of Selmun are bound by the sea with Mgiebaħ Bay, Blata l-Bajda, St Paul's Islands, Rdum il-Bies and Mistra Bay. The hinterland areas provide large stretches of sloping agricultural land. The historical landmarks of Selmun Palace (built by the Knights of St John in 1870) and Fort Campbell (built in 1937 by the British) are located at the top of a relatively gentle sloping promontory with the highest elevation of 110 m close to Selmun Tower. The western side borders a high-end residential area known as Santa Marija Estate.

The physical setting of Selmun area is closely linked to the tectonic structure processes present in the northern part of the Maltese Islands. Selmun is located north of the Great Fault and forms part of the ridge-trough sequence made up of Bajda Ridge, the Miżieb syncline (depression), Mellieħa Ridge and part of the Mellieħa Valley. A set of five normal faults, mainly tending SW-NE, have created contrasting topographies at Selmun and conditioned the surface exposure of five different litho-stratigraphies: MGLM, UGLM, BC, UCL (Mtarfa Member and tal-Pitkal Member). The central part of Selmun is characterised by a relatively gentle promontory expanse of the Mtarfa Member of UCL, surrounded by gentle sloping relief in BC. UGLM outcrops on the coastal fringes of Blata l-Bajda whilst both UGLM and MGLM surround the inner recess of Mistra Bay.

The coastal geology of Selmun has been largely influenced by the above-discussed tectonic structure. A SSW-NNE fault line, running from Mistra Bay to St Paul's Islands, has a SE downthrow and interrupts the coastal surface exposure of UGLM and MGLM at Blata il-Bajda and Mistra Bay respectively and

exposes UCL as Ras il-Miġnuna, Rdum il-Bies and St Paul's Islands (Figure 4.2f). Ras il-Miġnuna, and the whole St Paul's Islands – situated at the easternmost extent of the Bajda Ridge – are made up of the Tal-Pitkal Member of UCL. Rdum il-Bies inlet also exhibits Tal-Pitkal Member in its upper sections and Mtarfa Member in the lower coastal sections. At St Paul's Islands the fault brings the UCL layer in direct contact with the BC and exposes UGLM in the lowest sections of the cliff face at shore level. As a result of this fault system, Mistra Bay is also enclosed by two headlands – Ras il-Miġnuna and Rdum Rxawn – both made up of UCLM. A central axis of fold syncline extends from the outer shores of Rdum il-Bies into a northerly direction through St Paul's Islands, shaping the centre of the islands with a gentle convex topography and sloping relief towards its north-east.

Beneath the BC slopes of Selmun and closer to the shoreline, outcrops of UGLM border the northern coastlines of Għajn Ħadid, Mġiebaħ Bay and up to Ras il-Griebeġ, But the most dominant exposure of UGLM at Selmun is at Blata l-Bajda, which takes its Maltese name (Blata means 'rock' and Bajda means 'white') after the presence of low but extensive sub-horizontal platforms, most in light pale yellow-cream coloured exposures units, created by UGLM (Figure 4.12a). The platform is surrounded by a wider expanse of shallow sub-tidal platform. The visible part of this platform was measured to have a perimeter of 1447 m and a surface area of 17,063 m^2 and reached depths of not more than 5m (Figure 4.2b). Based on the study by Prampolini *et al.* (2017), this sub-tidal platform forms part of a larger paleoplatform, submerged during the Holocene sea level rise. The latter study maps this platform extending c. 0.7 km beyond the shoreline, reaching offshore depths of 20m below sea level and covering a surface area of 339,035m^2. The entire paleoplatform is also bounded by the two SW-NE faults that continue to trend offshore in a north-easterly direction (Figure 4.12).

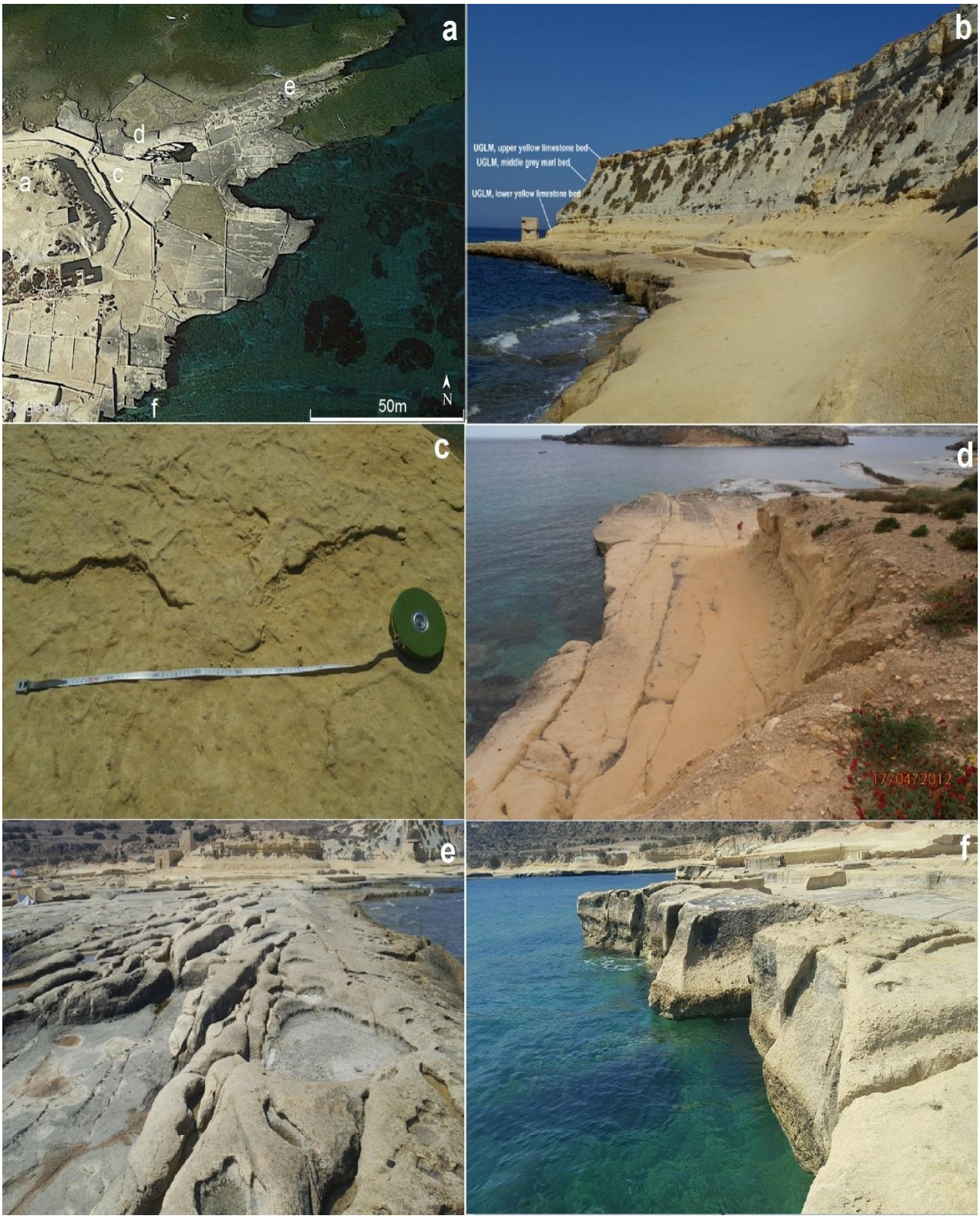

Figure 4.12: Main morphological characteristics of Blata l-Bajda platform a. Google Earth map with main features; b. The three main UGLM beds; c. Flaking and splintering on platform surface in lower yellow limestone bed; d. SE-NW fault-driven joints; e. Frontshore area of platform; f. Low-tide cliff with C_2 bed (Source: Photos taken by Author)

This platform is considered the most atypical from the five platforms chosen for this study in terms of its past history of intensive development. Blata l-Bajda was extensively developed into salinas in the 1930's by the Calafáto company. The company took over both platforms and transformed them into large salinas for tanning of animal hides for a tanning factory at Marsa. At the time, it was the only salinas that were developed for industrial purposes other than salt collection. A total of c.90 pans were developed over the entire platform. The units, mostly rectangular in shape, had dimensions ranging from 1 to 312 m^2. They were still in use up to the early nineties; a 1993 storm damaged the salinas beyond repair and operations were abandoned. The Blata l-Bajda coast is exposed in a north-easterly fetch from where the *Gregale* winds may deliver high impact waves. The area is in fact linked to the biblical narrative of St Paul's shipwreck by a *Gregale* storm. The islands opposite Blata l-Bajda, in fact take the name of the saint for such a reason. Interestingly, St Paul's Islands also feature a small UGLM shore platform and is joined with the rest of the paleoplatform present in the bay.

4.6.3 Morphological field assessment and mapping

Blata l-Bajda consists of smooth UGLM outcrops in the lower yellow bed and spatially make up of two distinct sections separated by a SW-NW fault line with a SE downthrow. The largest section is located north of the fault: it has an area of 17,158 m^2 and a coastal perimeter of 970 m (Figure 4.12 and Figure 4.13). The second part of the platform is situated south-east of the fault and has a relatively smaller surface area 8,887 m^2 and a perimeter of 475 m. They both exhibit a dip of 5^0, with an easterly direction at the largest section and a south-easterly direction at the second platform. In order to provide sufficient morphological detail related to this platform, only the largest section was chosen for this study. This section, apart from being the largest section, included most of the same morphological features (elaborated further in this section) which were present in the smaller sections and thus it was a good representation of the entire platform area.

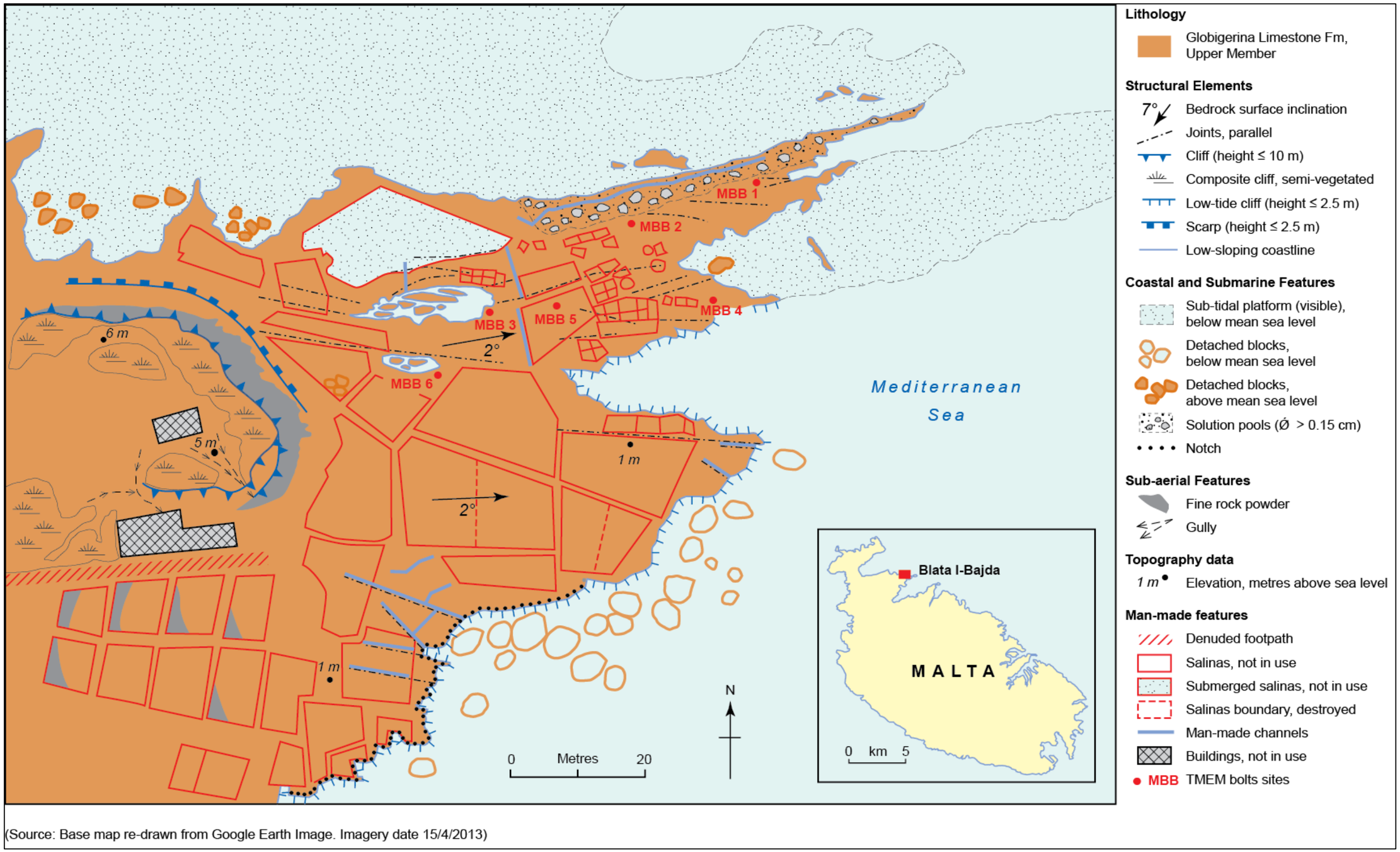

(Source: Base map re-drawn from Google Earth Image. Imagery date 15/4/2013)

Figure 4.13: Geomorphological map of Blata l-Bajda (Source: Base map from Google Earth and compiled by Author)

As explained in Chapter 2 (Section 2.6) shore platforms in UGLM are generally scant on the Maltese Islands. The shore platforms at Blata l-Bajda represent one of the few but most extensive platforms consisting of this geological unit. These sub-horizontal platforms are bound between three SE-NW faults and are also strongly geologically controlled. The platform of Blata l-Bajda has developed within the lower yellow limestone bed which is found very close to mean sea level and is relatively more resistant than the overlying grey marl bed. Differential erosion responses at sea level led to the formation of resistant sub-horizontal platforms by the lower yellow bed, with low cliffs of soft grey marl retreating further inland from these platforms. Horizontal alternation of the three member beds is visible along several parts of the cliff-platform junction, with the grey marl beds reaching elevations of up to 17 m a.m.s.l. at the very end of the western side of the platform of Blata l-Bajda (Figure 4.12b).

Towards a north-northwesterly direction, there are no significant topographic breaks and the platform slopes gentle towards the sea at a gradient of 2^0 to gentle shallow sub-tidal platforms. The UGLM lower yellow limestone bed, albeit relatively more resistant than the overlying UGLM grey marls, has a weathered, powdery surface. The backshore areas exhibit flaking weathering forms such as surface exfoliation and granular disintegration such as splintering (i.e. the detachment of irregular surface stones into splinters (Figure 4.12c). Fine yellow stone powder – presumably in UGLM – was observed deposited at the back of the platform, close to the break of slope between the UGLM yellow bed and the overlying grey marl bed. The overlying presence of steeper but softer UGLM grey marl layers, above the platform, also contributes to further input of fine sediment at the cliff-platform junction. However, the low marly cliffs are also channelled vertically by gullies which transport downwards boulder and coarse-grained sediment and deposit them as pockets of fanglomerates at the various points along the cliff-platform junction. Seasonal field visits have noticed how these deposits are subsequently reworked by other gully deposits but also by marine wave action.

The surface morphology of Blata l-Bajda has been largely influenced, not only by its lithology, but also by the SE-NW faults trending in the area (Figure 4.12d). Joints, inherent both by the site structure but also in the lithology are spaced at intervals ranging between 0.35 -1 m and are mostly oriented SW-NE in an cross-shore pattern to each other and give the platform the appearance of a blocky limestone pavement. The hewing of the salinas along these joints has further augmented such appearance and has not left much of the original solution pools. The joints in the gentle sloping foreshore zone, though tectonic in origin, have been considerable widened and excavated into a densely furrowed limestone pavement through a combination of mechanical wave action and solution weathering. The pavement channels were measured to have an average width range between 0.05 to 0.15 m. As they reach closer to sea level, they branch out into thinner strands of pitted and sinuous limestone dissections (Figure 4.12e). As a result of this, the foreshore zone surface morphology presents an irregularly shaped and hummocky terrain, contrasting with the smoother pale yellow topographies at the backshore. Most of the original jointed terrain (i.e. not modified by the salina construction) is visible mostly on the central part of the platform. It is on this type of natural terrain, that most of the TMEM bolts sites (5 out of 6) been installed.

The joints have also channelled seawater infiltration at subterranean levels, which has weakened parts of the platform by solution weathering and eventually led to the eventual collapse of the platform surface into the sea and the creation of an inland basin filled with collapsed boulders and regular sea water infiltration (Figure 4.12d). It is not altogether clear to what extent the operation works of the salina construction may have been deleterious to the widening of these subterranean joints and destabilising the structure of the platform. The perimeter of the collapsed basin confirms with the perimeter of abandoned salina, which would indicate that the hewing of these pans may have irrevocably weakened parts of the platform. Since the abandonment of the salinas, visible fractures trending SW-NE have developed at the base of the units, indicating the high degree of physical susceptibility to weathering of this

lithology. Some of the SW-NE joints have also sliced parts the platform edge into joint-bounded blocks, which then fell into the sea.

With a northerly dip, the platform edge rises into a low-tide cliff at its southern side (Figure 4.12f). It is along this side that the C_2 bed (between the lower yellow limestone bed and the MGLM) emerges above sea level and skirts upwards along the platform perimeter in a southerly direction and where it reaches maximum elevations of 2 m above sea level. A roof notch has developed where the resistant C_2 is c. 0.20 m above wave action; at such height, there is enough space for MGLM to be eroded by wave action. At its maximum elevation, this resistant conglomerate bed has sufficiently exposed the MGLM to wave quarrying to lead to rapid undercutting of the overlying UGLM and the eventual collapse of the UGLM cliff blocks into the sea. This process does not proceed further south because it is interrupted by the SW-NE fault, which downthrew the UGLM lower yellow limestone bed by 5 m and brought the two members in juxtaposition with each other.

Given the micro-tidal regime present of the islands and the sub-horizontal structure of Blata l-Bajda, the intertidal regime is quite limited in its vertical and horizontal extent across the platform. Pitted and sharp karst surfaces are mostly dominant in the low-lying perimeters of the platform in touch with the sea water. The elevated sides of the platform, in the southern sides of the platform display wave undercutting and rock falls have accumulated in inlet formation. Submerged boulders have also been observed close to the perimeter of the sub-tidal platform in the parts exposed to the E-NE fetch from where strong *Gregale* winds bring high impact waves.

4.7 Synthesis

This chapter has demonstrated how the five investigated platforms present a wide range of geomorphological characteristics, mainly dominated by the presence of specific erosion and weathering forms at various scales. Despite bring broadly assigned to the same litho-stratigraphic formation i.e. Globigerina Limestone, these findings highlight the complexity of the Globigerina limestone

lithology at member level and most importantly, explain in part why Globigerina platforms exhibit such a wide variety of surface morphologies. The shore platforms exhibit a wide range of surface forms that are mainly controlled by variations in lithological efficacy and, to a certain extent, by exposure to prevailing waves, zonation of wave splashes and sea spray action and structural controls.

Table 4.2 collates all the field evidence of these observed forms, in order to illustrate their spatial assemblage across the five platforms. The wide variety of these forms clearly demonstrate that rock resistance on shore platforms can be broadly generalised on the basis on their lithology, variations between sites are strongly mediated by local scale parameters. Questions arise on whether such complexities may potentially affect the lithological resistance to forces of surface change and elicit the need to look closer of how the measured data of surface change may relate with in sub-lithological context.

The morphological variations between sites therefore calls for further geo-technical investigations on the lithology properties of each platform and examine to what extent these properties can be held accountable for the observed variations at local scale parameters. The results of these tests, discussed in the next chapter, will also help to provide further insights on the likely control-process-form responses in terms of surface change.

Table 4.2: A summary of the main surface morphological forms at the studied platforms (Source: Compiled by Author)

Type of forms	Description	Ras il-Fenek	Ponta tal-Miġnuna	Ponta tal-Munxar	Ponta tal-Qammieħ	Blata l-Bajda
Tectonic structure	Joints (orthogonal or conjugate)		✓		✓	✓
	Joint-bounded boulders		✓			
	Micro-fissures		✓			✓
	Detachment scarps		✓		✓	
Weathering	Solution pits (Ø ≤ 0.15 cm)	✓	✓		✓	✓
	Solution pools (Ø > 0.15 cm)	✓	✓	✓	✓	✓
	Micropits (< 0.01 cm)	✓	✓	✓	✓	✓
	Flaking				✓	✓
	Crumbling	✓		✓	✓	✓
	Splintering					✓
Erosional	Marine Potholes				✓	
	Surf notch and visor	✓	✓	✓	✓	✓
	Foreshore limestone pavements	✓	✓	✓	✓	✓
	Scarp frontal erosion		✓	✓	✓	✓
Sub-aerial	Tafone	✓	✓			
	Slumping		✓			✓
	Gullies		✓			✓
Depositional	Rock fall or boulder fields	✓		✓		✓
	Coarse-grained sediment				✓	✓
	Gully fanglomerates		✓			✓
	Tafone rock meal	✓	✓			✓
	Fine rock powder	✓	✓			✓
	Posidonia banquettes			✓		
Biological	Trace fossil borings	✓	✓	✓		
	Vegetation	✓				
	Medilittoral organisms	✓	✓	✓	✓	✓
Sub-tidal	Sub-tidal terrace/reef	✓			✓	✓

5 Weather conditions during the study period and surface resistance assessment of the platforms

5.1 Introduction

The findings of the geomorphological investigations, presented in Chapter 4, provide evidence of the varied morphological assemblages present on the five studied shore platforms. In particular, the findings reveal how the surface character of the platform differs at multi-scale level in terms of grade and modes of surface weathering and erosion, structural weaknesses (especially in terms of joints presence), spatial extent of bedding thickness and exposure. All these properties determine to various degrees the rock mass resistance to both erosion and weathering processes (Augustinus, 1991). As discussed in Chapter 2, aspects related to rock mass resistance have been studied extensively in the study of shore platforms and there has been a growing recognition on the need to elucidate better the mechanisms between the forces operating on these platforms and the resistance responses to such forces driven by the platform properties (Trenhaile, 2011a). Central to this theme is the role of lithological properties that was observed to determine the efficiency of the processes operating on shore platforms.

In this study, an outline of the weather conditions of the Maltese Islands during the study period is presented in the first part of this chapter (Section 5.2). The weather data provides a better context of the outdoor and ambient conditions in which rates of surface change were measured throughout this study. A more detailed weather record compilation, based on data from private local companies Maltaweather.com and Malta Underground was also compiled for the field visit dates in which TMEM data was collected and presented in Appendix II.

The rest of the chapter (Section 5.3-5.5) describes how rock surface resistance was investigated in two methodical tiers as follows:

i. As a compositional assessment, whereby the physical fabric (i.e. surface hardness) and mineralogical constituents of the platform lithology are investigated; and
ii. As a dynamic assessment, in which rates and modes of rock decay were monitored and recorded over a period of 18 months.

Four different tests fed into this assessment:

i. Compositional tests: Near-infrared spectroscopy (NIR)(Section 5.3) and Schmidt Hammer rock hardness test (Section 5.4); and
ii. Dynamic test: exposure and micro-catchment experiment (Section 5.5).

5.2 Overview of weather conditions of the Maltese Islands during the study period: 2012-2016

The description of the weather conditions presented in this section is based on the official weather data sourced from the National Meteorological Office in Malta International Airport plc in Luqa. The presented data highlight whether the conditions experienced during the study period followed the typical trends of a Mediterranean climate and if not, what sort of climate anomalies were recorded. Monthly temperature and rainfall data were subsequently used to test out the possibility of correlation between seasonal trends and TMEM rates of surface change (See Section 6.3.2.6).

5.2.1 Overview of main weather trends

In terms of temperature trends, illustrated in Figure 5.1 and Figure 5.2, the conditions were quite typical of the dual seasonal Mediterranean climate, with warm drier summers and mildly cold wet winters. Annual temperature

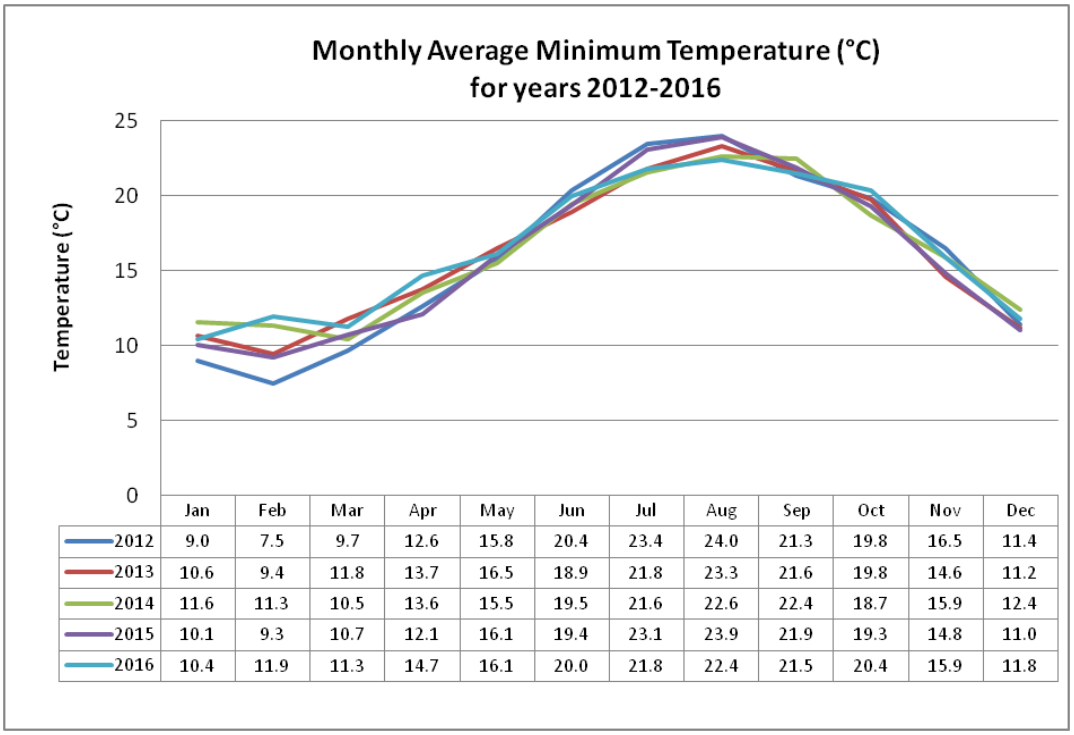

	Jan	Feb	Mar	Apr	May	Jun	Jul	Aug	Sep	Oct	Nov	Dec
2012	9.0	7.5	9.7	12.6	15.8	20.4	23.4	24.0	21.3	19.8	16.5	11.4
2013	10.6	9.4	11.8	13.7	16.5	18.9	21.8	23.3	21.6	19.8	14.6	11.2
2014	11.6	11.3	10.5	13.6	15.5	19.5	21.6	22.6	22.4	18.7	15.9	12.4
2015	10.1	9.3	10.7	12.1	16.1	19.4	23.1	23.9	21.9	19.3	14.8	11.0
2016	10.4	11.9	11.3	14.7	16.1	20.0	21.8	22.4	21.5	20.4	15.9	11.8

Figure 5.1: Monthly average maximum temperature for years 2012-2016

(Source: Mata National Meteorological Office, 2016)

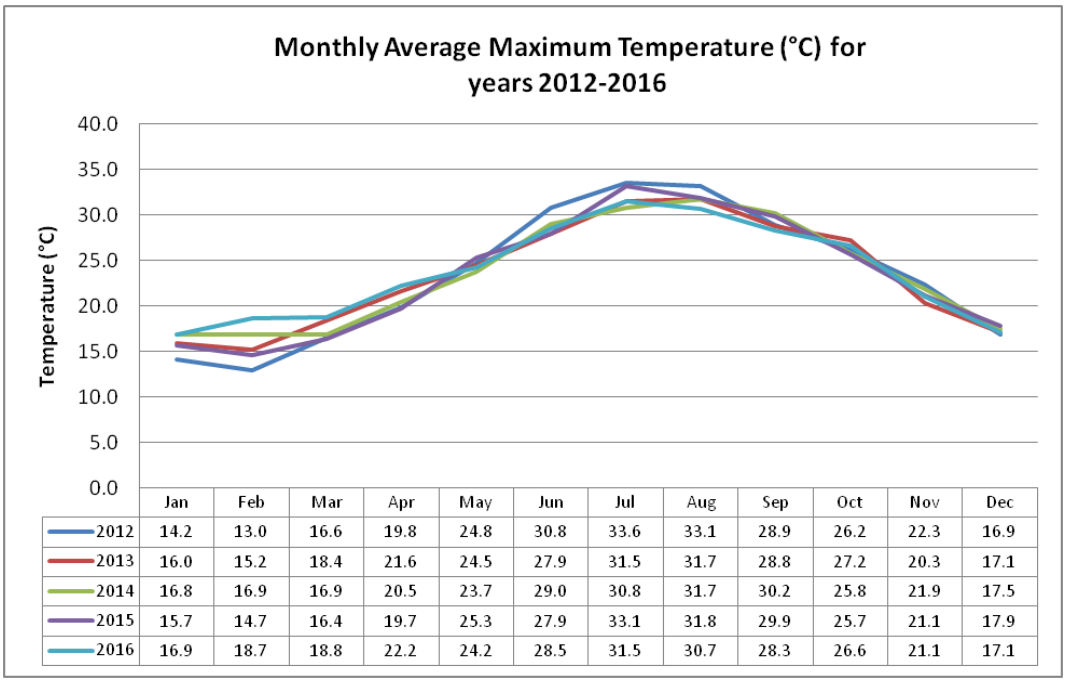

	Jan	Feb	Mar	Apr	May	Jun	Jul	Aug	Sep	Oct	Nov	Dec
2012	14.2	13.0	16.6	19.8	24.8	30.8	33.6	33.1	28.9	26.2	22.3	16.9
2013	16.0	15.2	18.4	21.6	24.5	27.9	31.5	31.7	28.8	27.2	20.3	17.1
2014	16.8	16.9	16.9	20.5	23.7	29.0	30.8	31.7	30.2	25.8	21.9	17.5
2015	15.7	14.7	16.4	19.7	25.3	27.9	33.1	31.8	29.9	25.7	21.1	17.9
2016	16.9	18.7	18.8	22.2	24.2	28.5	31.5	30.7	28.3	26.6	21.1	17.1

Figure 5.2: Monthly average maximum temperature for years 2012-2016

(Source Malta National Meteorological Office, 2016)

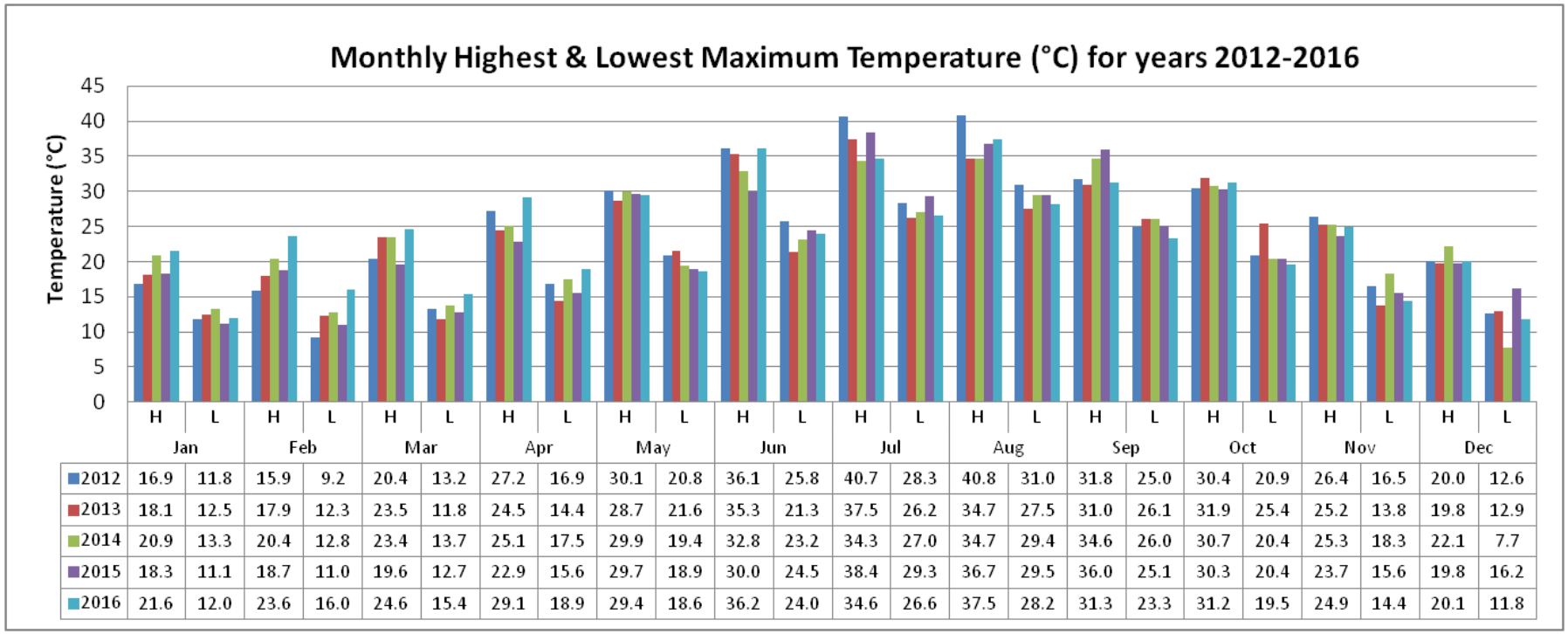

	Jan		Feb		Mar		Apr		May		Jun		Jul		Aug		Sep		Oct		Nov		Dec	
	H	L	H	L	H	L	H	L	H	L	H	L	H	L	H	L	H	L	H	L	H	L	H	L
2012	16.9	11.8	15.9	9.2	20.4	13.2	27.2	16.9	30.1	20.8	36.1	25.8	40.7	28.3	40.8	31.0	31.8	25.0	30.4	20.9	26.4	16.5	20.0	12.6
2013	18.1	12.5	17.9	12.3	23.5	11.8	24.5	14.4	28.7	21.6	35.3	21.3	37.5	26.2	34.7	27.5	31.0	26.1	31.9	25.4	25.2	13.8	19.8	12.9
2014	20.9	13.3	20.4	12.8	23.4	13.7	25.1	17.5	29.9	19.4	32.8	23.2	34.3	27.0	34.7	29.4	34.6	26.0	30.7	20.4	25.3	18.3	22.1	7.7
2015	18.3	11.1	18.7	11.0	19.6	12.7	22.9	15.6	29.7	18.9	30.0	24.5	38.4	29.3	36.7	29.5	36.0	25.1	30.3	20.4	23.7	15.6	19.8	16.2
2016	21.6	12.0	23.6	16.0	24.6	15.4	29.1	18.9	29.4	18.6	36.2	24.0	34.6	26.6	37.5	28.2	31.3	23.3	31.2	19.5	24.9	14.4	20.1	11.8

Figure 5.3 : Monthly highest and lowest maximum temperature for years 2012-2016 (Source: Malta National Meteorological Office, 2016)

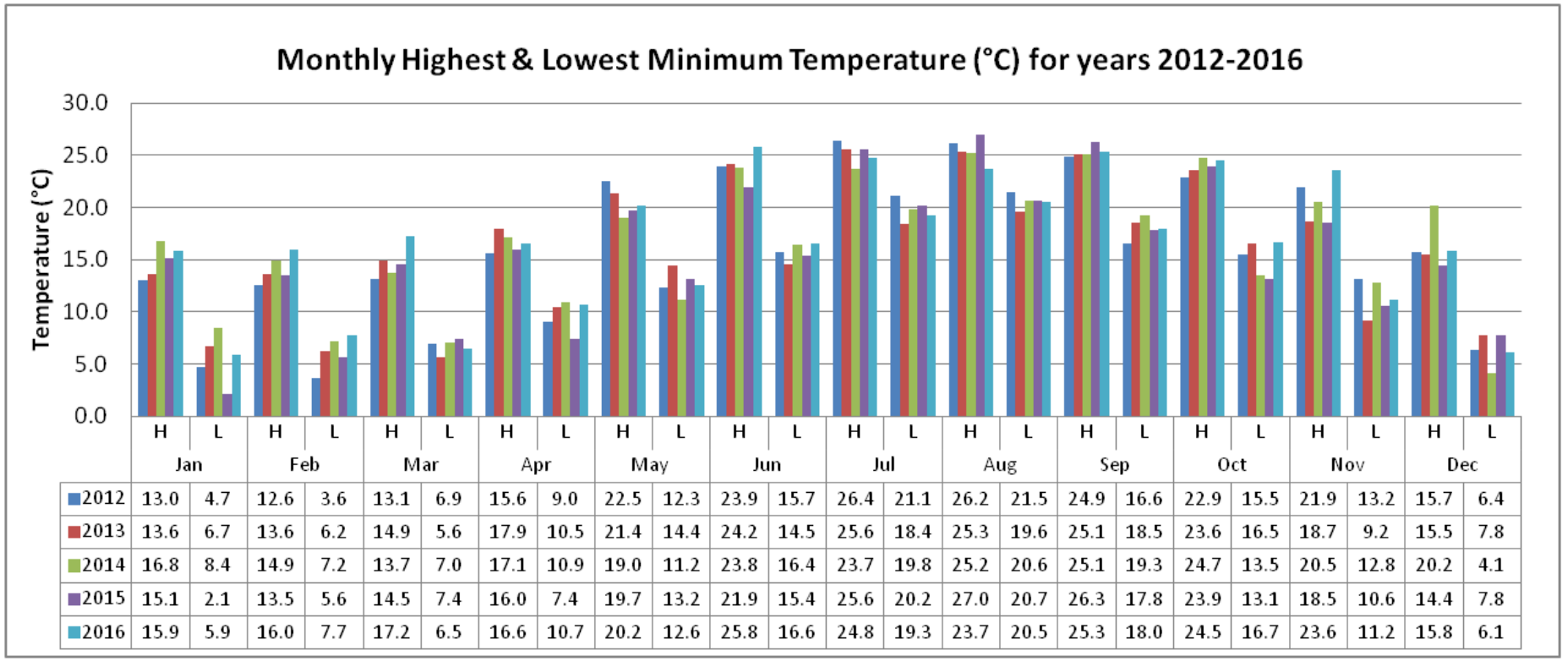

	Jan		Feb		Mar		Apr		May		Jun		Jul		Aug		Sep		Oct		Nov		Dec	
	H	L	H	L	H	L	H	L	H	L	H	L	H	L	H	L	H	L	H	L	H	L	H	L
2012	13.0	4.7	12.6	3.6	13.1	6.9	15.6	9.0	22.5	12.3	23.9	15.7	26.4	21.1	26.2	21.5	24.9	16.6	22.9	15.5	21.9	13.2	15.7	6.4
2013	13.6	6.7	13.6	6.2	14.9	5.6	17.9	10.5	21.4	14.4	24.2	14.5	25.6	18.4	25.3	19.6	25.1	18.5	23.6	16.5	18.7	9.2	15.5	7.8
2014	16.8	8.4	14.9	7.2	13.7	7.0	17.1	10.9	19.0	11.2	23.8	16.4	23.7	19.8	25.2	20.6	25.1	19.3	24.7	13.5	20.5	12.8	20.2	4.1
2015	15.1	2.1	13.5	5.6	14.5	7.4	16.0	7.4	19.7	13.2	21.9	15.4	25.6	20.2	27.0	20.7	26.3	17.8	23.9	13.1	18.5	10.6	14.4	7.8
2016	15.9	5.9	16.0	7.7	17.2	6.5	16.6	10.7	20.2	12.6	25.8	16.6	24.8	19.3	23.7	20.5	25.3	18.0	24.5	16.7	23.6	11.2	15.8	6.1

Figure 5.4: Monthly highest and lowest minimum temperature for years 2012-2016 (Source: Malta National Meteorological Office, 2016)

variability is linked to the regional weather patterns in the Central Mediterranean, and the moderating warming influence of the sea in winter and cooling during the summer period (Galdies, 2011). During the study period, July was recorded as the hottest month with a mean monthly maximum temperature of 32.1 ^{0}C over the five-year study period. The month of February was observed as being the coldest, with a mean monthly maximum temperature of 15.7 ^{0}C. The hottest month was July 2012 with a mean monthly temperature of 40.7 ^{0}C (Figure 5.1). With regard to monthly minimum temperatures, February also registered the lowest records, with a mean monthly minimum temperature of 9.9 ^{0}C and with February 2012 considered as the coldest with 9.2 ^{0}C (Figure 5.1). Monthly records of temperature variability are important to consider for this study as temperature fluctuations are considered significant drivers of weathering processes, especially in terms of thermal fatigue (Stephenson, Dickson and Trenhaile, 2013a). Within this context, it is important to note therefore the existence of temperature extremes recorded within the same month. As displayed in Figure 5.3 and Figure 5.4, monthly minimum and maximum temperatures may vary quite significantly across different months and most importantly, there is no defining season that may account more than other for higher variability. Just to mention a few examples: December 2014 recorded the largest variability, for both its highest-lowest minimum temperatures (16.1 ^{0}C) and its highest-lowest maximum temperature records (14.4 ^{0}C). Yet, large variable records can also be observed in other months: July 2012 (12.4 ^{0}C), June and July 2016 (12.2 ^{0}C and 12.4 ^{0}C respectively) for highest-lowest maximum temperatures and January 2015 (13.0 ^{0}C) and November 2016 (12.4 ^{0}C) for highest-lowest minimum temperatures.

Rainfall records during the study period, follow the dual seasonal trend of wet winters and relatively drier summers (Figure 5.5). However, the rainfall distribution with some monthly torrential peaks is worth noting, both in terms of total rainfall and number of rainy days. November 2013 was the rainiest month with 182 mm of rain falling over 19 days. Other months

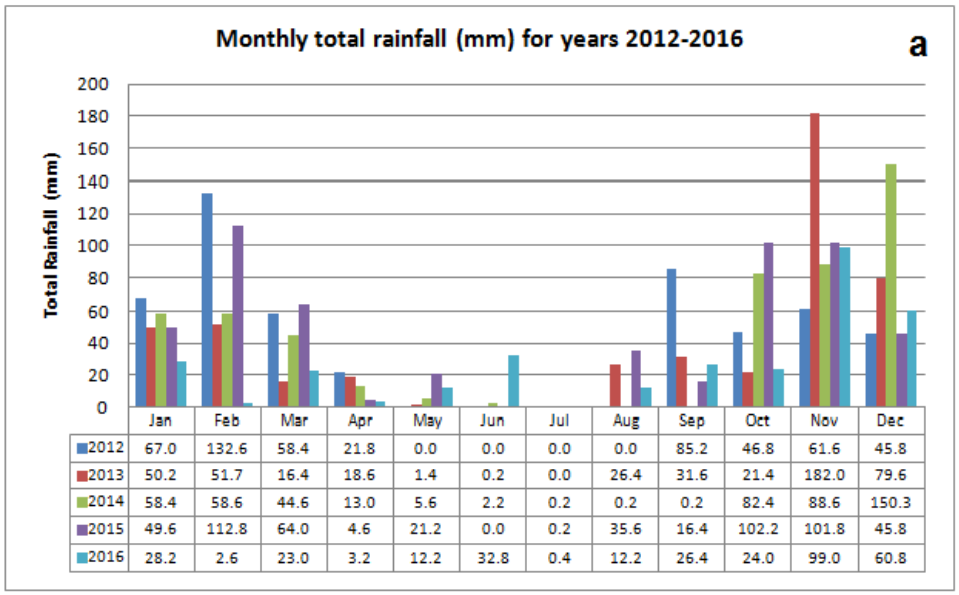

	Jan	Feb	Mar	Apr	May	Jun	Jul	Aug	Sep	Oct	Nov	Dec
2012	67.0	132.6	58.4	21.8	0.0	0.0	0.0	0.0	85.2	46.8	61.6	45.8
2013	50.2	51.7	16.4	18.6	1.4	0.2	0.0	26.4	31.6	21.4	182.0	79.6
2014	58.4	58.6	44.6	13.0	5.6	2.2	0.2	0.2	0.2	82.4	88.6	150.3
2015	49.6	112.8	64.0	4.6	21.2	0.0	0.2	35.6	16.4	102.2	101.8	45.8
2016	28.2	2.6	23.0	3.2	12.2	32.8	0.4	12.2	26.4	24.0	99.0	60.8

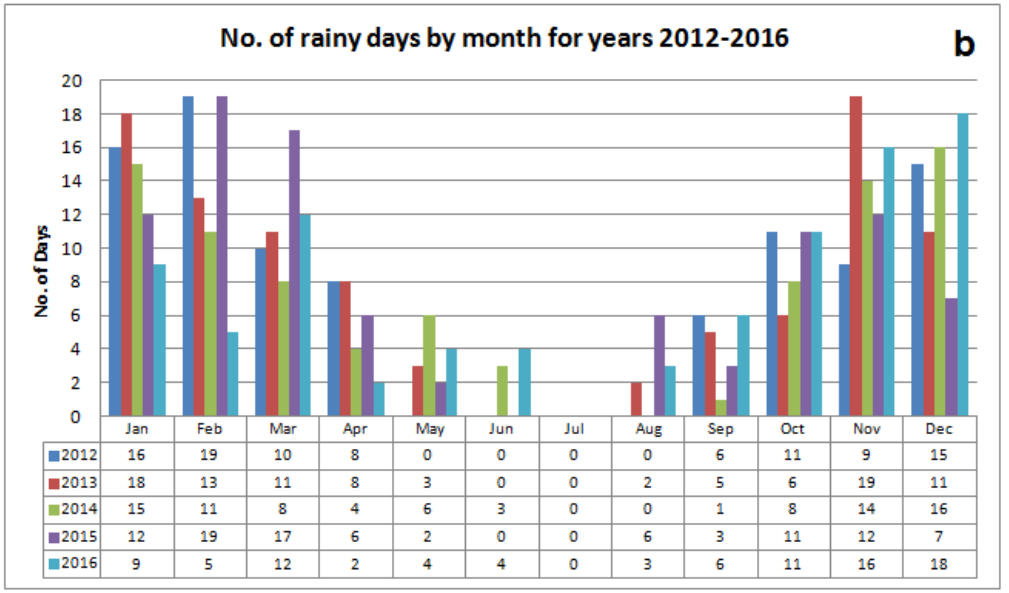

	Jan	Feb	Mar	Apr	May	Jun	Jul	Aug	Sep	Oct	Nov	Dec
2012	16	19	10	8	0	0	0	0	6	11	9	15
2013	18	13	11	8	3	0	0	2	5	6	19	11
2014	15	11	8	4	6	3	0	0	1	8	14	16
2015	12	19	17	6	2	0	0	6	3	11	12	7
2016	9	5	12	2	4	4	0	3	6	11	16	18

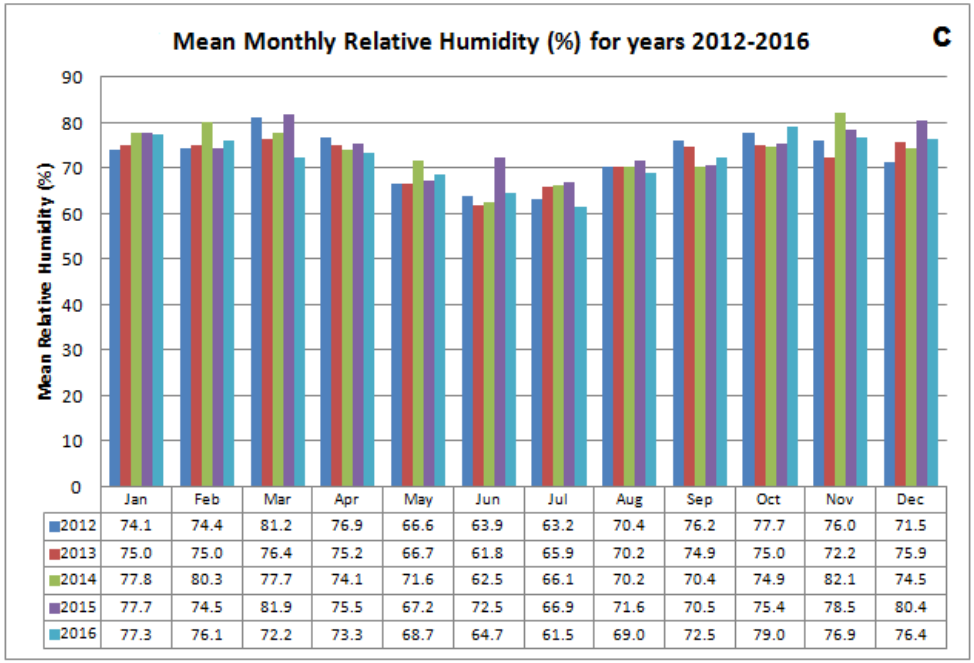

	Jan	Feb	Mar	Apr	May	Jun	Jul	Aug	Sep	Oct	Nov	Dec
2012	74.1	74.4	81.2	76.9	66.6	63.9	63.2	70.4	76.2	77.7	76.0	71.5
2013	75.0	75.0	76.4	75.2	66.7	61.8	65.9	70.2	74.9	75.0	72.2	75.9
2014	77.8	80.3	77.7	74.1	71.6	62.5	66.1	70.2	70.4	74.9	82.1	74.5
2015	77.7	74.5	81.9	75.5	67.2	72.5	66.9	71.6	70.5	75.4	78.5	80.4
2016	77.3	76.1	72.2	73.3	68.7	64.7	61.5	69.0	72.5	79.0	76.9	76.4

Figure 5.5: (a) Trends for monthly rainfall, (b) number of rainy days, (c) mean monthly relative humidity for the study period 2012-2016.

(Source: National Meteorological Office, 2017).

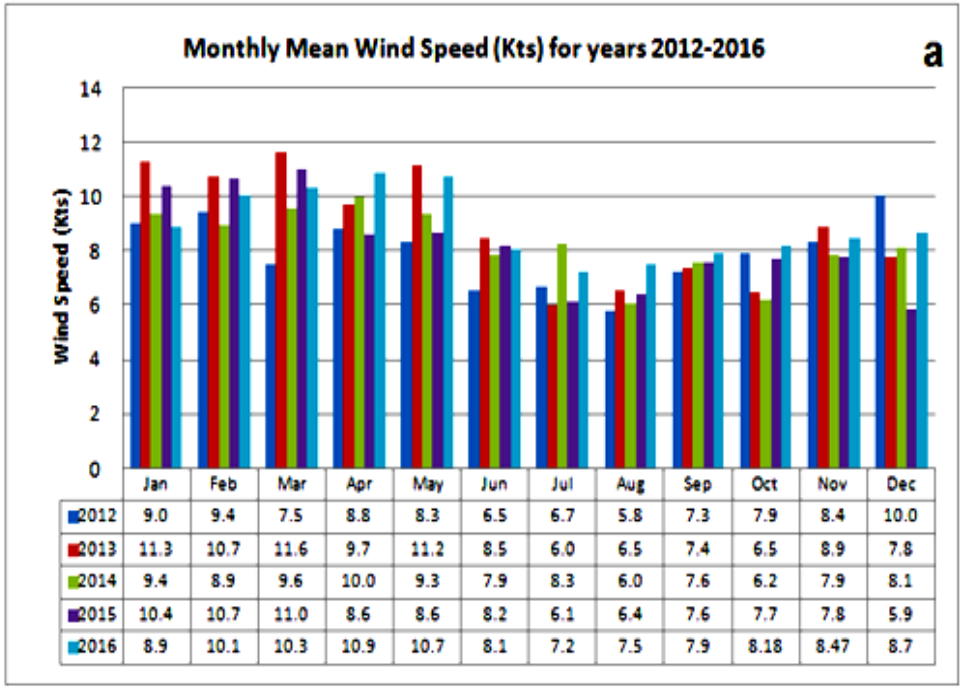

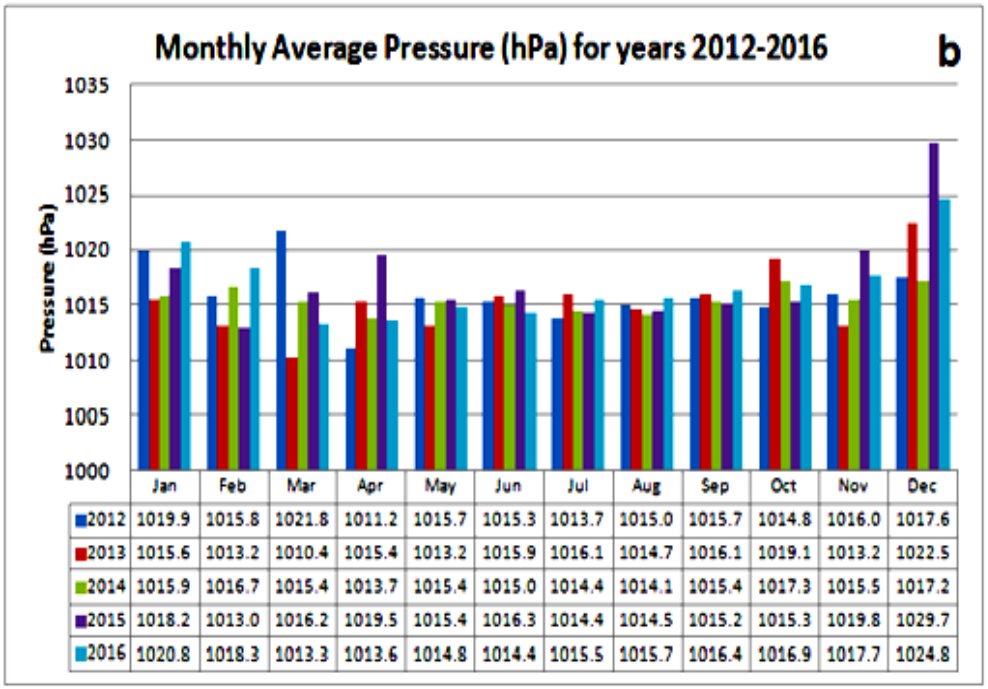

Mean Wind Directions (°)												
Year	Jan	Feb	Mar	Apr	May	Jun	Jul	Aug	Sep	Oct	Nov	Dec
2012	290	290	290	300	280	310	310	220	310	90	280	300
2013	280	280	280	80	300	300	280	310	310	120	240	230
2014	280	300	280	290	280	310	300	170	290	290	200	320
2015	310	290	310	310	320	320	320	50	320	310	310	320
2016	300	310	310	80	310	320	320	320	310	150	150	310

c

Figure 5.5: Mean wind speed (a), mean pressure (b) and mean wind direction (c) during the study period 2012-2016 (Source: Malta National Meteorological Office, 2017)

with relatively heavy rainfall and a higher number of rainy days included December 2014 with 150 mm (over 16 days) and February 2012 with 132.6 mm (19 days). High number of rainy days does not always equate with high records of rainfall: for example, December 2016 had 18 days of rain but only 60.1 mm of rain. Conversely, months with less rainfall totals may have been more torrential over a shorter span of days for example the 85 mm of rainfall in September 2012 and 82.4 mm in October 2014, fell in just over 8 days respectively. An important anomaly which occurred during the study period is a shortage of rain in 2016, totalling no more than 324.8 mma^{-1}. This total is far inferior than the average of 550 mma^{-1} for a 30-year climate period between 1961-1990 (Galdies, 2011). The 2016 year was reported as being the fifth driest year since 1923 and its winter was four times drier than that of 2015. Specifically, between January and April 2016, it recorded the driest winter drought in the last 50 years with a total rainfall of 57 mm (in 2015, those same months recorded 231 mm of rain). This dry spell coincided also with the presence of a relatively higher than normal atmospheric pressure between December 2015 and February 2016 (Figure 5.5).

The five year trends of humidity, winds speeds, wind directions were observed to be similar to those observed for the periods 1961-1990 (Galdies, 2011). Humidity averaged 73% over the study period with records ranging from 61.5% (July 2016) to 82.1% (November 2014). As displayed in Figure 5.5c, this range of humidity records and their variability follows the general trends observed for longer records, with the highest monthly variability between January and June. Average winds speeds were of 8.4 knots (8.8 knots for 1961-1990) and mean wind directions were mainly from the north-westerly.

5.2.2 Synthesis and context

Overall, the weather conditions during the study period were characterised by typical Mediterranean dual seasonal trends, albeit with an unusually drier 2016. Given that the platform surfaces being investigated are at supratidal level,

climate trends have an important bearing on the behaviour of their surface change, As reviewed in Chapter 2 (Section 2.4.3), coastal weathering mechanisms at supratidal levels are heavily influenced by atmospheric conditions such as solar radiation, rainfall and winds. Winds also have a bearing on the propagation of waves breaking on shore and in influencing their breaking energy, it partially determines the extent of the spray and splash zone across the platform. In addition to that, this information is needed to understand the geochemical and geomechanical behaviour of rock decay observed in the experimental part of this study. Lastly, climate data needs to be kept into perspective when it comes to comparing the rates of surface change observed in this study with those of other studies though the latter may have similar site-specific boundary conditions, but may still operate in a climate regime different from that of the Maltese Islands.

5.3 Near-infrared spectroscopy (NIR): Results

Rock strength and susceptibility to erosion and weathering are known to be partially determined by the mineralogical composition. It is well known that although limestone is composed mainly of calcite, it may show significant variations in minor mineral composition and texture, resulting in a complex and contrasting weathering behaviour (Kramar *et al.*, 2010). NIR test were undertaken to determine the mineralogical composition of the platform surfaces and identify to what extent they may affect patterns of surface change when corroborated with the TMEM surface measurements. An additional input in this investigation was the testing the weathered samples at the end of the exposure experiment order to examine how the geochemical properties of the weathered samples may have altered and potentially infer which properties of the rock are more susceptible to weathering. This investigation aims to address hypothesis no. 4 in determining how compositional properties may affect patterns of surface change (Table 3.3).

Two sets of spectroscopy results are presented: the first are the results of samples extracted from the shore platforms and the second set of results are

related to the samples collected from the sixteen experimental slabs which were exposed to inland subaerial conditions for a period of a year and a half (Sections 3.5.2 and 3.5.3).

5.3.1 Platforms samples: NIR spectral signature results

Table 5.1 displays the spectroscopy results for the samples collected from the shore platforms. The percentage results provide an estimate of how much the spectral signature is thought to result from the listed minerals. The results associate strongly the surface of the five shore platforms to the carbonate mineral group and also having a varying percentage association with sulphate content, which ranges from small to significant amounts. As seen in Figure 5.6 and Figure 5.7, all but one sample, the 'Fired Limestone' of MPQ5 have broadly similar signatures. Three types of carbonate minerals were found as follows:

i. Calcite ($CaCO_3$): Calcite is a common constituent of sedimentary rocks, especially of limestone, much of which is formed from the shells of dead marine organisms. As expected, this type of carbonate was present on all the five platforms as well; MH-3);

ii. Ankerite [$Ca(Fe,Mg,Mn)(CO_3)_2$]: it is a carbonate similar to dolomite (on the basis of its crystallographic and physical characters) but where magnesium (Mg) is replaced by iron (Fe). This was present in most samples on all the five platforms (MH-3.5-4); and

iii. Siderite ($FeCO_3$): In sedimentary rocks, this iron-rich carbonate is mostly known to form at shallow burial depths and its elemental composition is often related to the depositional environment of the enclosing sediments. It was mostly found in the samples derived from Ponta tal-Qammieħ. (MH-4).

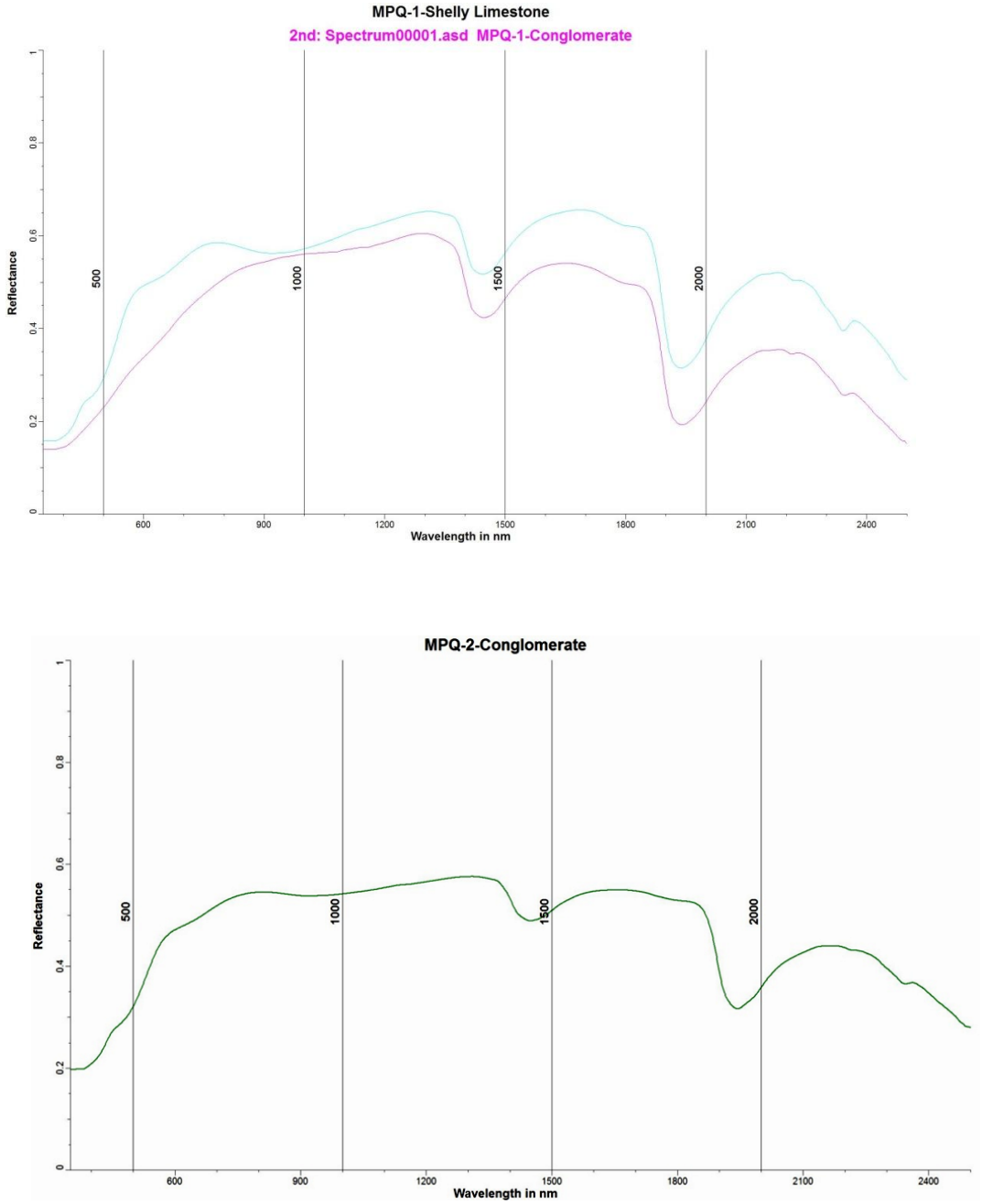

Figure 5.6: Spectra signatures for MPQ1 shelly limestone and MPQ 1 conglomerate (TOP) and MPQ2 conglomerate (BOTTOM).

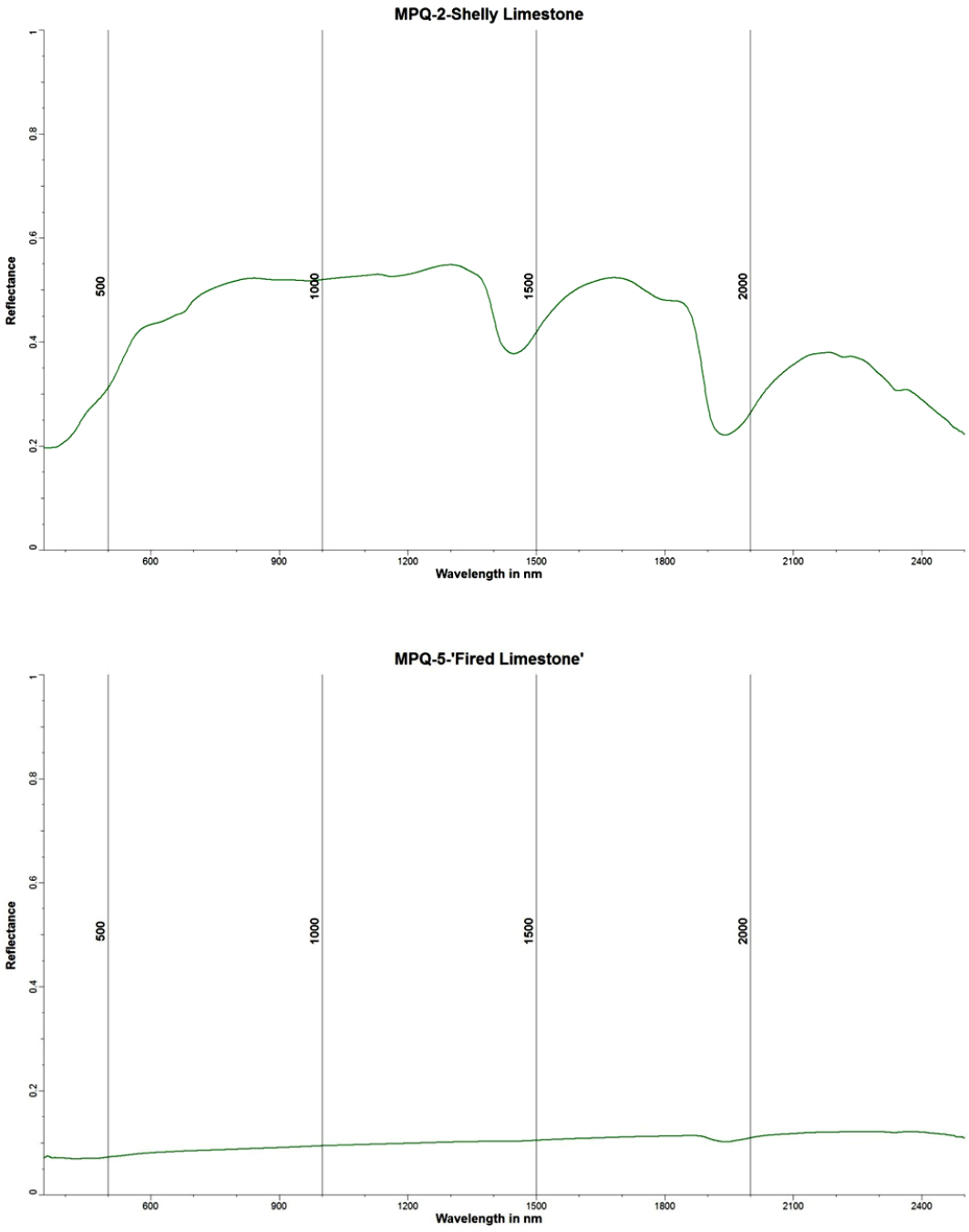

Figure 5.7: Spectra signatures for MPQ2 shelly limestone (TOP) and MPQ5 Fired Limestone (BOTTOM).

Table 5.1: Percentage of samples extracted from the platform containing mineral and mineral groups as indicated by the TheSpectralGeologist Core® software according to shore platform site

Shore platforms	% of samples containing mineral		% of samples containing mineral group	
Ras il-Fenek	Ankerite	57.1	Carbonate	78.6
	Gypsum	42.9	Sulphate	42.9
	Calcite	21.4		
Ponta tal-Munxar	Calcite	50.0	Carbonate	83.3
	Ankerite	33.3	Sulphate	16.7
	Gypsum	16.7		
Ponta tal-Miġnuna	Ankerite	50.0	Carbonate	100.0
	Calcite	50.0	Sulphate	50.0
	Gypsum	50.0	White-Mica	16.7
	Muscovite	16.7		
Blata l-Bajda	Gypsum	85.7	Sulphate	85.7
	Ankerite	14.3	Carbonate	14.3
Ponta tal-Qammieħ	Gypsum	90.9	Sulphate	90.9
	Ankerite	72.7	Carbonate	81.8
	Calcite	50.0		
	Siderite	9.1		

The presence of muscovite [$KAl_2(AlSi_3O_{10})(F,OH)_2$] (MH-2) was found at Ponta tal-Miġnuna. Muscovite is one of the most common of the micas and is a hydrated phyllosilicate mineral of aluminium and potassium. It occurs over a large range of geological conditions and is a principal constituent of the fine-grained sediments. Muscovite is not especially resistant to chemical weathering and is quickly transformed into clay minerals (Yoder and Eugster, 1955). Its presence in sedimentary rocks is usually an indication of their immature diagenesis and of not having been subjected to severe weathering

The results also point to a significant percentage of sulphate content, with the samples belonging to Ponta tal-Qammieħ and Blata l-Bajda having the highest content i.e. 90.9% and 85.7%. In all cases the spectroscopy signature

assigned was that of gypsum. Table 5.2 classifies the platform samples on their rock type characteristics and most of the samples were classified as having shelly limestone attributes and their spectral signature came back as carbonate-rich rocks with high sulphate content. Gypsum, ankerite and calcite were the main minerals detected from most type of limestones, with some traces of muscovite close to MPM3 and siderite in close to MPQ5. Figure 5.8 displays the resultant spectra signatures with all the samples combined together. Columns are listed in a sequence starting on the left hand side with the test number, location number and site code, a line pictogram of the data, rock type and the final two lists are automatically generated mineral indices representing as Min1 sTSAS (mineral index for TSA singleton match or primary mixture component) and Min2 sTSAS (mineral index for secondary mixture component).

The spectra signature attributed to gypsum called for some further careful considerations, due to a number of reasons. Local literature on Maltese limestone (ex. Bennett, 1979; Pedley and Bennett, 1985; Pedley and Clarke, 2002) never reported gypsum growth on Maltese limestone. The presence of this signature was thus suspected to be linked to environmentally-derived salts.

Carbonate minerals in limestone rocks have important implications in terms of rock surface weathering dynamics as they may contribute to processes of either dissolution (carbonates dissolve when they come contact with acidity present in ambient carbon dioxide) or else, under the right conditions, of precipitation (carbonates, especially calcite, may form mineral crust, that cement the existing rock grains together or fill fractures). The latter has been widely researched in the context of Maltese Globigerina limestone buildings, as discussed in Chapter 2 (Section 2.7).

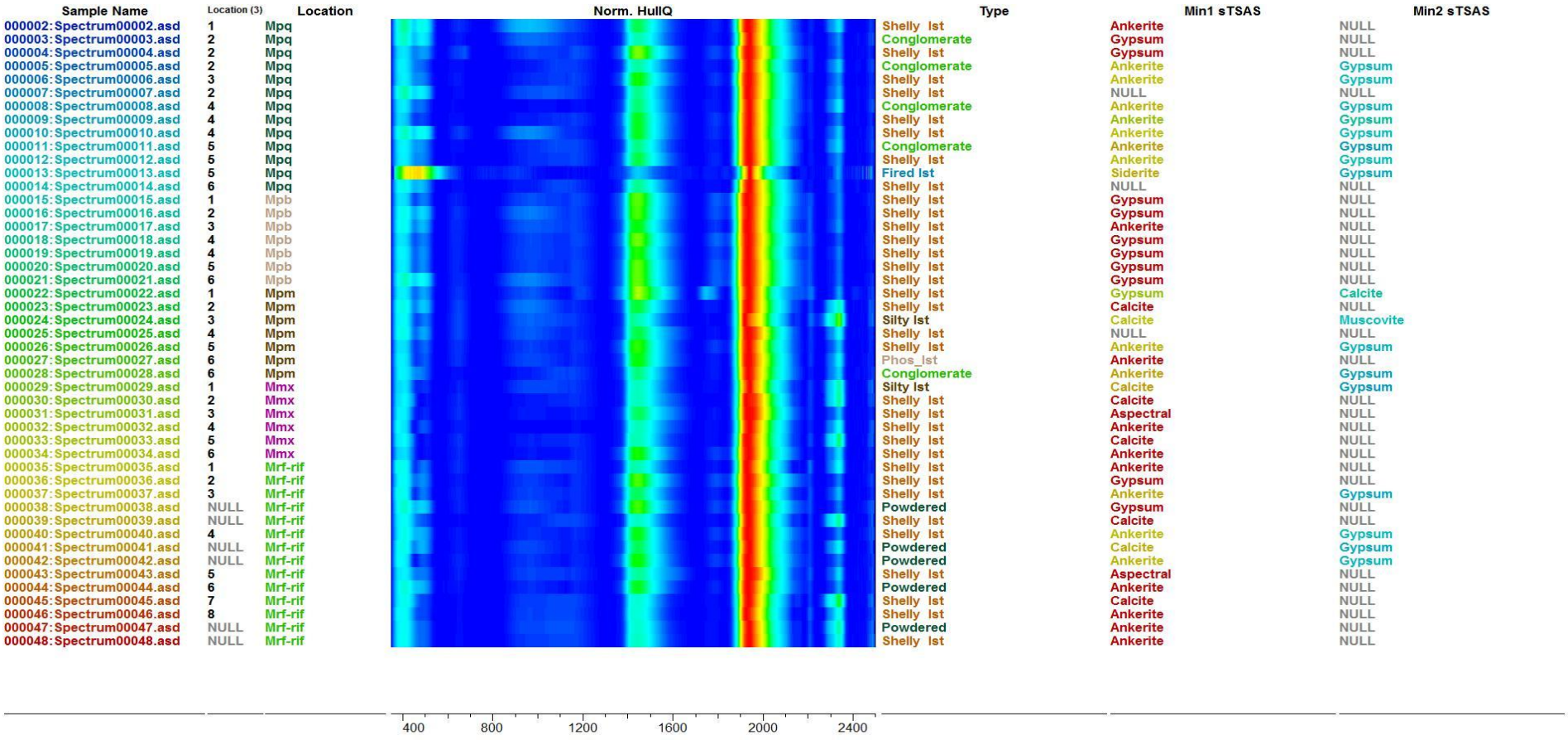

Figure 5.8: Spectral signature of the platform samples

Table 5.2: Percentage of samples containing mineral and mineral groups, as indicated by the TheSpectralGeologist Core® software, according to geological characteristics of the samples.

Type of Limestone	Platform Sites	Location	% of samples containing mineral		% of samples containing mineral group	
Conglomerate	Ponta tal-Qammieh Ponta tal-Mignuna	MPQ2 (2), MPQ4 (2) MPM6	Gypsum Ankerite	100.0 80.0	Sulphate Carbonate	100.0 80.0
Shelly Limestone	All	All	Gypsum Ankerite Calcite	53.3 46.7 20.0	Carbonate Sulphate	66.7 53.3
Silty Limestone	Ponta tal-Munxar Ponta tal-Mignuna	MMX1 MPM3	Calcite Muscovite Gypsum	100.0 50.0 50.0	Carbonate White-Mica Sulphate	100.0 50.0 50.0
Powdery	Ras il-Fenek	MRF NULL (4), MRF 6	Ankerite Gypsum Calcite	60.0 60.0 20.0	Carbonate Sulphate	80.0 60.0

Sulphate mineral group, listed in Table 5.2, was one the main mineral groups present on all of the five platforms. It presence was suspected to be related to the salt-related minerals derived from sea water and salt-laden winds present in coastal environments and which would have been absorbed by the limestone surfaces. XRD tests were performed to investigate further the presence of this gypsum signature. The XRD results of six tested samples are displayed in Table 5.3, whilst Figure 5.9 displays the signature outputs of the test for the six samples. The test confirms calcium carbonate as the primary mineral for all six samples; more importantly, it identifies sodium chloride as secondary mineral for samples MBB1, MPM3 and MBB4. No secondary mineral was detected for MPM3 and MMX2 and calcium phosphate for found for MPQ5 as a secondary mineral. In all samples, gypsum was not identified. No gypsum was found in the building sample either. This result confirms the initial

suspicion that the gypsum signal in the NIR was in actual fact indicative of salt mineral presence rather than gypsum.

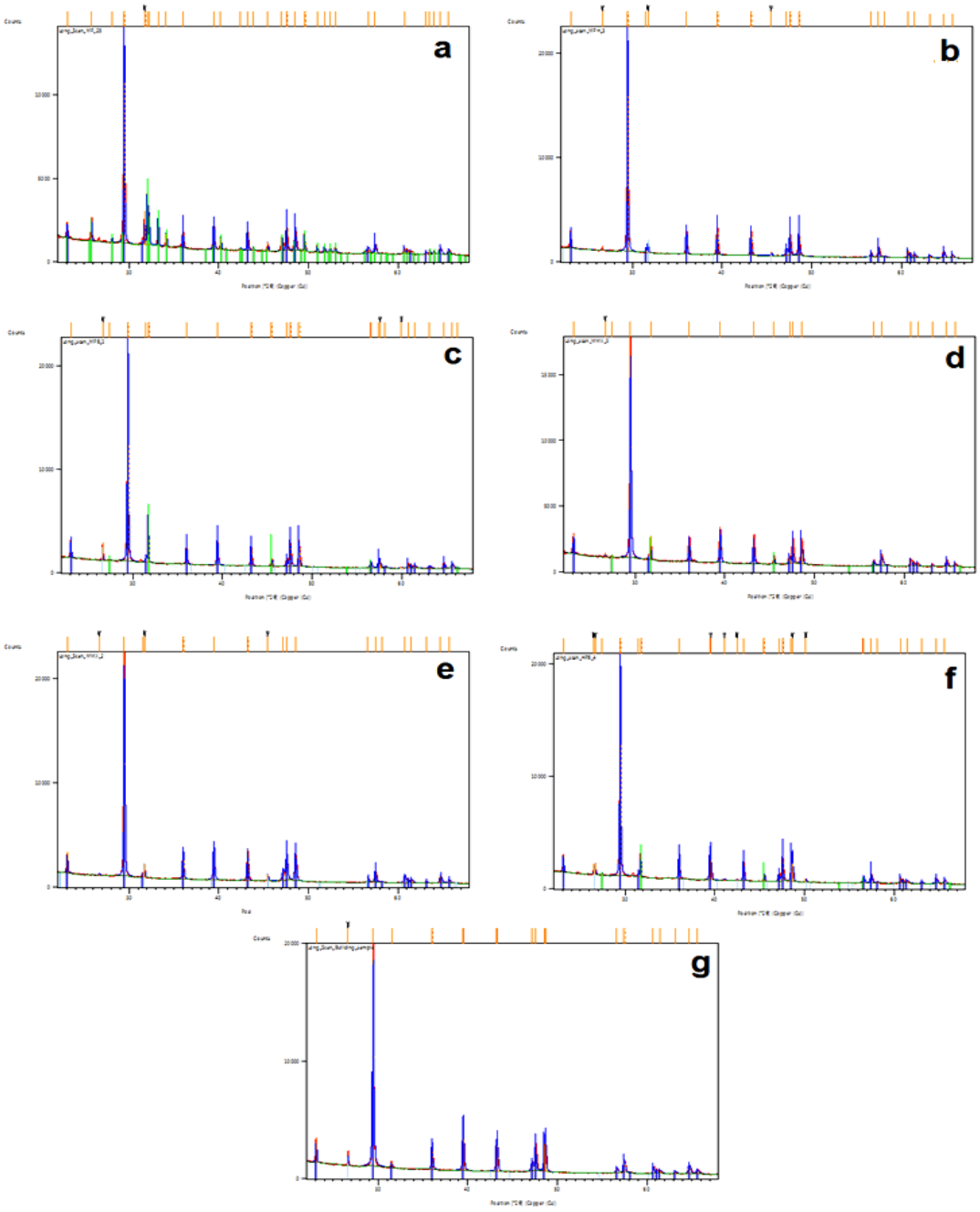

Figure 5.9: XRD Signatures of roof samples (a) MPQ5 (b) MPM3 (c) MPB1 (d) MMX3 (e) MMX2 (f) MPB4 (g) Building Sample

Table 5.3: XRD results for six tested limestone samples

XRD Test Name	Sample Name	Primary Mineral	Secondary Mineral
Long_Scan_MP_25	MPQ5	Calcium Carbonate $CaCO_3$	Calcium Phosphate $CaPO_4$
Long_scan_MPH_3	MPM3	Calcium Carbonate $CaCO_3$	
Long_scan_MPB_1	MBB1	Calcium Carbonate $CaCO_3$	Sodium Chloride NaCL
Long Scan MMX3	MMX3	Calcium Carbonate $CaCO_3$	Sodium Chloride NaCL
MMX2	MMX2	Calcium Carbonate $CaCO_3$	
HPB 4	MBB4	Calcium Carbonate $CaCO_3$	Sodium Chloride NaCL
Building Sample	Black Crust	Calcium Carbonate $CaCO_3$	

The result of these tests raises important questions about the role of salt weathering on these platforms. The marked presence of salt minerals in some of the platform samples and the absence of this mineral from other samples, have important implications in regard to how the different limestone lithologies are responding to the presence of salt in their respective surface environment. So far such information has only been provided through lab investigations of building stones in LGLM and no information yet exists on how other Maltese limestone lithologies in their natural state behave in response to environmentally-derives salt inputs.

5.3.2 Exposure experiment slabs' results

Sixteen weathered samples were tested with NIR in order to compare how weathering may affect the mineralogical composition of the lithology present on the platforms. Overall, NIR results of the weathered experimental slabs, as illustrated in Table 5.4, confirmed that the weathered samples still retained a good percentage composition of calcite as either their primary mineral (13 out of 15 samples) or as a secondary mineral (MPB1 and MRF1) (Figure 5.10). These latter samples were also confirmed as having muscovite as their primary mineral.

Table 5.4: Percentage of samples, from the experiment slabs, containing mineral and mineral groups, as indicated by the TheSpectralGeologist Core® software, according to geological characteristics of the samples.

Platform	Mineral Level	% of Sample Signature	Mineral Group Level	% of Sample Signature	Number of Samples
Blata l-Bajda	Muscovite	18	White Mica	18	• MBB
	Smectite	27	Smectite	27	• MBB 1
	Calcite	55	Carbonate	55	• MBB 3
Ponta tal-Miġnuna	Muscovite	19.3	White Mica	19.3	• MPM 6
	Smectite	10.8	Smectite	10.8	• MPM3
	Calcite	69.8	Carbonate	69.8	• MPM 1
Ponta tal-Munxar	Muscovite	18.5	White Mica	18.5	• MMX 4
	Smectite	8.9	Smectite	8.9	• MMX 2
	Calcite	72.6	Carbonate	72.6	• MMX 3
Globigerina Block	Calcite	100	Carbonate	100	
Ras il-Fenek	Muscovite	8.4	White Mica	8.4	• MRF 1
	Calcite	85.3	Carbonate	85.3	• MRF 7
	Gypsum	6.3	Sulphate	6.3	• MRF 4
Ponta tal-Qammieħ	Muscovite	20.8	White Mica	20.8	• MPQ 3
	Calcite	58.4	Carbonate	58.4	• MPQ 1
	Gypsum	20.9	Sulphate	20.9	

The mineral assemblage of the experimental slabs was primarily different from that of the platform samples on two accounts. First, some samples (MPB1, MPM6, MMX4 and MPM3) show the marked presence of montmorillonite $\{(Na,Ca)_{0.33}(Al,Mg)_2(Si_4O_{10})(OH)_2 \cdot nH_2O\}$. Montmorillonite is considered a mineral belonging to the smectite group and is known as an expansive clay mineral that is prone to large volume changes (swelling and shrinking), the latter known be caused by changes in water content. It may have the most dramatic shrink-swell capacity (Norrish, 1954). None of the platform samples had evidence of smectite, although its presence may have been mostly 'smothered' or dominated by the mineral responsible for the sulphate signature.

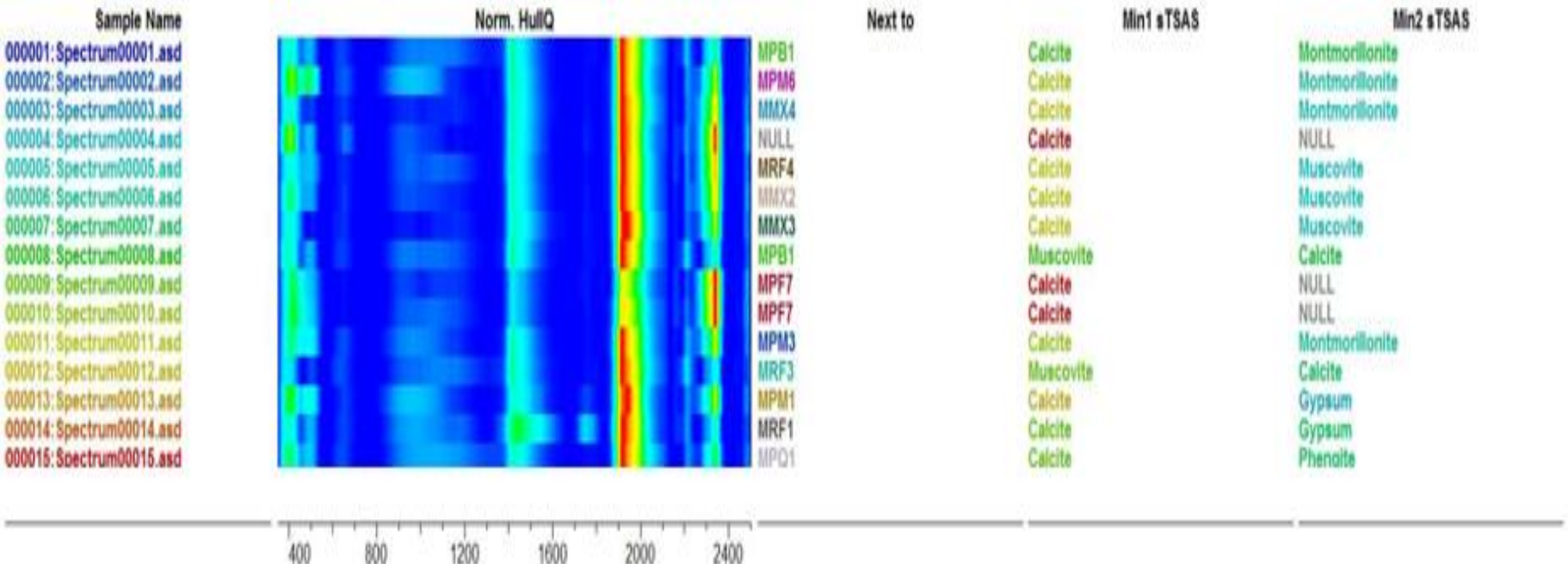

Figure 5.10: Spectral signature of the fifteen experimental slabs.

The second recorded difference was the absence in all but one sample of gypsum. In view of the XRD results obtained for the platform samples, the absence of gypsum from the weathered samples confirms that the NIR signature is salt and that these salts were removed from the experimental slabs by during the exposure process. This may also indicate that the platform samples were dominated by salts and would explain why most of the experimental weathered slabs were clean from the salt signature. Such a pattern does indicate fairly strongly that the sulphate signal is environmentally derived from saltwater or salt spray covering the samples. It also suggests the extent to which the platform samples absorb salt and thus may be susceptible to alterations and break down by salt weathering mechanisms.

5.3.3 Synthesis of main findings

i. The mineralogical tests characterise the five studied platform as carbonates, with a strong influence from sodium chloride;
ii. Notwithstanding that spectral signatures of the tested platform samples were found to be closely related (with the exception of MPQ5), the exposure experiment confirmed different levels of sodium chloride present in the samples and would indicate different processes related to salt input rates;
iii. The rock exposures of Blata l-Bajda were found to be the most susceptible to weathering and Ras il-Fenek as the least susceptible; potentially this may be linked to salt-weathering susceptibility on the basis on their sodium chloride presence in the slabs;
iv. The mineralogical composition of the Lower Globigerina Limestone block was made of 100% calcite, whereas the platform samples had lower content of calcite and other minerals present;
v. High carbonate content was similarly found in the weathered slabs but the lack of presence of sodium chloride indicate that salts have probably weathered away after exposure; and

vi. Montmorillonite (an expansive clay) was found in some of the exposed slabs as a secondary mineral. This may contribute to different modes of breakdown and resultant rates of surface change.

5.4 Surface hardness: Schmidt Hammer N type results

As explained in Chapter 2 (Section 2.5) and Chapter 3 (Section 3.5.1), determining the level and spatial extent of surface hardness properties across a platform may elicit a better understanding how the control-process dynamics between rock resistance and the forces operating on the platforms may influence their rates of surface change. The following section provides the results of the rock surface hardness as measured with a N-Type Schmidt Hammer

5.4.1 Descriptive statistics

Rock hardness measurements were recorded along ten transects from the frontshore to the backshore in a cross-shore direction and with each platform represented by two transects (Section 3.5.1; Table 3.6). The lowest mean R value at single test points was measured at Blata l-Bajda platform at (21.1, with standard deviation, SD=3.7) whilst the highest value of 43.4, (SD=2.7) was recorded at Ras il-Fenek platform. Table 5.5 lists down the descriptive data based on all the single R values collected. Both transects along the UGLM surface of Ras il-Fenek recorded the highest mean R values with 36.8 (SD=3.53) and 36.66 (SD=3.03) in Transect 1 and Transect 2 respectively. At the other end of the mean data spectrum, the lowest mean values were recorded on another UGLM platform i.e. at Blata l-Bajda, with the mean of both transects being the lowest two of the set.

Table 5.5: Descriptive statistics calculated on all R values per platform and transect

Descriptive statistics calculated on all R-values per platform and transect														
Platform-Transect	Mean	Median	Mode	Range	Minimum	Maximum	Std. Deviation	Sample Variance	Cofficient of Variation	UCS*	Density*	Sample Size	Kurtosis	Skewness
							±	%	%	MPa	kg m^{-3}			
Ras il-Fenek Tr1	36.78	37.28	38.14	14.79	28.29	43.08	3.53	12.38	9.59	25.98	1841.99	550	-1.26	0.66
Ras il-Fenek Tr2	36.66	36.86	37.24	12.28	29.88	42.16	3.03	9.70	8.27	25.75	1837.16	550	2.73	1.69
Ponta tal-Miġnuna Tr1	33.77	33.96	33.66	13.05	26.51	39.56	2.92	8.66	8.65	21.21	1729.50	500	-0.26	1.15
Ponta tal-Miġnuna Tr2	31.49	31.61	31.30	12.92	24.77	37.69	3.07	9.49	9.74	18.55	1638.04	500	0.73	1.37
Ponta tal-Munxar Tr1	32.73	32.75	32.59	12.01	25.93	37.94	2.59	6.87	7.93	19.79	1688.65	600	1.52	1.40
Ponta tal-Munxar Tr2	33.81	33.79	33.32	12.36	26.80	39.16	2.63	7.20	7.78	21.27	1730.99	576	2.41	1.72
Ponta tal-QammieħTr1	29.72	29.78	29.14	15.67	21.95	37.62	3.77	15.28	12.68	16.17	1562.65	750	-1.35	0.41
Ponta tal-QammieħTr2	30.39	30.29	30.11	15.25	22.69	37.94	3.84	15.14	12.64	16.91	1591.53	750	0.01	0.90
Blata l-Bajda Tr1	25.38	25.31	25.06	9.97	20.94	30.91	2.08	4.65	8.21	12.09	1355.82	700	-0.37	1.30
Blata l-Bajda Tr2	24.02	23.96	23.77	7.97	20.15	28.12	1.78	3.29	7.43	11.03	1283.99	600	2.52	1.78

Table 5.6: Percentage distribution of all recorded R values per class intervals measured at each transect. Highlighted class intervals cover >85% of measured R values, with the highest percentage highlighted in darker grey.

Shore Platform and Transect No.	20-24	25-29	30-34	35-39	40-44	45-49	50-54	Total
	%	%	%	%	%	%	%	%
Ras il-Fenek Tr1	0.0	2.5	9.3	20.2	37.6	28.9	1.5	100
Ras il-Fenek Tr2	0.0	0.0	4.9	24.5	55.5	14.9	0.2	100
Ponta tal-Miġnuna Tr1	0.0	1.0	14.8	48.6	34.8	0.8	0.0	100
Ponta tal-Miġnuna Tr2	0.0	2.4	33.0	52.6	12.0	0.0	0.0	100
Ponta tal-Munxar Tr1	0.0	0.8	21.2	53.2	24.3	0.5	0.0	100
Ponta tal-Munxar Tr2	0.2	0.7	8.8	60.2	29.8	0.3	0.0	100
Ponta tal-Qammieħ Tr1	1.5	22.1	34.4	24.4	12.5	4.9	0.1	100
Ponta tal-Qammieħ Tr2	1.1	12.0	41.6	25.6	18.5	1.2	0.0	100
Blata l-Bajda Tr1	1.7	42.6	53.3	1.9	0.6	0.0	0.0	100
Blata l-Bajda Tr2	3.2	64.8	31.8	0.2	0.0	0.0	0.0	100
ALL	0.84	16.1	26.7	29.9	21.4	4.9	0.16	100

As seen in Table 5.5, its mean R values were 24.02 (SD=1.78) for Transect 2 and 25.38 (SD=2.08) for Transect 1. Blata l-Bajda was also the platform which registered the lowest variability in its data spread, with 4.54% and 3.29% for sample variance and 8.21% and 7.43% for coefficient of variation. Comparatively, both transects at the platform in LGLM and conglomerate of Ponta tal-Qammieħ recorded the highest degree of data variance with 15.28% and 15.14% in sample variance and 12.68% and 12.64% as its coefficient of variation.

As expected, this wide data spread in R values has influenced the parameters of the UCS and density for the above mentioned platforms, bringing up the same distinction between Ras il-Fenek having the highest values for UCS (25.98 MPa and 25.75 MPa) and for density (1841.00 and 1837.16 kg m^{-3}). Blata l-Bajda platform registered the lowest UCS (12.09 MPa and 11.03 MPa) and density (1283.99 kg m^{-3} and 1355.82 kg m^{-3}). The two shore platforms at St Thomas Bay - Ponta tal-Miġnuna and Ponta tal-Munxar – do not just seem to share a common location but also similar surface hardness properties. The differences between the highest mean R value (Transect 2 of Ponta tal-Munxar) and the lowest mean R value (Transect 1 of Ponta tal-Miġnuna) is only of 2.32. Their UCS and density values are similarly and relatively very close (Table 5.5). The median and range values for the ten transects also trend in a similar pattern with Ras il-Fenek and Blata l-Bajda positioned on both ends of the data spectrum and the three other platforms grouped relatively more in the centre of the data structure.

On the sole basis of these surface hardness results, one would expect a few specific patterns of surface change to emerge between the five platforms. The platforms of Ras il-Fenek and Blata l-Bajda, though both in UGLM, were found to be the hardest and softest respectively in terms on surface hardness. This would suggest that Ras il-Fenek, in being relatively the hardest as a platform, may result in lower rates of surface change. Conversely, Blata l-Bajda platforms may produce relatively higher rates of surface change given that is was found to conisit of softer limestone exposures. The remaining three platforms produced

mixed results in terms of surface strength but their R values are not so statistically distant from each other. Hence, the expected outcome in terms of surface change for these three platforms would be varied results i.e. with no specific dominant pattern emerging from one platform but that the range of results would not be wide-ranging as much as for the UGLM platforms.

Analysing better the data composition of the R values in each dataset may provide a clearer picture of the level of variability in rock surface strength at each platform and understand to what extent this level of variability may affect the level of susceptibility to rock surface change. The following sections, Sections 5.4.3 to 5.4.10 provide the results of such analyses. Frequency distribution, skewness and kurtosis provide the appropriate descriptive means to analyse the data structure, whilst cluster analyses of this data help to infer similarities and differences between platforms. The data distribution will provide a better insight of the variability of surface hardness measurements within the dataset and how potentially it may influence the behaviour of surface change. Finally, these analyses will address the study hypotheses (no. 2 and no. 3, Table 3.3) related to whether the investigated Globigerina platforms share similar properties of surface hardness.

5.4.2 R values distribution: a platform-transect comparison

In order to understand better the data composition of the R values per platform-transect, all individual R values were grouped and classified in percentage distribution datasets. In order to visualise better the differences in the shape of the R value data between platforms, the measured R values were grouped into percentage composition based on seven interval classes of 5 R values each and covering a range from 20 to 54.

The percentage data, listed in Table 5.6, were then converted into a horizontal bar graph, Figure 5.12, in order to illustrate better the difference in rock hardness per transect. In terms of total percentage distribution, the most frequent rock hardness values belonged to the 35-39 categories (29.9%),

followed by those in 30-34 group (26.7%) and between 40-44 (21.4%). Such data composition means that 78% of the all individual R values centred around a range between 35 to 44 and that the highest and lowest categories i.e. that of 20-24 and 50-54, recorded the lowest percentages of 0 and 0.16% respectively. This result would broadly indicate a unimodal data distribution in terms of the whole dataset. However, as seen in both Table 5.6 and Figure 5.12, such a uniform distribution does not apply when data classes are examined at platform-transect level.

As seen in Table 5.6, the platform of Blata Bajda recorded the highest percentages for the lower end categories of 25-29 (Transect 1, 64%) and 30-34 (Transect 2, 53.3%). No values were recorded for the higher end categories, especially for R values which fall in the 45-49 and 50-54 intervals. A substantial percentage increase towards the higher end intervals were mostly recorded at Ras il-Fenek, with 80% of the values of Transect 1 within the 35-44 classes and 66.5% of those in Transect 2, measured within the 40-49 groups. Conversely, Ras il-Fenek platform did not produce R values in the 20-24 interval and only 2.5% were recorded in the 25-29 category. These statistical results seem to confirm the initial distinctive groupings observed in the descriptive statistics (Table 5.5), and which placed these two platforms as most distant from each other and from the rest of the platforms in terms rock hardness properties.

Figure 5.11 also shows how the centrality of the data distribution within the 30-44 cluster (which makes up 78% of the whole dataset) is strongly driven by two of its classes i.e. the 30-34 and 35-39 intervals, which together add up to 56.6% of the total dataset. Two platforms, Ponta tal-Miġnuna and Ponta tal-Munxar, show strong similar patterns in this respect, with their highest percentages recorded in the 35-39 interval across all four transects: 48.6% and 52.6% for Ponta tal-Miġnuna and 53.6% and 60.2% for Ponta tal-Munxar. Ponta tal-Qammieħ platform had the widest spread in terms of data distribution, with R values recorded in all the seven classes, and with the majority ($< 93\%$) spread across four intervals from 25-44.

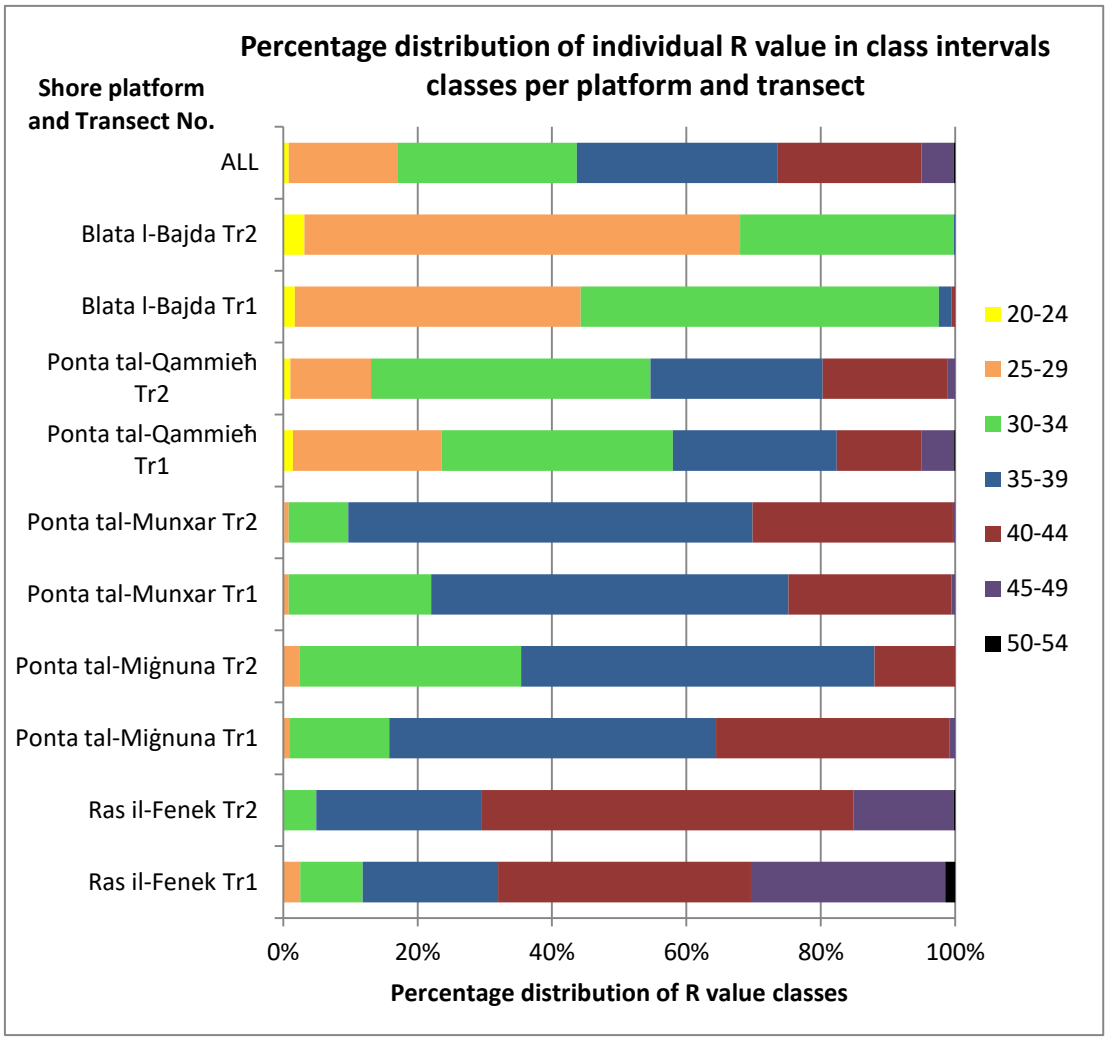

Figure 5.11: Horizontal bar graph showing percentage distribution of individual R values in class intervals per platform-transect. Distribution of the whole dataset included at the top.

5.4.3 Frequency distribution, skewness and kurtosis of R values

In view of the varied percentages obtained in terms of data distribution of total R values for each transect, frequency graphs were plotted in order to examine better the shape of each dataset and quantify the symmetry level in terms of skewness and kurtosis. Figure 5.12 and Figure 5.13 display ten frequency graphs calculated from all R values per transect. The histograms show an unimodal type of data shape for all transects, with only one peak value

recorded for one specific interval. This shape is in line with the general trend observed earlier for the whole dataset (Table 5.5).

In four out of five platforms, there is a good agreement between their respective transects in terms of peakedness at one specific class interval: both transects at Ras il-Fenek registered most values in the class interval 40-44; the R values of platforms of Ponta tal-Miġnuna and Ponta tal-Munxar scored mostly within the 35-39 bracket, whereas at Ponta tal-Qammieħ, the peak numbers of R values are best represented by the 30-34 interval. The transects of Ponta tal-Munxar and Ponta tal-Miġnuna are also reasonable similar, with the same category reaching peak values in both transects. Transect 2 of Ponta tal-Miġnuna did record a larger composition in the lower category 30.34. This is rather surprising given that Transect 2 covers a thicker conglomerate bed than Transect 1. The only plausible reason for these relatively lower values may be the surface roughness of the thicker conglomerate which may have impacted on rebound values. The platform of Blata l-Bajda is shown to be the only outlier in this pattern, with Transect 1 and Transect 2 registering different R values peaks in the 30-34 and 25-29 respectively.

In terms of skewness, the data pattern is more variable than peak frequency data. In using Bulmer's skewness classification, Figure 5.12 and Figure 5.13 display how seven out of ten transects were found to be have a strong positive skew. This was confirmed in the skewness values calculated in the descriptive statistics (Table 5.5) and reproduced hereunder in Table 5.7. As mentioned in the previous section, the distribution of R values for Ponta tal-Qammieħ were the only one to be considered as approximately symmetric and this was confirmed by skewness calculation of 0.41. On the other hand, Ras il-Fenek Transect 1 and Ponta tal-Qammieħ Transect 2 were found to be the inferiorly skewed compared to the rest of the transects (0.66 and 0.90 respectively). With regards to kurtosis (Table 5.5), the results are even more varied than those produced for skewness.

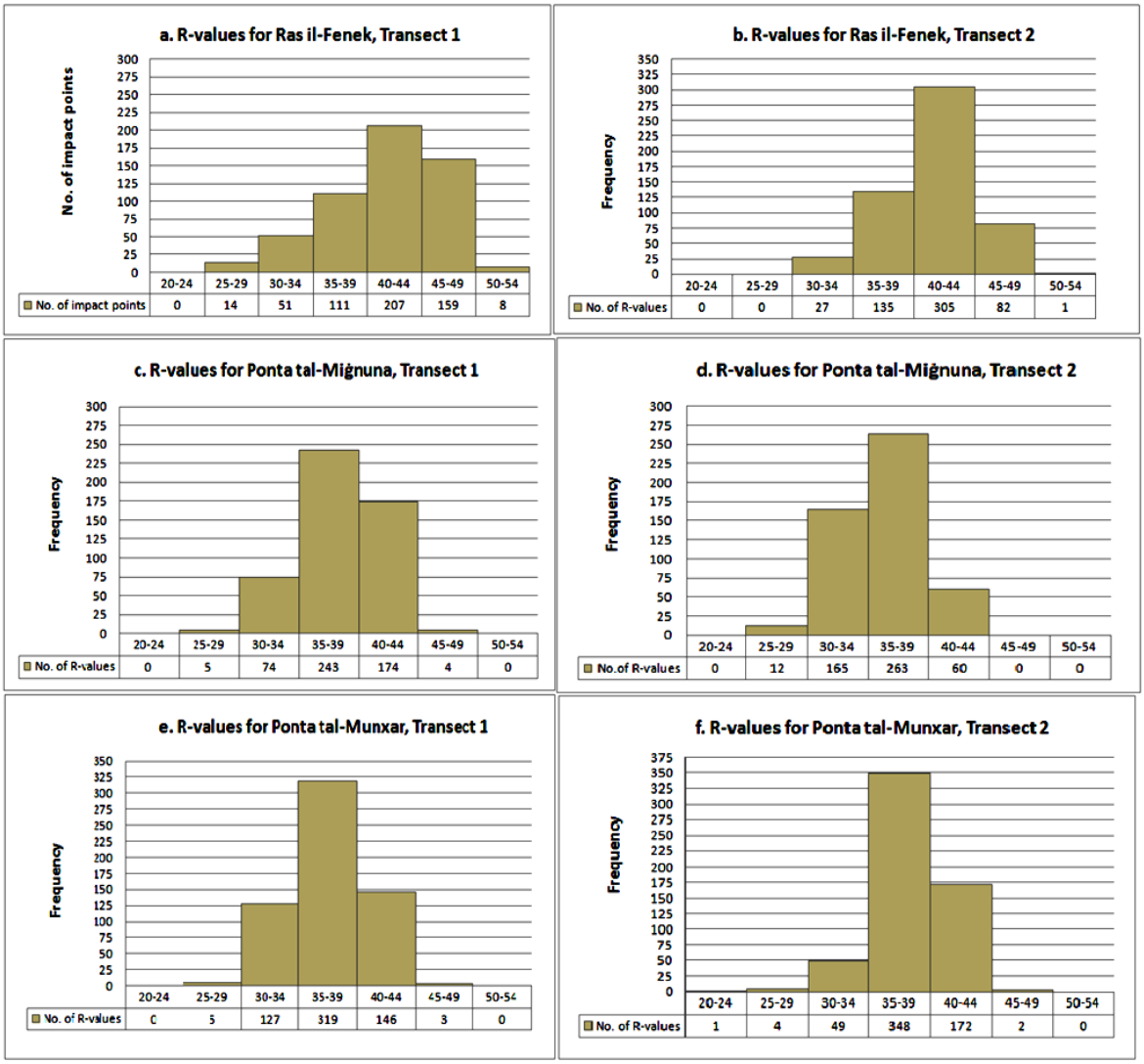

Figure 5.12: Frequency graphs showing distribution of all R values into class intervals for each transect: Ras il-Fenek, Ponta tal-Miġnuna and Ponta tal-Munxar.

This current study uses the recent interpretation of kurtosis by Westfall (2014), which states that kurtosis is more defined by the tails of the distribution rather by its peakedness. The tails provide information on the extremes, or outliers of a distribution. Based on such interpretation the kurtosis results classify the platforms in the following groups:

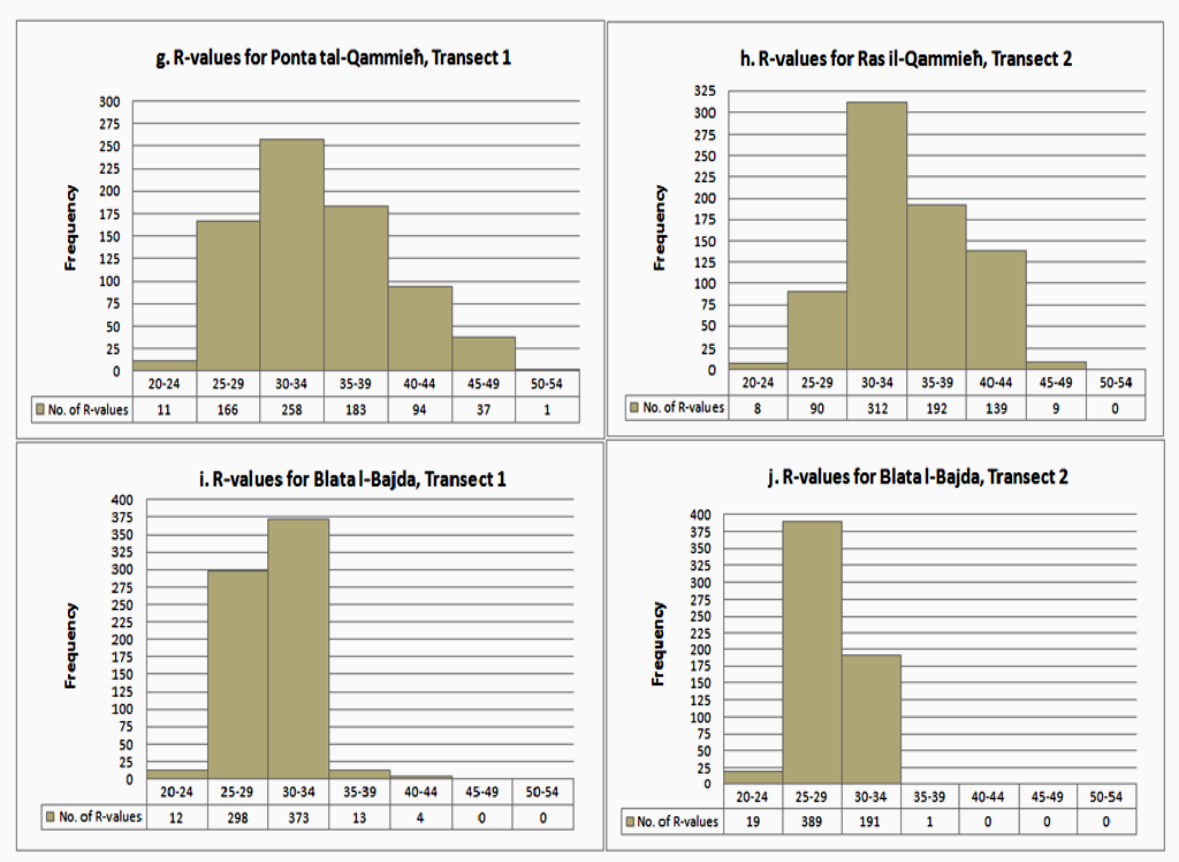

Figure 5.13: Frequency graphs showing distribution of all R values into class intervals for each transect: Ras il-Fenek, Ponta tal-Miġnuna and Ponta tal-Munxar

i. Platforms with a positive kurtosis: they indicate too few R values in the tails and/or alternatively a narrow and tall distribution curve (leptokurtic): These platforms would correspond to Ras il-Fenek Transect 1 (2.73), Blata l-Bajda Transect 2 (2.52) and Ponta tal-Munxar Transect 2 (2.41) and Ponta tal-Munxar Transect 1 (1.52);
ii. Platforms with a negative kurtosis: they indicate too many cases of R values in the tails and/or alternatively a flatter distribution curve (platykurtic). The platforms that would align with such a definition would be Ponta tal-Qammieħ Transect 1 (-1.35), Ras il-Fenek Transect 1 (-1.26); and
iii. Platforms close to a zero distribution, which would roughly have the same shape as a normal distribution. In this case, the following platforms would conform to such category, with some slightly deviating to both the negative or positive side of the zero distribution: Ras il-Qammieħ (0.01),

Ponta tal-Miġnuna (-0.26), Blata l-Bajda (-0.37) and Ponta tal-Miġnuna (0.73).

Table 5.7: Interpretation of skewness of R values dataset per transect

Skewness Level	Parameters	Platform-transect	Skewness
Highly skewed	Less than −1 or greater than +1	Ras il-Fenek Tr2	1.69
		Ponta tal-Miġnuna Tr1	1.15
		Ponta tal-Miġnuna Tr2	1.37
		Ponta tal-Munxar Tr1	1.40
		Ponta tal-Munxar Tr2	1.72
		Blata l-Bajda Tr1	1.30
		Blata l-Bajda Tr2	1.78
Moderately skewed	Between −1 and -0.5 or between +0.5 and +1	Ras il-Fenek Tr1	0.66
		Ponta tal-Qammieħ Tr2	0.90
Approximately symmetric	Between −0.5 and +0.5	Ponta tal-QammieħTr1	0.41

The implications of the above results would be that platforms with a positive kurtosis are likely to have a narrower range of surface strength parameters and therefore surface change behaviour will be less varied. On the other hand, platform with a negative kurtosis would have more spread of R value across a larger range of strength values and thus the rates of surface change may be expected to be equally varied. These assumptions are once again on the sole basis of rock surface strength and do not take into considerations all the other site-specific processes that additionally influence rates of surface change.

5.4.4 Mean R values per transect: a temporal comparison

As outlined in the methodology (Chapter 3, Section 3.5.1.1), one of the listed objectives of this rock hardness study was to test whether surface hardness on shore platforms may respond in any way to seasonal processes. In being micro-tidal, these shore platforms are relatively less affected by diurnal changes in tidal levels and more subject to seasonal induced influences and processes such as temperature fluctuations, moisture changes brought by

storm-wave sea spray and wave splashes. Capturing any variability in rock surface hardness and testing whether it is linked to specific seasons may shed light on whether platform surfaces are sensitive to effects of seasonality, the latter being so typical of the Mediterranean climate. If the level of surface hardness is found to be seasonal-dependent, then it may also imply that measurement of surface change may be also seasonal-dependent in response to such temporal variability in surface strength. If on the other hand, there is no seasonality effects on surface strength, then any seasonal rates of surface change encountered has to be attributed to other seasonal-dependent factors which do not include surface hardness.

Six measurement sessions were taken- spanning from February 2014 till August 2015. A cross-examination of any temporal trends through these six periods has been done at platform-transect level for each period and displayed as six box-plots in Figure 5.14 to Figure 5.19. The dataset is based on mean R values recorded along each test point per transect for each period. An initial cross-comparison between the different box plots shows a similar trend throughout the periods. In following the relative position of each transect, there seem to be no major shifts in their alignment with the overall mean. The mean R value of the whole dataset also did not experience such marginal shifts either, with levels ranging from 30.6 (in the 6th period) to 31.7 in the 10th period. The platforms of Ras il-Fenek and Blata l-Bajda retained their respective distant and isolated position in comparison with the overall mean and the rest of the platforms. Ras il-Fenek platforms remained fairly in the region of 6/7 points above the dataset mean, whilst Blata l-Bajda remained 6/7 points below the data set mean. The rest of the platforms do not seem exhibit such significant shifts across time periods, although some variations in the quartile range extent and standard error bars can be observed. This result may suggest that the assumption of seasonality as a potential issue in influencing surface hardness and resultant rates of surface change may be discounted. Section 5.4.9 presents a statistical test to see whether such a conclusion about the lack of seasonal variability in surface hardness is statistically valid.

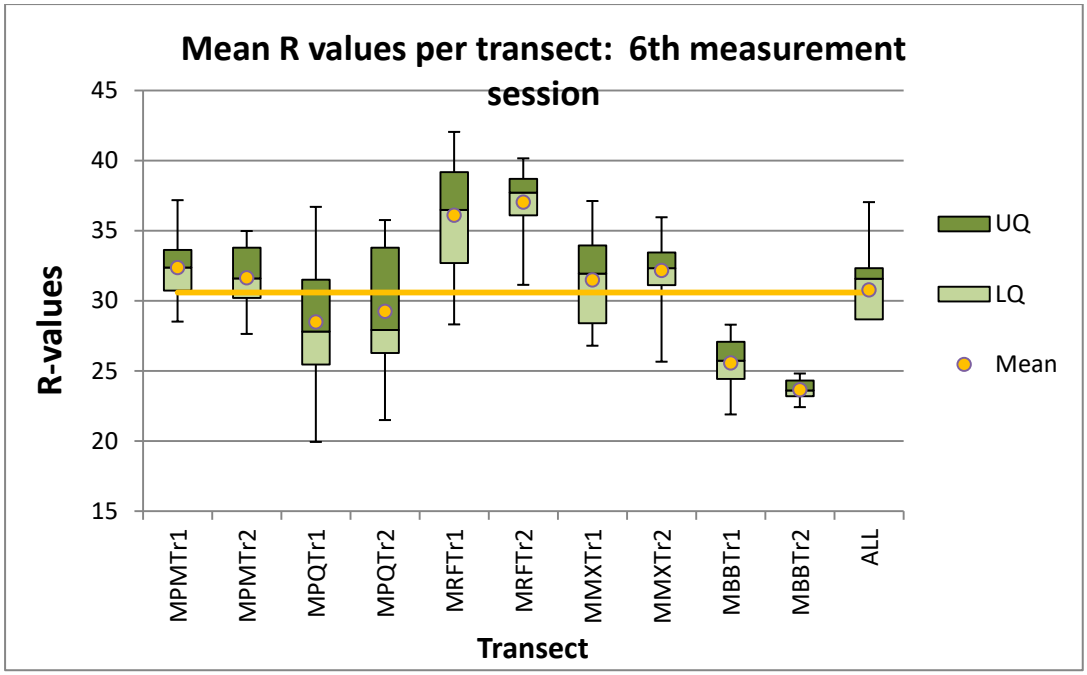

Figure 5.14: Mean R values per platform-transect across the 6th measurement session

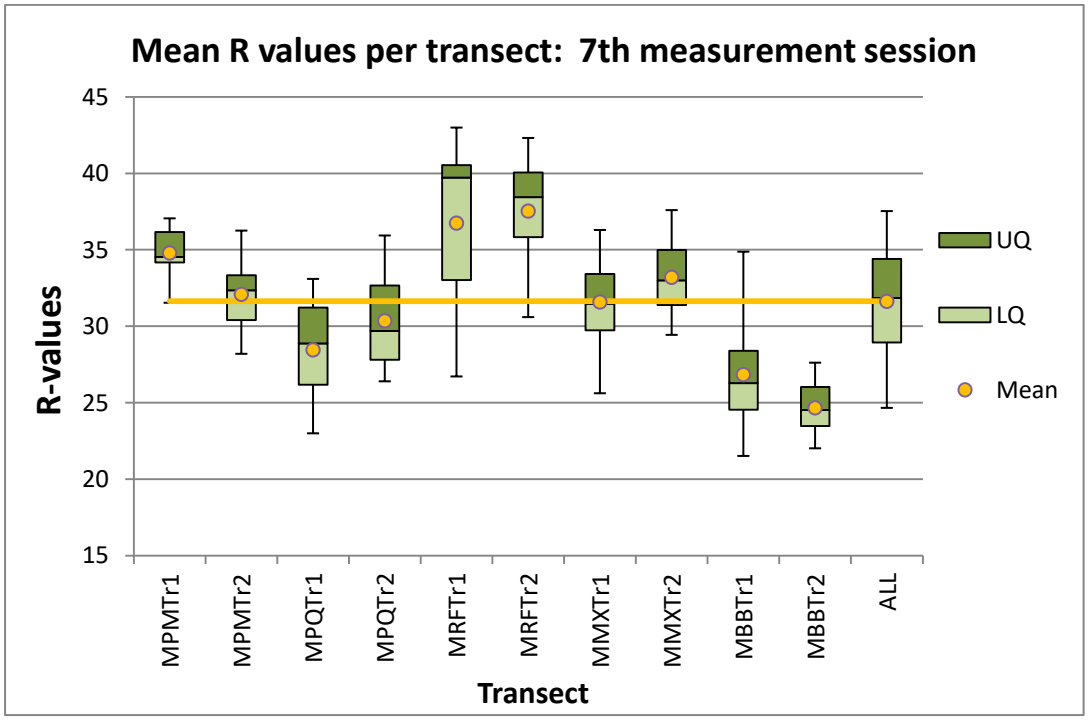

Figure 5.15: Mean R values per platform-transect across the 7th measurement session

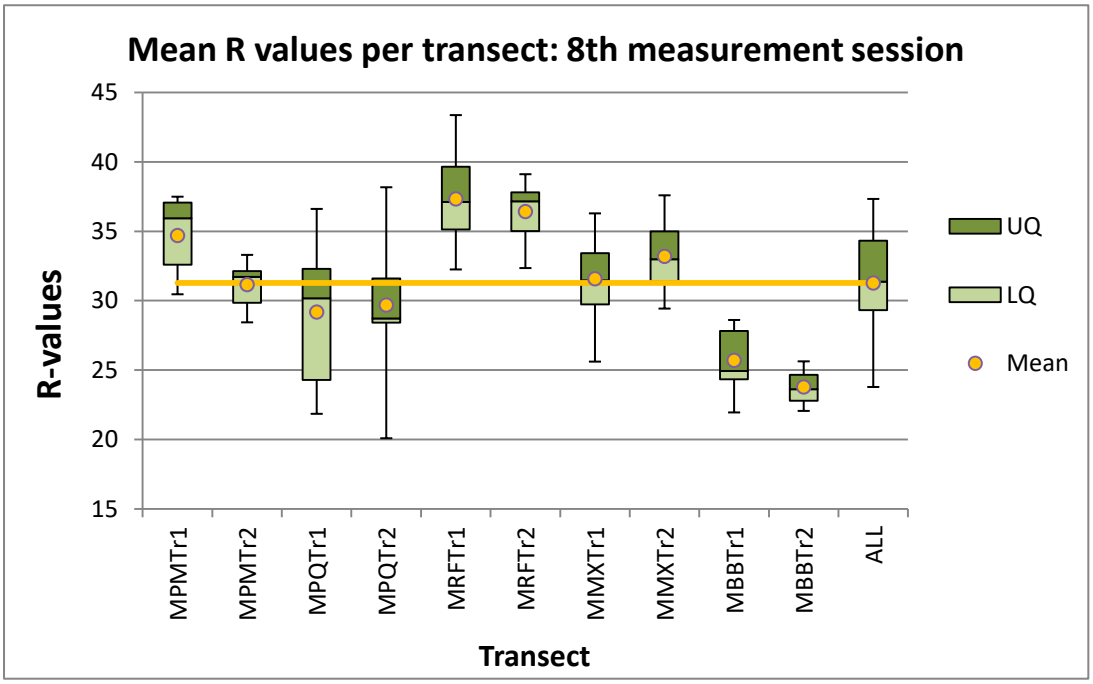

Figure 5.16: Mean R values per platform-transect across the 8th measurement session

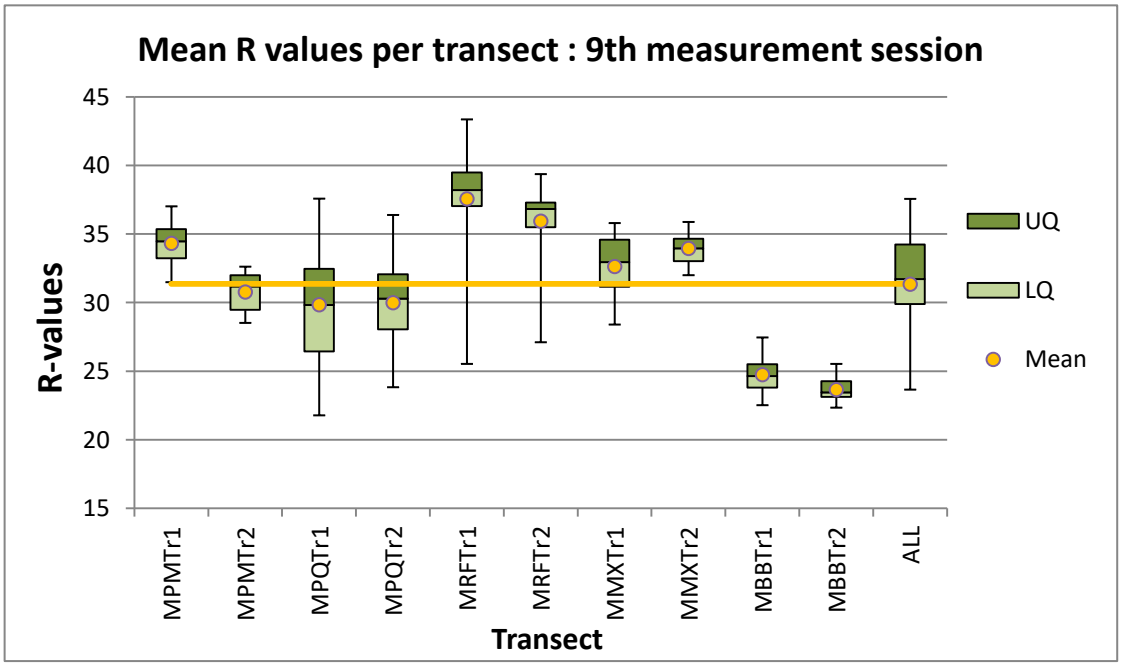

Figure 5.17: Mean R values per platform-transect across the 9th measurement session

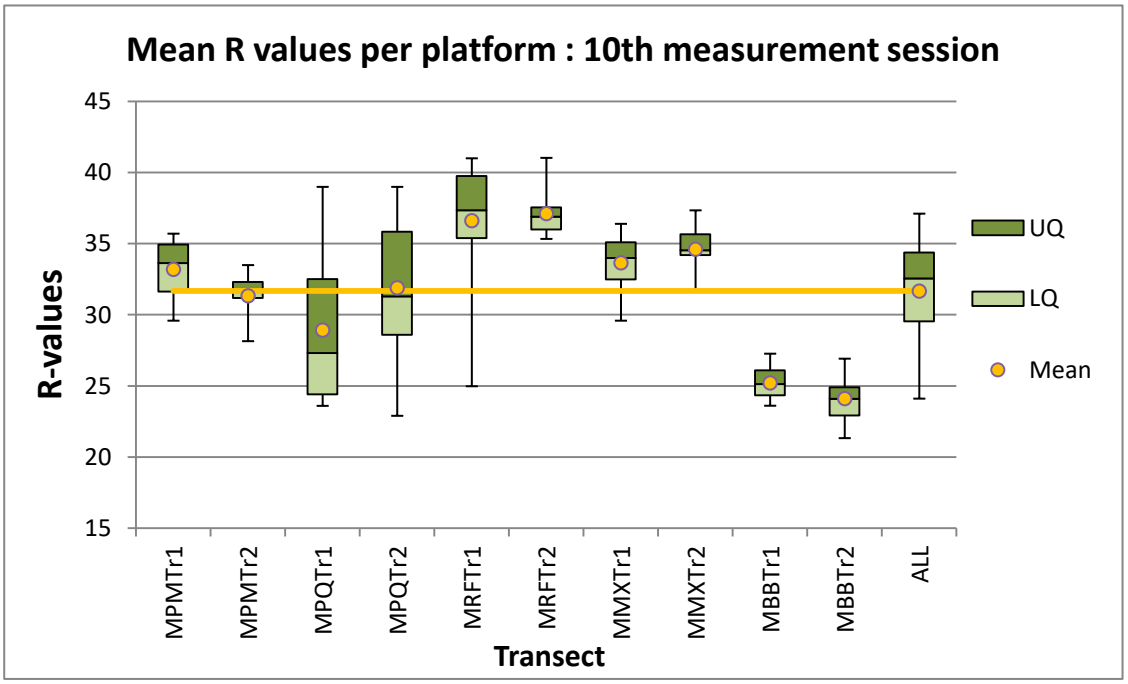

Figure 5.18: Mean R values per platform-transect across the 10th measurement session

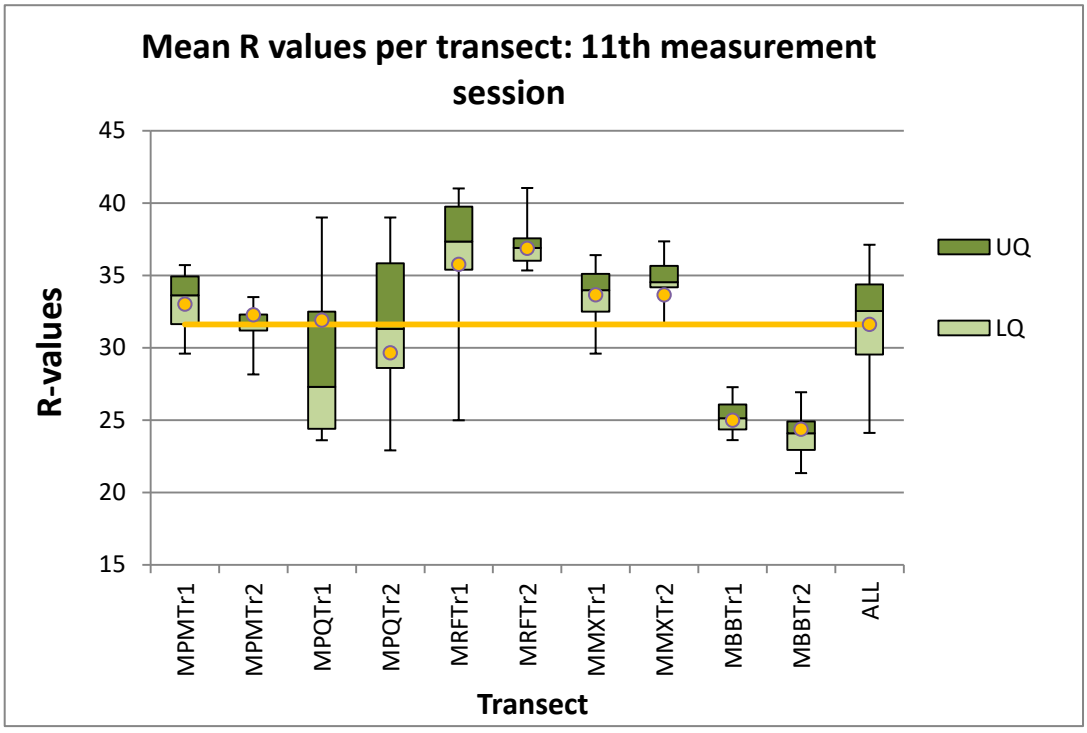

Figure 5.19: Mean R values per platform-transect across the 11th measurement session

5.4.5 Mean R values for TMEM stations

During the systematic collection of the R values across the platforms in a cross-shore direction, the relative position and R values of all *in situ* impact points in the vicinity of the TMEM stations were also recorded. This was done in order to get a more accurate measure of the rock hardness properties surrounding the TMEM stations. As explained in the Methodology chapter (Chapter 3, Section 3.5.1.1), this data would then be triangulated with the TMEM results in order to examine in a more site-specific manner the relationship between the rock surface mechanical strength and rock surface change rates. The other objective outlined was to identify any cross-shore differences in rock surface hardness by comparing the R values recorded in the foreshore areas with those in the backshore areas.

A total of 1550 impact points were measured close to 31 TMEM stations in situ, with 50 impacts points at each station recorded over a period of six measurement periods (18 months). As shown in Table 5.8 and Figure 5.20, more than 85% of the measured R values centred around four intervals from 25-44. This pattern is generally in agreement with the overall pattern observed at transect level (Table 5.6). The percentage groups that add up more 85% of the R values have been highlighted in grey in Table 5.8 (with peak percentage of R values in darker grey) for better identification of data distribution between the 31 TMEM stations.

Similar to the observations made earlier (Sections 5.4.2 and 5.4.3), the platform of Ras il-Fenek has recorded the largest representation of higher end R values. The measurements of TMEM stations at Ras il-Fenek, MRF 1-7, confirm this trend with a high percentage of R values in MRF 1, 3, 4, 5, 6 within the 40-44 interval whilst MRF1 and MRF7 registering the highest proportion the whole dataset with values in the 44-49 interval. Another identified pattern that was confirmed was that of the lower end R values being recorded at Blata l-Bajda platform. Similarly to the data produced at transect level, the data at the TMEM

stations fall within the intervals of 25-29 bracket (MBB 3, 5 and 6) and 30-34 bracket (MBB1, 2 and 4). The TMEM stations at Blata l-Bajda

Table 5.8: Percentage distribution of all individual R values per class intervals, recorded in the vicinity of each TMEM station. Highlighted class intervals cover >85% of measured R values, with the highest percentage highlighted in dark grey.

TMEM	20-24	25-29	30-34	35-39	40-44	45-49	50-55	Total
	%	%	%	%	%	%	%	
MPM1	0.0	0.0	26.0	48.0	24.0	2.0	0.0	100
MPM2	0.0	0.0	2.0	32.0	66.0	0.0	0.0	100
MPM3	0.0	0.0	6.0	36.0	56.0	2.0	0.0	100
MPM4	0.0	2.0	28.0	60.0	10.0	0.0	0.0	100
MPM5	0.0	4.0	32.0	50.0	14.0	0.0	0.0	100
MPM6	0.0	4.0	18.0	64.0	14.0	0.0	0.0	100
MRF1	0.0	2.0	12.0	36.0	44.0	6.0	0.0	100
MRF2	0.0	0.0	12.0	16.0	28.0	44.0	0.0	100
MRF3	0.0	0.0	2.0	12.0	54.0	32.0	0.0	100
MRF4	0.0	0.0	0.0	8.0	68.0	24.0	0.0	100
MRF5	0.0	0.0	8.0	38.0	52.0	2.0	0.0	100
MRF6	0.0	0.0	6.0	16.0	48.0	30.0	0.0	100
MRF7	0.0	0.0	0.0	12.0	24.0	60.0	4.0	100
MMX1	0.0	0.0	12.0	26.0	60.0	2.0	0.0	100
MMX5	0.0	0.0	8.0	60.0	32.0	0.0	0.0	100
MMX3	0.0	0.0	10.0	56.0	32.0	2.0	0.0	100
MMX2	0.0	2.0	12.0	58.0	28.0	0.0	0.0	100
MMX6	0.0	0.0	0.0	68.0	32.0	0.0	0.0	100
MMX4	0.0	0.0	6.0	46.0	46.0	2.0	0.0	100
MPQ1	0.0	2.0	24.0	60.0	14.0	0.0	0.0	100
MPQ2	0.0	0.0	38.0	54.0	8.0	0.0	0.0	100
MPQ3	0.0	30.0	54.0	16.0	0.0	0.0	0.0	100
MPQ4	0.0	4.0	50.0	22.0	24.0	0.0	0.0	100
MPQ5	0.0	4.0	54.0	34.0	8.0	0.0	0.0	100
MPQ6	0.0	22.0	54.0	18.0	6.0	0.0	0.0	100
MBB1	0.0	14.0	84.0	2.0	0.0	0.0	0.0	100
MBB2	0.0	4.0	96.0	0.0	0.0	0.0	0.0	100
MBB3	0.0	84.0	14.0	2.0	0.0	0.0	0.0	100
MBB4	0.0	40.0	60.0	0.0	0.0	0.0	0.0	100
MBB5	2.0	74.0	24.0	0.0	0.0	0.0	0.0	100
MBB6	14.0	84.0	2.0	0.0	0.0	0.0	0.0	100
ALL	0.5	12.1	24.3	30.6	25.5	6.7	0.1	100

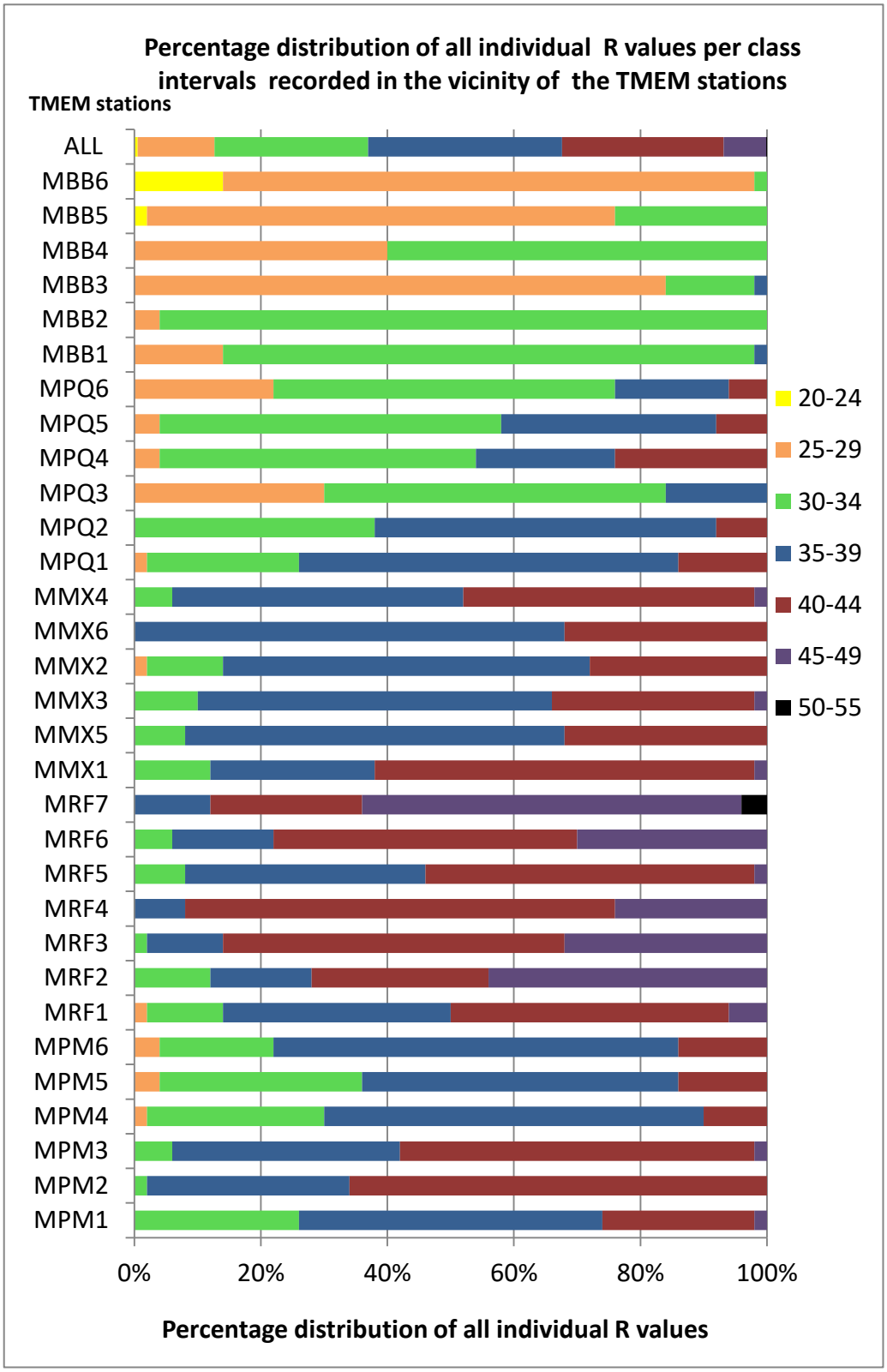

Figure 5.20: Percentage distribution of all individual R values recorded in situ vicinity of the TMEM stations. Percentage distribution of the whole TMEM dataset included at the top.

registered also the highest concentration of R values within one class interval: 96% of R values in class interval 30-34 at MBB2 and 84% at MBB1, 3 and 6. This distribution was relatively more highly concentrated than the one observed at transect level (Table 5.6). Both the relatively lower R values and their narrow variability within the values spectrum may be considered as the two main reasons while this shore platform was found to be so distinct from the rest of the investigated platforms.

As seen in Table 5.8 and Figure 5.20, the second closest platform to Blata l-Bajda in terms of measured rock hardness near TMEM stations was Ponta tal-Qammieħ, with four stations out of six recording the largest proportion of their R values within the 30-34 interval. Compared to Blata l-Bajda platform however, the distribution of >85% of the R values at Ponta tal-Qammieħ covers a wider range of class intervals, i.e. from 25-44. Within the wider distribution, R values in the upper class interval of 40-44 were only recorded only at MPQ 1 (14%) and MPQ 4 (24%).

Whilst a variable distribution of R values continues to be present in the remaining three platforms - Ponta tal-Munxar, Ras il-Fenek and Ponta tal-Miġnuna –Table 5.8 and Figure 5.20 display a noticeable data shift from Ponta tal-Qammieħ platform, with rock hardness values represented more in the 30-34 and 35-39 intervals at Ponta tal-Munxar and Ras il-Fenek platform. Two striking exceptions in this distribution are MRF2 and MRF7 which registered their largest percentage groups (44% and 60% respectively) outside the mentioned two class intervals and within the 40-44 intervals. MRF2 was also the station from the whole dataset which registered the widest range in its R values distribution, covering four intervals from 25-44. The TMEM stations at Ponta tal-Miġnuna were the ones which showed mostly a weighted spread of percentage groups across the 30-44 intervals, with MPM1, 4, 5 and 6 showing relatively more similar data structure compared to MPM2 and 3.

The variable levels of surface hardness measured in this study may imply that lithological resistance to processes of surface change may vary between

platforms but also within the same platform. In terms of variability of surface change between platforms, the strongest result can be attributed to the two UGLM platforms of Ras il-Fenek and Blata l-Bajda, which resulted as the hardest and the least hard respectively amongst the selected platforms. With regards to the variability within the same platform, the three LGLM platforms exhibited a wider spectrum of R values in the data structure. This may hence imply a larger variety of surface hardness properties and as a result the rates of surface change not only would be also equally variable but they would also be dependent on site-specific parameters of lithological resistance.

5.4.6 Cluster analysis of surface hardness properties and R value results

From the descriptive statistics presented in previous sections (Sections 5.4.1- 5.4.5) patterns of differences and similarities between platforms have emerged. In this section, a non-hierarchical clustering method, the K-means clustering method (SPSS®), was undertaken in order to confirm whether such patterns of differences and similarities are statistically significant. The results presented in Table 5.5 were run in a clustering procedure by aggregating platform data into two, three and four groups. The results are presented in Table 5.9. The row of those transects which remained consistently clustered together throughout the test, are highlighted for ease of reference.

The initial two-group clustering step detached the two transects of Blata l-Bajda platform from the rest of the eight transects. This first result confirms a pattern, identified in the previous sections, which indicated this platform as the most distant from the whole group and it remained a separate cluster throughout the three step procedure (Table 5.9). The result also confirms that there is a good degree of similarity between its two main transects, as previously observed in the frequency diagrams (Figure 5.12 and Figure 5.13).

Table 5.9: Cluster analysis of the platform according to their properties

Cluster membership into a 2-, 3- and 4-group of each transect						
Shore platform and Transect No.	2 Group Cluster	Distance	3 Group Cluster	Distance	4 Group Cluster	Distance
Ras il-Fenek Tr1	1	139.818	1	57.430	1	3.880
Ras il-Fenek Tr2	1	134.967	1	52.452	1	3.880
Ponta tal-Miġnuna Tr1	1	27.075	1	55.587	3	13.321
Ponta tal-Miġnuna Tr 2	1	64.675	2	18.086	4	41.004
Ponta tal-Munxar Tr1	1	14.760	2	68.827	3	27.808
Ponta tal-Munxar Tr2	1	28.817	1	54.186	3	14.695
Ponta tal-QammieħTr1	1	140.341	2	57.873	4	34.936
Ponta tal-QammieħTr2	1	111.420	2	29.056	4	6.306
Blata l-Bajda Tr1	2	36.019	3	36.019	2	36.019
Blata l-Bajda Tr2	2	36.019	3	36.019	2	36.019

From the three-group clustering, the platforms of Ras il-Fenek, Ponta tal-Qammieħ emerge as two separate clusters, whilst Ponta tal-Mignuna and Ponta tal-Munxar are closer and overlap each other and with Ras il-Fenek as aggregates. This second result continues to confirm that Blata l-Bajda platform is relatively more statistically distant from Ras il-Fenek platform. It also classifies Ras il-Fenek platform as statistically closer to two other platforms and not as strongly distinct as originally suspected in Section 5.4.1. In the final clustering step, Ras il-Fenek platform becomes a distinct cluster (Table 5.9). However, Ponta tal-Qammieħ platform continued to share its cluster with Ponta tal-Miġnuna Transect 2, whilst both transects at Ponta tal-Munxar re-grouped together and re-aligned with Ponta tal-Miġnuna Transect 1. This result further confirms the close statistical affinity, initially observed in Section 5.4.1 between the platforms of Ponta tal-Miġnuna, Ponta tal-Munxar and Ponta tal-Qammieħ and the larger differences present between Ras il-Fenek and Blata l-Bajda. If the rates of surface change are strongly controlled by surface hardness, then a similar pattern of surface change between the five platforms would likewise emerge i.e. Ras il-Fenek recording the lowest rates of surface change, Blata l-Bajda would record the highest rates of surface change, whilst the remaining three platforms would comparable record rates of surface change.

5.4.7 Percentage distribution of R values per platform and TMEM stations

A second clustering test was performed by using the percentage distribution of the R value classes presented in Table 5.6. The results confirm some of these results obtained in the previous clustering exercise. Similarly to the results presented in previous sections, these findings confirm that on the basis of surface hardness, the UGLM platforms of Ras il-Fenek and Blata l-Bajda should potentially produce relatively higher and lower rates of surface change respectively, whilst the rates of surface change at the LGLM platforms may produce less contrasting results but a wider mix of magnitudes.

Table 5.10: Cluster analysis of the platform according to their R values records

Cluster membership into a 2, 3 and 4 group cluster per platform						
Shore platform and Transect No.	2 Group Cluster	Distance	3 Group Cluster	Distance	4 Group Cluster	Distance
Ras il-Fenek Tr1	1	32.880	2	11.855	2	11.855
Ras il-Fenek Tr2	1	36.164	2	11.855	2	11.855
Ponta tal-Miġnuna Tr1	1	15.207	3	14.415	3	11.791
Ponta tal-Miġnuna Tr2	1	25.449	3	15.699	3	19.004
Ponta tal-Munxar Tr1	1	16.754	3	6.381	3	2.077
Ponta tal-Munxar Tr2	1	25.950	3	20.435	3	13.325
Ponta tal-Qammieħ Tr1	1	30.280	1	28.158	1	7.162
Ponta tal-Qammieħ Tr2	1	27.606	3	30.363	1	7.162
Blata l-Bajda Tr1	2	15.497	1	15.709	4	15.497
Blata l-Bajda Tr2	2	15.497	1	25.099	4	15.497

The platforms of Bajda l-Bajda and Ras il-Fenek became two distinct clusters by the third-grouping order and similarly Ponta tal-Miġnuna and Ponta tal-Munxar. The only difference in the final result between the two clustering tests is found in the position of Ponta tal-Miġnuna (Transect 2), which in the first test remained grouped with Ponta tal-Qammieħ platform, whilst in the second test, the four transects Ponta tal-Miġnuna and Ponta tal-Munxar remain clustered together. The slight difference may be attributed to the close similarities that exist between these three platforms. With the K-mean being a

multivariate test, it is to be expected that platforms with similar properties may create borderline situations in such a manner, that when there is a slight change in the variables base, a slight shift of cases may occur from one cluster to another. In this case the change was due to the first test having a multi-variable base (made up of 13 variables) whilst the second was primarily based on R values percentage classes only. Nevertheless, the principal common outcome for both tests remain unchanged: the platforms of Ras il-Fenek and Blata l-Bajda remain two distinct groups in terms of surface hardness whilst Ponta tal-Qammieħ, Ponta tal-Miġnuna and Ponta tal-Munxar occupy a more central region of similarities between them.

5.4.8 Percentage distribution of R values per TMEM stations

The third clustering analysis consisted of testing out which of the 31 TMEM stations may be more statistically close on the basis of the percentage distribution of their individual R value in interval classes, reproduced in Table 5.8. Table 5.11 displayed two clustering groups as follows:

i. Clustering of individual stations belonging to the same platform: TMEM stations from the same platform remained grouped together throughout the three step grouping; and
ii. Clustering of individual stations belonging to different platforms: TMEM stations from different platforms formed a cluster and remained together through the three-step grouping.

One of the main results which emerged is that stations primarily branch out into two main categories: stations that did not associate with other stations other than the ones found on the same platform and stations that have closer affinity both with other stations on the same platform and from other platforms. 13 out of 31 TMEM stations from all platforms with the exception of Ponta tal-Miġnuna has stations that remained clustered together primarily with other stations belonging to the same platform. This would indicate a strong similarity

Table 5.11: Results of K-mean clustering analysis according to percentage distribution of individual R values per TMEM station. TMEM stations are classified into clustering patterns, indicating which group of stations remained unchanged as a cluster group throughout the analysis. Colour codes indicate which stations shared the same association at each group level. Cluster number at each group level is indicated by a number.

Type of Clustering	Name of Platform	TMEM	5 Group Cluster	Distance	6 Group Cluster	Distance	7 Group Cluster	Distance
Within the same platform	Blata l-Bajda	MBB3	4	6.464	2	6.464	5	6.464
		MBB5	4	13.030	2	13.030	5	13.030
		MBB6	4	14.667	2	14.667	5	14.667
		MBB1	2	23.222	3	7.874	2	7.874
		MBB2	2	36.814	3	7.874	2	7.874
	Ponta tal-Qammieh	MPQ4	2	28.302	4	23.671	4	32.949
		MPQ5	2	26.808	4	22.634	4	26.070
	Pont tal-Munxar	MMX5	3	16.339	1	16.339	3	10.388
		MMX3	3	15.012	1	15.012	3	7.667
		MMX2	3	10.496	1	10.496	3	12.668
		MMX6	3	24.815	1	24.815	3	19.196
	Ras il-Fenek	MRF2	1	10.583	5	10.583	1	10.583
		MRF7	1	10.583	5	10.583	1	10.583
Between different platforms	Ras il-Fenek and Ponta tal-Munxar	MRF1	5	15.857	6	14.139	3	17.870
		MRF5	5	14.139	6	15.857	3	19.608
		MMX4	5	22.229	6	22.229	3	10.053
	Ponta tal-Qammieh/Blata l-Bajda	MPQ3	2	17.948	4	12.725	7	5.497
		MPQ6	2	12.733	4	2.592	7	11.813
		MBB4	2	27.544	4	28.515	7	15.348
	Ras il-Fenek/Ponta tal-Mignuna/Munxar	MRF3	5	26.498	6	26.498	6	20.281
		MRF4	5	27.663	6	27.663	6	19.408
		MRF6	5	23.303	6	23.303	6	19.305
		MMX1	5	12.180	6	12.180	6	15.599
		MPM2	5	16.757	6	16.757	6	19.816
		MPM3	5	12.325	6	12.325	6	19.579
	Ponta tal-Qammieh/Ponta tal-Mignuna	MPQ1	3	8.424	1	8.424	4	14.718
		MPQ2	3	22.781	1	22.781	4	9.572
		MPM4	3	12.319	1	13.877	4	12.674
		MPM5	3	13.877	1	16.363	4	13.215
		MPM6	3	16.363	1	9.704	4	2.574
		MPM1	3	9.704	1	12.319	4	21.809

that kept being constant throughout the analysis and irrespective of the transect in which they are located. This result confirms earlier analysis which showed a good degree of grouping between transects of the same platform.

Though these stations did form group associations with other platform stations (indicated by the colour code) at each separate group level, these associations kept changing from one group level to another. Ponta tal-Munxar was the platform with the strongest statistical affinity between its respective stations, by having the largest cluster of four stations grouped together, whilst the platform of Blata l-Bajda had stations paired up into a 3-2 set, with stations MBB3, 5 and 6 forming no associations with stations from other platforms at any level. On the hand MBB1 and 2, initially paired up with stations from Ponta tal-Qammieħ (MPQ3, 4, 5 and 6) and MBB4, but then remained distinct in the final two stages of the analysis. Two of the four composite clusters were relatively large and had six stations each: one group with Ponta tal-Qammieħ (MPQ1 and MPQ2) and Ponta tal-Miġnuna (MPM1, 4, 5, 6) and another group with three platforms: Ras il-Fenek (MRF3, MRF4 and MRF6), Ponta tal-Miġnuna (MPM2) and Ponta tal-Munxar (MMX1). One station from Blata l-Bajda (MBB4) paired up with Ponta tal-Qammieħ (MPQ3 and MPQ5) and another station from Ponta tal-Munxar (MMX4) paired up with Ras il-Fenek (MRF1 and MRF5).

Such a mix of results may be potentially attributed to the fact that measurements were taken at specific points on the platform. Differences from the relatively broader results at transect level were noticed. 18 stations from different platforms remained grouped together throughout the analysis and were classified under the second pattern indicating association between platforms. Yet, two observations can be confirmed from these results. First, Blata l-Bajda platform remains distinct even at a station level. The second observation confirmed is about the borderline properties of the Ponta tal-Miġnuna platform, which kept switching statistical associations with other

platforms, and primarily with Ponta tal-Munxar, Ponta tal-Qammieħ and Ras il-Fenek. This was also indicated already in the previous two clustering tests when these four platforms were separated from Blata l-Bajda into two distinct clusters (Table 5.9 and Table 5.10).

5.4.9 Temporal differences in mean R values per transect

In Section 5.4.4, the descriptive results seem to suggest that there seem to be no seasonal effect on the surface hardness values per platform. A series of Independent Sample T-tests were carried out to compare the mean R values collected from three measurement periods, in order to determine whether there is statistical evidence that mean R values are significantly different due to seasonality. The chosen measurment periods were, 7th and 11th (summer measurement sessions i.e. July/August 2014 and July/August 2015 respectively) and the 9th session (winter period i.e. Feb/March 2014). KS Test confirmed the normal distribution of the datasets for this test and appropriate use of Indepedent Sample T-test. The results displayed in Table 5.12, indicate that all tests did not result in any significant differences between the datasets representing the three seasonal periods. The *p* value scores were all above the 0.05, indicating no difference in R values between the different periods and hence winter-summer dual seasonality does not have any significant bearing on the surface hardness. Some degree of variability between the dataset was picked up and these are represented by the range of *p* value results obtained (from 0.06 to 0.77) for each transect. Yet this variability was not statistically significant enough to infer seasonality as a determining factor in rock surface hardness change. The outcome of this analysis is that rock strength as measured using R values can be treated as a constant once measured on a temporal scale and that levels of surface strength did not significantly change over the course of the study period due to seasonal effects. In using the Schmidt Hammer as a geomorphological tool to measure surface hardness, many platform studies had assumed this lack of seasonal effect; however it was never tested out to rule it out in an empirical way, as this study has done.

Table 5.12: Comparisons of mean R values between 7th, 9th and 11th measurement sessions

Comparisons of mean R values between 7th, 9th and 11th measurement sessions: Independent Sample T-tests results per platform and transect				
Shore platform and Transect No.	7th vs 9th measurement sessions*		9th vs 11th measurement sessions	
	P value	Mean, Standard Deviation, Degrees of Freedom	*P value*	Mean, Standard Deviation, Degrees of Freedom
Ras il-Fenek Tr1	0.70	(M=36.75, SD=5.47), t(20)=-0.39	0.34	(M=37.60, SD=4.57), t(20)= 0.99
Ras il-Fenek Tr2	0.29	(M=37.51, SD=3.55), t(20)=1.09	0.39	(M=35.95, SD=3.19), t(20)=-0.89
Ponta tal-Miġnuna Tr1	0.55	(M=34.80, SD=1.70), t(18)=0.61	0.12	(M=34.34, SD=1.68), t(18)=1.65
Ponta tal-Miġnuna Tr2	0.19	(M=32.11, SD=2.68), t(18)=1.37	0.20	(M=30.78, SD=1.48), t(18)=-2.47
Ponta tal-Munxar Tr1	0.36	(M=31.57, SD=3.24), t(22)=-0.94	0.42	(M=33.65, SD=2.32), t(22)=-0.82
Ponta tal-Munxar Tr2	0.34	(M=33.21, SD=2.38), t(22)= -0.97	0.66	(M=33.96, SD=1.29), t(22)=0.45
Ponta tal-Qammieħ Tr1	0.34	(M=28.46, SD=3.07), t(28)= -0.97	0.38	(M=30.01, SD=3.33), t(28)=-0.89
Ponta tal-Qammieħ Tr2	0.77	(M=30.36, SD=3.01), t(28)=0.29	0.38	(M=28.46, SD=3.07), t(28)=-0.97
Blata l-Bajda Tr1	0.06	(M=28.85, SD=3.66), t(26)=1.98	0.69	(M=24.76, SD=1.46), t(26)=-0.41
Blata l-Bajda Tr2	0.12	(M=24.66, SD=1.84), t(22)=1.63	0.18	(M=23.65, SD=0.09), t(22)=-1.40
** Dates: 7th = July/August 2014; 9th = Feb/March 2015; 11th = July/August 2015*				

5.4.10 Cross shore differences in R values analysis between foreshore with backshore stations

Due to their supratidal conditions in a micro-tidal regime, these platforms have a very restricted foreshore area, mainly affected by sea wave splashes and sea spray. Moisture, for example, is known to have an effect on the surface properties especially on porous rocks due to inter-grain sliding, which softens the grains and looses skeletal bonding (plasma) that holds the grains together (Aydin, 2009). Salt weathering is also known to be fairly localised in the foreshore at supratidal levels (Moses and Smith, 1994). It is not however clear to what extent surface resistance may vary across supratidal cross-shore surfaces. The structure of the platform in terms of elevation, edge morphology, gradient and orientation act as compounding factors limiting or extending moisture by direct wave reach extent. An independent sample t-test was undertaken to test whether surface hardness within the foreshore zones (influenced by, wave splashes, sea spray and salt weathering) is different from that in the backshore areas of the platform. A winter measurement period was chosen, the 9th (February/March 2015), as it provides the right conditions to test the foreshore area under rougher dynamic conditions with relatively more wave action and sea spray due to rougher sea conditions.

Table 5.13 displays the results of mean R values between the first test point in the foreshore area compared to the last test point in the backshore area along the ten transects. The 6th measurement session (also taken in winter) was also included as an initial comparison. The trend observed from the data is that there seem to be a decrease in the rebound values between foreshore and backshore areas. This reduction is quite variable and ranges from -0.2 (Ponta tal-Munxar Tr1) to -14.2 (Ponta tal-Qammieħ Tr 1) for the 6th session and -1.1 (Ponta tal-Miġnuna Tr2) to -14.3 (Ponta tal-Qammieħ Tr1). When comparing the data in Table 5.13 Ponta tal-Qammieħ stands out as an outlier in the dataset, with high values both in terms of cross shore decline in R values and also the relatively higher standard

deviation values. Not all differences resulted in a cross shore reduction of the R values. In the 9th session, Ras il-Fenek (Tr 1), Ponta tal-Munxar and Ponta tal-Miġnuna registered an increase, albeit not substantial (1.1-2.9) in the 9th session.

Table 5.13: Difference in mean R-values between foreshore and backshore zones per platform

Difference in mean R-values between foreshore and backshore zones per platform										
Platform and transect	6th session*					9th session*				
	Foreshore	St. Dev.	Backshore	St. Dev.	Diff.	Foreshore	St. Dev.	Backshore	St. Dev.	Diff.
Ras il-Fenek Tr1	39.3	1.7	42.0	1.0	-2.7	36.5	2.2	43.4	3.0	-6.9
Ras il-Fenek Tr2	38.0	2.6	39.7	1.8	-1.7	38.2	2.4	37.0	2.5	1.2
Ponta tal-Miġnuna Tr1	28.9	1.9	32.1	2.4	-3.2	34.8	2.9	33.5	1.6	1.3
Ponta tal-Miġnuna Tr2	29.9	3.7	31.2	2.4	-1.3	30.8	3.5	29.7	1.6	1.1
Ponta tal-Munxar Tr1	26.8	2.4	27.0	1.1	-0.2	31.3	2.4	28.4	2.1	2.9
Ponta tal-Munxar Tr2	25.7	4.5	32.5	1.3	-6.8	35.6	2.2	33.1	1.5	2.5
Ponta tal-Qammieħ Tr1	22.3	3.2	36.7	4.4	-14.4	21.8	1.9	36.1	4.3	-14.3
Ponta tal-Qammieħ Tr2	21.5	2.9	35.8	4.7	-14.3	23.9	1.6	30.9	3.0	-7.0
Blata l-Bajda Tr1	23.5	2.0	24.8	0.4	-1.3	22.5	1.7	25.5	1.5	-3.0
Blata l-Bajda Tr2	24.8	1.9	23.6	1.4	1.2	25.6	0.9	23.3	1.8	2.3

The result of the independent sample t-test for the 9th session was that there was no significant difference in the mean R values for foreshore areas (M= 30.10, SD=6.20) and backshore areas (M=32.09, SD= 5.89); t(18)= -0.736, p = 0.471. In other words, the observed reductions were not statistically significant. Not wanting to leave this result just based on a chance, a second independent sample t test was conducted by taking the R values recorded during the 6th measurement session (Feb/March 2014). The outcome of this second test confirms the first test: there

was no significant difference in the mean R values between foreshore areas (M= 28.07, SD=6.18) and backshore areas (M=32.54, SD= 6.16) conditions; t(18)=-1.620, p = 0.123. These two results would therefore suggest that the overall weathering and erosion conditions produced by waves and sea spray conditions and salt weathering at supratidal levels during winter may not be sufficient to establish a significant difference in R values between the foreshore areas and the backshore. The implication of these findings would potentially be that surface hardness in a cross-shore direction may not vary to the extent of influencing the rates of surface change across the platform

5.4.11 Synthesis of main findings

i. 78% of all individual R values measured on the platforms fell in the category 35-44, suggesting not a large difference in levels of surface hardness across the five platforms;
ii. UGLM platforms recorded opposite qualities of surface hardness: Blata l-Bajda recorded the lowest R values, whereas Ras il-Fenek platform recorded the highest R values. This trend was confirmed at station level;
iii. The two platforms of St Thomas Bay exhibited strong similar rates and patterns in terms of surface hardness even though they have a different structure;
iv. No seasonal difference in mean R values was measured on all the platforms;
v. No cross-shore difference in the mean R values was measured across the platforms. Spatial difference in rock hardness values between foreshore and backshore of platforms was not statistically significant; and
vi. Blata l-Bajda was found to be the most distinct in terms of surface hardness properties; the least distinct were found to be the platforms of St Thomas Bay.

5.5 Exposure experiment with micro-catchment: Results

5.5.1 Description of weathering state of exposed slabs.

The aim of this exposure experiment was to monitor surface change responses to inland subaerial conditions and quantify their susceptibility to weathering. As explained in Chapter 3 (Section 3.5.2), the variability of the responses to sub-aerial weathering may shed important indications about the geotechnical behaviour of rock and related breakdown responses (Pinho *et al.*, 2006). The underlying assumption would be that the observed rates and modes of physical alterations would provide important leads to potential behaviour patterns of surface change at platform level.

Over a total exposure period of 18 months, the sixteen limestone slabs manifested variable signs of denudation. This present section provides a visual inspection account of the variable state of weathering exhibited by the rock samples and summarised in Table 5.14. The weathered slabs were classified as follows: two as W1, nine were classified as W2, two samples were classified as W3, and 3 samples and specimens were classified as W4. No samples were classified as W5. The result of this ISRM (1981) classification-based assessment indicated some strong differences between the samples in terms of weathering states. The 16 slabs exhibited variable signs of deterioration in terms of colour, texture, firmness and form; all features which tend to indicate a decline in the mechanical properties of a rock cause by both physical and chemical weathering (Appendix VII). As displayed in Figure 5.21, the most common signs of weathering shared by most samples were as follows: discolouration to one to two shades lighter than the original one; increase in pitting and rougher surface; splinter breaks at the perimeter; debris loss and reduction in weight.

The UGLM samples of Blata l-Bajda platform were the ones which underwent the most intense alterations after exposure. Two of its samples, no. 9 and no. 12,

were the only two slabs from the whole experiment sample to grade as highly weathered (W4). These samples were discontinued from TMEM measurements after the first exposure period given that the rapid denudation destabilised the control points of the TMEM (Figure 5.21). Apart from rapid discolouration, the samples produced substantial powdering and fine surface flaking, accompanied by subsequent perimeter breakages and substantial form reduction. This rapid denudation produced substantial weight loss and debris loss throughout the exposure period (See Section 5.5.2).

Table 5.14: Description of weathering state of the experimental slabs according to ISRM (1981) classification system

Sample no.	Shore platform and sample position	Globigerina Limestone Member	Description of weathering state				
			W1	W2	W3	W4	W5
1	Blata l-Bajda - Front	Upper					
2	Ponta tal-Qammieh - Front	Lower					
3	Ponta tal-Mignuna - Back	Lower					
4	Ponta tal-Munxar - Back	Lower					
5	Globigerina Block Sample	Lower					
6	Ras il-Fenek - Front	Upper					
7	Ponta tal-Munxar - Back	Lower					
8	Ponta tal-Munxar - Front	Lower					
9	Blata l-Bajda -Front	Upper					
10	Ras il-Fenek - Back	Upper					
11	Ponta tal-Mignuna -Back	Lower					
12	Blata l-Bajda -Back	Upper					
13	Ponta tal-Mignuna - Front	Lower					
14	Ras il-Fenek - Front	Upper					
15	Ponta tal-Qammieh - Back	Lower					
16	Ponta tal-Qammieh - Front	Lower					

Slab Photo Before Exposure	Slab Photo After Exposure	Weathering State Description	Grade ISRM (1981)	Colour	Texture
		•Minor signs of alterations •Form and perimeter intact and retained 95% of original shape •Minor loss of weight •Minor loss of debris	W1	•Light greyish cream •Only slight signs of discolouration in some parts	•No alterations from original texture •No flaking, or powdering •Minor pitting
		•Visible signs of perimeter alterations •Smoothing of rough edges by solution • Signs of chipping by minor fracturing	W2	•Evident signs of discolouration to one shade lighter than original colour	•Coarser •More visible pitting •Fresh fractured surfaces at the sides
		•Evident signs of rock physical breakdown with presence of fractures and splinter fragments •Loss of original •Partial loss of TMEM studs	W3	•Heavy discolouration to one or two shades lighter than original colour	•Presence of weathered powder. •Visible signs of pitting •Flaking
		•Slabs lose their original shape completely. •Remnants have fragile structure •Total loss of TMEM studs •Heavy loss of weight and debris	W4	•Total discolouration to two or more lighter shades. •Whitish colour observed	•Very friable •Coated with weathered powder both at the surface and around the perimeter

Figure 5.21: Photographic record of the following slabs and related descriptions of weathering effects after exposure period: Ras il-Fenek no. 10 (W1), Ponta tal-Miġnuna no. 3 (W2), Ponta tal-Munxar no. 8 (W3) and Blata l-Bajda no. 9 (W4).

This response seems to indicate the UGLM rocks at Blata l-Bajda platform which are relatively weakly cemented rocks, once extracted, were subject to physical (mechanical) weathering caused by differential expansion from pressure release (the latter brought by a reduction of the confining forces previously exerted from the platform). Evident signs of chemical weathering were also observed through the heavy production of weathered powdered debris, flaking and smoothing of sharp edges and discolouration due to washing away of minerals.The responses of the UGLM samples of Ras il-Fenek platform was very different. As mentioned in Chapter 4 (Section 4.2), although the lithology of Ras il-Fenek platform consists of UGLM, the hardground beds present at its various exposure levels create a compact layer which is considered much more resistant to sub-aerial weathering. This resistance level was evident in this experiment, especially for the back sample no. 10, which graded as W1 for its low weathering alterations (Figure 5.21). The front samples of Ras il-Fenek (no. 6 and no. 14) extracted from areas with less hardground cover, exhibited slightly higher weathered states (W2), albeit not as intense at the Blata l-Bajda samples (W3 and W4) (Appendix VII). This result confirms the geo-mechanical variability that exists within the same globigerina member (in comparing Blata l-Bajda and Ras il-Fenek) but also its variability even within the same platform as in the case of Ras il-Fenek platform.

The majority of the remaining slabs in LGLM exhibited slightly weathered states (W2), with most platform specimens ranging widely from slightly weathered (no. 2, 3, 7, 11, 13, 14, 15, and 16) to moderately weathered (no. 1, 4 and 8) and highly weathered states (no. 9 and 12). Interestingly, the Lower Globigerina Limestone block (no. 5) showed minimal signs of weathering state (W1) and this was also confirmed by the results of negligible loss of weight and debris (See Section 5.5.2). This result points therefore to different geo-mechanical behaviour in LGLM between quarried limestone blocks and natural rock surfaces, as in this case for platform surfaces. When compared to the platform specimen, the quarried limestone block kept a relatively more

compact appearance throughout the whole exposure periods and exhibited a less sensitive response to weathering processes.

In most cases, colour was also a good indicator of weathering state; the lighter the colour the more weathered the specimen. Most of the slabs - with the exception of the Globigerina block and Ponta tal-Qammieħ samples - got discoloured from pale gray/yellow to a pale yellow or off-white. Texture was also observed to be a good indicator of weathering; in general it was observed that as weathering progressed from one exposure period to the next the texture of the specimen became coarser and rougher, suggesting that surface voids and pitted surfaces were developing as a result of physical and chemical breakdown. In some specimen minor hair-like cracks and more evident fractures had also developed on the surface (Figure 5.21).

5.5.2 Weight loss and debris loss: results

Table 5.15 and 5.16 display the results of weight loss and debris loss of the exposed slabs. Table 5.15 illustrates the percentage weight loss undergone by each experimental slab from February 2015 to August 2016. As explained in the methodology section, weight changes from each slab were measured in August 2015 (six-months after initially exposed) and then measured again in August 2016 (one year after first exposure measurement). Table 5.16 displays the weight of debris loss from each experimental slab during the same study period. Rock material was observed to be mostly lost from the bottom and the sides of the sample. However, changes to more weathered states were also observed at the surface, especially in the relatively softer samples.

Table 5.15: Descriptive statistics of weight loss records per slab for exposure period February 2015 to August 2016

Sample No.	Platform Name	Sample Position	Before Exposure	First Exposure Period		Second Exposure Period		Periodic Sample Weight Loss				Total Sample Weight Loss	
			Feb-15	Feb-Aug 2015		Aug 2015-Aug 2016		Feb 15-Aug 15		Aug 2015-Aug 2016		Feb 2015-Aug 2016	
			Sample Weight (Kg)	Sample Weight (Kg)	Debris Weight (Kg)	Sample Weight (Kg)	Debris Weight (Kg)	(Kg)	%	(Kg)	%	(Kg)	%
1	Blata l-Bajda	Front	3.824	3.631	0.097	3.037	0.429	0.193	5.047	0.594	16.359	0.787	21.406
2	Ponta tal-Qammieħ	Front	6.340	6.200	0.027	n/a	n/a*	0.140	2.208	-	-	0.14****	-
3	Ponta tal-Miġnuna	Back	1.415	1.317	0.030	1.252	0.063	0.098	6.926	0.065	4.935	0.163	11.861
4	Ponta tal-Munxar	Back	2.056	1.979	0.039	1.758	0.181	0.077	3.745	0.221	11.167	0.298	14.912
5	Globigerina Block	None	2.763	2.755	0.011	2.753	0.012	0.008	0.290	0.002	0.073	0.010	0.362
6	Ras il-Fenek	Front	3.701	3.688	0.013	3.678	0.033	0.013	0.351	0.010	0.271	0.023	0.622
7	Ponta tal-Munxar	Back	3.779	3.702	0.025	3.629	0.074	0.077	2.038	0.073	1.972	0.150	4.009
8	Ponta tal-Munxar	Front	3.156	2.804	0.150	2.257	0.702	0.352	11.153	0.547	19.508	0.899	30.661
9	Blata l-Bajda	Front	3.428	2.085	0.354	0.924	0.888	1.343	39.177	1.161	55.683	2.504	94.861
10	Ras il-Fenek	Back	2.250	2.235	0.011	2.233	0.018	0.015	0.667	0.002	0.089	0.017	0.756
11	Ponta tal-Miġnuna	Back	1.287	1.241	0.024	1.188	0.102	0.046	3.574	0.053	4.271	0.099	7.845
12	Blata l-Bajda	Back	4.236	3.792	0.227	2.469	1.180	0.444	10.482	1.323	34.889	1.767	45.371
13	Ponta tal-Miġnuna	Front	3.267	3.235	0.020	3.218	0.063	0.032	0.979	0.017	0.526	0.049	1.505
14	Ras il-Fenek	Front	4.601	4.404	0.112	3.771	0.643	0.197	4.282	0.633	14.373	0.830	18.655
15	Ponta tal-Qammieħ	Back	n/a **	3.797	n/a***	3.239	0.585	-	-	0.558	14.696	0.558****	14.696
16	Ponta tal-Qammieħ	Front	n/a**	3.561	n/a ***	3.109	0.299	-	-	0.452	12.693	0.452****	12.693

** Sample discontinued*
*** Samples set up in August 2015*
**** No debris as it was a pre-exposure phase*

***** Partial results*

Table 5.16: Debris weight loss in grams

Sample No.	Platform Name	Sample Position	First Exposure Period	Second Exposure Period	Total Debris Lost
			Feb-Aug 2015	Aug 2015-Aug 2016	Feb 2015-Aug 2016
			Debris Weight (g)	Debris Weight (g)	Debris Weight (g)
1	Blata l-Bajda	Front	97	429	526
2	Ponta tal-Qammieħ	Front	27*		27****
3	Ponta tal-Miġnuna	Back	90	63	153
4	Ponta tal-Munxar	Back	39	181	220
5	Globigerina Block	None	11	12	23
6	Ras il-Fenek	Front	13	33	46
7	Ponta tal-Munxar	Back	25	74	99
8	Ponta tal-Munxar	Front	150	702	852
9	Blata l-Bajda	Front	354	888	1242
10	Ras il-Fenek	Back	11	18	29
11	Ponta tal-Miġnuna	Back	42	49	91
12	Blata l-Bajda	Back	227	1180	1407
13	Ponta tal-Miġnuna	Front	20	15	35
14	Ras il-Fenek	Front	112	643	755
15	Ponta tal-Qammieħ**	Back	n/a***	0.585****	585
16	Ponta tal-Qammieħ**	Front	n/a ***	0.299****	299

** Sample discontinued*

*** Samples set up in August 2015*

**** No debris as it was a pre-exposure phase*

***** Partial results*

Marked differences have been recorded between the five studied platforms in terms of both weight loss and debris loss. Though the mean of the total percentage weight loss for the five platforms was of 18.7%, large variations in percentages have been recorded between the sixteen slabs. These differences are better illustrated in Figure 5.23 where the three percentage

variables (i.e. first exposure, second exposure and total percentage) have been grouped according to each individual platform and their related samples. The most evident weight loss was recorded at the platform of Blata l-Bajda, with a major weight loss of 94.8% for one of its front section samples (No. 9, First exposure loss [FEL]=39.2%; Second exposure loss [SEL]=55.7%). The back section sample (No. 12) also recorded a heavy loss in weight of 45.4% (FEL=10.5%; SEL=34.9%). Interestingly, the third sample, from the front section (No.1), recorded a relatively much inferior percentage loss of 21.4% (FEL=5%; SEL=16.4%). As shown in Figure 5.23, the slabs of Blata l-Bajda would, in fact, account for the largest variability in terms of percentage weight loss amongst the slabs of the five studied platforms. This result would potentially indicate the existence of a degree of spatial variability in the properties of the platform and which may therefore lead to different responses to sub-aerial weathering processes. Such differences may potentially impact of the rates of surface change across the platform of Blata l-Bajda, with exposure susceptible to weathering recording relatively higher magnitudes of surface change when compared to other areas with a relative resistant surface. This may also mean that the rates of surface change across of the platform will not be homogenous but rather more localised to site-specific lithological efficacy.

Variable percentages in weight loss were also recorded at Ponta tal-Munxar, Ponta tal-Miġnuna and Ras il-Fenek, albeit less pronounced than those at Blata l-Bajda. The front section slab of Ponta tal-Munxar (no. 8) registered a total weight loss of 30.7% (FEL=11.2%; SEL=19.5%), whereas its two back section slabs recorded relatively less losses: 14.9% and 4.0% for slabs no. 4 and no. 7 respectively. A situation similar to Blata l-Bajda - whereby two slabs from the front section recorded variable percentage losses - was also observed in the samples of Ras il-Fenek: sample no. 14 recorded a loss of 18.7% (FEL=4.3%; SEL=14.4%), whereas sample no. 6 recorded a very low weight loss of 0.6% (FEL=0.3%; SEL=0.3%). The back section slab had a similar low percentage loss of 0.8% (FEL=0.7%; SEL=0.1%).

Conversely, the slabs at Ponta tal-Miġnuna (no. 3, 11 and 13) recorded higher losses in the back section samples (no. 11 and 13) i.e. 11.9 % and 7.8 % respectively and only 1.5% for the front section sample no. 3. The slabs of Ponta tal-Qammieħ cannot be compared for the whole study period as they had to be replaced due to their rock surfaces being too unstable for a proper use of the TMEM instrument. Only one record was included for the second exposure period, in which close figures were obtained between the front (no. 15) and back section (no. 16) of the platform: 14.7 % and 12.7 % respectively. The LGLM slab, recorded very minimal losses of 0.4% (FEL=0.3%; SEL=0.4%), indicating how a LGLM slab, purposely cut-out for building purposes, has a relatively higher resistance to sub-aerial weathering.

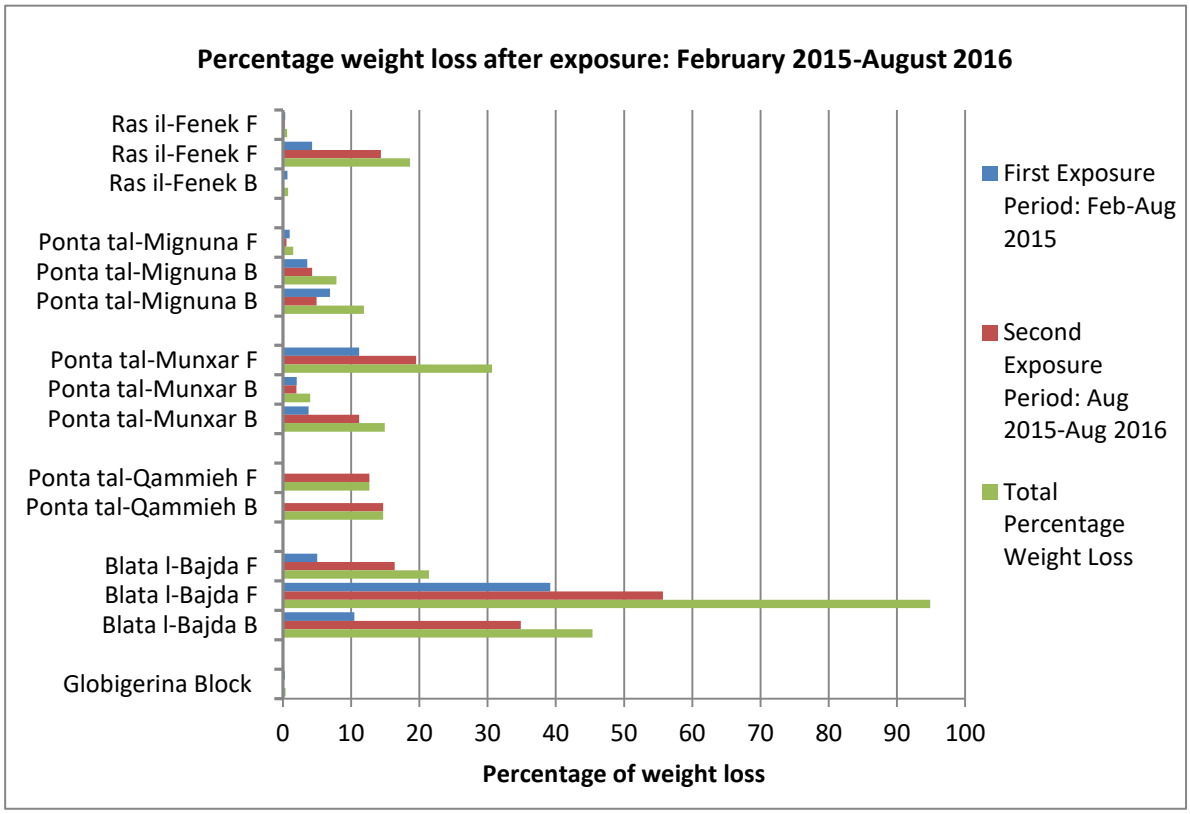

Figure 5.22: Percentage weight loss of experimental slabs, following exposure from February 2015 to August 2016. Recorded percentage values are for two exposure period. 'F' denotes slabs from the front section; 'B' for samples from the back section.

The mean percentage loss for the whole dataset during the first exposure period, which was of six months of duration, was of 6.8 % whilst the second exposure period, of one year record, registered a mean loss of 12.8%. Yet these figures belie the wide differences in the denudation rates recorded at platform levels, discussed earlier. The measured debris losses in grams are listed in Table 5.16 5.16 and grouped into platforms in Figure 5.23.

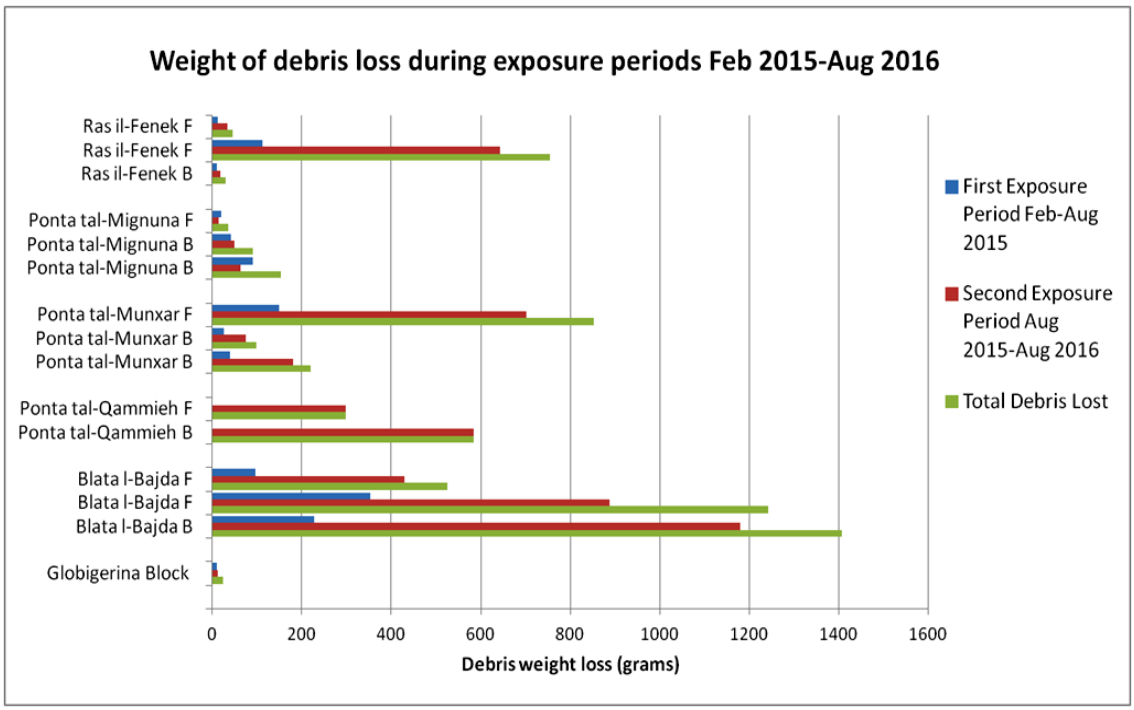

Figure 5.23: Weight of debris loss from experimental slabs following exposure from February 2015 to August 2016. Recorded values, in grams, are for two exposure periods. 'F' denotes slabs from the front section; 'B' for samples from the back section.

Comparisons are attempted with weight loss data in Figure 5.23. However, comparisons between the two graphs (Figure 5.23 and Figure 5.23) need to consider their proportional representation of the recorded losses displayed: the weight loss data was displayed as a percentage to the original weight before exposure whereas debris loss could not be tied to an original weight value and thus was presented as absolute values. Thus caution must be exercised when comparing percentages and absolute values of slabs which are substantially

different in sizes. The reason being that smaller samples which may have recorded high percentages of weight loss may still generate debris loss comparatively less in absolute weight when compared to larger slabs.

The relative pattern of debris loss per sample is very similar to the one described for percentage weight loss and have equally provided mixed results between platforms and differences between the slabs derived from the front and back sections. The slabs of Blata l-Bajda experienced the most debris loss as a result of their rapid denudation rates and thus account for the largest amount of debris loss in weight: 3,175 g out of a total 6385 g debris loss for all samples. The slabs from the front sections of Ponta tal-Munxar and Ras il-Fenek have also registered high debris loss (852 g and 755 g respectively) and these values align also with the patterns of weight loss recorded in the respective samples in Figure 5.23. Another similar identified pattern was that for Ponta tal-Miġnuna which registered also an opposite trend with slightly higher debris losses in the slabs derived from the back section. The Globigerina block produced minimal debris loss (23g) in line with the relatively small percentage loss and low denudation experienced by this slab.

5.5.3 Inferential analyses of inland subaerial experiment results: rates of weight and debris loss

The aims of the first analysis are two-fold: to establish whether a correlation exists between the weight loss experienced by the weathered slabs and the debris loss produced and secondly, to validate or otherwise the design of the debris catchment experiment used to capture the falling debris from overlying rock denuded samples. In order to provide a comparable analysis with the absolute values of the debris loss, the total weight loss per slab was left in absolute values as well. Only the datasets which cover the whole measurement period were considered and thus the slabs of Ponta tal-Qammieħ were not included in the test because their data does not cover the whole monitoring period.

A Kolmogorov-Smirnov test was carried out to check for data normality on the dependent variable, which in this case is the total debris loss. Debris loss dataset, $D(13) = 0.008$, $p > .05$, was found to have a non-normal distribution. A Spearman's correlation was run to assess the relationship between total weight loss and total debris loss using a small sample of 13 slabs from four platforms. There was a strong positive correlation between weight loss and debris loss, which was statistically significant, $r_s = 0.989$, $p = .000$. This result indicates that the there is a strong correlation between the amount of weight lost from the samples and that of = the debris that had accumulated in the catchment basins. This result illustrates how debris loss and weight loss were analogous and how their modes of losses may reflect in a similar behaviour of surface loss on the platform surface.

As discussed earlier, differences were observed in the weight-loss between the slabs from the front sections when compared with the back sections. This may indicate potential inherent lithological weaknesses present on the platform surfaces. The second statistical analysis presented in this section tests if such observed differences are statistical significant. The results for total weight loss (in grams) and percentage total weight loss were the two tested variables. Six samples from the front sections of the platforms (No. 4, 6, 8, 13, 1, 9) were tested against another six samples from the back sections (No. 3, 4, 7, 10, 11). Given the small sample size and the independence of both groups from each other, correlation tests were not considered adequate. A Kolmogorov-Smirnov test was used to test for normality of the two tested variables. Weight loss dataset, $D(12) = 0.189$, $p > .05$, was and percentage weight loss dataset, $D(12)=0.05$, $p >.05$ were found to have a normal distribution. The independent sample t-test was chosen as it requires a sample size of not less than six tested cases and it can also test if two independent groups are statistically different from each other.

For both tested variables, the differences were found not to be statistically significant. The T-test result for weight-loss showed no significant difference

between slabs from the front sections (M= 576.0, SD=474.9) and those from the backshore areas (M=520.3, SD= 693.8); t(10)= 0.162, p = 0.874. T-test result for percentage weight loss was similarly found to be not significant as follows: front sections (M=27.9, SD=34.8) and backshore areas (M=14.2, SD=16.1); t(10)= 0.883, p = 0.398.

The key findings behind these tests were the observed contrasting rates of denudation by the limestone slabs, ranging from overall relatively fast rates recorded by the slabs of Blata l-Bajda to very slow negligible rates of some samples from Ras il-Fenek and mixed denudation patterns within the same platform such as at Ponta tal-Miġnuna and Ponta tal-Munxar. In addition, as confirmed also by the Schmidt Hammer results, there are no cross-shore differences between the front and back samples in terms of differences in rates of weathering.

5.5.4 Synthesis of main findings

i. Rates of weight loss and debris loss from samples, confirm the overall surface hardness properties measured on the respective platforms. Patterns of debris loss from weathered slabs was correlated with percentage weight loss;
ii. The UGLM platforms at Blata l-Bajda and Ras il-Fenek are the most distant from each other in terms of loss records, whilst the other three platforms converge closer together; and
iii. Although some differences in weight and debris losses were observed, these differences were not found to be statistically significant in a cross-shore direction i.e. between the front and back sections of the platforms.

On the basis of the above results, the expectations about the magnitude of surface change rates would be as follows: rates of surface change on Blata l-Bajda platform would be relatively higher, those on Ras il-Fenek platform

would be relatively lower, whereas the rates at Ponta tal- Qammieħ, Ponta tal-Miġnuna and Ponta tal-Munxar would converge together and place in between the range of rates of the two UGLM platforms. Lastly, there would be not such a strong cross-shore pattern in the rates of surface across the platforms.

6 Rates of rock surface change: a spatio-temporal analyses

6.1 Introduction

The previous chapters – dealing with the morphological assessment (Chapter 4) and rock properties (Chapter 5) – have clearly demonstrated that the selected five shore platforms share different characteristics of surface features and variable levels of resistance, and this notwithstanding that they primarily belong to the same Globigerina limestone lithology. A quantified assessment of rates of rock surface change on shore platforms is key to a better understanding of the form-response systems operating on shore platform and related dynamics of change. It also allows for comparisons to be made both between different parts of one platform and consecutively, between different platforms.

As already outlined in Chapter 1, this current research is the first ever work to be undertaken in measuring rock surface change with the TMEM for Maltese limestone and specifically on Maltese shore platforms. This work not only aims to join the already widely established research community studying rates of surface change on shore platforms, but it aims to make a significant contribution to studies of shore platforms within both the Mediterranean context and islands` context (Section 1.4). In addition to what has been elicited in previous sections, it is also worth noting that as stated by Stephenson (2009) there are relatively few published data on rates of coastal erosion on islands.

This chapter presents the results for rates of rock surface change as measured with the TMEM across 41 selected field stations and over a study period between April 2012 and August 2016 (Appendix VIII). A large volume of individual data points – 7,182 – was collected over the course of 12 measurement periods (Section 3.4.2) and which provided a large range of

opportunities for detailed statistical analyses. A definition of the terms study periods, annual time-periods, semi-annual time-periods and individual time periods in provided in the Glossary section (pg xxi-xxiii).

As explained in Chapter 3, the three parameters of analysis were spatial variability for each platform, temporal variability for each platform and spatio-temporal variability across all platforms. The structure in this chapter follows these three parameters, according to which results are first presented hereby in a descriptive statistical format and then subsequently analysed through inferential statistics using tests such as Kruskal Wallis H and/or Mann Whitney tests (Section 3.6). These latter tests provided statistical comparisons of rates at both temporal and spatial levels (i.e. intra-platform and inter-platform).

Varying patterns of differences and similarities between stations and platforms are then discussed within each dimension. Table 6.12, Table 6.14, Table 6.20, Table 6.22, Table 6.24 and Table 6.26 present the inferential results as explained in Section 3.6. The 50 % threshold was used in order to quantify the percentage of p values that deviate from that threshold in terms of H_0 rejection and thus may imply a consistent presence or absence of a pattern.

6.2 Calibration trends within measurement sessions

As outlined in Section 3.4.2.6, a series of calibration measurements were undertaken to monitor the precision and calibration variations of the TMEM instrument. The main intent was to obtain comparable *in situ* measurements from one measurement session to the next. Table 6.1 illustrates the calibration variations measured during the course of study. Given the repetitive usage of the instrument every few months, checks started to be carried out from the 4^{th} measurement session onwards in order to test for any potential instrument error. The instrument was calibrated twice before each field session with 21 measurement points. This exceed the minimum number of precision levels which Trenhaile and Lankhan (2011) set at ten individual measurement points.

The instrument always performed within instrument error during double calibration throughout the study period (Table 6.1).

From the 10th measurement session onwards, three sets of double calibrations were performed: before the field visit (pre-situ), during the site visit (in situ) and after the field session (post situ). Mean differences in calibration were compared and calculated between pre-situ and post-situ in order to check calibration variations during the session on each respective platform. There was minimal variation in calibration with 19 of the 25 sessions recording shifts of less than 0.01 mm. Four sessions had a higher shift between 0.206 to -0.222 mm. These shifts, however, were observed consistently across the 21 measured calibration points. Thus, these four error shifts were interpreted as systematic and consistent and so could be corrected from in situ measurements.

The fact that these four error shifts happened in the last five sessions of the study, may imply some element of usage disturbance of the instrument. Though care was taken in the maintenance of the instrument, the salty ambient of the coastal environment is known to be harsh on instruments. It also suggests that the three-step calibration regime performed in the last five measurement sessions, was an appropriate method to identify any errors and be able to make the necessary corrections for comparable *in situ* data.

Issues related to the instrument accuracy are not a new thing in literature about rock surface measurements. Foote *et al.* (2001) found a range of calibration variation of 0.06 mm (SD= 0.01) and 0.85 mm (SD=0.195) on two MEMs over a period of 18 months. Other studies have relied on the long-term scale of observations to infer accuracy of measurements such by Smith *et al.* (1995) who reiterated that MEM observations taken over a number of years may help to reduce the effects of such errors. In fact for their 12-year study, they did not perform any calibration adjustments. This research has resulted in the set-up of a calibration procedure that is hoped will become a standard and ensure that any systematic changes in machine operation are identified and calibrated for rapidly within any study.

Table 6.1: Calibration variation measurements through each measurement session

Study Phase	Pilot study			Non-pilot study								
Calibration method	Single pre-situ calibration*					Double pre-situ calibration**			Double calibration - pre-situ, in situ, post-situ***			
Platform Site	Measurement sessions											
	1st	2nd	4th****	5th	6th****	7th	8th	9th	10th	11th	12th	13th	14th
Ras il-Fenek			0.003		0.000	0.001	0.001	0.000	0.000	-0.001	-0.129	-0.006	0.009
Ponta tal-Mignuna			-0.003		0.000	0.000	0.000	-0.001	0.004	0.007	-0.067	0.030	0.008
Pont tal-Munxar					0.000	0.000	0.000	0.000	-0.001	0.001	0.000	-0.007	0.206
Ponta tal-Qammieh						0.000	0.000	-0.001	-0.002	0.002	-0.001	0.002	-0.001
Blata l-Bajda			-0.001		0.000	0.000			-0.222	0.002	-0.159	0.008	0.008

** Between the 1st and 6th measurement session, one pre-situ calibration was done for each platform site*

*** Between the 6th and the 9th measurement session, a pre-situ double calibration was done for each platform site. Difference is between first and second calibration*

**** From 10th to 14th measurement session, difference between the first calibration of pre-situ and that of the post-situ*

***** Initial spot checks with double calibration*

6.3 Spatial patterns of surface change at station and platform level

6.3.1 Descriptive analysis of average rates of surface change at platform level

The following three sections present a description of the measured rates based on the average surface changes recorded by the 21 individual points per station. It also provides a description of how these rates trended spatially between TMEM sites and between different platforms (See Section 3.6.1.1). The spatial patterns analysed were those for rates between front, middle and back stations on each platform. The selection of these three spatial scales allowed comparisons between the relative position of station and evaluate how rates of surface change may trend differently or similarly within the spatial dimension. Statistical comparisons between the three TMEM stations with MWU and KWH tests provided the opportunity to infer of any significant spatial similarities within each platform and across the five platforms (See Table 3.13).

6.3.1.1 Across the study period

The mean rate of surface change for the 41 stations was of -0.237 mma^{-1}, with a standard deviation of 0.596 (Table 6.2). The mean rate was calculated as the difference in height between last measurement period and the first measurement period. Negative rates represent levels lower than the first measured period and indicate lowering of the rock surface, whist positive values represent higher surface levels than the first measurement period indicating rises (or accretion) of the rock surfaces. 35 out of 41 stations experienced surface lowering with rates ranging from -0.004 mma^{-1} (MRF3) to -3.247 mma^{-1} (MRF2a). The dataset mean rate is partially skewed by higher loss rates such as by ones recorded at MRF2a (-3.247 mma^{-1}) and MRF1a (-1.902 mma^{-1}). When the two rates were not included in the average calculations (MRF1a and MRF2a were also rates obtained from one measurement period only), the mean rate dropped down to -0.114 mma^{-1} and the standard deviation decreased from 0.596 to 0.102 (Table 6.2). This would imply that most

platforms have a closer range of rates of surface change. The following 12 stations were the ones which experienced relatively higher loss rates: at Blata l-Bajda (MBB 1a, 3, 4, 5 6a, 6b), at Ponta tal-Miġnuna (MPM 1, 3a and 3b), at Ponta tal-Qammieħ (MPQ2), at Ponta tal-Munxar (MMX 1b, 3b and 3c).

The average therefore did not fully capture the erosional behaviour of these surfaces which were highly variable in their rates of surface change and this was also illustrated by high standard deviations. 29 stations recorded lower than average standard deviation ranging from 0.016 to 0.102, leaving the remaining 11 stations with higher than average standard deviation and which had a stronger impact of the dataset mean. In fact, 8 stations with above average, rates of loss also recorded standard deviation values above average. With the modified mean, they go up to nine stations. This means that the rates of surface change produced a skewed distribution of sites for both averages and standard deviations implying that a few sites exhibited both high erosional losses and highly variable erosion rates such as MBB6a and 6b, MPM3a and 3b, MMX 3c.

In line with the modified mean, Blata l-Bajda platform had the most stations registering higher than average surface losses (6 out of 8 stations). MBB1a and MBB2 recorded the lowest rates of losses. Conversely, the platform at Ras il-Fenek had the largest number of stations (7 out of 9 stations) with relatively low rates of losses. The standard deviation values of these MRF stations also resulted below the modified average, with a relatively narrow range of 0.016 to 0.078. The latter result may indicate that rock surfaces which experience lower rates of losses in each station may also experience a lower magnitude of variability between individual measured points.

Table 6.2: Average rates of surface change during study period (April 2012 - August 2016). Shaded cells indicate values above average of total dataset

Platform Site	Station	Platform Position	Start Period	End Period	Rates of Surface Change* mm a $^{-1}$	Std Deviation ±	Rates of Surface Change** mm a $^{-1}$	Std Deviation ±
Blata l-Bajda	MBB 1a	Front	1st	2nd	-0.199	0.184	-0.199	0.184
	MBB 1b	Front	6th	14th	-0.090	0.056	-0.090	0.056
	MBB 2	Middle	1st	14th	-0.045	0.039	-0.045	0.039
	MBB 3	Back	1st	14th	-0.130	0.032	-0.130	0.032
	MBB 4	Front	6th	14th	-0.154	0.102	-0.154	0.102
	MBB 5	Middle	6th	14th	-0.160	0.038	-0.160	0.038
	MBB 6a	Back	6th	10th	-0.255	0.142	-0.255	0.142
	MBB 6b	Back	11th	14th	-1.002	0.273	-1.002	0.273
Ponta tal-Miġnuna	MPM 1	Front	2nd	14th	-0.285	0.097	-0.285	0.097
	MPM 2a	Middle	1st	7th	0.097	0.082	0.097	0.082
	MPM 2b	Middle	8th	14th	-0.039	0.083	-0.039	0.083
	MPM 3a	Back	4th	8th	-0.435	0.300	-0.435	0.300
	MPM 3b	Back	9th	14th	-0.448	0.300	-0.448	0.300
	MPM 4	Front	4th	14th	-0.097	0.051	-0.097	0.051
	MPM 5	Middle	4th	14th	-0.037	0.039	-0.037	0.039
	MPM 6	Back	5th	13th	-0.059	0.095	-0.059	0.095
Ponta tal-Qammieħ	MPQ 1	Front	1st	14th	-0.054	0.053	-0.054	0.053
	MPQ 2	Middle	1st	14th	-0.159	0.144	-0.159	0.144
	MPQ 3	Back	1st	14th	-0.023	0.031	-0.023	0.031
	MPQ 4	Front	6th	14th	0.094	0.030	0.094	0.030
	MPQ 5	Middle	6th	14th	-0.008	0.046	-0.008	0.046
	MPQ 6	Back	6th	14th	-0.025	0.029	-0.025	0.029
Munxar Headland	MMX 1a	Front	2nd	6th	0.060	0.063	0.060	0.063
	MMX 1b	Front	7th	14th	-0.120	0.098	-0.120	0.098
	MMX 2	Back	2nd	14th	-0.004	0.099	-0.004	0.099
	MMX 3a	Front	1st	6th	0.008	0.183	0.008	0.183
	MMX 3b	Front	7th	10th	-0.139	0.102	-0.139	0.102
	MMX 3c	Front	13th	14th	-0.380	0.507	-0.380	0.507
	MMX 4	Back	1st	14th	-0.037	0.044	-0.037	0.044
	MMX 5a	Front	6th	6th	n/a	n/a	n/a	n/a
	MMX 5b	Front	7th	14th	0.034	0.168	0.034	0.168
	MMX 6	Back	6th	14th	0.020	0.056	0.020	0.056
Ras il-Fenek	MRF 1a	Front	1st	2nd	-1.902	0.951		
	MRF 1b	Front	6th	14th	-0.021	0.020	-0.021	0.020
	MRF 2a	Middle	1st	2nd	-3.247	0.256		
	MRF 2b	Middle	6th	14th	-0.044	0.050	-0.044	0.050
	MRF 3	Back	6th	14th	-0.004	0.028	-0.004	0.028
	MRF 4	Front	6th	14th	-0.071	0.073	-0.071	0.073
	MRF 5	Middle	6th	14th	-0.027	0.078	-0.027	0.078
	MRF 6	Back	1st	14th	-0.009	0.016	-0.009	0.016
	MRF 7	Back	7th	14th	-0.086	0.034	-0.086	0.034
Average					-0.237	0.127	-0.114	0.102
St Deviation					0.596		0.196	
* Based on the whole dataset								
** Excluding MRF 1a and MRF 2a								

Ponta tal-Munxar and Ponta tal-Miġnuna recorded the largest spread in terms of rates, particularly the latter with mean rates ranging from slight gains (MPM2a and MPM4a) to relatively higher losses (MPM3a and 3b). Their standard deviation results were also similar in terms of variability. It was also interesting to observe that 11 stations recorded above average rates in terms of standard variability: nine of these stations recorded above average rates of losses, whereas the remaining two stations (MMX3a and MMX 5b) recorded net gains (Table 6.2).

The shore platform of Ponta tal-Munxar had the largest number of stations (4 stations) recording gains, with three of these stations (MMX1a, 3a and 5b) positioned at both the lowest elevation and in closest proximity to the sea level from all the stations in the dataset. In terms of variability of results, Ponta tal-Qammieħ may also be considered similar to these two platforms, although it has less pronounced losses in four of its stations (MPQ1, 3, 5 and 6) and MPQ4 and MPM2a experiencing minor surface rises. MPQ2 station recorded a surface lowering rate of -0.159 mma^{-1}. This may be due to its position in a likely erosional spot marked by backwearing scarp and close to the cliff edge of the platform. On the other hand, MPQ4 was the only anomaly from all the other stations at Ponta tal-Qammieħ in experiencing a gain rate of 0.094 mma^{-1}.

6.3.1.2 Annual rates

The mean rates across the whole study period, took only in consideration the measurement points collected at the beginning and the end of the survey i.e. at the 1st and 14th measurement period. Incorporating the other datasets collected in between these two measurement periods, may however help in defining better the responses of surface change across shorter timeframes such as annual, semi-annual and tri-monthly periods and quantify the magnitude of change at different temporal scales. The results presented in Section 6.3.1.1 indicate notable measured differences in the rates of surface change both at platform level and also at station level.

As outlined in the Methodology chapter (Section 3.6.1.1), a total 182 annual periods were examined. In terms of percentage distribution of periods resulting in surface lowering rates and those recording rates of surface rise, the whole dataset of mean annual rates revealed 79 % of rates with surface lowering trends (144 out of 182) and 21% with surface rises (38 out of 182). As shown in Table 6.3, the shore platforms of Ponta tal-Munxar and Ras il-Fenek had

Table 6.3 : Rates of surface change based on annual periods and scores of annual periods with surface lowering trends and surface rises.

Rates of surface change based on annual periods, and scores of periods with surface lowering (SL) and surface rises (SR)														
TMEM Station	**Rates of surface change**											**Total**	**SL**	**SR**
	A (5th-1st)	B (6th-2nd)	C (8th-4th)	D (9th-5th)	E (10th-6th)	F (11th-7th)	G (12th-8th)	H (13th-9th)	I (14th-10th)	Average	St Dev.			
MBB 1b					-0.076	-0.091	-0.021	-0.095	-0.107	-0.078	0.030	5	5	0
MBB 2	-0.131	-0.059	-0.029	0.038	-0.031	-0.050	0.012	-0.025	-0.025	-0.033	0.045	9	7	2
MBB 3	-0.161	-0.013	-0.148	-0.103	-0.096	-0.126	-0.086	-0.124	-0.119	-0.109	0.041	9	9	0
MBB 4					-0.208	-0.141	-0.058	-0.127	-0.141	-0.135	0.048	5	5	0
MBB 5					-0.122	-0.119	-0.063	-0.115	-0.086	-0.101	0.023	5	5	0
MBB 6a					-0.255					-0.255	0.000	1	1	0
Average	-0.146	-0.036	-0.089	-0.033	-0.131	-0.105	-0.043	-0.097	-0.096	-0.118	0.031			
Total												34	32	2
Percentage												100	94	6
Station	A (5th-1st)	B (6th-2nd)	C (8th-4th)	D (9th-5th)	E (10th-6th)	F (11th-7th)	G (12th-8th)	H (13th-9th)	I (14th-10th)					
MPM 1		0.687	0.053	0.046	-0.007	-0.100	0.136	0.160	-0.143	0.104	0.241	8	3	5
MPM 2a	0.011	0.369								0.190	0.179	2	0	2
MPM 2b							-0.091	0.254	-0.066	0.032	0.157	3	2	1
MPM 3a			-0.435							-0.435	0.000	1	1	0
MPM 3b								-0.439	-0.444	-0.442	0.003	2	2	0
MPM 4			-0.100	-0.114	-0.157	-0.118	-0.107	-0.105	-0.099	-0.114	0.018	7	7	0
MPM 5			-0.047	-0.030	-0.047	-0.025	-0.050	-0.054	-0.038	-0.042	0.010	7	7	0
MPM 6				-0.248	-0.031	-0.062	0.000	0.184		-0.031	0.138	5	3	2
Average	0.011	0.528	-0.132	-0.086	-0.060	-0.076	-0.022	0.000	-0.158	-0.092	0.093			
Total												35	25	10
Percentage												100	71	29
Station	A (5th-1st)	B (6th-2nd)	C (8th-4th)	D (9th-5th)	E (10th-6th)	F (11th-7th)	G (12th-8th)	H (13th-9th)	I (14th-10th)					
MPQ 1	-0.075	-0.140	-0.107	0.001	0.059	-0.092	-0.024	-0.085	-0.046	-0.043	0.058	9	7	2
MPQ 2	-0.172	-0.151	-0.217	-0.092	-0.056	-0.038	-0.041	-0.167	-0.193	-0.043	0.070	9	9	0
MPQ 3	0.027	-0.043	-0.085	-0.020	0.016	-0.025	0.055	-0.025	-0.031	-0.020	0.039	9	6	3
MPQ 4					0.006	0.040	0.043	-0.015	-0.037	-0.019	0.033	5	2	3
MPQ 5					0.014	-0.017	0.053	-0.020	-0.033	-0.052	0.037	5	3	2
MPQ 6					-0.007	-0.032	0.046	-0.042	-0.046	-0.059	0.038	5	4	1
Average	-0.073	-0.111	-0.136	-0.037	0.005	-0.027	0.022	-0.059	-0.064	-0.039	0.046			
Total												42	31	11
Percentage												100	74	26
Station	A (5th-1st)	B (6th-2nd)	C (8th-4th)	D (9th-5th)	E (10th-6th)	F (11th-7th)	G (12th-8th)	H (13th-9th)	I (14th-10th)					
MMX 1a		0.060								0.060		1	0	1
MMX 1b						-0.219	-0.174	-0.158	-0.187	-0.185	0.026	4	4	0
MMX 2		0.172	0.086	-0.056	-0.170	-0.054	-0.164	-0.088	-0.075	-0.044	0.118	8	6	2
MMX 3a	-0.039	-0.300								-0.169	0.184	2	2	0
MMX 4	-0.013	0.106	0.085	-0.028	-0.135	-0.052	-0.146	-0.078	-0.060	-0.036	0.087	9	7	2
MMX 5b						0.243	-0.028	-0.045	-0.073	0.024	0.147	4	3	1
MMX 6					0.084	-0.063	-0.135	-0.056	-0.057	-0.045	0.080	5	4	1
Average	-0.026	0.010	0.086	-0.042	-0.074	-0.029	-0.130	-0.085	-0.090	-0.056	0.107			
Total												33	26	7
Percentage												100	79	21
Station	A (5th-1st)	B (6th-2nd)	C (8th-4th)	D (9th-5th)	E (10th-6th)	F (11th-7th)	G (12th-8th)	H (13th-9th)	I (14th-10th)					
MRF 1b					-0.019	-0.115	-0.058	-0.008	-0.022	-0.044	0.039	5	5	0
MRF 2b					-0.042	-0.188	-0.178	-0.032	-0.046	-0.097	0.070	5	5	0
MRF 3					-0.037	-0.159	-0.115	0.028	0.036	-0.049	0.077	5	3	2
MRF 4					-0.042	-0.136	-0.203	-0.110	-0.107	-0.120	0.052	5	5	0
MRF 5					-0.028	-0.129	-0.064	0.009	-0.026	-0.048	0.047	5	4	1
MRF 6	-0.027	-0.125	0.015	-0.039	0.093	0.059	0.019	0.024	-0.004	0.002	0.059	9	4	5
MRF 7						-0.139	-0.118	-0.006	-0.005	-0.067	0.062	4	4	0
Average	-0.027	-0.125	0.015	-0.039	-0.013	-0.116	-0.102	-0.013	-0.025	-0.061	0.058			
Total												38	30	8
Percentage												100	79	21
TOTAL												182	144	38
Percentage												100	79	21

annual rates of surface lowering and surface rises with a percentage distribution similar to the overall dataset. Ponta tal-Qammieħ and Ponta tal-Miġnuna had a slightly lesser number of periods with annual rates of surface lowering.

However, Blata l-Bajda shore platform was a definite outlier amongst the five shore platforms, with 94% of annual periods recording rates of surface lowering and 6% with surface rises. In addition to this, the mean rate of surface lowering for Blata l-Bajda shore platform (based on annual period rates) was also relatively larger when compared with the remaining four platforms. In terms of variability of rates between annual periods, Blata l-Bajda shore platform had also the lowest standard deviation for its annual period rates, with 0.031 as mean standard deviation. Ponta tal-Munxar and Ponta tal-Miġnuna recorded the largest variability with mean standard deviation of 0.107 and 0.093 respectively. Once again, in terms of data, Blata l-Bajda was the most distant from all the platforms with regards to annual trends of surface change.

Figure 6.1 to Figure 6.5 show the results of mean rates of surface change for each TMEM stations according to annual periods. Three spatial trends - one main overall trend and two sub-trends - were identified as follows:

i. A surface lowering main trend: The first trend which emerged from the results displayed Figure 6.1 to Figure 6.5, shows how the dominant trend of surface lowering present on all shore platforms and that these rates of surface lowering seem to be more uniform on some shore platforms but more fluctuating on others. Although Blata l-Bajda and Ras il-Fenek were measured to have different magnitude of surface lowering (Figure 6.5), they both have stations which share similar trends of surface lowering across the annual periods. Stations MBB1b, 3 4 and 5 have temporal trends that which dip slightly in the G period but generally spike in the E,

F, H and I period. MRF1b, 2b, 4 and 7 recorded lowering trends inverse to those of Blata l-Bajda, with rates in a bell-shaped curves spiking in the F and G period and being less pronounced in the rest of the periods. Three other stations - MPQ2, MMX2 and MMX4 - seem to also share some typical highs and lows similar to those at Blata l-Bajda with a downward trend in the G period;

ii. A secondary trend of gains and losses: This trend – with relatively higher variability – was observed in the annual patterns at Ponta tal-Miġnuna (Figure 6.2) and Ponta tal-Munxar (Figure 6.4). This heterogeneous trend had already been identified in Section 6.3.1.1, when surface gains and losses were observed for mean rates across the whole study period. MPM4 and MMX5, although sharing slightly different magnitude levels of losses, are also relatively more consistent in their surface lowering patterns. MPM3a and 3b only share three annual periods (C for MPM3a, H and I for MPM3b) but their rates are a closer match in terms of magnitude of loss. The remaining three stations, MPM1, 2a, 2b and 6 display rather irregular trends of gains and losses. MPM1 and 2a are rather atypical in having more pronounced gains, especially in period B. The gains and losses recorded at Ponta tal-Munxar are relatively more systematic and clustered, with surface rises recorded in the earlier phases of the survey period such as in periods B, C and E, and surface lowering recorded in the later phases of the survey period; and

iii. An 'odd one out' sub-trend: These latter stations, MPM1 and 2a, can also be included in this third observed sub-trend, referred as the 'odd one out' sub-trend because one or two stations behave markedly different from the other nearby

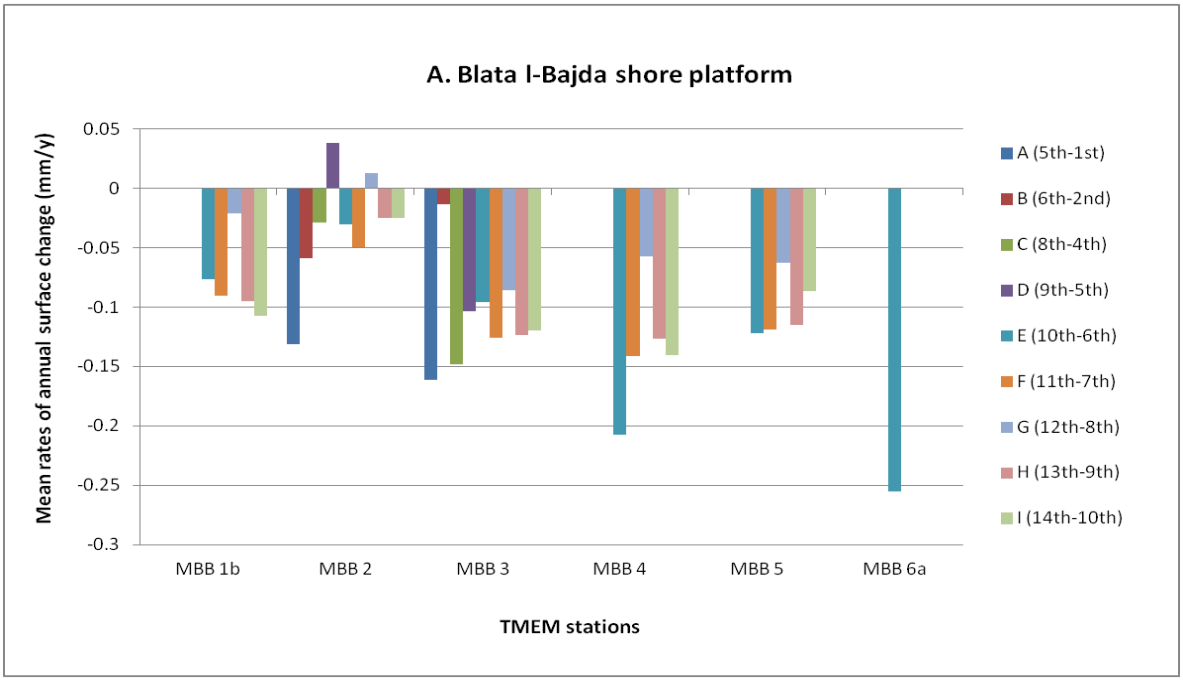

Figure 6.1: Mean annual rates of surface change on Blata l-Bajda shore platform

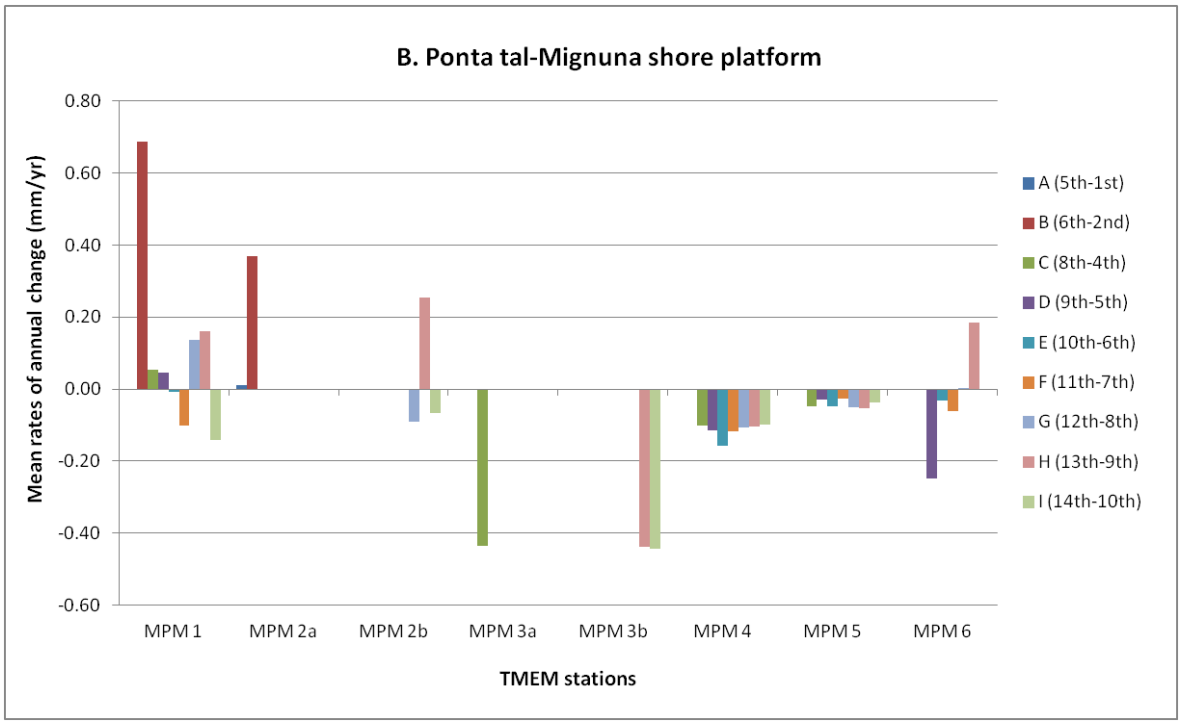

Figure 6.2: Mean annual rates of surface change on Ponta tal-Miġnuna shore platform

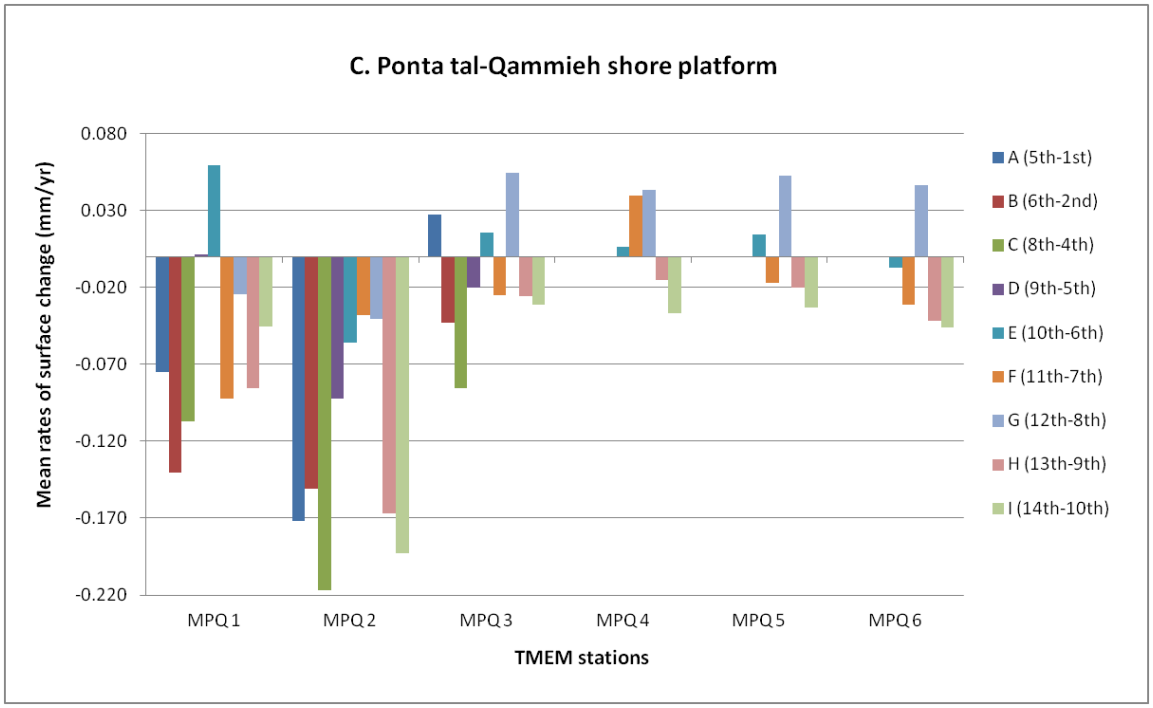

Figure 6.3: Mean annual rates of surface change on Ponta tal- Qammieħ shore platform

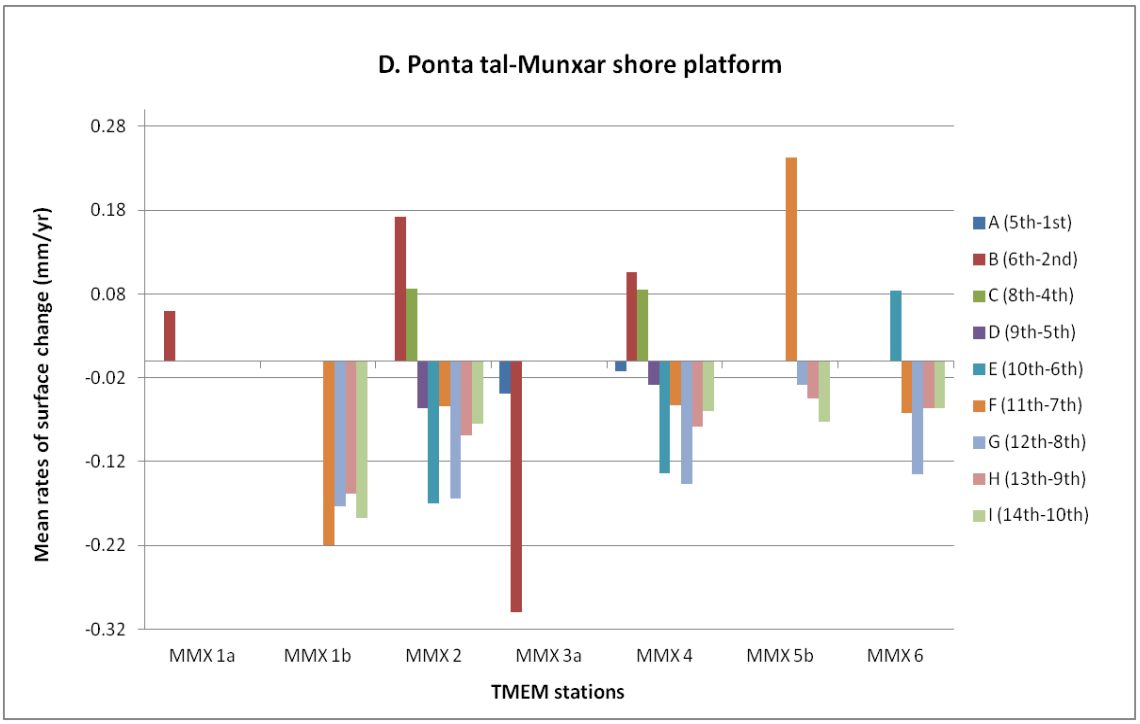

Figure 6.4: Mean annual rates of surface change on Ponta tal-Munxar shore platform

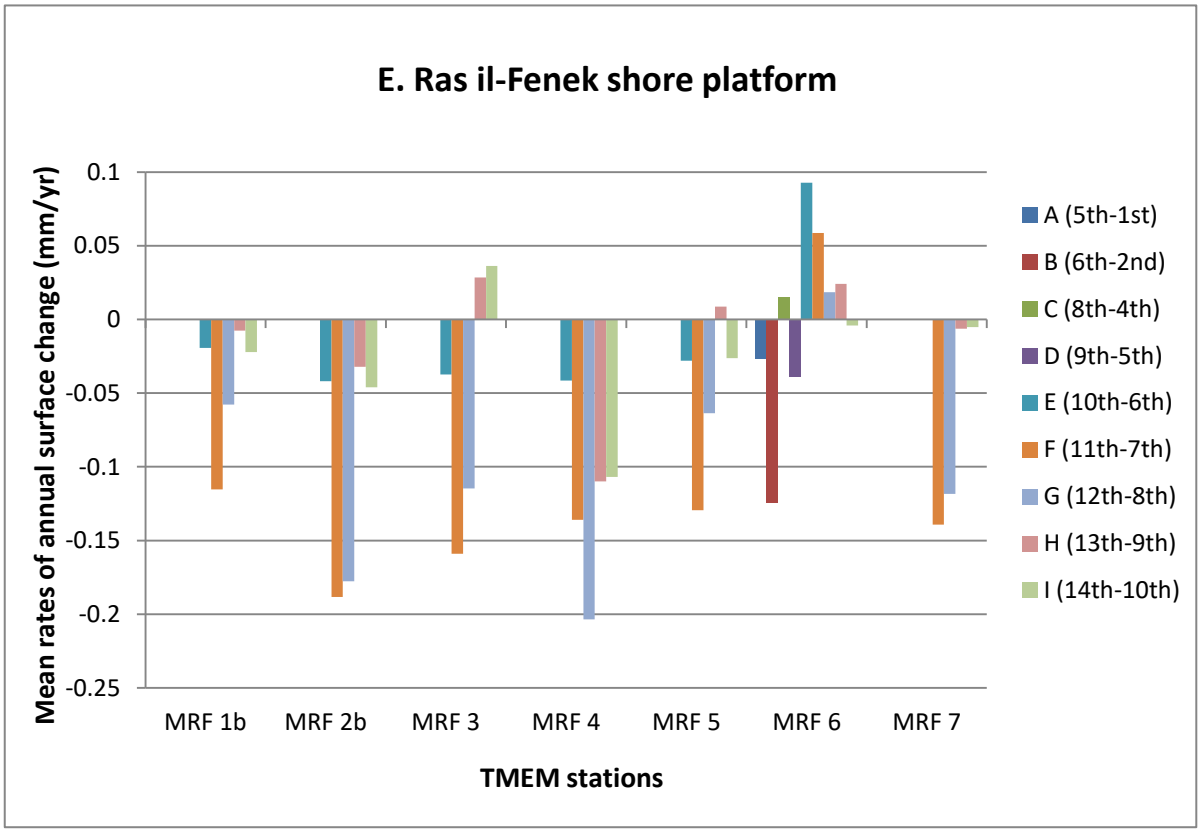

Figure 6.5: Mean annual rates of surface change on Ras il-Fenek shore platform

platform stations. As mentioned earlier in Section 6.3.1.1, station MPQ2 is surely to be considered as strikingly different from the other stations at Ponta Tal-Qammieħ in terms of both the magnitude of lowering rates but also the trends exhibited through the annual periods (Figure 6.3). MPQ1, 3, 4, 5, and 6 share similar patterns of alternating surface lowering and rises, with lowering rates for most of the annual periods and surface rises in the E and G period. MRF6 can also be considered the most atypical amongst the seven stations at Ras il-Fenek with a notable trend of rises in its last four annual periods (F- I).

6.3.1.3 Individual time period rates (3 -4 months)

The results of the mean rates of surface change at individual measurement periods are displayed in Figure 6.6 to Figure 6.10 according to each platform. A total of 292 periods were examined across the five stations (Section 3.6.1.1). 69 per cent of the total measurement periods recorded mean surface lowering rates and 31 per cent recorded mean rates of surface rises. At platform level, all five platforms recorded a higher percentage of surface lowering rates compared to the rates of surface rises. However, the percentage distribution of rates of surface lowering and that of rises varied. Blata l-Bajda shore platform recorded the highest percentage of surface lowering rates whereas Ras il-Fenek shore platform recorded the lowest percentage of surface lowering rates and the highest percentage of surface rises. The remaining three platforms fell in between these two extremes in terms of their respective rates of surface lowering and rises.

With regards to variability of rates per station, Ponta tal-Munxar and Ponta tal-Miġnuna recorded the highest mean standard deviation results and had some contrasting anomalies within the same stations in terms rates magnitude of lowering versus rises: particularly MPM 1, 2 and 6 and MMX 3b. These anomalies may have affected the standard deviation results per station and thus the overall mean standard deviation per platform. The mean standard deviation result of Blata l-Bajda shore platform was 0.295; however this relatively high value is not consistent with the lower variability displayed in the graph (Figure 6.6) and it has been substantially influenced by the high surface lowering rate recorded in MBB6b. When the results of MBB6b were not included in the mean calculations, the mean standard deviation for the remaining seven stations dropped to 0.133, indicating a much lower variability between individual periods per station. The same trend was observed at Ras il-Fenek shore platform with a very large surface lowering rates are MRF2a and MRF1a for the 1st measurement session. The variability without these two measurements was of 0.221, which is relatively lower when compared Ponta tal-Miġnuna and Ponta tal-Munxar.

Ponta tal-Qammieħ shore platform also recorded a relatively lower variability i.e. of 0.170. This variability was primarily affected by rates of the 5th and 7th measurement period which recorded rises on most stations of the platform. In fact, when eliminating these two measurement periods, the mean variability for the whole shore platform dropped to a mean standard deviation of 0.107.

At station level, Blata l-Bajda has also the stations with least variability of rates across the measurement periods, in particular MBB1b (SD=0.106) and MBB5 (SD=0.111) which were the stations with lowest variability from the whole dataset. Ponta tal-Munxar and Ponta tal-Miġnuna were the ones that had stations with the highest variability, and in particular MMX3b (SD=2.046), MPM2b (SD=0.804), MMX1a (SD=0.588), MPM6 (SD=0.583). In these cases, the variability was influenced by rates of surface lowering and rises across the measurement periods in each station.

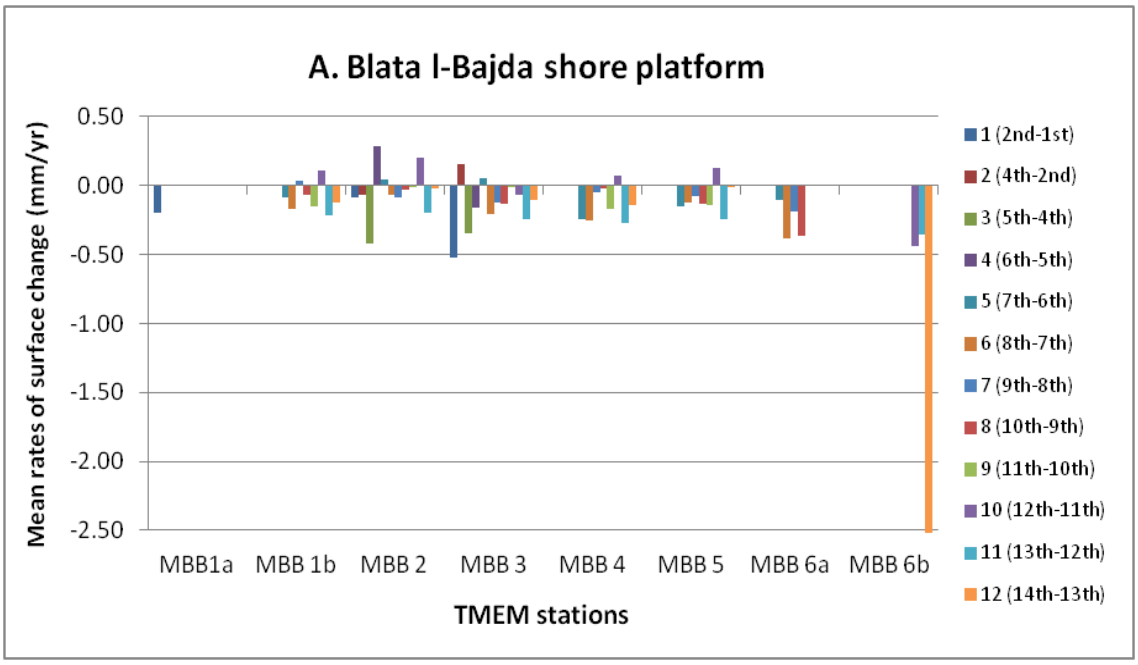

Figure 6.6: Mean rates of surface for each individual period on Blata l-Bajda shore platform

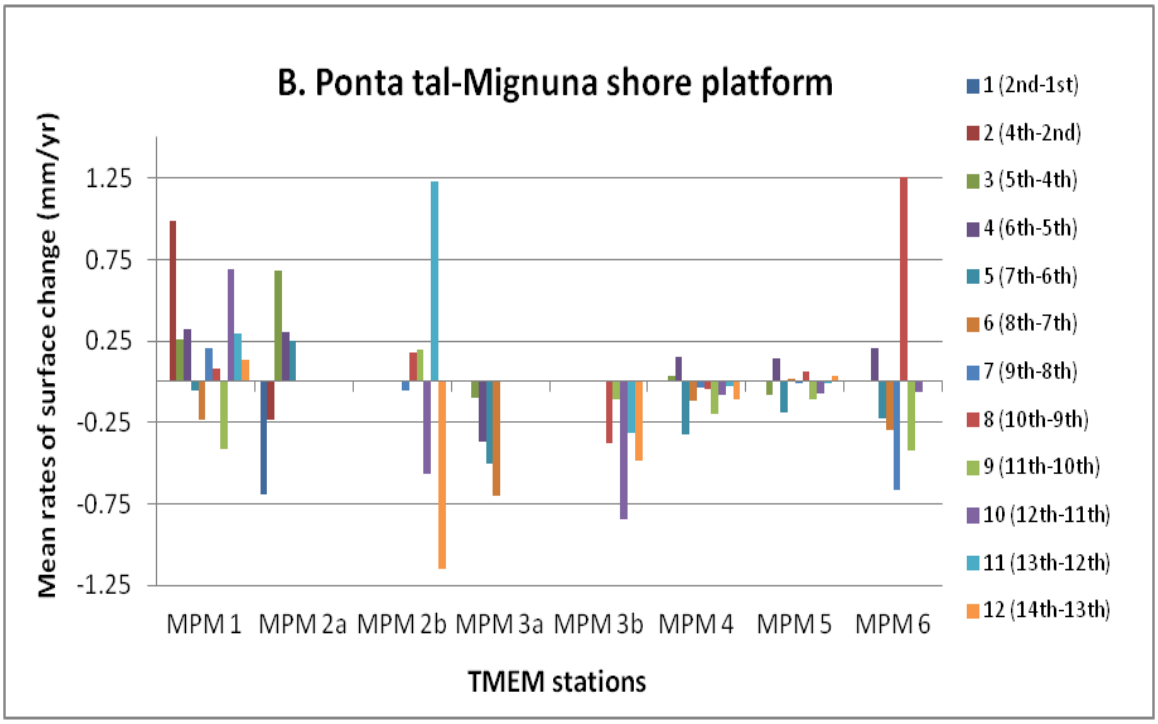

Figure 6.7: Mean rates of surface for each individual period on Ponta tal-Miġnuna shore platform

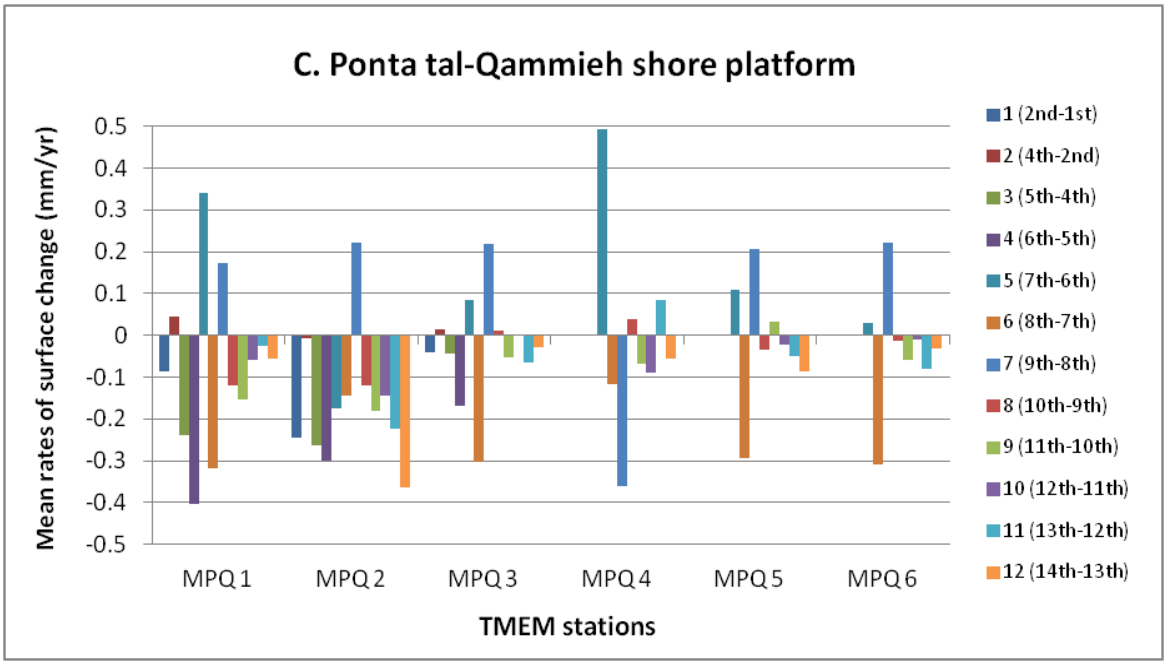

Figure 6.8: Mean rates of surface for each individual period on Ponta tal-Qammieħ shore platform

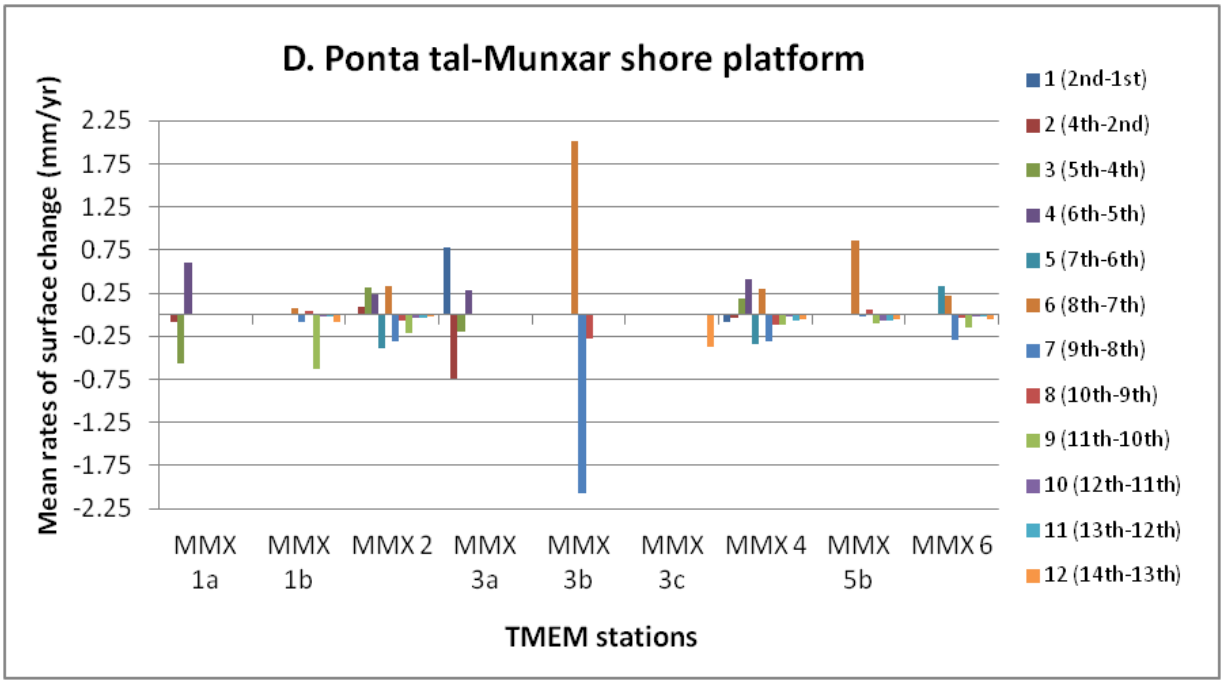

Figure 6.9: Mean rates of surface for each individual period on Ponta tal-Munxar shore platform

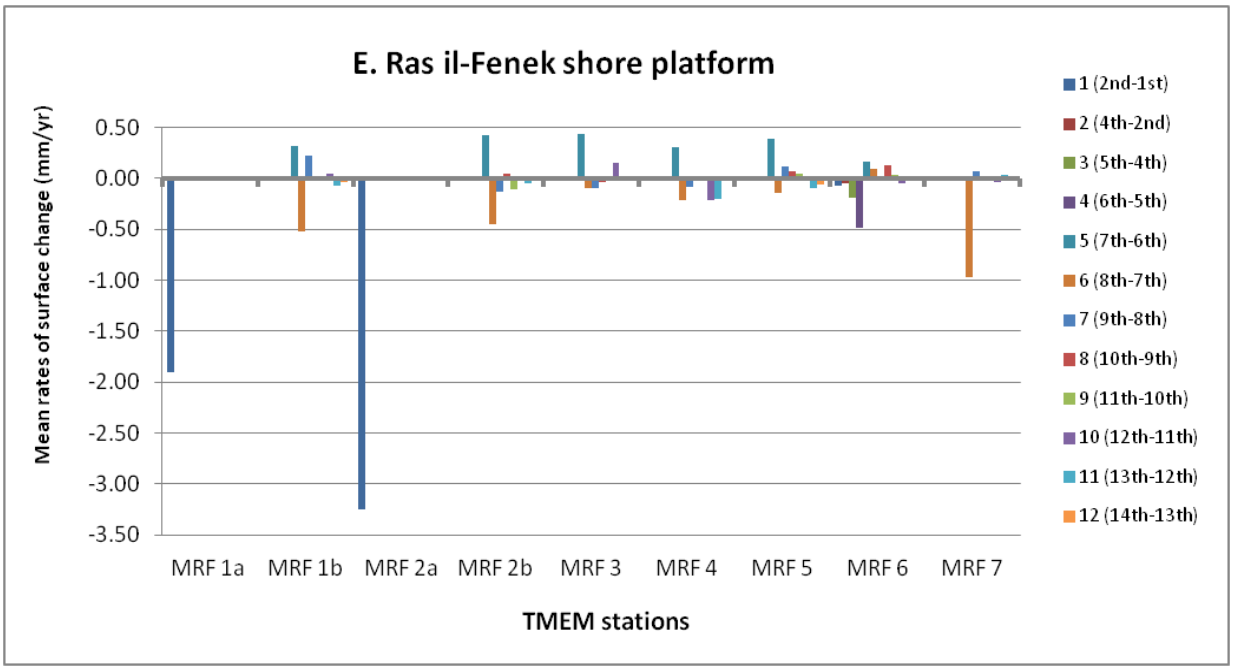

Figure 6.10: Mean rates of surface for each individual period on Ras il-Fenek shore platform

6.3.2 Descriptive analyses of average rates of surface change at station level

6.3.2.1 Across study-period: front, middle and back of platform

Table 6.4 and Figure 6.11- Figure 6.13 display the mean rates of surface change across the study period according to the cross-shore position of the TMEM stations in a front, middle or back position along each platform. Table 6.4 shows how 85% (34 out of 40) of the mean rates are rates of surface lowering and the remaining 16% are rates of surface rises. The overall mean rates of surface change are highest at the middle station group, with a mean surface lowering rate of -0.367 mma^{-1}. This rate was partially attributed to the relatively high rate of surface change 3.247 mma^{-1} at MRF2a and without which, the overall mean rate would decline to -0.047 mma^{-1}. The same situation can be observed in the front stations: its overall mean is of -0.207 mma^{-1}, which includes a high value of -1.902 mma^{-1} for MRF1a. Without the latter rate, the overall mean rate of surface change would drop to -0.094 mma^{-1}. The rates of MRF1a and MRF2a were measured during the first measurement period only and their high rates are attributed to two different but anomalous site-specific conditions: MRF1a was installed in the lowest level of the platform in almost high-tide conditions, reachable by frequent wave action whilst MRF2a was installed in a relatively lithological weak exposure of UGLM close to an access point on the platform, In both circumstances, the studs were lost after a few months: one due to suspected wave quarrying (MRF 1a)and another to tampering (MRF2a).

The results are also displayed in Table 6.4 and from Figure 6.11 to Figure 6.13. They show this overall tendency of surface change characterised by a dominant surface lowering trend and sporadic records of surface rises in specific stations. The back stations where the stations have an overall record of surface lowering rates for most stations with less surface rising rates. As shown in Figure 6.13, the largest rates of surface lowering were recorded at Blata l-Bajda and Ponta tal-Miġnuna. Another two stations at Blata l-Bajda shore

platform (MBB6a and MBB3a,b) recorded also relatively distinct surface lowering rates.

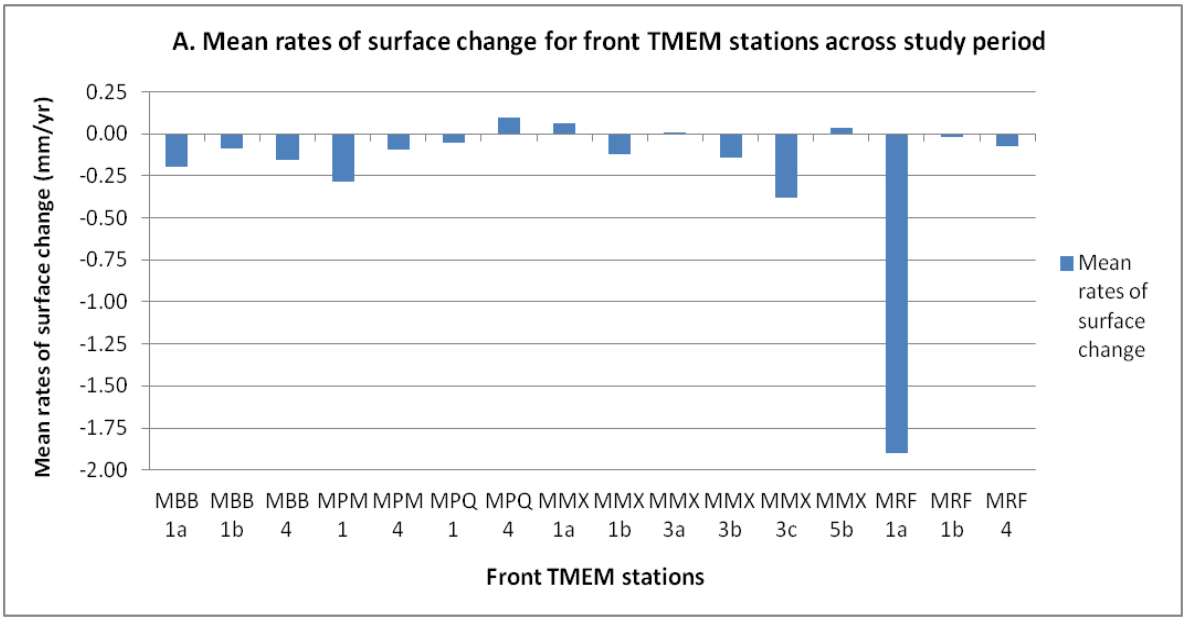

Figure 6.11: Mean rates of surface change for front TMEM stations across study period.

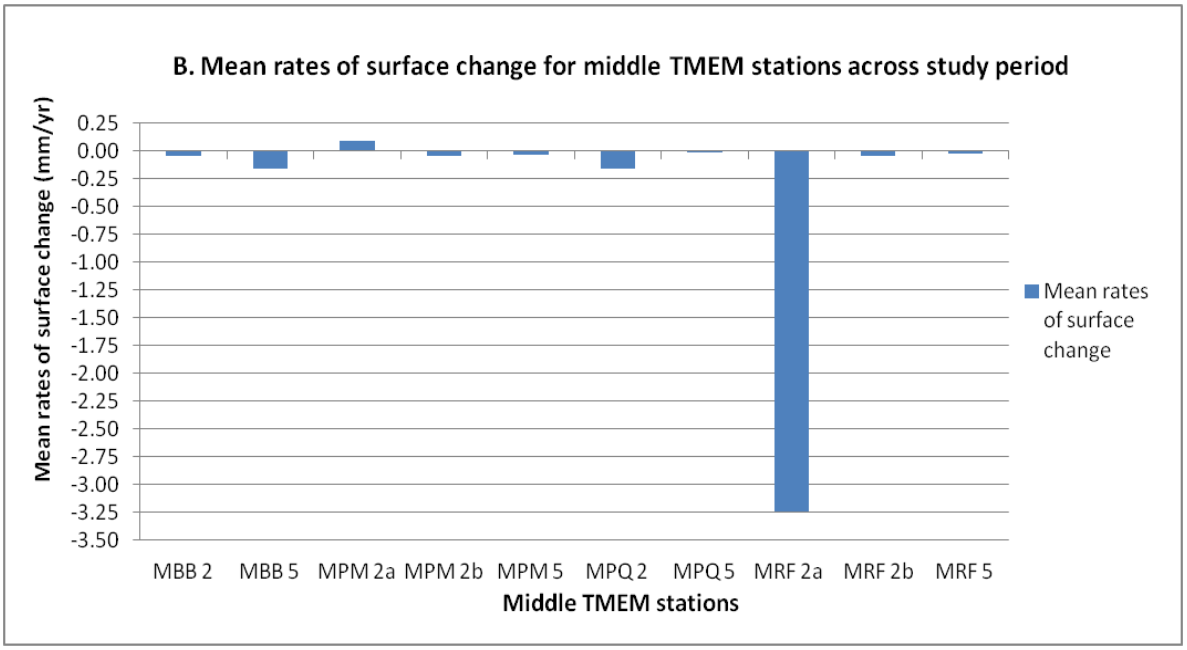

Figure 6.12: Mean rates of surface change for middle TMEM stations across study period.

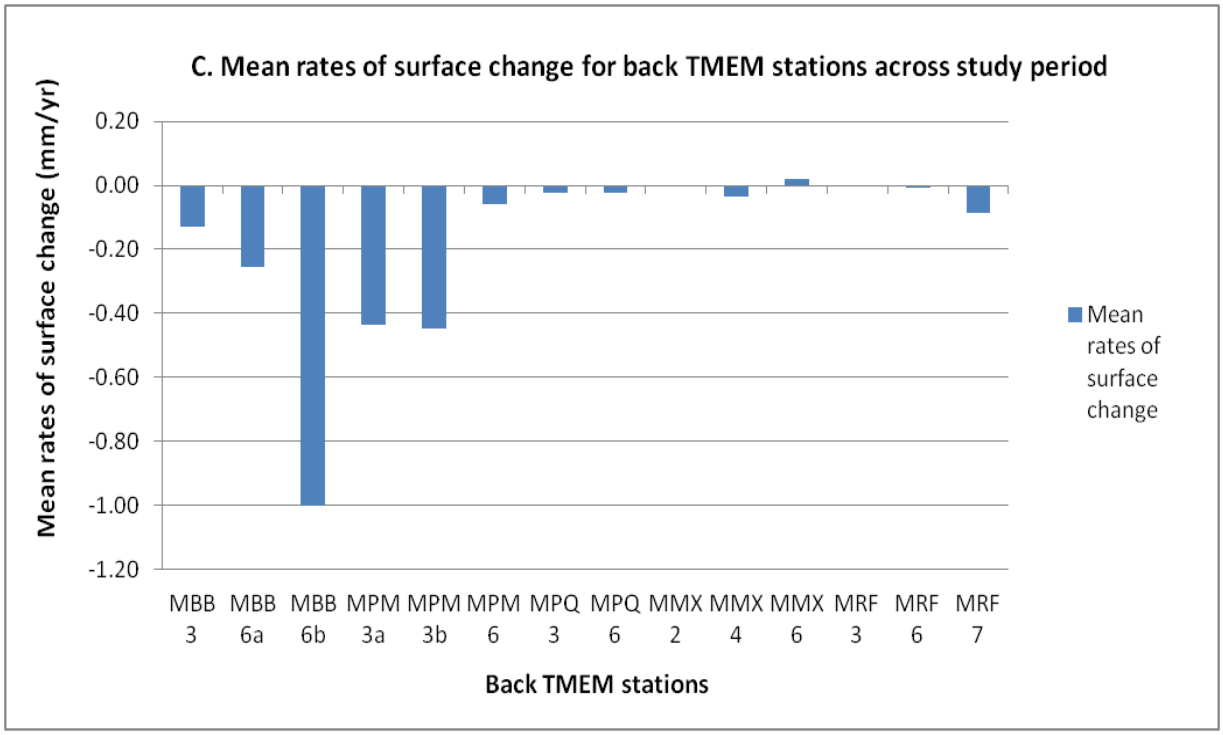

Figure 6.13: Mean rates of surface change for back TMEM stations across the study

The back stations at Ponta tal-Qammieħ and Ponta tal-Munxar had less pronounced surface lowering rates when compared to Blata l-Bajda and Ponta tal-Miġnuna (Figure 6.13). When taking into consideration the total number of back stations (i.e. of 14), the average rate of surface change was of -0.178 mma-1. This would mean that the back stations of Blata l-Bajda and Ponta tal-Miġnuna had above average lowering rates whereas the back stations of the remaining three shore platforms scored below average. With the exception of MPM2a, the 10 middle stations of the four selected platforms (Ponta tal-Munxar did not have middle stations) also had surface lowering rates which ranged from -0.008 mma^{-1} (MPQ5) to -3.247 mma^{-1} (MRF2a).

Table 6.4: Mean rates of surface change across study period according to front, middle and back positions across platform

Platform position	**TMEM stations**	**Mean rates of surface change mma $^{-1}$**	**Std Deviation ±**
Front Stations	MBB 1a	-0.199	0.184
	MBB 1b	-0.090	0.056
	MBB 4	-0.154	0.102
	MPM 1	-0.285	0.097
	MPM 4	-0.097	0.051
	MPQ 1	-0.054	0.053
	MPQ 4	0.094	0.030
	MMX 1a	0.060	0.063
	MMX 1b	-0.120	0.098
	MMX 3a	0.008	0.183
	MMX 3b	-0.139	0.102
	MMX 3c	-0.380	0.507
	MMX 5b	0.034	0.168
	MRF 1a	-1.902	0.951
	MRF 1b	-0.021	0.020
	MRF 4	-0.071	0.073
	Average	-0.207	0.171
Middle Stations	TMEM stations	Mean rates of surface change mm a $^{-1}$	Std Deviation
	MBB 2	-0.045	0.039
	MBB 5	-0.160	0.038
	MPM 2a	0.097	0.082
	MPM 2b	-0.039	0.083
	MPM 5	-0.037	0.039
	MPQ 2	-0.159	0.144
	MPQ 5	-0.008	0.046
	MRF 2a	-3.247	0.256
	MRF 2b	-0.044	0.050
	MRF 5	-0.027	0.078
	Average	-0.367	0.086
Back Stations	Back stations	Mean rates of surface change mm a $^{-1}$	Std Deviation
	MBB 3	-0.130	0.032
	MBB 6a	-0.255	0.142
	MBB 6b	-1.002	0.273
	MPM 3a	-0.435	0.300
	MPM 3b	-0.448	0.300
	MPM 6	-0.059	0.095
	MPQ 3	-0.023	0.031
	MPQ 6	-0.025	0.029
	MMX 2	-0.004	0.099
	MMX 4	-0.037	0.044
	MMX 6	0.020	0.056
	MRF 3	-0.004	0.028
	MRF 6	-0.009	0.016
	MRF 7	-0.086	0.034
	Average	-0.178	0.106

With the average rates of surface change amongst the middle stations being -0.367 mma^{-1}, only MRF2a has rates of surface change relatively above overall average. This would imply that the overall mean rate with MRF2a was not consistent with the overall trend of the other middle stations.

The overall mean rate of the front stations was of -0.207 $mma^{-1,}$ with rates ranging from -1.092 mma^{-1} (MRF1a) to 0.094 mma^{-1} (MPQ4). The 16 stations in all were the ones which showed most variability in terms of surface lowering rates versus surface rises (Figure 6.11). Apart from MPQ4, the front stations at Ponta tal-Munxar (MMX1a, 3a, 5b) recorded a surface rise which contrasted with the rates of surface lowering measured at the same platform at MMX1b, MMX3b and MMX5b. The platforms at Blata l-Bajda, Ponta tal-Miġnuna and Ras il-Fenek recorded surface lowering rates for all their front stations, with the rates of the first two mentioned platforms within or above average whilst the front stations at Ras il-Fenek scored below average.

6.3.2.2 Mean annual rates: front, middle and back of platform

Table 6.5 and Figure 6.14a-c illustrate the 182 annual time periods which were analysed and categorised as 60 periods in the front sections, 50 periods for the middle sections, and 72 periods for the back sections (Table 6.5). Overall, 79 % of the annual periods recorded rates of surface lowering, whilst the remaining 21% registered rates of surface rise. When analysing the distribution of rates in the three spatial categories, the front sections have a percentage distribution quite close to the overall dataset average i.e. 80 % and 20 %. The middle stations recorded a relatively higher percentage of surface lowering i.e. 84%, whilst the back stations recorded a lower percentage of surface lowering rates i.e. 75 % (Table 6.5).

However, the magnitude of surface lowering rates in the back stations was comparatively larger and measured as the highest from the three spatial

categories. The front and middle stations had an overall lower mean surface lowering rate of -0.059 mma^{-1} and -0.025 mma^{-1} and these results confirm the previous results of rates for the study period, (See Section 6.3.2.1).

The mean annual rates, displayed in Figure 6.14a-c, provide a more detailed picture when compared to the results previously presented in Section 6.3.1.1, for the overall study period. The most striking difference is the annual trends displayed for the back stations which show a higher degree of variability characterised by more surface rises recorded intermittently between surface lowering rates (Figure 6.14c). MMX2, MMX4 and MRF6 were the back stations which displayed more variability with alternating trends of surface lowering and surface rises across its annual rates. At platform level, Ponta tal-Qammieħ and Ponta tal-Munxar were the platforms which recorded highest variability in their back stations (Figure 6.14c). Blata l-Bajda shore platform on the other hand did not record any surface rises. MPM3a and MPM3b experienced the largest surface lowering rates, with the former station period C and periods H- I respectively.

The variability of surface change (with alternating surface lowering and rising rates) is less pronounced in the middle and front stations (Figure 6.14a, b). However, Ponta tal- Miġnuna has registered two high surface rise rates in period B for MPM1 and MPM2a and in period H for MPM2b. Ras il-Fenek stations representing the middle section (MRF2b and 5) and the front section (MRF1b and MRF4) retained surface lowering rates through all the annual periods, with only a marginal rise at MRF5 during period H. The same trend of consistent surface-lowering rates with no surface rises was observed at the front stations of Blata l-Bajda (MBB1b and MBB4) and at the middle station of MBB5. MBB2 also recorded most of its annual periods with surface lowering rates, with the exception of MBB2 which experiences a slight rise in period D.

Table 6.5: Mean rates of surface change based on annual periods for front, middle and back stations and with average, standard deviation, and scores for stations with surface lowering (SL) and surface rises (SR)

Mean rates of surface change based on annual periods for front, middle and back stations and with average, standard deviation and scores for stations with surface lowering (SL) and surface rises (SR)															
Front stations	A (5th-1st)	B (6th-2nd)	C (8th-4th)	D (9th-5th)	E (10th-6th)	F (11th-7th)	G (12th-8th)	H (13th-9th)	I (14th-10th)	Average	St Dev	Period	Total	SL	SR
MBB 1b					-0.076	-0.091	-0.021	-0.095	-0.107	-0.078	0.030	A	2	2	0
MBB 4					-0.208	-0.141	-0.058	-0.127	-0.141	-0.135	0.048	B	4	2	2
MPM 1		0.687	0.053	0.046	-0.007	-0.100	0.136	0.160	-0.143	0.104	0.241	C	3	2	1
MPM 4			-0.100	-0.114	-0.157	-0.118	-0.107	-0.105	-0.099	-0.114	0.018	D	3	1	2
MPQ 1	-0.075	-0.140	-0.107	0.001	0.059	-0.092	-0.024	-0.085	-0.046	-0.057	0.058	E	8	6	2
MPQ 4					0.006	0.040	0.043	-0.015	-0.037	0.007	0.031	F	10	8	2
MMX 1a		0.060								0.060	0.000	G	10	8	2
MMX 1b						-0.219	-0.174	-0.158	-0.187	-0.185	0.022	H	10	9	1
MMX 3a	-0.039	-0.300								-0.169	0.130	I	10	10	0
MMX 5b						0.243	-0.028	-0.045	-0.073	0.024	0.127		60	48	12
MRF 1b					-0.019	-0.115	-0.058	-0.008	-0.022	-0.044	0.039			80	20
MRF 4					-0.042	-0.136	-0.203	-0.110	-0.107	-0.120	0.052				
Average										-0.059	0.066				
Middle stations	A (5th-1st)	B (6th-2nd)	C (8th-4th)	D (9th-5th)	E (10th-6th)	F (11th-7th)	G (12th-8th)	H (13th-9th)	I (14th-10th)			Period	Total	SL	SR
MBB 2	-0.131	-0.059	-0.029	0.038	-0.031	-0.050	0.012	-0.025	-0.025	-0.033	0.045	A	3	2	1
MBB 5					-0.122	-0.119	-0.063	-0.115	-0.086	-0.101	0.023	B	3	2	1
MPM 2a	0.011	0.369								0.190	0.179	C	3	3	0
MPM 2b							-0.091	0.254	-0.066	0.032	0.157	D	3	2	1
MPM 5			-0.047	-0.030	-0.047	-0.025	-0.050	-0.054	-0.038	-0.042	0.010	E	7	6	1
MPQ 2	-0.172	-0.151	-0.217	-0.092	-0.056	-0.038	-0.041	-0.167	-0.193	-0.125	0.065	F	7	7	0
MPQ 5					0.014	-0.017	0.053	-0.020	-0.033	-0.001	0.031	G	8	6	2
MRF 2b					-0.042	-0.188	-0.178	-0.032	-0.046	-0.097	0.070	H	8	6	2
MRF 5					-0.028	-0.129	-0.064	0.009	-0.026	-0.048	0.047	I	8	8	0
Average										-0.025	0.070		50	42	8
														84	16
Back stations	A (5th-1st)	B (6th-2nd)	C (8th-4th)	D (9th-5th)	E (10th-6th)	F (11th-7th)	G (12th-8th)	H (13th-9th)	I (14th-10th)			Period	Total	SL	SR
MBB 3	-0.161	-0.013	-0.148	-0.103	-0.096	-0.126	-0.086	-0.124	-0.119	-0.109	0.041	A	4	3	1
MBB 6a					-0.255					-0.255	0.000	B	5	3	2
MPM 3a			-0.435							-0.435	0.000	C	6	3	3
MPM 3b								-0.439	-0.444	-0.442	0.003	D	6	6	0
MPM 6				-0.248	-0.031	-0.062	0.000	0.184		-0.031	0.138	E	10	7	3
MPQ 3	0.027	-0.043	-0.085	-0.020	0.016	-0.025	0.055	-0.025	-0.031	-0.015	0.039	F	10	9	1
MPQ 6					-0.007	-0.032	0.046	-0.042	-0.046	-0.016	0.034	G	10	6	4
MMX 2		0.172	0.086	-0.056	-0.170	-0.054	-0.164	-0.088	-0.075	-0.044	0.110	H	11	8	3
MMX 4	-0.013	0.106	0.085	-0.028	-0.135	-0.052	-0.146	-0.078	-0.060	-0.036	0.082	I	10	9	1
MMX 6					0.084	-0.063	-0.135	-0.056	-0.057	-0.045	0.071		72	54	18
MRF 3					-0.037	-0.159	-0.115	0.028	0.036	-0.049	0.077			75	25
MRF 6	-0.027	-0.125	0.015	-0.039	0.093	0.059	0.019	0.024	-0.004	0.002	0.059				
MRF 7						-0.139	-0.118	-0.006	-0.005	-0.067	0.062				
Average										-0.119	0.055				
Total													182	144	38
Percentage													100	79	21

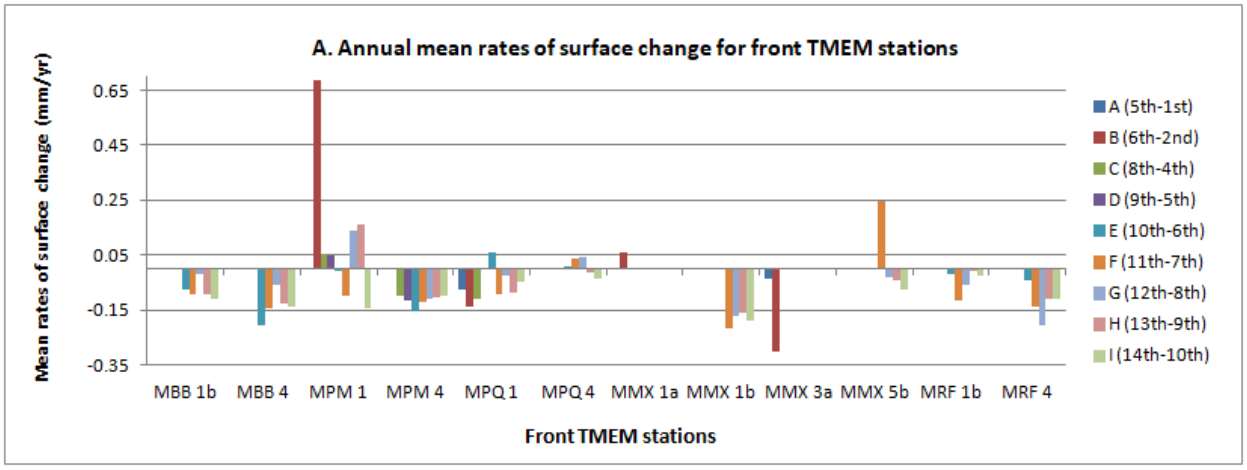

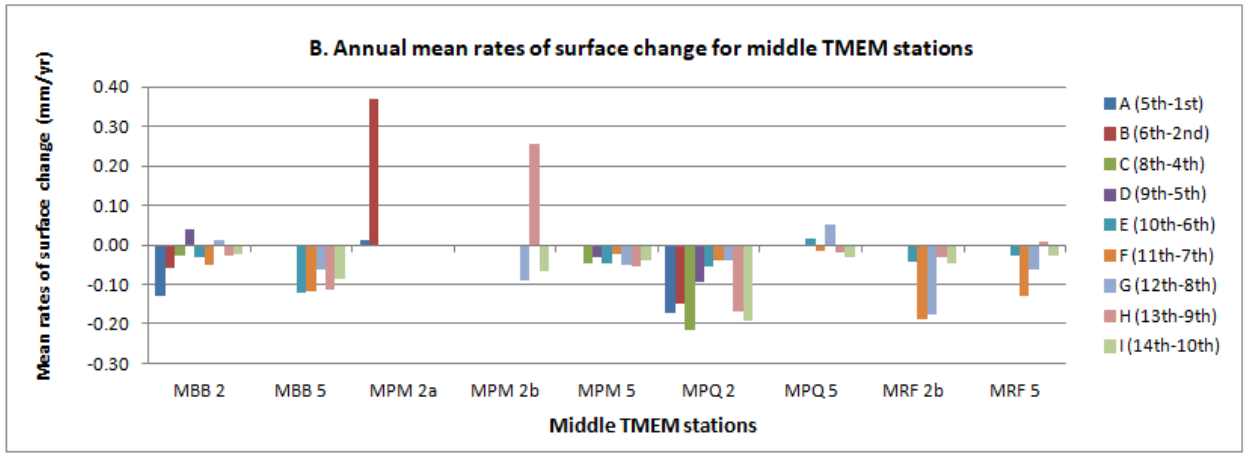

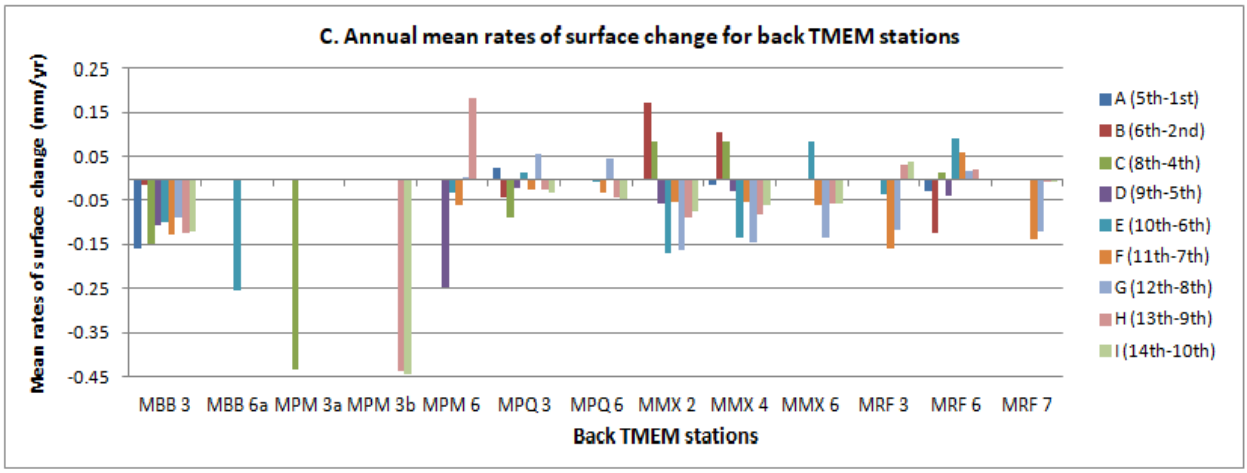

Figure 6.14: Mean rates of surface change based on annual periods for front, middle and back stations.

6.3.2.3 Individual time periods: front, middle and back of platform

Figure 6.15 to Figure 6.17 show the 292 individual time periods (3-4 months) distributed according to 16 TMEM stations in the front part of the platform, 10 TMEM stations representing the middle section of the platforms and 14 TMEM stations representing the back part of the platforms. A total of 101 measurement periods were analysed for the front TMEM stations, 78 periods for the middle stations and 113 representing the back stations and the mean rates of surface change are displayed in Table 6.6. Ponta tal-Munxar platform did not have middle stations due to its narrow morphology and the higher number for the front and back stations includes also TMEM stations which were replaced in the same location.

The average rate of surface change measured for the different sections of the platforms were as follows: -0.177 mma^{-1} at the front stations, -0.354 mma^{-1} for the middle sections and -0.185 mma^{-1} for the back sections. The three mean rates of surface change would indicate that the rates of surface change is relatively higher in the middle section and that it is subject to more surface lowering processes. These three mean values however, hide some singular values of rates of surface change which have impacted on the resultant mean rates of surface change for each section. These would include MRF1a (-1.902 mma^{-1}) in the front sections, MRF2a (-3.247 mma^{-1}) in the middle sections and MBB6 (-1.104 mma^{-1}) in the back sections.

The rates of these stations were obtained from very short measurement periods (one for MRF1a and MRF2a and three for MBB6b). When these outliers were removed from the overall mean calculations, the results of the overall mean rates adjusted as follows: 0.062 mma^{-1} for the front sections, -0.033 mma^{-1} for the middle sections and -0.115 mma^{-1} for the back sections. This would suggest a number of things: first that the back section is subject to most surface lowering than the middle and the front; secondly that the front section is

subject to an overall trend of surface rise; and thirdly, that there seems to be a positive correlation between distance from shoreline and rates of surface lowering.

A closer examination of the individual measurement periods in each front station, which combined together resulted in a mean overall surface change rate of 0.062 mma^{-1}, reveal a more complex picture. Out of the 101 measurements, 67 % of them recorded rates of surface lowering, whilst only 33% recorded surface rises (Table 6.6). Out of the 15 stations, only one station i.e. MPM1, had more measurement periods with surface rise rather than surface losses (8 out of 11) and which resulted in a mean rate of surface change of 0.207 mma^{-1} (Figure 6.15). Another two stations – MMX3a and MMX5b – have also recorded mean surface rises of 0.028 mma^{-1} and 0.089 mma^{-1} respectively but MMX3a had only two out of four periods recording surface gains, whereas MMX5b only had two periods out of seven recording surface gains (Figure 6.15).

The remaining 11 stations, although they have experienced some periods with rates of surface rises, have recorded a mean rate of surface lowering and which when combined together, give an overall surface rate of change of -0.104 mma^{-1}. This result would therefore imply that the overall mean rate of surface change of 0.062 mma^{-1} was affected by the magnitude of positive surface change experienced by the mentioned three stations i.e. MPM1, MMX3a and MMX5b and reversing to positive the overall mean rate of surface change.

The middle TMEM stations also had two stations with an overall mean rate of surface rise: MPM2a (0.064 mma^{-1}) and MRF5 (0.041 mma^{-1}). As seen in Figure 6.16, they were also the only two stations, amongst the middle ones, which had more periods with surface rises rather than surface lowerings. Yet their mean rate of surface rise was not strong enough to reverse the overall trend of mean surface lowering rates recorded for most of the middle stations. The group of back stations was the one with the highest number of periods with

rates of surface lowering i.e. 71%, and the lowest number periods with surface rises (29 %)(Table 6.6).

Table 6.6: Mean rates of surface change based on individual time periods for front middle and back stations and with average, standard deviation, and scores for stations with surface lowering (SL) and surface rises (SR)

Mean rates of surface change based on individual periods for front, middle and back stations and with average, standard deviation and scores for stations with surface lowering (SL) and surface rises (SR)																
Front station	1 (2nd-1st)	2 (4th-2nd)	3 (5th-4th)	4 (6th-5th)	5 (7th-6th)	6 (8th-7th)	7 (9th-8th)	8 (10th-9th)	9 (11th-10th)	10 (12th-11th)	l1 (13th-12th	12 (14th-13th)	Average	St Dev	Total	SL	SR
MBB1a	-0.199												-0.199	0.000	1	1	0
MBB 1b					-0.081	-0.166	0.033	-0.071	-0.153	0.106	-0.214	-0.120	-0.083	0.106	8	6	2
MBB 4					-0.242	-0.248	-0.044	-0.024	-0.167	0.071	-0.269	-0.140	-0.133	0.123	8	7	1
MPM 1		0.991	0.257	0.327	-0.051	-0.237	0.203	0.081	-0.413	0.693	0.295	0.131	0.207	0.393	11	3	8
MPM 4			0.031	0.153	-0.322	-0.122	-0.040	-0.048	-0.194	-0.077	-0.031	-0.107	-0.076	0.127	10	8	2
MPQ 1	-0.085	0.046	-0.239	-0.404	0.342	-0.317	0.174	-0.121	-0.152	-0.059	-0.025	-0.056	-0.075	0.204	12	9	3
MPQ 4					0.493	-0.116	-0.361	0.039	-0.068	-0.089	0.086	-0.055	-0.009	0.242	8	5	3
MMX 1a		-0.081	-0.569	0.601									-0.016	0.588	4	3	1
MMX 1b						0.079	-0.082	0.036	-0.629	-0.024	-0.022	-0.086	-0.104	0.239	7	5	2
MMX 3a	0.782	-0.747	-0.199	0.276									0.028	0.654	4	2	2
MMX 3b						2.009	-2.074	-0.271					-0.112	2.046	3	2	1
MMX 3c												-0.380	-0.380	0.000	1	1	0
MMX 5b						0.856	-0.001	0.062	-0.107	-0.069	-0.063	-0.055	0.089	0.342	7	5	2
MRF 1a	-1.902												-1.902	0.000	1	1	0
MRF 1b					0.319	-0.519	0.218	0.013	-0.019	0.042	-0.071	-0.041	-0.007	0.247	8	4	4
MRF 4					0.305	-0.214	-0.079	-0.004	-0.023	-0.215	-0.203	0.013	-0.053	0.174	8	6	2
Average													-0.177	0.343			
Total															101	68	33
Percentage															100	67	33
Middle stations	1 (2nd-1st)	2 (4th-2nd)	3 (5th-4th)	4 (6th-5th)	5 (7th-6th)	6 (8th-7th)	7 (9th-8th)	8 (10th-9th)	9 (11th-10th)	10 (12th-11th)	l1 (13th-12th	12 (14th-13th)	Average	St Dev			
MBB 2	-0.086	-0.063	-0.424	0.287	0.043	-0.066	-0.082	-0.025	-0.011	0.204	-0.195	-0.024	-0.037	0.171	12	9	3
MBB 5					-0.148	-0.123	-0.078	-0.134	-0.145	0.125	-0.244	-0.009	-0.094	0.103	8	7	1
MPM 2a	-0.690	-0.232	0.684	0.304	0.254								0.064	0.476	5	2	3
MPM 2b							-0.058	0.175	0.200	-0.571	1.230	-1.153	-0.029	0.734	6	3	3
MPM 5			-0.079	0.142	-0.187	0.020	0.000	0.062	-0.113	-0.077	-0.013	0.038	-0.021	0.090	10	6	4
MPQ 2	-0.244	-0.008	-0.264	-0.301	-0.176	-0.143	0.222	-0.121	-0.180	-0.144	-0.224	-0.363	-0.162	0.146	12	11	1
MPQ 5					0.109	-0.295	0.207	-0.035	0.033	-0.024	-0.051	-0.086	-0.018	0.138	8	5	3
MRF 2a	-3.247												-3.247	0.000	1	1	0
MRF 2b					0.425	-0.455	-0.135	0.045	-0.109	-0.024	-0.051	-0.004	-0.039	0.227	8	6	2
MRF 5					0.388	-0.138	0.114	0.067	0.052	0.004	-0.092	-0.064	0.041	0.153	8	3	5
Average													-0.354	0.224			
Tota;															78	53	25
Percentage															100	68	32
Back station	1 (2nd-1st)	2 (4th-2nd)	3 (5th-4th)	4 (6th-5th)	5 (7th-6th)	6 (8th-7th)	7 (9th-8th)	8 (10th-9th)	9 (11th-10th)	10 (12th-11th)	l1 (13th-12th	12 (14th-13th)	Average	St Dev			
MBB 3	-0.522	0.155	-0.346	-0.162	0.056	-0.208	-0.123	-0.128	-0.007	-0.071	-0.240	-0.108	-0.142	0.171	12	10	2
MBB 6a					-0.108	-0.380	-0.184	-0.364					-0.259	0.116	4	4	0
MBB 6b										-0.434	-0.353	-2.526	-1.104	1.006	3	3	0
MPM 3a			-0.098	-0.367	-0.508	-0.702							-0.419	0.220	4	4	0
MPM 3b								-0.378	-0.110	-0.847	-0.312	-0.482	-0.426	0.243	5	5	0
MPM 6				0.204	-0.222	-0.294	-0.666	1.257	-0.424	-0.060	0.006		-0.025	0.545	8	5	3
MPQ 3	-0.042	0.015	-0.043	-0.168	0.085	-0.304	0.218	0.011	-0.053	0.000	-0.065	-0.028	-0.031	0.121	12	7	5
MPQ 6					0.028	-0.309	0.222	-0.013	-0.057	-0.011	-0.079	-0.032	-0.031	0.136	8	6	2
MMX 2		0.093	0.316	0.231	-0.386	0.335	-0.309	-0.072	-0.207	-0.040	-0.036	-0.021	-0.009	0.228	11	7	4
MMX 4	-0.092	-0.037	0.185	0.409	-0.345	0.303	-0.307	-0.122	-0.114	-0.012	-0.064	-0.048	-0.020	0.213	12	9	3
MMX 6					0.335	0.215	-0.290	-0.043	-0.152	-0.028	-0.004	-0.047	-0.002	0.184	8	6	2
MRF 3					0.434	-0.097	-0.092	-0.037	0.021	0.152	-0.020	-0.011	0.044	0.164	8	5	3
MRF 6	-0.074	-0.043	-0.190	-0.490	0.168	0.094	0.004	0.124	0.031	-0.053	-0.015	0.022	-0.035	0.165	12	6	6
MRF 7						-0.970	0.072	-0.018	0.002	-0.038	0.031	-0.014	-0.133	0.343	6	3	3
Average													-0.185	0.275			
Total															113	80	33
Percentage															100	71	29
Dataset Total															292	201	91
Dataset Percentage															100	69	31

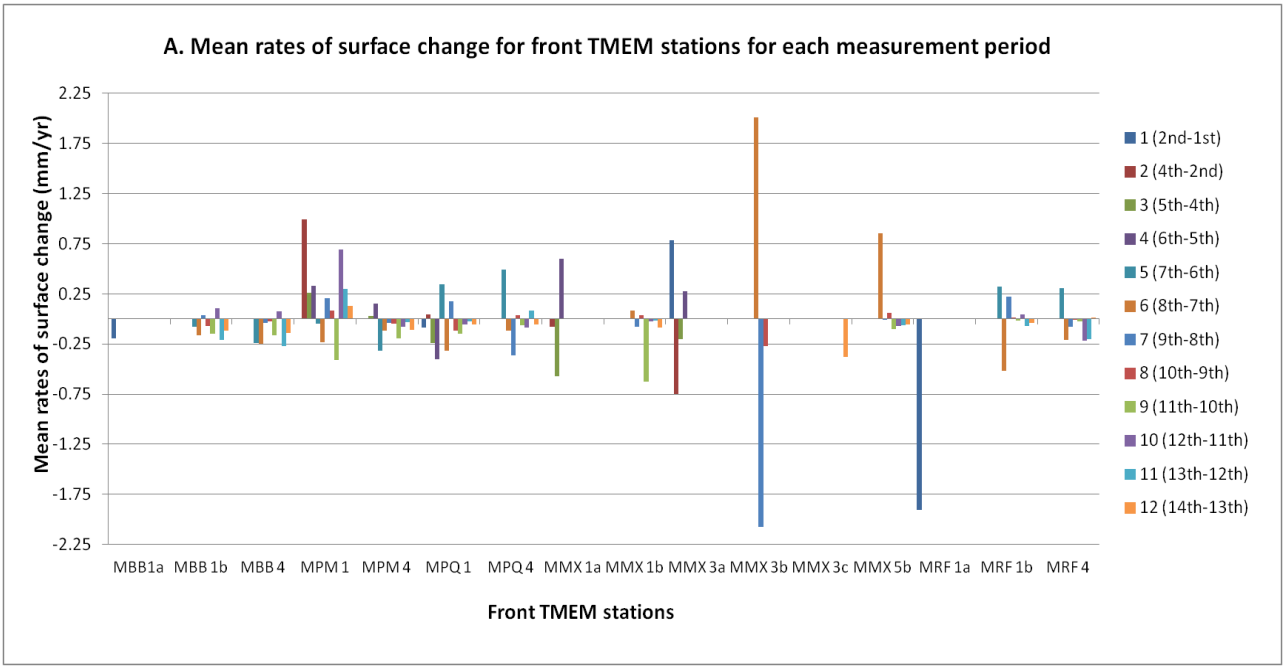

Figure 6.15: Mean rates of surface change based on individual time periods for front TMEM stations.

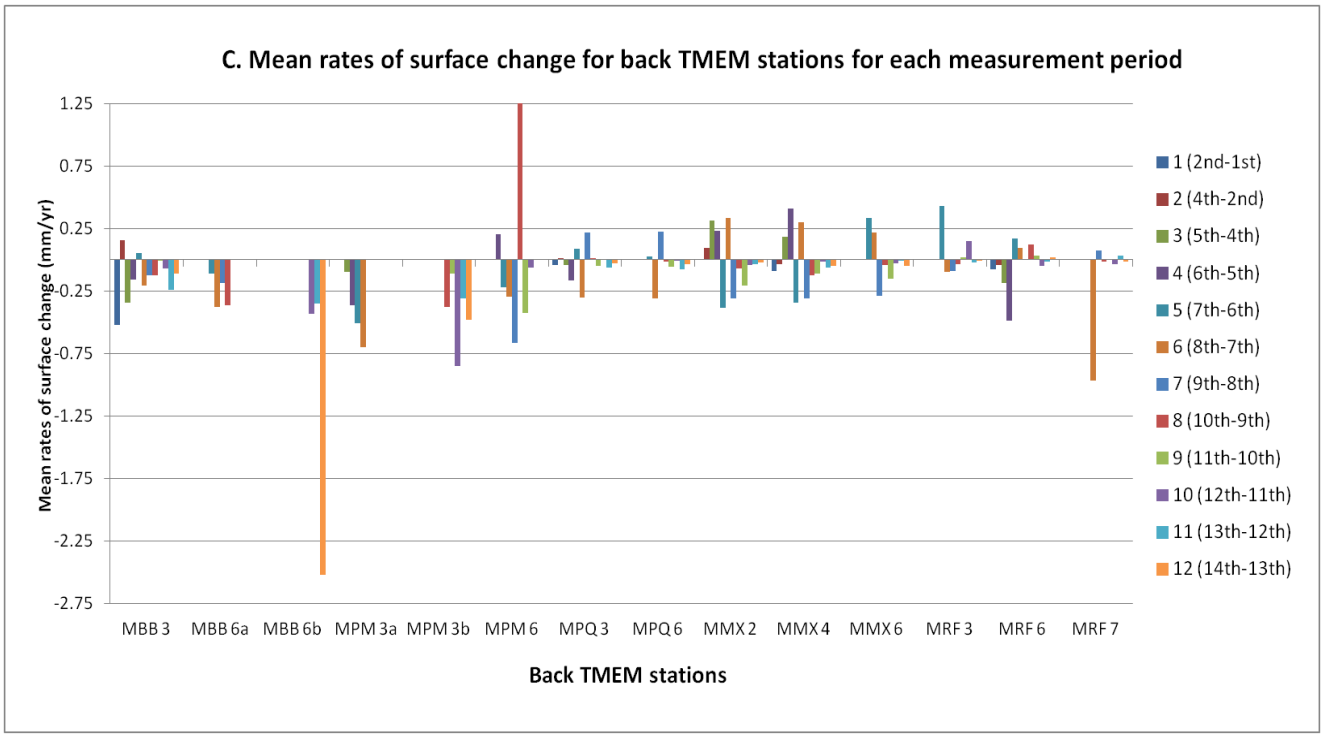

Figure 6.16: Mean rates of surface change based on individual time periods for middle TMEM stations.

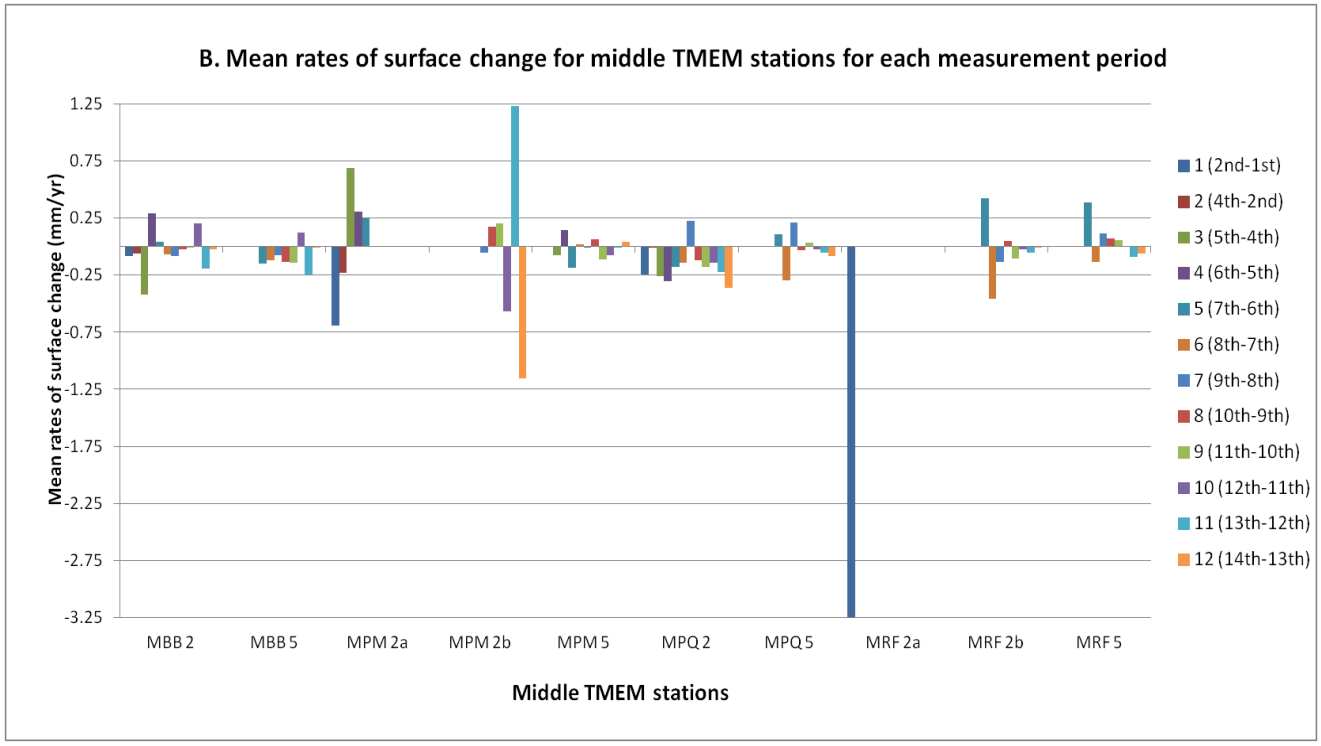

Figure 6.17: Mean rates of surface change based on individual time periods for back TMEM stations.

The back stations of Blata l-Bajda were the ones with most periods recording surface lowering (17 out of 19) (Figure 6.17) and with 69% and 31% of the rates recorded surface lowering and surface rise respectively. MRF6 and MRF7 had both equal number of periods with surface rises and surface lowering; however their mean rate of surface change still trended towards surface lowering, with -0.035 mma^{-1} for MRF6 and -0.133 mma^{-1} for MRF7. All stations recorded a mean overall surface lowering rate, with the exception of MRF 3 which recorded a mean rate of surface rise of 0.044 mma^{-1}. Though five of its eight measurement periods were rates of surface lowering, the overall mean rate of surface lowering was diminished by the rate of 0.434 mma^{-1} during the 5^{th} measurement period.

The analyses presented in this section has demonstrated how much rates of surface change need to be examined at individual period level given that an

overall mean value may mask singular magnitudes of change and the latter may lead the overall mean rate of surface change to become a misrepresentation of the overall dataset. On the other hand, as previously explained in Section 6.3.1.3, the overall rates indicating surface lowering was of 69% and that 31% of the periods represented rates of surface rises. This section has provided evidence that this percentage distribution is also similarly represented at spatial level when the stations were categorised into front, middle and back stations.

6.3.3 Inferential analyses of average rates of surface change at station level

In the following sub-sections, five statistical tests were done in order to analyse if there are any statistical significant patterns amongst the TMEM stations when examining rates of surface of change across annual and individual periods. The aims of these tests are to test out the hypotheses as illustrated in Table 3.13. These analyses aim to confirm or reject the following five null hypotheses:

i. There is no statistical difference in the annual rates of surface change between the stations at each platform (Section 6.3.3.1);
ii. There is no statistical difference in the individual rates of surface change between the stations at each platform (See Section 6.3.3.2);
iii. There is no statistical difference in the individual rates of surface change between the front and middle stations of each platform (See Section 6.3.3.3);
iv. There is no statistical difference in the individual rates of surface change between the front and back stations of each platform (See Section 6.3.3.4); and
v. There is no statistical difference in the individual rates of surface change between the middle and back stations of each platform (See Section 6.3.3.5).

For the above tests, the first two (i and ii) were analysed using the non-parametric Kruskal Wallis H (KWH) test, whilst the last three tests (iii-v) were carried out with paired statistical comparisons by using the non-parametric Mann-Whitney U (MWU) tests. For each of these tests, the rates of surface change across the 21 points per station were analysed (See Table 3.13).

6.3.3.1 Comparisons of annual rates between front, middle and back of platform

For this analysis, 40 KWH tests were conducted in order to evaluate the null hypothesis (H_0) stating that there is no difference in terms of measured annual rates (periods A-I) between the TMEM stations found on each platform. The *p* value results are listed in Table 6.7. Out of 40 *p* value results, 36 of them show a *p* value of less than 0.05. For results with *p* value of less than 0.05, the H_0 of no difference is rejected. Thus these results provide enough statistical evidence to conclude that the annual rates between the stations on each platform are different. The *p* value results ranged from 0.000 – 0.024, with 33 of them scoring *p* values of 0.000. From these KWH results, the following two conclusions can be elicited:

i. That there are no spatial similarities in the annual rates measured at the majority of the stations, even though the distances between them are not relatively large; and
ii. There are no spatial similarities in the annual rates across the majority of the periods i.e. seven out of nine annual periods.

Table 6.7: Kruskall Wallis H results for comparison of annual rates of surface change between front, middle and back stations per platform

Kruskall Wallis H results for comparison of annual rates of surface change between front, mid and back stations per platform. Grey shaded cells indicate *p* value results with no statistical difference between stations in terms of annual rates of surface change.

Annual Rates	Ponta tal-Munxar		Blata l-Bajda		Ponta tal-Miġnuna		Ponta tal-Qammieħ		Ras il-Fenek	
	Stations	KWH	Stations	KWH	Stations	KWH	Stations	KWH	Stations	KWH
		p value		*p* value		*p* value		*p* value		*p* value
Period A	Back Station MMX3a Tr1 Front Station MMX4 Tr2	0.597	Middle Station MBB2 Tr 1 Back Station MBB3 Tr1	0.065	n/a		Front Station MPQ1 Tr1 Middle Station MPQ2 Tr1 Back Station MPQ3 Tr1	0.000	n/a	
Period B	Middle Station MMX2 Tr1 Back Station MMX3a Tr1 Front Station MMX4 Tr 2	0.006	Middle Station MBB2 Tr1 Back Station MBB3 Tr1	0.250	Front Station MPM1 T1 MIddle Station MBB2a/b Tr1	0.022	Front Station MPQ1 Tr1 Middle Station MPQ2 Tr1 Back Station MPQ3 Tr1	0.000	n/a	
Period C	Middle Station MMX2 Tr1 Front Station MMX4 Tr2	0.222	Middle Station MBB2 Tr1 Back Station MBB3 Tr1	0.000	Front Station MPM1 T1 Front Station MPM4 Tr2 Middle Station MPM5 Tr2	0.000	Front Station MPQ1 Tr1 Middle Station MPQ2 Tr1 Back Station MPQ3 Tr1	0.000	n/a	
Period D	Middle Station MMX2 Tr1 Front Station MMX4 Tr2	0.024	Front Station MBB4 Tr2 Middle Station MBB5 Tr2	0.000	Front Station MPM1 T1 Front Station MPM4 Tr2 Middle Station MPM5 Tr2 Back Station MPM 6 Tr2	0.000	Front Station MPQ1 Tr1 Middle Station MPQ2 Tr1 Back Station MPQ3 Tr1	0.000	n/a	
Period E	Middle Station MMX2 Tr1 Front Station MMX4 Tr2 Back Station MMX6 Tr2	0.000	Front Station MBB1b Tr1 Middle Station MBB2 Tr1 Back Station MBB3 Tr1	0.000	Front Station MPM1 T1 Front Station MPM4 Tr2 Middle Station MPM5 Tr2 Back Station MPM 6 Tr2	0.000	Front Station MPQ1 Tr1 Middle Station MPQ2 Tr1 Back Station MPQ3 Tr1 Front Station MPQ4 Tr2 Middle Station MPQ5 Tr2 Back Station MPQ6 Tr2	0.000	Front Station MRF1b Tr1 Middle Station MRF2b Tr1 Back Station MRF3 Tr1 Front Station MRF4 Tr2 Middle Station MRF5 Tr2 Back Station MRF6 Tr2	0.000
Period F	Front Station MMX1b Tr1 Middle Station MMX2 Tr1 Front Station MMX4 Tr2 Middle Station MMX5a Tr2 Back Station MMX6 Tr2	0.000	Front Station MBB1b Tr1 Middle Station MBB2 Tr 1 Back Station MBB3 Tr1 Front Station MBB4 Tr2 Middle Station MBB5 Tr2	0.000	Front Station MPM1 T1 Front Station MPM4 Tr2 Middle Station MPM5 Tr2 Back Station MPM 6 Tr2	0.000	Front Station MPQ1 Tr1 Middle Station MPQ2 Tr1 Back Station MPQ3 Tr1 Front Station MPQ4 Tr2 Middle Station MPQ5 Tr2 Back Station MPQ6 Tr2	0.000	Front Station MRF1b Tr1 Middle Station MRF2b Tr1 Back Station MRF3 Tr1 Front Station MRF4 Tr2 Middle Station MRF5 Tr2 Back Station MRF6 Tr2 Back Station MRF7 Tr2	0.000
Period F	Front Station MMX1b Tr1 Middle Station MMX2 Tr1 Front Station MMX4 Tr2 Middle Station MMX5a Tr2 Back Station MMX6 Tr2	0.000	Front Station MBB1b Tr1 Middle Station MBB2 Tr 1 Back Station MBB3 Tr1 Front Station MBB4 Tr2 Middle Station MBB5 Tr2	0.000	Front Station MPM1 T1 MIddle Station MBB2a/b Tr1 Front Station MPM4 Tr2 Middle Station MPM5 Tr2 Back Station MPM 6 Tr2	0.000	Front Station MPQ1 Tr1 Middle Station MPQ2 Tr1 Back Station MPQ3 Tr1 Front Station MPQ4 Tr2 Middle Station MPQ5 Tr2 Back Station MPQ6 Tr2	0.000	Front Station MRF1b Tr1 Middle Station MRF2b Tr1 Back Station MRF3 Tr1 Front Station MRF4 Tr2 Middle Station MRF5 Tr2 Back Station MRF6 Tr2 Back Station MRF7 Tr2	0.000
Period H	Front Station MMX1b Tr 1 Middle Station MMX2 Tr1 Front Station MMX4 Tr2 Middle Station MMX5a Tr2 Back Station MMX6 Tr2	0.000	Front Station MBB1b Tr1 Middle Station MBB2 Tr 1 Back Station MBB3 Tr1 Front Station MBB4 Tr2 Middle Station MBB5 Tr2	0.000	Front Station MPM1 T1 MIddle Station MBB2a/b Tr1 Back Station MPM3b Tr1 Front Station MPM4 Tr2 Middle Station MPM5 Tr2 Back Station MPM 6 Tr2	0.000	Front Station MPQ1 Tr1 Middle Station MPQ2 Tr1 Back Station MPQ3 Tr1 Front Station MPQ4 Tr2 Middle Station MPQ5 Tr2 Back Station MPQ6 Tr2	0.000	Front Station MRF1b Tr1 Middle Station MRF2b Tr1 Back Station MRF3 Tr1 Front Station MRF4 Tr2 Middle Station MRF5 Tr2 Back Station MRF6 Tr2 Back Station MRF7 Tr2	0.000
Period I	Front Station MMX1b Tr 1 Middle Station MMX2 Tr1 Front Station MMX4 Tr 2 Middle Station MMX5a Tr2 Back Station MMX6 Tr2	0.000	Front Station MBB1b Tr1 Middle Station MBB2 Tr 1 Back Station MBB3 Tr1 Front Station MBB4 Tr2 Middle Station MBB5 Tr2	0.000	Front Station MPM1 T1 MIddle Station MBB2a/b Tr1 Back Station MPM3b Tr1 Front Station MPM4 Tr2 Middle Station MPM5 Tr2	0.000	Front Station MPQ1 Tr1 Middle Station MPQ2 Tr1 Back Station MPQ3 Tr1 Front Station MPQ4 Tr2 Middle Station MPQ5 Tr2 Back Station MPQ6 Tr2	0.000	Front Station MRF1b Tr1 Middle Station MRF2b Tr1 Back Station MRF3 Tr1 Front Station MRF4 Tr2 Middle Station MRF5 Tr2 Back Station MRF6 Tr2 Back Station MRF7 Tr2	0.000

These results would also imply that the behaviour of limestone surface change at supratidal conditions is not as homogenous as one would expect from stations belonging to the same limestone lithology on each respective platform. On the other hand, this test does not indicate clearly how these patterns of differences in rates translate spatially, when considering stations in specific positions on the platform (i.e. front, middle and back stations). For this type of analysis, other statistical tests have been undertaken (See Section 6.3.3.3, 6.3.3.4 and 6.3.3.5).

6.3.3.2 Comparison of individual time period rates between front, middle and back of platform

As displayed in Table 6.8, a total of 55 KWH tests were undertaken to examine the null hypothesis for spatial patterns between stations based on their respective individual measurement periods (3-4 months). Out of 55 *p* value results obtained, 49 results scored a *p* value of less than 0.05. These *p* value ranged from 0.000 to 0.033, with 42 results recording a *p* value of 0.000 (Table 6.8). The null hypothesis of no statistical difference between stations can be rejected and it can be concluded that stations of each respective platform experienced variable rates of surface change across the individual measurement periods.

Ponta tal-Miġnuna was the platform which scored differences in all its measurement periods and in addition to that, with all its *p* values not exceeding the 0.000. At Ponta tal-Munxar, the last three measurement periods scored *p* values higher than 0.05 i.e. 0.719, 0.721 and 0.390. With *p* values higher than 0.05, in this case the null hypothesis is accepted and it can be concluded that there is no difference in the rates of surface change between the stations. This result is quite unique on two accounts:

Table 6.8: Kruskall Wallis H results for comparison of individual rates of surface change between front, middle and back stations per platform

Kruskall Wallis H results for comparison of individual rates of surface change between front, mid and back stations per platform. Grey shaded cells indicate *p* value results with no statistical difference between stations in terms of individual rates of surface change.										
Individual Rates	**Ponta tal-Munxar**		**Blata l-Bajda**		**Ponta tal-Miġnuna**		**Ponta tal-Qammieħ**		**Ras il-Fenek**	
	Stations	**KWH**	**Stations**	**KWH**	**Stations**	**KWH**	**Stations**	**KWH**	**Stations**	**KWH**
		p value		*p* value		*p* value		*p* value		*p* value
RATES2_1	Back Station MMX 3a Tr1 Front Station MMX 4 Tr2	0.020	Middle Station MBB 2 Tr1 Back Station MBB 3 Tr1	0.001	n/a	n/a	Front Station MPQ1 Tr1 Middle Station MPQ2 Tr1 Back Station MPQ3 Tr1	0.003	n/a	n/a
RATES4_2	Front Station MMX 1a Tr1 Middle Station MMX 2 Tr1 Back Station MMX 3a Tr1 Front Station MMX 4 Tr2	0.000	Middle Station MBB 2 Tr1 Back Station MBB 3 Tr1	0.006	Front Station MPM 1 Tr1 Middle Station MPM 2a Tr1	0.000	Front Station MPQ1 Tr1 Middle Station MPQ2 Tr1 Back Station MPQ3 Tr1	0.322	n/a	n/a
RATES5_4	Front Station MMX 1a Tr1 Middle Station MMX 2 Tr1 Back Station MMX 3a Tr1 Front Station MMX 4 Tr2	0.000	Middle Station MBB 2 Tr1 Back Station MBB 3 Tr1	0.240	Front Station MPM 1 Tr1 Middle Station MPM 2a Tr1 Back Station MPM 3a Tr1 Front Station MPM 4 Tr2 Middle Station MPM 5 Tr2	0.000	Front Station MPQ1 Tr1 Middle Station MPQ2 Tr1 Back Station MPQ3 Tr1	0.000	n/a	n/a
RATES6_5	Front Station MMX 1a Tr1 Middle Station MMX 2 Tr1 Back Station MMX 3a Tr1 Front Station MMX 4 Tr2	0.000	Middle Station MBB 2 Tr1 Back Station MBB 3 Tr1	0.000	Front Station MPM 1 Tr1 Middle Station MPM 2a Tr1 Back Station MPM 3a Tr1 Front Station MPM 4 Tr2 Middle Station MPM 5 Tr2 Back Station MPM 6 Tr2	0.000	Front Station MPQ1 Tr1 Middle Station MPQ2 Tr1 Back Station MPQ3 Tr1	0.000	n/a	n/a
RATES7_6	Middle Station MMX 2 Tr1 Front Station MMX 4 Tr2	0.004	Front Station MBB 1b Tr1 Middle Station MBB 2 Tr1 Back Station MBB 3 Tr1 Front Station MBB 4 Tr2 Middle Station MBB 5 Tr2 Back Station MBB 6a Tr2	0.000	Front Station MPM 1 Tr1 Middle Station MPM 2a Tr1 Back Station MPM 3a Tr1 Front Station MPM 4 Tr2 Middle Station MPM 5 Tr2 Back Station MPM 6 Tr2	0.000	Front Station MPQ1 Tr1 Middle Station MPQ2 Tr1 Back Station MPQ3 Tr1	0.000	Front Station MRF1b Tr1 Middle Station MRF2b Tr1 Back Station MRF3b Tr1 Front Station MRF4 Tr2 Middle Station MRF5 Tr2 Back Station MRF6 Tr2	0.000
RATES8_7	Front Station MMX1b Tr1 Middle Station MMX 2 Tr1 Back Station MMX 3b Tr1 Front Station MMX 4 Tr2 Middle Station MMX 5 Tr2 Back Station MMX 6 Tr2	0.000	Front Station MBB 1b Tr1 Middle Station MBB 2 Tr1 Back Station MBB 3 Tr1 Front Station MBB 4 Tr2 Middle Station MBB 5 Tr2 Back Station MBB 6a Tr2	0.000	Front Station MPM 1 Tr1 Back Station MPM 3a Tr1 Front Station MPM 4 Tr2 Middle Station MPM 5 Tr2 Back Station MPM 6 Tr2	0.000	Front Station MPQ1 Tr1 Middle Station MPQ2 Tr1 Back Station MPQ3 Tr1 Front Station MPQ4 Tr2 Middle Station MPQ5 Tr2 Back Station MPQ6 Tr2	0.000	Front Station MRF1b Tr1 Middle Station MRF2b Tr1 Back Station MRF3b Tr1 Front Station MRF4 Tr2 Middle Station MRF5 Tr2 Back Station MRF6 Tr2 Back Station MRF7 Tr2	0.000
RATES9_8	Front Station MMX1a Tr1 Middle Station MMX 2 Tr1 Back Station MMX 3b Tr1 Front Station MMX 4 Tr2 Middle Station MMX 5 Tr2 Back Station MMX 6 Tr2	0.000	Front Station MBB 1b Tr1 Middle Station MBB 2 Tr1 Back Station MBB 3 Tr1 Front Station MBB 4 Tr2 Middle Station MBB 5 Tr2 Back Station MBB 6a Tr2	0.000	Front Station MPM 1 Tr1 Middle Station MPM 2b Tr1 Front Station MPM 4 Tr2 Middle Station MPM 5 Tr2 Back Station MPM 6 Tr2	0.000	Front Station MPQ1 Tr1 Middle Station MPQ2 Tr1 Back Station MPQ3 Tr1 Front Station MPQ4 Tr2 Middle Station MPQ5 Tr2 Back Station MPQ6 Tr2	0.000	Front Station MRF1b Tr1 Middle Station MRF2b Tr1 Back Station MRF3b Tr1 Front Station MRF4 Tr2 Middle Station MRF5 Tr2 Back Station MRF6 Tr2 Back Station MRF7 Tr2	0.000
RATES10_9	Front Station MMX1b Tr1 Middle Station MMX 2 Tr1 Back Station MMX 3b Tr1 Front Station MMX 4 Tr2 Middle Station MMX 5 Tr2 Back Station MMX 6 Tr2	0.000	Front Station MBB 1b Tr1 Middle Station MBB 2 Tr1 Back Station MBB 3 Tr1 Front Station MBB 4 Tr2 Middle Station MBB 5 Tr2 Back Station MBB 6a Tr2	0.000	Front Station MPM 1 Tr1 Middle Station MPM 2b Tr1 Back Station MPM 3b Tr1 Front Station MPM 4 Tr2 Middle Station MPM 5 Tr2 Back Station MPM 6 Tr2	0.000	Front Station MPQ1 Tr1 Middle Station MPQ2 Tr1 Back Station MPQ3 Tr1 Front Station MPQ4 Tr2 Middle Station MPQ5 Tr2 Back Station MPQ6 Tr2	0.010	Front Station MRF1b Tr1 Middle Station MRF2b Tr1 Back Station MRF3 Tr1 Front Station MRF4 Tr2 Middle Station MRF5 Tr2 Back Station MRF6 Tr2 Back Station MRF7 Tr2	0.000
RATES11_10	Front Station MMX1b Tr1 Middle Station MMX 2 Tr1 Front Station MMX 4 Tr2 Middle Station MMX 5 Tr2 Back Station MMX 6 Tr2	0.000	Front Station MBB 1b Tr1 Middle Station MBB 2 Tr1 Back Station MBB 3 Tr1 Front Station MBB 4 Tr2 Middle Station MBB 5 Tr2	0.000	Front Station MPM 1 Tr1 Middle Station MPM 2b Tr1 Back Station MPM 3b Tr1 Front Station MPM 4 Tr2 Middle Station MPM 5 Tr2 Back Station MPM 6 Tr2	0.000	Front Station MPQ1 Tr1 Middle Station MPQ2 Tr1 Back Station MPQ3 Tr1 Front Station MPQ4 Tr2 Middle Station MPQ5 Tr2 Back Station MPQ6 Tr2	0.000	Front Station MRF1b Tr1 Middle Station MRF2b Tr1 Back Station MRF3 Tr1 Front Station MRF4 Tr2 Middle Station MRF5 Tr2 Back Station MRF6 Tr2 Back Station MRF7 Tr2	0.000
RATES12_11	Front Station MMX1b Tr1 Middle Station MMX 2 Tr1 Front Station MMX 4 Tr2 Middle Station MMX 5 Tr2 Back Station MMX 6 Tr2	0.719	Front Station MBB1b Tr1 Middle Station MBB2 Tr 1 Back Station MBB3 Tr1 Front Station MBB4 Tr2 Middle Station MBB5 Tr2	0.000	Front Station MPM 1 Tr1 Middle Station MPM 2b Tr1 Back Station MPM 3b Tr1 Front Station MPM 4 Tr2 MIddle Station MPM 5 Tr2 Back Station MPM 6 Tr2	0.000	Front Station MPQ1 Tr1 Middle Station MPQ2 Tr1 Back Station MPQ3 Tr1 Front Station MPQ4 Tr2 Middle Station MPQ5 Tr2 Back Station MPQ6 Tr2	0.016	Front Station MRF1b Tr1 Middle Station MRF2b Tr1 Back Station MRF3 Tr1 Front Station MRF4 Tr2 Middle Station MRF5 Tr2 Back Station MRF6 Tr2 Back Station MRF7 Tr2	0.000
RATES13_12	Front Station MMX1b Tr1 Middle Station MMX 2 Tr1 Front Station MMX 4 Tr2 Middle Station MMX 5 Tr2 Back Station MMX 6 Tr2	0.721	Front Station MBB 1b Tr1 Middle Station MBB 2 Tr1 Back Station MBB 3 Tr1 Front Station MBB 4 Tr2 Middle Station MBB 5 Tr2 Back Station MBB 6b Tr2	0.004	Front Station MPM 1 Tr1 Middle Station MPM 2b Tr1 Back Station MPM 3b Tr1 Front Station MPM 4 Tr2 MIddle Station MPM 5 Tr2 Back Station MPM 6 Tr2	0.000	Front Station MPQ1 Tr1 Middle Station MPQ2 Tr1 Back Station MPQ3 Tr1 Front Station MPQ4 Tr2 Middle Station MPQ5 Tr2 Back Station MPQ6 Tr2	0.033	Front Station MRF1b Tr1 Middle Station MRF2b Tr1 Back Station MRF3 Tr1 Front Station MRF4 Tr2 Middle Station MRF5 Tr2 Back Station MRF6 Tr2 Back Station MRF7 Tr2	0.000
RATES14_13	Front Station MMX1b Tr 1 Middle Station MMX2 Tr1 Front Station MMX4 Tr 2 Middle Station MMX5a Tr2 Back Station MMX6 Tr 2	0.390	Front Station MBB 1b Tr1 Middle Station MBB 2 Tr1 Back Station MBB 3 Tr1 Front Station MBB 4 Tr2 Middle Station MBB 5 Tr2 Back Station MBB 6b Tr2	0.000	Front Station MPM 1 Tr1 Middle Station MPM 2b Tr1 Back Station MPM 3b Tr1 Front Station MPM 4 Tr2 MIddle Station MPM 5 Tr2	0.000	Front Station MPQ1 Tr1 Middle Station MPQ2 Tr1 Back Station MPQ3 Tr1 Front Station MPQ4 Tr2 Middle Station MPQ5 Tr2 Back Station MPQ6 Tr2	0.000	Front Station MRF1b Tr1 Middle Station MRF2b Tr1 Back Station MRF3 Tr1 Front Station MRF4 Tr2 Middle Station MRF5 Tr2 Back Station MRF6 Tr2 Back Station MRF7 Tr2	0.295

i. No difference between stations was confirmed for three measurement periods, whilst the other platforms (with the exception of Ponta tal-Miġnuna) recorded statistical similarities for one period only; and

ii. These periods were consecutive and this may indicate the presence of physical processes of change which were constant enough over the period of the last nine months of the survey to create comparable rates of surface change across stations of Ponta tal-Munxar. The potential factor in this case may be the long period of dry weather experienced in 2016, which may have produced less variable conditions that would have otherwise been produced by storm induced sea splashes or sea spray and/or wetness by rainfall. However such pattern was not encountered on the other platforms during the same climate periods.

Apart from the above-mentioned statistical exception, the analysis of temporal changes over different time-periods converges on similar conclusions. The KWH test based on the individual measurement periods confirms the conclusion reached by the KWH tests on periods annual (Section 6.3.3.1): rates of surface change across stations are statistical different from each other when tested as one group at platform level.

6.3.3.3 Paired comparisons of rates of individual time periods between front and middle of platforms

This section and the ones that follow (Section 6.3.3.4 and 6.3.3.5) examine the possibility of spatial relations between stations according to their relative position using the Mann Whitney U Test (MWU). In this section, a total of 72 MWU tests were undertaken in order to test the null hypothesis of no spatial difference between the front and middle stations on each respective platform, based on their individual rates of surface change. MWU tests confirm that no striking pattern of similar or contrasting behaviour between the front and middle stations (Table 6.9). Although some similarities were captured, this result continues to confirm the results obtained in the previous two sections, in that each station seems to behave independently in terms of surface change and that the individual rates measured are not determined by the spatial position in which each station is located on the platform.

Table 6.9: Results of MWU *p* values for comparison of front and middle stations based on individual period rates and with scores of *p* value results in H_0 and H_1

Results of MWU *p* values for comparisons of front and middle stations* based on individual period rates and with scores for *p* value results in H0 and H1																
Name of Platform	TMEM Stations	RATES2_1	RATES4_2	RATES5_4	RATES6_5	RATES 7_6	RATES8_7	RATES9_8	RATES10_9	RATES11_10	RATES12_11	RATES13_12	RATES14_13	Total	H0	H1
Blata l-Bajda	MBB 1b bv MBB2					0.018	0.000	0.042	0.177	0.001	0.000	0.614	0.009	8	2	6
	MBB 4 vs MBB5					0.953	0.193	0.027	0.038	0.496	0.851	0.888	0.033	8	5	3
Ponta tal-Miġnuna	MPM1 vs MPM2a+b		0.000	0.005	0.796	0.000		0.082	0.062	0.000	0.000	0.000	0.000	10	3	7
	MPM4 vs MPM5			0.007	0.103	0.032	0.002	0.040	0.001	0.142	0.787	0.105	0.146	10	5	5
Ponta tal-Qammieħ	MPQ 1 vs MPQ2	0.004	0.313	0.445	0.690	0.000	0.001	0.095	0.071	0.589	0.589	0.009	0.001	12	7	5
	MPQ 4 vs MPQ5					0.000	0.000	0.000	0.690	0.070	0.480	0.201	0.007	8	4	4
Ras il-Fenek	MRF 1b vs MRF2b					0.991	0.124	0.001	0.062	0.655	0.003	0.655	0.452	8	6	2
	MRF4 vs MRF5					0.218	0.044	0.000	0.004	0.006	0.015	0.222	0.181	8	3	5
Total		1	2	3	3	8	7	8	8	8	8	8	8	72	35	37
** Munxar has no middle stations.*																

Table 6.10: Percentage of *p* values accepting H_0 (no difference) between front and middle stations.

Name of Platform	TMEM Stations Front vs Middle	Percentage of *p* values accepting H_0				
		0-25%	26-49%	50%	51-75%	76-100%
Blata l-Bajda	MBB 1b vs MBB2					
	MBB 4 vs MBB5					
Ponta tal-Miġnuna	MPM1 vs MPM2a+b					
	MPM4 vs MPM5					
Ponta tal-Qammieħ	MPQ 1 vs MPQ2					
	MPQ 4 vs MPQ5					
Ras il-Fenek	MRF 1b vs MRF2b					
	MRF4 vs MRF5					

Table 6.9 displays the *p* values obtained for each test, Out of a total of 72 tests, 49% (35) of the *p* values confirm the null hypothesis of no difference in rates of surface change between the front and middle stations. The remaining 51% (37) resulted in *p* values of less than 0.05 and thus confirm differences between stations This result can be considered as a rather borderline result, with the confirmation of the H_0 being only marginally higher than that of H_1. Table 6.10 shows a diverse pattern of no differences between front and middle stations and there was no single platform that had both front stations comparable with its middle stations. Three comparisons confirm H_0 with a percentage group of H_0 results above 51%, another three comparisons accept H_1 with percentage scores below 49%. Only two comparisons scored no pattern of difference within the 50% groups. The rates of Ponta l-Bajda proved to be the most contrasting, with the front and middle stations of Transect 1 (MPB1b vs MPB2) exhibiting statistical significant differences whilst the front and middle stations of Transect 2 (MPB4 vs MPB5) resulting in differences in their rates of surface change. Similar to the latter stations, the stations of Transect 1 at Ponta tal-Qammieħ (MPQ1 vs MPQ2) and at Ras il-Fenek (MRF1b vs MRF2b) also confirmed statistical similarities in their rates of surface change.

6.3.3.4 Paired comparisons of individual period rates between front and back of platforms

A total of 98 MWU tests were undertaken to compare the individual time period rates of the front stations with those of the back stations on each respective platform. These tests aim to answer whether there is statistical significant difference in rates of surface change between the front and back stations measured over the same time-periods (See Table 3.13).

The overall H_1 result of statistical differences between the front and back stations seems to be disproportionately affected by the results obtained from the tests of Ponta tal-Miġnuna, Ras il-Fenek and Ponta tal-Munxar and

Table 6.11: Results of MWU *p* values for comparison of front with back stations based on individual period rates and with scores of *p* value results in H_0 and H_1

Results of MWU *p* values for comparisons of front and back stations* based on individual period rates and with scores for p value results in H0 and H1																
Name of Platform	TMEM Stations	RATES2_1	RATES4_2	RATES5_4	RATES6_5	RATES 7_6	RATES8_7	RATES9_8	RATES10_9	RATES11_10	RATES12_11	RATES13_12	RATES14_13	Total	H0	H1
Munxar	MMx 1a+b vs MMX2		0.064	0.000	0.000		0.000	0.000	0.003	0.000	0.209	0.879	0.072	10	4	6
	MMX 3a+6 vs MMX 4	0.020	0.012	0.000	0.006		0.013	0.002	0.013					7	0	7
	MMX 5b vs MMX 6						0.021	0.000	0.015	0.336	0.549	0.181	0.565	7	4	3
Blata l-Bajda	MBB 1b bv MBB 3					0.017	0.110	0.000	0.078	0.014	0.001	0.981	0.823	8	4	4
	MBB 4 vs MBB 6a+b					0.209	0.103	0.013	0.000		0.000	0.016	0.000	7	2	5
Ponta tal-Mignuna	MPM1 vs MPM3a+b			0.001	0.000	0.001	0.000		0.000	0.439	0.000	0.000	0.000	9	1	8
	MPM4 vs MPM6				0.066	0.003	0.016	0.000	0.000	0.006	0.003	0.001		8	1	7
Ponta tal-Qammieh	MPQ 1 vs MPQ3	0.972	0.118	0.000	0.001	0.000	0.265	0.832	0.018	0.004	0.011	0.181	0.285	12	6	6
	MPQ 4 vs MPQ 6					0.000	0.000	0.000	0.098	0.250	0.488	0.121	0.028	8	4	4
Ras il-Fenek**	MRF1b vs MRF3b						0.000	0.002	0.000	0.000	0.000	0.001	0.046	7	0	7
	MRF4 vs MRF 6					0.000	0.000	0.004	0.000	0.000	0.010	0.001	0.860	8	1	7
	MRF4 vs MRF7						0.000	0.001	0.647	0.008	0.173	0.000	0.991	7	3	4
Total		2	3	4	5	7	12	11	12	10	11	11	10	98	30	68

Table 6.12: Percentage of *p* values accepting H_0 (no difference) between front and back stations.

Name of Platform	TMEM Stations Front vs Back	Percentage of *p* values accepting H_0				
		0-25%	26-49%	50%	51-75%	76-100%
Munxar	MMX 1a+b vs MMX2					
	MMX 3a+6 vs MMX 4					
	MMX 5b vs MMX 6					
Blata l-Bajda	MBB 1b vs MBB3					
	MBB 4 vs MBB 6a+b					
Ponta tal-Miġnuna	MPM1 vs MPM3a+b					
	MPM4 vs MPM6					
Ponta tal-Qammieħ	MPQ1 vs MPQ3					
	MPQ4 vs MPQ 6					
Ras il-Fenek*	MRF1b vs MRF3b					
	MRF4 vs MRF 6					
	MRF4 vs MRF7					

**Ras il-Fenek has an extra station at the back*

much less by those of Ponta tal-Miġnuna and Blata l-Bajda. As displayed in Table 6.11, out of 98 *p* value results, 31% (30 out of 98) scored *p* value higher than 0.05 and thus they confirm the null hypothesis of no difference in the rates of surface change between the front and back stations. The remaining 69 % of the results (68 out of 98) scored *p* values lower than 0.05 and thus suggesting statistical significant differences between the stations.

All tested stations of Ponta tal-Miġnuna, Ras il-Fenek and Ponta tal-Munxar conform with the alternative hypothesis in experiencing statistically significant differences in their rates of surface change, especially MPM1 vs MPM3a+b, MPM4 vs MPM6, MRF1b vs MRF3b, MRF4 vs MRF6 and MMX3a+6 vs MMX4 (Table 6.12). Only one paired comparison resulted in a definite H_0 result: that of Ponta tal-Munxar (MMX5b vs MMX6) and which contrasts with the results of differences obtained on the same platform when comparing with the other four stations. The results may be summarised as follows:

i. Statistical analyses of the rates of surface erosion between front and back stations on platforms tend to show statistically significant differences;
ii. The MWU results partially confirm the results of statistical difference obtained for the KWH tests for annual rates (Section 6.3.3.1), especially for the stations of Ponta tal-Miġnuna, Ras il-Fenek and Ponta tal-Munxar; and
iii. They also show how the results of significant differences observed in Ponta tal-Miġnuna and Blata l-Bajda with KWH tests in Section 6.3.3.1 actually mask other different statistical sub-trends when comparing the front and back stations only.

Another result that may be highlighted is the result of no spatial pattern observed at Ponta tal-Qammieħ. As illustrated in Table 6.12, both tests result in a 50% composition for *p* values, leading to an equal acceptance of H_0 in as much as that of H_1. This result partially echoes the no pattern observed previously for

the front and middle station comparison of MPQ4 and MPQ5 (Table 6.8) but it also contrasts with the other result (MPQ1 vs MPQ2) which had recorded a stronger *p* value groups of no difference (Table 6.8). The results of Blata l-Bajda, on the other hand, fall either within 25-49 % groups of moderate similar behaviour (MBB4 vs MBB 6a+b) or the 50 % groups of no pattern (MBB1b vs MBB3).

6.3.3.5 Paired comparisons of individual time period rates between middle and back of platforms

A total of 77 MWU tests were carried out to compare the individual time period rates of middle and the back stations on each platform. These tests aim to answer whether there is statistical significant difference in rates of surface change between the middle and back stations measured over the same time periods (See Table 3.13). The *p* value results are displayed in Table 6.13 and Table 6.14. The key findings of this test are as follows:

i. In terms of H_1/H_0 percentage groups, the pattern of differences between middle and back stations analyses suggests that the greatest variability in differences in rates of surface change occurs between the middle and back stations. In examining the results of stations such as MPB5 vs MPB6a+b, MPM2a+b vs MPM3a+b, MPM5 vs MPM6 and MRF5 vs MRF6, it was noticed that more than 80% of their respective measurement periods had *p* values lower than 0.05, thus suggesting strong statistical differences in rates across most of the measurement time periods (Table 6.14);

Table 6.13: Results of MWU *p* values for comparison of middle with back stations based on individual period rates and with scores of *p* value results in H_0 and H_1

Results of MWU *p* values for comparisons of middle and back stations* based on individual period rates and with scores for *p* value results in H0 and H1																
Name of Platform	Stations	RATES2_1	RATES4_2	RATES5_4	RATES6_5	RATES 7_6	RATES8_7	RATES9_8	RATES10_9	RATES11_10	RATES12_11	RATES13_12	RATES14_13	Total	H0	H1
Blata l-Bajda	MPB 1b bv MPB 3	0.001	0.006	0.240	0.000	0.614	0.000	0.000	0.001	0.751	0.000	0.707	0.032	12	4	8
	MPB 5 vs MPB 6a+b					0.000	0.000	0.003	0.000		0.000	0.000	0.000	7	0	7
Ponta tal-Miġnuna	MPM2a+b vs MPM3a+b				0.000	0.000			0.000	0.024	0.307	0.000	0.018	7	1	6
	MPM5 vs MPM6				0.020	0.113	0.001	0.000	0.000	0.003	0.001	0.007		8	1	7
Ponta tal-Qammieħ	MPQ2 vs MPQ3	0.002	0.963	0.000	0.000	0.020	0.250	0.159	0.209	0.000	0.017	0.084	0.001	12	5	7
	MPQ 5 vs MPQ 6					0.000	0.366	0.017	0.255	0.698	0.605	0.925	0.597	8	6	2
Ras il-Fenek**	MRF2b vs MRF 3b					0.004	0.000	0.991	0.000	0.001	0.000	0.000	0.240	8	2	6
	MRF5 vs MRF6					0.002	0.003	0.000	0.018	0.022	0.000	0.000	0.078	8	1	7
	MRF4 vs MRF7						0.000	0.003	0.000	0.796	0.285	0.000	0.796	7	3	4
Total		2	2	2	4	8	8	8	9	8	9	9	8	77	23	54
** Munxar has no middle stations.*																
***Ras il-Fenek has an extra station at the back*																

Table 6.14: Percentage of *p* values accepting H_0 (no difference) between middle and back stations.

Name of Platform	TMEM Stations Middle vs Back	Percentage of *p* values accepting H_0				
		0-25%	26-49%	50%	51-75%	76-100%
Blata l-Bajda	MBB 1b vs MBB 3					
	MBB 5 vs MBB 6a+b					
Ponta tal-Miġnuna	MPM2a+b vs MPM3a+b					
	MPM5 vs MPM6					
Ponta tal-Qammieħ	MPQ2 vs MPQ3					
	MPQ 5 vs MPQ 6					
Ras il-Fenek	MRF2b vs MRF 3b					
	MRF5 vs MRF6					
	MRF4 vs MRF7					

ii. In terms of H_1/H_0 percentage groups (Table 6.14), differences in rates of surface change for the middle and back stations tend to be stronger and less variable. The strongest result was that of 70 % of the total *p* values of the dataset (54 out of 77) which were less than 0.05 and thus confirm that there are differences in rates of surface change between the middle and back stations of each platform (Table 6.13); and
iii. There are some similarities between rates of surface change between stations (such as Ponta tal-Qammieħ) but these tend to be isolated occurrences and it is difficult to discern a general pattern in them.

This third MWU analysis continues to mainly confirm the key findings of the previous KWH and MWU tests discussed in the earlier sections as follows:

i. Both KWH and MWU tests show a pattern of differences in rates of surface change between the three types of stations;
ii. The analysis of spatial patterns of surface rates tends to show that the position of the station on the platform has little impact on the statistical differences observed; and
iii. The degree of statistical differences is time-scale-dependent. KWH results for annual and individual rates for front, middle and back stations scored higher H_1 outcome (90 % and 81% respectively), whilst the paired MWU tests scored lower H_1 results: front and middle comparison had a slightly higher H_0 result (51%) whilst front with back and middle with back comparisons had a higher H_1 result of 69% and 70% respectively. This implies that annual and individual rates are more likely to be statistically different from each other between stations whilst rates in same time-periods between certain parts of the platform are more likely to be statistically similar.

6.4 Temporal patterns of rock surface change at each platform

The following two sections present the results of measured rates based on the average surface changes recorded per station across three different timeframes: annual periods, semi-annual periods and individual measurement periods (See Section 3.6.1.1). A total of 3,943 MWU tests and 36 KWH tests were carried out for paired comparisons of annual, semi-annual and individual periods. The selection of these three time-frames allows comparisons between shorter and longer temporal scales and evaluate how rates of surface change may trend differently or similarly within the spatial dimension. Statistical comparisons between the three selected time-frames with the MWU test and KWH test provided the opportunity to infer any significant temporal similarities within each platform and across the five platforms (See Table 3.13).

6.4.1 Descriptive analyses of average rates of surface change

6.4.1.1 Annual rates

A total of 45 annual time periods (nine per platform) were compared. Their rates are listed in Table 6.15 and their trends are displayed in Figure 6.18 to Figure 6.22. As observed in Section 6.3.1.1, the majority of the annual rates registered surface lowering trends, with minor trends of rises in specific periods or at some specific stations. Table 6.15 shows how, out of a total of 45 periods, 36 registered surface-lowering rates (80%) and only five measurement periods (11%) recorded rates of surface rise at specific periods (B period at Ponta tal-Miġnuna, E and G periods at Ponta tal-Qammieħ, period C at Ponta tal-Munxar and Ras il-Fenek). The remaining four periods experienced equal number of mean rates with lowering and rising trends.

Table 6.15: Rates of surface change based on annual periods with average and standard deviation values for each period

Rates of surface change based on annual periods, with average and standard deviation values for each period.																
TMEM Station	**Rates of surface change**										Period	Total	SL	SR	SL	SR
	A (5th-1st)	B (6th-2nd)	C (8th-4th)	D (9th-5th)	E (10th-6th)	F (11th-7th)	G (12th-8th)	H (13th-9th)	I (14th-10th)	Average						
MBB 1b					-0.076	-0.091	-0.021	-0.095	-0.107		A	2	2	0	100	0
MBB 2	-0.131	-0.059	-0.029	0.038	-0.031	-0.050	0.012	-0.025	-0.025		B	2	2	0	100	0
MBB 3	-0.161	-0.013	-0.148	-0.103	-0.096	-0.126	-0.086	-0.124	-0.119		C	2	2	0	100	0
MBB 4					-0.208	-0.141	-0.058	-0.127	-0.141		D	2	1	1	50	50
MBB 5					-0.122	-0.119	-0.063	-0.115	-0.086		E	6	6	0	100	0
MBB 6a					-0.255						F	5	5	0	100	0
Average	-0.146	-0.036	-0.089	-0.033	-0.131	-0.105	-0.043	-0.097	-0.096	-0.086	G	5	4	1	80	20
St Deviation	0.021	0.033	0.084	0.100	0.084	0.036	0.039	0.042	0.044	0.054	H	5	4	1	80	20
											I	5	5	0	100	0
Station	A (5th-1st)	B (6th-2nd)	C (8th-4th)	D (9th-5th)	E (10th-6th)	F (11th-7th)	G (12th-8th)	H (13th-9th)	I (14th-10th)							
MPM 1		0.687	0.053	0.046	-0.007	-0.100	0.136	0.160	-0.143		A	1	1	0	100	0
MPM 2a	0.011	0.369									B	2	0	2	0	100
MPM 2b							-0.091	0.254	-0.066		C	4	3	1	75	25
MPM 3a			-0.435								D	4	3	1	75	25
MPM 3b								-0.439	-0.444		E	4	4	0	100	0
MPM 4			-0.100	-0.114	-0.157	-0.118	-0.107	-0.105	-0.099		F	4	4	0	100	0
MPM 5			-0.047	-0.030	-0.047	-0.025	-0.050	-0.054	-0.038		G	5	3	2	60	40
MPM 6				-0.248	-0.031	-0.062	0.000	0.184			H	6	3	3	50	50
Average	0.011	0.528	-0.132	-0.086	-0.060	-0.076	-0.022	0.000	-0.158	0.000	I	6	3	3	50	50
St. Deviation			0.212	0.126	0.066	0.041	0.098	0.257	0.165	0.138						
Station	A (5th-1st)	B (6th-2nd)	C (8th-4th)	D (9th-5th)	E (10th-6th)	F (11th-7th)	G (12th-8th)	H (13th-9th)	I (14th-10th)							
MPQ 1	-0.075	-0.140	-0.107	0.001	0.059	-0.092	-0.024	-0.085	-0.046		A	3	2	1	67	33
MPQ 2	-0.172	-0.151	-0.217	-0.092	-0.056	-0.038	-0.041	-0.167	-0.193		B	3	3	0	100	0
MPQ 3	0.027	-0.043	-0.085	-0.020	0.016	-0.025	0.055	-0.025	-0.031		C	3	3	0	100	0
MPQ 4					0.006	0.040	0.043	-0.015	-0.037		D	3	2	1	67	33
MPQ 5					0.014	-0.017	0.053	-0.020	-0.033		E	6	2	4	33	67
MPQ 6					-0.007	-0.032	0.046	-0.042	-0.046		F	6	5	1	83	17
Average	-0.073	-0.111	-0.136	-0.037	0.005	-0.027	0.022	-0.059	-0.064	-0.054	G	6	2	4	33	67
St. Deviation	0.100	0.059	0.071	0.049	0.037	0.042	0.043	0.059	0.063	0.058	H	6	6	0	100	0
											I	6	6	0	100	0
Station	A (5th-1st)	B (6th-2nd)	C (8th-4th)	D (9th-5th)	E (10th-6th)	F (11th-7th)	G (12th-8th)	H (13th-9th)	I (14th-10th)							
MMX 1a		0.060														
MMX 1b						-0.219	-0.174	-0.158	-0.187		A	2	2	0	100	0
MMX 2		0.172	0.086	-0.056	-0.170	-0.054	-0.164	-0.088	-0.075		B	4	2	2	50	50
MMX 3a	-0.039	-0.300									C	3	0	3	0	100
MMX 4	-0.013	0.106	0.085	-0.028	-0.135	-0.052	-0.146	-0.078	-0.060		D	2	2	0	100	0
MMX 5b						0.243	-0.028	-0.045	-0.073		E	3	2	1	67	33
MMX 6					0.084	-0.063	-0.135	-0.056	-0.057		F	5	4	1	80	20
Average	-0.026	0.010	0.086	-0.042	-0.074	-0.029	-0.130	-0.085	-0.090	-0.042	G	5	5	0	100	0
St. Deviation	0.018	0.211	0.001	0.020	0.138	0.168	0.058	0.045	0.055	0.079	H	5	5	0	100	0
											I	5	5	0	100	0
Station	A (5th-1st)	B (6th-2nd)	C (8th-4th)	D (9th-5th)	E (10th-6th)	F (11th-7th)	G (12th-8th)	H (13th-9th)	I (14th-10th)							
MRF 1b					-0.019	-0.115	-0.058	-0.008	-0.022		A	1	1	0	100	0
MRF 2b					-0.042	-0.188	-0.178	-0.032	-0.046		B	1	1	0	100	0
MRF 3					-0.037	-0.159	-0.115	0.028	0.036		C	1	0	1	0	100
MRF 4					-0.042	-0.136	-0.203	-0.110	-0.107		D	1	1	0	100	0
MRF 5					-0.028	-0.129	-0.064	0.009	-0.026		E	6	5	1	83	17
MRF 6	-0.027	-0.125	0.015	-0.023	0.093	0.059	0.019	0.024	-0.004		F	7	6	1	86	14
MRF 7						-0.139	-0.118	-0.006	-0.005		G	7	6	1	86	14
Average	-0.027	-0.125	0.015	-0.023	-0.013	-0.116	-0.102	-0.013	-0.025	-0.048	H	7	4	3	57	43
St. Deviation					0.052	0.080	0.076	0.047	0.044	0.060	I	7	6	1	86	14

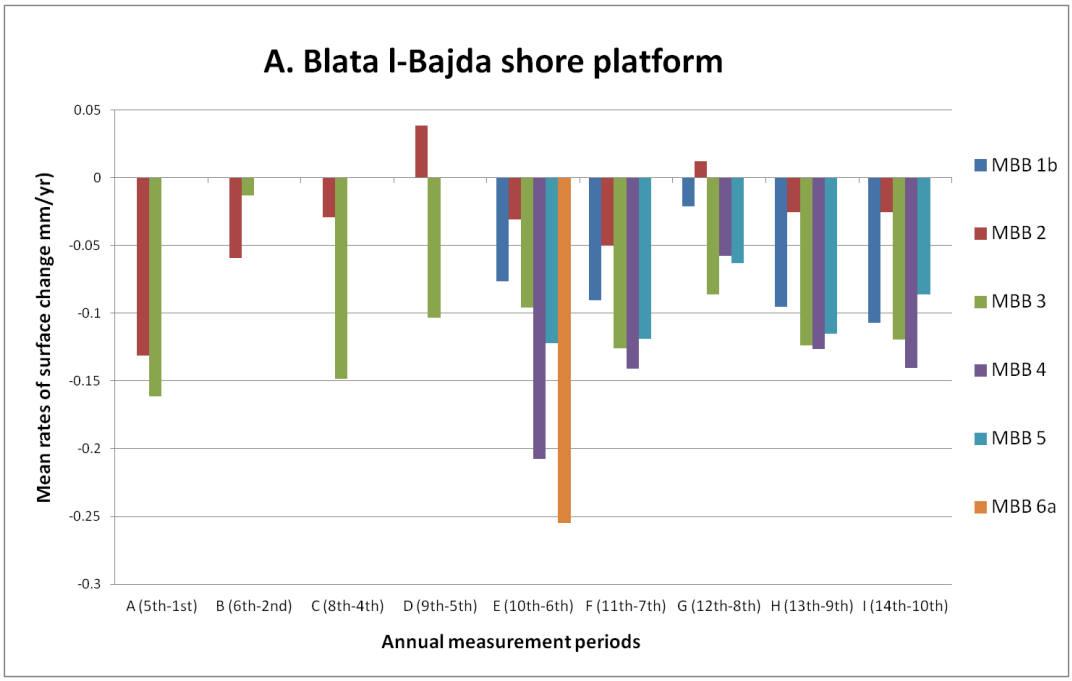

Figure 6.18: Temporal trends of surface change based on annual periods at Blata l-Bajda shore platform

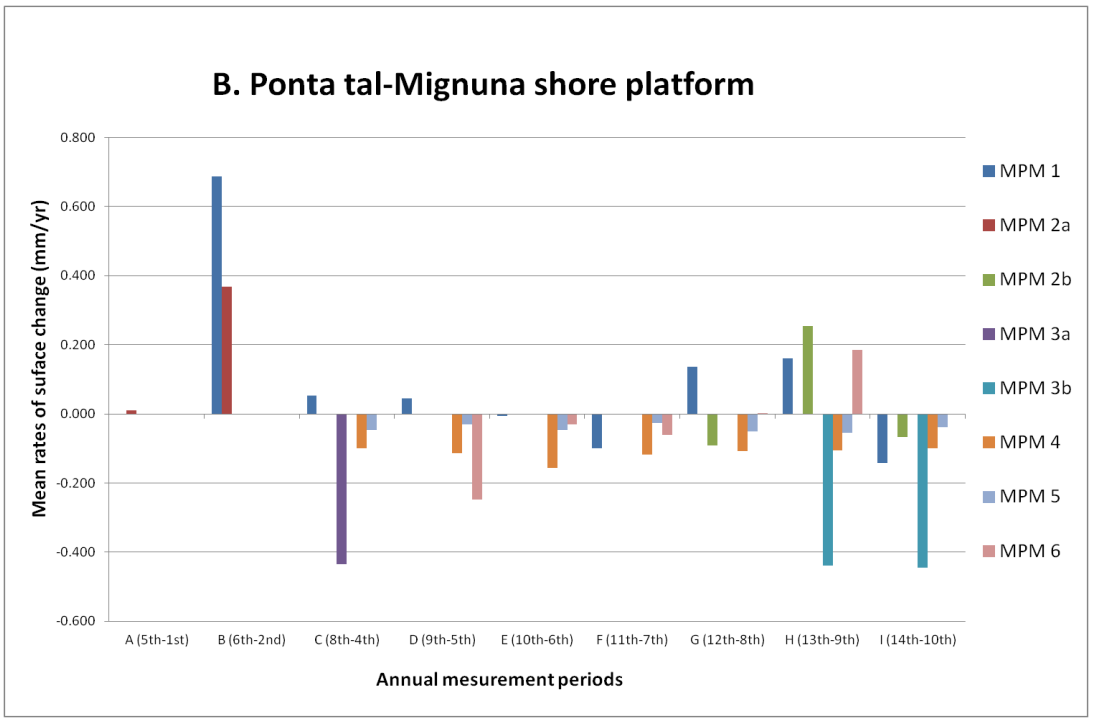

Figure 6.19: Temporal trends of surface change based on annual periods at Ponta tal- Miġnuna shore platform

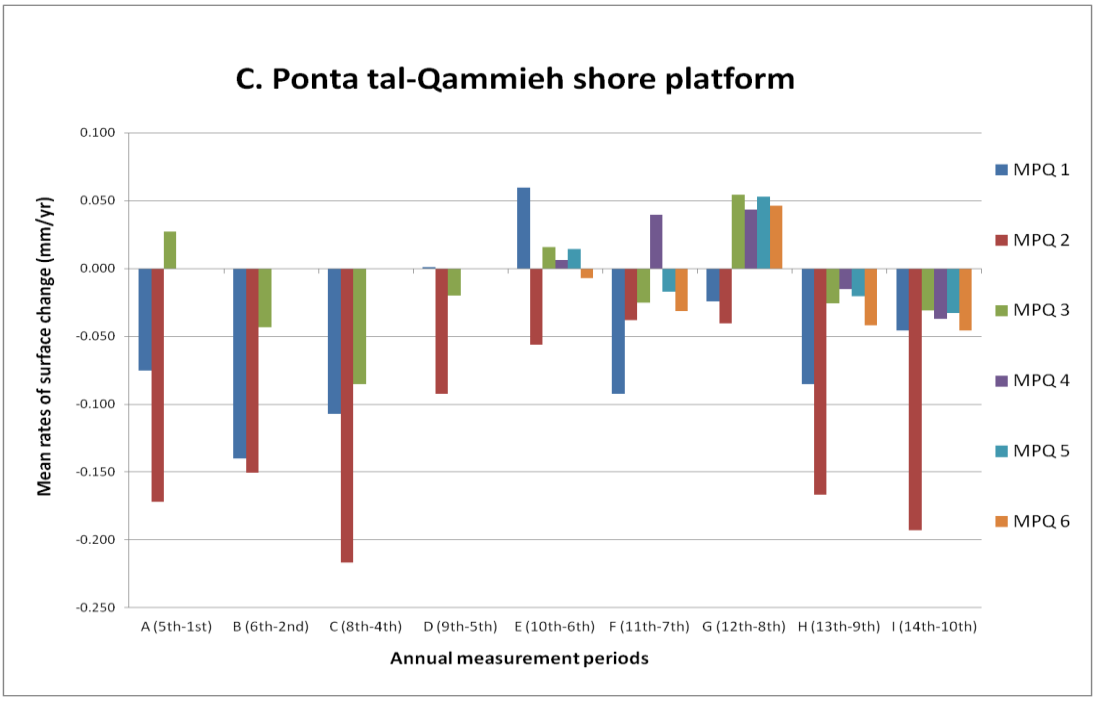

Figure 6.20: Temporal trends of surface change based on annual periods at Ponta tal- Qammieħ shore platform

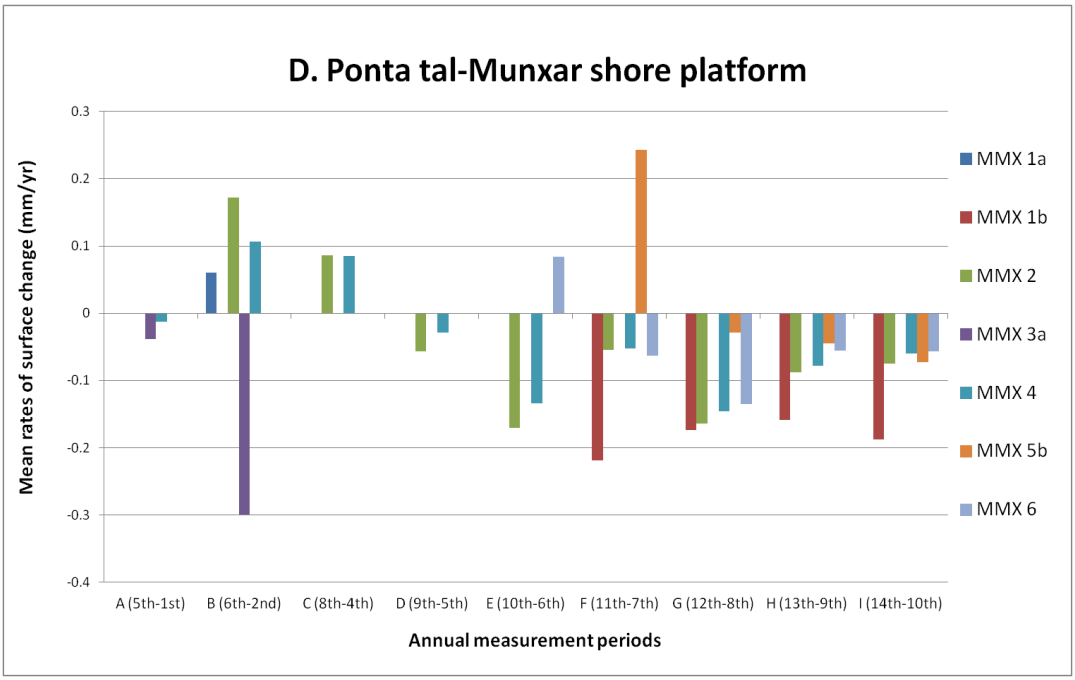

Figure 6.21: Temporal trends of surface change based on annual periods at Ponta tal- Munxar shore platform

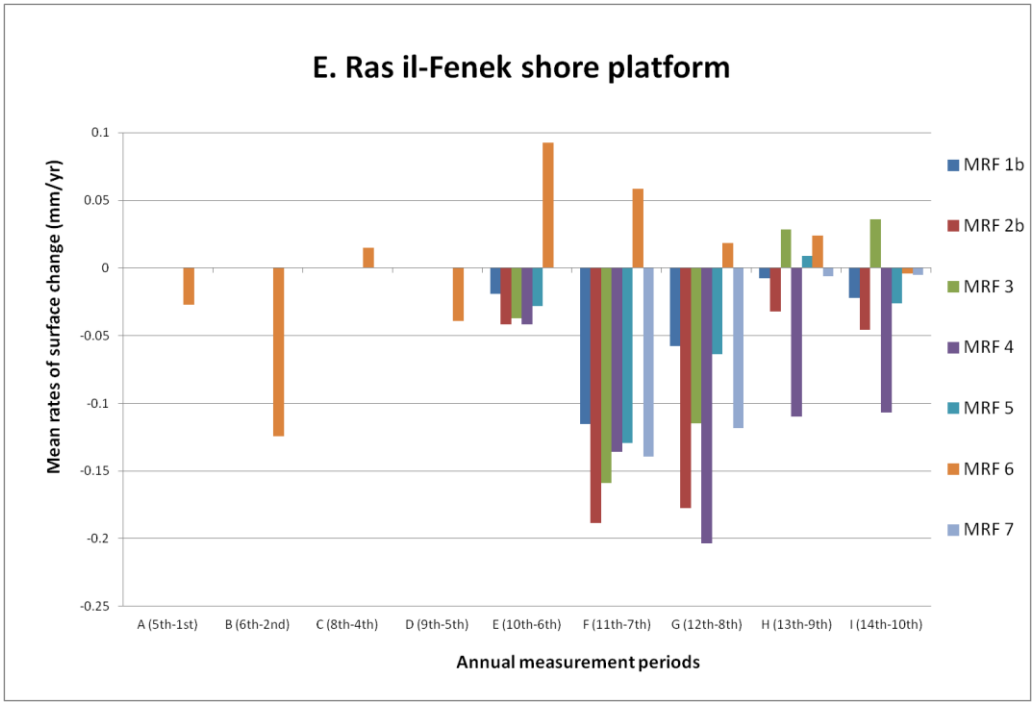

Figure 6.22: Temporal trends of surface change based on annual periods at Ras il-Fenek shore platform

In examining the overall mean rates of surface change based on mean temporal rates, Blata l-Bajda platform scored the largest rate of downwearing and lowest mean standard deviation between its mean temporal rates. The mean rates of surface change across the annual measurement periods for each shore platform were highly variable and there is no specific period or periods which have a common pattern across stations (Figure 6.18 to Figure 6.22). Ponta tal-Qammieħ had the largest mean rates of downwearing in the first three periods A-C (Figure 6.20), whilst Ponta tal-Munxar (Figure 6.21) recorded its largest mean rates of surface change in the last three periods (G, H and I). The other three platforms have mean rates interspersed throughout the survey period: Blata l-Bajda (A, E, F), Ponta tal-Miġnuna (B, C and I) and Ras il-Fenek (B, F and G). In terms of trends, periods E, F and G have recorded the largest trends in surface lowering rates, especially at the shore platforms of Ras il-Fenek (Figure 6.22) and Blata l-Bajda (Figure 6.18). Periods H and I were then also quite pronounced at Blata l-Bajda and Ponta tal-Qammieħ platform.

The temporal trends at Qammieħ platform recorded for periods F and G can be considered an inverse trend to that observed at Blata l-Bajda and Ras il-Fenek. F and G measurement periods registered the lowest levels of downwearing rates and also had some rises trends. Most of the notable downwearing rates were experienced in the earlier periods of the study (periods A, B and C) and the latter part of the survey period i.e. in H and I. Similar to Ras il-Fenek and Blata l-Bajda, the highest rates of surface change at Ponta tal-Munxar were recorded in periods G, H and I.

Some stations recorded both rises and losses throughout the survey period: such as MPM1, MMX2, MMX4 and MRF6. In terms of rises across the study period, Blata l-Bajda shore platform was the one with relatively less records of rises (Table 6.16). The rest of the stations had relatively more records of rises, although limited to one of two specific stations at each platform, such as period E and G at Ponta tal-Qammieħ, period C and H at Ras il-Fenek and period B and C for Ponta tal-Munxar platform.

Table 6.16: Percentage of surface rises from total recorded rates of surface change on each platform based on annual and semi-annual time periods.

Name of platform	Annual Time Periods											Semi-Annual time periods										
	A	B	C	D	E	F	G	H	I	%*		A2	B2	C1	C2	D2	E2	F2	G2	H2	I2	%*
Blata l-Bajda	0	0	0	50	0	0	20	20	0	10		0	0	50	0	0	0	0	20	0	17	7
Ponta tal-Mignuna	0	100	25	25	0	0	40	50	50	33		33	80	33	0	25	80	33	17	33	33	37
Pontatal-Qammieh	33	0	0	33	67	17	67	0	0	27		33	0	33	33	33	100	0	17	0	17	27
Ponta tal-Munxar	0	50	100	0	33	20	0	0	0	21		25	100	0	33	50	17	0	0	0	0	22
Ras il-Fenek	0	0	100	0	17	14	14	43	14	21		0	0	0	17	14	57	29	43	14	29	27
** Percentage from total measured rates on platform*																						

6.4.1.2 Semi-annual rates

Ten temporal trends for semi-annual rates, labelled from A2 to I2, were analysed (Table 6.17, Figure 6.23 and Figure 6.24). A total of 241 semi-annual

rates were examined and it was observed that the temporal trends for semi-annual rates are not markedly different from those observed for the annual rates in terms of surface lowering and rising patterns. As displayed in Table 6.17, 75% of the total number of semi-annual rates (181) recorded rates of surface lowering and the remaining 25% (60) were rates of surface rise. These two percentage results were not so distant from the 79% and 21% results obtained from the annual rates (See Section 6.3.1.2).

All the five platforms recorded more surface lowering trends whilst records of rises were clustered in specific periods or for specific stations Figure 6.23 and Figure 6.24). As displayed in Table 6.17, the shore platforms of Ras il-Fenek, Ponta tal-Munxar and Ponta tal-Qammieħ have all percentage distributions close to the overall average of the dataset. The percentages of Ponta tal-Miġnuna shore platform are less close to the dataset average (with 63% of the rates being surface lowering and 37% being rates of surface rise) whilst the Blata l-Bajda shore platform remains the most distant with 93% and 7% respectively and confirms the results analysed at annual level (See Section 6.3.1.2).

In examining temporal rates at station level, the semi-annual rates of Blata l-Bajda platform (Figure 6.23) were similar to the annual rates in being mostly surface lowering rates and with only one semi-annual period, period C1, recording a mean surface rise of 0.055 mma^{-1}. Only three individual rates (out of a total of 43) measured a surface rise: MBB2 in period C1 and C2 and MBB3 in J. At the shore platform of Ponta tal-Miġnuna (Figure 6.23), period B and F resulted as outliers in having four out of five individual rates recording surface rises. Period A2 and I2 also recorded a mean surface rise but they were largely influenced by high rates of surface rises recorded in MPM1.

Table 6.17: Rates of surface change based on semi-annual periods, with average and standard deviation per period ands cores for periods with surface lowering (SL) and surface rises (SR)

Rates of surface change based on semi-annual periods with average and standard deviation per periods and scores for periods with surface lowering (SL) and surface rises (SR)															
TMEM station	**Rates of surface change according to semi-annnual periods**											**Periods**	**Total**	**SL**	**SR**
	A2 (4th-2nd)	B2 (6th-4th)	C1 (7th-5th)	2 (8th-6th)	2 (9th-7th	2 (10th-8th	2 (11th-9th	2 (12th-10t	2 (13th-11th	2 (14th-12th)	Average	A2	2	2	0
MBB 1b				-0.122	-0.076	-0.018	-0.108	-0.025	-0.083	-0.176		B2	2	2	0
MBB 2	-0.063	-0.054	0.148	-0.011	-0.066	-0.056	-0.018	0.095	-0.032	-0.125		C1	2	1	1
MBB 3	-0.186	-0.171	-0.039	-0.072	-0.125	-0.169	-0.073	-0.038	-0.250	0.155		C2	5	5	0
MBB 4				-0.245	-0.156	-0.036	-0.123	-0.049	-0.130	-0.217		D2	5	5	0
MBB 5				-0.136	-0.103	-0.106	-0.139	-0.012	-0.093	-0.148		E2	5	5	0
MBB 6a						-0.272	-0.291	-0.241				F2	5	5	0
MBB 6b									-1.235	-0.325		G2	5	4	1
Average	-0.125	-0.113	0.055	-0.117	-0.105	-0.110	-0.125	-0.045	-0.304	-0.139	-0.113	H2	6	6	0
St Dev	0.087	0.083	0.132	0.087	0.037	0.096	0.092	0.109	0.462	0.160	0.135	I2	6	5	1
												Total	43	40	3
Station	A2 (4th-2nd)	B2 (6th-4th)	C1 (7th-5th)	2 (8th-6th)	2 (9th-7th	2 (10th-8th	2 (11th-9th	2 (12th-10t	2 (13th-11th	2 (14th-12th)		A2	3	2	1
MPM 1	0.991	0.292	0.094	-0.124	-0.014	0.145	-0.198	0.170	0.488	0.214		B2	5	1	4
MPM 2a	-0.232	0.491	0.273									C1	6	4	2
MPM 2b						0.054	0.143	-0.206	0.342	0.062		C2	4	4	0
MPM 3a	-0.235	-0.454	-0.584									D2	4	3	1
MPM 3b							-0.298	-0.498	-0.572	-0.295		E2	5	1	4
MPM 4		0.093	-0.141	-0.244	-0.080	-0.044	-0.161	-0.133	-0.053	-0.068		F2	6	4	2
MPM 5		0.033	-0.061	-0.106	0.010	0.029	-0.065	-0.094	-0.044	0.012		G2	6	5	1
MPM 6			-0.059	-0.250	-0.482	0.253	0.414	-0.232	-0.026			H2	6	4	2
Average	0.175	0.091	-0.080	-0.181	-0.142	0.087	-0.028	-0.166	0.023	-0.015	-0.023	I2	6	4	2
St Deviation	0.707	0.354	0.288	0.077	0.230	0.115	0.263	0.217	0.370	0.187	0.281	Total	51	32	19
Station	A2 (4th-2nd)	B2 (6th-4th)	C1 (7th-5th)	2 (8th-6th)	2 (9th-7th	2 (10th-8th	2 (11th-9th	2 (12th-10t	2 (13th-11th	2 (14th-12th)		A2	3	2	1
MPQ 1	0.046	-0.308	0.056	0.068	-0.058	0.049	-0.136	-0.099	-0.044	-0.041		B2	3	3	0
MPQ 2	-0.008	-0.279	-0.224	-0.162	0.049	0.076	-0.150	-0.159	-0.180	-0.293		C1	3	2	1
MPQ 3	0.015	-0.095	-0.012	-0.077	-0.029	0.130	-0.021	-0.022	-0.029	-0.047		C2	6	4	2
MPQ 4				0.240	0.081	0.165	-0.014	-0.080	-0.016	0.009		D2	6	4	2
MPQ 5				-0.059	-0.030	0.104	-0.001	0.001	-0.036	-0.069		E2	6	0	6
MPQ 6				-0.112	-0.029	0.122	-0.035	-0.031	-0.047	-0.062		F2	6	6	0
Average	0.018	-0.227	-0.060	-0.017	-0.002	0.108	-0.060	-0.065	-0.059	-0.084	-0.045	G2	6	5	1
St Dev	0.027	0.115	0.146	0.147	0.055	0.041	0.066	0.059	0.060	0.106	0.082	H2	6	6	0
												I2	6	5	1
												Total	51	37	14
Station	A2 (4th-2nd)	B2 (6th-4th)	C1 (7th-5th)	2 (8th-6th)	2 (9th-7th	2 (10th-8th	2 (11th-9th	2 (12th-10t	2 (13th-11th	2 (14th-12th)		A2	4	3	1
MMX 1a	-0.081	0.243										B2	4	0	4
MMX 1b					-0.003	-0.027	-0.298	-0.333	-0.023	-0.053		C1	2	2	0
MMX 2	0.093	0.275	-0.125	-0.053	0.019	-0.199	-0.140	-0.126	-0.038	-0.029		C2	3	2	1
MMX 3a	-0.747	0.281										D2	6	3	3
MMX 3b					-0.081	-1.240						E2	6	5	1
MMX 4	-0.037	0.292	-0.057	-0.068	0.003	-0.222	-0.118	-0.064	-0.040	-0.056		F2	5	5	0
MMX 5b					0.477	0.030	-0.023	-0.088	-0.066	-0.059		G2	5	5	0
MMX 6				0.284	-0.033	-0.176	-0.098	-0.091	-0.015	-0.025		H2	5	5	0
Average	-0.193	0.273	-0.091	0.054	0.064	-0.306	-0.135	-0.140	-0.036	-0.044	-0.055	I2	5	5	0
St Dev	0.377	0.021	0.047	0.199	0.206	0.469	0.101	0.110	0.019	0.016	0.157	Total	45	35	10
Station	A2 (4th-2nd)	B2 (6th-4th)	C1 (7th-5th)	2 (8th-6th)	2 (9th-7th	2 (10th-8th	2 (11th-9th	2 (12th-10t	2 (13th-11th	2 (14th-12th)		A2	1	1	0
MRF 1b				-0.124	-0.125	0.114	-0.002	0.013	-0.013	-0.056		B2	1	1	0
MRF 2b				-0.040	-0.237	-0.044	-0.027	-0.065	-0.038	-0.027		C1	1	1	0
MRF 3				-0.016	-0.197	-0.064	-0.010	0.089	0.068	-0.015		C2	6	5	1
MRF 4				-0.042	-0.153	-0.041	-0.013	-0.123	-0.209	-0.092		D2	7	6	1
MRF 5				-0.121	-0.200	0.090	0.060	0.027	-0.043	-0.078		E2	7	3	4
MRF 6	-0.043	-0.132	-0.115	0.129	0.045	0.047	0.081	-0.012	-0.034	0.004		F2	7	5	2
MRF 7					-0.162	0.027	-0.008	-0.018	-0.004	0.008		G2	7	4	3
Average	-0.043	-0.132	-0.115	-0.036	-0.147	0.018	0.012	-0.013	-0.039	-0.037	-0.053	H2	7	6	1
St Dev				0.092	0.092	0.070	0.041	0.068	0.084	0.039	0.070	I2	7	5	2
												Total	51	37	14
Total													241	181	60

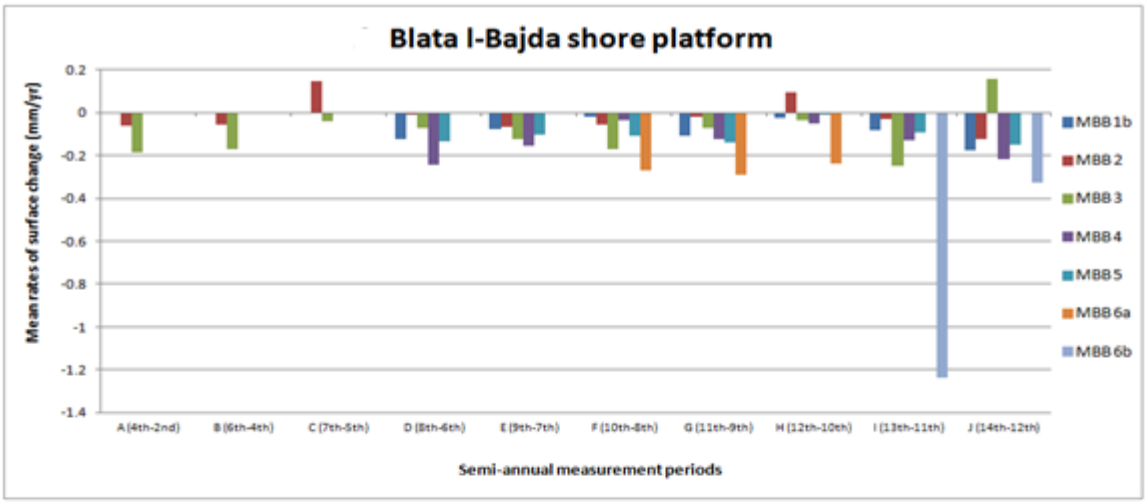

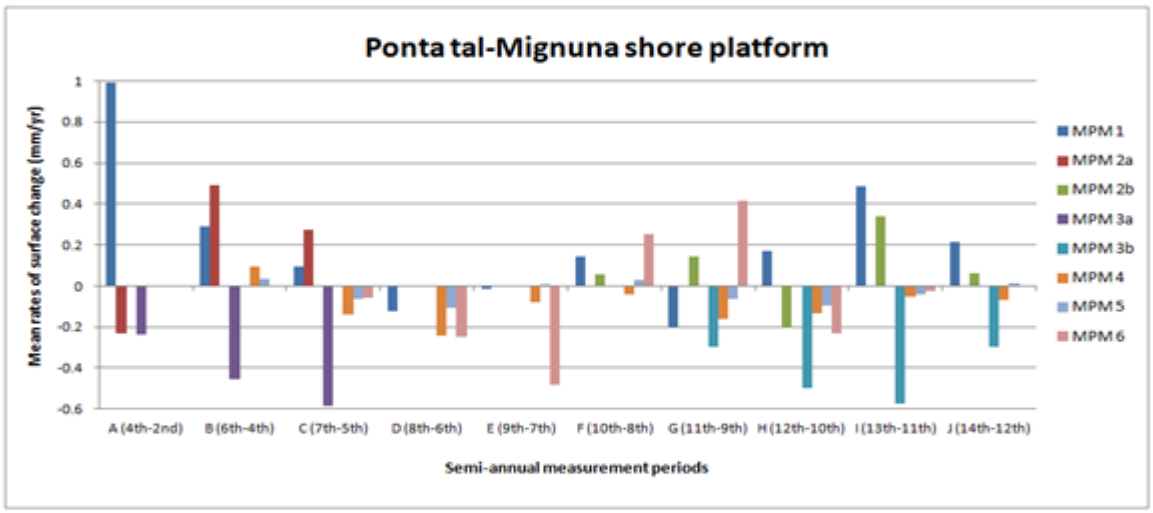

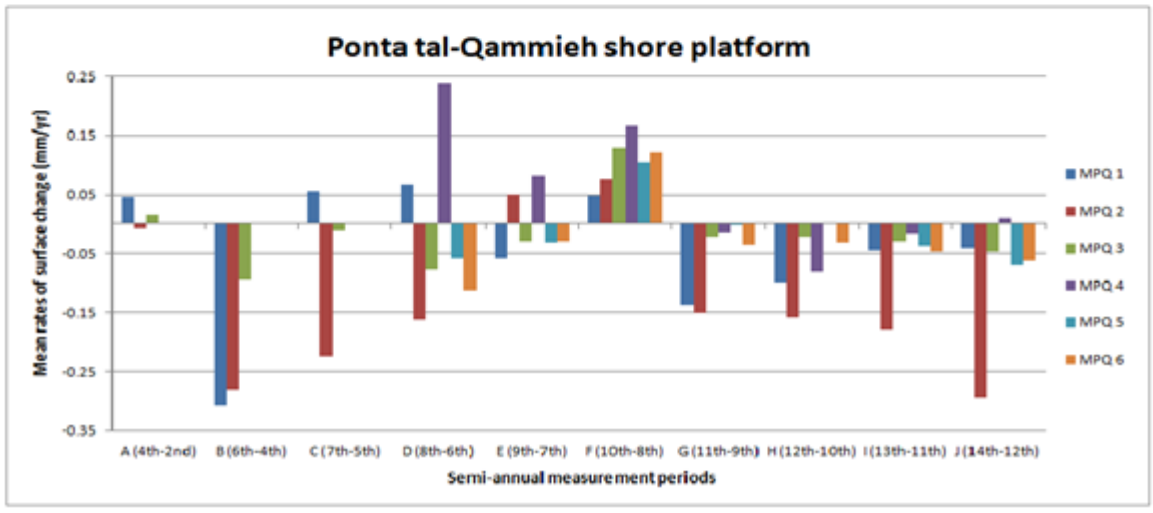

Figure 6.23: Temporal trends of semi-annual periods for Blata l-Bajda, Ponta tal- Miġnuna and Ponta tal-Qammieħ shore platforms

Figure 6.24: Temporal trends of semi-annual periods for Ponta tal-Munxar and Ras il-Fenek shore platforms

Periods A2 and E2 proved also to be an anomaly in the overall trend of surface lowering at Ponta tal-Qammieħ (Figure 6.23) with overall mean rates of 0.018 mma^{-1} (A2) and 0.10 mma^{-1} (E2). Semi-annual rates at Ponta tal-Qammieħ displayed also a temporal trend similar to the annual one (Figure 6.3), with largest rates of surface lowering in early periods B2, C1, C2 and later

period G2, H2 and I2, an inverse trend of surface rises in period F and less pronounced rises in less stations in periods A2, C1, C2 and D2. Period E2 and F2 were also the only two periods which registered a mean rate of surface rise at Ras il-Fenek. The semi-annual trends of Ras il-Fenek platform (Figure 6.24) are different from the annual rates on two accounts: firstly, it displays more variability at semi-annual levels, with more rises recorded in E2 and G2 and secondly, the trend of surface lowering rates is larger in period E and less pronounced in periods E2 and F2. Ponta tal-Miġnuna also displays relatively more rises in period B2 and F2 (Table 6.16).

This would suggest that the semi-annual rates capture more variability in rock surface change, which otherwise is more masked when surface change is calculated on an annual time-frame. In fact in just taking Ponta tal-Miġnuna and Ponta tal-Munxar (Figure 6.24d) as an example, the mean standard deviation of their semi-annual rates (the highest from the whole dataset) was almost double than that for their annual rates: 0.281 (semi-annual) and 0.138 (annual) for Ponta tal-Miġnuna and 0.157 (semi-annual) and 0.057 (annual).

6.4.1.3 Individual time periods (3-4 months)

Table 6.18 and Figure 6.25 to Figure 6.29 display the temporal trends of each measurement period with surface change rates for each station grouped together under each period. 12 measurement periods were examined with a total of 292 individual temporal periods. In analysing both the variability trend across these measurement periods and the sequence of rates of surface lowering and surface rises, there does not seem to be any defined pattern of surface change. In terms of variability, some of the early measurement periods such as period 1, 2, 4, and 5 were observed to have variable rates above platform average and this was observed across different shore platforms. However, above-average variability in rates of surface change was also recorded in measurement periods towards the end of the survey such as the 10th and 12th measurement periods in particular at Blata l-Bajda and Ponta tal-Miġnuna.

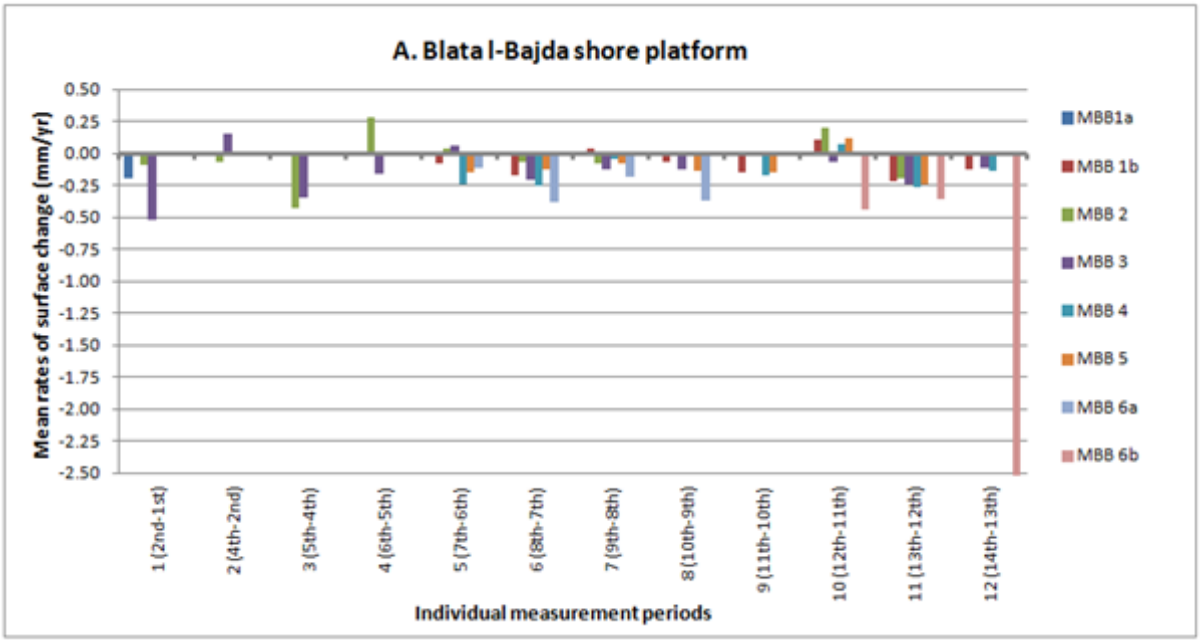

Figure 6.25: Temporal trends of individual time periods for Blata l-Bajda shore platform

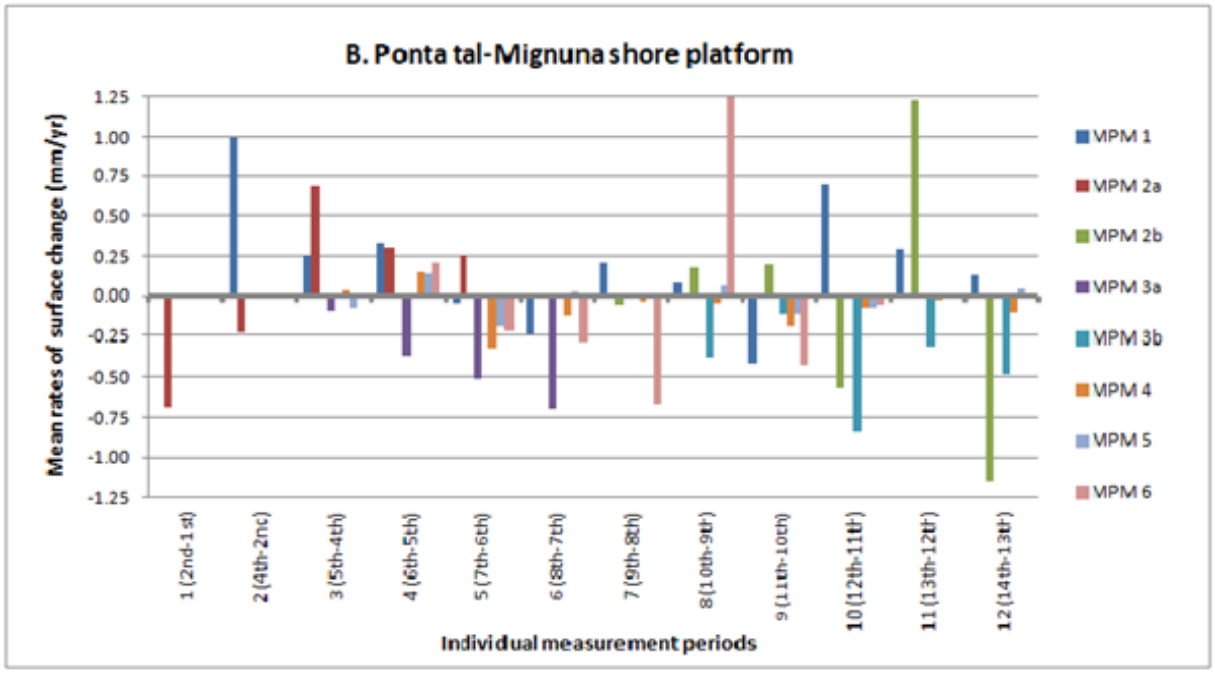

Figure 6.26: Temporal trends of individual time periods for Ponta tal-Miġnuna shore platform

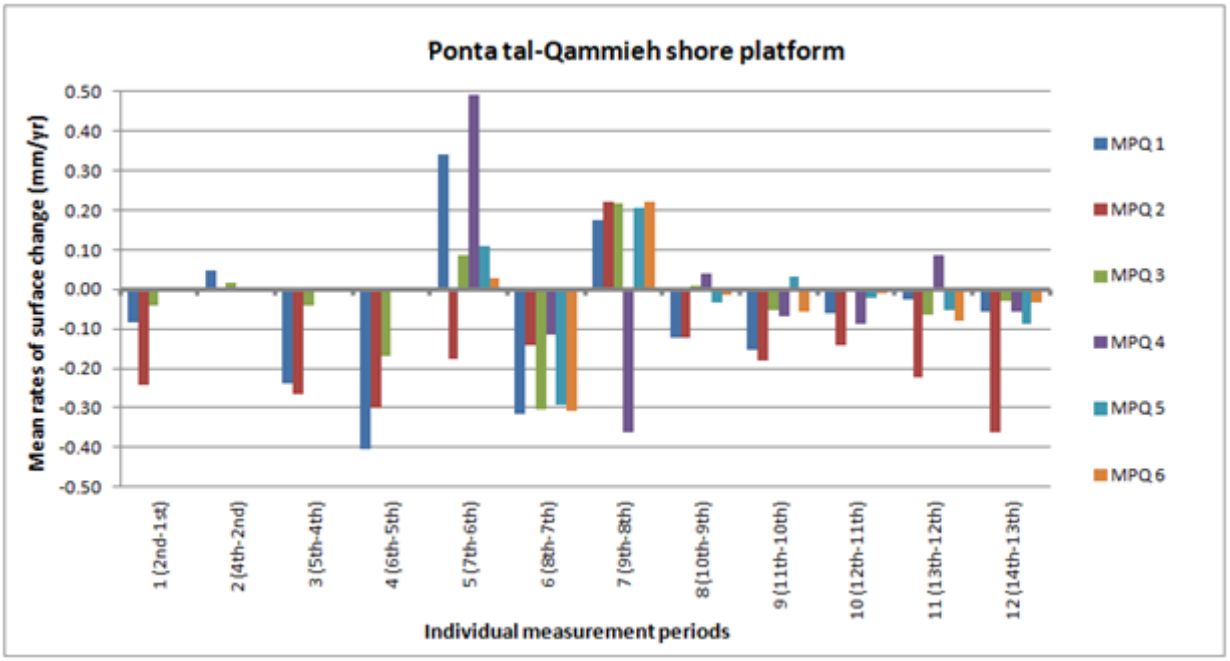

Figure 6.27: Temporal trends of individual time periods for Ponta tal-Qammieħ shore platform

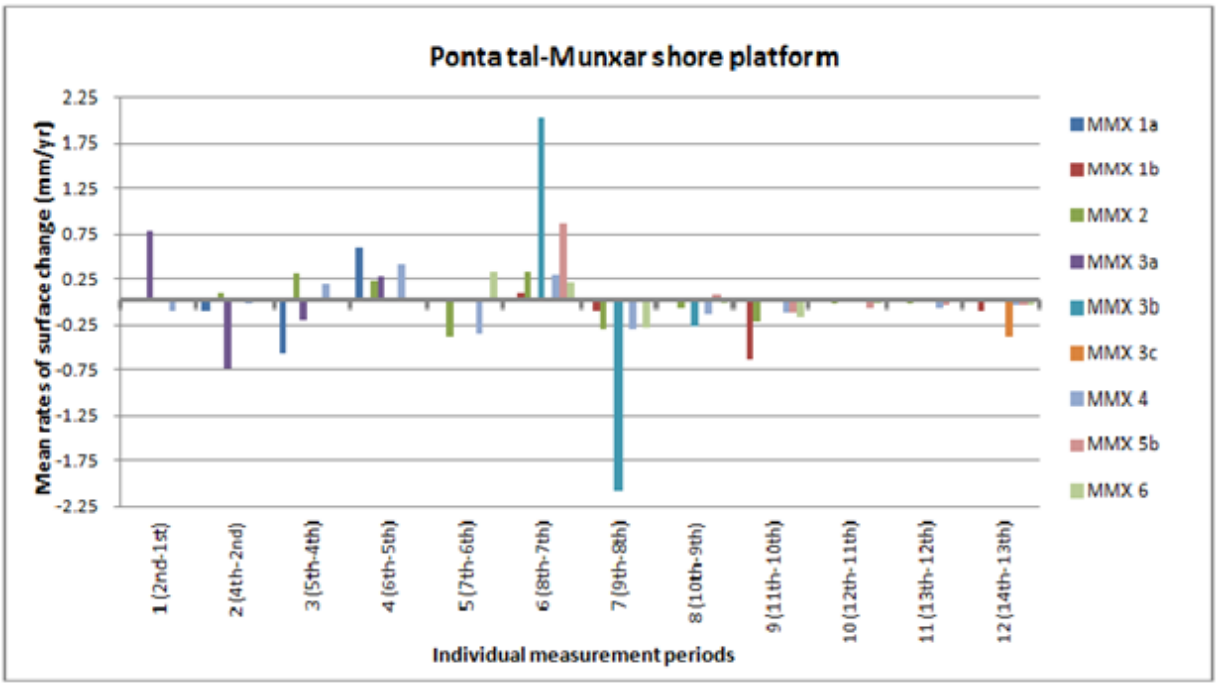

Figure 6.28: Temporal trends of individual time periods for Ponta tal-Munxar shore platform

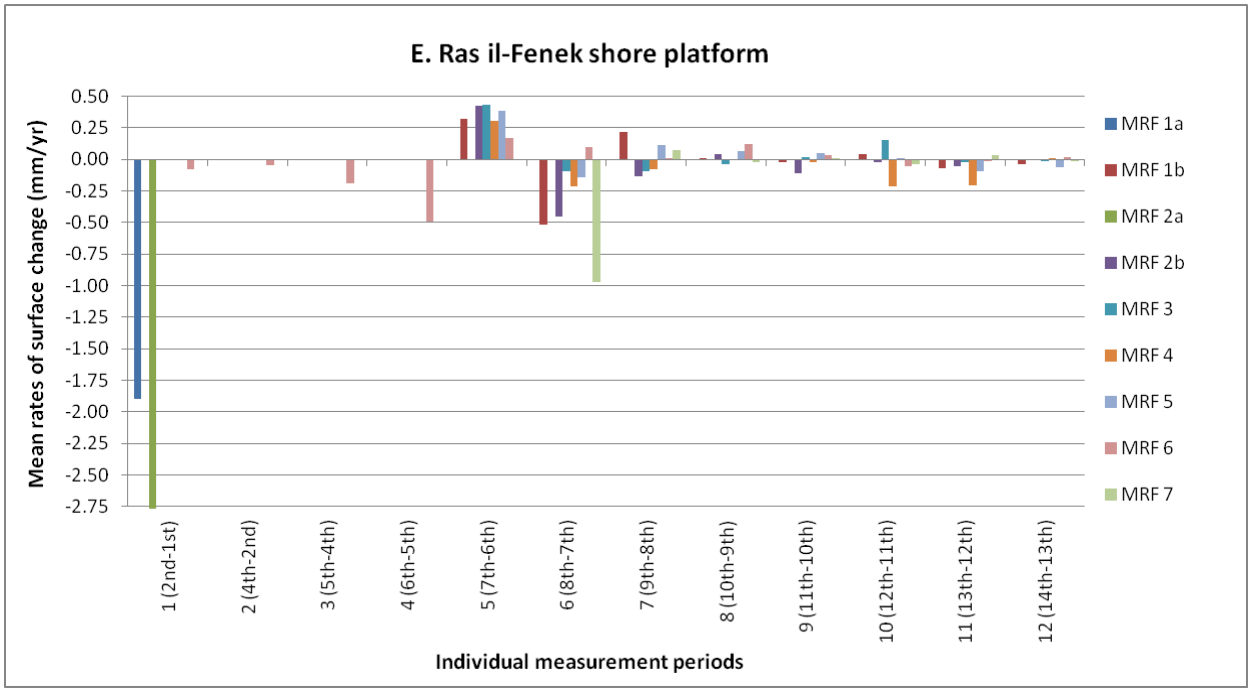

Figure 6.29: Temporal trends of individual time periods for Ras il-Fenek shore platform

With regard to the trend between rates of surface-lowering versus those of surface-rises, 70% of the individual temporal periods recorded surface-lowering rates (See Section 6.2.1.3). Exceptions to this trend were one or two periods per station in which relatively more rates of surface change although no time-period emerged consistently in the measurement of these rises.

Table 6.18: Rates of surface change based on individual time periods with average and standard deviation per periods and scores for periods with surface lowering (SL) and surface rises (SR)

Rates of surface change based on individual time periods with average and standard deviation per periods and scores for periods with surface lowering (SL) and surface rises (SR)														Period	No of Rates	SL	SR	SL	SR
Station	1 (2nd-1st)	2 (4th-2nd)	3 (5th-4th)	4 (6th-5th)	5 (7th-6th)	6 (8th-7th)	7 (9th-8th)	8 (10th-9th)	9 (11th-10th)	10 (12th-11th)	11 (13th-12th)	12 (14th-13th)	Average					%	%
MBB1a	-0.199													1	3	3	0	100	0
MBB 1b					-0.081	-0.166	0.033	-0.071	-0.153	0.106	-0.214	-0.120		2	2	1	1	50	50
MBB 2	-0.086	-0.063	-0.424	0.287	0.043	-0.066	-0.082	-0.025	-0.011	0.204	-0.195	-0.024		3	2	2	0	100	0
MBB 3	-0.522	0.155	-0.346	-0.162	0.056	-0.208	-0.123	-0.128	-0.007	-0.071	-0.240	-0.108		4	2	1	1	50	50
MBB 4					-0.242	-0.248	-0.044	-0.024	-0.167	0.071	-0.269	-0.140		5	6	4	2	67	33
MBB 5					-0.148	-0.123	-0.078	-0.134	-0.145	0.125	-0.244	-0.009		6	6	6	0	100	0
MBB 6a					-0.108	-0.380	-0.184	-0.364						7	6	5	1	83	17
MBB 6b										-0.434	-0.353	-2.526		8	6	6	0	100	0
Average	-0.269	0.046	-0.385	0.063	-0.080	-0.199	-0.080	-0.124	-0.097	0.000	-0.252	-0.488	-0.155	9	5	5	0	100	0
St Deviation	0.226	0.154	0.055	0.317	0.114	0.109	0.073	0.127	0.080	0.231	0.056	1.000	0.212	10	6	2	4	33	67
														11	6	6	0	100	0
														12	6	6	0	100	0
															56	47	9	84	16
Station	1 (2nd-1st)	2 (4th-2nd)	3 (5th-4th)	4 (6th-5th)	5 (7th-6th)	6 (8th-7th)	7 (9th-8th)	8 (10th-9th)	9 (11th-10th)	10 (12th-11th)	11 (13th-12th)	12 (14th-13th)		1	1	1	0	100	0
MPM 1		0.991	0.257	0.327	-0.051	-0.237	0.203	0.081	-0.413	0.693	0.295	0.131		2	2	1	1	50	50
MPM 2a	-0.690	-0.232	0.684	0.304	0.254									3	5	2	3	40	60
MPM 2b							-0.058	0.175	0.200	-0.571	1.230	-1.153		4	6	5	1	83	17
MPM 3a			-0.098	-0.367	-0.508	-0.702								5	6	5	1	83	17
MPM 3b								-0.378	-0.110	-0.847	-0.312	-0.482		6	5	4	1	80	20
MPM 4			0.031	0.153	-0.322	-0.122	-0.040	-0.048	-0.194	-0.077	-0.031	-0.107		7	5	4	1	80	20
MPM 5			-0.079	0.142	-0.187	0.020	0.000	0.062	-0.113	-0.077	-0.013	0.038		8	6	2	4	33	67
MPM 6				0.204	-0.222	-0.294	-0.666	1.257	-0.424	-0.060	0.006			9	6	5	1	83	17
Average	-0.690	0.379	0.159	0.127	-0.173	-0.267	-0.112	0.192	-0.176	-0.156	0.196	-0.315	-0.070	10	6	5	1	83	17
St Deviation		0.864	0.326	0.254	0.259	0.271	0.326	0.556	0.231	0.528	0.542	0.524	0.426	11	6	3	3	50	50
														12	5	3	2	60	40
															59	40	19	68	32
Station	1 (2nd-1st)	2 (4th-2nd)	3 (5th-4th)	4 (6th-5th)	5 (7th-6th)	6 (8th-7th)	7 (9th-8th)	8 (10th-9th)	9 (11th-10th)	10 (12th-11th)	11 (13th-12th)	12 (14th-13th)		1	3	3	0	100	0
MPQ 1	-0.085	0.046	-0.239	-0.404	0.342	-0.317	0.174	-0.121	-0.152	-0.059	-0.025	-0.056		2	3	1	2	33	67
MPQ 2	-0.244	-0.008	-0.264	-0.301	-0.176	-0.143	0.222	-0.121	-0.180	-0.144	-0.224	-0.363		3	3	3	0	100	0
MPQ 3	-0.042	0.015	-0.043	-0.168	0.085	-0.304	0.218	0.011	-0.053	0.000	-0.065	-0.028		4	3	3	0	100	0
MPQ 4					0.493	-0.116	-0.361	0.039	-0.068	-0.089	0.086	-0.055		5	6	1	5	17	83
MPQ 5					0.109	-0.295	0.207	-0.035	0.033	-0.024	-0.051	-0.086		6	6	6	0	100	0
MPQ 6					0.028	-0.309	0.222	-0.013	-0.057	-0.011	-0.079	-0.032		7	6	1	5	17	83
Average	-0.124	0.018	-0.182	-0.291	0.147	-0.247	0.114	-0.040	-0.080	-0.054	-0.060	-0.104	-0.075	8	6	4	2	67	33
St Deviation	0.107	0.027	0.121	0.118	0.237	0.092	0.233	0.067	0.077	0.055	0.100	0.129	0.114	9	6	5	1	83	17
														10	6	5	1	83	17
														11	6	5	1	83	17
														12	6	6	0	100	0
															60	43	17	72	28
Station	1 (2nd-1st)	2 (4th-2nd)	3 (5th-4th)	4 (6th-5th)	5 (7th-6th)	6 (8th-7th)	7 (9th-8th)	8 (10th-9th)	9 (11th-10th)	10 (12th-11th)	11 (13th-12th)	12 (14th-13th)		1	2	1	1	50	50
MMX 1a		-0.081	-0.569	0.601										2	4	3	1	75	25
MMX 1b						0.079	-0.082	0.036	-0.629	-0.024	-0.022	-0.086		3	4	2	2	50	50
MMX 2		0.093	0.316	0.231	-0.386	0.335	-0.309	-0.072	-0.207	-0.040	-0.036	-0.021		4	4	0	4	0	100
MMX 3a	0.782	-0.747	-0.199	0.276										5	3	2	1	67	33
MMX 3b						2.009	-2.074	-0.271						6	6	0	6	0	100
MMX 3c												-0.380		7	6	6	0	100	0
MMX 4	-0.092	-0.037	0.185	0.409	-0.345	0.303	-0.307	-0.122	-0.114	-0.012	-0.064	-0.048		8	6	4	2	67	33
MMX 5b						0.856	-0.001	0.062	-0.107	-0.069	-0.063	-0.055		9	5	5	0	100	0
MMX 6					0.335	0.215	-0.290	-0.043	-0.152	-0.028	-0.004	-0.047		10	5	5	0	100	0
Average	0.345	-0.193	-0.067	0.379	-0.132	0.633	-0.511	-0.068	-0.242	-0.035	-0.038	-0.106	-0.003	11	5	5	0	100	0
St Deviation	0.618	0.377	0.400	0.166	0.405	0.724	0.777	0.121	0.220	0.022	0.026	0.136	0.333	12	5	5	0	100	0
															55	38	17	69	31
Station	1 (2nd-1st)	2 (4th-2nd)	3 (5th-4th)	4 (6th-5th)	5 (7th-6th)	6 (8th-7th)	7 (9th-8th)	8 (10th-9th)	9 (11th-10th)	10 (12th-11th)	11 (13th-12th)	12 (14th-13th)		1	3	3	0	100	0
MRF 1a	-1.902													2	1	1	0	100	0
MRF 1b					0.319	-0.519	0.218	0.013	-0.019	0.042	-0.071	-0.041		3	1	1	0	100	0
MRF 2a	-3.247													4	1	1	0	100	0
MRF 2b					0.425	-0.455	-0.135	0.045	-0.109	-0.024	-0.051	-0.004		5	6	6	0	100	0
MRF 3					0.434	-0.097	-0.092	-0.037	0.021	0.152	-0.020	-0.011		6	6	5	0	83	17
MRF 4					0.305	-0.214	-0.079	-0.004	-0.023	-0.215	-0.203	0.013		7	7	3	4	43	57
MRF 5					0.388	-0.138	0.114	0.067	0.052	0.004	-0.092	-0.064		8	7	3	4	43	57
MRF 6	-0.074	-0.043	-0.190	-0.490	0.168	0.094	0.004	0.124	0.031	-0.053	-0.015	0.022		9	7	3	4	43	57
MRF 7						-0.970	0.072	-0.018	0.002	-0.038	0.031	-0.014		10	7	4	3	57	43
Average	-1.741	-0.043	-0.190	-0.490	0.340	-0.328	0.015	0.027	-0.007	-0.019	-0.060	-0.014	-0.209	11	7	6	1	86	14
St Deviation	1.593				0.100	0.353	0.127	0.056	0.053	0.111	0.075	0.030	0.277	12	7	5	2	71	29
															60	41	18	68	32

.

6.4.2 Inferential analyses of average rates of surface change across measurement periods

In the following sub-sections, five statistical analyses were undertaken in order to evaluate whether there are any temporal patterns examining rates of surface of change at each TMEM stations based on three types of measurement periods: annual, semi-annual and individual time periods (See Table 3.13). These analyses aimed to confirm or reject the following five null hypotheses:

i. There is no statistical difference in the individual rates of surface change between annual periods measured at each station (Section 6.4.2.1);
ii. There is no statistical difference in the individual rates of surface change between semi-annual periods measured at each station (See Section 6.4.2.2);
iii. There is no statistical difference in the individual rates of surface change when comparing the annual rates with the semi-annual periods (See Section 6.4.2.3);
iv. There is no statistical difference in the individual rates of surface change based on individual measurement periods (See Section 6.4.2.4);
v. There is no statistical difference in the individual rates of surface change across all time-periods for each station (See Section 6.4.2.5); and
vi. There is no correlation between seasonal trends (temperature and rainfall) and individual rates of surface change measures on each station (See Section 6.4.2.6).

For the above tests, the first four (i to iv) were carried out by undertaking paired statistical comparisons using the non-parametric Mann-Whitney U (MWU) tests. The fifth test (v) was done using the Kruskal Wallis H (KWH) test. The last test (vi) was carried using by using Spearman Rank Correlation (Table 3.13).

6.4.2.1 Paired comparisons of annual rates

A total of 504 MWU tests were undertaken in order to compare the annual rates of surface change measured at each TMEM station across the nine annual periods previously described in Section 6.4.1.1. TMEM stations which could not provide annual rates due to shorter survey periods were not included in the test. The first result from these tests is that out of 504 tests, 331 results scored a *p* value less than 0.05. This would mean that 66% of the dataset reject the null hypothesis of no difference and accept that there are temporal differences in the rate of surface change between the annual periods. Period F with B was the only paired test which recorded 100% of its results accepting H_1. Other cross-tested pairs with a relative higher percentage composition of H_1 results were period G when tested with A, B and F, period E when tested with periods B, C and D, period H with B and period F with A. Ponta tal-Qammieħ was the only shore platform which more than 50% of its results accepting H_1 in all its stations. The results ranged from 58% for MPQ2 to 90% for MPQ4.

The remaining 34% of the MWU results show periods with similar rates and thus confirm no statistical differences in the rates of surface change (Table 6.19). Table 6.20 shows 30 paired periods with less than 50% of *p* values with H_0 result. This result once again confirms the strong result presented in the Table 6.19, whereby 83% of the tested pairs give evidence of differences between the annual rates. Periods E and F seem to be the only two periods with a relative high number of H_0 results, with 8 out of 16 tested pairs resulting in H_0 acceptance of results of less than 25%. Only five out 36 tested periods resulted with a H_0 result of no difference. The MWU result of period I with H provided the strongest result with no difference in the rate of surface change. Another result of no pattern (50%) saves for the tested comparison between period G and D. Such type of result was also observed previously in Section 6.3.3 in the spatial analysis, whereby the no pattern groups were proportionately less populated with inferential results, when compared to the other four groups.

Table 6.19: Summary of *p* value results from MWU tests, based on paired comparisons between annual rates of surface change and with scores for *p* value results in H_0 and H_1

Summary of *p* value results for Mann-Whitney U test: Comparison between annual periods and with scores for *p* value results in H0 and H1																																	
Annual Periods	**Ponta tal-Munxar TMEM Stations**						**Blata l-Bajda TMEM Stations**					**Ponta tal-Mignuna TMEM Stations**							**Ponta tal-Qammieh TMEM Stations**						**Raf il-Fenek TMEM Stations**							H0	H1	Total
	MMX 1b	MMX 2	MMX 3a	MMX 4	MMX 5b	MMX 6	MBB 1b	MBB 2	MBB 3	MBB 4	MBB 5	MPM 1	MPM 2a	MPM 2b	MPM 3b	MPM 4	MPM 5	MPM 6	MPQ 1	MPQ 2	MPQ 3	MPQ 4	MPQ 5	MPQ 6	MRF 1b	MRF 2b	MRF 3	MRF 4	MRF 5	MRF 6	MRF 7			
Period B with A			0.159	1.000				0.000	0.002				0.019						0.002	0.950	0.000									0.000		3	6	9
Period C with A				0.000				0.000	0.467										0.146	0.011	0.000									0.027		2	5	7
Period C with B		0.065		0.000				0.003	0.004			0.000							0.015	0.024	0.154									0.000		2	7	9
Period D with A				0.851				0.000	0.004										0.000	0.099	0.002									0.082		3	4	7
Period D with B		0.000		0.065				0.000	0.043			0.000							0.000	0.138	0.003									0.000		2	7	9
Period D with C		0.000		0.000				0.000	0.030			0.481				0.425	0.155		0.000	0.000	0.000									0.004		3	8	11
Period E with A				0.000				0.000	0.000			.							0.000	0.000	0.144									0.000		1	6	7
Period E with B		0.000		0.001				0.002	0.067			0.000							0.000	0.002	0.000									0.000		1	8	9
Period E with C		0.000		0.000				0.139	0.002			0.040				0.000	0.916		0.000	0.000	0.000									0.000		2	9	11
Period E with D		0.000		0.000				0.001	0.231			0.004				0.002	0.280	0.000	0.001	0.032	0.000									0.000		2	10	12
Period F with A				0.025				0.000	0.028										0.201	0.001	0.000									0.000		1	6	7
Period F with B		0.000		0.027				0.012	0.013			0.000							0.006	0.003	0.001									0.000		0	9	9
Period F with C		0.000		0.009				0.474	0.177			0.000				0.209	0.005		0.002	0.000	0.000									0.003		3	8	11
Period F with D		0.733		0.000				0.000	0.280			0.000				0.639	0.031	0.000	0.000	0.061	0.734									0.000		5	7	12
Period F with E		0.000		0.000		0.000	0.166	0.042	0.020	0.673	0.534	0.002				0.010	0.004	0.121	0.000	0.615	0.000	0.000	0.000	0.006	0.000	0.000	0.000	0.000	0.000	0.018		5	19	24
Period G with A				0.000				0.000	0.000										0.000	0.001	0.056									0.000		1	6	7
Period G with B		0.000		0.001				0.000	0.069			0.000							0.000	0.005	0.000									0.000		1	8	9
Period G with C		0.000		0.000				0.000	0.001			0.027				0.673	0.391		0.000	0.000	0.000									0.050		3	8	11
Period G with D		0.000		0.000				0.690	0.170			0.000				0.725	0.824	0.000	0.729	0.131	0.000									0.000		6	6	12
Period G with E		0.411		0.173		0.000	0.024	0.000	0.474	0.002	0.000	0.000				0.001	0.467	0.054	0.001	0.428	0.000	0.000	0.000	0.000	0.084	0.000	0.000	0.000	0.124	0.000		8	16	24
Period G with F	0.372	0.000		0.000	0.001	0.000	0.000	0.000	0.026	0.001	0.002	0.000				0.360	0.012	0.005	0.000	0.900	0.000	0.009	0.000	0.000	0.004	0.851	0.000	0.002	0.001	0.016	0.025	4	23	27
Period H with A				0.009				0.000	0.026										0.163	0.201	0.001									0.000		2	5	7
Period H with B		0.000		0.008				0.005	0.017			0.000					.		0.003	0.186	0.030									0.000		1	8	9
Period H with C		0.000		0.000				0.897	0.142			0.008				0.842	0.542		0.003	0.285	0.000									0.005		5	6	11
Period H with D		0.152		0.002				0.002	0.565			0.000				0.411	0.614	0.000	0.001	0.015	0.633									0.000		5	7	12
Period H with E		0.000		0.000		0.000	0.354	0.379	0.087	0.265	0.318	0.000				0.001	0.518	0.000	0.000	0.000	0.000	0.000	0.001	0.023	0.072	0.177	0.000	0.159	0.553	0.000		10	14	24
Period H with F	0.690	0.080		0.411	0.000	0.411	0.842	0.489	0.656	0.392	0.664	0.000				0.265	0.009	0.000	0.603	0.000	0.706	0.000	0.991	0.605	0.000	0.000	0.000	0.004	0.000	0.069	0.000	15	12	27
Period H with G	0.681	0.000		0.000	0.385	0.000	0.001	0.000	0.029	0.010	0.001	0.385		0.000		0.614	0.778	0.000	0.001	0.000	0.000	0.000	0.000	0.000	0.024	0.000	0.000	0.000	0.005	0.205	0.000	6	22	28
Period I with A				0.127				0.000	0.016										0.027	0.385	0.000									0.177		3	4	7
Period I with B		0.000		0.023				0.001	0.020			0.000							0.000	0.414	0.144									0.000		2	6	8
Period I with C		0.000		0.000				0.751	0.100			0.000				0.549	0.209		0.000	0.182	0.002									0.707		6	5	11
Period I with D		0.291		0.093				0.000	0.725			0.000				0.227	0.778		0.001	0.020	0.097									0.005		6	5	11
Period I with E		0.000		0.000		0.000	0.100	0.302	0.201	0.534	0.004	0.000				0.003	0.227		0.000	0.000	0.000	0.000	0.002	0.451	0.953	0.725	0.000	0.177	0.366	0.000		10	13	23
Period I with F	0.100	0.201		0.597	0.000	0.379	0.543	0.342	0.606	0.796	0.030	0.005				0.149	0.089		0.624	0.000	0.048	0.000	0.981	0.734	0.000	0.000	0.000	0.001	0.000	0.001	0.000	14	13	27
Period I with G	0.166	0.000		0.000	0.020	0.000	0.000	0.000	0.100	0.005	0.060	0.000		0.869		0.360	0.342		0.001	0.000	0.000	0.000	0.000	0.000	0.100	0.000	0.000	0.000	0.573	0.040	0.000	8	19	27
Period I with H	0.011	0.725		0.227	0.181	0.944	0.565	1.000	0.725	0.681	0.067	0.000		0.000	0.907	0.489	0.265		0.863	0.910	0.178	0.087	0.991	0.805	0.197	0.360	0.018	0.824	0.016	0.009	0.255	22	6	28
Total	6	28	1	36	6	10	10	36	36	10	10	28	1	3	1	21	21	10	36	36	36	10	10	10	10	10	10	10	10	36	6	173	331	504

Table 6.20: Percentage of *p* values accepting H_0 (no difference) between annual rates of surface change

Annual Periods	Percentage of *p* values accepting H0				
	0-25%	26-49%	50%	51-75%	76-100%
Period B with A					
Period C with A					
Period C with B					
Period D with A					
Period D with B					
Period D with C					
Period E with A					
Period E with B					
Period E with C					
Period E with D					
Period F with A					
Period F with B					
Period F with C					
Period F with D					
Period F with E					
Period G with A					
Period G with B					
Period G with C					
Period G with D					
Period G with E					
Period G with F					
Period H with A					
Period H with B					
Period H with C					
Period H with D					
Period H with E					
Period H with F					
Period H with G					
Period I with A					
Period I with B					
Period I with C					
Period I with D					
Period I with E					
Period I with F					
Period I with G					
Period I with H					

6.4.2.2 Paired comparisons of semi-annual rates

The field survey generated ten semi-annual periods with rates of surface change that were described in Section 6.4.1.2. Temporal differences in the rate of surface change between the ten semi-annual periods were cross-compared at each TMEM station with the MWU tests. These paired tests are listed in Table 6.21 and have generated a dataset of 824 MWU results across the five shore platforms.

These results confirm the same statistical trend previously observed in the MWU results for the annual periods (Section 6.4.2.1), in which more than two-thirds of the dataset confirm differences in the rates of surface change between the paired tested periods. From this result, one can also conclude that the statistical trends observed at annual level are not very different from the ones observed at semi-annual level and that long-term trends do not produce significantly different results from shorter ones. Table 6.21 illustrates how out of 824 MWU tests, 67% (555) of the tests resulted in p values of less than 0.05. This would reject the null hypotheses of no difference between the tested semi-annual periods and confirm that there are differences in the semi-annual rates for a sizeable majority of the cross-compared periods. The remaining 33 % (269) accept the H_0 result (Table 6.21). Ponta tal-Munxar and Ponta tal-Qammieħ were the only two platforms which recorded H_1 in more than 50% of the results in each station. Table 6.22 groups the 824 MWU results into percentage groups of H_0 acceptance. Out of the 45 periods, 40 fall under the category on low H_0 acceptance made up of the 0-25% (19 paired periods) and 26-49% groups (21 paired periods). Once again, this result draws out a very strong message about the extent to which the semi-annual rates behave differently from each other.

Table 6.21: Summary of *p* value results from MWU tests based on paired comparisons between semi-annual annual rates of surface change and with scores for *p* value results in H_0 and H_1

Summary of *p* value results for Mann-Whitney U test: Comparison between semi-annual periods and with scores for *p* value results in H0 and H1																																								
Semi-annual periods	Ponta tal-Munxar TMEM Stations								Blata l-Bajda TMEM Stations							Ponta tal-Mignuna TMEM Stations								Ponta tal-Qammiegh TMEM Stations						Raf il-Fenek TMEM Stations							Total	H0	H1
	MMX1a	MMX 1b	MMX 2	MMX 3a	MMX 3b	MMX 4	MMX 5b	MMX 6	MBB 1b	MBB 2	MBB 3	MBB 4	MBB 5	MBB 6a	MBB 6b	MPM 1	MPM 2a	MPM 2b	MPM 3a	MPM 3b	MPM 4	MPM 5	MPM 6	MPQ 1	MPQ 2	MPQ 3	MPQ 4	MPQ 5	MPQ 6	MRF 1b	MRF 2b	MRF 3	MRF 4	MRF 5	MRF 6	MRF 7			
Period B2 with A2	0.000		0.018	0.000		0.000				0.860	0.000					0.000	0.000						0.000	0.000	0.000									0.000		12	1	11
Period C1 with A2			0.021			0.173				0.000	0.014					0.000	0.000						0.030	0.000	0.037									0.003		10	1	9
Period C1 with B2			0.000			0.000				0.000	0.000					0.016	0.000		0.091		0.000	0.001		0.000	0.030	0.133									0.159		13	3	10
Period C2 with A2			0.091			0.201				0.004	0.005					0.000								0.043	0.001	0.000									0.000		9	2	7
Period C2 with B2			0.000			0.000				0.023	0.000					0.000			0.003		0.000	0.000		0.000	0.000	0.302									0.000		12	1	11
Period C2 with C1			0.000			0.348				0.000	0.664					0.000			0.291		0.001	0.860	0.000	0.885	0.010	0.130									0.000		13	6	7
Period D2 with A2			0.630			0.002				0.173	0.000					0.000								0.034	0.734	0.388									0.093		9	5	4
Period D2 with B2			0.000			0.000				0.452	0.003					0.000					0.000	0.549		0.000	0.000	0.000									0.000		11	2	9
Period D2 with C1			0.000			0.127				0.000	0.000					0.004					0.047	0.010	0.000	0.000	0.000	0.245									0.000		12	2	10
Period D2 with C2			0.000			0.001		0.000	0.209	0.076	0.000	0.121	0.156	0.372		0.000					0.000	0.000	0.000	0.000	0.000	0.001	0.000	0.078	0.000	0.060	0.000	0.000	0.000	0.005	0.003		25	7	18
Period E2 with A2			0.003			0.000				0.005	0.000					0.000								0.008	0.128	0.000									0.002		9	1	8
Period E2 with B2			0.000			0.000				0.064	0.000					0.051					0.000	0.664		0.000	0.000	0.000									0.000		11	3	8
Period E2 with C1			0.000			0.000				0.000	0.006					0.098					0.003	0.001	0.000	0.001	0.000	0.000									0.000		12	1	11
Period E2 with C2			0.000			0.000		0.000	0.002	0.391	0.009	0.000	0.067	0.699		0.000					0.000	0.000	0.000	0.027	0.000	0.000	0.016	0.000	0.000	0.000	0.324	0.000	0.518	0.000	0.000		25	5	20
Period E2 with D2		0.860	0.000		0.001	0.000	0.001	0.000	0.001	0.227	0.010	0.014	0.673	0.656		0.001					0.265	0.265	0.000	0.000	0.011	0.026	0.000	0.000	0.000	0.000	0.000	0.000	0.000	0.000	0.944	0.000	29	7	22
Period F2 with A2			0.020			0.103				0.007	0.004					0.000								0.563	0.005	0.154									0.000		9	3	6
Period F2 with B2			0.000			0.000				0.103	0.000					0.000					0.000	0.004		0.000	0.000	0.000									0.000		11	1	10
Period F2 with C1			0.519			0.008				0.000	0.769					0.000					0.589	0.231	0.000	0.000	0.011	0.000									0.000		12	4	8
Period F2 with C2			0.000			0.024		0.000	0.742	0.192	0.972	0.010	0.573			0.097					0.004	0.005	0.000	0.000	0.466	0.000	0.000	0.000	0.000	0.001	0.095	0.760	0.222	0.000	0.000		24	9	15
Period F2 with D2		0.000	0.000			0.000	0.000	0.000	0.366	0.379	0.000	0.639	0.209			0.049					0.006	0.008	0.000	0.003	0.003	0.086	0.008	0.000	0.000	0.000	0.000	0.000	0.000	0.000	0.213	0.000	27	6	21
Period F2 with E2		0.000	0.001			0.000	0.108	0.000	0.000	0.398	0.005	0.015	0.074			0.000		0.418			0.000	0.001	0.003	0.000	0.000	0.000	0.000	0.000	0.000	0.002	0.121	0.000	0.019	0.000	0.000	0.103	28	6	22
Period G with A2			0.027			0.398				0.000	0.033					0.000								0.001	0.000	0.541									0.606		9	3	6
Period G with B2			0.000			0.000				0.000	0.000					0.014					0.000	0.000		0.000	0.008	0.000									0.000		11	0	11
Period G with C1			0.953			0.496				0.379	0.432					0.017					0.302	0.639	0.000	0.000	0.326	0.050									0.000		12	8	4
Period G with C2			0.000			0.833		0.000	0.015	0.000	0.152	0.000	0.000			0.000					0.000	0.093	0.227	0.000	0.213	0.000	0.000	0.000	0.000	0.001	0.519	0.000	0.860	0.001	0.000		24	7	17
Period G with D2		0.000	0.000			0.008	0.000	0.004	0.008	0.000	0.001	0.013	0.003			0.000					0.542	0.000	0.001	0.070	0.000	0.159	0.000	0.000	0.087	0.000	0.000	0.000	0.000	0.000	0.034	0.000	27	4	23
Period G with E2		0.000	0.000			0.000	0.010	0.000	0.614	0.000	0.001	0.879	0.001			0.330		0.002			0.105	0.000	0.000	0.000	0.000	0.000	0.000	0.000	0.000	0.006	0.778	0.000	0.360	0.000	0.000	0.005	28	6	22
Period G with F2		0.379	0.496			0.051	0.159	0.769	0.005	0.000	0.093	0.025	0.000			0.000		0.000		0.152	0.087	0.108	0.000	0.001	0.152	0.000	0.000	0.000	0.003	0.869	0.084	0.000	0.197	0.024	0.000	0.860	29	14	15
Period H2 with A2			0.197			0.062				0.065	0.000					0.000								0.708	0.006	0.489									0.324		9	6	3
Period H2 with B2			0.000			0.000				0.197	0.000					0.067					0.000	0.000		0.000	0.003	0.000									0.000		11	2	9
Period H2 with C1			0.000			0.439				0.000	0.000					0.000					0.001	0.036	0.002	0.005	0.122	0.050									0.001		12	3	9
Period H2 with C2			0.181			0.057		0.000	0.385	0.348	0.001	0.021	0.045			0.000					0.000	0.000	0.000	0.007	0.950	0.001	0.000	0.000	0.000	0.002	0.438	0.000	0.027	0.087	0.000		24	7	17
Period H2 with D2		0.897	0.017			0.605	0.000	0.086	0.860	0.460	0.496	0.418	0.805			0.000					0.060	0.002	0.000	0.001	0.003	0.833	0.001	0.000	0.019	0.000	0.000	0.000	0.005	0.000	0.001	0.000	27	10	17
Period H2 with E2		0.869	0.000			0.000	0.018	0.000	0.029	0.760	0.124	0.170	0.673			0.000		0.124			0.125	0.000	0.000	0.000	0.000	0.000	0.000	0.000	0.000	0.002	0.445	0.000	0.029	0.000	0.000	0.202	28	9	19
Period H2 with F2		0.000	0.000			0.007	0.446	0.000	0.265	0.925	0.000	0.681	0.087			0.000		0.372		0.149	0.000	0.330	0.000	0.297	0.763	0.639	0.091	0.020	0.360	0.037	0.082	0.000	0.003	0.000	0.000	0.760	29	15	14
Period H2 with G2		0.000	0.000			0.152	0.307	0.000	0.044	0.000	0.000	0.082	0.004			0.000		0.000		0.833	0.018	0.240	0.000	0.000	0.563	0.489	0.010	0.185	0.170	0.055	0.760	0.072	0.096	0.000	0.001	0.573	29	14	15
Period I2 with A2			0.265			0.372				0.039	0.000					0.000								0.488	0.000	0.011									0.418		9	4	5
Period I2 with B2			0.000			0.000				0.173	0.013					0.265					0.000	0.318		0.000	0.333	0.006									0.000		11	4	7
Period I2 with C1			0.000			0.935				0.000	0.000					0.001					0.003	0.002		0.000	0.571	0.664									0.000		11	3	8
Period I2 with C2			0.189			0.418		.0.000	0.039	0.159	0.000	0.630	0.842			0.000					0.000	0.000		0.001	0.030	0.173	0.000	0.014	0.006	0.043	0.170	0.130	0.108	0.425	0.000		23	10	13
Period I2 with D2		0.130	0.027			0.302	0.000	0.285	0.000	0.541	0.573	0.113	0.067			0.000					0.105	0.142		0.050	0.000	0.019	0.000	0.045	0.742	0.000	0.000	0.000	0.000	0.000	0.076	0.000	26	12	14
Period I2 with E2		0.093	0.000			0.000	0.022	0.000	0.000	0.589	0.009	0.000	0.026			0.073		0.511			0.255	0.431		0.000	0.000	0.000	0.000	0.000	0.000	0.000	0.481	0.001	0.103	0.000	0.015	0.981	27	10	17
Period I2 with F2		0.000	0.000			0.034	0.360	0.000	0.017	0.769	0.000	0.021	0.431			0.000		0.222		0.542	0.001	0.039		0.945	0.014	0.000	0.004	0.000	0.002	0.062	0.378	0.133	0.016	0.000	0.000	0.360	28	10	18
Period I2 with G2		0.000	0.000			0.511	0.549	0.002	0.000	0.000	0.000	0.000	0.000			0.519		0.001		0.047	0.024	0.000		0.010	0.119	0.127	0.218	0.656	0.639	0.074	0.445	0.000	0.324	0.001	0.681	0.069	28	13	15
Period I2 with H2		0.082	0.888			0.751	0.787	0.411	0.006	0.796	0.189	0.019	0.014		0.000	0.000		0.073		0.050	0.606	0.002		0.284	0.047	0.027	0.291	0.116	0.118	0.285	0.275	0.001	0.366	0.197	0.037	0.130	29	19	10
Total																																					824	269	555

Table 6.22: Percentage of *p* values accepting H_0 (no difference) between semi-annual rates of surface change

Semi-annual periods	Percentage of *p* values accepting H_0				
	0-25%	26-49%	50%	51-75%	76-100%
Period B2 with A2					
Period C1 with A2					
Period C1 with B2					
Period C2 with A2					
Period C2 with B2					
Period C2 with C1					
Period D2 with A2					
Period D2 with B2					
Period D2 with C1					
Period D2 with C2					
Period E2 with A2					
Period E2 with B2					
Period E2 with C1					
Period E2 with C2					
Period E2 with D2					
Period F2 with A2					
Period F2 with B2					
Period F2 with C1					
Period F2 with C2					
Period F2 with D2					
Period F2 with E2					
Period G2 with A2					
Period G2 with B2					
Period G2 with C1					
Period G2 with C2					
Period G2 with D2					
Period G2 with E2					
Period G2 with F2					
Period H2 with A2					
Period H2 with B2					
Period H2 with C1					
Period H2 with C2					
Period H2 with D2					
Period H2 with E2					
Period H2 with F2					
Period H2 with G2					
Period I2 with A2					
Period I2 with B2					
Period I2 with C1					
Period I2 with C2					
Period I2 with D2					
Period I2 with E2					
Period I2 with F2					
Period I2 with G2					
Period I2 with H2					

Only four cross-compared periods had H_0 results: period H2 with A2, F2 and I2, and period G2 with C1. No tested periods produced results in the 50% (no pattern) groups. Additionally, no paired test produced an H_0 result strong enough to qualify in the 76-100% HO acceptance groups (Table 6.22).

The next sub-section, Section 6.4.2.3, aims to test out whether rates of surface change observed as annual rates are comparable with those over a semi-annual period, by using the same cross-comparison techniques with MWU tests. Such cross-comparisons will determine whether the measured rates of surface change at annual time-scale behave similarly to those at shorter time-scales (6 months) and thus be able to infer that processes of surface change do not impact differently across different time-scales.

6.4.2.3 Paired comparisons of annual rates with semi-annual rates

A total of 1464 MWU tests were carried out in order to test whether there are differences in the rates of surface change when annual rates are compared with semi-annual rates. As seen in Table 6.23, a total of 90 cross-paired comparisons were set up using nine annual periods and ten semi-annual periods. Out of 1464 *p* value results, 65% (i.e. 963 results) had *p* values lower than 0.05 and thus reject the null hypothesis that there are no differences between the annual and semi-annual rates. The remaining 35% (510 results) accept the null hypothesis of no difference with *p* value results ranging from 0.054 to 1.000.

This result confirms that the rates of surface change measured on two different time scales i.e. annual and semi-annual provide different trends in the rates on surface change. This would all the more confirm the importance of the choice criteria when deciding which temporal scale should be selected to measure rates of surface change. It also implies that rates of surface change taken on shorter time-scales at supratidal conditions do not necessarily reflect

Table 6.23: Summary of *p* value results from MWU tests based on paired comparisons between annual and semi-annual annual rates of surface change and with scores for *p* value results in H_0 and H_1

Annual vs Semi-Annual Rates	Ponta tal-Munxar TMEM Stations							Blata l-Bajda TMEM Stations						Ponta tal-Miġnuna TMEM Stations							Ponta tal-Qammieħ TMEM Stations							Ras il-Fenek TMEM Stations							H0	H1	Total
	MMX 1a	MMX 1b	MMX 2	MMX 3a	MMX 4	MMX 5b	MMX 6	MBB 1b	MBB 2	MBB 3	MBB 4	MBB 5	MBB 6a	MPM 1	MPM 2a	MPM 2b	MPM 3b	MPM 4	MPM 5	MPM 6	MPQ 1	MPQ 2	MPQ 3	MPQ 4	MPQ 5	MPQ 6	MRF 1b	MRF 2b	MRF 3	MRF 4	MRF 5	MRF 6	MRF 7			
Period A with A2				0.007	0.005				0.003	0.000					0.000						0.013	0.000	0.320									0.796		2	7	9
Period A with B2				0.000	0.000				0.002	0.000					0.000						0.000	0.000	0.000									0.000		0	9	9
Period A with C1					0.474				0.000	0.000					0.000						0.000	0.044	0.001									0.001		1	7	8
Period A with C2					0.053				0.000	0.000											0.000	0.392	0.000									0.000		2	5	7
Period A with D2					0.250				0.000	0.573											0.325	0.000	0.285									0.006		4	3	7
Period A with E2					0.000				0.000	0.123											0.000	0.000	0.000									0.000		1	6	7
Period A with F2					0.001				0.000	0.001											0.017	0.232	0.406									0.000		2	5	7
Period A with G2					0.121				0.000	0.000											0.506	0.489	0.000									0.296		4	3	7
Period A with H2					0.879				0.000	0.833											0.002	0.554	0.326									0.051		5	2	7
Period A with I2					0.557				0.000	0.218											0.065	0.070	0.000									0.250		5	2	7
Period B with A2	0.000			0.091	0.027				0.823	0.071				0.012	0.000						0.000	0.001	0.001									0.000		3	8	11
Period B with B2	0.000			0.000	0.200				0.972	0.000				0.000	0.460						0.000	0.000	0.003									0.014		3	8	11
Period B with C1					0.050				0.000	0.467				0.000	0.250						0.000	0.043	0.990									0.769		5	4	9
Period B with C2					0.019				0.002	0.133				0.000							0.000	0.546	0.112									0.000		3	5	8
Period B with D2					0.166				0.103	0.003				0.000							0.009	0.001	0.037									0.000		2	6	8
Period B with E2					0.000				0.003	0.021				0.000							0.000	0.000	0.000									0.000		0	8	8
Period B with F2					0.003				0.003	0.121				0.000							0.002	0.339	0.000									0.000		2	6	8
Period B with G2					0.024				0.000	0.467				0.000							0.008	0.320	0.002									0.000		2	6	8
Period B with H2					0.076				0.043	0.004				0.010							0.000	0.950	0.024									0.000		2	6	8
Period B with I2					0.047				0.012	0.002				0.000							0.000	0.056	0.860									0.000		2	6	8
Period C with A2					0.000				0.002	0.000				0.000							0.000	0.000	0.000									0.330		1	7	8
Period C with B2			0.000		0.000				0.118	0.000				0.004				0.000	0.000		0.000	0.005	0.263									0.000		2	9	11
Period C with C1			0.000		0.000				0.000	0.000				0.581				0.156	0.011		0.000	0.687	0.371									0.000		4	7	11
Period C with C2			0.000		0.000				0.113	0.001				0.000				0.000	0.000		0.000	0.004	0.521									0.000		2	9	11
Period C with D2			0.000		0.000				0.372	0.205				0.042				0.385	0.001		0.009	0.000	0.002									0.209		4	7	11
Period C with E2			0.000		0.000				0.348	0.113				0.033				0.009	0.000		0.000	0.000	0.000									0.000		2	9	11
Period C with F2			0.000		0.000				0.851	0.000				0.001				0.018	0.313		0.000	0.004	0.000									0.000		2	9	11
Period C with G2			0.000		0.000				0.000	0.000				0.001				0.842	0.452		0.370	0.606	0.000									0.103		5	6	11
Period C with H2			0.000		0.000				0.907	0.787				0.000				0.002	0.155		0.000	0.068	0.001									0.000		4	7	11
Period C with I2			0.000		0.000				0.760	0.069				0.000				0.012	0.000		0.003	0.555	0.178									0.751		5	6	11
Period D with A2					0.003				0.000	0.001				0.000							0.258	0.014	0.571									0.117		3	5	8
Period D with B2			0.000		0.000				0.000	0.000				0.003				0.000	0.000		0.000	0.000	0.000									0.000		0	11	11
Period D with C1			0.000		0.342				0.001	0.016				0.108				0.354	0.004	0.000	0.001	0.002	0.029									0.001		3	9	12
Period D with C2			0.944		0.013				0.015	0.080				0.000				0.000	0.000	0.534	0.008	0.216	0.000									0.000		4	8	12
Period D with D2			0.000		0.296				0.001	0.002				0.022				0.098	0.003	0.000	0.000	0.006	0.268									0.003		3	9	12
Period D with E2			0.000		0.000				0.001	0.534				0.004				0.001	0.000	0.000	0.000	0.000	0.000									0.000		1	11	12
Period D with F2			0.000		0.000				0.000	0.025				0.000				0.067	0.707	0.035	0.023	0.753	0.000									0.000		3	9	12
Period D with G2			0.000		0.069				0.001	0.005				0.000				0.481	0.116	0.000	0.000	0.054	1.000									0.001		5	7	12
Period D with H2			0.185		0.860				0.005	0.028				0.000				0.000	0.769	0.000	0.563	0.044	0.687									0.245		6	6	12
Period D with I2			0.113		0.673				0.001	0.001				0.000				0.006	0.005		0.061	0.004	0.048									0.037		3	8	11
Period E with A2					0.001				0.003	0.001				0.000							0.023	0.218	0.104									0.000		2	6	8
Period E with B2			0.000		0.000				0.045	0.000				0.001				0.000	0.000		0.000	0.000	0.000									0.000		0	11	11
Period E with C1			0.001		0.000				0.000	0.142				0.001				0.398	0.014	0.059	0.212	0.000	0.000									0.000		4	8	12
Period E with C2			0.000		0.000		0.000	0.197	0.673	0.213	0.201	0.597	0.734	0.000				0.001	0.000	0.000	0.525	0.002	0.000	0.142	0.000	0.000	0.004	0.925	0.004	0.597	0.704	0.001		11	14	25
Period E with D2			0.000		0.000		0.000	0.716	0.096	0.000	0.606	0.265	0.639	0.589				0.000	0.001	0.000	0.000	0.232	0.064	0.000	0.000	0.000	0.000	0.000	0.000	0.000	0.000	0.116		9	16	25
Period E with E2			0.019		0.000		0.000	0.016	0.565	0.051	0.005	0.124	0.769	0.000				0.000	0.000	0.000	0.034	0.000	0.000	0.042	0.000	0.000	0.001	0.296	0.009	0.742	0.000	0.000		6	19	25
Period E with F2			0.015		0.496		0.000	0.185	0.154	0.110	0.177	0.796		0.015				0.573	0.197	0.000	0.000	0.032	0.290	0.000	0.000	0.021	0.019	0.064	0.003	0.042	0.000	0.201		11	13	24
Period E with G2			0.001		0.002		0.000	0.024	0.000	0.016	0.004	0.000		0.000				0.039	0.444	0.000	0.000	0.002	0.000	0.000	0.002	0.005	0.025	0.354	0.000	0.734	0.000	0.000		3	21	24
Period E with H2			0.000		0.000		0.000	0.824	0.589	0.007	0.213	0.089		0.000				0.000	0.152	0.069	0.001	0.017	0.372	0.000	0.236	0.944	0.573	0.285	0.000	0.039	0.907	0.000		12	12	24
Period E with I2			0.000		0.003		0.000	0.001	0.312	0.000	0.265	0.425		0.000				0.001	0.000		0.000	0.000	0.000	0.000	0.012	0.076	0.425	0.149	0.003	0.091	0.047	0.000		7	16	23
Period F with A2					0.260				0.030	0.000				0.000							0.130	0.019	0.686									0.004		3	5	8
Period F with B2			0.000		0.000				0.250	0.000				0.000				0.000	0.213		0.000	0.000	0.000									0.000		2	9	11
Period F with C1			0.000		0.425				0.000	0.002				0.000				0.425	0.093	0.664	0.000	0.000	0.023									0.000		4	8	12
Period F with C2			0.907		0.869		0.000	0.496	0.057	0.004	0.080	0.285		0.024				0.000	0.001	0.000	0.000	0.010	0.000	0.000	0.000	0.000	0.925	0.000	0.000	0.000	0.391	0.000		8	16	24
Period F with D2		0.000	0.000		0.001	0.121	0.002	0.218	0.823	0.013	0.673	0.379		0.074				0.049	0.193	0.000	0.138	0.090	0.148	0.196	0.000	0.003	0.000	0.000	0.000	0.000	0.000	0.614	0.000	12	15	27
Period F with E2		0.000	0.000		0.000	0.015	0.000	0.000	0.162	0.542	0.003	0.265		0.000				0.001	0.291	0.000	0.000	0.000	0.000	0.000	0.000	0.000	0.000	0.000	0.000	0.000	0.000	0.851	0.000	5	22	27
Period F with F2		0.001	0.000		0.021	0.001	0.078	0.935	0.398	0.004	0.280	0.630		0.526				0.146	0.107	0.000	0.085	0.050	0.000	0.022	0.000	0.001	0.000	0.000	0.000	0.000	0.000	0.093	0.000	11	16	27
Period F with G2		0.000	0.000		0.760	0.000	0.245	0.002	0.000	0.001	0.004	0.000		0.000				0.398	0.044	0.000	0.104	0.003	0.706	0.000	0.108	0.318	0.000	0.000	0.000	0.003	0.000	0.000	0.000	7	20	27
Period F with H2		0.000	0.255		0.056	0.000	0.001	0.481	0.664	0.146	0.302	0.162		0.000				0.001	0.010	0.000	0.010	0.036	0.715	0.002	0.142	0.133	0.000	0.000	0.000	0.189	0.000	0.000	0.000	11	16	27
Period F with I2		0.002	0.145		0.372	0.000	0.003	0.003	0.787	0.010	0.089	0.185		0.000				0.005	0.725		0.223	0.000	0.044	0.000	0.489	0.565	0.001	0.000	0.000	0.007	0.573	0.006	0.000	10	16	26
Period G with A2					0.000				0.000	0.002				0.000							0.271	0.017	0.038									0.053		2	6	8
Period G with B2			0.000		0.000				0.000	0.000				0.049				0.000	0.000		0.000	0.000	0.000									0.000		0	11	11
Period G with C1			0.012		0.000				0.000	0.307				0.082				0.218	0.098	0.907	0.001	0.000	0.000									0.000		5	7	12
Period G with C2			0.000		0.000		0.000	0.001	0.005	0.565	0.000	0.000		0.000				0.000	0.001	0.000	0.006	0.016	0.000	0.000	0.000	0.000	0.110	0.000	0.000	0.000	0.118	0.000		3	21	24
Period G with D2	0.000	0.000	0.000		0.000	0.000	0.000	0.001	0.000	0.001	0.005	0.069		0.000				0.152	0.002	0.000	0.000	0.053	0.064	0.474	0.000	0.000	0.000	0.000	0.000	0.001	0.000	0.398	0.000	6	21	27
Period G with E2	0.000	0.009			0.000	0.133	0.000	0.833	0.000	0.030	0.778	0.023		0.725		0.030		0.004	0.000	0.000	0.000	0.000	0.000	0.000	0.000	0.000	0.002	0.000	0.000	0.000	0.000	0.000	0.000	4	24	28
Period G with F2	0.001	0.084			0.133	0.778	0.002	0.000	0.000	0.496	0.007	0.000		0.000		0.009		0.036	0.597	0.000	0.018	0.064	0.005	0.000	0.000	0.015	0.017	0.000	0.000	0.000	0.000	0.000	0.000	6	22	28
Period G with G2	0.000	0.011			0.000	0.024	0.001	0.460	0.000	0.043	0.860	0.018		0.222		0.054		0.698	0.213	0.000	0.000	0.004	0.000	0.000	0.000	0.000	0.015	0.000	0.000	0.001	0.000	0.000	0.000	6	22	28
Period G with H2	0.000	0.000			0.000	0.255	0.000	0.023	0.002	0.004	0.067	0.149		0.000		0.004		0.001	0.879	0.312	0.506	0.039	0.080	0.000	0.000	0.003	0.041	0.000	0.000	0.022	0.438	0.000	0.000	8	20	28
Period G with I2	0.000	0.000			0.001	0.177	0.000	0.000	0.000	0.000	0.000	0.000		0.016		0.056		0.009	0.002		0.075	0.000	0.000	0.000	0.000	0.000	0.460	0.000	0.000	0.000	0.245	0.240	0.000	6	21	27
Period H with A2					0.698				0.020	0.000				0.000							0.154	0.000	0.138									0.030		3	5	8
Period H with B2			0.000		0.000				0.142	0.000				0.087				0.000	0.000		0.000	0.001	0.000									0.000		2	9	11
Period H with C1			0.015		0.121				0.000	0.004				0.018				0.205	0.124	0.000	0.000	0.326	0.155									0.000		5	7	12
Period H with C2			0.116		0.432	.	0.000	0.573	0.218	0.012	0.024	0.189		0.000				0.000	0.001	0.000	0.000	0.105	0.000	0.000	0.000	0.000	0.002	0.280	0.000	0.113	0.002	0.000		8	16	24
Period H with D2	0.000	0.001			0.000	0.000	0.057	0.557	0.398	0.012	0.673	0.614		0.000				0.385	0.001	0.000	0.130	0.000	0.763	0.000	0.000	0.130	0.000	0.000	0.000	0.000	0.000	0.503	0.000	10	17	27
Period H with E2	0.000	0.000			0.000	0.039	0.000	0.001	0.778	0.907	0.027	0.291		0.907		0.033		0.025	0.000	0.201	0.000	0.000	0.000	0.000	0.000	0.000	0.002	0.647	0.000	0.136	0.000	0.002	0.008	7	21	28
Period H with F2	0.000	0.005			0.060	0.769	0.030	0.760	0.879	0.003	0.935	0.467		0.000		0.213	0.307	0.025	0.385	0.000	0.212	0.072	0.000	0.000	0.000	0.002	0.255	0.181	0.000	0.013	0.001	0.000	0.701	14	15	29
Period H with G2	0.000	0.014			0.385	0.117	0.103	0.005	0.000	0.001	0.023	0.000		0.418		0.000	0.734	0.778	0.372	0.000	0.010	0.940	0.940	0.024	0.647	0.953	0.366	0.690	0.000	0.250	0.145	0.000	0.888	16	13	29
Period H with H2	0.000	0.033			0.022	0.725	0.003	0.606	0.916	0.142	0.614	0.231		0.000		0.851	0.656	0.002	0.760	0.000	0.034	0.358	0.326	0.372	0.193	0.201	0.213	0.398	0.001	0.418	0.002	0.000	0.496	19	10	29
Period H with I2	0.000	0.014			0.170	0.511	0.015	0.005	0.805	0.005	0.024	0.078		0.078		0.006	0.096	0.013	0.001		0.370	0.199	0.131	0.647	0.734	0.690	0.016	0.879	0.431	0.953	0.003	0.205	0.008	17	11	28
Period I with A2					0.200				0.009	0.001				0.000							0.354	0.000	0.013									0.467		3	5	8
Period I with B2			0.000		0.000				0.093	0.000				0.000				0.000	0.002		0.000	0.002	0.000									0.000		1	10	11
Period I with C1			0.006		0.656				0.000	0.012				0.000				0.096	0.093		0.000	0.242	0.466									0.000		5	6	11
Period I with C2			0.240		0.716		0.000	0.963	0.177	0.038	0.091	0.005		0.189				0.000	0.001		0.000	0.125	0.001	0.000	0.001	0.000	0.004	0.897	0.000	0.197	0.027	0.000		9	14	23
Period I with D2	0.000	0.000			0.033	0.000	0.084	0.152	0.245	0.009	0.972	0.438		0.000				0.879	0.007		0.050	0.000	0.489	0.000	0.001	0.270	0.000	0.000	0.000	0.000	0.000	0.057	0.000	10	16	26
Period I with E2	0.000	0.000			0.000	0.005	0.000	0.000	0.751	0.805	0.016	0.639		0.000		0.076		0.372	0.000		0.000	0.000	0.000	0.000	0.000	0.000	0.001	0.542	0.000	0.159	0.000	0.000	0.152	8	19	27
Period I with F2	0.030	0.003			0.013	0.307	0.049	0.981	0.851	0.017	0.656	0.024		0.851		0.017	0.336	0.025	0.707		0.246	0.061	0.000	0.000	0.000	0.003	0.046	0.089	0.000	0.015	0.000	0.000	0.526	11	17	28
Period I with G2	0.000	0.007			0.716	0.851	0.145	0.002	0.000	0.003	0.012	0.001		0.000		0.044	0.589	0.542	0.053		0.000	1.000	0.066	0.366	0.557	0.869	0.093	0.557	0.001	0.296	0.001	0.597	0.222	16	12	28
Period i with H2	0.000	0.057			0.189	0.318	0.008	0.372	0.953	0.056	0.405	0.769		0.000		0.004	0.526	0.139	0.405		0.034	0.372	0.163	0.041	0.302	0.170	0.664	0.557	0.170	0.270	0.342	0.101	0.597	22	6	28
Period I with I2	0.000	0.033			0.481	0.647	0.017	0.022	0.698	0.005	0.098	0.001		0.000		0.054	0.087	0.149	0.014		0.525	0.227	0.450	0.439	0.639	0.716	0.444	0.282	0.028	0.664	0.054	0.760	0.255	19	9	28
Total	2	24	63	4	90	24	35	35	90	90	35	35	3	80	6	15	8	63	63	35	90	90	90	35	35	35	35	35	35	35	35	90	24	501	963	1464

Table 6.24: Percentage of *p* values accepting H_0 (no difference) between annual and semi-annual rates of surface change

Annual with Semi-Annual periods	Percentage of p values accepting H0				
	0-25%	26-49%	50%	51-75%	76-100%
Period A with A2					
Period A with B2					
Period A with C1					
Period A with C2					
Period A with D2					
Period A with E2					
Period A with F2					
Period A with G2					
Period A with H2					
Period A with I2					
Period B with A2					
Period B with B2					
Period B with C1					
Period B with C2					
Period B with D2					
Period B with E2					
Period B with F2					
Period B with G2					
Period B with H2					
Period B with I2					
Period C with A2					
Period C with B2					
Period C with C1					
Period C with C2					
Period C with D2					
Period C with E2					
Period C with F2					
Period C with G2					
Period C with H2					
Period C with I2					
Period D with A2					
Period D with B2					
Period D with C1					
Period D with C2					
Period D with D2					
Period D with E2					
Period D with F2					
Period D with G2					
Period D with H2					
Period D with I2					
Period E with A2					
Period E with B2					
Period E with C1					
Period E with C2					
Period E with D2					
Period E with E2					
Period E with F2					
Period E with G2					
Period E with H2					
Period E with I2					
Period F with A2					
Period F with B2					
Period F with C1					
Period F with C2					
Period F with D2					
Period F with E2					
Period F with F2					
Period F with G2					
Period F with H2					
Period F with I2					
Period G with A2					
Period G with B2					
Period G with C1					
Period G with C2					
Period G with D2					
Period G with E2					
Period G with F2					
Period G with G2					
Period G with H2					
Period G with I2					
Period H with A2					
Period H with B2					
Period H with C1					
Period H with C2					
Period H with D2					
Period H with E2					
Period H with F2					
Period H with G2					
Period H with H2					
Period H with I2					
Period I with A2					
Period I with B2					
Period I with C1					
Period I with C2					
Period I with D2					
Period I with E2					
Period I with F2					
Period I with G2					
Period i with H2					
Period I with I2					

those for longer time-scales and thus one should be cautious in extrapolating these results collected for shorter time-scales. Table 6.24 shows the grouping of all the *p* values in percentage composition of H_0 acceptance. Out of 90 cross-compared periods, 89% have percentage composition of H_0 values of between 0-25% (41%) or 26-49% (48%).

No paired test scored full percentage of *p* values accepting the null hypothesis. The highest percentage reached was period I with H2 with a percentage composition of 79% having *p* value with H_0 results (Table 6.23). The tested periods with resulted in H_0 results were mainly eight: annual period A with semi-annual periods G2, H2, I2, annual period I with G2, H2 and I2, annual period A with D2 and annual period B with D2 (Table 6.24). The presence of these eight tested periods out of 90 does not make it sufficiently strong to conclude that there is an overall agreement between the different temporal rates.

6.4.2.4 Paired comparisons of rates between individual time periods

For this test, 66 cross-temporal comparisons between the 12 individual periods were statistically examined using the MWU tests. A total of 1151 MWU tests were undertaken across the five shore platforms and the *p* value results of these tests are displayed in Table 6.25. From these *p* values results, it emerges that 74% of the results (855) accept the H_1 hypothesis in showing temporal differences between the individual periods in the rate of rock surface change. The remaining 26% of *p* value results (296 in total) accepted the H_0 hypothesis of no difference between the temporal periods (Table 6.25).

Table 6.26 shows the grouping of all the *p* values in percentage composition of H_0 acceptance for the individual periods. Similarly to the previous analyses for other temporal periods, the majority of the *p* values fall under the 0-25% groups (34 out of 66 cross-paired periods) or the 26-49% groups (27 out of 66). Only five resulted in 'no pattern' group of 50%.

Table 6.25 Summary of *p* value results from MWU tests based on paired comparisons between individual rates of surface change and with scores for *p* value results in H_0 and H_1

Single vs Single Periods	Ponta tal-Munxar TMEM Stations								Blata l-Bajda TMEM Stations							Ponta tal-Miġnuna TMEM Stations								Ponta tal-Qammieħ TMEM Stations						Raf il-Fenek TMEM Stations							Total	H0	H1
	MMX1a	MMX 1b	MMX 2	MMX 3a	MMX 3b	MMX 4	MMX 5b	MMX 6	MBB 1b	MBB 2	MBB 3	MBB 4	MBB 5	MBB 6a	MBB 6b	MPM 1	MPM 2a	MPM 2b	MPM 3a	MPM 3b	MPM 4	MPM 5	MPM 6	MPQ 1	MPQ 2	MPQ 3	MPQ 4	MPQ 5	MPQ 6	MRF 1b	MRF 2b	MRF 3	MRF 4	MRF 5	MRF 6	MRF 7			
RATES5_4_2_1				0.006		0.260				0.000	0.098						0.001							0.000	0.418	0.557									0.000		9	4	5
RATES6_5_2_1				0.000		0.003				0.000	0.006						0.009							0.001	0.100	0.003									0.000		9	1	8
RATES6_5_4_2	0.000		0.050	0.000		0.000				0.000	0.001					0.000	0.000							0.000	0.001	0.002									0.000		12	1	11
RATES7_6_2_1						0.026				0.000	0.000						0.009							0.000	0.007	0.173									0.000		8	1	7
RATES7_6_4_2			0.000			0.021				0.000	0.231					0.000	0.000							0.000	0.053	0.121									0.000		10	3	7
RATES7_6_5_4			0.000			0.000				0.000	0.000					0.001	0.001		0.025		0.000	0.007		0.000	0.001	0.121									0.000		13	1	12
RATES8_7_2_1						0.022				0.496	0.006													0.001	0.405	0.015									0.000		7	2	5
RATES8_7_4_2			0.005			0.006				0.630	0.000					0.000								0.000	0.003	0.105									0.003		9	2	7
RATES8_7_5_4			0.833			0.017				0.000	0.021					0.000			0.000		0.001	0.004		0.093	0.065	0.105									0.000		12	4	8
RATES8_7_6_5			0.000			0.002				0.000	0.673					0.000			0.004		0.000	0.796	0.000	0.418	0.003	0.166									0.000		13	4	9
RATES9_8_2_1						0.031				0.004	0.001													0.000	0.000	0.000									0.000		7	0	7
RATES9_8_4_2			0.000			0.026				0.004	0.001					0.000								0.000	0.003	0.000									0.698		9	1	8
RATES9_8_5_4			0.000			0.000				0.000	0.000					0.418					0.014	0.065		0.000	0.000	0.000									0.000		11	2	9
RATES9_8_6_5			0.000			0.000				0.000	0.004					0.173					0.000	0.000	0.000	0.000	0.000	0.000									0.000		12	1	11
RATES9_8_7_6			0.000			0.796		0.000	0.023	0.040	0.000	0.003	0.008	0.043		0.001					0.000	0.000	0.001	0.003	0.000	0.000	0.000	0.000	0.000	0.105	0.000	0.000	0.000	0.020	0.000		25	2	23
RATES10_9_2_1						0.324				0.100	0.001													0.002	0.001	0.000									0.000		7	2	5
RATES10_9_4_2			0.074			0.925				0.170	0.001					0.000								0.003	0.769	0.000									0.000		9	4	5
RATES10_9_5_4			0.000			0.000				0.000	0.000					0.004					0.009	0.000		0.000	0.001	0.000									0.000		11	0	11
RATES10_9_6_5			0.000			0.000				0.000	0.006					0.004					0.000	0.033	0.000	0.001	0.007	0.000									0.000		12	0	12
RATES10_9_7_6			0.000			0.000		0.000	0.280	0.000	0.000	0.053	0.438	0.000		0.127					0.000	0.000	0.000	0.001	0.009	0.916	0.000	0.549	0.064	0.000	0.000	0.000	0.000	0.000	0.760		25	8	17
RATES10_9_8_7		0.000	0.000		0.000	0.000	0.004	0.000	0.002	0.098	0.008	0.029	1.000	0.070		0.002					0.222	0.205	0.000	0.000	0.004	0.039	0.000	0.000	0.000	0.000	0.000	0.000	0.000	0.037	0.796	0.000	29	6	23
RATES11_10_2_1						0.411				0.001	0.001													0.049	0.398	0.360									0.000		7	3	4
RATES11_10_4_2			0.005			0.814				0.000	0.035					0.000								0.014	0.006	0.916									0.031		9	2	7
RATES11_10_5_4			0.000			0.000				0.000	0.000					0.000					0.000	0.851		0.044	0.181	0.916									0.000		11	3	8
RATES11_10_6_5			0.000			0.000				0.000	0.000					0.000					0.000	0.000	0.000	0.001	0.037	0.000									0.000		12	0	12
RATES11_10_7_6			0.000			0.000		0.000	0.113	0.003	0.010	0.549	0.860			0.017					0.000	0.037	0.034	0.000	0.069	0.037	0.000	0.000	0.002	0.000	0.000	0.000	0.000	0.000	0.000		24	4	20
RATES11_10_8_7		0.000	0.000			0.000	0.000	0.000	0.034	0.000	0.000	0.398	0.589			0.557					0.981	0.007	0.690	0.001	0.907	0.074	0.002	0.000	0.000	0.000	0.000	0.000	0.000	0.065	0.009	0.000	27	8	19
RATES11_10_9_8		0.000	0.000			0.000	0.005	0.000	0.000	0.121	0.000	0.003	0.006			0.000		0.146			0.006	0.041	0.057	0.000	0.000	0.000	0.000	0.000	0.000	0.002	0.003	0.000	0.004	0.000	0.000	0.049	28	3	25
RATES12_11_2_1						0.725				0.000	0.006													0.260	0.166	0.136									0.017		7	4	3
RATES12_11_4_2			0.118			0.145				0.000	0.010					0.011								0.155	0.009	0.742									0.076		9	5	4
RATES12_11_5_4			0.000			0.000				0.000	0.000					0.001					0.000	0.972		0.004	0.078	0.000									0.000		11	2	9
RATES12_11_6_5			0.000			0.000				0.707	0.017					0.007					0.000	0.000	0.000	0.006	0.016	0.086									0.000		12	2	10
RATES12_11_7_6			0.000			0.000		0.000	0.002	0.000	0.009	0.000	0.000			0.000					0.000	0.001	0.000	0.000	0.275	0.039	0.000	0.000	0.003	0.000	0.000	0.000	0.000	0.000	0.000		24	1	23
RATES12_11_8_7		0.716	0.000			0.000	0.001	0.000	0.000	0.000	0.003	0.000	0.000			0.000					0.981	0.001	0.000	0.004	0.707	0.000	0.000	0.000	0.000	0.000	0.000	0.000	0.002	0.270	0.000	0.000	27	4	23
RATES12_11_9_8		0.716	0.000			0.000	0.008	0.000	0.006	0.000	0.034	0.006	0.000			0.000		0.014			0.006	0.000	0.000	0.000	0.000	0.000	0.000	0.000	0.000	0.006	0.000	0.000	0.004	0.000	0.028	0.000	28	1	27
RATES12_11_10_9		0.255	0.205			0.003	0.071	0.015	0.000	0.000	0.037	0.000	0.000			0.000		0.000		0.051	0.152	0.000	0.000	0.000	0.008	0.000	0.000	0.000	0.000	0.411	0.002	0.000	0.474	0.019	0.000	0.707	29	8	21
RATES13_12_2_1						0.614				0.001	0.006													0.015	0.087	0.156									0.000		7	3	4
RATES13_12_4_2			0.372			0.425				0.000	0.001					0.000								0.038	0.159	0.152									0.502		9	5	4
RATES13_12_5_4			0.000			0.002				0.001	0.051					0.751					0.005	0.098		0.000	0.031	0.152									0.000		11	4	7
RATES13_12_6_5			0.000			0.000				0.000	0.879					0.432					0.000	0.000	0.000	0.000	0.023	0.000									0.000		12	2	10
RATES13_12_7_6			0.000			0.000		0.000	0.001	0.000	0.000	0.108	0.056			0.000					0.000	0.000	0.000	0.000	0.935	0.324	0.000	0.057	0.518	0.000	0.000	0.000	0.000	0.000	0.000		24	7	17
RATES13_12_8_7		0.664	0.000			0.000	0.001	0.000	0.291	0.000	0.925	0.432	0.005			0.000					0.001	0.002	0.000	0.000	0.348	0.074	0.000	0.000	0.000	0.000	0.000	0.000	0.177	0.733	0.000	0.000	27	8	19
RATES13_12_9_8		0.372	0.000			0.000	0.029	0.000	0.000	0.000	0.022	0.000	0.000			0.372		0.000			0.769	0.016	0.000	0.012	0.000	0.001	0.000	0.000	0.000	0.001	0.000	0.000	0.078	0.000	0.005	0.127	28	5	23
RATES13_12_10_9		0.250	0.127			0.043	0.074	0.022	0.000	0.000	0.053	0.000	0.001			0.000		0.000		0.372	0.222	0.000	0.000	0.690	0.213	0.385	0.879	0.166	0.452	0.000	0.000	0.188	0.001	0.000	0.000	0.087	29	14	15
RATES13_12_11_10		0.000	0.000			0.110	0.526	0.000	0.013	0.000	0.001	0.037	0.009			0.000		0.000		0.707	0.006	0.354	0.000	0.000	0.460	0.291	0.001	0.166	0.041	0.004	0.250	0.000	0.003	0.000	0.000	0.814	29	9	20
RATES14_13_2_1						0.597				0.003	0.001													0.064	0.234	0.011									0.003		7	3	4
RATES14_13_4_2			0.260			0.439				0.002	0.005					0.000								0.025	0.001	0.004									0.681		9	3	6
RATES14_13_5_4			0.000			0.002				0.000	0.000					0.027					0.156	0.011		0.004	0.760	0.004									0.000		11	2	9
RATES14_13_6_5			0.000			0.000				0.000	0.001					0.049					0.001	0.029		0.000	0.360	0.000									0.000		11	1	10
RATES14_13_7_6			0.000			0.000		0.000	0.189	0.001	0.000	0.336	0.001			0.023					0.000	0.000		0.000	0.001	0.086	0.000	0.000	0.000	0.000	0.000	0.000	0.000	0.000	0.003		23	3	20
RATES14_13_8_7		0.033	0.000			0.000	0.001	0.000	0.012	0.003	0.000	0.181	0.026			0.000					0.133	0.133		0.000	0.033	0.105	0.105	0.000	0.000	0.000	0.000	0.000	0.000	0.833	0.018	0.000	26	6	20
RATES14_13_9_8		0.108	0.000			0.000	0.010	0.000	0.000	0.048	0.116	0.057	0.053			0.133		0.001			0.981	0.149		0.000	0.000	0.000	0.000	0.000	0.000	0.001	0.005	0.001	0.005	0.000	0.360	0.149	27	9	18
RATES14_13_10_9		0.018	0.076			0.146	0.091	0.296	0.944	0.259	0.065	0.751	0.001			0.049		0.000		0.656	0.606	0.606		0.001	0.002	0.000	0.000	0.000	0.000	0.280	0.116	0.015	0.108	0.013	0.003	0.348	28	15	13
RATES14_13_11_10		0.000	0.000			0.245	0.526	0.002	0.972	0.048	0.019	0.302	0.000			0.000		0.000		0.133	0.089	0.018		0.647	0.091	0.000	0.002	0.002	0.041	0.639	0.139	0.589	0.082	0.023	0.438	0.673	28	14	14
RATES14_13_12_11		0.028	0.301			0.291	0.690	0.805	0.000	0.000	0.404	0.000	0.000		0.000	0.000		0.026		0.185	0.089	0.005		0.255	0.042	0.000	0.000	0.000	0.006	0.265	0.240	0.001	0.009	0.201	0.038	0.035	29	11	18
RATES4_2_1				0.000		0.796				0.372	0.000						0.222							0.707	0.001	0.557									0.001		9	5	4
RATES5_4_2	0.000		0.013	0.064		0.041				0.000	0.000					0.000	0.000							0.000	0.000	1.000									0.000		12	2	10
RATES6_5_4	0.000		0.010	0.000		0.000				0.000	0.065					0.565	0.001		0.606		0.000	0.000		0.019	0.152	0.002									0.000		15	4	11
RATES7_6_5			0.000			0.000				0.000	0.000					0.003	0.597		0.270		0.000	0.000	0.000	0.000	0.003	0.173									0.000		14	3	11
RATES8_7_6			0.000			0.000		0.012	0.003	0.000	0.000	0.597	0.425	0.003		0.039			0.181		0.000	0.001	0.127	0.000	0.033	0.907	0.000	0.000	0.000	0.000	0.000	0.000	0.000	0.000	0.690		26	6	20
RATES9_8_7		0.534	0.000		0.000	0.000	0.002	0.000	0.000	0.003	0.003	0.004	0.218	0.031		0.000					0.010	0.012	0.012	0.000	0.000	0.024	0.000	0.000	0.000	0.000	0.000	0.000	0.391	0.000	0.000	0.000	29	3	26
RATES10_9_8		0.189	0.000		0.001	0.000	0.511	0.000	0.000	0.022	0.681	0.030	0.013	0.011		0.051		0.142			0.541	0.000	0.000	0.027	0.003	0.000	0.000	0.000	0.000	0.000	0.000	0.001	0.003	0.000	0.000	0.039	30	6	24
RATES11_10_9		0.000	0.000			0.833	0.036	0.015	0.963	0.006	0.000	0.240	0.411			0.002		0.963		0.241	0.152	0.000	0.000	0.000	0.007	0.000	0.000	0.005	0.000	0.000	0.001	0.000	0.581	0.597	0.000	0.275	29	10	19
RATES12_11_10		0.000	0.000			0.007	0.270	0.000	0.000	0.000	0.467	0.000	0.000			0.000		0.000		0.006	1.000	0.070	0.000	0.270	0.511	0.896	0.010	0.269	0.796	0.000	0.605	0.000	1.000	0.019	0.000	0.000	29	11	18
RATES13_12_11		0.814	0.307			0.716	0.814	0.035	0.000	0.000	0.039	0.000	0.000		0.302	0.000		0.000		0.012	0.006	0.003	0.716	0.000	0.526	0.681	0.006	0.080	0.121	0.000	0.013	0.000	0.028	0.000	0.000	0.000	30	10	20
RATES14_13_12		0.057	0.503			0.453	0.991	0.018	0.002	0.000	0.005	0.009	0.000		0.000	0.000		0.000		0.254	0.760	0.100		0.004	0.039	0.001	0.001	0.001	0.010	1.000	0.080	0.052	0.001	0.733	0.488	0.925	29	13	16
Total	3	21	55	6	3	66	21	28	28	66	66	28	28	6	3	55	10	15	6	10	45	45	28	66	66	66	28	28	28	28	28	28	28	28	66	21	1151	296	855

Table 6.26: Percentage of *p* values accepting H_0 (no difference) between individual rates of surface change

Single vs Single Periods	**Percentage of *p* values accepting H0**				
	0-25%	26-49%	50%	51-75%	76-100%
RATES5_4_2_1					
RATES6_5_2_1					
RATES6_5_4_2					
RATES7_6_2_1					
RATES7_6_4_2					
RATES7_6_5_4					
RATES8_7_2_1					
RATES8_7_4_2					
RATES8_7_5_4					
RATES8_7_6_5					
RATES9_8_2_1					
RATES9_8_4_2					
RATES9_8_5_4					
RATES9_8_6_5					
RATES9_8_7_6					
RATES10_9_2_1					
RATES10_9_4_2					
RATES10_9_5_4					
RATES10_9_6_5					
RATES10_9_7_6					
RATES10_9_8_7					
RATES11_10_2_1					
RATES11_10_4_2					
RATES11_10_5_4					
RATES11_10_6_5					
RATES11_10_7_6					
RATES11_10_8_7					
RATES11_10_9_8					
RATES12_11_2_1					
RATES12_11_4_2					
RATES12_11_5_4					
RATES12_11_6_5					
RATES12_11_7_6					
RATES12_11_8_7					
RATES12_11_9_8					
RATES12_11_10_9					
RATES13_12_2_1					
RATES13_12_4_2					
RATES13_12_5_4					
RATES13_12_6_5					
RATES13_12_7_6					
RATES13_12_8_7					
RATES13_12_9_8					
RATES13_12_10_9					
RATES13_12_11_10					
RATES14_13_2_1					
RATES14_13_4_2					
RATES14_13_5_4					
RATES14_13_6_5					
RATES14_13_7_6					
RATES14_13_8_7					
RATES14_13_9_8					
RATES14_13_10_9					
RATES14_13_11_10					
RATES14_13_12_11					
RATES4_2_1					
RATES5_4_2					
RATES6_5_4					
RATES7_6_5					
RATES8_7_6					
RATES9_8_7					
RATES10_9_8					
RATES11_10_9					
RATES12_11_10					
RATES13_12_11					
RATES14_13_12					

Period 9-8th and 12-11th were the periods with highest results of differences in at least five (sequential) cross-comparisons. On an individual level, the periods with 100% of their p value results resulting in H_1 were the following four: period 9-8th with 2-1st, period 10-9th with 5-4th and 6-5th and period 11-10th with 6-5th (Table 6.26). No individual tested period had 100% of its *p* value accepting H_0. With a total of 92% of the tested periods accepting the H_1 hypothesis of differences between periods, one can conclude that the rates of surface change across individual temporal periods are variable and follow no temporal, cyclical or seasonal trend. The results, presented in Table 6.27, display how the relationship between time periods is the same for all bar individual time periods, which are slightly more distinct from each other in terms of proportion of statistically significant different rates of surface change.

Table 6.27: Percentage distribution of results with H_0 acceptance levels (also expressed in percentage) H_1 for the four cross-paired analysis of the temporal periods

Temporal cross-comparisons	Percentage of *p* values for each H_0 acceptance groups				
	0-25%	26-49%	50%	51-75%	76-100%
Annual vs Annual	44	39	3	11	3
Semi-annual vs Semi-annual	42	46	0	11	0
Annual vs Semi-annual	41	48	2	9	0
Individual vs Individual	52	40	0	8	0

The main conclusions that can be inferred from the results displayed in Table 6.28 are as follows:

i. Individual measurement periods show more statistically significant differences between rates of surface change between sites than do longer time periods. This may reflect the greater variability of rates of surface change as measured over shorter time periods. Over longer time periods this variability seems to be reduced;

ii. Comparison of annual rates of surface change exhibit a wider spread of statistically significant and statistically not-significant differences;
iii. As the time period of analysis increases, the number of relationships with statistically significant differences in rates of surface change declines suggesting that in longer time period there is a tendency for rates of surface change to converge; and
iv. The convergence of rates of surface change seems to be consistent between semi-annual and annual time periods suggesting that these time periods may be comparable in their temporal patterns in the rates of surface change.

Table 6.28**:** Percentage composition of MWU results accepting H_0 or H_1 for the four cross-paired analysis of the temporal periods.

Temporal cross-comparisons	H_0	H_1
	%	
Annual vs Annual	33	66
Semi-annual vs Semi-Annual	33	67
Annual vs Semi-Annual	34	65
Individual vs Individual	26	74

6.4.2.5 Comparisons of rates across all individual time periods

A total of 36 TMEM stations were analysed by using KWH tests in order to compare rates of surface change across all individual time periods and thus identify any key time periods which may have be statistically similar. As seen in Table 6.29, all the KWH results had *p* values lower than 0.05. These results confirm that there are significant differences across individual temporal periods at each station and thus the null hypothesis of no difference can be rejected. This result confirms the results obtained in the previous sections with the MWU test (Section 6.4.2.4) and which recorded high percentage of H_0 rejections across the individual temporal periods.

Table 6.29: KWH results for comparisons of rates of surface change across the respective individual period for each TMEM station

Ponta tal-Munxar			Blata l-Bajda			Ponta tal-Miġnuna			Ponta tal-Qammieħ			Ras il-Fenek		
TMEM stations	Time-periods	KWH	TMEM stations	Time-periods	KWH	TMEM stations	Time-periods	KWH	TMEM stations	Time-periods	KWH	TMEM stations	Time-periods	KWH
		p value			*p* value			*p* value			*p* value			*p* value
MMX1a	4_2	0.000	MBB 1b	7_6	0.000	MPM 1	5_4	0.000	MPQ 1	2_1	0.000	MRF 1b	9_8	0.000
	5_4			8_7			6_5			4_2			10_9	
	6_5			9_8			7_6			5_4			11_10	
MMX 1b	8_7	0.000		10_9			8_7			6_5			12_11	
	9_8			11_10			9_8			7_6			13_12	
	10_9			12_11			10_9			8_7			14_13	
	11_10			13_12			11_10			9_8		MRF 2b	7_6	0.000
	12_11			14_13			12_11			10_9			8_7	
	13_12		MBB 2	2_1	0.000		13_12			11_10			9_8	
	14_13			4_2			14_13			12_11			10_9	
MMX 2	4_2	0.000		5_4		MPM 2a	2_1	0.000		13_12			11_10	
	5_4			6_5			4_2			14_13			12_11	
	6_5			7_6			5_4		MPQ 2	2_1	0.000		13_12	
	7_6			8_7			6_5			4_2			14_13	
	8_7			9_8			7_6			5_4		MRF 3	7_6	0.000
	9_8			10_9		MPM 2b	9_8	0.000		6_5			8_7	
	10_9			11_10			10_9			7_6			9_8	
	11_10			12_11			11_10			8_7			10_9	
	12_11			13_12			12_11			9_8			11_10	
	13_12			14_13			13_12			10_9			12_11	
	14_13		MBB 3	2_1	0.000		14_13			11_10			13_12	
MMX 3a	2_1	0.000		4_2		MPM 3a	5_4	0.001		12_11			14_13	
	4_2			5_4			6_5			13_12		MRF 4	7_6	0.000
	5_4			6_5			7_6			14_13			8_7	
	6_5			7_6			8_7		MPQ 3	2_1	0.000		9_8	
MMX 3b	9_8	0.000		8_7		MPM 3b	10_9	0.036		4_2			10_9	
	8_7			9_8			11_10			5_4			11_10	
	10_9			10_9			12_11			6_5			12_11	
MMX 4	14_13	0.000		11_10			13_12			7_6			13_12	
	13_12			12_11			14_13			8_7			14_13	
	12_11			13_12		MPM 4	5_4	0.000		9_8		MRF 5	7_6	0.000
	11_10			14_13			6_5			10_9			8_7	
	10_9		MBB 4	7_6	0.000		7_6			11_10			9_8	
	9_8			8_7			8_7			12_11			10_9	
	8_7			9_8			9_8			13_12			11_10	
	7_6			10_9			10_9			14_13			12_11	
	6_5			11_10			11_10		MPQ 4	7_6	0.000		13_12	
	5_4			12_11			12_11			8_7			14_13	
	4_2			13_12			13_12			9_8		MRF 6	2_1	0.000
	2_1			14_13			14_13			10_9			4_2	
MMX 5b	8_7	0.000	MBB 5	7_6	0.000	MPM 5	5_4	0.000		11_10			5_4	
	9_8			8_7			6_5			12_11			6_5	
	10_9			9_8			7_6			13_12			7_6	
	11_10			10_9			8_7			14_13			8_7	
	12_11			11_10			9_8		MPQ 5	7_6	0.000		9_8	
	13_12			12_11			10_9			8_7			10_9	
	14_13			13_12			11_10			9_8			11_10	
MMX 6	7_6	0.000		14_13			12_11			10_9			12_11	
	8_7		MBB 6a	7_6	0.000		13_12			11_10			13_12	
	9_8			8_7			14_13			12_11			14_13	
	10_9			9_8		MPM 6	6_5	0.000		13_12		MRF 7	8_7	0.000
	11_10			10_9			7_6			14_13			9_8	
	12_11		MBB 6b	12_11	0.000		8_7		MPQ 6	7_6	0.000		10_9	
	13_12			13_12			9_8			8_7			11_10	
	14_13			14_13			10_9			9_8			12_11	
							11_10			10_9			13_12	
							12_11			11_10			14_13	
							13_12			12_11				
										13_12				
										14_13				

The implication of this result is that the platform responses to processes of surface change are not consistent on a temporal level and that short-term time frames do not produce predictable or comparable rates of surface change from one time period to another. Superimposed on this outcome, there is also no spatial pattern: no temporal pattern of comparability was found irrespective of the relative position in which the stations are located on the platform. Hence, the rates of surface change are variable both spatially and temporarily. The number of measured time periods also did not affect the result. As shown in Table 6.29, whether a station was tested with three time periods, such as MBB6b, or with the full set of twelve stations, as in the case of most stations, the results of differences were produced in all the tested datasets.

The understanding from all this is that the supratidal surfaces at the sites measured of the selected platform operates almost independently and their responses to processes of surface change are both site-specific and time-specific. A further test between seasonal trends and individual rates of surface change was done in order to examine whether individual rates of surface change reflect any seasonal parameters (Section 6.4.2.6). Finally, in order to corroborate the site-specific element, cross-comparisons between platforms were done in Section 6.5. The aim of these last tests was to test whether comparability of surface change behaviour exists between stations with the same relative position.

6.4.2.6 Correlation between seasonal trends (temperature and rainfall) with individual rates of surface change

In Chapter 5 (Section 5.2), a description of the weather data collected for this study confirmed the dual seasonal trends present during the study period and a marked drier period in the last eight months of the study i.e. in 2016. Correlation tests were carried out in order to analyse whether these trends impacted on the rates of the individual time periods at each TMEM station. Given that the dual seasonality of the Maltese Islands is largely represented by temperature and rainfall trends and that the 2016 registered an anomaly in

Table 6.30: Spearman rank correlation coefficient results for monthly mean temperature and rainfall records with rates of surface change measured by TMEM stations

TMEM Stations	Temperature	Rainfall	N
MBB2	-0.10	-0.23	12
MBB3	-0.07	-0.45	12
MBB1b	0.04	0.34	8
MBB4	-0.08	0.19	8
MBB5	0.18	0.09	8
MPM1	-0.38	0.26	11
MPM4	-0.55	0.39	10
MPQ1	-0.14	0.05	12
MPQ4	0.34	0.11	7
MMX1b	-0.58	0.29	7
MMX5b	0.22	0.22	7
MRF1b	-0.38	0.18	8
MRF4	0.56	-0.20	7
MBB5	0.18	0.09	8
MPM2b	-0.30	0.06	6
MPM5	-0.26	-0.27	10
MPQ2	-0.27	0.47	12
MPQ5	-0.40	0.39	8
MRF2	-0.22	-0.33	8
MRF5	-0.10	0.15	8
MPM6	-0.15	-0.48	8
MPQ3	0.45	-0.57	11
MPQ6	-0.55	0.45	8
MMX2	0.07	0.13	11
MMX4	0.03	0.03	12
MMX6	0.21	-0.26	8
MRF3	0.12	-0.18	8
MRF6	0.33	-0.33	12
MRF7	-0.36	-0.10	7
N	95% significance level		
6	0.73		
7	0.67		
8	0.62		
9	0.58		
10	0.55		
11	0.52		
12	0.50		

terms of drier rainfall records, these two weather elements were selected for the correlation tests. Table 6.30 displays the correlation coefficient results for monthly mean temperature and rainfall with the rates of surface change 31 TMEM stations. Only those stations which had at least a continuous record of six or more individual time periods were tested. The results displayed in Table 6.30 show that with the exception of two TMEM stations, the correlation of rates of surface change with temperature and rainfall records were not considered to be statistically significant. Temperature resulted in more negative co-efficient when compared to rainfall but given the non-significant results, one cannot attribute any form of seasonality effect to such rates. The results of these tests would therefore imply that *in situ* rates are not driven by seasonality as one of the main controls on the rates of surface change. It also means that the drier 2016 did not have such an effect on the overall rates of surface change at any of these stations. Finally, it also means that though the shore platforms may have slightly different surface lithologies in terms of surface hardness, their level of response to processes of surface change were independent from seasonal trends.

6.5 Spatio-temporal patterns of surface change between platforms

6.5.1 Inferential analyses of rates across platforms to determine spatio-temporal patterns.

In the following-sub-sections, Kruskal Wallis H (KWH) tests were done in order to evaluate if there are any spatio-temporal patterns examining rates of surface of change between platforms. These analyses aim to confirm or reject the following four null hypotheses:

i. There is no statistical difference in the individual rates of surface change of each time period between front, mid and back of platforms (See Section 6.5.1.1);

ii. There is no statistical difference in the individual rates of surface change for each time period between the front of platforms (See Section 6.5.1.2);
iii. There is no statistical difference in the individual rates of surface change for each time period between the middle of platforms (See Section 6.5.1.2); and
iv. There is no statistical difference in the individual rates of surface change for each time period between the back of platforms (See Section 6.5.1.2).

6.5.1.1 Comparisons of rates for individual time periods between front, middle and back stations across platforms

Table 6.31 lists the 12 KWH results for a statistical comparison between front, middle and back stations for each individual periods. The 12 results showed all *p* value of less than 0.05. Therefore, these results are all in agreement that the null hypothesis of no difference should be rejected and that there is a statistical difference in all the stations for each time period. No time period provided any similarities in the rates of surface change between stations. These results confirm those previously discussed in Section3 6.3 and 6.4, in which rates of surface change for each time periods were compared at spatial level for each station. In other words, the behaviour of rock surface change in each period behaved differently at station level, platform level and temporal level. Thus, the rates of surface change at each station were statistically different between stations, between platforms and between time periods.

6.5.1.2 Comparisons of rates for individual time periods between all front, middle and back stations across platforms

A total of 12 KWH tests were undertaken to compare the rates of all the front stations and the results displayed in Table 6.32. Similarly to the results in Section 6.5.1.1, all the results provided *p* values of less than 0.05. 11 individual periods resulted in *p* values of 0.000 whilst period 4-2nd resulted in a *p* value of

Table 6.31: Comparison of rates of surface change for each time period between front, mid and back of platforms using KWH test

Shore Platform	TMEM stations according to each individual time period											
	RATES 2_1	**RATES 4_2**	**RATES 5_4**	**RATES 6_5**	**RATES 7_6**	**RATES 8_7**	**RATES 9_8**	**RATES 10_9**	**RATES 11_10**	**RATES 12_11**	**RATES 13_12**	**RATES 14_13**
Ponta tal-Munxar	MMX3a Tr2	MMX1a Tr1	MMX1a Tr1	MMX1a Tr1	MMX2 Tr 1	MMX1b Tr1	MMX1b Tr1	MMX1b Tr1	MMX1b Tr1	MMX1b Tr1	MMX1b Tr1	MMX1b Tr1
	MMX4 Tr2	MMX2 Tr 1	MMX2 Tr 1	MMX2 Tr 1	MMX4 Tr2	MMX2 Tr 1	MMX2 Tr 1	MMX2 Tr 1	MMX2 Tr 1	MMX2 Tr 1	MMX2 Tr 1	MMX2 Tr 1
		MMX3a Tr2	MMX3a Tr2	MMX3a Tr2	MMX6 Tr3	MMX3b Tr2	MMX 3b Tr2	MMX 3b Tr2	MMX4 Tr2	MMX4 Tr2	MMX4 Tr2	MMX 3c Tr2
		MMX4 Tr2	MMX4 Tr2	MMX4 Tr2		MMX4 Tr2	MMX4 Tr2	MMX4 Tr2	MMX 5b Tr3	MMX 5b Tr3	MMX 5b Tr3	MMX4 Tr2
						MMX 5b Tr3	MMX 5b Tr3	MMX 5b Tr3	MMX6 Tr3	MMX6 Tr3	MMX6 Tr3	MMX 5b Tr3
						MMX6 Tr3	MMX6 Tr3	MMX6 Tr3				MMX6 Tr3
Blata l-Bajda	MBB2 Tr1	MBB2 Tr1	MBB2 Tr1	MBB2 Tr1	MBB1b Tr1	MBB1b Tr1	MBB1b Tr1	MBB1b Tr1	MBB1b Tr1	MBB1b Tr1	MBB1b Tr1	MBB1b Tr1
	MBB3 Tr1	MBB3 Tr1	MBB3 Tr1	MBB3 Tr1	MBB2 Tr1	MBB2 Tr1	MBB2 Tr1	MBB2 Tr1	MBB2 Tr1	MBB2 Tr1	MBB2 Tr1	MBB2 Tr1
					MBB3 Tr1	MBB3 Tr1	MBB3 Tr1	MBB3 Tr1	MBB3 Tr1	MBB3 Tr1	MBB3 Tr1	MBB3 Tr1
					MBB4 Tr2	MBB4 Tr2	MBB4 Tr2	MBB4 Tr2	MBB4 Tr2	MBB4 Tr2	MBB4 Tr2	MBB4 Tr2
					MBB5 Tr2	MBB5 Tr2	MBB5 Tr2	MBB5 Tr2	MBB5 Tr2	MBB5 Tr2	MBB5 Tr2	MBB5 Tr2
					MBB6a Tr2	MBB6a Tr2	MBB6a Tr2	MBB6a Tr2		MBB6b Tr2	MBB6b Tr2	MBB6b Tr2
Ponta tal-Miġnuna	MPM1 Tr1	MPM1 Tr1	MPM1 Tr1	MPM1 Tr1	MPM1 Tr1	MPM1 Tr1	MPM1 Tr1	MPM1 Tr1	MPM1 Tr1	MPM1 Tr1	MPM1 Tr1	MPM1 Tr1
	MPM2a Tr1	MPM2a Tr1	MPM2a Tr1	MPM2a Tr1	MPM2a Tr1	MPM3a Tr1	MPM2b Tr1	MPM2b Tr1	MPM2b Tr1	MPM2b Tr1	MPM2b Tr1	MPM2b Tr1
			MPM3a Tr1	MPM3a Tr1	MPM3a Tr1	MPM4 Tr2	MPM4 Tr2	MPM3b Tr1	MPM3b Tr1	MPM3b Tr1	MPM3b Tr1	MPM3b Tr1
			MPM4 Tr2	MPM4 Tr2	MPM4 Tr2	MPM5 Tr2	MPM5 Tr2	MPM4 Tr2	MPM4 Tr2	MPM4 Tr2	MPM4 Tr2	MPM4 Tr2
			MPM5 Tr2	MPM5 Tr2	MPM5 Tr2	MPM6 Tr2	MPM6 Tr2	MPM5 Tr2	MPM5 Tr2	MPM5 Tr2	MPM5 Tr2	MPM5 Tr2
				MPM6 Tr2	MPM6 Tr2			MPM6 Tr2	MPM6 Tr2	MPM6 Tr2	MPM6 Tr2	
Ponta tal-Qammieħ	MPQ1 Tr1	MPQ1 Tr1	MPQ1 Tr1	MPQ1 Tr1	MPQ1 Tr1	MPQ1 Tr1	MPQ1 Tr1	MPQ1 Tr1	MPQ1 Tr1	MPQ1 Tr1	MPQ1 Tr1	MPQ1 Tr1
	MPQ2 Tr1	MPQ2 Tr1	MPQ2 Tr1	MPQ2 Tr1	MPQ2 Tr1	MPQ2 Tr1	MPQ2 Tr1	MPQ2 Tr1	MPQ2 Tr1	MPQ2 Tr1	MPQ2 Tr1	MPQ2 Tr1
	MPQ3 Tr1	MPQ3 Tr1	MPQ3 Tr1	MPQ3 Tr1	MPQ3 Tr1	MPQ3 Tr1	MPQ3 Tr1	MPQ3 Tr1	MPQ3 Tr1	MPQ3 Tr1	MPQ3 Tr1	MPQ3 Tr1
					MPQ4 Tr2	MPQ4 Tr2	MPQ4 Tr2	MPQ4 Tr2	MPQ4 Tr2	MPQ4 Tr2	MPQ4 Tr2	MPQ4 Tr2
					MPQ5 Tr2	MPQ5 Tr2	MPQ5 Tr2	MPQ5 Tr2	MPQ5 Tr2	MPQ5 Tr2	MPQ5 Tr2	MPQ5 Tr2
					MPQ6 Tr2	MPQ6 Tr2	MPQ6 Tr2	MPQ6 Tr2	MPQ6 Tr2	MPQ6 Tr2	MPQ6 Tr2	MPQ6 Tr2
Ras il-Fenek	MRF6 Tr2	MRF6 Tr2	MRF6 Tr2	MRF6 Tr2	MRF1b Tr1	MRF1b Tr1	MRF1b Tr1	MRF1b Tr1	MRF1b Tr1	MRF1b Tr1	MRF1b Tr1	MRF1b Tr1
					MRF2b Tr 1	MRF2b Tr1	MRF2b Tr1	MRF 2b Tr1	MRF2b Tr1	MRF2b Tr1	MRF2b Tr1	MRF2b Tr1
					MRF3b Tr1	MRF3b Tr1	MRF3b Tr1	MRF3b Tr1	MRF3b Tr1	MRF3b Tr1	MRF3b Tr1	MRF3b Tr1
					MRF4 Tr2	MRF4 Tr2	MRF4 Tr2	MRF4 Tr2	MRF4 Tr2	MRF4 Tr2	MRF4 Tr2	MRF4 Tr2
					MRF5 Tr2	MRF5 Tr2	MRF5 Tr2	MRF 5 Tr2	MRF5 Tr2	MRF5 Tr2	MRF5 Tr2	MRF5 Tr2
					MRF6 Tr2	MRF6 Tr2	MRF6 Tr2	MRF6 Tr2	MRF6 Tr2	MRF 6 Tr2	MRF6 Tr2	MRF6 Tr2
						MRF7Tr2	MRF7Tr2	MRF7 Tr2	MRF7 Tr2	MRF7 Tr2	MRF7 Tr2	MRF7 Tr2
KWH *p* value	0.000	0.000	0.000	0.000	0.000	0.000	0.000	0.000	0.000	0.000	0.000	0.000

Table 6.32: Comparison of rates of surface change for each time period between front of platforms using KWH test

Shore platform	TMEM front stations according to each individual time period											
	RATES 2_1	**RATES 4_2**	**RATES 5_4**	**RATES 6_5**	**RATES 7_6**	**RATES 8_7**	**RATES 9_8**	**RATES 10_9**	**RATES 11_10**	**RATES 12_11**	**RATES 13_12**	**RATES 14_13**
Ponta tal-Munxar	MMX3a Tr2	MMX1a Tr1	MMX1a Tr1	MMX1a Tr1		MMX1b Tr1	MMX1b Tr1	MMX1b Tr1	MMX1b Tr1	MMX1b Tr1	MMX1b Tr1	MMX1b Tr1
		MMX3a Tr2	MMX3a Tr2	MMX3a Tr2		MMX3b Tr2	MMX 3b Tr2	MMX 3b Tr2	MMX 5b Tr3	MMX 5b Tr3	MMX 5b Tr3	MMX 3c Tr2
						MMX 5b Tr3	MMX 5b Tr3	MMX 5b Tr3				MMX 5b Tr3
Blata l-Bajda					MBB1b Tr1	MBB1b Tr1	MBB1b Tr1	MBB1b Tr1	MBB1b Tr1	MBB1b Tr1	MBB1b Tr1	MBB1b Tr1
					MBB4 Tr2	MBB4 Tr2	MBB4 Tr2	MBB4 Tr2	MBB4 Tr2	MBB4 Tr2	MBB4 Tr2	MBB4 Tr2
Ponta tal-Miġnuna	MPM1 Tr1	MPM1 Tr1	MPM1 Tr1	MPM1 Tr1	MPM1 Tr1	MPM1 Tr1	MPM1 Tr1	MPM1 Tr1	MPM1 Tr1	MPM1 Tr1	MPM1 Tr1	MPM1 Tr1
			MPM4 Tr2	MPM4 Tr2	MPM4 Tr2	MPM4 Tr2	MPM4 Tr2	MPM4 Tr2	MPM4 Tr2	MPM4 Tr2	MPM4 Tr2	MPM4 Tr2
Ponta tal-Qammieħ	MPQ1 Tr1	MPQ1 Tr1	MPQ1 Tr1	MPQ1 Tr1	MPQ1 Tr1	MPQ1 Tr1	MPQ1 Tr1	MPQ1 Tr1	MPQ1 Tr1	MPQ1 Tr1	MPQ1 Tr1	MPQ1 Tr1
					MPQ4 Tr2	MPQ4 Tr2	MPQ4 Tr2	MPQ4 Tr2	MPQ4 Tr2	MPQ4 Tr2	MPQ4 Tr2	MPQ4 Tr2
Ras il-Fenek					MRF1b Tr1	MRF1b Tr1	MRF1b Tr1	MRF1b Tr1	MRF1b Tr1	MRF1b Tr1	MRF1b Tr1	MRF1b Tr1
					MRF4 Tr2	MRF4 Tr2	MRF4 Tr2	MRF4 Tr2	MRF4 Tr2	MRF4 Tr2	MRF4 Tr2	MRF4 Tr2
KWH p value	0.000	0.032	0.000	0.000	0.000	0.000	0.000	0.000	0.000	0.000	0.000	0.000

Table 6.33: Comparison of rates of surface change for each time period between middle of platforms using KWH test

Shore platform	TMEM middle stations according to each individual time period											
	RATES2_1	**RATES4_2**	**RATES5_4**	**RATES6_5**	**RATES7_6**	**RATES8_7**	**RATES9_8**	**RATES10_9**	**RATES11_10**	**RATES12_11**	**RATES13_12**	**RATES14_13**
Blata l-Bajda	MBB2 Tr1	MBB2 Tr1	MBB2 Tr1	MBB2 Tr1	MBB2 Tr1	MBB2 Tr1	MBB2 Tr1	MBB2 Tr1	MBB2 Tr1	MBB2 Tr1	MBB2 Tr1	MBB2 Tr1
					MBB5 Tr2	MBB5 Tr2	MBB5 Tr2	MBB5 Tr2	MBB5 Tr2	MBB5 Tr2	MBB5 Tr2	MBB5 Tr2
Ponta tal-Miġnuna	MPM2a Tr1	MPM2a Tr1	MPM2a Tr1	MPM2a Tr1	MPM2a Tr1	MPM3a Tr1	MPM2b Tr1	MPM2b Tr1	MPM2b Tr1	MPM2b Tr1	MPM2b Tr1	MPM2b Tr1
			MPM4 Tr2	MPM4 Tr2	MPM4 Tr2	MPM4 Tr2	MPM4 Tr2	MPM4 Tr2	MPM4 Tr2	MPM4 Tr2	MPM4 Tr2	MPM4 Tr2
Ponta tal-Qammieħ	MPQ2 Tr1	MPQ2 Tr1	MPQ2 Tr1	MPQ2 Tr1	MPQ2 Tr1	MPQ2 Tr1	MPQ2 Tr1	MPQ2 Tr1	MPQ2 Tr1	MPQ2 Tr1	MPQ2 Tr1	MPQ2 Tr1
					MPQ4 Tr2	MPQ4 Tr2	MPQ4 Tr2	MPQ4 Tr2	MPQ4 Tr2	MPQ4 Tr2	MPQ4 Tr2	MPQ4 Tr2
Ras il-Fenek					MRF2b Tr 1	MRF2b Tr1	MRF2b Tr1	MRF 2b Tr1	MRF2b Tr1	MRF2b Tr1	MRF2b Tr1	MRF2b Tr1
					MRF5 Tr2	MRF5 Tr2	MRF5 Tr2	MRF 5 Tr2	MRF5 Tr2	MRF5 Tr2	MRF5 Tr2	MRF5 Tr2
KWH *p* value	0.024	0.000	0.000	0.000	0.000	0.000	0.000	0.000	0.000	0.000	0.000	0.000

Table 6.34: Comparison of rates of surface change for each time period between back of platforms using KWH test

Shore platform	TMEM back stations according to each individual time period											
	RATES 2_1	**RATES 4_2**	**RATES 5_4**	**RATES 6_5**	**RATES 7_6**	**RATES 8_7**	**RATES 9_8**	**RATES 10_9**	**RATES 11_10**	**RATES 12_11**	**RATES 13_12**	**RATES 14_13**
Ponta tal-Munxar	MMX4 Tr2	MMX2 Tr 1	MMX2 Tr 1	MMX2 Tr 1	MMX2 Tr 1	MMX2 Tr 1	MMX2 Tr 1	MMX2 Tr 1	MMX2 Tr 1	MMX2 Tr 1	MMX2 Tr 1	MMX2 Tr 1
		MMX4 Tr2	MMX4 Tr2	MMX4 Tr2	MMX4 Tr2	MMX4 Tr2	MMX4 Tr2	MMX4 Tr2	MMX4 Tr2	MMX4 Tr2	MMX4 Tr2	MMX4 Tr2
					MMX6 Tr3	MMX6 Tr3	MMX6 Tr3	MMX6 Tr3	MMX6 Tr3	MMX6 Tr3	MMX6 Tr3	MMX6 Tr3
Blata l-Bajda	MBB3 Tr1	MBB3 Tr1	MBB3 Tr1	MBB3 Tr1	MBB3 Tr1	MBB3 Tr1	MBB3 Tr1	MBB3 Tr1	MBB3 Tr1	MBB3 Tr1	MBB3 Tr1	MBB3 Tr1
					MBB6a Tr2	MBB6a Tr2	MBB6a Tr2	MBB6a Tr2		MBB6b Tr2	MBB6b Tr2	MBB6b Tr2
Ponta tal-Miġnuna			MPM3a Tr1	MPM3a Tr1	MPM3a Tr1	MPM3a Tr1	MPM6 Tr2	MPM3b Tr1	MPM3b Tr1	MPM3b Tr1	MPM3b Tr1	MPM3b Tr1
				MPM6 Tr2	MPM6 Tr2	MPM6 Tr2		MPM6 Tr2	MPM6 Tr2	MPM6 Tr2	MPM6 Tr2	
Ponta tal-Qammieħ	MPQ3 Tr1	MPQ3 Tr1	MPQ3 Tr1	MPQ3 Tr1	MPQ3 Tr1	MPQ3 Tr1	MPQ3 Tr1	MPQ3 Tr1	MPQ3 Tr1	MPQ3 Tr1	MPQ3 Tr1	MPQ3 Tr1
					MPQ6 Tr2	MPQ6 Tr2	MPQ6 Tr2	MPQ6 Tr2	MPQ6 Tr2	MPQ6 Tr2	MPQ6 Tr2	MPQ6 Tr2
Ras il-Fenek	MRF6 Tr2	MRF6 Tr2	MRF6 Tr2	MRF6 Tr2	MRF3b Tr1	MRF3b Tr1	MRF3b Tr1	MRF3b Tr1	MRF3b Tr1	MRF3b Tr1	MRF3b Tr1	MRF3b Tr1
					MRF6 Tr2	MRF6 Tr2	MRF 6 Tr2	MRF 6 Tr2	MRF 6 Tr2	MRF 6 Tr2	MRF6 Tr2	MRF6 Tr2
						MRF7Tr2	MRF7Tr2	MRF7 Tr2	MRF7 Tr2	MRF7 Tr2	MRF7 Tr2	MRF7 Tr2
KWH *p* value	0.002	0.000	0.137	0.000	0.000	0.000	0.000	0.000	0.000	0.000	0.000	0.000

0.032. Since all the results are below 0.05, the null hypothesis of no difference can be rejected. All front stations differed in their rates of surface change across all time periods. This would therefore imply that although the relative position of the stations on the platform was the common denominator, other site-specific factors, may have a stronger determining role in the rates of rock surface change at each station or platform.

Similar to the tests undertaken in Section 6.5.1.1 and 6.5.1.2, the rates of the middle stations were also tested out in 12 KWH tests. Out of 12 *p* value results, 11 of them had *p* values close to 0.000, i.e. lower than the 0.05 (Table 6.33). The first measurement period 2-1st resulted in a *p* value of 0.024, which is still lower than 0.05. Thus all the 12 results reject the H_0 hypothesis of no difference and conclude that there are differences between all the middle stations in each respective time period. A similar conclusion to that elaborated in Section 6.3, can be argued in the relation to the role of the relative position of the station as not being a driver of rates of surface change and no period provided significant similar patterns.

Table 6.31 lists the results of the 12 KWH tests undertaken for all the back stations across individual temporal periods. Ten results show *p* value of 0.000 and thus reject the null hypothesis of no difference. Another result, that of 2-1st had a slightly higher *p* value of 0.002, which is nonetheless still lower than 0.05 and thus accepts the H_1 result of difference between its middle stations. The result of period 5-4th proved to be the only different result not only from the back stations dataset. With a *p* value of 0.137, it shows that the rates of surface change had significant similar patterns and that in being above 0.05, the null hypothesis is accepted and there are no differences in the rates of surface change between the 6 back stations during the 5-4th time period.

The interpretation of this result was subsequently tested the context of the rest of temporal periods being examined. Given that this result stands out as a single result for specific six stations, the trend of previous and successive

periods is not comparable given that less or more back stations were included in the test in the remaining periods. The only way to test out the validity of similarity between the six stations in question was to sample them for other KWH test for other periods. An additional 3 KWH tests were done for periods 6-5th, 7-6th and 8-7th which together with 5-4th period provide an analyses of an annual time-scale. In all the three KWH tests, the *p* value results came back as 0.000 and thus rejecting the null hypothesis of no difference. So the observed behaviour measured in the 5th-4th period was singular in the context of an annual time-scale. This continues to confirm how rates calculated over short-term scales may not necessarily represent rates over of longer time-frames.

6.6 Observed rates of surface changes on experimental slabs

As explained in Section 3.5.2 the aim of this exposure experiment was to monitor more closely the responses of Globigerina limestone samples (extracted from each platform) to weathering, in order to both understand whether (and to what extent) their rates and modes of surface change may be influenced by weathering processes and record changes in quantified outcomes (See Table 3.1). The following sections present the results of the TMEM measurements recorded from January 2015 and August 2016 (Appendix IX). The aim of this analysis is to identify whether or not platforms shared similar rates of surface change throughout the different exposure periods (Section 3.5.2.2). The findings may offer further insights about the results of the rock properties presented in Chapter 5.

6.6.1 Spatial patterns of rock surface change on experimental slabs of each platform

The following section presents the results for rates of surface change based on an examination of how these rates trended on each platform. The spatial scale observed was between the front and back section of the platforms. This section presents the results of KWH tests in order to compare the rates between each position and examine if statistical differences exist across each platform.

The analyses aim to test out whether there is no difference in the rates of surface change between stations on each platform (Table 3.13).

6.6.1.1 Descriptive analysis of overall mean rates of surface change

This section presents results for the mean rates of surface change across the platforms obtained for the total exposure period, on an annual level and for the three individual exposure periods. Similarities and differences in overall mean rates of surface change between platforms were also identified and subsequently also discussed at sample level.

i. Comparison of samples from each platform across total exposure period (18 months)

Only 12 results produced rates of surface gains, which are within a relatively narrower range of data spread from 0.002 to 0.414 mma^{-1}. Overall, almost all samples, with the exception of the front sample of Ponta tal-Qammieħ (sample no. 16) registered a mean rate of surface loss throughout the whole exposure period. The mean rates of surface change representing the individual exposure periods and the whole exposure period are illustrated in Table 6.35. From 73 mean values, 84% of the mean values registered relatively high surface losses, with a proportion of 61 results recording changes, which ranged widely from -9.061 to 0.026 mma^{-1}.

Apart from sample no. 9 of Blata l-Bajda, only another sample registered losses above the dataset mean rates of surface loss: the front sample no. 8 of Ponta tal-Munxar. The rate of breakdown of the bottom section of the sample no. 8 was also rather rapid and measurements could not be continued after the first exposure period. The dataset mean was mostly affected by the high values obtained for sample no. 1 and no. 9 (Blata l-Bajda) and sample no. 8 for Ponta

Table 6.35: Mean rates of surface change across individual exposure periods and across total exposure periods

	Mean rates of surface change across individual exposure periods and the total exposure period									
Sample no.	Shore platform and sample position	No. of TMEM stations	Position on sample	Exposure Period 1* mma^{-1}	Exposure Period 2** mma^{-1}	Exposure Period 3*** mma^{-1}	Exposure Period**** mma^{-1}	SL	SR	Overall spatial mean rate mma^{-1}
1	Blata l-Bajda - Front	2	Left	-1.729	-1.667	-1.102	-1.918	4	0	-1.604
			Right	-1.755	-2.555	-0.255	-1.563	4	0	-1.532
2	Ponta tal-Qammieh - Front	3	Left	Discontinued						
			Centre							
			Right							
3	Ponta tal-Mignuna - Back	1		-1.026	-0.357	-0.248	-0.535	4	0	-0.541
4	Ponta tal-Munxar - Back	1		0.114	-1.313	-0.207	-0.099	3	1	-0.376
5	Globigerina Block Sample	2	Left	-0.308	-0.043	0.054	-0.306	3	1	-0.151
			Right	-0.420	0.017	-0.042	-0.124	3	1	-0.142
6	Ras il-Fenek - Front	1		-0.310	-0.631	-0.252	-0.183	4	0	-0.344
7	Ponta tal-Munxar - Back	2	Left	-0.793	-0.029	-0.026	-0.241	4	0	-0.272
			Right	-2.071	-0.040	-0.081	-0.607	4	0	-0.700
8	Ponta tal-Munxar - Front	2	Top	-2.359	-1.814	-1.139	-1.750	4	0	-1.766
			Bottom	-2.978	Discontinued			1	0	-2.978
9	Blata l-Bajda -Front	2	Top	-8.079	Discontinued			1	0	-8.079
			Bottom	-9.061				1	0	-9.061
10	Ras il-Fenek - Back	2	Left	-0.824	0.213	-0.279	-0.110	3	1	-0.250
			Right	-0.631	0.255	0.002	-0.075	2	2	-0.112
11	Ponta tal-Mignuna -Back	1		-2.411	0.067	-0.159	-0.667	3	1	-0.792
12	Blata l-Bajda -Back	3	Left	Discontinued						
			Centre							
			Right							
13	Ponta tal-Mignuna - Front	2	Left	-0.635	0.412	-0.623	-0.260	3	1	-0.276
			Right	-1.039	0.414	0.020	-0.120	2	2	-0.181
14	Ras il-Fenek - Front	1		-2.035	-0.639	-1.503	-1.316	4	0	-1.373
15	Ponta tal-Qammieh - Back	1		Not set-up	-0.417	-0.439	-0.426	3	0	-0.427
16	Ponta tal-Qammieh - Front	1			0.199	-0.166	0.074	1	2	0.036
	Surface Loss (SL)		61	18	11	15	17	61	12	-1.473
	Surface Rise (SR)		12	1	7	3	1			
	Temporal Mean Rate			-2.018	-0.482	-0.365	-0.617			-0.871

** First exposure measurement- Pre-exposure measurement*

*** Second exposure measurement - First exposure measurement*

**** Final exposure measurement- Second exposure measurement*

***** Final exposure measurement-Pre-exposure measurement*

tal-Munxar. On the other hand, the samples extract from the back of the platform – sample no. 4 and no. 7, had relatively lower rates of surface loss. As listed in Table 6.35, the shore platform which registered the largest rates of surface loss was that of Blata l-Bajda: sample no. 1 and sample no. 9. Similarly to sample no. 8, the breakdown rate for this sample was very rapid and it was not possible to obtain further measurements after the first exposure period, The sample extracted from the back of the platform, sample no. 12, was equally rapid in its breakdown and disintegrated before surface measurements could be taken at the end of the first exposure period.

In terms of platform samples, the lowest mean rates of surface lowering mostly account for the back section of Ras il-Fenek shore platform (sample no. 10). However the rates were proportionately higher after the first exposure period and then eventually became more variable in the successive exposure periods with surface gains in the second period and lower surface losses in the third exposure period and an overall lower rates for the study period. The same trend was also observed in sample no. 13 (Ponta tal-Miġnuna – Front) which also recorded relatively low mean rates of surface but which were affected by surface gains during the second exposure period. Given that the surface deterioration of these samples was noticeable throughout the study period and the higher number of other surface measurements resulting in surface losses, these surface gains records during the second measurement period could only be attributed to an operator error during the data collection stage. Such an error could have derived from physical instability of the rock sample due weathering process.

As explained in Chapter 3, a freshly cut Lower Globigerina Limestone block (sample no. 5), was included in the experiment for a comparison with the platforms rocks and build on the numerous discussion related to deterioration Lower Globigerina Limestone (Section 2.7), This comparative work is a first in comparing rates of deterioration across the different rocks in Globigerina Limestone and also using TMEM a tool to measure rock surface change for both. It aimed to test whether behaviour of rock surface change varies across a number of

Globigerina samples and if so, to what extent were rates and modes of surface change different. The measured rates of surface change of sample no. 5 were different from the platform sample on the following two accounts:

i. Their overall mean rates of surface change were much lower than those recorded by the platform samples: -0.151 mma^{-1} and -0.142 mma^{-1}; and
ii. The two resultant mean rates of surface change were relatively closer, whilst samples with two stations – such as sample no. 7, 8, 9 10 and 13, resulted in mean rates of surface change more distant from each other.

These two results would imply that the surface deterioration of freshly cut surfaces in LGL respond differently from naturally untouched surfaces represented by the platform rock surfaces. It also confirms that the variability which exists within the deterioration process of the Globigerina limestone and that studies on the deterioration of Globigerina building blocks provide only one insight to the otherwise complex behaviour of surface responses to weathering and erosion processes. The statistical results which emerged from this exposure experiment provide initial confirmation that rock surfaces in Globigerina limestone from each platform operate differently in terms of surface change.

ii. Comparisons between front and back samples of each platform

When comparing the overall mean rates of surface change between the samples taken from the front section with those extracted from the back section of each platform, some differences can be observed for some platforms and reverse trends of such differences on other platforms. As seen in Figure 6.30, the front samples of Ras il-Fenek and Ponta tal-Munxar have experienced higher rates of surface loss, when compared with the losses recorded for the back samples. The largest differences were those observed between the samples of Ponta tal-Munxar: -1.766 mma^{-1} and -2.978 mma^{-1} for the front samples and -0.376, -0.272 and -0.700 mma^{-1} for the back samples. Conversely, it was observed that the measured rates

of surface losses recorded for the back samples of Ponta tal-Qammieħ and Ponta tal-Miġnuna were overall higher than those for the front samples. Though statistical comparisons for Blata l-Bajda samples were not possible (given that the back stations deteriorated too quickly to extract any measured rates), one can also conclude that the rate of breakdown of the back samples at Blata Bajda was relatively higher than that of its front samples. This does not overrule the fact that the rates of surface losses at Blata l-Bajda were experienced the highest surface losses nonetheless.

Figure 6.30: Overall mean rates of surface change per platform sample

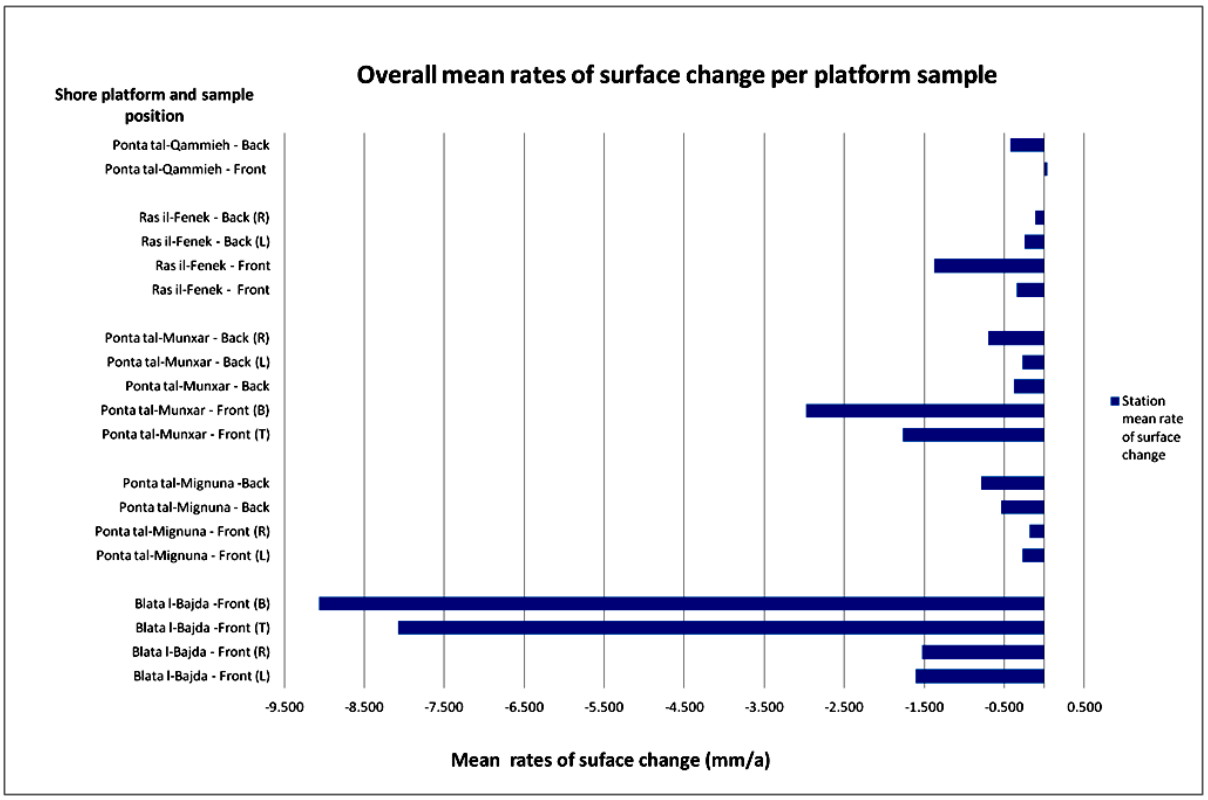

Variable rates of rock breakdown from the same platform can relatively confirm the different levels of rock resistance present within the same limestone platform. This variability as reflected in the rates of surface change that were measured within the same samples (i.e. for samples with more than one TMEM station) and this may be a strong indication of the small scale at which surface

change variability operates, especially for limestone rocks which are confined within *in situ* physical properties. Variability of surface responses to processes of change can be considered as a key characteristic of these slabs and therefore, the likelihood *in situ* surfaces operating in differential responses can be confirmed.

6.6.1.2 Inferential analysis of rates of surface change of each platform sample

KWH tests were undertaken in order to confirm that the rates of surface change provide a statistically significant pattern. The null hypothesis (H_0) in this case was that there is no difference in the rates of surface change on each of the selected platforms.

Table 6.36 summarises the p value results of the 17 KWH tests, undertaken in order to examine whether there are statistical differences in the rates of surface change for samples belonging to the same platform.

Table 6.36: KWH *p* value results for comparison of rates of surface change of individual exposure per platform

Shore platform	Sample No.	Exposure Period 1	Exposure Period 2	Exposure Period 3	Total Exposure Period
Blata l-Bajda	1, 9	0.000	0.021	n/a	n/a
Ponta tal-Mignuna	3, 11, 13	0.000	0.000	0.000	0.000
Ponta tal-Munxar	4, 7, 8	0.000	0.000	0.000	0.000
Ponta tal-Qammieh	15, 16	n/a	0.000	0.001	0.000
Ras il-Fenek	6, 10, 14	0.000	0.000	0.000	0.000

This test determined whether or not the experiment slabs which belonged to the same platform had similar or different rates of rock denudation by using TMEM surface measurements as vertical records of such breakdown. All the 17 KWh tests resulted in *p* value of less than 0.005. This result means that, for each platform, the tested slabs exhibited different rates of surface change and such statistical

difference was consistent for all the three individual exposure periods and for the total exposure period.

6.6.2 Temporal patterns of rock surface change on each platform

The following section presents the results for rates of surface change based on an examination of how these rates trended over specific temporal scales. The main time-frames discussed are the mean rate of surface changes based on four exposure periods, the rates calculated from two annual trends and the trends from each individual exposure period. This section presents the results of MWU tests in order to compare the rates measured across individual, annual and total exposure time periods and examine if statistical differences exist between each temporal period. The analyses aim to test the following null hypotheses:

i. There is no differences in the rates of surface change between each exposure period at each platform (Section 6.6.2.2); and
ii. There is no difference in the rates of surface change between each exposure period and total exposure period at each platform (Section 6.6.2.2).

6.6.2.1 Descriptive analysis of mean rates of surface change across temporal periods

i. Across individual and total exposure periods

The first exposure period i.e. the period from pre-exposure to the first exposure measurement, was the one which marked the highest rates of surface change across most of the experimental slabs. The overall mean rate for the first -2.018 mma^{-1}, followed by -0.482 mma^{-1}, -0.365 $mma^{-1}$and -0.617 mma^{-1} for the second, third and total exposure period. Arguably, the slowing down of rates of surface loss in these latter periods may also be partially attributed to the discontinuation of samples and stations such as sample no. 9 and the bottom station of sample no. 8 which recorded relatively higher rates of surface losses in the first exposure period.

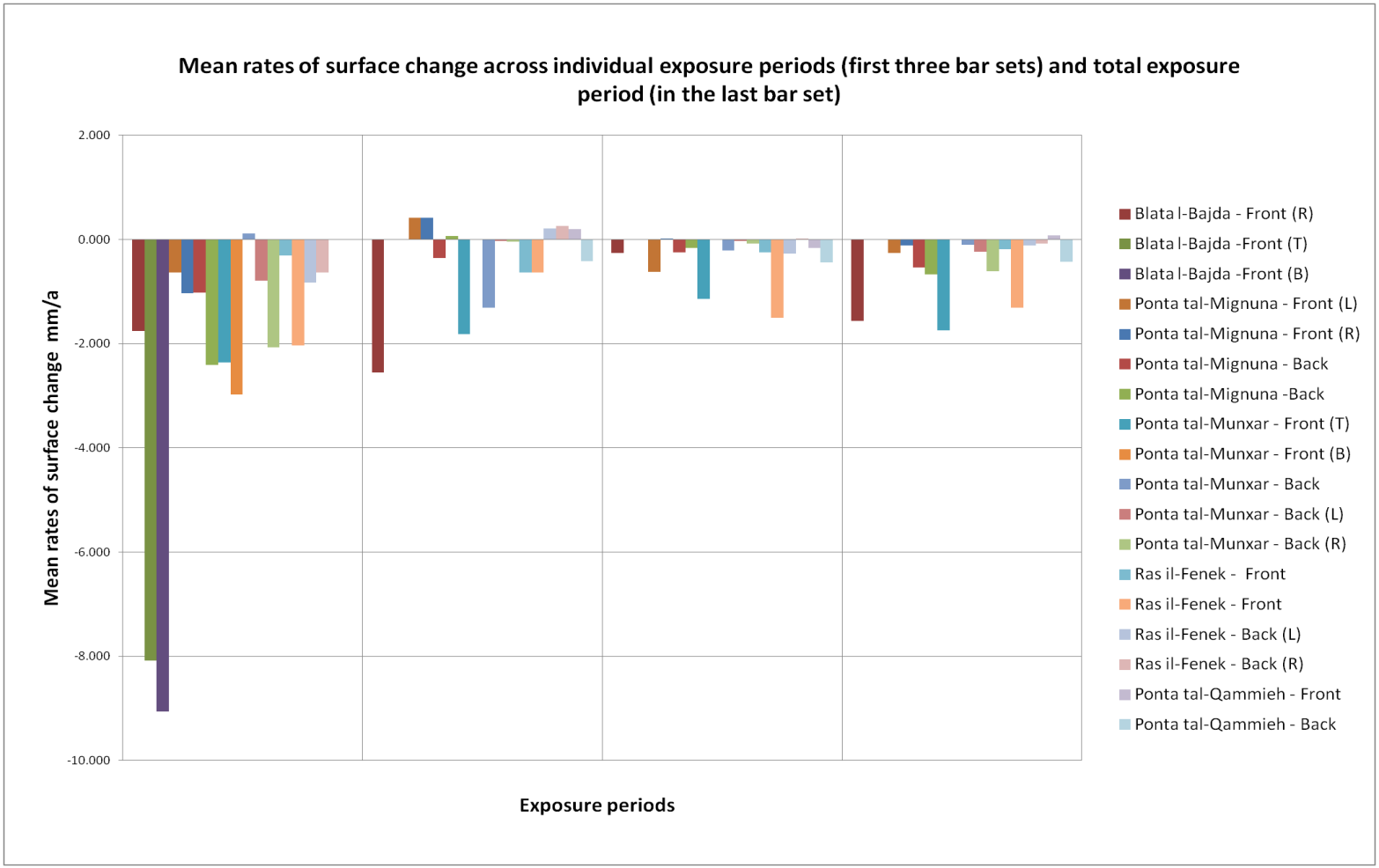

Figure 6.31: Mean rates of surface change across each individual exposure period and across total exposure period.

Table 6.37: Mean rates of surface change across individual exposure periods for front and back samples

Samples	Exposure Period 1	Exposure Period 2	Exposure Period 3	Total Exposure Period
	mma^{-1}	mma^{-1}	mma^{-1}	mma^{-1}
Front	-2.998	-0.926	-0.693	-1.016
Back	-1.092	-0.203	-0.179	-0.345

However, even if these rates had to be removed from the mean calculations, the mean rate of surface change for the first exposure period would still be the record the highest rate of surface change with a result of -1.139 mma^{-1}. Some of the samples which experienced amongst the highest rates of surface loss during the first exposure period - such as Blata l-Bajda-Front (sample no. 1), Ponta tal-Munxar – Front (sample no. 8) and Ras il-Fenek-Front (sample no. 14) - continued to experience relatively higher rates of surface loss (albeit lower compared to the fist exposure period) in the subsequent periods (Figure 6.31).

This result seems to indicate that the most intense denudation responses to sub-aerial weathering occurred in the initial phase of exposure and then slowed down to lower rates. This type of response may indicate a sort of 'acclimatisation' response, in which the samples experienced intense adjustments due the shift of environmental conditions from the coastal-platform confined ambient to non-coastal unconfined conditions following pre-exposure. These adjustments led to intense rates of surface change and immediate visible signs of surface flaking or powdering, discoloration or splintering. The first exposure period also coincides with winter–spring conditions. Conditions such as rainfall and fluctuating daily temperatures, may have also coincided with higher incidence of solution weathering than in subsequent exposure periods. The samples may have subsequently

experienced lower rates of surface change due to lesser adjustments required after the first exposure period.

When calculated separately, the overall mean rate of surface losses for the front samples was relatively higher when compared to the back sample and this trend was consistent for each temporal period (Table 6.37). However, as already explained in Section 6.6.1.1, this trend does not apply consistently when rates are examined at individual sample level, although higher rates of surface losses during the first exposure period is a strong trend even at sample level as evidenced by Figure 6.31. This result once again confirms the variability of the responses of the tested limestones to processes of change.

Rates of surface losses were high, also during the third exposure period with 17 periods (out of a total of 18), recording surface losses (Table 6.38). As a trend this is very close to what was experienced in the first exposure period, with 18 out of 19 periods experiencing surface losses. It was the second exposure period, the results were relatively more mixed with 11 out of 18 rates recording surface losses and 7 registering surface rises (mostly from samples no. 10, no. 11 and no. 13) (Figure 6.31).

ii. Across annual periods

Rates of surface change across two annual periods were also calculated for each sample and are listed in Table 6.38. Annual period a corresponds to a measurement period from pre-exposure to second exposure (373 days) and annual period B covers a measurement period from first exposure to third exposure (400 days). The overall mean rates of surface change for the two periods were not substantially different. However, these overall rates tend to a wide range of individual rates of surface change per sample and which include rates of surface rises in the annual period A for sample such as no. 5, 6, 10 and 13. Apart from the latter inconsistencies, the trend of surface lowering measured across both annual periods is quite in line with that examined across the whole exposure period, especially for samples no. 1, 3, 4, 8, 11, 14 and 15.

Table 6.38: Mean rates of surface change across annual exposure periods

Sample no.	Shore platform and sample position	Position on sample	Annual Period A mma^{-1}	Annual Period B mma^{-1}
1	Blata l-Bajda - Front	Left	-1.701	-2.025
		Right	-2.256	-1.661
3	Ponta tal-Mignuna - Back		-0.295	-0.264
4	Ponta tal-Munxar - Back		-0.375	-0.814
5	Globigerina Block Sample	Left	0.187	-0.001
		Right	0.184	0.009
6	Ras il-Fenek - Front		0.201	-0.133
7	Ponta tal-Munxar - Back	Left	0.002	0.023
		Right	-0.535	-0.039
8	Ponta tal-Munxar - Front	Top	-1.697	-1.514
10	Ras il-Fenek - Back	Left	0.131	0.166
		Right	0.236	0.140
11	Ponta tal-Mignuna -Back		-0.206	-0.044
13	Ponta tal-Mignuna - Front	Left	0.327	-0.115
		Right	0.160	0.235
14	Ras il-Fenek - Front		-0.872	-1.037
15	Ponta tal-Qammieh - Back			-0.429
16	Ponta tal-Qammieh - Front			0.074
	Temporal Mean Rate		-0.407	-0.413

6.6.2.2 Inferential analyses of rates of surface change across exposure periods

i. Paired comparisons in the rates of surface change between individual exposure time periods

A total of 46 MWU tests were undertaken to cross-compare the three exposure periods per platform sample. The results of these tests are displayed in Table 6.39. Out of 46 tests, 36 tests resulted in *p* value below 0.000 and indicating differences in the rate of surface change between the paired tests. The number of H_0 results is relatively low in each temporal comparison and only slight variations exist between each temporal comparison and another. The comparison between exposure period 2 and 3 yielded the highest number of H_0 results, with 3 out of 5 results deriving from the Ponta tal-Munxar

Table 6.39: MWU test p value results for cross-comparisons between individual exposure periods and with total exposure period. Shaded cells indicate p value results large than 0.05 and thus accepting the H_0 hypothesis of no difference in surface rates between tested periods

MWU test p value results for cross-comparisons between individual exposure periods and with total exposure period							
Sample No.	Name of platform and slab position	Exp Per 1 vs 2	Exp 1 vs 3	Exp Per 2 vs 3	Total	H_0	H_1
		p values	p values	p values			
1	Blata l-Bajda - Front (L)	0.260	n/a	n/a			
1	Blata l-Bajda - Front (R)	0.006	n/a	n/a			
9	Blata l-Bajda -Front (T)	n/a	n/a	n/a			
9	Blata l-Bajda -Front (B)	n/a	n/a	n/a	2	1	1
13	Ponta tal-Miġnuna - Front (L)	0.000	0.543	0.000			
13	Ponta tal-Miġnuna - Front (R)	0.000	0.000	0.000			
3	Ponta tal-Miġnuna - Back	0.000	0.000	0.663			
11	Ponta tal-Miġnuna -Back	0.000	0.000	0.002	12	10	2
8	Ponta tal-Munxar - Front (T)	0.096	0.000	0.074			
8	Ponta tal-Munxar - Front (B)	n/a	n/a	n/a			
4	Ponta tal-Munxar - Back	0.000	0.003	0.000			
7	Ponta tal-Munxar - Back (L)	0.000	0.000	0.534			
7	Ponta tal-Munxar - Back (R)	0.140	0.026	0.096	12	7	5
6	Ras il-Fenek - Front	0.000	0.012	0.000			
14	Ras il-Fenek - Front	0.000	0.067	0.002			
10	Ras il-Fenek - Back (L)	0.000	0.000	0.000			
10	Ras il-Fenek - Back (R)	0.000	0.000	0.000	12	11	1
16	Ponta tal-Qammieħ - Front	n/a	n/a	0.270			
15	Ponta tal-Qammieħ - Back	n/a	n/a	0.000	2	1	1
5	Globigerina Block Sample - Left	0.000	0.000	0.000			
5	Globigerina Block Sample - Right	0.000	0.000	0.000	6	0	6
	Total	16	14	16	46	30	16
	H_0	3	2	5	10		
	H_1	13	12	11	36		

samples no. 7 and no. 8. These samples also resulted in two H_1 results in the comparison between exposure period 1 and 2.

The rest of the samples recorded H_0 p values in isolated patterns throughout the three exposure period comparisons. Overall the results seem to indicate that although the dominant behaviour seems one of rapid surface loss; both the breakdown pattern and rate of surface change of most samples operate differently from one temporal period to another. Once again, the variability in responses of the experimental samples provides further evidence on how the mechanisms of surface change on each shore platform may result in different rates and modes of surface change. It confirms the initial assumption that they though these platforms belong to the same lithological unit, their surfaces exhibit a wide variety of measurable responses to processes of change.

6.6.3 Spatio-temporal patterns of rock surface change between platforms of experimental samples

6.6.3.1 Inferential analyses of rates of surface change between all platforms

i. Comparison of rates across all stations for each exposure time period

Four KWH tests were performed in which the rates of surface change for all platforms were statistically compared across each exposure time period and for the total exposure time period. All the p values of the four KWH tests show values lower than 0.005 and no temporal pattern was identified across stations for each exposure period. This result confirms the previous results obtained in spatial analysis (presented in Section 6.6.2.1) whereby no pattern was identified at spatial level for each platform according to the four exposure periods.

ii. Comparisons of mean rates of surface change across individual time periods between front and back samples

Table 6.40 displays the *p* value results from KWH analysis in which the mean rates of surface change listed in Table 6.35 were tested for differences between the front and back samples across the four exposure time periods. All the four KWH tests resulted in *p* values larger than 0.005 and which therefore accept the null hypothesis of no difference in the rates of surface change between the front and back samples. It is important to note that in these tests only one value of mean rates of surface change was used for each station (listed in Table 6.35) and thus surface change variability across the 22 measurement points within each stations is not sufficiently represented and nor tested out at individual level as it was done for Section 6.6.1.2.

Table 6.40: KWH result of mean rates of surface change between front and back samples according to each exposure period

Sample position	Sample No.	Exposure Period 1	Exposure Period 2	Exposure Period 3	Total Exposure Period
Front samples	1, 6, 8, 9, 13, 14, 16	0.143	0.186	0.125	0.634
Back samples	3, 4, 7, 10, 11, 15				

iii. Comparisons of mean rates of surface change across annual exposure periods between front and back samples

Table 6.41 lists the results of two KWH test done when comparing the mean rates over two annual periods for front and back stations. Both results came back with *p* values higher than 0.05. Similarly to the results obtained for the mean rates of the individual exposure periods, these results also confirm that there are no differences in the mean rates of surface change between the front and back samples.

Table 6.41: KWH results for comparison of mean rates of surface change per annual exposure period between front and back samples.

Sample position	Sample No.	Annual Period A	Annual Period B
Front samples	1, 6, 8, 9, 13, 14, 16	0.482	0.208
Back samples	3, 4, 7, 10, 11, 15		

6.7 Summary of main findings

6.7.1 Rates of surface change on platforms

From the study period calculations, the mean rate of surface change for the 41 stations was measured and found to be -0.237 mma^{-1} but this overall result included rates and standard deviations primarily skewed by the relatively higher losses recorded in 14 out of 41 stations.

Variability in results was observed both at spatial and temporal scales. At platform level, all five platforms recorded a higher percentage of surface lowering rates compared to the rates of surface rises.

Out of a total of 184 rates of surface change obtained for annual periods, 78% (143) registered surface-lowering rates and only 22% (41) recorded rates of surface-rise. 75% of the 241 semi-annual rates (181) recorded rates of surface-lowering and the remaining 25% (60) were rates of surface rise.

Given the similar percentage results obtained for surface rises and surface lowering, the semi-annual rates can be considered comparable to annual rates in capturing rock surface change. However, the percentage results of the rates for individual periods captured slightly less percentage in surface losses and more in surface rises.

In terms of individual time periods, Blata l-Bajda shore platform had the highest percentage of losses (84%) and Ras il-Fenek shore platform had the least percentage of losses (59%) and highest records (41%) in terms of rises. Such difference may be lithologically related due to the presence of hardground beds at Ras il-Fenek, whereas these beds are absent at Blatal-Bajda. This point will be further elaborated in the next chapter (Chapter 7).

The stations with the largest variability in rates of surface change across the individual measurement periods (such as MPM2b, MPM6, MMX1a, MMX3a, MMX3b) were more likely to be those which experienced rock-surface rises and losses across their respective periods, rather than those which recorded only rates of surface losses or rises.

Stations which experienced higher rates of surface change across the study period, also recorded higher standard deviations. This may suggest that rock surfaces with higher rates of loss or gains may result in higher variability of surface change amongst its measured individual points.

In terms of percentage distribution of results with surface lowering rates and those recording surface rise, there was a slight difference between the annual and the individual periods: the whole dataset of mean annual rates revealed 79% of rates with surface lowering trends and 21% with surface rises, whilst the individual periods resulted in a lower percentage of losses (69%) and higher percentage in rises (31%). This confirms that the annual rates tend to mask other individual surface rises.

The variability of annual rates between stations with similar platform position was relatively lower than those obtained for the whole study period due to the omission of rates that could not be used for annual calculations (due to their shorter survey duration), some of which had a high magnitude such as MBB6b, MMX3b, MMX 3c and MPB 1a.

Three spatial trends - one main overall and two secondary ones - were identified for the annual periods: a main trend of surface lowering (in which most rates recorded surface losses), a variable secondary trend of gains and losses (in which stations recorded surface rises and surface lowering across the study period) and an 'odd one out' secondary trend (in which surfaces behaved markedly different from the other nearby platform stations).

At individual period level, the percentage distribution of surface rises and losses is slightly less pronounced in the middle and front stations when compared with the back stations. At annual scales, an inverse picture was found, with more pronounced percentage losses at front and middle stations. In these cases the percentage distribution of losses is relatively higher when compared with that of the individual periods. This confirms that rises are more captured at individual period level.

The average rate of surface change measured across the individual periods for the different sections of the platforms were as follows: -0.177 mma^{-1} at the front stations, -0.354 mma^{-1} for the middle sections and -0.185 mma^{-1} for the back sections. These three mean values however, hide some singular high values of rates of surface change which have impacted on the resultant mean rates of surface change for each section.

The shore platforms of Ponta tal-Miġnuna, Ponta tal-Munxar and Ponta tal-Qammieħ provided rates of surface change which were extremely variable across the three examined temporal time-frames: annual, semi-annual and individual periods.

Percentage results of surface losses were relatively higher when analysed on an annual time period (78%) than at individual time periods (69%). The percentage results for semi-annual time periods (75%) were closer to the annual time periods. This may indicate more comparability between the two time periods, when compared with the individual time periods. It may also

suggest that annual time periods tend to mask other individual variabilities such as surface rises. The analyses of the rates of surface change based on individual periods have shown that the overall mean rates may mask variability of rates and may lead to misrepresentation of patterns of surface change within the whole dataset. This result has clearly demonstrated the importance to examine rates of surface change at individual period level to have a better picture of rock surface behaviour.

The stations with the largest variability in rates of surface change across the individual measurement periods (such as MPM2b, MPM6, MMX1a, MMX3a, MMX3b) were more likely to be those which experienced relatively more surface rises and losses across their respective periods. They also recorded higher standard deviations, which would suggest that rock surfaces with higher rates of losses and gains may result in higher variability of surface change amongst its measured individual points.

In terms of overall rates of change across the study period, the back TMEM stations were the stations to have an overall record of more surface lowering rates for most stations and less for surface rises. At individual period level, the percentage distribution of surface rises and losses is slightly less pronounced in the middle and front stations when compared with the back stations. At annual scales, the percentage losses at front and middle stations were relatively higher when compared with that of the individual periods. This confirms that rises are more captured at individual period level.

A total of 247 paired MWU tests were undertaken comparing individual rates for front-middle, front-back and middle-back stations at each platform. MWU results were as follows: 49% (HI) for front-middle, 69% (H_1) for front-back and 70% (HI) for middle-back. A total of 95 KWH results were also carried out to compare front-middle-back station rates on an annual and individual period. The KWH results showed 90% of the annual rates had HI results and 89% of the individual rates had HI result. When compared with KWH test, the

MWU tests had a lower percentage of H_1 results. This may suggest that test pairing between specific stations brought out more similarities between stations (hence a larger H_0) than the all-inclusive KWH test. The rates of surface change across stations are statistically different from each other when tested as one group at platform level.

The MWU results confirm that pattern of surface difference between stations dominates more than that for similar surface behaviour. Although some similarities were captured, each station seems to behave independent of its platform position in terms of surface change. Thus the individual rates measured are not determined by the spatial position in which each station is located on the platform.

Twelve individual measurement periods were examined with a total of 292 individual temporal periods. In analysing both the variablity trend across these measurement periods and the sequence of rates of surface lowering and rises, there does not seem to be any defined temporal pattern of surface change. With regards rates of surface lowering versus those of surface rises, 70% of the individual temporal periods recorded surface lowering rates of variable magnitude. A total of 3,943 MWU tests were carried out for paired comparisons of annual, semi-annual and individual periods. The test revealed similar percentage results of H_0 and H_1 for annual and semi-annual comparison and a slightly higher percentage of H_0 reject when comparing individual measurement periods as follows:

i. 504 MWU tests for comparisons between annual rates of surface change recorded 66% of the results rejecting H_0 and confirming differences in the rate of surface change between the annual periods;
ii. 824 MWU tests compared semi-annual rates. 67% (555) of the tests resulted in H_0 rejection as well and confirmed that there are differences in the semi-annual rates;

iii. 1464 paired MWU tests compared annual with semi-annual rates. 65% (i.e. 963 results) had *p* values lower than 0.05 and thus reject H_0 of no differences between the annual and semi-annual rates; and
iv. From the 1151 MWU tests for individual periods, 74% of the results (855) rejected H_0 hypothesis and showed temporal differences between the individual periods. The higher percentage result of H_0 may mean that the individual measurement periods picked up differences in rates which are then converged when calculating rates on a semi-annual or annual time-frame.

A total of 48 KWH tests were used to test out difference between all platforms in their respective front, middle and back TMEM stations. All the front and middle stations resulted in differences in all their results. For the back stations, one result had an H_0 acceptance, suggesting similar rates. When this was tested across three other consecutive individual periods, H_1 result was obtained. Thus the singular H_0 result was considered a chance result.

6.7.2 Rates of surface change of exposure slabs

The main findings are as follows:

i. Rates of surface change on slabs operate differently from those on platform due to physical weathering and pressure release conditions brought by a reduction of the confined pressure;
ii. The rates were markedly high during the first exposure period and subsequently lower during the second and third exposure period. This may indicate an acclimatisation process during the first exposure period and which gradually subsided in the following periods;
iii. The geo-mechanical response to weathering from the Blata l-Bajda slabs in UGLM were markedly higher than that for the rest of the

samples, with fast denudation signs and high rates of surface losses during the first exposure period;

iv. Other UGLM slabs, at Ras il-Fenek has much slower responses, conditioned by the hard ground beds covering the UGLM exposures of the platform;
v. The LGLM limestone block has very slow rates of surface change compared to the natural rock surfaces and thus comparisons of limestone deterioration studies need to be handles with caution;
vi. There were no temporal similarities between each exposure period although Ponta tal-Munxar recorded more temporal similarities than the rest of the platforms;
vii. No differences of overall mean rates of surface change were observed when slabs were tested according to a front and back position. Thus the cross-shore position of the tested slabs does not influence the resultant mean rates of surface change; and
viii. Statistical comparisons of datasets based on individual measurement results yielded more statistical differences (H_1) than when the overall mean of the datasets were compared. This may indicate that mean rates of surface change may belie significant levels of variability of surface change which are measured at individual point level.

7 Discussion

7.1 Research hypotheses recalled

The previous three chapters have presented in detail the findings of this research based on four main hypotheses strands: the morphological landscape (form), the geo-mechanical properties of their rock exposures (control), the rates of surface change and their related measurement approach (method). These four strands addressed the key hypotheses framing this research which are being reproduced in Table 7.1. The next sections discuss the connections between the different sets of findings and also their relevance within the context of international research on platform studies.

Table 7.1: The originally formulated hypotheses, covering the main research themes presented in this thesis (Source: Developed by Author)

Research Theme	Hypothesis	
Geomorphological features	1	Globigerina shore platforms share common geomorphological features, primarily inherent of their geological characteristics
Mineralogical and geo-mechanical properties	2	Globigerina shore platforms share similar properties of surface hardness
	3	Surface hardness on Globigerina shore platforms is subject to spatio-temporal variability
	4	Globigerina shore platforms consist of a limestone lithology susceptible to similar rates of weathering
	5	The mineralogical properties of the Globigerina shore platforms influence lithological control and rates of surface change
Rates of surface change	6	Rates of surface change are directly related to cross-shore spatial dynamics across each platform
	7	Rates of surface change on each platform are influenced by temporal parameters
	8	Platforms share common spatio-temporal patterns of surface change

7.2 Morphological features and their spatial context to infer surface processes of change

The field observations presented in Chapter 4 provided a detailed account of the erosional and weathering assemblages present on each platform. Table 4.2 illustrated how the nature and extent of the observed surface forms changed spatially and were primarily diversified by the coupling mechanisms between site-specific structure, *in situ* lithological controls and locally dominant processes. The main conclusions reached from all the observations of morphologically forms were mainly three:

i. The five studied platform exhibited varied morphological landscapes with localised morpho-dynamic responses to processes of change and resultant surface forms;
ii. Erosional forms are more site-specific and restricted in spatial extent and their distribution is dependent on the platform structure (and how this structure creates differing exposures to wave action) and lithological control in creating beds of variable resistance, determining surface roughness and generating coarse material for abrasive action; and
iii. Weathering forms, on the other hand are less spatially restricted although the front and middle sections of the platforms present a larger variety of weathering forms than the back sections of the platforms and this is partially determined by the effect of wave splashes and sea spray deposits.

Although it may not be possible to definitively relate control-process-form to each observed form without specific observations of each process (Stephenson, 2000), the observed surface form provide an important meso-scale context against which to infer and explain the rates and modes of surface change measured at each site with the TMEM.

All platforms were observed to lie within the vicinity of well-identified fault systems, which primarily trended in the WSW-ENE direction (Figure 4.2).

Platform properties, such as gradient, elevation and exposure have all conditioned differently the degree of exposure to processes, in particular the position of the platform surfaces in relation to contemporary sea level and prevailing wave action. Field studies have noted how the investigated platforms (with the exception of Ras il-Fenek) combine both sloping and sub-horizontal surfaces, as observed in other studies such as by Chelli *et al.* (2010), Chelli, Pappalardo and Pannacciulli (2012) and Kennedy and Dickson (2006).

Structure surely conditioned erosional effectiveness to a certain extent, with some of TMEM stations recording relatively larger surface lowering rates independent of their cross-shore position; - such as MPQ 2 (middle) and MMX3b and 3b (back) - which were situated along the scarped seaward edges facing prevailing wave exposure. Trenhaile (1980, 1999) in fact argue that the susceptibility of platforms to wave attack is determined also by how strike and dip are oriented relative to the direction of wave approach.

This argument however does not explain the surface lowering rates measured in other similarly positioned stations such as MMX2 and MMX6: they actually recorded mixed results of very low rates of surface lowering or surface rises (Table 6.2). It was however observed how site-specific structure has protected the platform of Ponta tal-Munxar against direct wave erosion (Figure 4.8). The dipped bed to the south, with its highest seaward edge in a prominent strike parallel to the dominant wave approach (NE) may have provided more protection from the direct erosional impact on waves, as explained by Naylor and Stephenson (2010). Yet, some of the 'less exposed' MMX stations located at the lowest end of the dip (away from direct wave action, but still in close proximity to the shoreline) still recorded relatively higher rates of surface lowering.

Elevation and proximity to wave action surely impacted on the rates recorded by some stations. For example, MRF 1a was installed at the lowest section of the platform and thus strongly subject to incoming wave action. The

high rates of surface lowering recorded over just one individual time period, show the differences in wave exposure between this part and the remaining elevated parts of the platform which recorded much lower rates of surface lowering. A slightly different situation was observed at the front stations of Munxar platform: the front stations of MMX1b, 3b and 3c were similarly positioned very close to the shoreline (but not directly exposed to prevailing wave action) and still recorded higher rates of surface lowering nonetheless (Table 6.2). However, the rates of MMX5b (also close to shoreline) recorded mixed results, suggesting variability of surface change across stations.

Lithological efficacy may seem to have an effect larger that the spatial dimension. For example, MRF2a, though found at an elevated position on the platform (front section), was installed on UGLM exposure which is not covered by hardground bedding and thus is less resistant to processes of change. In fact the exposure block of Ras il-Fenek no. 6 (taken from the front part) recorded higher denudation losses in the exposure experiment (Table 6.35) when compared with other samples from the same platform. The same argument of lithological efficacy may be attributed to the back stations of Blata l-Bajda (MBB 6a and 6b), the back stations Ponta tal-Miġnuna (MPM3a and 3b) and the front stations of Ponta tal-Munxar (MMX1b, 3b and 3c. These stations, irrespective whether of their elevation and exposure all recorded relatively higher rates of surface lowering (Table 6.2) and exposure samples from such platform positions also recorded substantial denudation losses (Table 6.35). Surface hardness at these stations provided mixed results with relatively lower R-values for MBB6 and MMX3, but then relatively higher for MPM3 and MMX 1 (Table 7.24). The difference in R value between the two sets was not observed to be substantial though.

The presence of specific surface forms point to the combined role of lithological control and structure in incrementing rates of surface change: such as the development of scarps formed by step erosion located at seaward edge with exposed contact points between two units in Globigerina i.e. either

between hardground/phosphate bed and the LGLM (Munxar, Qammieħ and Miġnuna platforms) or hardground/UGLM/hardground in Ras il-Fenek. Such lithologically-controlled step erosion was also observed by Causon Deguara and Gauci (2017) on the south-east coast of Malta, who reported how exposed but receding seaward scarps were formed along the contact point between LGLM and LCL beds. The presence of step-backwearing scarps and the higher magnitude of erosion rates of MPQ 2 (positioned at the foot of the scarp) confirm how the spatial occurrence of erosion is localised to these site-specific areas. They are largely ascribed to a combined work of structure, lithological resistance and exposure to wave action. These are bound to vary within the spatial extent of the platform and would account for one of the main reasons why rates of surface change behaved in non-homogenous spatial patterns throughout the study period.

Another example of localised erosional forms resulting from the combination of elevation, lithology and exposure, are marine potholes, observed only at Ponta tal-Qammieħ. The landward extent of pothole formation in relation to site-specific processes and controls should therefore not be underestimated. Unfortunately, no TMEM stations were located close to these potholes but the presence of these forms confirm how measurement of surface change on these surfaces may necessitate to adopt a less standard systematic sampling and be more site-specific in setting up TMEM stations. Specific research on these erosion forms is absent on the Maltese Islands and still very scant and not recent at international level (such as Elston, 1917; Wentworth, 1944; Abbott and Pottratz, 1969 amongst the most cited works). Recent studies such as by Cooper and Green (2016) have reported their occurrence at supratidal levels and may infer important dynamic processes over such surfaces.

Though lithologically similar, the platforms of Ponta tal-Qammieħ, Ponta tal-Munxar and Ponta tal-Miġnuna were found to be diversified by the presence of discontinuities forming joint bounded blocks, even on areas where subaerial

weathering dominates their morphology. In studies such as Trenhaile and Kanyaya (2007), Kennedy, Paulik and Dickson (2011) and Cooper and Green (2016) boulder–strewn perimeters were not ascribed to the occurrence of a weaker lithology but rather to a combined effect between joints and higher exposure to wave action. This is particularly the case of Ponta tal-Mignuna, where the jointed part of the platform is found in thicker conglomerate beds and thus is more lithologically resistant to direct wave action than other areas on the same platform. Field studies with SH results confirm and recorded higher R values and UCS results the outer parts of the platform (Table 5.8). Due to more lithological resistance, the rates of surface change of the TMEM stations in the heavily jointed exposed area (MPM4, 5, and 6) were relatively lower than the those in the more sheltered less jointed area (MPM 1, 2 and 3) (Table 6.2). Wave action in this exposed part of the platform resulted more effective in dislodging blocks along these joints but not in producing higher erosion rates at TMEM stations level. This confirms once again how lithological efficacy had a more dominant effect over structure and exposure in the rates of surface change.

Other signs of a dynamic wave environment included dissected limestone pavements due to eroded joints, blowholes and internal collapsed features along the main discontinuities at l-Blata l-Bajda platform. However, these were also signs of a weaker geological structure of the UGLM. Surface hardness at Blata l-Bajda was observed to be relatively lower, with the rates of surface change at the back stations relatively higher (MBB3 and MBB6). However they were also relatively high on other platform positions: MBB1 and MBB 4(front) and MBB5 (middle). With these results indicating no cross-shore patterns both in surface hardness and rates of surface change, it is difficult to separate the effect of wave action from lithological efficacy. It can be safely said however that lithological control does not operate as a constant on these surfaces.

This study has collected evidence of how salt and related forms of sub-aerial weathering have contributed to create morphologies at supratidal level

which were distinct at each platform and were determined by the interplay between sea water inputs (from wave splashes and sea spray), atmospheric conditions, structure (elevation, gradient and discontinuities) and lithological controls (surface roughness and strength).

Though the specific role of weathering processes, and how they interact synergistically to create forms, remains elusive (Robinson and Moses, 2011). Authors such as Stephenson and Kirk (2000b) have shown that weathering may reduce the compressive strength of the rocks by as much as 50% and thus can make platforms more susceptible to erosional processes. In this study, the elevated surfaces outside the direct reach of wave action, but within the splash zone, were dominated by weathering forms such as pitting and solution pools. This was observed to be a common characteristic on all the elevated surfaces within the splash zone independent of the lithological unit.

It was observed how these features, especially solution pools, are restricted mostly in the front and middle part of the platforms, and they disappear above the level which is not reached by wave splashes. The presence of these forms would indicate that the rates of surface change are mainly influenced by dynamic interaction between sub-aerial weathering and episodic wetting by wave splashes and then this interaction would decrease further landward. Sea spray seems is considered not enough to produce wetting conditions. Kennedy and Dickson (2006) reported that active downwearing or lack of cycles of wetting and drying would inhibit the formation of such pools. Trenhaile (1987) also considers high evaporation levels as a significant role in this mechanism. Thus rock surfaces within these areas would therefore be susceptible to similar processes with rates and modes of surface change dependent on the occurrence, intensity and sequence of wave splash wetting and evaporation drying events.

Many authors agree that weathering is an important pre-condition to the effectiveness of erosion (Robinson and Moses, 2011). In this case, on three platforms the resultant weathered forms contributed to the release of rock

material which potentially acts as abrasive material whilst being transported mainly by winds in a landward direction across the platforms. This process was particularly evident in various forms, such as follows:

i. Coarse-clastic pockets of fine gravel sediment transported and deposited along the cliff platform junction at Ponta tal-Qammieħ (Figure 4.11);
ii. Fine silt/rock powder pockets at Blata l-Bajda trapped in specific corners of the abandoned saline (Figure 4.13); and
iii. Rock powder on the tafoni floor along the cliff face areas of Ponta tal-Miġnuna and Ras il-Fenek and (Figure 4.6 and Figure 4.4).

The size, texture and distribution of material is dependent on lithology, whereby conglomerate is more likely to produce coarse material while the softer exposure of UGLM and MGLM are likely to produce fine rock powder deposits. Clearly, the gravel material may produce more abrasion than the powdery one across the platform, as the lighter material is more likely to be transported in suspension whilst the gravel material may move in surface creep motion. To what extent this may contribute to surface change across the platform is difficult to infer comprehensively. However a few stations such as stations MPQ3 and MPQ6 were observed to have nearby deposits of such material in the vicinity and therefore this study could locate which stations may potentially be affected by such abrasive deposits. Their overall rates of surface lowering are not however substantially higher to infer the additional process input of abrasion (Table 6.2).

In providing a morphological assessment this study has demonstrated how much there is considerable variability in the surface morphology on the studied platforms and this notwithstanding that they belong to the same rock type. Prior to this study, the Maltese shore platforms were generally described as low-lying near-horizontal surfaces, characterised by an outward seaward edge that terminate into a steep scarp (Said and Schembri, 2010). This comparative

study identified much more complex and varied settings and equally complex process-control-form responses at different spatial scales. Insights to platform morphology provided an important context against which other investigations of lithological control and measurements of surface changes can be corroborated in a more integrated manner.

7.3 The role of geo-mechanical properties

7.3.1 Surface rock hardness

In literature there is a general consensus that Schmidt Hammer tests, in recording rock surface strength, are indirectly assessing the state of the surface which would include degree of weathering, moisture content, texture and presence of fractures (Taylor, 2003; Viles *et al.*, 2011; Goudie, 2013, 2016). This research dealt with five Globigerina limestone platforms, formed in UGLM and LGLM in order to identify the factors driving these morphological differences with a comparative analysis of rock surface strength with a Schmidt Hammer test (Chapter 5, Section 5.4).

7.3.1.1 Surface hardness properties

The SH findings confirm the extent to which rock surface resistance to erosion is determined primarily by surface hardness as an investigation parameter in its own right rather directly related to a specific rock type. Table 5.5 presented the mean *R* value for the five selected five platforms and which ranged from 24.02 $\pm$ 1.78 (Blata l-Bajda, Transect 1) to 36.8 $\pm$ 3.53 (Ras il-Fenek, Transect 1) (Section 5.4). Based on the ISRM (1978) Schmidt hardness classification, their rock exposure belongs to the 'slightly strong rock' category for R values (20-40 class). As a biomicritic limestone, the resultant R values aligned comparatively well with those of other *in situ* limestone exposures in several published studies, such as 34.2 for biocrimitic limestones (Day, 1980), 29 for reef limestone in micro-tidal conditions Bjärget, Sweden (Cruslock *et al.*,

2010), 28.5 and 31 for limestone platforms in micro-tidal Kaikoura (Stephenson and Kirk, 2003 and Taylor, 2003 respectively). Chelli *et al.* (2010), on the other hand, reported a wider range of R values i.e. from 39 to up to 53, for the limestone platforms situated in the micro-tidal Gulf of La Spezia (Italy). This spread of mean R values seem to confirm the variability of limestone surface hardness, previously reviewed across many studies by Guney *et al.* (2005) and Goudie (2006).

The results for density (Table 5.5) suggest that limestone exposures are typical of the soft limestones with low densities: from 1.3 at Blata l-Bajda to 1.8 at Ras il-Fenek. These results placed at the lower end within the limestone category when compared with other density results obtained for limestones outcrops; for example, Ersoy and Waller (1995) (2.23) and Yagiz (2011) (2.3) on soft limestones, or Sopacı and Akgün (2016) (1.8 to 2.0) for karstic limestone. The analyses of the surface hardness properties of the five selected platforms lead to the following expectations in terms of rates surface change:

i. The variability in surface hardness on the conglomerate and hardground surfaces as measured with the Schmidt Hammer would explain the variability in the rates of surface changes measured with the TMEM;
ii. The relatively highest R values of Ras il- Fenek would explain why the measured rates amongst the lowest in the dataset;
iii. The coarse grained surface of Ras il-Fenek would explain the variability recorded not only by the Schmidt Hammer but also by the rates of surface change; and
iv. With Blata l-Bajda recorded the lowest R values from the dataset, the relatively higher rates of surface change measured with the TMEM can also be confirmed.

The strongest evidence of this, produced by this study, was the fact that though both Ras il-Fenek and Blata l-Bajda platforms are both attributed to

UGLM, the mean R value results to be variable by more than 12 units, with the hardground laminates responsible for a higher mean R value result. The R values obtained for the conglomerates/hardground platforms are Ponta tal-Qammieħ (thickly developed conglomerate), Ponta tal-Miġnuna (thinly developed conglomerate) and Ponta tal-Munxar (non-homogenous hardground only) are not so distant from those published by Özbek (2009) for clast-supported conglomerates (34-38). The surface hardness findings were also mirrored by the results of the exposure experimental results, with the samples of Ras il-Fenek and Blata l-Bajda exhibiting the lowest and highest rates of susceptibility to weathering (Section 5.5).

7.3.1.2 Surface texture

Another widely reported aspect in the study of rock surface strength is that surface hardness is considered to be also a function of lithological texture (Williams and Robinson, 1983; Goudie, 2006; Viles *et al.*, 2011; Moses, Robinson and Barlow, 2014). The heterogeneous surface observed at a meso-scale on the five Globigerina limestone platforms is a very typical characteristic of sedimentary rocks, in consisting of more than one type of surface and exhibiting alternate laminations or exposed beds of variable strength due to variations in the natural forming processes during depositional stages (Liang *et al.*, 2015). As Dickson (2002) argued, SH results for these type of surface must be assessed conservatively given that smoother and compact surfaces may be more amenable to the technique rather than rougher coarser ones. As discussed in Chapter 4, this study has identified three types of texture forms at meso-scale as follows:

i. the smoother and fine-grained UGLM exposures at Blata l-Bajda;
ii. the rougher and coarse-grained hardgrounds laminates at Ras il-Fenek; and
iii. the irregular but rather non-homogenous (hummocky-type) surfaces of the hardground/conglomerate beds at Ponta tal-Qammieħ, Ponta tal-Miġnuna and Ponta tal-Munxar.

The wide scatter of rebound values, presented in Chapter 5 (Section 5.4) is considered as an expected outcome when rebound tests are conducted *in situ* due to the presence of weathering states, weakness planes and variation in the surface structure (Sheorey *et al.,* 1984). In this study, the above-described surface heterogeneity has two mean effects on the readings. The first one is related to the highest levels of mean SD results produced by three conglomerate bed platforms. The second outcome is related to the mean SD values of Ras il-Fenek platform, which were also amongst the highest values due to the coarser texture produced by the hardground bed at Ras il-Fenek. Coarse-grained surface are in fact acknowledged in literature to produce a wider scatter of rebound values (Aydin, 2009).

However, the variable effects observed at Ras il-Fenek and at the three hardground/conglomerate platforms are conditioned by different mechanical causes. The rebound variability at the first three platforms would have been conditioned by the fact that the conglomerate exposure is a non-homogenous surface, and therefore the plunger impact may have been weakened by a surrounding non-visible void present at various test points. Rebound values are also known to vary on conglomerates as the latter constitute a combination of large pieces of aggregate and softer matrix (ASTM, 2014). Özbek (2009) also demonstrated that conglomerates do not behave as a linear elastic medium but rather as an anisotropic mass (with anomalies in their physical behaviour) depending on rock property differences such as their clast matrix or sediment imbrications. This in turn produces different R values depending on the original depositional direction of the material. This finding confirms that SH values are influenced by the rock properties which extend below the surface (Hack and Huisman, 2002).

In the case of Ras il-Fenek, the rough coarse-grained surface at micro-level would have minimized the contact point between the rock and the plunger point and thus weakened its impact. As Hucka (1965) explained, *in situ*

measurements are based on an imperfectly elastic impact between the mass of the test hammer and the solid face of the rock. Irregularities of the rock surface affect that impact. In fact Viles *et al.* (2011) reported surface irregularities are often also crushed before the plunger tip reaches the rock surface, resulting in some loss of impact energy and this my account for the variable SD values recorded at Ras il-Fenek. Aydin (2009) also explains how in coarse-grained materials, grains with sizes comparable to the plunger tip diameter may significantly deviate from the average, depending on their strength relative to the matrix or dominant grain size.

Lithological variability in surface exposure within the same platform was also observed on two accounts. The first was that the three hardground/conglomerate covered platforms backed by Middle Globigerina Limestone cliffs are relatively softer compared to the underlying platform beds. The transition to the MGLM is not sharp at the cliff-platform junction but rather the member start to gradually transit from one of two meters at the back of the platform. It was observed that this lowered the R value by a few units and so potentially obfuscating any cross-shore pattern. An evidence of this came out also in the cluster analysis (Chapter 5, Section 5.4.6) when the mean R values of MBB4 (Blata l-Bajda) paired up with those of MPQ 3 and MPQ6 (Ponta tal-Qammieħ), which are the back stations closest to Middle Globigerina cliffs).

Secondly, at Ras il-Fenek, there were exposures of weathered UGL with the removal of the hardground cover at one test point close to MRF2. This recorded lower *R* values (within the range recorded at Blata l-Bajda) and simultaneously widened the range of R values recorded. This latter result was not enough to distant significantly the overall mean R values between the two transects and the level of the resultant mean SD values in relation to those for the rest of the platforms. Nevertheless, it is yet another evidence of how much surface hardness is controlled by the lithological variability at platform scale, and that it would be misleading to attribute a whole platform to one single rock unit.

The third outcome is that the mean SD values of the above-mentioned four platforms are however still comparatively high when compared to the smoother surfaces of the Blata l-Bajda platform. This latter platform had the lowest mean SD values, in line with also its lower mean *R* values. The plunger impact left more visible marks at the test points, which indicates that weaker surfaces are present at Blata l-Bajda. In addition to being lithologically weaker, the marks were evident signs of some minor surface crushing which may have lowered the R value (Viles *et al.*, 2011).

The above three outcomes pull out another important conclusion i.e. that the mean SD values provide a better representation than the mean R values in assessing how surface heterogeneity impacts surface hardness readings, especially when studying lithologically similar platforms, as postulated by other scholars such as Aydin (2009) and Hebib, Belhai and Alloul (2017). As explained earlier, this study found that lithological surface heterogeneity between and within platforms has influenced measured rates of surface change.

7.3.1.3 Wetting conditions by waves

The *in situ* wetting conditions by waves and how they may influence surface hardness and related processes of surface change were also examined in this study. The SH test is reported to be sensitive to moist surfaces especially in weaker rocks (Sumner and Nel, 2002) or weathered, porous, loosely cemented rocks (Aydin, 2009). In this study, no statistical correlation was found in surface hardness along the cross-shore direction from the low tide cliff to the cliff line in the ten transects delineated. Though it is widely acknowledged in the literature that moisture affects surface hardness, a number of studies have similarly not found a correlation between moisture and *in situ* surface hardness such as in studies by Kennedy and Beban (2005), Kennedy and Milkins (2015). Studies that have found cross-shore spatial patterns attributed these findings to processes (some of them combined) of weathering, abrasion or bio-erosion rather than to moisture *per se* (Dickson, 2002; Blanco-Chao *et al.*, 2007; Chelli *et al.*, 2010).

In the context of this study, the findings can be explained in various ways. The first explanation is that the range of hardness values may have not been varied enough to be bring enough statistical differences between the front shore and the back shore areas. No test point was taken below the spring tide level at each platform. Chelli *et al.* (2010) and Causon Deguara and Gauci (2017) also reported such a procedure in delineating the boundary of their investigation on micro-tidal platforms. Due to the small tidal range (0.206 m during spring tide and 0.046 m during neap tides as per Drago, 2009), spring tide level was normally lower than the lowest elevation required at each investigated platform. This would have restricted the likelihood of testing rocks which are continuously moist during the winter season in the front section of the cross-shore profiles.

Due to the very small tidal range, Maltese shore platforms are more likely to be exposed to wetting conditions only through incoming storms waves or frequent wave splashes at best in the front sections. The wave regime is predominantly the result of wind-generated wave action rather than long-period swell (Malta Maritime Authority, 2003). Storm-generated waves generally occur from September to March (Galdies, 2011). A study by Drago *et al.* (2013) found a strong seasonal pattern, with the majority of wave energy concentrated during the six months of winter from November to April. Drago *et al.* (2013) reported mean offshore significant wave height of 1.22 m over a period of one year and 1.92 m for the winter season. Causon Deguara and Gauci (2017) reported significant offshore wave heights during storm events between 20/09/11 and 13/05/2013 which reached highest maximum between 5.75 m and 7.75 m and which come from variable wind directions.

With regard to inshore waves, Sammut *et al.* (2017) reported storm waves events during 2014 which were calculated through SWAN modelling to have generated inshore maximum wave heights ranging from 0.42 m to 2.84 m. It was observed that offshore waves decrease in height as they propagate towards inshore areas of the Maltese Island and change direction due to inshore

refraction caused by bathymetric variations and diffraction by coastal configuration. Variability in inshore wave dynamics was also confirmed by recent study done by Pace *et al.* (2017) in which they found clear differences in inshore wave climate amongst four NE sites of the Maltese Islands despite these sites shared similar geo-morphological characteristics and depth ranges (with the area of Selmun being one the study areas). Similar conclusions about wave energy dissipation through shoaling and refraction were also reported in other parts of the world, whereby offshore waves decrease in height and dissipate energy before reaching the platforms (Stephenson *et al.*, 2004; Marshall and Stephenson, 2011).

The second reason is linked to the wave dynamics that operate at supratidal levels on Maltese shore platforms. Generally, it was observed that, at supratidal conditions, most of the waves break on the low-tide cliff at the seaward edge of the sub-horizontal platforms during all micro-tidal stages, and thus most of the platform surface is exposed more to atmospheric conditions than to marine ones by direct wave action. The site characteristics of the seaward edge of the platforms have an important controlling role in delimiting the wetting effect by incoming waves (Kennedy, 2016). The platforms of Ras il-Fenek and Ponta tal-Miġnuna have low-tide cliff perimeters which range from 1 to 4 m above sea level, whereas the seaward edge of Ponta tal-Munxar (0-2 m) is aligned against the prevailing wind-generated waves.

The third reason may be linked to the fact that moisture content of the rock depends on its microstructure. Rocks with a higher permeability are more sensitive to the moisture-induced effects of inter-grain sliding which cause softening of grains and loosening of plasma grain-holding ability (Aydin, 2009). The level of permeability of the platform rocks may not have been high enough to create contrasting conditions of moisture between the front relatively wetter parts and back drier parts of the platform. Though pitting and solution pools were frequent features on the front parts of the studied platforms, they are mostly attributed to irregular events characterized by storm-wave driven

wetting and subsequent prolonged drying periods rather than a sign of some permanence or regularity of wetting processes.

All the above findings may imply that waves play a variable role at a local scale and, as a result, the process-form dynamics examined one platform may not necessarily apply to another. This study has demonstrated that the wetting dynamics on the Maltese shore platforms are driven by variable wave conditions, dependent on the occurrence, intensity and direction of storm-generated waves and, on the other hand, controlled by platform elevation in relation to minimal tidal range, their orientation to incoming waves, coastal configuration and surrounding bathymetry. Prevailing winds affect the extent of the sea-spray distribution and evapo-transpiration rates (which are quite high due to prolonged rainless Mediterranean days).

It is for this reason, therefore, that patterns of surface change can vary on lithologically similar platforms. The differences in surface hardness between temporal periods were also not found to be statistically significant and thus seasonal fluctuations in temperature do not significantly alter the surface hardness of the platform. This result seem to fit with the conclusions by Day (1980) who concluded that temperature has no appreciable influence on R values. The SH test has nonetheless enabled quantitative comparisons to be made across the lithologically-similar platforms and assess the surface hardness variability within and between Globigerina limestone platforms. It demonstrated the relationship between surface hardness and the measured rates of surface change presented in Chapter 6.

7.3.2 Lithological susceptibility to weathering

As explained in Section 3.5.2 and Section 5.5, this experimental study was carried out to observe the effects of the weathering process on a set of limestone slabs extracted from the front and back sections of the five studied platforms. This study used a simple methodology based on exposure trials,

micro-catchment and non-destructive analyses. SH data indicated a lithological variability of the surface hardness on each platform exposure (Table 5.5). Used in combination with this weathering experiment, a more detailed comparison of each rock exposure facilitated the understanding of the properties of each rock exposure respond and ultimately is altered by weathering mechanisms.

The significance of the results reported in Chapter 5 (Section 5.5) lies not so much in the actual observed values, although they are important in illustrating the range of losses experienced by the exposed slabs, but rather in demonstrating how varied and complex the responses of the exposed Globigerina slabs were over various time-scales and at platform scale. There were similarities and differences in these responses, with some more complex than originally expected. The weathering data was positively skewed, with a fairly small proportion of the rock samples experiencing rapid breakdown (mostly Blata l-Bajda samples) whereas the majority of the slabs experienced a slower but varied response. Ras il-Fenek slabs were considered the more durable platform rocks, recording a very slow rate of weight and debris loss, whilst other platforms such as Ponta tal-Munxar showed mixed results, suggesting localized variability in rock properties at platform scale.

Similar to Goudie (1999), the average percentage weight loss in this study was used as one of the prime determinants in ranking the slabs according to their weathering grade. As seen in Table 5.15 (Chapter 5) and here in Table 7.2, the rate of weathering on a spatial level recorded Blata l-Bajda slabs as the ones most responsive to weathering (with much higher losses than originally anticipated), whilst those of Ras il-Fenek and the LGL slabs were the least responsive in their alterations. On a temporal level, the heavy losses of weight loss and material debris were mostly observed during the first exposure period (Table 7.2).

The weathering experiment results, especially in terms of percentage weight loss, mirrored well the findings of the SH test on a number of levels.

Firstly, the weathering results presented in Chapter 5 (Section 5.5) confirmed the difference in surface hardness between the two UGLM platforms of Blata l-Bajda and Ras il-Fenek. The SH results provided the lowest R value for the rock exposure of Blata l-Bajda and the weathering experiment confirmed the weaker signature of these slabs as they were the ones most susceptible to weathering by breaking down comparatively quicker than the rest of the exposed samples. Conversely, the highest R values recorded at Ras il-Fenek were reconfirmed in the weathering experiment by recording the slowest response to weathering. Only one slab recorded a higher percentage of weight loss (18%) and it corresponded to a front slab where the hardground is relatively thinner, more weathered (as demonstrated by the individual R value results in Section 5.4.1). In being less compact, this UGLM rock slab was similarly susceptible to weathering as the UGLM slabs of Blata l-Bajda platform.

Table 7.2: Mean and range of R values recorded in situ by the Schmidt Hammer and the sample weight loss recorded in the exposure experiment.

Platform-Transect	Mean	Range	Std. Deviation	Total Sample Weight Loss of each sample		
				%	%	%
Ras il-Fenek Tr1	36.78	14.79	3.53	0.62	0.76	18.66
Ras il-Fenek Tr2	36.66	12.28	3.03			
Ponta tal-Miġnuna Tr1	33.77	13.05	2.92	11.86	7.85	1.51
Ponta tal-Miġnuna Tr2	31.49	12.92	3.07			
Ponta tal-Munxar Tr1	32.73	12.01	2.59	14.92	4.01	30.66
Ponta tal-Munxar Tr2	33.81	12.36	2.63			
Ponta tal-QammieħTr1	29.72	15.67	3.77	14.70	12.69	
Ponta tal-QammieħTr2	30.39	15.25	3.84			
Blata l-Bajda Tr1	25.38	9.97	2.08	21.41	94.86	45.37
Blata l-Bajda Tr2	24.02	7.97	1.78			

The relative positional ranking in terms of surface hardness for Ponta tal-Qammieħ, Ponta tal-Munxar and Ponta tal-Miġnuna reflected in a likewise positional ranking in terms of denudation rates for their respective exposure slabs (Table 7.2). However, some anomalies were also recorded such as the

relatively higher weight loss (30.66%) for one of the slabs at Ponta tal-Munxar (Sample no. 8, Front) or the relatively low weight loss for one of Ponta tal-Miġnuna slabs (Sample no. 13, Front). The reason for such anomalies may be related to having selected weaker or stronger specimen for the experiment; this may be a possibility as both platforms exhibited a variable range of surface hardness as demonstrated in the range and standard deviation results (Table 7.2). This does not seem to apply to the Ponta tal-Qammieħ samples, which exhibited more or less similar loss of weight from August 2015 to August 2016, even though their range and standard deviation results of surface hardness are the highest from the whole dataset. The weight loss results also tie in with the cluster analyses results according to surface hardness, which distinguished Blata l-Bajda, Ras il-Fenek and Ponta tal-Qammieħ as distinct platforms and grouped together Ponta tal-Miġnuna and Ponta tal-Munxar on the basis of similarity in both having a variable nature.

The weathering mode was also very different, with the slabs of Blata l-Bajda powdering heavily and splinting rapidly, whilst the rest of the samples manifested much slower mechanical changes, with the slabs of Ras il-Fenek showing very minimal signs of visual signs of disintegration (Section 5.5.1). These variable trends exhibited by the Globigerina limestone members in an experimental setting are not very different from what was observed in limestones in other studies such as by Smith *at al.* (1995), Goudie (1999) and Nicholson (2001). Though the experiment techniques were slightly different from the one in this current study, both cited studies concluded that different types of limestone have a wide spectrum of relative resistance to weathering and that their durability is affected by factors such as modulus of elasticity, water absorption capacities, density, salt uptakes and pore structure.

It is also important to explain the behaviour of the rock properties in the context of the weather parameters to which the rocks were exposed. This was also reiterated by Nicholson (2001) who observed that, apart from a variable resistance to weathering, the studied limestone types also exhibited difference

in resistance to particular weathering processes. In the case of the limestone slabs used in this study, it is worth pointing out the following weather conditions to which the limestones were exposed:

i. The first exposure period - February to August 2015 - recorded an unusually higher rainfall record in February 2015 (112.8 mm). This month alone totalled the highest amount of rainfall for the whole experiment period (See Section 5.2). March 2015 and August 2015 also had a higher than usual rainfall records and as a result, the first exposure period recorded a total of 238.4 mm of rain out of an annual total of 554 mm i.e. of 43% of annual rainfall. In terms of number of rainy days it was 50 out of an annual record of 95 days i.e. 53%;
ii. The second exposure period – (end) August 2015 – August 2016 was characterized by a drier rainfall regime which dominated the 2016 year, with not more than an annual total of 324.8 mm (42% less than the annual norm). This meant that during the second exposure period (12 months), the total amount of rainfall was of 380.8 mm, with months of January 2016 to August 2016 characterized by only 114.6 mm of rainfall (30% of rain for the whole study period); and
iii. The year 2015, apart from recording relatively higher rainfall trends, had also experienced RH levels above the 75% in March (81.9), April (75.5), October (75.4), November (78.5) and December (80.4); and
iv. The year 2016, apart from being the driest year, also recorded higher values of temperature both in terms of minimum and maximum temperature regimes, especially from January to April 2016.

A number of consequences resulted from this weather trend in terms of weathering effects. First, the weathering rates during the first exposure period were dominated by torrential rainfall that would have exposed the slabs to heavy amounts of wetting and moisture movement. This weakened the exposed

slabs but particularly those with the highest water absorption capacity, as water in this case was responsible in accelerating the weathering processes during the first exposure period. The heavy weight and debris losses sustained in the first exposure period seem to indicate that the Globigerina slabs are particularly prone to breakdown in association with the absorption of water. Cabello-Briones and Viles (2017) similarly reported that exposed Globigerina slabs were particular sensitive to weathering and that dissolution of limestone in rainfall was considered to be one of the main causes of deterioration when the limestone was exposed in the wet temperate climate of Witney, UK.

The successive occurrence of a relatively drier and warmer 2016 may have however weakened the slabs through a different set of weathering processes related to prolonged desiccation, higher temperatures and resultant wider thermal fluctuations. Temperature is considered to be a significant control on mechanical rock breakdown, with laboratory evidence pointing towards positive links between high temperatures and rock fatigue, due to continuing expansion and contraction of fissures and pores (Warke and Smith, 1998; Mottershead, 2013; McAllister, Warke and McCabe, 2017) and rates of salt crystallisation (such as by Goudie, 1993). A major factor in controlling thermal conductivity in sedimentary rocks is the high variability of porosity as porous rocks can retain surface cooling for longer times than quick drying less porous ones (Coombes and Naylor, 2012). Various studies have confirmed the high porosity of the Globigerina Limestone (Rothert *et al.*, 2007). Specifically on thermal-induced changes, Franzoni *et al.* (2013) did not find significant changes in the mechanical properties (especially pore size distribution) of the LGLM and attributed this to high porosity which allows deformation of calcite crystals without causing stress in the stone. Thus high temperatures as a stand-along weathering agent does not produce dramatic weathering changes and this may be partially the reason for the recorded slower rates of change of the exposure slabs during the second exposure period, which was characterised by higher temperatures values and lower rainfall input.

The weathering patterns experienced by the slabs would have resulted from the interactions between a variety of weathering processes but also in relation to inherited properties of saline conditions from the coastal platforms. Sea water is a mixture of five salts, although studies have shown that NaCl is the most dominant in coastal weathering (Mottershead, 1982; Robinson and Williams, 2000). Though marine salts do not reach supratidal platforms through direct wave action, coastal salt deposition can still reach onshore through a number of factors such as episodes of high winds, high surf, and precipitation which delivers salt to coastal sites. Though such quantified studies are not available locally, the salt-tolerant angiosperm *Inula crithmoides* (Golden Samphire) (which grows also under the influence of sea spray), is considered as an indicator of the inland limit of the coastal zone and is reported to grow kilometres inland (Schembri, 2003; ERA, 2012a). This would imply that the studied platforms may be well within the range of being exposed to maximum values of salt deposition.

What is relatively still unknown is whether there are variations in the salt content across the different globigerina platforms (and if so, to what extent). Salt crystallization is recognised in various studies as the main weathering process in LGLM building stone (Cassar, 2002; Rothert *et al.*, 2007) but it has rarely been examined on other globigerina exposures and in states other than quarried building stone specimen. This appears to represent a gap in current knowledge on globigerina rock and reflects a wider situation in which there are still limited observations how salt content of coastal rocks vary in different lithologies or with varying degrees of exposure (Mottershead, 2013).

The first exposure period was presumably the period in which the slabs may have held variable amount of coast-derived salts depending on their surface hardness and resultant porosity. This period, with high rainfalls and high humidity, may have accelerated dissolution in some of the most porous samples due to a higher degree of salt saturation. From the weathering grade results obtained, it was clear that the mechanical properties of Blata l-Bajda

slabs were the most sensitive to these processes and conducive to weathering, with an observed rapid reduction of density, hardness and strength of the rocks. The visible fractures that were observed to have developed would have exacerbated water intrusion rates, porosity and thus accelerated the dissolution process. On the other hand, slabs such as those of Ras il-Fenek, exhibited a more durable surface that was less conducive to developing similar fractures and thus inhibited further water intrusion, and related dissolution process. At this stage however is difficult to detach the effects of wetting and drying from salt weathering as porous limestone are rarely free from water containing salts in marine setting (Robinson and Moses, 2011).

The denudation behaviour between the LGLM block and the platform was found to be strikingly different. As reported such as by Cassar (2002) and Cabello-Briones and Viles (2017), it withstood exposure comparatively well, slowly acquired a darker yellow shade, kept a relatively resistant surface and experienced little weight loss. Reports of increase of surface hardness of LGL blocks were recently reported by Cabello-Briones and Viles (2017) in their deterioration study of exposed LGLM samples in the outdoor conditions of Hagar Qim temples. This comparative aspect proves the extent to which the properties of LGLM building stone (Franka) respond differently to weathering when compared to those of the studied platforms and this is another confirmation of the variability within the Globigerina limestone properties. In the light of the different altered responses observed in the limestone samples of the studied shore platforms, it can therefore be concluded with more certainty that weathering studies on the durability of LGLM building blocks do not provide sufficient comparable insights to cover the complex variability exhibited by the globigerina lithology of the selected Maltese shore platforms.

The main causes of Globigerina samples deterioration, as observed in the exposure experiment, were identified to be the combined effect of rainfall, prolonged dry periods to relatively higher temperature, and potential presence of salts (which contributed to the initial physical breakdown and dissolution

during the first exposure period). In literature, such type of combined interaction is acknowledged to create a complex synergistic linkages, which are challenging to detach into singular processes or quantify (Viles, 2013). Though it is still too early to determine which stresses were the most significant in leading to the rapid deterioration of some of the samples, the range of weathering modes, identified in the context of the main environmental stresses, may support the following interpretations:

i. Frequent torrential rains in 2015 caused rapid calcite precipitation and dissolution, the effects of which were examined in various studies on Globigerina Limestone;
ii. Drying phases in between these torrential periods were then causing more repetitive expansion of salts in the rock pores (subflorescence), the latter affect also reported in various studies on Globigerina limestone;
iii. Drying phases in between the torrential rainfall events were potentially causing more complete evaporation and thus exposing the rock to aggressive late-stage brine (efflorescence); and
iv. Prolonged higher temperatures in 2016 were directly creating greater thermal stresses.

In addition to environmental conditions, a second set of variables – more related to the rock lithological properties – may then have determined the relative influence of each of these environmental stresses and accounted for the variable rates of denudation recorded throughout the experimental study; such as the samples of Blata l-Bajda being the most susceptible to these stresses and those of Ras il-Fenek and the LGL block as being the least susceptible.

These initial results provide scope for further geo-technical analysis to provide a clear picture of each weathering effects. In addition to the susceptibility to salt crystallization, sedimentary rocks are also known to be subject to stress relief: where unequal release of confining pressures (in this

case by extraction from the platform surface) of once confined rock exposures can lead to exfoliation and splitting (Smith, 2009). These latter effects were also observed to be relatively more pronounced on the Blata l-Bajda samples but it not clear if they were induced by stress relief, wetting and drying and or a possible combination of both.

To summarize, the preceding discussion has shown how these initial experiment results fulfil the initial scope set out for this experiment: to provide a useful comparison of different responses of Globigerina samples to weathering processes. The occurrence of skewed weather trends over the study period became a chance opportunity in which it was observed how the Globigerina limestone properties responded to a non-linear weather regime which sequentially and cumulatively inflicted extreme effects when shifting from one micro-climatic event (torrential rainfall) to another (desiccation period). The outcomes of this study surely reaffirm the conclusion reached by Smith, Warke and Moses (2000) to look beyond a simplistic climate regime in order to explain the complexity of weathering processes and consider the spatial and temporal variability of micro-climate at the rock/air interface.

Though the results of the weathering experiment were not meant to explain the processes happening on the platform *per se*, they surely demonstrated how much they are governed by lithological units which have differential responses to weathering processes. Despite the complexity of the effects observed, one overriding conclusion that can be drawn up is that the lithological properties of the platforms are distinct enough in defining the relative efficiency of these rocks to weathering mechanisms. Clearly, the different weathering responses amongst the Globigerina slabs warrant more attention, with long-term set of exposure trials to provide a more detailed assessment of the processes of surface change of Globigerina limestone.

7.3.3 The role of mineralogical properties

Mineral content is an important parameter in the mechanical behaviour of rocks, and studies have shown it can influence rock strength and deformability. Different minerals tend to also vary in their susceptibility to weathering (Williams and Robinson, 1983).

As reviewed in Chapter 2, numerous studies on LGLM agree this member exhibits a large variety of weathering patterns (Section 2.7), mainly controlled by the mineralogy and/or geochemical composition. The mineralogical picture that comes out of these results is not a straightforward one to link to the morphological and SH results provided in the course of this study. But this challenge in itself provides more scope for investigation and discussion since it confirms the initial hypothesis of the variable nature of these platforms.

Analysis of NIR experimental data for the mineral composition of the samples extracted from the platform and experimental slabs show a mix of expected and unexpected results. The expected results were related to the largely known presence of carbonates (as a mineral group) and specifically of calcite, ankerite and siderite (as minerals) in various levels (Table 5.1). Ankerite was noted to be more present in the conglomerate/hardground samples, especially in the well developed conglomerate beds of Ponta Tal-Qammieħ (72.7) and the coarse-grained hardgrounds of Ras il-Fenek platform (57.1). The unexpected side of the experimental data was that apparently similar conglomerate platforms such as Ponta tal-Munxar, Ponta tal-Miġnuna and Ponta tal-Qammieħ have variable levels of minerals and this confirms the views made by Pratt (1990) that hardground mineralization is perhaps one of the most variable features of hardgrounds in general and largely controlled by environmental and temporal factors in their diagenesis. Also, Pratt (1990) reported francolite and glauconite minerals for the conglomerate beds of Qammieħ but the signature of these minerals was not picked up in the NIR experiment.

The percentage distribution composition of minerals also indicate the presence of sodium chloride in all samples, with Blata l-Bajda and Ponta tal-Qammieħ having a larger composition of sodium chloride, followed by Ras il-Fenek in that order. The presence of sodium chloride is also an expected result given the coastal conditions of the platform and also the widely reported saline conditions (leading to limestone deterioration) reported for the Maltese Islands, for example Rothert *et al.* (2007). However, the variability of sodium chloride may also suggest different geo-chemical responses to saline exogenous conditions. Higher percentages of sodium chloride may suggest higher salt absorption properties. In that case the platforms of Ponta tal-Qammieħ and Blata l-Bajda, though they are not similar in their limestone properties (one in LGLM with conglomerate, and the other is UGLM), they share properties of higher salt intake. The high levels of sodium chloride at Blata l-Bajda platforms may also have resulted in a stronger signature, obfuscating the mineralogical presence of carbonates in the Blata l-Bajda samples.

Clearly, the rocks are salt-dominated and a good part of the surface morphologies observed on the platforms point to visible evidence of a salt-weathered environment in a supratidal conditions. Yet, the mineralogical results indicate also that the susceptibility to salt weathering by some of these platforms may be more than surficial given higher salt content. Also, distinct platforms (such as those of Blata l-Bajda and Qammieħ) share similar mineral properties whilst apparently similar ones (such as conglomerate platforms of Qammieħ, Miġnuna and Munxar) revealed a more complex variety.

The weathering experiment data of the weathered samples produced different results when compared to the platform ones. The signature of muscovite and smectite is present in all the samples, with the exception of the LGLM block. These two minerals are ascribed to the weathering states of the samples in which these minerals crystallised from limestone dissolution. The presence of sodium chloride is less strong due to weathering state of the samples. This confirms that the salts present in the platform samples were

environment derived and have been washed away from the blocks after exposure and before samples were tested for NIR. The experimental data also brings out stark differences between the platform rocks and the LGLM blocks and similarly, to the weathering experimental results, it confirms the differences which exist between the platform limestone types and the LGL building type of limestones. The removal of calcite by dissolution can also dramatically increase the porosity and permeability of the rock. This may account for the faster decay of some of the experimental slabs, together with the development of fissures that allow further water circulation and facilitates the breakdown process.

The reason for slower responses to rock decay in the weathering experiment and the higher SH by the conglomerates may also reside in the diagenetic cementing properties of the hardground surfaces. Hardness is in fact acknowledged to be controlled by factors such as mineral composition and related cementing material and density (Demirdag, Yavuz and Altindag, 2009). The carbon cementing properties of Maltese hardgrounds and related conglomerate beds are amply acknowledged in the petrographic literature (Carbone *et al.*, 1987; Pratt, 1990; Rehfeld and Janssen, 1995; Umran Dogan *et al.*, 2006; Gruszczyński *et al.*, 2008). These properties may in part explain why hardgrounds and/or conglomerate samples with high levels of salt intake broke down relatively slower, when compared to samples from Blata l-Bajda, which had similar levels of sodium chloride but non-hardground properties. It could therefore imply that the specific physico-mechanical properties of the hardgrounds slowed down the geo-chemical processes responsible for limestone salt weathering.

The variable rates of rock decay of the conglomerates observed in the weathering experiment may also indicate that these properties are not uniform and, in consequence, their inconsistencies may determine their susceptibility to faster or slower rates of decay by weathering. Laboratory tests on the strength and hardness of limestone hardgrounds in Turkey by Dogan *et al.* (2006)

revealed variable strength results and claim that petrographic assessments of these rocks may belie important differences in their physic-mechanical properties.

The NIR data have surely started to address long-overdue questions about their physico-chemical properties of the Maltese platforms and their responses to weathering within and outside the *in situ* conditions. These questions warrant more research to properly understand the rock properties of these platforms.

7.4 Rates of surface change: platform and exposure slabs

7.4.1 The role of spatio-temporal parameters on platforms and exposure blocks

This current study analysed rates of surface change at three levels i.e. spatial, temporal and spatio-temporal. Almost all comparative tests resulted in statistical differences for annual, semi-annual and individual rates (Sections 6.3, 6.4 and 6.5 and Table 7.3). A number of implications follow from these results. Rock surfaces at supratidal levels on the studied Globigerina platforms were observed to behave non-homogenously in terms of surface change. This was also confirmed by the measurements done on the experimental slabs in which variability of denudation was evidenced.

The fastest mean downwearing rates were recorded in the soft-grained UGL limestone of Blata l-Bajda platform whilst the slowest rates were measured in the hardground covered UGL rocks of Ras il-Fenek (Table 6.1). These results were consistent with the findings of the Schmidt Hammer and the weathering experiment as follows:

Table 7.3: Summary of results obtained from inferential tests.

Results summary of inferentials tests		H0	H1
		%	%
Spatial	Comparisons of annual rates between front, middle and back of the platform	10	90
	Comparisons of individual time rates between front,middle and back of platform	14	86
	Paired comparisons of rates of individual periods beterrn front and middle of platforms	49	51
	Paired comparisons of individual periods between front and back of platform	31	69
	Paired comparions of individual periods between middle and back of the platform	30	70
Temporal	Paired comparisons of annual rates	33	66
	Paired comparisons of semi-annual rates	33	67
	Paired comparisons of annual rates with semi-annual rates	34	65
	Paired comparisons of rates between individual measurement periods	26	24
	Comparisons of rates across all individual measurement periods	H1	
Spatio-temporal	Comparisons of rates for individual time periods between front, middle and back stations across platforms	0	100
	Comparisons of rates for individual time periods between all front stations across platforms	0	100
	Comparisons of rates for individual time periods between all middle stations across platforms	0	100
	Comparisons of rates for individual time periods between all back stations across platforms	0	100
	Comparisons of overall rates of surface change between front. middle and back stations between all platforms	100	0

i. The percentage loss of weight and debris resulted from the experimental slabs, with the largest losses resulting from Blata l-Bajda samples and Ras il-Fenek samples registering amongst the lowest losses. Ras il-Fenek sample (No. 14) was not covered in hardground and thus recorded relatively higher rates of change both *in situ* and heavier losses of sample weight and weathering debris loss ; and

ii. The Schmidt Hammer R results are consistent with the *in situ* downwearing rates, with the lowest R values corresponding to the Blata l-Bajda (24.02) and the highest R values corresponding to the Ras il-Fenek platform (36.8).

The magnitude of mean rates of surface change recorded in this study (listed in Table 6.1) were comparatively much lower than those published by Micallef and Williams (2009) and Furlani *et al.*, (2014). Both authors published

relatively higher erosion rates (9.16 mma^{-1} and 9.0-14.0 mma^{-1} respectively) for MGLM outcrops. MGLM outcrops were not considered in this current study, as most platforms across the Maltese Islands have been generally observed to outcrop in either Lower and Upper Globigerina Limestone (Said and Schembri, 2010; S.Scerri, Pers. Comm., 12/12/2011). Comparisons of rates for UGLM surfaces were however not possible, given that both cited studies did not investigate lowering rates of platforms surfaces in UGLM.

The magnitude of the lowering rates of LGLM surfaces published by Micallef and Williams (2009), i.e. of 0.49-1.09 mma^{-1}, were also proportionately higher than those recorded for this study, specifically on the LGLM platforms of Ponta tal-Qammieħ, (from 0.094 mma^{-1} to -0.159 mma^{-1}), Ponta tal-Munxar (0.060 mma^{-1} to -0.380 mma^{-1}) and Ponta tal-Miġnuna (from 0.097 mma^{-1} to -0.448 mma^{-1}). The reasons for such discrepancy may be attributed to one or both of the following reasons:

i. The LGLM platforms used in this study were covered in conglomerate beds and hardgrounds of variable thickness, whist the LGLM platforms used by Micallef and Williams (2009) (indicated in their Figure 1, pg 738) were sites in which LGLM outcrops are not covered by such beds. The conglomerate beds may have therefore provided more resistance that LGLM outcrops and thus explain the lower rates of surface change measured in this study; and
ii. Secondly, the instrument used by Micallef and Williams (2009) was a rock profiler and therefore the comparability of measured data remains relative to the instrument used. No empirical study exists on the data comparability of the two techniques and therefore whether or not both techniques are capable of producing similar results remains speculative. The single TMEM rate published by Furlani *et al.* (2014) for MGLM surfaces may indicate a comparability potential but as Williams, Swantesson and Robinson (2000) have pointed out erosion rates often display notable spatial

variations, even at short distances, and more sampling sites may be needed to validate such comparisons.

The magnitude of rates reported in this current study were found to be comparable with those of other limestone lithologies in a supratidal conditions such by Shakesby and Walsh (1986) and Swantesson *et al.* (2006) (Table 2.3). In addition to this, the rates were measured with a MEM, although Swantesson *et al.* (2006) also used a laser scanner. Though it must be acknowledged that the range bracket of the published rates were relatively wide (Table 2.3), their magnitudes are still relatively lower than those published by Micallef and Williams (2009).

With reference to erosion rates on platforms in the Western Mediterranean and the Baltic, Robinson (2002) also reported rates close to those found in this present study i.e. from 0.16 to 0.38 mma^{-1}. He reiterated that erosion rates in the supratidal zone are on the low side of this bracket when compared to those in the inter-tidal zone. Shakesby and Walsh (1986) found however a contrary situation on the carboniferous limestone platforms in South Wales, with erosion rates greater in the supratidal zone. Their published values of 0.020-0.297 mma^{-1} remain nonetheless comparable with those found in the current study.

Micallef and Williams (2009) observed no correlation between exposure to wave action and mean surface lowering rates on LGLM outcrops. They ascribed rates to weathering processes rather than wave action. In this current study, rates controlled by wave-dominated exposure were tested out by comparing TMEM rates in a cross-shore direction to the prevailing wind-driven onshore waves. As seen in Table 6.1, patterns of statistical differences between bolts sites were significant when compared at annual and individual time periods. However, at paired comparisons of the p values percentages between front-middle, middle-back and front-back stations, a slightly stronger similarity was found between the front and middle stations (Section 6.3.3.3). This result may

imply a degree of exposure which may have influenced rates in the first half of the platform zone.

Table 6.9 indicates also that elevation and orientation may not have favoured such similarities, given that comparable rates of surface change were observed on platforms with different elevations and orientation i.e. at Blata l-Bajda, Ponta tal-Qammieħ and Ras il-Fenek. In view of the similarity-difference percentage result of 49-51, exposure may not have been dominant above other processes across the platforms. It may however indicate that – to certain extent - the effect of exposure on some of the shore platforms was spatially limited to the first half of the platform zone and the back sections are located in relatively less exposed conditions and thus subject to more weathering processes.

Various authors have produced results on the ineffectiveness of waves on micro-tidal shore platforms: for example Stephenson and Kirk (2000) demonstrated that, on the micro-tidal platforms of Kaikoura Peninsula (New Zealand), most of wave energy was dissipated by shoaling and refraction and less than 10% of it arrived on the coast. Closer to the Mediterranean, Pappalardo et al. (2017) concluded that waves do not directly erode the small micro-tidal shore platforms in the NW of Italy. As previously mentioned in Section 7.3.1.3, Pace *et al.* (2017) also found clear differences in inshore wave climate amongst four NE sites of the Maltese Islands.

In this current study, the Schmidt Hammer test and the weathering experiment did not indicate any strong cross-shore differences in the rate of weathering of the platform; morphologically, however, micro-pitting and solution pools were observed more present in the front part of the platforms. Thus, the effect of exposure at supratidal conditions may still have produced some zonal effects from sub-aerial processes directly linked to other processes such as the drying effect of winds, sea spray and wave swashes. These may not necessarily operate as a constant across the whole platform and their spatial influence may vary temporally from hours, days to seasonal periods. The

exposure-erosion-weathering relationship may thus actually be masked by the combined effects of a much wider range of mechanisms. Porter *et al.* (2010b) reiterate that, should one or two mechanisms be identified, patterns of downwearing rates may still be obfuscated by spatial variations in the chemical and physical characteristics of the rocks. Gomez-Pujol, Stephenson and Fornos (2007) pointed out that much of the detail of how these processes operate and interact still remains to be properly understood.

In the field, it was observed that other site-specific parameters played a stronger local in rates control such as lithological susceptibility to weathering or the relative position of the TMEM stations close to evident erosional and/or weathering zones on the platform. In first instance, variable rates of rock breakdowns between specimens from the same platform were in fact observed during the experiment (such as Ponta tal-Munxar samples). The reason for such difference was attributed to having selected weaker rocks for the experiments and this observation further confirmed the lithological variability present within the same bedrock. A similar experimental observation was made by Porter *et al.* (2010) in their weathering experiments on the argillaceous rocks on the upper intertidal shore platform at Mont Louis.

With regard to localised spots of erosion and/or weathering, various examples were observed such as the comparatively higher rates measured at MPQ2: it was installed close to the platform low-tide cliff edge where LGLM surfaces are free from conglomerates. The spot was also marked by morphological evidence of erosional and weathering processes such as a retreating scarp line and solution pools. The relatively higher rates of surface change at MPQ2 would therefore be the result of a dynamic interplay between weathering and erosion and would confirm the validity of looking at site-specific morphological surfaces to understand better such interplay. Though lithologically similar, this study has shown that *in situ* conditions of these platforms should not be regarded as a constant parameter and this is confirmed by other rock studies which have shown that in situ conditions of rocks not only

varies widely with the seasons, but also exhibits wide spatial variations (Ojo and Brook, 1990).

The statistical results of the temporal scales confirm the complex behaviour of change operating at annual and individual time scales. Temporal anomalies in surface change rates were also captured. For ex. the platform of Ponta tal-Miġnuna did return statistically similar results in the last three measurement periods (Section 6.4.2.4). This may imply specific site and short-term responses which resulted in homogenous surface change behaviour across the platform during the last nine-months of the survey. This period coincided with a drier spell period which occurred in winter 2016-2017 (See Section 5.2). Yet, similar responses during this dry period were not measured on other Globigerina platforms. Temporal variability was also observed by Stephenson *et al.* (2004) for the supratidal surfaces of Apollo Bay (Australia), in which changes were recorded to range from daily changes of substantial magnitude to periods of no significant changes at all. The authors argued that results with such variability were not surprising given the supratidal conditions of their studied surfaces during the monitoring period.

The dynamic nature of rock surface change observed this study was also highlighted by rock surface rises. This finding opens a new dimension in the understanding of processes of surface change on Maltese shore platforms, particularly because surface rises are still relatively unquantified in studies on Globigerina Limestone surfaces. Porter *et al.* (2010) argued that since platform surfaces can only be lowered over the long-term, surface rises are temporary conditions of swelling events. In their study on eastern Canada platforms records of surface gains were excluded when calculating mean downwearing rates. This study has taken a different approach in presenting mean rates of surface change and included surface lowering and surface rises in the statistical calculations. Rock surface rise, albeit temporary, was considered important in this study to better understand its contributory role to rock fatigue and resultant rock surface change.

As reviewed by Stephenson and Finlayson (2009) and Stephenson, Dickson and Trenhaile (2013), surface rise is a relatively common phenomenon on shore platforms and has become increasingly measured with MEM and TMEM in various platform studies. Interestingly, various interpretations on the mechanisms of such a process are evolving with more published works. Some of the earliest but still on-going works link surface rises to wetting and drying processes in intertidal zones (Kirk, 1977; Mottershead, 1989; Stephenson and Kirk, 2001; Kanyaya and Trenhaile, 2005; Trenhaile, 2006; Porter and Trenhaile, 2007; Porter *et al.*, 2010a). However, other interpretations are postulated for supratidal zones: mainly salt crystallisation, thermal changes and biological influences. Trenhaile (2001) argued that salt weathering causes disaggregation of rocks in supratidal zones and that hydration and dehydration of trapped salts absorption of water by hydration causes salt crystals to swell and to exert pressures against the constraining walls of rock capillaries. Mottershead (1989) measured episodic swelling of up to 0.1 mm from monthly to annual timescales on the supratidal greenschists and ascribed such process to rock desiccation during dry period and salt crystallisation. Thermoclastic processes were considered such as by Hemmingsen, Eikaas and Hemmingsen (2007) and Williams and Davies (1987). Moses and Smith (1993), Gomez-Pujol, Stephenson and Fornos, (2007) and Mayaud, Viles and Coombes (2014) have investigated surface rises controlled by biological influences at supratidal exposed conditions.

Given that chosen areas of the bolt sites were free from any biological growth at visible surface level, the role of biological influence in surface rises has to be excluded. Comparisons of the temporary surface rises between *in situ* surface and experimental slabs provide the following characteristics:

i. The order of magnitude of surface rises on the exposure slabs was much lower than that for surface lowering rates, indicating that the processes of rock denudation on the slabs were most stronger and rapid throughout the experiment;

ii. The occurrence of surface rises on the platforms was more irregular on a temporal scale compared to the slabs; surface rises on the experimental slabs were recorded primarily in the second and third exposure period whilst rates at individual, annual and semi-annual time scales were found not to be statistically comparable;
iii. Surface rises on the platform and on the slabs did not show any particular cross-shore spatial pattern, although they were evident at on the LGLM block, Ras il-Fenek and Ponta tal-Miġnuna slabs ;
iv. On platform level, the percentage composition of surface rises differed when calculated on annual scale and individual time period scale: on an annual scale the back stations of the platform had a higher percentage composition of surface rises (25%) compared to the middle (16%) and front sections (20%), whereas in the individual time periods, the front and middle stations had a very close percentage composition of 33% and 32% respectively, whereas back stations had a slightly lower percentage (29%). This confirmed how much scaling up measurement from individual to annual time-frames may then result in a different outcome of results at spatial level; and
v. At bolts site level, the order of magnitude of surface rise for the individual time period confirmed the temporal patterns of surface change (described in iv) i.e. with the front and middle bolts site recording larger magnitude of surface rises: ex. MPM1 (front) and MPM 2a (middle) at annual level and MPM1, MMX1b, MMX3b, and MMX5b (front bolts site) and MPM2b (middle) at individual time period level.

The implications of the above findings are several. Though the magnitude of surface lowering rates measured on the slabs were higher than those on the platform, the relative patterns of rates according to the platform fit well with those measured *in situ* . However, the patterns and magnitudes of surface rises

of the exposure slabs and the platforms were relatively less straightforward to compare. The different temporal patterns of surface rise between the slabs and the platforms may indicate that the set of altering processes operating on the slabs may have had a different effect than on the platform. In particular, the weathering processes operating on the slabs impacted heavily in the first exposure period and contributed to rapid rock decay losses and heavy surface losses (Table 5.15). However, they became less dominant in the second and third exposure period. In this case, the role of temperature and rainfall may have also been determining factor as lower temperatures and torrential rains characterized the first exposure period, and the latter period was followed with higher temperatures and drier periods during the second and third periods (See Section 5.2).

In view of this, one may argue that the higher temperatures and drier periods corresponded to more surface rises on the slabs and this argument would be in line with other observations of rock surface behaviour attributed to insolation weathering, in which maximum rock surface expansion was observed to occur during the hottest hours of the day (Bland and Rolls, 1998; Hall and Hall, 1991; Winkler, 1997) and also coupled with salt weathering (Goudie and Viles, 1997). Cabello-Briones (2015) and Cabello-Briones and Viles (2017) have reported increase of weight for exposed slabs in LGLM and attribute salt accumulation in combination with temperature fluctuations as responsible for the final slight changes of weight.

However, applying such interpretations of this current study require caution, in view of the evident physical alterations that the samples have undergone during the first exposure period. These alterations may have conditioned surface change responses in a cumulative effect in the subsequent two exposure periods. The spectroscopy tests of the weathered samples, in fact, show a slight mineralogical difference in the weathered slabs when compared to the platform samples. This small mineralogical difference indicate geo-

chemical alterations in the slabs during the weathering experiment and which may have in turn influenced the surface change responses of the slabs.

In this study, correlation of rates of surface change on the platforms with mean monthly temperature and rainfalls were not found to be statistically significant. This may confirm the extent to which *in situ* limestone surfaces may behave differently from experimental rock surfaces. The exposure trials provided a good indication of the relative resistance of different limestone surfaces (within the Globigerina) but in terms of susceptibility levels, the slabs were observed to be more susceptible to denudation and not comparable with *in situ* parameters.

Spatial results on platforms showed mixed patterns: similar frequencies of surface rises and lowering were measured in the front and middle stations and both were less similar with the back stations. This pattern seems to match well with the mean annual downwearing rates (Table 6.5) in which the back stations have a relatively higher mean rates compared to the front and middle stations, which recorded closer results as rates (Table 6.5).

The rates of surface change between front and middle platforms were also found to be relatively more statistical similar when compared with the back (Table 7.3). The combination of results would suggest that front and middle parts exhibit more similar patterns of surface change than when compared with the back stations. Comparisons with overall mean rates at individual level (Table 6.6) are more ambivalent and do not tie in well with the percentage of results of rises and lowering at both temporal scales. This is partially attributed to the fact that overall mean values were skewed by three single rates of high magnitude (at MRF1a, MRF2a and MBB6b).

The recorded non-homogenous rates of surface change measured on the Globigerina shore platforms suggest processes which operate at different temporal and spatial scales and with different magnitudes. This view is in

agreement with those already expressed in geomorphological literature on how scale, magnitude and frequency have become essential when investigating rock surface change (Goudie and Viles, 1999; Viles, 2001; Robinson, 2002; Stephenson and Finlayson, 2009; Robinson and Moses, 2011). Robinson (2002) also reviewed such a situation for the Mediterranean platforms studied in the ESPED project. Within the context of the Maltese Islands, Micallef and Williams (2009) similarly observed a considerable range of surface lowering data at each site and similarly to the previous authors, they inferred that a high spatial variability of rates exists at micro-scale, on the same bedrock and even at the same profiling site.

In their review of weathering studies, Hall, Thorn and Sumner (2012) raised a valid point in saying that they '*believe that weathering studies have reached a point where we need better questions rather than better answers*' (2012: 9). The direction of this current study should not be any different. Numerous questions emerge from this work which can help to point to future directions in this study. What is the level of interaction between insolation and salt weathering? What is the extent of the direct effect of short-term events such as dry spells in winter or infrequent episodic storm wave events? How would these short-term processes impact on TMEM measurements in terms of rates of surface change at shorter temporal scales? What role does the cumulative effect of specific processes of change operating at short-term sequences have at supratidal conditions?

The results of surface change on the selected supratidal platforms and those on the exposure slabs would indicate that the temporal scales of investigation are very important and that longer-term rates of surface change should consider short-term surface changes during monitoring in order to capture if and how the measured dynamic behaviour contributed to an under- or over-estimation of the rates (Gomez-Pujol, Stephenson and Fornos, 2007). The focus of this study was on monthly scales and it has managed to capture variability of rates at individual time periods. Other temporal scales of

measurements may be considered in future such as hourly scales, episodic ones (ex. post storm waves, post torrential rainfall or during dry spell conditions) in order to capture better the responses of supratidal rock exposures to these dynamic processes.

7.5 Research hypotheses answered

Table 7.4 reviews the main findings according to the explored research themes and tested hypotheses. The findings provide a good evidence of the morphological diversity present on Globigerina shore platforms. A synergy of marine and weathering processes is represented by morphological evidence, although the interpretation of their process efficacy is not easy to decipher (Viles, 2013). The efficacy of wave erosion is demonstrated by the presence of meso-scale erosion forms such as marine potholes, step backwearing scarps, notches, detached boulders and blowholes (often the result of wave quarrying). Superimposed on these forms, weathering is dominant at micro-scale with the presence of micro-pits, solution pools and salt-filled depressions.

Structure remains an important control driving the broader platform geometry and related shape dynamics at meso-scale level. Exposure seems to influence the rates of surface change at the front and middle bolts sites although Schmidt Hammer reading did not capture any cross-shore differences in rock surface hardness. The mean rates of surface change measured on the platform are in line with those published in other international studies on surface erosion at supratidal levels. Sample weight and debris loss measured by the weathering experiment have confirmed the *in situ* readings in terms of surface losses although the magnitude of loss where much higher on the exposure slabs. They also confirm the lithological variability present on the five selected shore platforms.

The mineralogy tests confirmed subtle differences in the geo-chemical composition of the tested platform surfaces and even more differences were

observed on the weathered samples. This would explain the occurrence of rapid alterations of the rocks during the experiment. The rates of surface change behaved non-homogenously across spatial, temporal and spatio-temporal levels. The front and middle bolts sites were considered relatively more comparable at individual time periods, although no specific temporal periods was found comparable.

Table 7.4: Summary of the research hypotheses and findings, together with resultant inferences (Source: Developed by Author)

Research Theme		Hypothesis	Research Findings	Resultant inference
Geomorphological features	1	Globigerina shore platforms share common geomorphological features, primarily inherent of their geological characteristics	UGLM platforms were very different from each other due to presence of resistant lithological bedding and structure which conditioned jointing and elevation	Globigerina shore platforms displayed a highly varied geomorphological landscape at meso scale
			LGLM platforms were variable and mostly dependent on presence and thickness of conglomerate beds	
			Presence of erosional and weathering forms were influenced by lithological resistance, structure and exposure	
Mineralogical and geo-mechanical properties	2	Globigerina shore platforms share similar properties of surface hardness	UGLM platforms were found to be the hardest (Ras il-Fenek) and the softest (Blata l-Bajda) of the five platforms	Globigerina shore platforms share different properties of surface hardness
			The LGLM platforms covered in conglomerate converged in surface hardness levels but site-specific variability was observed on all platform surfaces	
	3	Surface hardness on Globigerina shore platforms is subject to spatio-temporal variability	R values in cross shore direction between foreshore and backshore of platforms were found to be statistically significant	Intact surface rock strength on Globigerina shore platforms was not influenced by spatio-temporal variability.
			R value comparisons between measurement periods were not found to be statistically significant	
	4	Globigerina shore platforms consist of a limestone lithology susceptible to similar rates of weathering	Blata l-Bajda samples deteriorated relatively very rapidly. Ras il-Fenek weathered very slowly	Globigerina shore platforms show different responses to denudation.
			The conglomerates and hardground beds were susceptible variable rates of denudation	
	5	The mineralogical properties of the Globigerina shore platforms influence lithological control and rates of surface change	Mineralogy showed that platforms shared broadly similar properties in terms of calcite percentage as primary mineral but variations were observed in secondary minerals	The mineralogical properties of the Globigerina shore platforms influence rate of denudation change and rates of surface change
			Samples of Blata l-Bajda scored higher salt content, suggesting better absorption to salt intake than other relatively harder samples such as Ras il-Fenek	
Rates of surface change	6	Rates of surface change are directly related to cross-shore spatial dynamics across each platform	Rates for individual periods were more comparable between front vs middle, rather than between front vs back or middle vs back	There were no strong cross-shore similarities across platform
			Rates on an annual basis were spatially different from each other, with no evident cross-shore pattern	
	7	Rates of surface change on each platform are influenced by temporal parameters	Rates were not found to be comparable at annual, semi-annual or individual time period	There were no strong temporal similarities between different temporal scales.
			No correlation was found between rates of surface change and temperature/rainfall trends over the seasonal periods	Seasonality does not impact on rates of surface change
	8	Platforms share common spatio-temporal patterns of surface change	No strong statistical similarities were found between platforms on a spatio-temporal level	Platforms do not share common spatio-temporal patterns of surface change.

8 Conclusion

8.1 Reflections on the findings and recommendations

Overall this study has fulfilled the aims laid out in Chapter 1. The morphological features of Globigerina shore platforms have been better identified and mapped for the first time, the rock properties have been tested for mineralogy and resistance whilst the rates of surface change on their limestone exposures are better known and quantified on a spatio-temporal scale thanks to the use of the TMEM. The geomorphological mapping, the platform geo-mechanical properties and rates of surface change have all served the ultimate purpose to be combined together to provide the cross-scalar linkages with the platforms at landform scale (Viles, 2013) .

Though Kennedy, Stephenson and Naylor (2014) state that at a regional level, climate and tidal range tend to have greater similarities at this spatial scale, this present study has demonstrated that, at local scale and within the same tidal range and lithology, differences in platform characteristics may still exist, ranging from morphology, structure, surface hardness, patterns of weathering to rates of surface change. On the other hand it has also confirmed the important role of lithology in the surface resistance of sub-horizontal platforms and especially with reference to bedding and jointing.

The final overall rates of surface change were lower than those published by Micallef and Williams (2009) for the Maltese Islands with a rock profiler but were within the range of other published works for limestone exposure at supratidal conditions. The UGLM surfaces recorded the highest and lowest values of surface change, with the lowest rates of surface change determined by the lithological resistant of their hardground beds. The LGLM surfaces were also conditioned by the presence of the conglomerate beds and variable rates and mode of surface change were recorded in between the range of highest and lowest values produced by the UGLM surfaces.

The understanding of the interplay of processes and their relative contribution, rather than trying to identify a single process, is in fact becoming more central in studies concerning platform development (Trenhaile, 2002a). In this study, the results from the TMEM have been interpreted to infer with caution processes of surface change, whilst keeping in mind that rates and modes of surface change respond indiscriminately to such processes, irrespective whether the latter are operating individually or in tandem across spatio-temporal scales

Measurements of surface change were taken every three to four months for a period of three years. The rates and modes of surface change however may not necessarily have operate with a similar regularity given that the bolt sites were located at supratidal level, where processes are known to behave sporadically from no change to episodic-driven high changes. No rates were found to be statistically comparable on a temporal level i.e. at an annual rate, semi-annual or individual measurement period. This may imply that the processes operating at supratidal levels were largely variable over the measurement period of three years and the timing of the data collection may have captured a variety of modes of surface change such as a recent event of surface change in an otherwise stable period or an episode of surface rises that may have masked any previous period of lowering or no change.

The measurement period coincided with a year of torrential episodes of rains in 2015, followed by a period with long dry spells during the first eight months 2016. Though the effect on the denudation rates of some samples during the monitoring experiment were more tangible, these responses of the *in situ* surfaces to such episodes were more elusive. This may imply that, on the platform, the interplay of local conditions may be adding a layer of other responses above those produced by climatic conditions. As explained by Coombes, (2014) a wetter climate increases the likelihood of solution in the supratidal zones of carbonate coasts, whereas while more extreme and variable temperatures may enhance rock breakdown due to heat and moisture

fluctuations (via thermal cycling, salt crystallization and wetting and dying). This part of the investigation may require a more direct investigation with monitoring *in situ* ambient conditions and measurements taken on shorter time scales marking the episode in order to understand better the short-term responses.

Long-term climate change may reverse present sub-aerial processes as well. Since the late 1970s, mean sea surface temperatures is known to have increased by 0.05 ^{0}C per year (Anon, 2017b). Specifically, on the Maltese Islands, they have reached record highs of 30 ^{0}C in August 2017 and with temperatures in shallower waters reaching one or two degrees higher (Anon, 2017b). This may reduce the effectiveness of sea water in dissolving calcium carbonates as warmer seas contain a higher context of dissolved carbonates and thus are less able to dissolve limestone outcrops; they may instead precipitate carbonates on coastal outcrops, reducing the effect of solution weathering.

The presence of surface rises surely adds another layer of complexity and merits more investigation to this effect. Though the phenomenon is documented in international literature as a very common phenomenon, it was never reported in works for Globigerina surfaces. This is the first work that provides evidence and quantification of surface rises on such limestone surfaces and more research is needed to investigate further this phenomenon in order to determine the exact causes of these rises and if they are efflorescence or sub-efflorescence in nature. More detailed study of specific properties such as porosity may help to explain better the susceptibility of the rocks to specific processes such as moisture absorption and salt crystallisation.

Also, with shorter scale measurements, such as hourly or diurnal, one would capture better the behaviour responses of the surface change to processes such as diurnal thermal changes (especially in summer) or episodic based measurements such as pre-storm and post-storm events. Such scales of investigation may provide a more direct understanding of how supratidal

surfaces respond to specific processes and will help to provide important clues about what extent waves erode material from supratidal surfaces that have been previously weakened by weathering.

The role of subaerial weathering processes has been successfully assessed at a broader meso-scale level by mapping out all the geomorphological forms present on the platform, measuring surface roughness as well as by monitoring and quantifying changes in the exposure experiment. The results of the weathering experiment are also interpreted with caution, as the denudation rates measured by weight loss, debris loss and rates of surface change are not comparable with rates examined on the platform. However the relative behaviour response (i.e. faster or slower rates of change) exhibited by the exposure blocks do align sufficiently well with both the TMEM measurements recorded *in situ* and the Schmidt Hammer readings in terms of rock surface strength,

In addition to the above, both the presence of micro-pits and solution pools in the first half section of the platforms and the relatively more comparable rates of surface change measured by TMEM in the front and middle bolts sites (at individual measurement period) seem to point to a more active processes operating between the front and middle section of the platform and distinct from the back section. Why the rates and modes of surface change (lowering and rises) between the front and middle bolt sites become less comparable at annual time scales need to be better understood. Wetting and drying cycles in the front parts of the platform were inferred morphologically, particularly with the present of micro-pitting. It would be much preferred if field instrumentation is developed that would directly record the degree of *in situ* moisture present within the first few millimetres in depth of rock surfaces in order to provide better relation with measurements of rock surface strength and rates of surface change on a spatio-temporal level.

It has to be acknowledged that both the rock surface hardness test and the TMEM measurements relied on surfaces which were relatively smoother and homogenous enough to measure from. Depressions, voids, cavities within the platform surface were all avoided, as per normal instrument procedures. However, in these spots and lines of weakness, weathering may actually be more operative and thus have also an important role in contributing to the overall surface weakness of the platform and resultant erosion products at meso-scale level. It would be interesting in future therefore to gauge and quantify how surface roughness and joint strengths may determine the rate and extent of weathering across these rough surfaces and how this related with the meso-scale erosional dynamics produced by waves and related erosion products such as blocks, plucking scars and step-backwearing scarps.

How the geo-mechanical properties are contributing to the rates of surface change is not altogether so evident, given the overall similar properties found in the platform samples. The higher levels of salts in some of the samples, such as at Blata l-Bajda, may indicate that such rocks have higher absorption capacities and thus the breakdown mechanism of this UGLM rock may be more internal compared to relatively harder rock in hardground and conglomerates. With less absorption, it may be inferred (with some caution) that salts may crystallise and weather at more efflorescence level rather than internally. The presence of solution pools on exposure in harder rocks may indicate that solution pools develop on rocks with lower absorption capacities and therefore salt accumulation acts more surficial to create weathering forms. However, hardground and conglomerate rocks were also observed to have a rougher surface and so the surface roughness may have facilitated the entrapment of more saline water and as a result concentrated salt weathering in the front parts of the platforms.

The presence of different minerals on the weathered exposure blocks may also indicate that the limestone exposures are susceptible to some degree of chemical alteration by weathering, when removed away from the *in situ*

conditions and from the confined strength of the platform landmass. The need to test Globigerina rock exposure in order to determine their role in the physical and mechanical properties of platforms cannot be emphasized enough in this study. This study has shown that, like in many other studies, the Schmidt Hammer can be used to measure the strength and other engineering properties of rocks, and remain a reliable tool for *in situ* measurements to otherwise expensive laboratory testing procedures and equipments. Further assessment of the efficiency of particular weathering processes on Globigerina shore platforms would be of use as laboratory studies have so far been generally biased towards testing of LGLM building blocks only. Experiments and monitoring of rock decay of a greater range of variety of Globigerina exposures would also be of value, with particular attention being given to the operation of mechanical and chemical breakdown under Mediterranean climate regime. In this study, the role of salt weathering was inferred by morphological features on platform surfaces and the results of the mineralogy tests. The efficiency and relative contributions of rock breakdown by thermal cycling under Mediterranean warming regime is relatively unknown, for example, and the influence of supratidal conditions of salt crystallization changes on rock platforms is yet to be explored.

While this thesis has succeeded in fulfiling its targeted aims, it has also provided a better context in which to better frame future research questions to be investigated. Clearly the role of salt weathering is very important on these platforms although the wider implication of this result will need to be tested to other platforms. What is also needed in future is to quantify the surface responses of long-term weathering phenomenon against shorter term ones produced by episodic effects of storm waves, torrential rainfall and dry spells. In the present realities of climate change, anomalies in climate trends impose a different way how to measure rates of surface change and which would require considering the cumulative effect of one process when followed by another. No attempt was made to investigate directly the biological factors influencing surface change on these platforms but it should not preclude the possibility of

detailed investigations of the role of biology affecting platform erosion in future, especially along the vertically low-tide cliffs where biological forms were observed to be more present.

Finally, it must be acknowledged that part of the academic challenge of this work was to underpin the results within the context of those previously published in other platform studies - as illustrated in Figure 2.3 - given the different boundary conditions of these studies. Just to mention a few examples, the micro-tidal platforms of Kaikoura Peninsula (New Zealand) are energetic open oceanic coasts, much wider (up to 10 times), more continuous than in the Mediterranean, and their elevation above sea level is relatively lower. Trenhaile and Kanyaya (2007) and Porter *et al.* (2010a) investigated the micro-tidal platform of the Gaspe Peninsula in eastern Canada, which faces the Atlantic Ocean in argillite lithology. Kennedy and Dickson (2006) discuss structure and lithological controls for the micro-tidal platform in Shag Point, New Zealand made up of mudstone and sandstone. The argument recently elicited by Pappalardo (2017) applies in this study as well: that due to lack of studies on Mediterranean shore platforms, where boundary conditions are very specific, the results presented in this study cannot be extrapolated completely to other micro-tidal environments or compared with results obtained in different environments.

8.2 Evaluation of the instruments: limitations and opportunities

8.2.1 Geomorphological mapping at platform scale

This study represents the first contribution to the knowledge of the large-scale geomorphology of Maltese shore platforms. In detail, it has shown the importance of large-scale geomorphological mapping in revealing the platform's structural features and the morphological variations. The mapping of structural, erosional and weathering forms has permitted to identify the linkages between processes and lithological controls according to specific forms.

Base maps needed to be produced from scratch as the largest scales available were 1:2500. The scale of these available maps was not considered adequate as they do not include enough meso-scale features such as detachment scarps, precise boulder perimeters, joints, spot heights or proper shoreline perimeter. They were constructed from Google Earth images and then updated though regular field checks. The local geological map of the Maltese Islands also had to be corrected given that the information was extracted from a map of 1:25,000 and, at that scale, geological attributes of some platforms were incorrectly marked. The platforms of Blata l-Bajda and Munxar were incorrectly marked at MGLM.

This large-scale mapping approach has so far been scantily adopted by platform researchers and, to date, there is still a lack of examples of geomorphological maps at shore platform scale. Few platform studies have to date actually produced mapping results, such as Cruslock *et al.* (2010), Gómez-Pujol, Fornós and Swantesson (2006) and Hénaff, Lageat and Costa (2006). They demonstrated the varied morphological setting of the investigated platforms. Similarly to such works, the resultant differences in structure and morphological settings between lithologically similar platforms justified the choice of creating these maps an important empirical contribution to the overall study.

8.2.2 Schmidt Hammer

The application of this instrument in the field of geomorphology has been amply reviewed over the past decades (McCarroll, 1987; Goudie, 2006, 2013b) and therefore this section will only highlight issues and learnt lessons that have been encountered in the field and not previously documented or published.

Schmidt Hammer data was collected with sufficient awareness that it is recording the surface hardness of rocks rather than their overall resistance, which depends on many other properties of the rock surface and also their

meso-scale structure. The experiment fulfilled the intended objective to quantify the variability of rock hardness between the different globigerina platform surfaces, which previously were not examined scientifically and inferred to be similar just on a lithological basis.

Although the experimental design tried to minimise any form of bias in the selection of the impact points in a cross-shore direction, some selective sampling was unavoidable. These primarily concerned choosing surfaces away from discontinuities and smoother surfaces as advised in the mentioned literature. Specifically for the conglomerate beds, the depressions and hollowed spaces were avoided given that TMEM stations were not installed on such microforms. Yet, future studies with Schmidt Hammer may need to include these microforms and how they are affecting rock surface hardness.

8.2.3 Rock block exposure and micro-catchment

The use of rock block exposures and micro-catchments to monitor and quantify weathering changes are considered established techniques in geomorphology (Halsey, 2000; Moses, 2000). They employ a range of methods, the latter primarily dictated by the purpose of the study in question. This current study designed a multi-method approach to incorporate three tests. Given the different scopes and methods employed in the other studies, a comparative analysis to gauge the effectiveness this current method is not considered appropriate and representative. Comparison with the results of earlier workers is difficult because of the varying experimental conditions employed (Moses, 2000; Moses, Robinson and Barlow, 2014).

The implications of a multi-method approach provided a number of advantages and disadvantages. The advantages were that it was possible to cross-compare results of different experiments: specifically between weight and debris loss and weather trends, weight and debris loss with surface hardness results and weight and debris loss with rates of surface change. Block exposures

had to be chosen of an adequate size in order to provide a surface area large enough to measure surface change within the TMEM triangle space (Smith *et al.*, 1995). On the other hand, the requirement of such dimensions facilitated visual comparisons and gave a more realistic representation of the natural rock outcrop (Moses, 2000). Another value was that the method provided a relatively cost-effective and rapid way to obtain results of weathering changes and they could be readily analysed for other laboratory techniques such as NIR. The strong positive correlation between weight loss and debris loss, reported in Chapter 5 (Section 5.5) confirms the effectiveness of the experiment as a comparable measurement for the two tested variables of losses. In view of the rapid breakdowns of some of the blocks, the catchment design provided a good opportunity to examine visually the large broken splinters that temporarily got detached from the blocks but remained on the steel grid, before breaking further into smaller pieces and fall through the grid into the basin.

Disadvantages included selecting rock outcrops with a suitable smooth surface to install the TMEM studs and facilitate proper readings within the reaching limits of the probe, transporting the blocks from the site without damaging them and ensure that they are placed in a proper horizontal position on the steel grid. Direct Schmidt Hammer readings on the samples were not possible due to damage risks. The first sample of Qammieħ had to be replaced, as its micro-topography could not provide an adequate surface over which to measure the vertical heights with the TMEM probe. Due to the rapid rock decay of Blata l-Bajda samples, the possibility of measuring rates of surface change with TMEM over annual timescales was not possible. Moses, Robinson and Barlow (2014) pointed out the occurrence of this limitation for other works such on limestone and mudstone at Kaikoura Peninsula, New Zealand (Stephenson and Kirk, 1996b; Stephenson *et al.*, 2010) and on reef limestone on Aldabra Atoll, Indian Ocean (Viles and Trudgill, 1984). One has to see whether this will occur *in situ* with the TMEM stations set up on the UGLM platform at Blata l-Bajda.

The micro-catchment basins were made of plastic and their exposure to outdoor elements necessitated frequent replacement to maintain an optimum condition. Given that the basins had no water outflow, rainwater had to be emptied from the basins after a rainy event, without disturbing the debris sediment that would have accumulated at the bottom of the basin. Emptying the basins from the debris for proper weighing was laborious and time-consuming and was possible only during dry phases. Though a strong correlation was found between the weight and debris loss, the author does not rule out that some of the finer debris may have been blown away from the sample surface by strong winds. A refinement of this method would include drilling holes in the mid-way edge sections of the basins to act as outflows for precipitation water, without losing the depositing weathering debris.

8.2.4 NIR

Our work has demonstrated the potential of diffuse reflectance spectroscopy, using the NIR, to efficiently acquire mineralogy information on rock samples. The experiment results have shown how qualitative interpretations may aid with the identification and assignment of spectral bands to mineral constituents. In comparison to other lengthier tests such as XRD, NIR was less laborious as it required less sample preparation and provided rapid results output. This approach was well suited for this research due to the need to examine a large number of samples in a relatively short period of research time. In being a non-destructive method, it also did not exclude for other tests to be done in parallel or subsequently, as it has been the case for this research with XRD.

Other potential avenues to be explored would be to undertake NIR spectroscopy in the field, as it has been similarly done in various soil studies (Viscarra Rossel *et al.*, 2009 and references therein). As pointed out by Stenberg *et al.*, (2010) environmental and technical issue regarding sample preparations should not deter from measuring directly in the field in order to capture

influences of *in situ* variations in mineralogy, water, organic matter and, not least, of their interactions.

8.2.5 TMEM

A number of authors have reviewed the advantages and disadvantages of using TMEM for rock coast erosion studies the most recent being Stephenson and Finlayson (2009) and Stephenson, 2013). Whilst there is limited scope in repeating such published information, this section will focus on elaborating on instrument issues that were encountered during the course of this research and how they were addressed to ensure maximum accuracy and continuous length of recorded data.

As explained in Chapter 3, the data collection procedure was initially set up based on published procedures (Furlani and Cucchi, 2008; Furlani *et al.*, 2009; Furlani, Cucchi and Biolchi, 2011). A pilot study of three measurement periods was set up as an early phase of the data collection period in order to address operation issues related to bolt stations set up and use of TMEM. Similarly to Viles and Trudgill (1984), one of the first concerns that needed to be addressed in the pilot test was the loss of bolts between the measurement periods, primarily due to storm dislocation or human disturbances (tampering). Similar field issues were also reported in other local studies such as by Magri *et al.* (2008)and Micallef and Williams (2009). A few stations needed to have their bolts re-installed, with the exception of Ponta tal-Qammieh as it is very difficult to reach. Some of the bolts were installed too close to the well-beaten track on the platforms and were thus easily spotted by visitors. This issue was partially resolved by transferring the bolt sites to less visible locations on the platform and coating the bolts with a thin coating film of diluted grey cement in order to camouflage the shine of the titanium bolts. This however required careful polishing off when measurements needed to be taken. On quite a few occasions, this thin cement coating just plucked off, as cement attaches very lightly to titanium surface of the bolts. But it did provide some intermittent 'camouflage

protection' especially during the summer periods when the platforms were used for recreational bathing.

Another limitation was related to the choice of rock surface for the bolt sites. Whilst all possible care was exercised to select the best representative surfaces for each shore platform, conglomerates have very non-homogeneous clastic surfaces which required specific selection in order to measure a surface that can be reached by the instrument probe transversally in three directions. This morphological characteristic has conditioned in part the selection of the surfaces, opting for relatively smoother surfaces, thinner conglomerates with less clastic protrusions. Salt-filled depressions and voids in between the hummocky surfaces were also avoided as their surfaces may get covered and disrupt the data collection. A few stations installed at the back of the platform had to be relocated as well, as they were too close to the powdery MGLM cliffs and got covered by MGM cliff debris.

All these issues justified the scope of having a pilot study. The above procedure ensured a proper surface coverage reach by the instrument, albeit not a total coverage in a couple of cases. A few position points were either not reached by the instrument probe or else they had lowered away from its reach. Stephenson and Kirk (1996) mention an adjustment to this operational issue by using a ruler to take a measurement alongside the exposed bolt but they also admit that the inclusion of such procedure is questionable. For this study, it was opted to leave out the immeasurable position points from the surface change calculations.

Crucial was the calibration regime to provide accurate field measurements. Checks to the instrument were also done twice during the course of study with S. Furlani (supplier of the instrument). Given the monitoring of 31 stations over a period of 3.5 years for 14 consecutive measurement periods, the instrument required constant checks for calibration variations and for whicih field measurements needed to be corrected. Four deviations (out of 25) were found

to be higher (c. 0.2 mm) in the last five measurement sessions but these were observed to be systematic and thus corrected from the field measurements (Section 6.2). The learning outcome from this was that calibration regime in the last five measurement sessions was found to be the most appropropriate in capturing potential variations. The final surface change results were significant at scales large enough to exclude any other form of instrument error. Not much information is available on the calibration procedures of the TMEM. It is hoped that this study sheds better light on the functionality of the TMEM from this angle and provides avenues for more information sharing about its accuracy.

8.3 Shore platform erosion: implications for coastal management

Substantial research has been devoted over the years to the study of platform development and related processes and change. Yet, few works have attempted to put all this research within the context of coastal management. Whenever this was done as part of geomorphological studies, the treatment of the topic was rather superficial. However, recent works by Brew *et al.* (2004) and Defra (2007) on the defence and conservation strategies for cohesive platforms, Kennedy *et al.* (2013) on rocky coast hazards and Kennedy *et al.* (2017) on wave hazards on micro-tidal shore platforms have surely paved the way for this overdue discussion about the relationship between shore platform erosion dynamics and risk management.

Like on many other densely populated islands such as the Maltese Islands, any study related to processes of change on coastal landscapes would translate into a meaningful narrative when these changes impact on the community life with loss of property, recreational or historical assets and loss of life. A recent experience of this in the local context was the collapse of the Azure Window (Dwejra, Gozo) on the 8th of March 2017, which triggered unprecedented distressing reactions from both the local and international community (Anon, 2017a). More specific to the studied platforms, the destroyed salini at the Blata

l-Bajda platform due to a 1993 storm is example of coastal assets destroyed by the impactful force of storm waves (Chapter 4).

The accessible nature and sub-horizontal morphology of shore platforms on the Maltese Islands is a magnet for various forms of recreational and sports activities all year round such as bathing, barbecuing, fishing, diving, outdoor strolling and fitness workouts. In additional, intense coastal infrastructure has also been built close or onto these platforms in the hope to maximise military operations, recreational and property revenue. This was done during time in which minimal consideration was given to the exposure pressures impacting on this development. Sad to say but there is still very limited awareness related to the exposure dangers of rocky shores to local unstable conditions. 'Unseasonable rough seas' and 'freak waves' have become common terms to describe the sudden occurrence of large waves with strong underwater currents during apparently calm days (such as May and August) and which often take shoreline strollers (mostly foreigners) by surprise (Martin, 2017). It is reported that this phenomenon is, in part, the reason why fatalities such as drowning and falling accidents from rocky shores are becoming more common on the Maltese Islands. Nine of the 12 people who tragically drowned in 2016 were foreigners (MINS, 2017), although the phenomenon of foreigners being more likely to drown is not a new one. Back in 2013, a local media newspaper reported that, between 2003 and 2013, more than 70 per cent of drowning cases (i.e. 42 out of 57 victims) were foreigners (Martin, 2017).

The implications of erosion and weathering of Globigerina shore platforms on the functioning of the wider coastal system has largely been ignored to date and much remains to be done also in the context on scientific work on coastal erosion (Micallef *et al.*, 2018). In this current study, the following issues are considered as highly critical in justifying the scope for specific management actions on the protection and conservation of Maltese shore platforms:

i. Disruption of platform equilibrium with lowering of platform surfaces and resultant decline in the abilities of the platform geometry to regulate cliff erosion;
ii. More incidents of flooding and inundation due to projected increase in sea level rise (with waves breaking further inshore due to increase in water depth) and increasing incidence of storminess related to climate change;
iii. Loss of land through cliff recession, also due to the relatively short distances between the platform edge and the cliff line;
iv. Dangers to or loss of life due to exposure risks related to platform surface collapse, block detachment from platform edges, rock falls from cliff faces or onshore wave breaking;
v. Loss of recreational space for local and international community;
vi. Damage to or loss of infrastructure amenities built close or upon shore platforms;
vii. Damage to or loss of archaeological and historical sites;
viii. Damage to or loss of artisanal practices such as salini works;
ix. Loss or damage to geological sites with landscape aesthetic value;
x. Disruption or loss of supratidal habitats; and
xi. Loss of recreational revenue for tourism activities.

More scientific research is thus needed to examine also the influence of wave exposure and how platform elevation and sub-tidal morphology is influencing the extent of onshore wave-breaking across Maltese shore platforms. In a recent work by Micallef *et al.* (2018) on erosion-hazard assessment of the Maltese coasts, the five studied platforms have been scored very high in terms of hazard levels of erosion according to parameters such as wave exposure, geological layout and storm climate. Coastal outcrops in Globigerina Limestone are considered as "*softer geological strata*" (2017: 9) and are assigned a high index of erosion hazard level. No distinction is provided for the different members. Additionally, narrow platforms with soft backshores

are recommended as priority areas of coastal erosion management. These recommendations emphasize all the more the need to monitor rates of surface change on Maltese shore platforms on a long-term basis in order to scientifically feed future policies of coastal erosion management.

Policy provision for mitigation of coastal erosion is very minimal on many levels and they can be briefly summarised as follows:

i. The recently published local regulatory framework, Strategic Plan for Environment and Development – SPED document (MEPA, 2015) has outlined three objectives for the coastal zone but no specific targets were set to mitigate coastal erosion as key designated tasks. Coastal Objective 1 only mentions priorities to be given to uses that do not accelerate erosion;
ii. Coastal erosion does not feature as one of the main environmental issues identified in the SPED Strategic Environmental Assessment report (see pg 6, Table 1 of the said report) (MEPA, 2015);
iii. In the EU Environmental Implementation Review Country Report for Malta (EC, 2017), the concept of 'natural capital' for the Islands is still only tied to EU Biodiversity Strategy to 2020 and erosion concerns only address soil resources; and
iv. Erosion of shore platforms are totally unaccounted for in the guidelines for coastal erosion management practices in Europe, published by the European Commission under the EUrosion project (EUrosion, 2004a, 2004b). The types of coasts examined were mainly beaches, cliffs and deltas (in that order). The Maltese Islands presented case-studies for Xemxija and Ghajn Tuffieha beaches (Serra *et al.*, 2003).

8.4 Epilogue

The environmental and socio-economic costs related to platform erosion on the Maltese Islands should not remain underestimated. The current state of knowledge related the rates and mode of Globigerina platform erosion and the resultant consequences are largely insufficient to fulfil the necessary decision making process at national scale. It is hoped that this current work provides the start of this much-needed process.

References

Abbott, A. T. and Pottratz, S. W. (1969) 'Marine Pothole Erosion, Oahu, Hawaii', *Pacific Science*, 23(3), pp. 276–290.

Agar, R. (1960) 'Post-glacial erosion of the North Yorkshire coast from the Tees estuary to Ravenscar', in *Proceedings of the Yorkshire Geological and Polytechnic Society*. Geological Society of London, pp. 409–427.

Amaral, P. M., Rosa, L. G. and Fernandes, J. C. (1999) 'Determination of Schmidt rebound hardness consistency in granite', *International Journal of Rock Mechanics and Mining Sciences*. Pergamon, 36(6), pp. 833–837.

Andriani, G. F. and Walsh, N. (2007) 'Rocky coast geomorphology and erosional processes: A case study along the Murgia coastline South of Bari, Apulia — SE Italy', *Geomorphology*, 87(3), pp. 224–238. doi: 10.1016/j.geomorph.2006.03.033.

Anon (2017a) 'Ripples from the Azure Window's collapse spread across the globe', March 8th, *Times of Malta*.

Anon (2017b) 'Sea temperatures soars beyond 30C'. August 7th, Times of Malta.

ASTM (2005) *Determination of Rock Hardness by Rebound Hammer Method*.

ASTM (2014) *Standard test method for determination of rock hardness by rebound hammer method D5873-14*, *Vol. 4.09*.

Augustinus, P. C. (1991) 'Rock resistance to erosion: Some further considerations', *Earth Surface Processes and Landforms*, 16(6), pp. 563–569. doi: 10.1002/esp.3290160608.

Aydin, A. (2009) 'ISRM Suggested method for determination of the Schmidt hammer rebound hardness: Revised version', *International Journal of Rock Mechanics and Mining Sciences*, 46(3), pp. 627–634. doi: 10.1016/j.ijrmms.2008.01.020.

Aydin, A. and Basu, A. (2005) 'The Schmidt hammer in rock material characterization', *Engineering Geology*, 81(1), pp. 1–14. doi: 10.1016/j.enggeo.2005.06.006.

Baldassini, N. (2012) *Biostratigraphy of the Oligo-Miocene Globigerina Limestone Formation (Maltese Archipelago) based on calcareous nannofossils*. Unpublished PhD Thesis, Universita di Siena.

Baldassini, N., Mazzei, R. and Foresi, L. M. (2013) 'Calcareous plankton bio-chronostratigraphy of the Maltese Lower Globigerina Limestone member', *Acta Geologica Polonica*, *63*(1), 105-135, doi: 10.2478/agp-2013-0004.

Baldassini, N. and Di Stefano, A. (2015) 'New insights on the Oligo-Miocene succession bearing phosphatic layers of the Maltese Archipelago', *Italian Journal of Geosciences*, 134(2), pp. 355–366. doi: 10.3301/IJG.2014.52.

Baldassini, N. and Di Stefano, A. (2017) 'Stratigraphic features of the Maltese Archipelago: a synthesis', *Natural Hazards*, 86, pp. 203–231. doi: 10.1007/s11069-016-2334-9.

Bartrum, J. A. (1916) 'High water rock platforms: a phase of shoreline erosion', in *Transactions of the New Zealand Institute*, pp. 132–134.

Bartrum, J. A. (1924) 'The shore platform of the west coast near Auckland: its storm wave origin', *Report Australian New Zealand Association for the Advancement of Science*, 16, pp. 493–495.

Bartrum, J. A. (1926) '"Abnormal" Shore Platforms', *The Journal of Geology*, 34(8), pp. 793–806.

Bartrum, J. A. (1935) 'Shore platforms'. Meeting of the Australian and New Zealand Association for the Advancement of Science 22, 135-143.

Bartrum, J. A. (1936) Honeycomb weathering of rocks at the shoreline. New Zealand Journal of Science and Technology 18, 593-600.

Bartrum, J. A. and Turner, F. J. (1928) 'Pillow lavas, peridotites, and associated rocks from northernmost New Zealand', *Transactions*, New Zealand Institute 59, 98-138.

Basu, A. and Aydin, A. (2004) 'A method for normalization of Schmidt hammer rebound values', *International Journal of Rock Mechanics and Mining Sciences*, 41(7), pp. 1211–1214. doi: 10.1016/j.ijrmms.2004.05.001.

Beetham, E. P. and Kench, P. S. (2011) 'Field observations of infragravity waves and their behaviour on rock shore platforms', *Earth Surface Processes and Landforms*, 36(14), pp. 1872–1888. doi: 10.1002/esp.2208.

Ben-Dor, E. and Banin, A. (1990) 'Near-Infrared Reflectance Analysis of Carbonate Concentration on Soils'. *Applied Spectroscopy,* 44, (6), pp. 1064-1068.

Bennett, S. M. (1979) 'Palaeoenvironmental studies in maltese mid-tertiary carbonates.' PhD Thesis, Royal Holloway, University of London.

Bianucci, G., Gatt, M., Catanzariti, R., Sorbi, S., Bonavia, C. G., Curmi, R. and Varola, A. (2011) 'Systematics, biostratigraphy and evolutionary pattern of the Oligo-Miocene marine mammals from the Maltese Islands', *Geobios*. Elsevier, 44(6), pp. 549–585.

Biolchi, S., Furlani, S., Antonioli, F., Baldassini, N., Causon Deguara, J., Devoto, S., Di Stefano, A., Evans, J., Gambin, T. and Gauci, R. (2015) 'Boulder accumulations related to extreme wave events on the eastern coast of Malta', *Natural Hazards and Earth System Sciences Discussions*, 3, pp. 5977–6019.

Biolchi, S., Furlani, S., Devoto, S., Gauci, R., Castaldini, D. and Soldati, M. (2016) 'Geomorphological identification, classification and spatial distribution of coastal landforms of Malta (Mediterranean Sea)', *Journal of Maps*. Taylor & Francis, 12(1), pp. 87–99.

Bird, E. C. F. (2011) *Coastal geomorphology: an introduction*. John Wiley & Sons.

Bird, E. C. F. and Dent, O. F. (1966) 'Shore platforms on the south coast of New South Wales', *The Australian Geographer*. Taylor & Francis, 10(2), pp. 71–80.

Blanco-Chao, R., Pérez-Alberti, A., Trenhaile, A. S., Costa-Casais, M. and Valcárcel-Díaz, M. (2007) 'Shore platform abrasion in a para-periglacial environment, Galicia, northwestern Spain', *Geomorphology*, 83(1–2), pp. 136–151. doi: 10.1016/j.geomorph.2006.06.028.

Boissevain, J. (2004) 'Hotels, tuna pens, and civil society: Contesting the foreshore in Malta', *Contesting the Foreshore*, p. 233.

Brew, D.S., Balson, P. S., Pearson, S., Hobbs, P., Williams, R., Robinson, D., Moses, C. and Walkden, M. (2004) 'The implications of cohesive shore platform erosion for coastal management'. *Proceedings of Littoral 2004,* Vol 2 Aberdeen, Scotland, pp. 590-595.

Briones, C. (2015) 'The Effects of Open Shelters on the Preservation of Limestone Remains at Archaeological Sites'. PhD Thesis, Geography and the Environment, University of Oxford.

Brooke, B. P., Young, R. W., Bryant, E. A., Murray-Wallace, C. V. and Price, D. M. (1994) 'A Pleistocene origin for shore platforms along the northern Illawarra coast, New South Wales', *The Australian Geographer*. Taylor & Francis, 25(2), pp. 178–185.

Bulmer, M. G. (1979) *Principles of statistics*. Courier Corporation.

Bunaciu, A., Udriştioiu, E. G. and Aboul-Enein, H. Y. (2015) 'X-Ray Diffraction: Instrumentation and Applications', *Critical Reviews in Analytical Chemistry*. Taylor & Francis, 45(4), pp. 289–299. doi: 10.1080/10408347.2014.949616.

Buttigieg, M., Vassallo, M. and Schembri, J. A. (1997) 'Basic Geomorphological Studies of Shore Platforms in the Maltese Islands', in *Third International Conference on the Mediterranean Coastal Environment MEDCOAST 97*, pp. 79–88.

Cabello-Briones, C. and Viles, H. A. (2017) 'Evaluating the Effects of Open Shelters on Limestone Deterioration at Archaeological Sites in Different Climatic Locations', *International Journal of Architectural Heritage*. Taylor & Francis, 0(0), pp. 1–13. doi: 10.1080/15583058.2017.1300710.

Carbone, S., Grasso, M., Lentini, F. and Pedley, H. M. (1987) 'The distribution and palaeoenvironment of early miocene phosphorites of southeast sicily and their relationships with the maltese phosphorites', *Palaeogeography, Palaeoclimatology, Palaeoecology*, 58(1–2), pp. 35–53. doi: 10.1016/0031-0182(87)90004-6.

Carter, N. E. A. and Viles, H. A. (2005) 'Bioprotection explored: the story of a little known earth surface process', *Geomorphology*. Elsevier, 67(3), pp. 273–281.

Cassar, J. (2002) 'Deterioration of the Globigerina limestone of the Maltese Islands', *Geological Society, London, Special Publications*. Geological Society of London, 205(1), pp. 33–49. doi: 10.1144/GSL.SP.2002.205.01.04.

Causon Deguara, J. and Gauci, R. (2017) 'Evidence of extreme wave events from boulder deposits on the south-east coast of Malta (Central Mediterranean)', *Natural Hazards*. Springer, 86(2), pp. 543–568.

Chelli, A., Pappalardo, M., Llopis, I. A. and Federici, P. R. (2010) 'The relative influence of lithology and weathering in shaping shore platforms along the coastline of the Gulf of La Spezia (NW Italy) as revealed by rock strength', *Geomorphology*. 118(1–2), pp. 93–104. doi: 10.1016/j.geomorph.2009.12.011.

Chelli, A., Pappalardo, M. and Pannacciulli, F. (2012) 'Le piattaforme litorali mediterranee: indagare i processi responsabili del loro modellamento per utilizzarle come indicatori dei paleo livelli del mare', in D'Angelo, S. and Fiorentino, S. (eds) *Contributi al Meeting Marino, 25–26 Ottobre 2012*. Roma: ISPRA, pp. 19–24.

Choi, K. H. and Seong, Y. B. (2014) 'Chapter 11: The rock coast of Korea', *Geological Society, London, Memoirs* , 40(1), pp. 193–202. doi: 10.1144/M40.11.

Clark, R. N. (1999) 'Spectroscopy of rocks and minerals, and principles of spectroscopy', *Manual of remote sensing*, 3, pp. 3–58.

Cooke, R. U. and Smalley, I. J. (1968) 'Salt weathering in deserts', *Nature*. Springer, 220(5173), pp. 1226–1227.

Cook, T.D., (1979) Exploration history of south Texas Lower Cretaceous carbonate platform. *AAPG Bulletin*, *63* (1), pp.32-49.

Coombes, M. A. (2014) 'Chapter 5: The rock coast of the British Isles: weathering and biogenic processes', *Geological Society, London, Memoirs* , 40(1), pp. 57–76. doi: 10.1144/M40.5.

Coombes, M. A. and Naylor, L. A. (2012) 'Rock warming and drying under simulated intertidal conditions, part II: weathering and biological influences on evaporative cooling and near-surface micro-climatic conditions as an example of biogeomorphic ecosystem engineering', *Earth Surface Processes and Landforms*. Wiley Online Library, 37(1), pp. 100–118.

Cooper, J. A. G. and Green, A. N. (2016) 'Geomorphology and preservation potential of coastal and submerged aeolianite: Examples from KwaZulu-Natal, South Africa', *Geomorphology*. Elsevier B.V., 271, pp. 1–12. doi: 10.1016/j.geomorph.2016.07.028.

Cotton, C. A. (1963) 'Levels of planation of marine benches', *Zeitschrift für Geomorphologie*, 7, pp. 97–111.

Cruslock, E. M., Naylor, L. A., Foote, Y. L. and Swantesson, J. O. H. (2010) 'Geomorphologic equifinality: A comparison between shore platforms in Höga Kusten and Fårö, Sweden and the Vale of Glamorgan, South Wales, UK',

Geomorphology, 114(1–2), pp. 78–88. doi: 10.1016/j.geomorph.2009.02.019.

Dana, J. D. (1849) *Geology of the United States-Exploring expedition during the years 1836, 1840, 1841, 1842, under the command of Charles Wilkes, USN*. XI.

Dasgupta, R. (2010) 'Whither shore platforms?', *Progress in Physical Geography*, 35(2), pp. 183–209. doi: 10.1177/0309133310375730.

Davies, P., Sunamura, T., Takeda, I., Tsujimoto, H., & Williams, A. (2006) Controls of Shore Platform Width: The Role of Rock Resistance Factors at Selected Sites in Japan and Wales, UK. *Journal of Coastal Research,* 160-164. Retrieved from http://www.jstor.org/stable/25741554

Day, M. J. (1980) 'Rock hardness: Field assessment and geomorphic importance', *Professional Geographer*, 32(1), pp. 72–81. doi: 10.1111/j.0033-0124.1980.00072.x.

Defra (2007) *Understanding and Predicting Beach Morphological Change Associated with the Erosion of Cohesive Shore Platforms*, *R&D Technical Report FD1926/TR*.

De La Beche, H. T. (1839) *Report on the geology of Cornwall, Devon and West Somerset*. HM Stationery Office, Longman, Orme, Brown, Green, and Longmans.

Demirdag, S., Yavuz, H. and Altindag, R. (2009) 'The effect of sample size on Schmidt rebound hardness value of rocks', *International Journal of Rock Mechanics and Mining Sciences*, 46(4), pp. 725–730. doi: 10.1016/j.ijrmms.2008.09.004.

Devoto, S., Biolchi, S., Bruschi, V. M., Díez, A. G., Mantovani, M., Pasuto, A., Piacentini, D., Schembri, J. A. and Soldati, M. (2013) 'Landslides along the north-west coast of the Island of Malta', in *Landslide science and practice*. Springer, pp. 57–63.

Devoto, S., Biolchi, S., Bruschi, V. M., Furlani, S., Mantovani, M., Piacentini, D., Pasuto, A. and Soldati, M. (2012) 'Geomorphological map of the NW Coast of the Island of Malta (Mediterranean Sea)', *Journal of Maps*. Taylor & Francis, 8(1), pp. 33–40.

Dickson, M. E. and Stephenson, W. J. (2014) 'The rock coast of New Zealand', in Kennedy, D. M., Stephenson,W.J. & Naylor, L. A. (eds) 2014. (ed.) *Rock Coast Geomorphology: A Global Synthesis.* Geological Society of London, pp. 225–234.

Dickson, M. E. (2002) *The development of rock coast morphology on Lord Howe Island, Australia*. University of Wollongong.

Dickson, M. E. (2006) 'Shore platform development around Lord Howe Island, southwest Pacific', *Geomorphology*, 76(3–4), pp. 295–315. doi: 10.1016/j.geomorph.2005.11.009.

Dickson, M. E., Kennedy, D. M. and Woodroffe, C. D. (2004) 'The influence of rock resistance on coastal morphology around Lord Howe Island, Southwest Pacific', *Earth Surface Processes and Landforms*, 29(5), pp. 629–643. doi:

10.1002/esp.1058.

Dickson, M. E. and Woodroffe, C. D. (2005) 'Rock coast morphology in relation to lithology and wave exposure, Lord Howe Island, southwest Pacific', *Zeitschrift für Geomorphologie, NF*. Schweizerbart'sche Verlagsbuchhandlung, pp. 239–251.

Dornbusch, U. and Robinson, D. A. (2011) 'Block removal and step backwearing as erosion processes on rock shore platforms: a preliminary case study of the chalk shore platforms of south-east England', *Earth Surface Processes and Landforms*, 36(5), pp. 661–671. doi: 10.1002/esp.2086.

Drago, A., Azzopardi, J., Gauci, A., Tarasova, R. and Bruschi, A. (2013) 'Assessing the offhore wave energy potential for the Maltese Islands', in *Sustainable Energy Conference 2013: The ISE Annual Conference*, pp. 16–27.

Dramis, F., Guida, D. and Cestari, A. (2011) 'Nature and aims of geomorphological mapping', *Geomorphological mapping: Methods and applications*. Elsevier London, pp. 39–73.

EC (2017) *The EU Environmental Implementation Review Country Report - MALTA*.

Edwards, A. B. (1941) 'Storm wave platforms', *Journal of Geomorphology*, 4, pp. 223–236.

Edwards, A. B. (1951) 'Wave action in shore platform formation', *Geological Magazine*. Cambridge University Press, 88(1), pp. 41–49.

Elston, E. D. (1917) 'Potholes : Their Variety, Origin and Significance', *The Scientific Monthly*, 5(6), pp. 554–567.

Emery, K. O. (1941) 'Rate of surface retreat of sea cliffs based on dated inscriptions', *Science*. American Association for the Advancement of Science, 93(2426), pp. 617–618.

Emery, K. O. and Kuhn, G. G. (1982) 'Sea cliffs: their processes, profiles, and classification', *Geological Society of America Bulletin*. Geological Society of America, 93(7), pp. 644–654.

ERA (2012a) *BioSnippet*. Malta.

ERA (2012b) *Rdumijiet ta' Malta: Mir-Ramla taċ-Ċirkewwa sar-Ramla tal-Mixquqa*. Malta.

Ersoy, A. and Waller, M. D. (1995) 'Textural characterisation of rocks', *engineering geology*. Elsevier, 39(3–4), pp. 123–136.

EUrosion (2004a) *A guide to coastal erosion management practices in Europe*.

EUrosion (2004b) *Living with coastal erosion in Europe: Sediment and Space for Sustainability - A guide to coastal erosion management practices in Europe*.

Everard, C. E., Lawrence, R. H., Witherick, M. E. and Wright, L. W. (1964) 'Raised

beaches and marine geomorphology', *Present Views on Some Aspects of the Geology of Cornwall and Devon. Royal Geological Society of Cornwall, Truro*, pp. 283–310.

Farrugia, M. T. (2008) 'Coastal erosion along northern Malta: geomorphological processes and risks', *Geografia Fisica e Dinamica Quaternaria*, 31(2), pp. 149–160.

Felix, R. (1973) 'Oligo-Miocene stratigraphy of Malta and Gozo'. H. Veenman.

Fener, M., Kahraman, S., Bilgil, A. and Gunaydin, O. (2005) 'A comparative evaluation of indirect methods to estimate the compressive strength of rocks', *Rock Mechanics and Rock Engineering*, 38(4), pp. 329–343. doi: 10.1007/s00603-005-0061-8.

Foote, Y., Plessis, E. and Robinson, D. (2001) 'Rates and patterns of cliff erosion and downwearing of chalk shore platforms: comparisons between France and England', in *European Rock Coasts 2001 Conference, Brighton, England*, pp. 24–25.

Foresi, L. M., Baldassini, N., Sagnotti, L., Lirer, F., Di Stefano, A., Caricchi, C., Verducci, M., Salvatorini, G. and Mazzei, R. (2014) 'Integrated stratigraphy of the St. Thomas section (Malta Island): A reference section for the lower Burdigalian of the Mediterranean Region', *Marine Micropaleontology*. Elsevier B.V., 111, pp. 66–89. doi: 10.1016/j.marmicro.2014.06.004.

Foresi, L. M., Verducci, M., Baldassini, N., Lirer, F., Mazzei, R., Gianfranco, S., Ferraro, L. and Da Prato, S. (2011) 'Integrated stratigraphy of St. Peter's Pool section (Malta): new age for the Upper Globigerina Limestone member and progress towards the Langhian GSSP', *Stratigraphy*, 8(2–3), pp. 125–143.

Forti, F., Furlani, S. and Cucchi, F. (2006) 'Lowering Rates Of Limestone Along the Western Istrian shoreline and the Gulf of Trieste', *Geografia Fisica e Dinamica Quaternaria*, (211116), pp. 61–69.

Franzoni, E., Sassoni, E., Scherer, G. W. and Naidu, S. (2013) 'Artificial weathering of stone by heating', *Journal of Cultural Heritage*. Elsevier, 14(3), pp. e85–e93.

Fronteau, G., Schneider-Thomachot, C., Chopin, E., Barbin, V., Mouze, D. and Pascal, A. (2010) 'Black-crust growth and interaction with underlying limestone microfacies', *Geological Society, London, Special Publications*, 333(April), pp. 25–34. doi: 10.1144/SP333.3.

Furlani, S., Antonioli, F., Biolchi, S., Gambin, T., Gauci, R., Presti, V. Lo, Anzidei, M., Devoto, S., Palombo, M. and Sulli, A. (2013) 'Holocene sea level change in Malta', *Quaternary International*. Elsevier, 288, pp. 146–157.

Furlani, S., Chersicla, D., Bressan, G. and Biolchi, S. (2011) 'Shore Grykes Along The Western Istrian Coast Obalni Grajki Ob Zahodni Istrski Obali', *Acta Carsologica*, 40(1), pp. 29–42.

Furlani, S. and Cucchi, F. (2008) 'TMEM Surveying On Sandstones'. *Proceedings*

of the 10th International Symposium on Pseudokarts, Gorizia, pp. 147-156

Furlani, S., Cucchi, F. and Biolchi, S. (2011) 'Morfologie Carsiche Costiere Intertidali Lungo Le Coste Del Golfo Di Trieste', *Atti e Mormorie della Commissione Grotte 'E. Boegan"*, 43, pp. 151–168.

Furlani, S., Cucchi, F., Forti, F. and Rossi, A. (2009) 'Comparison between coastal and inland Karst limestone lowering rates in the northeastern Adriatic Region (Italy and Croatia)', *Geomorphology*. Elsevier, 104(1), pp. 73–81.

Furlani, S., Pappalardo, M., Gómez-Pujol, L. and Chelli, A. (2014) 'Chapter 7: The rock coast of the Mediterranean and Black seas', *Geological Society, London, Memoirs*, 40(1), pp. 89–123. doi: 10.1144/m40.7.

Galdies, C. (2011) *The Climate of Malta: statistics, trends and analysis 1951-2010*. National Statistics Office, Malta.

Galve, J. P., Tonelli, C., Gutiérrez, F., Lugli, S., Vescogni, A. and Soldati, M. (2015) 'New insights into the genesis of the Miocene collapse structures of the island of Gozo (Malta, central Mediterranean Sea)', *Journal of the Geological Society*. Geological Society of London, 172(3), pp. 336–348.

Gatt, P. A. (2006) 'Model of limestone weathering and damage in masonry : Sedimentological and geotechnical controls in the Globigerina Limestone Formation (Miocene) of Malta', *Xjenza*, 11, pp. 30–39.

Gauci, R., Schembri, J. A. and Inkpen, R. (2017) 'Traditional use of shore platforms: a study of the artisanal management of salinas on the Maltese Islands (Central Mediterranean)', *SAGE Open*. SAGE Publications Sage CA: Los Angeles, CA, 7(2), p. 2158244017706597.

Gerada Gatt, E. (2014) 'The Mystery of St Paul's shipwreck', *Think Magazine*.

Gianelli, L., Salvatorini, G., Giannelli, L. and Salvatorini, G. (1972) 'I foraminiferi planctonici dei sedimenti terziari dell'arcipelago Maltese', *Atti della Societa Toscana di Scienze Naturali*, LXXIX(79), pp. 49-74-.

Gill, E. D. (1967) 'The dynamics of the shore platform process, and its relation to changes in sea-level', *Proceedings of the Royal Society of Victoria*, 80, pp. 183–192.

Gill, E. D. (1972) 'The relationship of present shore platforms to past sea levels', *Boreas*, 1(1), pp. 1–25. doi: 10.1111/j.1502-3885.1972.tb00141.x.

Gill, E. D. and Lang, J. G. (1983) 'Micro-erosion meter measurements of rock wear on the Otway coast of southeast Australia', *Marine Geology*, 52, pp. 141-156.

Gomez-Heras, M., Smith, B. J., Viles, H. A, Lukaszewicz, J. W. and Niemcewicz, P. (2008) 'Laboratory modelling of gypsum crust growth on limestone related to soot pollution and gaseous sulphur: implications of "cleaner" environments for stone decay', *Proceedings of the 11th international Congress on Deterioration and Concervation of Stone*, Torun, pp. 105–112.

Gómez-Pujol, L., Fornós, J. J. and Swantesson, J. O. H. (2006) 'Rock surface millimetre-scale roughness and weathering of supratidal Mallorcan carbonate coasts (Balearic Islands)', *Earth Surface Processes and Landforms*. John Wiley & Sons, Ltd., 31(14), pp. 1792–1801. doi: 10.1002/esp.1379.

Gómez-Pujol, L., Stephenson, W. J. and Fornós, J. J. (2007) 'Two-hourly surface change on supra-tidal rock (Marengo, Victoria, Australia)', *Earth Surface Processes and Landforms*, 32(1), pp. 1–12. doi: 10.1002/esp.1373.

Goudie, A. S. (1993) 'Salt weathering simulation using a single-immersion technique', *Earth Surface Processes and Landforms*. Wiley Online Library, 18(4), pp. 369–376.

Goudie, A. S. (1999) 'Experimental salt weathering of limestones in relation to rock properties', *Earth Surface Processes and Landforms*. Chichester, Sussex; New York: Wiley, c1981-, 24(8), pp. 715–724.

Goudie, A. S. (2006) 'The Schmidt Hammer in geomorphological research', *Progress in Physical Geography*, 30(6), pp. 703–718. doi: 10.1177/0309133306071954.

Goudie, A. S. (2013) *The Schmidt Hammer and Related Devices in Geomorphological Research*, *Treatise on Geomorphology*. Elsevier Ltd. doi: 10.1016/B978-0-12-374739-6.00398-5.

Goudie, A. S. (2014) 'Alphabetical Glossary of Geomorphology Version 1.0', p. 84. Available at: http://www.geomorph.org/wp-content/uploads/2015/06/GLOSSARY_OF_GEOMORPHOLOGY1.pdf. Last accessed: 19th June 2018.

Goudie, A. S. (2016) 'Quantification of rock control in geomorphology', *Earth-Science Reviews*. Elsevier B.V., 159, pp. 374–387. doi: 10.1016/j.earscirev.2016.06.012.

Goudie, A. S. and Viles, H. A. (1999) 'The frequency and magnitude concept in relation to rock weathering', *Zeitschrift für Geomorphologie Supplement Volumes*. Schweizerbart'sche Verlagsbuchhandlung, pp. 175–189.

Gruszczyński, M., Marshall, J. D., Goldring, R., Coleman, M. L., Małkowski, K., Gaździcka, E., Semil, J. and Gatt, P. (2008) 'Hiatal surfaces from the Miocene Globigerina Limestone Formation of Malta: Biostratigraphy, sedimentology, trace fossils and early diagenesis', *Palaeogeography, Palaeoclimatology, Palaeoecology*, 270(3–4), pp. 239–251. doi: 10.1016/j.palaeo.2008.01.035.

Guney, A., Altındağ, R., Yavuz, H. and Saraç, S. (2005) 'Evaluation of the Relationships between Schmidt Hardness Rebound Number and Other (Engineering) Properties of Rocks', *The 19th International Mining Congress and Fair of Turkey, IMCET2005, İzmir, Turkey*, (June 09-12), pp. 83–90.

Hack, R. and Huisman, M. (2002) 'Estimating the intact rock strength of a rock mass by simple means', Proceedings 9th Congress of the International Association for Engineering Geology and the Environment, Durban, South

Africa, 16-20th September 2002, pp. 1971-1977.

Hall, K., Thorn, C. and Sumner, P. (2012) 'On the persistence of "weathering"', *Geomorphology*. Elsevier, 149, pp. 1–10.

Halsey, D. P. (2000) 'Studying rock weathering with microcatchment experiments (with 5 figures and 1 table)', *Zeitschrift Fur Geomorphologie Supplementband*, pp. 23–32.

Hawkins, J. (1827) 'On changes which appear to have taken place in the primitive form of the Cornish peninsula', *Transactions of the Royal Geological Society of Cornwall*, 3, 1-16.

Hebib, R., Belhai, D. and Alloul, B. (2017) 'Estimation of uniaxial compressive strength of North Algeria sedimentary rocks using density, porosity, and Schmidt hardness', *Arabian Journal of Geosciences*, 10(17), p. 383. doi: 10.1007/s12517-017-3144-4.

Hemmingsen, S. A., Eikaas, H. S. and Hemmingsen, M. a. (2007) 'The influence of seasonal and local weather conditions on rock surface changes on the shore platform at Kaikoura Peninsula, South Island, New Zealand', *Geomorphology*, 87(4), pp. 239–249. doi: 10.1016/j.geomorph.2006.09.010.

Hénaff, A., Lageat, Y. and Costa, S. (2006) 'Geomorphology and shapping processes of chalk shore platforms of the Channel coasts.', *Annales de Géomorphologie/Annals of Geomorphology/Zeitschrift für Geomorphologie*, 144, pp. 61–91.

High, C. and Hanna, F. K. (1970) 'Method for the direct measurement of erosion on rock surfaces'. Published for the British Geomorphological Research Group by Geo Abstracts.

Hills, E. S. (1949) 'Shore platforms', *Geological Magazine*. Cambridge University Press, 86(3), pp. 137–152.

Hills, E. S. (1972) 'Shore platforms and wave ramps', *Geological Magazine,*. Cambridge University Press, 109(2), pp. 81–88.

Hodgkin, E. P. (1964) 'Rate of erosion of intertidal limestone', *Zeitschrift für Geomorphologie*, 8(4), pp. 385–392.

Hucka, V. (1965) 'A rapid method of determining the strength of rocks in situ', *International Journal of Rock Mechanics & Mining Sciences*, 2, pp. 127–134. doi: 10.1016/0148-9062(65)90009-4.

Hunt, G. R. and Salisbury, J. W. (1971) 'Visible and near-infrared spectra of minerals and rocks II: Carbonates'. *Modern Geology*, 2, pp. 23-30.

Hunt, G. R. and Salisbury, J. W. (1976). Visible and near-infrared spectra of minerals and rocks XI: Sedimentary Rocks. *Modern Geology*, 5, pp. 211-217.

Inkpen, R. J., Stephenson, W. J., Kirk, R. M., Hemmingsen, M. a. and Hemmingsen, S. a. (2010) 'Analysis of relationships between micro-topography and short- and

long-term erosion rates on shore platforms at Kaikoura Peninsula, South Island, New Zealand', *Geomorphology*. Elsevier B.V., 121(3–4), pp. 266–273. doi: 10.1016/j.geomorph.2010.04.023.

International Society for Rock Mechanics (2007) *The complete ISRM suggested methods for rock characterization, testing and monitoring: 1974-2006*. International Society for Rock Mechanics, Commission on Testing Methods.

James, N. P. (1972) 'Holocene And Pleistocene Calcareous Crust (Caliche) Profiles: Criteria For Subaerial Exposure', *Journal for Sedimentary Research*, 42(4).

John, C. M., Mutti, M. and Adatte, T. (2003) 'Mixed carbonate-siliciclastic record on the North African margin (Malta) - Coupling of weathering processes and mid Miocene climate', *Bulletin of the Geological Society of America*, 115(2), pp. 217–229. doi: 10.1130/0016-7606(2003)115<0217:MCSROT>2.0.CO;2.

Johnson, D. W. (1919) *Shore processes and shoreline development*. John Wiley & Sons, Incorporated.

Johnson, D. W. (1938) 'Shore platforms-Discussion' *I. Geomorph*, 1, pp. 268-72.

Jutson, J. T. (1939) 'Shore platforms near Sydney', *New South Wales. Journal of Geomorphology*, 2, pp. 237–250.

Jutson, J. T., (1954) 'The shore platform of Lorne, Victoria, and the processes of erosion operating thereon', *Royal Soc. Victoria Proc*. 65, pp.125–134.

Kanyaya, J. I. and Trenhaile, A. S. (2005) 'Tidal wetting and drying on shore platforms: an experimental assessment', *Geomorphology*. Elsevier, 70(1), pp. 129–146. doi: 10.1016/j.geomorph.2005.04.005.

Karaman, K. and Kesimal, A. (2015) 'A comparative study of Schmidt hammer test methods for estimating the uniaxial compressive strength of rocks', *Bulletin of Engineering Geology and the Environment*. Springer Berlin Heidelberg, 74(2), pp. 507–520. doi: 10.1007/s10064-014-0617-5.

Katz, O., Reches, Z. and Roegiers, J.-C. (2000) 'Evaluation of mechanical rock properties using a Schmidt Hammer', *International Journal of Rock Mechanics and Mining Sciences*, 37, pp. 723–730.

Kennedy, D. M. (2010) 'Geological control on the morphology of estuarine shore platforms: Middle Harbour, Sydney, Australia', *Geomorphology*. Elsevier B.V., 114(1–2), pp. 71–77. doi: 10.1016/j.geomorph.2009.02.012.

Kennedy, D. M. (2016) 'The subtidal morphology of microtidal shore platforms and its implication for wave dynamics on rocky coasts', *Geomorphology*. Elsevier B.V., 268, pp. 146–158. doi: 10.1016/j.geomorph.2016.06.003.

Kennedy, D. M. and Beban, J. G. (2005) 'Shore platform morphology on a rapidly uplifting coast, Wellington, New Zealand', *Earth Surface Processes and Landforms*, 30(7), pp. 823–832. doi: 10.1002/esp.1192.

Kennedy, D. M. and Dickson, M. E. (2006) 'Lithological control on the elevation of shore platforms in a microtidal setting', *Earth Surface Processes and Landforms*. John Wiley & Sons, Ltd., 31(12), pp. 1575–1584. doi: 10.1002/esp.1358.

Kennedy, D. M., Ierodiaconou, D., Weir, A. and Brighton, B. (2017) 'Wave hazards on microtidal shore platforms: testing the relationship between morphology and exposure', *Natural Hazards*. Springer Netherlands, 86(2), pp. 741–755. doi: 10.1007/s11069-016-2714-1.

Kennedy, D. M. and Milkins, J. (2015) 'The formation of beaches on shore platforms in microtidal environments', *Earth Surface Processes and Landforms*, 40(1), pp. 34–46. doi: 10.1002/esp.3610.

Kennedy, D. M. and Paulik, R. (2007) 'Estuarine shore platforms in Whanganui Inlet, South Island, New Zealand', *Geomorphology*, 88(3–4), pp. 214–225. doi: 10.1016/j.geomorph.2006.11.007.

Kennedy, D. M., Paulik, R. and Dickson, M. E. (2011) 'Subaerial weathering versus wave processes in shore platform development: reappraising the Old Hat Island evidence', *Earth Surface Processes and Landforms*, 36(5), pp. 686–694. doi: 10.1002/esp.2092.

Kennedy, D. M., Sherker, S., Brighton, B., Weir, A. and Woodroffe, C. D. (2013) 'Rocky coast hazards and public safety: Moving beyond the beach in coastal risk management', *Ocean & Coastal Management*, 82, pp. 85–94. doi: 10.1016/j.ocecoaman.2013.06.001.

Kennedy, D. M., Stephenson, W. J. and Naylor, L. A. (2014a) 'Rock Coast Geomorphology: A Global Synthesis', in. Geological Society Memour, No. 40, Geological Society of London.

Kennedy, D. M., Stephenson, W. J. and Naylor, L. A. (2014b) 'Chapter 1 Introduction to the rock coasts of the world', *Geological Society, London, Memoirs*, 40(1), pp. 1–5. doi: 10.1144/M40.1.

Kirk, R. M. (1977) 'Rates and forms of erosion on intertidal platforms at Kaikoura Peninsula, South Island, New Zealand', *New Zealand Journal of Geology and Geophysics*. Taylor & Francis, 20(3), pp. 571–613.

Kramar, S., Urosevic, M., Pristacz, H. and Mirtič, B. (2010) 'Assessment of limestone deterioration due to salt formation by micro-Raman spectroscopy: application to architectural heritage', *Journal of Raman spectroscopy*. Wiley Online Library, 41(11), pp. 1441–1448.

Liang, M., Mohamad, E. T., Khun, M. C. and Alel, M. N. A. (2015) 'Estimating uniaxial compressive strength of tropically weathered sedimentary rock using indirect tests', *Jurnal Teknologi*, 72(3), pp. 49–58.

Malta Environment and Planning Authority (1995). *Marsaxlokk Bay Local Plan*. Malta.

Malta Environment and Planning Authority (2006) *South Malta Local Plan*.

Malta.

Malta Environment and Planning Authority (2015) *Strategic Environmental Assessment, Environment Report, SPED*. Floriana.

Magri, O., Mantovani, M., Pasuto, A. and Soldati, M. (2008) 'Geomorphological investigation and monitoring of lateral spreading along the north-west coast of Malta', *Geografia Fisica e Dinamica Quaternaria*, 31(2), pp. 171–180.

Marshall, R. J. E. and Stephenson, W. J. (2011) 'The morphodynamics of shore platforms in a micro-tidal setting: Interactions between waves and morphology', *Marine Geology*. Elsevier B.V., 288(1–4), pp. 18–31. doi: 10.1016/j.margeo.2011.06.007.

Martin, I. (2017) 'Three of every four people who drowned in Malta last year were foreign', February 18th, *Times of Malta*.

Mayaud, J. R., Viles, H. A. and Coombes, M. A. (2014) 'Exploring the influence of biofilm on short-term expansion and contraction of supratidal rock: An example from the Mediterranean', *Earth Surface Processes and Landforms*, 39(10), pp. 1404–1412. doi: 10.1002/esp.3602.

McAllister, D., Warke, P. and McCabe, S. (2017) 'Stone temperature and moisture variability under temperate environmental conditions: Implications for sandstone weathering', *Geomorphology*. Elsevier B.V., 280, pp. 137–152. doi: 10.1016/j.geomorph.2016.12.010.

McCarroll, D. (1987) 'The Schmidt hammer in geomorphology: five sources of instrument error', *British Geomorphological Research Group Technical Bulletin*, 36, pp. 16–27.

McKenna, J., Carter, R. W. G. and Bartlett, D. (1992) 'Coast erosion in Northeast Ireland:-Part II Cliffs and shore platforms', *Irish Geography*. Taylor & Francis, 25(2), pp. 111–128.

Micallef, A., Foglini, F., Le Bas, T., Angeletti, L., Maselli, V., Pasuto, A. and Taviani, M. (2013) 'The submerged paleolandscape of the Maltese Islands: Morphology, evolution and relation to Quaternary environmental change', *Marine Geology*. Elsevier, 335, pp. 129–147.

Micallef, A. and Williams, A. T. (2009) 'Shore platform denudation measurements along the Maltese coastline', *Journal of Coastal Research*. JSTOR, 56(2), pp. 737–741.

Micallef, S., Micallef, A., Galdies, C., (2018) 'Application of the Coastal Hazard Wheel to assess erosion on the Maltese coast', *Ocean and Coastal Management*. Elsevier Ltd, 156, pp. 209-222. doi: 10.1016/j.ocecoaman.2017.06.005

MINS (2017) *Report of drownings in Maltese waters for 2016*.

Moses, C. A. (2000) 'Field rock block exposure trials', *Zeitschrift fur Geomorphologie*, 120, pp. 33–50.

Moses, C. A. (2013) 'Tropical rock coasts: Cliff, notch and platform erosion dynamics', *Progress in Physical Geography*, 37(2), pp. 206–226. doi: 10.1177/0309133312460073.

Moses, C. A. (2014) 'Chapter 4: The rock coast of the British Isles : shore platforms', in *Rock Coast Geomorphology: A Global Synthesis*, pp. 39–56. doi: 10.1144/M40.4.

Moses, C. A., Robinson, D. A., Williams, R. B. G. and Marques, F. (2006) 'Predicting rates of shore platform downwearing from rock geotechnical properties and laboratory simulation of weathering and erosion processes (with 5 tables)', *Zeitschrift fur Geomorphologie Supplementband*, 144, p. 19.

Moses, C. A. and Smith, B. J. (1993) 'A note on the role of the lichen collema auriforma in solution basin development on a carboniferous limestone substrate', *Earth Surface Processes and Landforms*, 18(4), pp. 363–368. doi: 10.1002/esp.3290180405.

Moses, C., Robinson, D. and Barlow, J. (2014) 'Methods for measuring rock surface weathering and erosion: A critical review', *Earth-Science Reviews*. Elsevier B.V., 135, pp. 141–161. doi: 10.1016/j.earscirev.2014.04.006.

Moses, C., Robinson, D., Kazmer, M. and Williams, R. (2015) 'Towards an improved understanding of erosion rates and tidal notch development on limestone coasts in the Tropics: 10 years of micro-erosion meter measurements, Phang Nga Bay, Thailand', *Earth Surface Processes and Landforms*. Wiley Online Library, 40(6), pp. 771–782.

Moses, C. and Smith, B. J. (1994) 'Limestone weathering in supra-tidal zone: an example from Mallorca', in *Rock Weathering and Landform Evolution.* Wiley & Sons, pp. 433–452.

Mottershead, D. (1982) 'Coastal spray weathering of bedrock in the supratidal zone at East Prawle, South Devon', *Field studies*, 5, pp. 663–684.

Mottershead, D. (1989) 'Rates and patterns of bedrock denudation by coastal salt spray weathering: A seven-year record', *Earth Surface Processes and Landforms*. Wiley Online Library, 14(5), pp. 383–398.

Mottershead, D. (2013) 'Coastal weathering', in *Treatise on geomorphology. Volume 4, Weathering and soils geomorphology*. Elsevier.

Moura, D., Gabriel, S. and Jacob, J. (2011) 'Coastal morphology along the Central Algarve rocky coast : Driver mechanisms', *Journal of Coastal Research, Suppl. Special Issue*. Fort Lauderdale (64), pp. 790–794.

Naylor, L. A. (2005) 'The contributions of biogeomorphology to the emerging field of geobiology', *Palaeogeography, Palaeoclimatology, Palaeoecology*. Elsevier, 219(1), pp. 35–51.

Naylor, L. A. and Stephenson, W. J. (2010) 'On the role of discontinuities in mediating shore platform erosion', *Geomorphology*. Elsevier B.V., 114(1–2), pp. 89–100. doi: 10.1016/j.geomorph.2008.12.024.

Naylor, L. A., Coombes, M. A. and Viles, H. A. (2012) 'Reconceptualising the role of organisms in the erosion of rock coasts: A new model', *Geomorphology*. Elsevier B.V., 157–158, pp. 17–30. doi: 10.1016/j.geomorph.2011.07.015.

Naylor, L. A., Kennedy, D. M. and Stephenson, W. J. (2014) 'Synthesis and conclusion to the rock coast geomorphology of the world', *Geological Society, London, Memoirs*, 40, pp. 283–286. doi: 10.1144/M40.17.

Naylor, L. A., Stephenson, W. J. and Trenhaile, A. S. (2010) 'Rock coast geomorphology: Recent advances and future research directions', *Geomorphology*, 114(1), pp. 3–11. doi: 10.1016/j.geomorph.2009.02.004.

Naylor, L. A., Viles, H. A. and Carter, N. E. A. (2002) 'Biogeomorphology revisited: looking towards the future', *Geomorphology*. Elsevier, 47(1), pp. 3–14.

Nicholson, D. T. (2001) 'Pore properties as indicators of breakdown mechanisms in experimentally weathered limestones', *Earth Surface Processes and Landforms*. Wiley Online Library, 26(8), pp. 819–838.

Niedzielski, T., Migoń, P. and Placek, A. (2009) 'A minimum sample size required from Schmidt hammer measurements', *Earth Surface Processes and Landforms*. Wiley Online Library, 34(13), pp. 1713–1725.

Noormets, R., Crook, K. A. W. and Felton, E. A. (2004) 'Sedimentology of rocky shorelines: 3. Hydrodynamics of megaclast emplacement and transport on a shore platform, Oahu, Hawaii', *Sedimentary Geology*, 172(1–2), pp. 41–65. doi: 10.1016/j.sedgeo.2004.07.006.

Norrish, K. (1954) 'The swelling of montmorillonite', *Discussions of the Faraday society*. Royal Society of Chemistry, 18, pp. 120–134.

NSO (2012) *Census of Population and Housing: Preliminary Report*. Malta.

O'Rourke, J. E. (1989) 'Rock index properties for geoengineering in underground development', *Min. Eng.(Littleton, Colo.);(United States)*. Woodward-Clyde Consultants, Oakland, CA (US), 41(2).

Odediran, O. A. and Mopa, B. (2014) 'Preliminary Field Measurement of the Uniaxial Compressive Strength of Migmatite Using N-type Schmidt Rebound Hammer', *The International Journal of Engineering and Science*, 3(8), pp. 11–17.

Ojo, O. and Brook, N. (1990) 'The effect of moisture on some mechanical properties of rock', *Mining Science and Technology*, 10(2), pp. 145–156. doi: 10.1016/0167-9031(90)90158-O.

Özbek, A. (2009) 'Variation of Schmidt hammer values with imbrication direction in clastic sedimentary rocks', *International Journal of Rock Mechanics and Mining Sciences*, 46(3), pp. 548–554. doi: 10.1016/j.ijrmms.2008.09.003.

Pace, M., Borg, J. A., Galdies, C. and Malhotra, A. (2017) 'Influence of wave climate on architecture and landscape characteristics of Posidonia oceanica meadows', *Marine Ecology*, 38(1), pp. 1–14. doi: 10.1111/maec.12387.

Pappalardo (2017) 'Development of Shore Platforms along the NW Coast of Italy: The Role of Wind Waves', *Journal of Coastal Research*. doi: 10.2112/JCOASTRES-D-16-00113.1.

Pedley, H. M. (1975) 'Oligocene-Miocene stratigraphy of the Maltese islands', Unpublished Ph. D. Dissertation, University of Hull.

Pedley, H. M. (1993) 'Geological Map of the Maltese Islands. Sheet 1. Malta, Scale 1:25,000'. Malta: Oil Exploration Directorate, Office of the Prime Minister, Malta.

Pedley, H. M. (2011) 'The Calabrian Stage, Pleistocene highstand in Malta: a new marker for unravelling the Late Neogene and Quaternary history of the islands', *Journal of the Geological Society*, 168(4), pp. 913–926. doi: 10.1144/0016-76492010-080.

Pedley, H. M. and Bennett, S. M. (1985) 'Phosphorites, hardgrounds and syndepositional solution subsidence: a palaeoenvironmental model from the Miocene of the Maltese Islands', *Sedimentary Geology*. Elsevier, 45(1–2), pp. 1–34. doi: 10.1016/0037-0738(85)90022-3.

Pedley, H. M., House, M. R. and Waugh, B. (1976) 'The geology of Malta and Gozo', *Proceedings of the Geologists' Association*. Elsevier, 87(3), pp. 325–341.

Pedley, H. M., House, M. R. and Waugh, B. (1978) 'The Geology of the Pelgian Block: The Maltese islands', *The ocean basins and margins : the Western Mediterranean, Vol. 4B*, pp. 417–433.

Pedley, H. M. and Clarke, M. H. (2002) *Limestone Isles in a Crystal Sea: the geology of the Maltese Islands*. Publishers Enterprises Group.

Pinho, A., Rodrigues-Carvalho, J. A., Gomes, C. and Duarte, I. M. (2006) 'Overview of the evaluation of the state of rock weathering by visual inspection', *IAEG 2006 Engineering Geology for Tomorrow's Cities*.

Pirazzoli, P. A. (1986) 'Marine notches', in Van de Plassche, O. (ed.) *Sea-Level Research: A Manual for the Collection and Evaluation of Data.* Norwich: Geo Books, pp. 361–400.

Pirazzoli, P. A. (1993) 'Global sea-level changes and their measurement', *Global and Planetary Change*, 8(3), pp. 135–148. doi: 10.1016/0921-8181(93)90021-F.

Pomar, F., Gómez-Pujol, L., Fornós, J. J., Del Valle, L. and Nogales, B. (2017) 'Limestone biopitting in coastal settings: A spatial, morphometric, SEM and molecular microbiology sequencing study in the Mallorca rocky coast (Balearic Islands, Western Mediterranean)', *Geomorphology*. Elsevier B.V., 276, pp. 104–115. doi: 10.1016/j.geomorph.2016.10.014.

Poole, R. W. and Farmer, I. W. (1980) 'Consistency and repeatability of Schmidt Hammer rebound data during field testing', *International Journal of Rock Mechanics and Mining Sciences*, 17(3), pp. 167–171. doi: 10.1016/0148-9062(80)91363-7.

Porter, N. J. and Trenhaile, A. S. (2007) 'Short-term rock surface expansion and contraction in the intertidal zone'. *Earth Surface Processes and Landforms*, 32: 1379-1397, pp. 1379–1397. doi: 10.1002/esp.

Porter, N. J., Trenhaile, A. S., Prestanski, K. J. and Kanyaya, J. I. (2010a) 'Shore platform downwearing in eastern Canada: Micro-tidal Gaspé, Québec', *Geomorphology*. Elsevier B.V., 116(1–2), pp. 77–86. doi: 10.1016/j.geomorph.2009.10.010.

Porter, N. J., Trenhaile, A. S., Prestanski, K. and Kanyaya, J. I. (2010b) 'Patterns of surface downwearing on shore platforms in eastern Canada', *Earth Surface Processes and Landforms*, 35(15), pp. 1793–1810. doi: 10.1002/esp.2018.

Prampolini, M., Foglini, F., Biolchi, S., Devoto, S., Angelini, S. and Soldati, M. (2017) 'Geomorphological mapping of terrestrial and marine areas, northern Malta and Comino (central Mediterranean Sea)', *Journal of Maps*. Taylor & Francis, 13(2), pp. 457–469.

Pratt, S. K. (1990) 'Hardground genesis in pelagic carbonates from the Miocene of Malta and Cretaceous of southern England'. PhD Thesis, Royal Holloway, University of London. EThOS ID: uk.bl.ethos.555690

Ramsay, S. A. C. (1846). *On the denudation of South Wales and the adjacent counties of England*. Longman, Brown, Green, and Longmans.

Reich, G. (2005) Near-infrared spectroscopy and imaging: basic principles and pharmaceutical applications. *Advanced drug delivery reviews*, *57*(8), pp.1109-1143.

Rehfeld, U. and Janssen, A. W. (1995) 'Development of phosphatized hardgrounds in the miocene Globigerina Limestone of the maltese archipelago, including a description of Gamopleura melitensis sp. nov. (Gastropoda, Euthecosomata)', *Facies*, 33(1), pp. 91–106. doi: 10.1007/BF02537445.

Revelle, R. and Emery, K. O. (1957) *Chemical erosion of beach rock and exposed reef rock: Bikini and nearby atolls, Marshall Islands*. US Government Printing Office.

Rizzo, C. (1932) 'Geology of the Maltese Islands', *Government Printing Office, Malta*.

Robinson, D. A. (2002) *European Shore Platform Dynamics, Final Report: Work Package 6*. Available at: http://www.sussex.ac.uk/geography/researchprojects/coastview/shoreplatform/dave.pdf. Last accessed: 19th June 2018.

Robinson, D. A. and Lageat, Y. (2006) 'European shore platform dynamics', *Zeitschrift für Geomorphologie*, (144), pp. 1–257.

Robinson, D. A. and Moses, C. A. (2011) 'Rock surface and weathering: process and form', *The SAGE Handbook of Geomorphology. SAGE, London*, pp. 291–309.

Robinson, D. A. and Williams, R. B. G. (2000) 'Experimental weathering of

sandstone by combinations of salts', *Earth Surface Processes and Landforms*. Wiley Online Library, 25(12), pp. 1309–1315.

Robinson, L. A. (1976) 'The micro-erosion meter technique in a littoral environment', *Marine Geology*. Elsevier, 22(3), pp. M51–M58.

Robinson, L. A. (1977a) 'Erosive processes on the shore platform of northeast Yorkshire, England', *Marine Geology*. Elsevier, 23(4), pp. 339–361. doi: 10.1016/0025-3227(77)90038-X.

Robinson, L. A. (1977b) 'Marine erosive processes at the cliff foot', *Marine Geology*, 23(3), pp. 257–271. doi: 10.1016/0025-3227(77)90022-6.

Rose, E. P. F., Pratt, S. K. and Bennett, S. M. (1992) 'Evidence for sea-level changes in the Globigerina Limestone Formation (Miocene) of the Maltese Islands', *Paleontologia i Evolució*, 24, p. 25.

Rothert, E., Eggers, T., Cassar, J., Ruedrich, J., Fitzner, B. and Siegesmund, S. (2007) 'Stone properties and weathering induced by salt crystallization of Maltese Globigerina Limestone', *Geological Society, London, Special Publications*. Geological Society of London, 271(1), pp. 189–198. doi: 10.1144/GSL.SP.2007.271.01.19.

Said, G. and Schembri, J. (2010) 'Malta', in *Encyclopedia of the World's Coastal Landforms*. Springer, pp. 751–759.

Sammut, S., Gauci, R., Drago, A., Gauci, A. and Azzopardi, J. (2017) 'Pocket beach sediment: A field investigation of the geodynamic processes of coarse-clastic beaches on the Maltese Islands (Central Mediterranean)', *Marine Geology*. Elsevier, 387, pp. 58–73.

Schembri, J. A. (2003) 'Coastal land use in the Maltese Islands: A description and appraisal'. University of Durham. Available at http://etheses.dur.ac.uk/4417.

Schembri, P. J., Deidun, A., Mallia, A. and Mercieca, L. (2005) 'Rocky shore biotic assemblages of the Maltese Islands (Central Mediterranean): a conservation perspective', *Journal of Coastal Research*, 21 (1) pp. 157–166.

Schwartz, M. (2006) *Encyclopedia of coastal science*. Springer Science & Business Media.

Selçuk, L. and Nar, A. (2016) 'Prediction of uniaxial compressive strength of intact rocks using ultrasonic pulse velocity and rebound-hammer number', *Quarterly Journal of Engineering Geology and Hydrogeology*, 49(1), pp. 67–75. doi: 10.1144/qjegh2014-094.

Serra, J., Montori, C., Arends, A., Gelizo, O., Roca, E. and Luisi, T. (2003) 'Eurosion: Review of experience in erosion management', *WIT Transactions on the Built Environment*, 70, pp. 325–334.

Shakesby, R. A. and Walsh, R. P. D. (1986) 'Micro-erosion meter measurements of erosion of limestone, Oxwich Point, Gower: some technical considerations and preliminary results', *Cambria*, 13(2), pp. 213–224.

Sheorey, P. R., Barat, D., Das, M. N., Mukherjee, K. P. and Singh, B. (1984) 'Schmidt hammer rebound data for estimation of large scale in situ coal strength', in *International Journal of Rock Mechanics and Mining Sciences & Geomechanics Abstracts*. Elsevier, pp. 39–42.

Short, A. (2013) 'Water-Layer Weathering', *Encyclopedia of Geomorphology*.

Smith, B. J. (2009) 'Weathering processes and forms', in *Geomorphology of desert environments*. Springer, pp. 69–100.

Smith, B. J., Heras, M. G., Viles, H. A. and Cassar, J. (2010) 'Limestone in the built environment: present-day challenges for the preservation of the past', in. Geological Society of London, Special Publication 331, London.

Smith, B. J., Warke, P. A. and Moses, C. A. (2000) 'Limestone weathering in contemporary arid environments: a case study from southern Tunisia', *Earth Surface Processes and Landforms*. Wiley Online Library, 25(12), pp. 1343–1354.

Smith, D. I., Greenaway, M. A., Moses, C. and Spate, A. P. (1995) 'Limestone weathering in eastern Australia. Part 1: Erosion rates', *Earth Surface Processes and Landforms*. Wiley Online Library, 20(5), pp. 451–463.

So, C. L. (1965) 'Coastal platforms of the Isle of Thanet, Kent', *Transactions of the Institute of British Geographers*. JSTOR, pp. 147–156.

Soldati, M., Tonelli, C. and Galve, J. P. (2013) 'Geomorphological evolution of palaeosinkhole features in the Maltese archipelago (Mediterranean Sea)', *Geografia Fisica e Dinamica Quaternaria*, 36(1), pp. 189–198.

Sopacı, E. and Akgün, H. (2016) 'Engineering geological characterization of the Antalya karstic rocks, southern Turkey', *Environmental Earth Sciences*. Springer, 75(5), p. 366.

Spencer, T. (1981) 'Micro-topographic change on calcarenites, grand Cayman Island, West Indies', *Earth Surface Processes and Landforms*. Wiley Online Library, 6(1), pp. 85–94.

Spencer, T. (1985) 'Weathering rates on a Caribbean reef limestone: Results and implications', *Marine Geology*, 69(1–2), pp. 195–201. doi: 10.1016/0025-3227(85)90142-2.

Spencer, T. and Viles, H. (2002) 'Bioconstruction, bioerosion and disturbance on tropical coasts: coral reefs and rocky limestone shores', *Geomorphology*. Elsevier, 48(1), pp. 23–50.

Spiteri, S. (2012) *Campaigning for Rihama Battery*, *Military architecture*. Available at: http://www.militaryarchitecture.com/index.php/Conservation/campaigning-for-rihama-battery.html. Last accessed: 19th June 2018.

Stenberg, B., Viscarra Rossel, R. A., Mouazen, M. and Wetterlind, J. (2010) 'Visible and Near Infrared Spectroscopy in Soil Science', *Advances in Agronomy*,

107(10), pp. 163–215. doi: 10.1016/s0065-2113(10)07005-7.

Stephenson, W. (2013) 'The Micro and Traversing Erosion Meter', *Treatise on Geomorphology*, 14, pp. 164–169. doi: 10.1016/B978-0-12-374739-6.00381-X.

Stephenson, W. J. (1997) 'Improving the traversing micro-erosion meter', *Journal of Coastal Research*. JSTOR, pp. 236–241.

Stephenson, W. J. (2000) 'Shore platforms: a neglected coastal feature?', *Progress in Physical Geography*, 24(3), pp. 311–327. doi: 10.1177/030913330002400301.

Stephenson, W. J., Dickson, M. E. and Denys, P. H. (2017) 'New Insights on the Relative Contributions of Coastal Processes and Tectonics to Shore Platform Development following the Kaikoura Earthquake', *Earth Surface Processes and Landforms*. doi: 10.1002/esp.4176.

Stephenson, W. J., Dickson, M. E. and Trenhaile, A. S. (2013) 'Rock Coasts', in *Treatise on Geomorphology*. Elsevier, pp. 289–307. doi: 10.1016/B978-0-12-374739-6.00284-0.

Stephenson, W. J. and Finlayson, B. L. (2009) 'Measuring erosion with the micro-erosion meter—Contributions to understanding landform evolution', *Earth-Science Reviews*. Elsevier B.V., 95(1–2), pp. 53–62. doi: 10.1016/j.earscirev.2009.03.006.

Stephenson, W. J. and Kirk, R. M. (1996) 'Measuring erosion rates using the micro-erosion meter: 20 years of data from shore platforms, Kaikoura Peninsula, South Island, New Zealand', *Marine Geology*, 131(1984), pp. 209–218.

Stephenson, W. J. and Kirk, R. M. (1998) 'Rates and patterns of erosion on inter-tidal shore platforms, Kaikoura Peninsula, South Island, New Zealand', *Earth Surface Processes and Landforms*, 23(12), pp. 1071–1085.

Stephenson, W. J. and Kirk, R. M. (2000a) 'Development of shore platforms on Kaikoura Peninsula, South Island, New Zealand Part One: The role of waves', *Geomorphology*, 32(1–2), pp. 21–41. doi: 10.1016/S0169-555X(99)00061-6.

Stephenson, W. J. and Kirk, R. M. (2000b) 'Development of shore platforms on Kaikoura Peninsula , South Island , New Zealand Part Two: The role of subaerial weathering', *Geomorphology*, 32, pp. 43–56.

Stephenson, W. J. and Kirk, R. M. (2001) 'Surface swelling of coastal bedrock on inter-tidal shore platforms, Kaikoura Peninsula, South Island, New Zealand', *Geomorphology*, 41(1), pp. 5–21. doi: 10.1016/S0169-555X(01)00100-3.

Stephenson, W. J. and Kirk, R. M. (2006) 'Shore platforms', *Encyclopedia of Coastal Science*.

Stephenson, W. J., Kirk, R. M., Hemmingsen, S. A. and Hemmingsen, M. A. (2010) 'Decadal scale micro erosion rates on shore platforms', *Geomorphology*. Elsevier B.V., 114(1–2), pp. 22–29. doi: 10.1016/j.geomorph.2008.10.013.

Stephenson, W. J. and Naylor, L. A. (2010) 'Rock coast geomorphology', *Geomorphology*. Elsevier B.V., 114(1–2), pp. 1–2. doi: 10.1016/j.geomorph.2009.02.013.

Stephenson, W. J., Taylor, A. J., Hemmingsen, M. A., Tsujimoto, H. and Kirk, R. M. (2004) 'Short-term microscale topographic changes of coastal bedrock on shore platforms', *Earth Surface Processes and Landforms*, 29(13), pp. 1663–1673. doi: 10.1002/esp.1120.

Stephenson, W. J. and Thornton, L. E. (2005) 'Australian rock coasts: review and prospects', *Australian Geographer*. Taylor & Francis, 36(1), pp. 95–115.

Stoner, E. R. & Baumgardner, M. F. (1981) 'Characteristic variation in reflectance of surface soils'. *Journal of the Soil Science Society of America*, 45, pp. 1161-1165.

Sumner, P. and Nel, W. (2002) 'The effect of rock moisture on Schmidt hammer rebound: Tests on rock samples from Marion Island and South Africa', *Earth Surface Processes and Landforms*, 27(10), pp. 1137–1142. doi: 10.1002/esp.402.

Sunamura, T. (1973) 'Coastal cliff erosion due to waves-field investigations and laboratory experiments.', *Jour. Fac. Eng. Univ. Tokyo (B)*, 32, pp. 1–85.

Sunamura, T. (1975) 'A laboratory study of wave-cut platform formation', *The Journal of Geology*. University of Chicago Press, 83(3), pp. 389–397.

Sunamura, T. (1978a) 'A mathematical model of submarine platform development', *Mathematical Geology*. Springer, 10(1), pp. 53–58.

Sunamura, T. (1978b) 'Mechanisms of shore platform formation on the southeastern coast of the Izu Peninsula, Japan', *The Journal of Geology*. University of Chicago Press, 86(2), pp. 211–222.

Sunamura, T. (1983) 'Processes of sea cliff and platform erosion', *CRC Handbook of coastal processes and erosion*. CRC Press, pp. 233–266.

Sunamura, T. (1991) 'The elevation of shore platforms: a laboratory approach to the unsolved problem', *The Journal of Geology*. 99(5), pp. 761-766.

Sunamura, T. (1992) *Geomorphology of Rocky Coasts*. John Wiley & Son Ltd.

Sunamura, T., Tsujimoto, H. and Aoki, H. (2014) 'Chapter 12 The rock coast of Japan', *Geological Society, London, Memoirs* , 40(1), pp. 203–223. doi: 10.1144/M40.12.

Swantesson, J. O. H., Moses, C. A., Berg, G. E. and Jansson, K. M. (2006) 'Methods for measuring shoreplatform micro-erosion; a comparison of the micro-erosion meter and the laser scanner', *Zeitschrift fur Geomorphologie Supplementband*, 144, pp. 1–17.

Swirad, Z. M., Rosser, N. J., Brain, M. J. and Vann Jones, E. C. (2016) 'What controls the Geometry of Rocky Coasts at the Local Scale?', *Journal of Coastal*

Research, 75(sp1), pp. 612–616. doi: 10.2112/SI75-123.1.

Takahashi, K., Suzuki, T. and Matsukura, Y. (1994) 'Erosion rates of a sandstone used for a masonry bridge pier in the coastal spray zone.', *Rock Weathering and Landform Evolution.* John Wiley and Sons, pp. 175–192.

Takahashi, T. (1977) 'Shore Platforms in Southwestern Japan–Geomorphological Study', *Coastal Landform Study Society of Southwestern Japan, Osaka*.

Taylor, A. J. (2003) *Change and processes of change on shore platforms*. PhD Thesis, University of Canterbury. Geography.

Thornton, L. E. and Stephenson, W. J. (2006) 'Rock Strength: A Control of Shore Platform Elevation', *Journal of Coastal Research*, 221, pp. 224–231. doi: 10.2112/05A-0017.1.

Torabi, S. R., Ataei, M. and Javanshir, M. (2011) 'Application of Schmidt rebound number for estimating rock strength under specific geological conditions', *Journal of Mining and Environment*, 1(2), pp. 1–8.

Torunski, H. (1979) 'Biological erosion and its significance for the morphogenesis of limestone coasts and for nearshore sedimentation (Northern Adriatic)', *Senckenbergiana maritima*, 11(3/6), pp. 193–265.

Trenhaile, A. S. (1971) 'Lithological control of high-water rock ledges in the Vale of Glamorgan, Wales', *Geografiska Annaler. Series A. Physical Geography*. JSTOR, pp. 59–69.

Trenhaile, A. S. (1972) 'The shore platforms of the Vale of Glamorgan, Wales', *Transactions of the Institute of British Geographers* , 56, pp. 127–144.

Trenhaile, A. S. (1974) 'The geometry of shore platforms in England and Wales', *Transactions of the Institute of British Geographers*, 62, pp. 129–142.

Trenhaile, A. S. (1978) 'The Shore Platforms Of Gaspé, Québec', *Annals of the Association of American Geographers*. Taylor & Francis, 68(1), pp. 95–114.

Trenhaile, A. S. (1980) 'Shore platforms: a neglected coastal feature', *Progress in physical geography*. Sage Publications Sage: Thousand Oaks, CA, 4(1), pp. 1–23.

Trenhaile, A. S. (1987) *The geomorphology of rock coasts*. Oxford University Press, USA.

Trenhaile, A. S. (1997) *Coastal dynamics and landforms*. Oxford University Press on Demand.

Trenhaile, A. S. (1999) 'The width of shore platforms in Britain, Canada, and Japan', *Journal of Coastal Research*, 15 (2), pp. 355–364.

Trenhaile, A.S. (2000) 'Modelling the development of wave-cut shore platforms'. *Marine Geology*, 166, 163-178.

Trenhaile, A. S. (2001) 'Modelling the effect of eeathering on the evolution and

morphology of shore platforms', *Journal of Coastal Research*, 17(2), pp. 398–406.

Trenhaile, A. S. (2002) 'Rock coasts, with particular emphasis on shore platforms', *Geomorphology*. Elsevier, 48(1–3), pp. 7–22. doi: 10.1016/S0169-555X(02)00173-3.

Trenhaile, A. (2006a) 'Tidal wetting and drying on shore platforms: An experimental study of surface expansion and contraction', *Geomorphology*, 76(3–4), pp. 316–331. doi: 10.1016/j.geomorph.2005.11.006.

Trenhaile, A. S. (2006b) 'Shore platforms', *Encyclopedia of Geomorphology Volume 2*. Taylor & Francis.

Trenhaile, A. S. (2008) 'The development of subhorizontal shore platforms by waves and weathering in microtidal environments', *Zeitschrift für Geomorphologie*, 52(1), pp. 105–124.

Trenhaile, A. S. (2010) 'The effect of Holocene changes in relative sea level on the morphology of rocky coasts', *Geomorphology*, 114(1–2), pp. 30–41. doi: 10.1016/j.geomorph.2009.02.003.

Trenhaile, A. S. (2012) 'Cliffs and Rock Coasts', *Treatise on Estuarine and Coastal Science*. Elsevier Inc. doi: 10.1016/B978-0-12-374711-2.00309-0.

Trenhaile, A. S. (2015) 'Coastal notches: Their morphology, formation, and function', *Earth-Science Reviews*, 150, pp. 285–304. doi: 10.1016/j.earscirev.2015.08.003.

Trenhaile, A. S. and Kanyaya, J. I. (2007) 'The Role of Wave Erosion on Sloping and Horizontal Shore Platforms in Macro- and Mesotidal Environments', *Journal of Coastal Research*, 232, pp. 298–309. doi: 10.2112/04-0282.1.

Trenhaile, A. S., and Lakhan, V. C. (2011) 'Transverse micro-erosion meter measurements; determining minimum sample size'. *Geomorphology*, *134* (3-4), 431-439.

Trenhaile, A. S. and Layzell, M. G. J. (1980) 'Shore platform morphology and tidal-duration distributions in storm wave environments', *The coastline of Canadian Geol. Surv. Canada Paper*.

Trenhaile, A. S. and Layzell, M. G. J. (1981) 'Shore platform morphology and the tidal duration factor', *Transactions of the Institute of British Geographers*, 6 (1), pp. 82–102.

Trenhaile, A.S. and Porter, N.J. (2018) 'Shore platform downwearing in eastern Canada; A 9–14 year micro-erosion meter record'. *Geomorphology*, *311*, pp.90-102.

Trenhaile, A. S., Perez-Alberti, A., Martinez Cortizas, A., Costa-Casais, M. and Blanco Chao, R. (1999) 'Rock Coast Inheritance : An Example From Galicia , Northwestern Spain', *Earth Surface Processes and Landforms*, (24), pp. 605–621.

Trudgill, S. T. (1976) 'The marine erosion of limestones on Aldabra Atoll, Indian Ocean', *Zeischrift fur Geomorphologie*, Suppl. Bd. 26, pp. 164–200.

Trudgill, S. T. (1983) 'Preliminary estimates of intertidal limestone erosion, one tree island, southern Great Barrier Reef, Australia', *Earth Surface Processes and Landforms*, 8(2), pp. 189–193.

Trudgill, S. T., High, C. J. and Hanna, F. K. (1981) 'Improvements to the micro-erosion meter', *British Geomorphological Research Group Technical Bulletin*, 29, pp. 3–17.

Tsujimoto, H. (1987) 'Dynamic conditions for shore platform initiation', *Sci. Rept., Inst. Geosci., University of Tsukuba, Sec. A*, 8, pp. 45–93.

Umran Dogan, A., A, O., Meral, D., Karpuz C and Brenner, R. L. (2006) 'Classifications Of Hardgrounds Based Upon Their Strength Properties', *Carbonates and Evaporites*, 21(1), pp. 14–20.

Viles, H. A. (2001) 'Scale issues in weathering studies', *Geomorphology*, 41(1), pp. 63–72.

Viles, H. A. (2005) 'Microclimate and weathering in the central Namib Desert, Namibia', *Geomorphology*, 67(1), pp. 189–209.

Viles, H. A. (2013) *Synergistic Weathering Processes*, *Treatise on Geomorphology*. Elsevier Ltd. doi: 10.1016/B978-0-12-374739-6.00057-9.

Viles, H. A., Naylor, L. A., Carter, N. E. A. and Chaput, D. (2008) 'Biogeomorphological disturbance regimes: progress in linking ecological and geomorphological systems', *Earth Surface Processes and Landforms*, 33(9), pp. 1419–1435.

Viles, H. A. and Trudgill, S. T. (1984) 'Long term remeasurements of micro-erosion meter rates, Aldabra Atoll, Indian Ocean', *Earth Surface Processes and Landforms*, 9(1), pp. 89–94.

Viles, H. A., Goudie, A., Grab, S. and Lalley, J. (2011) 'The use of the Schmidt Hammer and Equotip for rock hardness assessment in geomorphology and heritage science : a comparative analysis Science Applications of Rock', 333(July 2010), pp. 320–333. doi: 10.1002/esp.2040.

Viscarra Rossel, R. A., Cattle, S. R., Ortega, A. and Fouad, Y. (2009) 'In situ measurements of soil colour, mineral composition and clay content by vis-NIR spectroscopy', *Geoderma*, 150(3–4), pp. 253–266. doi: 10.1016/j.geoderma.2009.01.025.

Warke, P. A. and Smith, B. J. (1998) 'Effects of direct and indirect heating on the validity of rock weathering simulation studies and durability tests', *Geomorphology*, 22(3–4), pp. 347–357. doi: 10.1016/S0169-555X(97)00078-0.

Wentworth, C. K. (1938) Marine bench-forming processes -water level weathering. *Journal of Geomorphology*, (1), pp. 5-32.

Wentworth, C. K. (1939) Marine bench-forming processes. II. Solution benching. *Journal of Geomorphology* , (2), pp. 3-25.

Wentworth, C. K. (1944) 'Potholes, pits, and pans: subaerial and marine', *The Journal of Geology*. University of Chicago Press, 52(2), pp. 117–130.

Westfall, P. H. (2014) 'Kurtosis as Peakedness, 1905–2014. *R.I.P.*', *The American Statistician*, 68(3), pp. 191–195. doi: 10.1080/00031305.2014.917055.

Williams, A. T. and Davies, P. (1987) 'Rates and mechanisms of coastal cliff erosion in Lower Lias rocks', in Kraus, N. (ed.) *Coastal Sediments '87: Proceedings of a Speciality Conference on Advances in Understanding of Coastal Sediment Processes*. New Orleans, L.A.: ASCE, pp. 1855–1870.

Williams, R. B. G., Swantesson, J. O. H. and Robinson, D. A. (2000) 'Measuring rates of surface downwearing and mapping microtopography: the use of micro-erosion meters and laser scanners in rock weathering studies', *Zeitschrift fur Geomorphologie Supplementband*, 120, pp. 51–66.

Williams, R. and Robinson, D. (1983) 'The effect of surface texture on the determination of the surface hardness of rock using the Schmidt Hammer', *Earth Surface Processes and Landforms*, 8 (3), pp. 289–292.

Woodroffe, C. D., Bryant, E. A., Price, D. M. and Short, S. A. (1992) 'Quaternary inheritance of coastal landforms, Cobourg Peninsula, northern territory', *The Australian Geographer*. Taylor & Francis, 23(2), pp. 101–115.

Woodward, J. (2009) *The physical geography of the Mediterranean*. Vol. 8. Oxford University Press on Demand.

Wright, L. W. (1967) 'Some characteristics of the shore platforms of the English Channel Coast and the northern part of the North Island, New Zealand', *Zeitschrift für Geomorphologie NF*, 11, pp. 36–46.

Yagiz, S. (2009) 'Predicting uniaxial compressive strength, modulus of elasticity and index properties of rocks using the Schmidt hammer', *Bulletin of Engineering Geology and the Environment*, 68(1), pp. 55–63. doi: 10.1007/s10064-008-0172-z.

Yagiz, S. (2011) 'Correlation between slake durability and rock properties for some carbonate rocks', *Bulletin of Engineering Geology and the Environment*. 70(3), pp. 377–383.

Yilmaz, N. G., Goktan, R. M., Yavuz, A. B. and Karaca, Z. (2016) 'Influence of rock cradle block geometry on rebound hardness', *Bulletin of Engineering Geology and the Environment*, 75(1), pp. 325–339. doi: 10.1007/s10064-015-0746-5.

Yılmaz, I. and Sendır, H. (2002) 'Correlation of Schmidt hardness with unconfined compressive strength and Young's modulus in gypsum from Sivas (Turkey)', *Engineering Geology*, 66(3), pp. 211–219.

Yoder, H. S. and Eugster, H. P. (1955) 'Synthetic and natural muscovites', *Geochimica et Cosmochimica Acta*, 8(5–6), pp. 225–280.

Young, R. W. and Bryant, E. A. (1993) ‘Coastal rock platforms and ramps of Pleistocene and Tertiary Age in southern New-South-Wales, Australia’, *Zeitschrift fur Geomorphologie*, 37(3), pp. 257–272.

Appendix

Submitted with main thesis in partial fulfillment of the requirements for the award of the degree of Doctor of Philosophy in Geography at the University of Portsmouth

March 2018

Appendix I: Ethics Review Approval Form and UPR16 (7 pages)

University of Portsmouth, Faculty of Science
Initial Ethics Review Filter: Geography & Earth Sciences

To be completed by all Staff and postgraduate students undertaking research

- You are required to undertake an ethics review of your Research Proposal. Before completing this checklist please read through the guidelines entitled "*Research Ethics Guidance for Geography staff and students*" on the K:drive at: *K:\Science\Staff\Geography\Geography Ethics*
- When you have completed the checklist, submit it via Dr Malcolm Bray
- *Ethical review is a University requirement for all research. This form constitutes a light touch mechanism to identify potential ethics issues.*

Name of Principal Investigator: Ritienne Gauci
Name of 1st Supervisor (if relevant): Dr Robert Inkpen
Research Title:
Identifying and quantifying rates of shore platform downwearing on the Maltese Islands through the use of a multi-approach analysis of rock surface change

Research Aims (give brief statement):
The overall aim of this research is to build a baseline study to investigate the morphological characteristics and geomorphic processes operating on selected shore platforms in various parts of the Maltese Islands. Central to this aim is the need to identify and quantify downwearing rates of selected shore platforms and how these rates may be conditioned by specific environmental parameters on a spatial and temporal basis.

Nature of data collection - give brief details:
Primary data collection mainly consists of measuring rock surface height through the use of a Transverse Micro-Erosion Meter and Next Engine Laser Scanner. Other aspects of data collection will include intact rock strength measurements with the use of Schmidt Hammer, roughness measurements with carpet profiles, and laboratory tests to determine geological characteristics of lithology under investigation.

Measurements of physical environment – The Next Engine Laser Scanner, the Schmidt Hammer and carpet profiler are strictly non-invasive and they leave the rock surface intact without any damage. The Transverse Micro-erosion Meter makes us of small (1cm radius) circular studs that act as control points for the TMEM to take its measurement. These small studs are drilled in the rock at about 2.5cm depth and they are made of titanium (they do not rust and hence do not pose any health hazard). Due to their small size, they do not pose any invasive damage to the landform under investigation.

Sampling of rocks, sediments or biological materials: 10 small samples of rock (15x15x15cm) has been collected from site to be examined in laboratory at Portsmouth.

(A) Please indicate Yes or No to the following:	Yes	No
Is the study likely to involve human participants? (participants are persons giving data, responding to interviews, or being experimented upon)	☐	☑

If 'Yes', please go to SECTION B

[2] Is the study likely to involve observations of people in non-public places? ☐ ☑

If 'Yes', please complete a full Science Faculty participant ethics review application

If 'No' to all of above please answer the following:-

1) Will the research be conducted within or could it potentially affect a protected area (local, regional, national or international), designated heritage site, geological geomorphological or landscape site and/or vulnerable habitat? ☐ ☑
2) Are there risks of damage to protected geological or geomorphological sites and/or habitats? ☐ ☑
3) Are there risks of damage to features of historical or cultural heritage? ☐ ☑
4) Are there risks of harm to sensitive/protected flora and/or fauna? ☐ ☑
5) Could the conduct of the research and/or its outputs potentially be harmful to third parties? ☐ ☑

If you have answered 'yes' to a), b), c) or d), then please provide details (in the space below) of the specific risks and how you plan to minimise them. You may attach additional information if necessary.

N/A

Now go to page 5 and sign the Declaration (Section E)

(B) You intend to involve human research participants or subjects. Will your data collection methods involve:-

TICK APPLICABLE BOXES

1. Secondary sources (i.e. data that have already been collected and are in the public domain such as the UK Census of Population, data from web-resources such as ONS Neighbourhood Statistics or the various Government Departments' statistical pages) ☐
2. Primary sources (e.g. face-to-face interviews or questionnaires, focus groups or observational methods)? ☐
3. Both secondary and primary collection methods:- ☐

*If you ticked statement **number 2 or 3**, please go to **SECTION C** on the next page (page 4).*

*If you ticked **number 1** then please indicate whether there are any other potential issues relating to research ethics:-*

Please indicate Yes or No :-	Yes	No
4. Will the research be conducted within or could it potentially affect a protected area (local, regional, national or international), designated heritage site, geological geomorphological or landscape site and/or vulnerable habitat?	☐	☐
5. Are there risks of damage to protected geological or geomorphological sites and/or habitats?	☐	☐
6. Are there risks of damage to features of historical or cultural heritage?	☐	☐
7. Are there risks of harm to sensitive/protected flora and/or fauna?	☐	☐
8. Could the conduct of the research and/or its outputs potentially be harmful to third parties?	☐	☐

If you have answered 'yes' to 4), 5), 6) or 7), then please provide details (in the space below) of the specific risks and how you plan to minimise them. You may attach additional information if necessary.

.....
.....
.....
.....
.....
.....
.....
.....
.....
.....
.....
.....
.....
.....

.....
.....
.....
.....
.....
.....
.....
.....
.....
.....

Now go to page 5 and sign the Declaration (Section D)

[C] In terms of the primary data collection methods on human participants, please answer the following indicating Yes or No:-

	Yes	No
1. Will the study involve NHS patients, staff or premises?	☐	☐
2. Do human participants/subjects take part in studies without their knowledge/consent at the time or will deception of any form be used?	☐	☐
3. Does the study involve vulnerable (e.g. children or people with learning difficulties) or dependent participants (e.g. students or employees)	☐	☐
4. Does the study involve inquiry concerning participants' sensitive sexual, political, financial, ethnic, illegal behaviour?	☐	☐
5. Are drugs, placebos or other substances (e.g. food, vitamins) to be administered to participants?	☐	☐
6. Will blood or tissue samples be obtained from participants?	☐	☐
7. Is pain or more than mild discomfort likely to result from the study?	☐	☐
8. Could the study induce psychological distress or anxiety in participants, and/or third parties?	☐	☐
9. Will the study involve prolonged or repetitive testing of participants?	☐	☐
10. Will financial inducements other than reasonable expenses be offered to participants?	☐	☐

Please indicate whether there are any other general problems relating to research ethics:-

11) Will the research be conducted within or could it potentially affect a protected area (local, regional, national or international), designated heritage site, geological geomorphological or landscape site and/or vulnerable habitat?	☐	☐
12) Are there risks of damage to protected geological or geomorphological sites and/or habitats?	☐	☐
13) Are there risks of damage to features of historical or cultural heritage?	☐	☐
14) Are there risks of harm to sensitive/protected flora and/or fauna?	☐	☐
15) Could the conduct of the research and/or its outputs potentially be harmful	☐	☐

to third parties?

If you have answered 'yes' to 2, 3, 4, 8, 9, 10, 11, 12, 13, 14, or 15 then you must provide additional details (in the space below) of the specific risks and how you plan to minimise them. Please attach any additional materials if necessary.

.....
.....
.....
.....
.....
.....
.....
.....

Now go to page 5 and sign the Declaration (Section D)

[D] Declaration

I confirm that the information provided is a complete and accurate record of my plans at present and that I shall resubmit an amended version of this form should my research alter significantly such that there is any significant variation of ethical risk. I confirm that I have read the University Ethics Policy (2011) and have read "Research Ethics Guidance, Geography Staff and Students" available at:
K:\science\Staff\Geography\Geography Ethics\Ethics Guidance)

Where necessary, I will also provide a covering letter/information leaflet and/or consent form for the participants in my research.

Signed Rihanne Lau (Principal Investigator)

Date 17/3/15

[E] REVIEW RECORD *(completed by Departmental Ethics Representative after you have submitted the checklist)*

Dr Malcolm Bray (Departmental Ethics Representative) will review your submitted ethics checklist and will tick one of the boxes below. If there is a recommendation to undertake clarification in terms of ethics consideration (e.g. undertaking to follow simple procedures to minimise risks) or undertaking a more detailed ethics review then instructions will be included with the returned form.

Favourable opinion : INSIGNIFICANT risk/issues arising	☑
Favourable opinion : INSIGNIFICANT risks subject to comments listed below	☐
Risks assessed as SIGNIFICANT referred for FACULTY Ethics Review	☐
Opinion not possible, or referred for detailed review – reasons specified below	☐

I wish you success with your research

PS. Apologies for the delay in returning to you.

Signed Malcolm Bray (Departmental Ethics Representative)

Date 28th May 2015

FORM UPR16

Research Ethics Review Checklist

University of Portsmouth

Please include this completed form as an appendix to your thesis (see the Postgraduate Research Student Handbook for more information

Postgraduate Research Student (PGRS) Information			Student ID:	UP 640208
PGRS Name:	RITIENNE GAUCI			
Department:	GEOGRAPHY	First Supervisor:	DR ROBERT INKPEN	
Start Date: (or progression date for Prof Doc students)	OCTOBER 2011			
Study Mode and Route:	Part-time ☑ Full-time ☐	MPhil ☐ PhD ☑	MD ☐ Professional Doctorate ☐	

Title of Thesis:	THE IDENTIFICATION AND QUANTIFICATION OF SURFACE CHANGE ON LIMESTONE SHORE PLATFORMS OF THE MALTESE ISLANDS.
Thesis Word Count: (excluding ancillary data)	91,167 words.

If you are unsure about any of the following, please contact the local representative on your Faculty Ethics Committee for advice. Please note that it is your responsibility to follow the University's Ethics Policy and any relevant University, academic or professional guidelines in the conduct of your study

Although the Ethics Committee may have given your study a favourable opinion, the final responsibility for the ethical conduct of this work lies with the researcher(s).

UKRIO Finished Research Checklist:
(If you would like to know more about the checklist, please see your Faculty or Departmental Ethics Committee rep or see the online version of the full checklist at: http://www.ukrio.org/what-we-do/code-of-practice-for-research/)

a) Have all of your research and findings been reported accurately, honestly and within a reasonable time frame?	YES ☑ NO ☐
b) Have all contributions to knowledge been acknowledged?	YES ☑ NO ☐
c) Have you complied with all agreements relating to intellectual property, publication and authorship?	YES ☑ NO ☐
d) Has your research data been retained in a secure and accessible form and will it remain so for the required duration?	YES ☑ NO ☐
e) Does your research comply with all legal, ethical, and contractual requirements?	YES ☑ NO ☐

Candidate Statement:

I have considered the ethical dimensions of the above named research project, and have successfully obtained the necessary ethical approval(s)

Ethical review number(s) from Faculty Ethics Committee (or from NRES/SCREC):	ETHICS DONE SEE APPENDIX I (THESIS)

If you have not submitted your work for ethical review, and/or you have answered 'No' to one or more of questions a) to e), please explain below why this is so:

Signed (PGRS):	Ritienne Gauci	Date:	27/3/2018

UPR16 – August 2015

Appendix II – Field session dates per platform, with description of daily means for weather and marine conditions (1 table)

Platform Site	Field Date	Sessions	Daily Mean								Maximum and Minimum							Marine Conditions				Field Date
			Temperature	Humidity	Dew Point	Pressure	Wind Speed	Gust Speed	Wind Direction	Wind Direction	Max. Temperature	Min. Temperature	Max.Heat Index	Max. Humidity	Min. Humidity	Max. Pressure	Min. Pressure	Wave Direction	Wave Height	Sea Temperature	Sea Conditions	
			°C	%	°C	hPa	km/hr	km/hr	°X	Card. Point	°C	°C	°C	%	%	hPa	hPa	Card . Point	(m)	°C		
Ponta tal-Qammieh (Marfa Ridge)	25/04/2012	1	19.5	62.0	11.6	1016.1	9.2	20.2	321	NW	27.1	13.6	27.1	86	43	1018.4	1013.1	n/a	n/a	n/a	n/a	25/04/2012
	02/02/2013	2	14.6	77.0	10.5	1007.4	1.9	5.5	228	SW	19.0	11.6	19.0	91	61	1016.4	1002.7	WSW to SW	2.0	15	Moderate to Rough	02/02/2013
	08/06/2013	3	22.7	70.0	16.3	1014.4	3.0	3.5	251	WSW	36.1	16.9	37.6	90	33	1015.7	1013.1	E to NE	1.0	19	Moderate to Slight	08/06/2013
	16/08/2013	4	28.9	59.0	19.4	1015.3	6.2	10.9	318	NW	36.1	23.9	38.1	81	34	1016.3	1014.3	WNW	0.5	28	Slight	16/08/2013
	21/12/2013	5	14.1	82.0	11.0	1029.9	18.6	28.7	116	ESE	17.7	10.8	17.7	88	41	1031.5	1028.0	ESE	2.0-2.5	18	Moderate	21/12/2013
	21/03/2014	6	15.0	80.0	11.4	1020.5	15.2	23.0	222	SW	19.6	11.9	19.6	90	65	1021.9	1019.4	ESE	0.5	16	Slight	21/03/2014
	13/08/2014	7	27.3	76.0	22.5	1011.7	11.6	18.8	212	SW	32.4	22.6	38.9	88	59	1013.0	1010.0	S	0.1-0.5	26	Calm	13/08/2014
	24/11/2014	8	17.5	84.0	14.7	1015.7	2.1	4.2	214	SW	22.5	13.9	23.8	92	70	1016.6	1013.6	SSE to E	0.3-0.4	22	Smooth	24/11/2014
	19/03/2015	9	13.7	84.0	10.9	1012.0	7.2	13.0	143	SE	17.6	9.4	17.6	91	72	1013.0	1010.9	ESE to E	1.4-1.0	15	Moderate to Slight	19/03/2015
	12/06/2015	10	24.2	71.0	18.2	1008.1	13.5	21.2	150	SSE	28.6	20.9	29.5	89	48	1009.4	1007.0	SSE	0.6-1.3	21	Slight to Moderate	12/06/2015
	04/09/2015	11	28.9	74.0	23.4	1007.1	9.7	16.2	209	SSW	36.5	24.6	43.2	90	21	1008.8	1006.1	WNW to SSW	0.6-0.3	28	Slight to Smooth	04/09/2015
	26/12/2015	12	13.4	78.0	9.3	1023.4	1.9	4.0	352	N	20.8	9.4	25.1	91	50	1025.0	1021.7	NE	0.4-0.7	19	Slight	26/12/2015
	29/03/2016	13	15.9	70.0	10.5	1019.7	4.9	10.7	281	W	19.1	13.5	24.8	76	63	1021.0	1018.0	WN to-SSW	0.3-0.5	16	Slight	29/03/2016
	29/06/2016	14	24.5	58.0	15.4	1015.1	11.2	17.6	250	WSW	29.0	21.9	28.8	72	38	1032.0	1014.0	NW	0.5-1.1	22	Slight	29/06/2016
Blata l-Bajda (Selmun)	07/06/2012	1	21.8	70.0	15.9	1014.5	2.7	3.2	210	SSW	30.4	16.2	31.3	88	47	1015.1	1013.4	n/a	n/a	n/a	n/a	07/06/2012
	12/12/2012	2	10.1	71.0	5.1	1018.2	4.8	11.4	321	NW	13.5	7.3	13.5	85	60	1021.4	1015.4	WNW	2.0-1.5	19	Rough to Moderate	12/12/2012
	14/06/2013	3	23.7	63.0	15.2	1015.6	3.4	3.9	182	S	34.2	17.1	34.1	90	32	1017.4	1014.3	WNW	0.75	20	Slight	14/06/2013
	06/09/2013	4	25.7	81.0	21.9	1012.7	5.7	10.5	132	SE	31.6	21.5	37.4	93	61	1014.2	1010.9	SE	1.0	26	Slight	06/09/2013
	06/12/2013	5	13.4	75.0	9.1	1018.2	10.5	18.4	304	NW	17.8	9.0	17.8	83	33	1020.6	1016.4	NW	2.0	19	Moderate	06/12/2013
	15/03/2014	6	14.3	83.0	11.4	1015.6	21.6	33.1	55	ENE	17.8	12.4	17.8	89	72	1017.4	1013.4	ESE	2.5-1.5	16	Rough to Moderate	15/03/2014
	24/07/2014	7	25.5	69.0	18.9	1011.5	11.8	20.3	310	NW	34.0	20.3	37.1	87	45	1013.0	1009.9	NW	1.6-0.6	24	Moderate to Slight	24/07/2014
	26/11/2014	8	16.2	90.0	14.6	1008.9	10.6	14.1	180	S	18.4	14.6	18.4	92	48	1011.1	1007.5	SSE to E	0.3-0.8	21	Smooth to Slight	26/11/2014
	09/03/2015	9	10.3	82.0	7.3	1008.8	8.8	15.9	12	NNE	14.6	6.7	14.6	91	44	1011.3	1006.9	NNE to N	1.0-1.8	15	Slight to Moderate	09/03/2015
	17/06/2015	10	24.5	71.0	18.5	1004.3	10.7	17.0	319	NW	30.9	20.1	33.1	91	48	1005.0	1003.4	WNW to NW	0.5-3.6	22	Slight to Rough	17/06/2015
	10/09/2015	11	24.4	68.0	18.0	1004.8	10.1	17.7	304	WNW	29.3	21.6	30.8	84	49	1008.8	1002.1	NE to NW	1.5	28	Moderate	10/09/2015
	02/12/2015	12	14.6	76.0	10.3	1020.7	10.3	16.4	304	WNW	19.1	11.6	19.1	85	39	1022.0	1019.6	NW	1.3-0.6	20	Moderate to Slight	02/12/2015
	31/03/2016	13	17.5	61.0	9.9	1019.9	9.1	9.3	240	WSW	19.8	15.7	26.1	69	49	1022.0	1018.0	SE	1.0-1.4	16	Slight to Moderate	31/03/2016
	21/06/2016	14	22.3	60.0	14.1	1018.2	8.7	8.9	252	WSW	26.2	19.5	26.4	75	41	1019.0	1017.0	NW	1.7-0.9	22	Moderate to Slight	21/06/2016
Ponta tal-Munxar (St Thomas Bay)	12/06/2012	1	24.8	66.0	17.7	1010.3	5.4	10.9	218	SW	33.4	19.3	34.2	88	38	1011.7	1009.4	n/a	n/a	n/a	n/a	12/06/2012
	07/12/2012	2	12.3	63.0	5.5	1016.3	7.1	17.1	316	NW	16.0	10.0	16.0	69	52	1018.1	1014.3	NW to W	3.0-3.5	19	Moderate to Rough	07/12/2012
	11/04/2013	3	17.3	67.0	10.7	1017.5	5.5	6.2	322	NW	26.8	17.4	26.8	85	39	1018.7	1016.4	SW to WNW	1.0-0.75	15	Slight	11/04/2013
	17/08/2013	4	28.5	57.0	18.9	1015.6	6.3	12.2	17	NNE	35.9	22.8	40.8	80	41	1016.8	1014.5	NW	0.5	28	Slight	17/08/2013
	27/11/2013	5	10.7	65.0	4.3	1019.8	12.3	19.0	331	NNW	15.2	7.8	15.2	73	54	1024.2	1015.7	NW	3.5-2.0	20	Rough to Moderate	27/11/2013
	28/02/2014	6	11.3	79.0	7.6	1016.6	8.2	14.8	328	NNW	15.6	8.3	15.6	91	61	1020.3	1011.7	SE to NW	1.5	16	Moderate	28/02/2014
	29/07/2014	7	25.8	71.0	19.6	1010.4	8.8	14.7	194	SSW	34.1	19.7	34.7	86	34	1012.3	1008.1	NW to S	1.0-0.8	25	Slight	29/07/2014
	19/11/2014	8	18.1	78.0	14.0	1010.2	7.2	12.3	323	NW	24.3	15.0	25.5	92	57	1012.8	1007.2	SE	1.3-0.7	22	Moderate to Slight	19/11/2014
	08/03/2015	9	11.0	73.0	6.1	1007.2	18.6	27.4	93	E	16.2	7.4	16.2	86	43	1008.6	1006.0	NNW to NE	2.2-1.0	15	Moderate to Slight	08/03/2015
	10/06/2015	10	24.6	64.0	16.7	1007.8	10.7	17.2	180	S	30.9	18.6	32.1	84	37	1009.1	1006.8	S to SSE	0.6	21	Slight	10/06/2015
	13/09/2015	11	25.4	71.0	19.7	1010.8	4.6	10.5	181	S	29.7	21.0	32.5	83	60	1012.1	1009.3	NE to E	0.2-0.4	28	Smooth	13/09/2015
	13/12/2015	12	13.0	79.0	9.4	1017.4	2.2	6.1	284	WNW	18.5	9.6	18.5	90	33	1019.1	1016.4	W to NW	0.8-1.4	19	Slight to Moderate	13/12/2015
	26/03/2016	13	14.0	60.0	6.3	1017.9	12.0	19.3	270	W	15.9	12.0	15.9	66	55	1020.0	1017.0	NW	1.3-1.1	16	Moderate to Slight	26/03/2016
	02/07/2016	14	24.9	70.0	18.9	1014.4	13.5	20.5	233	SW	28.0	22.6	29.6	84	45	1016.0	1013.0	SE to SSE	0.8-0.7	23	Slight	02/07/2016
Ponta tal-Mignuna (St Thomas Bay)	03/06/2012	1	21.8	75.0	17.1	1017.5	3.2	8.2	190	S	27.0	17.8	27.8	90	57	1019.1	1015.8	n/a	n/a	n/a	n/a	03/06/2012
	07/02/2013	2	12.3	63.0	5.5	1016.5	7.1	17.1	316	NW	14.9	12.5	14.9	69	52	1018.1	1014.3	WNW to W	3.0-4.0	15	Rough	07/02/2013
	01/06/2013	3	23.3	52.0	7.8	1014.9	7.6	13.5	340	NW	17.8	28.5	20.5	78	49	1016.0	1014.0	NW to WNW	1.5-2.5	19	Moderate to Rough	01/06/2013
	17/08/2013	4	28.5	57.0	18.9	1015.6	6.3	12.2	17	NE	35.9	22.8	40.8	80	41	1016.8	1014.5	NW	0.5	28	Slight	17/08/2013
	21/11/2013	5	16.9	63.0	9.7	1008.5	9.5	17.7	288	WNW	21.2	13.6	25.1	72	52	1010.2	1006.7	SW	2.0-3.0	22	Moderate	21/11/2013
	28/02/2014	6	11.3	79.0	7.6	1016.6	8.2	14.8	1	N	15.6	8.3	15.6	91	61	1020.3	1011.7	SE to NW	1.5	16	Moderate	28/02/2014
	07/08/2014	7	27.3	65.0	19.6	1010.7	19.4	27.4	346	NNW	34.3	22.4	36.2	88	36	1012.4	1008.6	NW	2.1-1.1	25	Moderate to Slight	07/08/2014
	18/11/2014	8	19.7	88.0	17.7	1004.9	4.9	9.2	294	WNW	25.1	16.5	26.1	93	65	1007.6	803.4	SE to NW	1.2-1.4	22	Slight to Moderate	18/11/2014
	04/03/2015	9	15.7	78.0	11.6	1014.4	12.7	20.5	245	WSW	21.9	11.6	24.7	87	33	1017.4	1008.2	W to SW	0.7-0.8	15	Slight	04/03/2015
	09/06/2015	10	25.0	69.0	18.5	1007.1	7.6	13.5	241	WSW	32.1	18.8	29.1	89	47	1008.3	1006.0	WNW to S	0.6	21	Slight	09/06/2015
	05/09/2015	11	28.8	77.0	24.1	1007.1	12.5	20.3	202	SSW	33.8	26.0	41.1	89	56	1008.5	1006.2	SSW to S	0.3-0.6	28	Smooth to Slight	05/09/2015
	12/12/2015	12	12.8	74.0	8.1	1019.5	8.9	15.8	318	NW	18.1	9.9	18.1	86	43	1020.6	1018.5	NW to W	1.4-0.8	19	Moderate to Slight	12/12/2015
	25/03/2016	13	13.8	57.0	5.4	1014.4	14.8	22.9	308	NW	16.4	11.9	16.4	61	51	1018.0	1011.0	WNW to NW	2.8-1.3	16	Rough to Moderate	25/03/2016
	02/07/2016	14	24.9	70.0	18.9	1014.4	13.5	20.5	233	SW	28.0	22.6	29.6	84	45	1016.0	1013.0	SE to SSE	0.8-0.7	23	Slight	02/07/2016
Ras il-Fenek (Delimara)	09/05/2012	1	20.5	67.0	13.7	1018.5	4.1	7.1	271	W	28.8	14.5	29.1	86	47	1020.4	1017.1	n/a	n/a	n/a	n/a	09/05/2012
	31/01/2013	2	13.4	84.0	10.7	1021.9	13.3	26.2	344	NNW	16.5	10.9	16.5	90	73	1024.3	1020.3	WNW	1.5-2.0	16	Rough	31/01/2013
	01/06/2013	3	17.8	52.0	7.8	1013.0	12.0	32.0	340	NNW	21.0	15.0	21.0	50	90	1014.0	1012.0	NW to WNW	1.5-2.0	19	Moderate to Rough	01/06/2013
	17/08/2013	4	28.5	57.0	18.9	1015.6	6.3	12.2	17	NNE	35.9	22.8	40.8	80	41	1016.8	1014.5	NW	0.5	28	Slight	17/08/2013
	04/12/2013	5	15.8	86.0	13.4	1020.4	14.5	22.4	26	NNE	17.8	11.8	17.8	99	68	1022.2	1018.1	NE	2.0-1.0	19	Moderate	04/12/2013
	07/03/2014	6	12.1	76.0	7.9	1013.2	10.2	16.1	1	N	17.9	8.1	17.9	89	44	1014.9	1011.7	NW	1.5	16	Moderate	07/03/2014
	08/07/2014	7	27.6	72.0	21.8	1013.2	16.3	24.6	236	WSW	35.0	22.9	42.1	90	48	1014.6	1012.0	SE to NW	1.0-1.2	24	Slight	08/07/2014
	23/11/2014	8	17.4	83.0	14.4	1016.3	9.6	14.4	89	E	22.3	14.3	23.9	92	67	1017.3	1015.5	S to SSE	0.5-0.4	22	Smooth	23/11/2014
	04/03/2015	9	15.7	78.0	11.6	1014.4	12.7	20.5	245	WSW	21.9	11.6	24.7	87	33	1017.4	1008.2	W to SW	0.7-0.8	15	Slight	04/03/2015
	16/06/2015	10	25.4	72.0	19.4	1005.8	11.2	16.8	52	NE	32.8	19.6	36.0	90	47	1007.1	1004.1	Se to WNW	0.7-0.5	22	Slight	16/06/2015
	14/09/2015	11	26.1	73.0	20.8	1009.1	10.8	18.4	186	S	30.0	23.5	33.7	82	63	1010.3	1007.8	NE to SSE	0.4	28	Smooth	14/09/2015
	20/12/2015	12	12.8	86.0	10.5	1017.9	9.3	16.0	143	NE	15.8	11.1	15.8	92	81	1019.8	1015.6	WNW to NW	0.9-3.9	27	Slight to Rough	20/12/2015
	22/03/2016	13	18.5	55.0	9.3	998.7	24.1	29.8	246	WSW	22.4	16.9	25.2	65	42	1006.0	992.0	NW	1.1-0.5	16	Moderate to Slight	22/03/2016
	28/06/2016	14	23.6	60.0	15.4	1014.3	18.5	28.1	321	NW	26.1	21.9	31.0	69	46	1016.0	1013.0	WNW to NW	1.1	22	Slight	28/06/2016

Appendix III– Photos of TMEM stations on site (5 figures)

Figure 1: TMEM stations at Ponta tal-Mignuna: MPM 1b (a). MPM 2b (b) , MPM3c (c), MPM4b (d), MPM5 (e) and MPM6b (f). Images of MPM 1a, 2a. 3a.3b, 4 a and 6

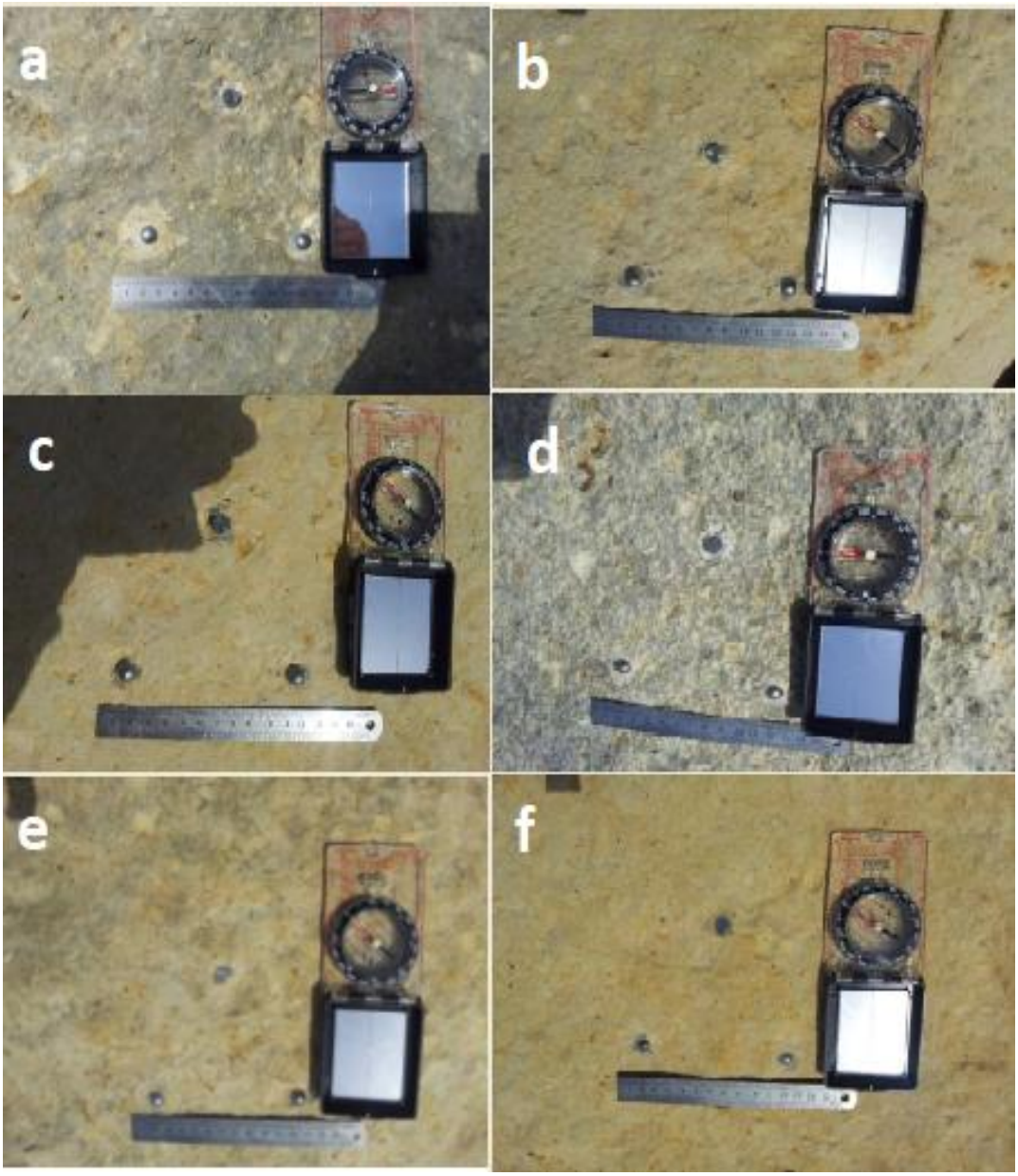

Figure 2. TMEM stations at Blata l-Bajda a. MBB1b (a). MBB2 (b), MBB3 (c), MBB4 (d), MBB5 (e), MBB 6c (f). Images of MBB 6a, b and MBB 1a were unavailable.

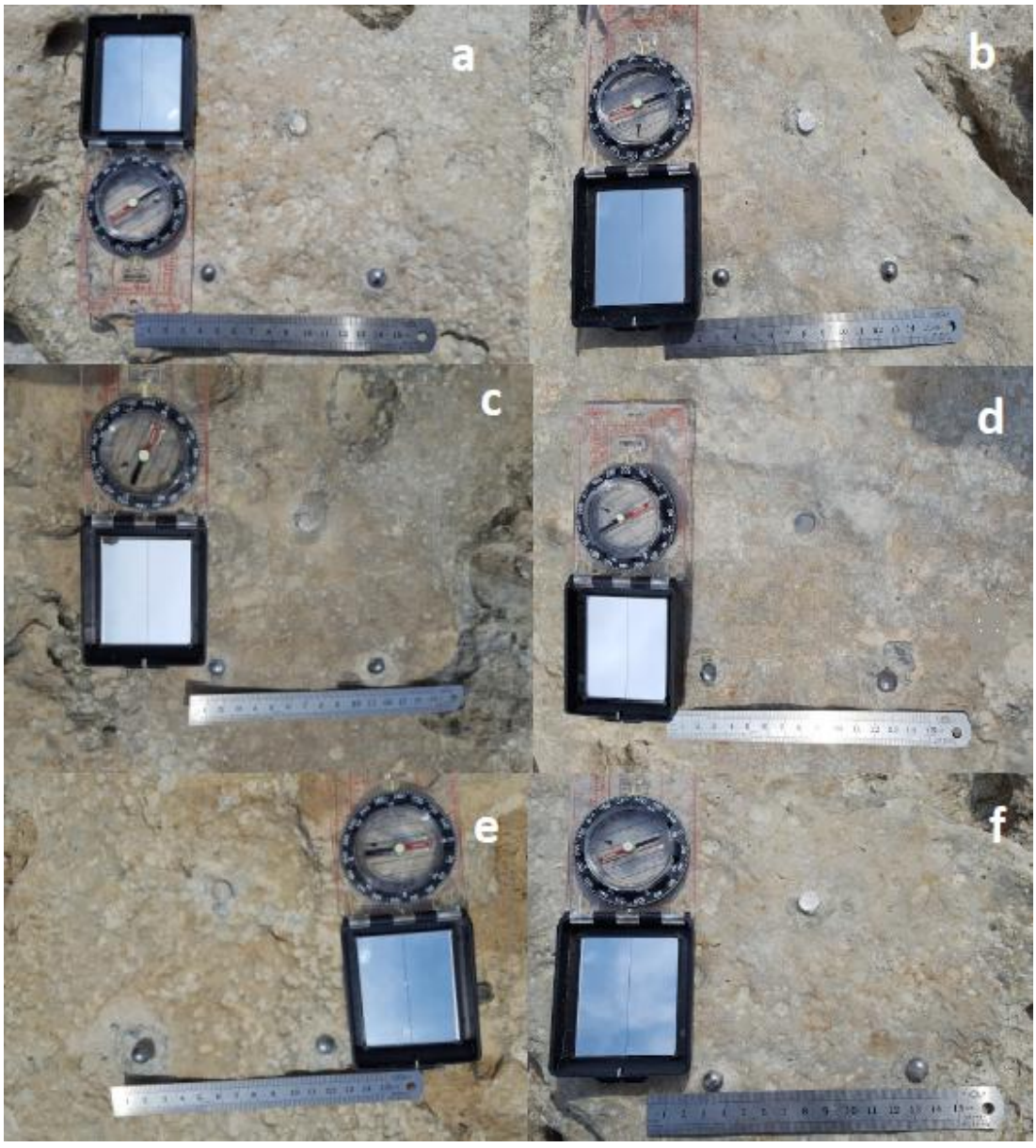

Figure 3: TMEM stations at Ponta tal-Munxar: MMX1b (a), MMX2 (b), MMX3c (c), MMX4 (d). MMX5b (e), MMX6 (f). Images of MMX1a, 3a, b, and 5a were unavailable.

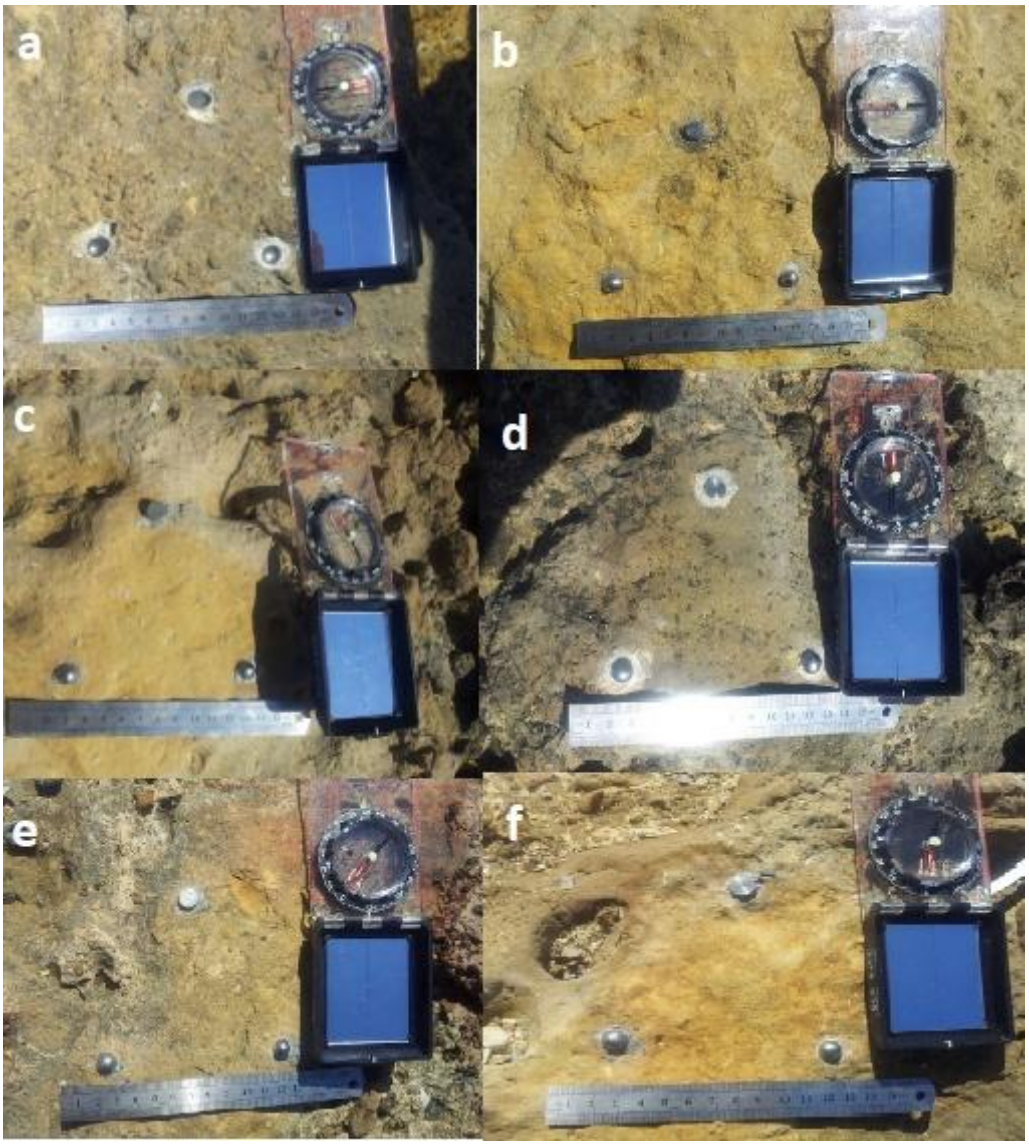

Figure 4: TMEM stations at Ponta tal-Qammieh, MPQ1 (a), MPQ2 (b), MPQ3 (c), MPQ4 (d), MPQ5 (e) and MPQ6 (f).

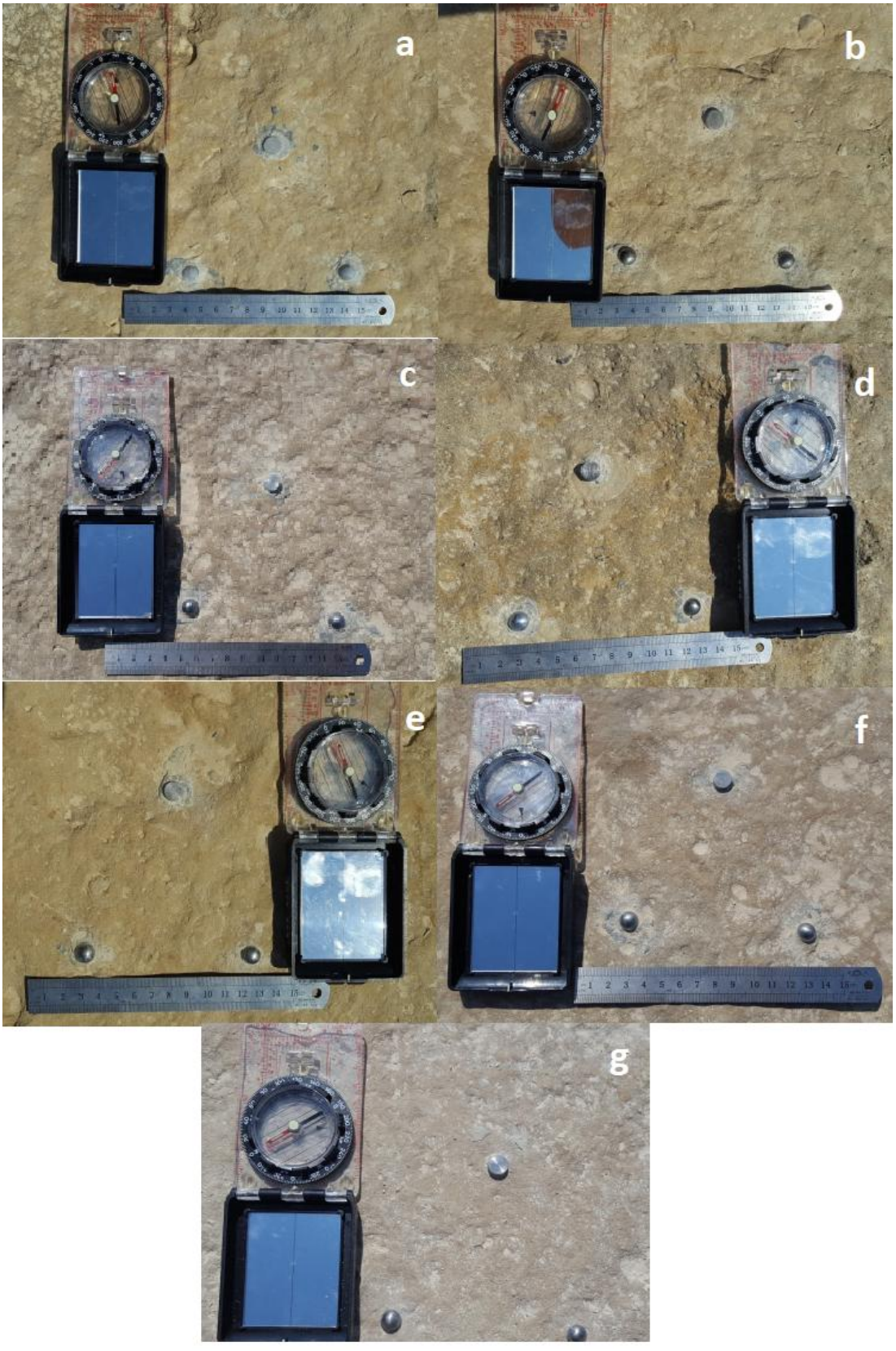

Figure 5: TMEM stations at Ras il-Fenek, MRF 1b (a), MRF 2b (b), MRF3 (c), MRF4 (d), MRF5 (e), MRF 6 (f) and MRF7 (g). Images of MRF1a and MRF2a were not available.

Appendix IV – A literature review matrix of the methods used to obtain a representative R value (2 pages)

Study Reference	Field method to collect a representative R value
Hucka (1965)	Select the peak rebound value from 10 continuous impacts at a point. Average the peaks of the three sets of tests conducted at three separate points
Deere and Miller (1966)	Record three readings along the length of an NX size core for each 45^0 rotation. Average a total of 24 readings, disregarding the erroneous readings
Fowell and McFeat Smith (1976)	Take the mean of the last five values from 10 continuous impacts at a point
Soiltest Inc (1976)	Record 15 rebound values from single impacts and average the highest ten. The maximum deviation from the mean should be less than 2.5
ISRM (1978, 2007)	20 rebound values from single impacts separated by at least a plunger diameter should be recorded and averaged the upper ten values.
Young and Fowell (1978)	Divide the rock mass surface into grids and average the single impacts from each grid
Poole and Farmer (1980)	The peak value from at least five continuous impacts at a point should be selected. Average the peaks of the three sets of tests conducted at three separated points.
Kazi and Al- Mansour (1980)	Record at least 35 rebound readings, drop the 10 lowest readings and average the remaining 25
Matthews and Shakesby (1984)	15 R-values for each sample, with 5 values that deviate most from the mean being discarded.
Goktan and Ayday (1993)	Record 20 rebound values from 20 single impacts separated by at least a plunger diameter. Reject outlier values by using Chauvenet's criterion, and average the remaining readings.
USBR (1998)	Ten readings at various locations on each surface. Discount the five lowest readings and average the highest five.

Study Reference	Field method to collect a representative R value
Sumner and Nel (2002)	Take 15 readings at different points and discard the five worst outliers to obtain a mean value from the remaining 10 values
Yavuz et al. (2006)	Collect 20 values and only used the top 10
Gupta (2009)	Collected 50 samples per site and discarded the upper 10 and the lower 10
Aydin (2009)	New (ISRM) method for the SH; 20 R-values from single impacts separated by at least a plunger width and all values should be used to calculate summary statistics and no values (high or low) should be discarded.
Niedzielski *et al.* (2009)	Appropriate minimum sample size:15 for sandstone and shales, 25 for weak and moderately strong rocks, and 30 for strong and coarse rocks
Katz *et al.* (2009)	Performed 32–40 individual impacts and averaged the upper 50%
ASTM D 5873 – 14 (2014)	Record at least 10 single impact readings, discarding those differing from the average by more than 7 units, and averaging those left

Appendix V: Current land use management of the five selected shore platforms (3 pages)

1) Delimara Peninsula: shore platform of Ras il-Fenek

The sub-circular coasts of Xrobb l-Għaġin are scheduled as Area of Ecological Importance (AEI) Level 2 and Site of Scientific Importance as defined by Structure Plan Policy ME01, as UGLM allows specific coastal vegetation communities to colonise. All of the vegetation on site has a higher degree of salt tolerance than equivalent inland habitats on the rest of the island. Generally the most dominant habitats are the steppe and garigue. The cliffs are also classified as Area of High Landscape Value (AHLV) Level 2 (i.e. protected or identified for protection in accordance with Policy RCO 1 of the Structure Plan) in accordance with Government Legal Notice 400 of 1996 (Anon, 1995). In accordance with Structure Plan Policy RCO14, the greater part of the Delimara Peninsula is designated as a National park, as outline in policy MD01 of the Marsaxlokk Local Plan (1995).

2) St Thomas Bay: shore platforms of Ponta tal-Miġnuna and Ponta tal-Munxar

A few coastal military structures (ex. Riħama Battery, St Thomas Tower and Battery, l-Għassa tal-Munxar) dating back the ruling period of the Knights of St John and that of the British still survive in proximity of these shore platforms, as a remembrance of the strategic importance of sheltered low-lying bays in preventing invading enemy forces from landing their troops ashore through the use of these (Spiteri, 2012). The northern part of the bay's inner recess has been mostly concreted over by a number of maritime-related structures such as jetties and slipways in order to facilitate fishing and water sports activities (ex. kayaking) in the foreshore area. Two narrow beaches, one with coarse sand and gravel deposits (c. 252ms long and 10 ms wide) and another with finer sand deposits (92.5ms long and 16.2 ms wide), fringe the central and southern side of littoral and service mostly bathers and snorkellers. Other pockets of sand or mixed deposits have formed naturally in more secluded pockets along the northern rocky littoral of the bay and together with the shore platforms, serve as focal recreational points for bathers from nearby villages of Fgura, Żabbar and Żejtun.

The recreational use of the shore platforms skirting St Thomas Bay was largely influenced by the growth of its closest town, Marsaskala, which grew very rapidly over the last five decades as a result of planned schemes of urban development dating back to early 60s. Such schemes contributed to an

exponential population growth in the 70s and 80s and very sharply in the 90s (MEPA, 2006). Between 1985 and 2011 the population increased by 571% i.e. from 1936 to 11056 inhabitants (NSO, 2012). This growth pushed for a lot of changes and pressure on the coast between Marsascala Bay and St Thomas Bay (MEPA, 2006). The overall planning strategy for St Thomas Bay is regulated by the South Malta Local Plan (MEPA, 2006), in which the bay is currently designated for built-up development as a Coastal Recreational Area (SMLP Policy code SMMS 08). Presently this part of the bay is contentiously occupied by 370 privately-owned boathouses that were built during the unregulated years prior to1992 and serve more as beachrooms rather than boat storages.

The platforms and ease of access to the sea by these landforms has contributed in part to this intense recreational growth. However, they are also considered sensitive areas for a variety of reasons. The rocky shores along the northern part of the bay (which include the studied shore platform of Ponta tal-Miġnuna) are scheduled as Green Area (SMLP Policy code SMSE 04) and as Area of Ecological Importance and Sites of Scientific Importance (SMLP Policy Code SMCO 03) (MEPA, 2006). The Munxar littoral in the southern part of the bay (where the second platform is situated), is situated in a more rural setting and scheduled as a National Park (SMLP Policy Code SMIA 13) primarily for informal recreation (e.g. walking, cycling). It is also classified as Area of Ecological Importance and Sites of Scientific Importance (SMLP Policy Code SMCO 03) due to its many Pleistocene deposits, endemic species and being one of the longest stretches of coast in Middle Globigerina Limestone cliffs along the promontory of l-Għassa tal-Munxar (MEPA, 2006). Clearly, a study about the processes of change of the shore platforms in the bay provides an additional scientific input to the present environmental legal scheduling of the bay.

3) Marfa Ridge: shore platform of Ponta tal-Qammieħ

The rdum area of Qammieħ forms part of one of the largest Natura 2000 Special Area of Conservation (SAC) that covers 4.13km^2 of rdum coasts on the western part of Malta (ERA, 2012). The site was designated as a SAC via Government Notice 112 of 2007, and as declared through the provisions of the Flora, Fauna and Natural Habitats Regulations of 2006 (Legal Notice 311 of 2006). The Qammieħ area was previously scheduled as Areas of High Landscape Value (in accordance with Section 46 of the Development Planning Act 1992) and as Scheduling of Coastal Cliffs as Area of Ecological Importance / Site of Scientific Importance (as per Government Legal Notice 400 of 1996). All the legal establishments for Qammieħ focus primarily on the fact that the inaccessible coastal cliffs and the sheltering rdum with their boulder scree support an important biotope based upon a wide array of Maltese endemic and sub-endemic species. The inaccessibility of these habitats makes them important for their ornithological value as well. A depression formed in the

elevated Globigerina platform along Rdum il-Qammieħ is also mentioned but only in relation to its role in creating freshwater wetland conditions that serve as a breeding ground for birds and for supporting rare and endangered species, (ERA, 2012b).

4) Selmun: shore platform of Blata l-Bajda

Selmun is designated as a Special Area of Conservation and Candidate Site of International Importance via Government Notice 112 of 2007, as declared through the provisions of the Flora, Fauna and Natural Habitats Regulations of 2006 (Legal Notice 311 of 2006). St Paul's Islands were designated as a Nature Reserve via LN 25 of 1993 and declared as a Specially Protected Area under the SPA Protocol (Barcelona Convention) since 1986. Specifically, the geomorphologic features coastal caves, rock platforms and low cliffs in the area falls within a Coastal Cliffs Area of High Landscape Value AHLV) (GN 400/96). Other landscape assets include the rich rural, archaeological and historical heritage present in the area.

Appendix VI – Schmidt Hammer Field Data: raw and normalised R values for each platform (10 tables)

{Raw data presented to examiners)

Appendix VII– Experimental Slabs: Description of weathering grades based on ISRM (1981) method (3 tables)

Slab Photo Before Exposure	Slab Photo After Exposure	Weathering State Description	Grade ISRM (1981)	Colour	Texture
		1. Blata l-Bajda - Front •Visible signs of perimeter alterations •Smoothing of rough edges by solution • Heavy powdering from surface	W3	•Heavy discolouration to one or two shades lighter than original colour	•Heavy powdered surface •Flaking
		4 . Ponta tal-Munxar – Back •Evident signs of rock physical breakdown with presence of fractures and splinter fragments •Partial loss of original shape	W3	•Evident signs of discolouration to one shade lighter than original colour	•Coarser •More visible pitting •Fresh fractured surfaces at the sides
		5. Globigerina Building Block •Minor signs of alterations •Form and perimeter intact and retained 95% of original shape •Minor loss of weight •Minor loss of debris	W1	•Colouration to one or two shades darker than original colour	•No alterations from original texture •No flaking, or powdering •Minor pitting
		6. Ras il-Fenek Front •Slabs lose their original shape completely. •Remnants have fragile structure •Total loss of TMEM studs •Heavy loss of weight and debris	W4	•Total discolouration to two or more lighter shades. •Whitish colour observed	•Very friable •Coated with weathered powder both at the surface and around the perimeter

Slab Photo Before Exposure	Slab Photo After Exposure	Weathering State Description	Grade ISRM (1981)	Colour	Texture
		7. Ponta tal-Munxar Back •Visible signs of perimeter alterations •Smoothing of rough edges by solution • Signs of chipping by minor fracturing	W2	•Evident signs of discolouration to one shade lighter than original colour	•Coarser •More visible pitting •Minor hairline cracks
		11. Ponta tal-Mignuna Back •Visible signs of perimeter alterations •Smoothing of rough edges by solution • Signs of chipping by minor fracturing	W2	•Evident signs of discolouration to one shade lighter than original colour	•Evident signs of discolouration to one shade lighter than original colour
		12. Blata l-Bajda Back •Slabs lose their original shape completely. •Remnants have fragile structure •Total loss of TMEM studs •Heavy loss of weight and debris	W4	•Heavy discolouration to one or two shades lighter than original colour	•Very friable •Coated with weathered powder both at the surface and around the perimeter
		13. Ponta tal-Mignuna Front •Visible signs of perimeter alterations •Smoothing of rough edges by solution • Signs of chipping by minor fracturing	W2	•Evident signs of discolouration to one shade lighter than original colour	•Evident signs of discolouration to one shade lighter than original colour

Slab Photo Before Exposure	Slab Photo After Exposure	Weathering State Description	Grade ISRM (1981)	Colour	Texture
		14. Ras il-Fenek Front •Visible signs of perimeter alterations •Smoothing of rough edges by solution • Signs of chipping by minor fracturing	W2	•Evident signs of discolouration to one shade lighter than original colour	•Coarser •More visible pitting •Fresh fractured surfaces at the sides
		15. Ponta tal-Qammieh Back •Visible signs of perimeter alterations •Smoothing of rough edges by solution • Signs of chipping by minor fracturing	W2	•Signs of colouration to one shade darker than original colour	•Coarser •More visible pitting •Fresh fractured surfaces at the sides
		16.Ponta tal-Qammieh Front •Visible signs of perimeter alterations •Smoothing of rough edges by solution • Signs of chipping by minor fracturing	W2	•Signs of colouration to one shade darker than original colour	•Coarser •More visible pitting •Fresh fractured surfaces at the sides

Appendix VIII – TMEM Data: Field Measurements and Final Surface Change for each station

(Raw data presented to examiners)

Appendix IX – TMEM Measurements on Experimental Slabs Surfaces

{Raw data presented to examiners)